

Waste Isolation Pilot Plant



# TRUPACT-II

## Safety Analysis Report



Revision 23  
April 2012

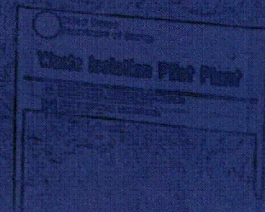


## TABLE OF CONTENTS

<b>1.0 GENERAL INFORMATION .....</b>	<b>1.1-1</b>
1.1 Introduction .....	1.1-1
1.2 Package Description .....	1.2-1
1.2.1 Packaging .....	1.2-1
1.2.1.1 Packaging Description.....	1.2-1
1.2.1.2 Gross Weight.....	1.2-5
1.2.1.3 Neutron Moderation and Absorption .....	1.2-5
1.2.1.4 Receptacles, Valves, Testing, and Sampling Ports .....	1.2-5
1.2.1.5 Heat Dissipation .....	1.2-6
1.2.1.6 Coolants.....	1.2-6
1.2.1.7 Protrusions.....	1.2-6
1.2.1.8 Lifting and Tie-down Devices.....	1.2-6
1.2.1.9 Pressure Relief System.....	1.2-7
1.2.1.10 Shielding.....	1.2-7
1.2.2 Operational Features.....	1.2-7
1.2.3 Contents of Packaging.....	1.2-8
1.3 Appendices .....	1.3-1
1.3.1 Packaging General Arrangement Drawings .....	1.3.1-1
1.3.2 Glossary of Terms and Acronyms.....	1.3.2-1
<b>2.0 STRUCTURAL EVALUATION .....</b>	<b>2.1-1</b>
2.1 Structural Design .....	2.1-1
2.1.1 Discussion .....	2.1-1
2.1.1.1 Containment Vessel Structure (ICV) .....	2.1-1
2.1.1.2 Non-Containment Vessel Structures (OCV and OCA).....	2.1-2
2.1.2 Design Criteria .....	2.1-3
2.1.2.1 Analytic Design Criteria (Allowable Stresses) .....	2.1-3
2.1.2.2 Miscellaneous Structural Failure Modes.....	2.1-4
2.2 Weights and Centers of Gravity .....	2.2-1
2.2.1 Effect of a Radial Payload Imbalance .....	2.2-1
2.2.2 Effect of an Axial Payload Imbalance.....	2.2-3
2.2.3 Significance of Package Center of Gravity Shifts.....	2.2-4
2.2.3.1 Lifting.....	2.2-4
2.2.3.2 Tie-down .....	2.2-4
2.2.3.3 Vibration.....	2.2-5
2.2.3.4 Free Drop and Puncture.....	2.2-5
2.3 Mechanical Properties of Materials.....	2.3-1
2.3.1 Mechanical Properties Applied to Analytic Evaluations .....	2.3-1

2.3.2	Mechanical Properties Applied to Certification Testing.....	2.3-2
2.4	General Standards for All Packages.....	2.4-1
2.4.1	Minimum Package Size.....	2.4-1
2.4.2	Tamper-indicating Feature.....	2.4-1
2.4.3	Positive Closure.....	2.4-1
2.4.4	Chemical and Galvanic Reactions.....	2.4-1
2.4.4.1	Packaging Materials of Construction.....	2.4-2
2.4.4.2	Payload Interaction with Packaging Materials of Construction....	2.4-3
2.4.5	Valves.....	2.4-3
2.4.6	Package Design.....	2.4-3
2.4.7	External Temperatures.....	2.4-3
2.4.8	Venting.....	2.4-4
2.5	Lifting and Tie-down Standards for All Packages.....	2.5-1
2.5.1	Lifting Devices.....	2.5-1
2.5.2	Tie-down Devices.....	2.5-2
2.5.2.1	Tie-down Forces.....	2.5-2
2.5.2.2	Tie-down Stress Due to a Vertical Tensile Load.....	2.5-3
2.5.2.3	Tie-down Stress Due to a Vertical Compressive Load.....	2.5-7
2.5.2.4	Tie-down Stresses Due to a Horizontal Compressive Load.....	2.5-8
2.5.2.5	Response of the Package if Treated as a Fixed Cantilever Beam.....	2.5-10
2.5.2.6	Summary.....	2.5-11
2.6	Normal Conditions of Transport.....	2.6-1
2.6.1	Heat.....	2.6-2
2.6.1.1	Summary of Pressures and Temperatures.....	2.6-2
2.6.1.2	Differential Thermal Expansion.....	2.6-3
2.6.1.3	Stress Calculations.....	2.6-3
2.6.1.4	Comparison with Allowable Stresses.....	2.6-4
2.6.1.5	Range of Primary Plus Secondary Stress Intensities.....	2.6-5
2.6.2	Cold.....	2.6-6
2.6.2.1	Stress Calculations.....	2.6-6
2.6.2.2	Comparison with Allowable Stresses.....	2.6-7
2.6.3	Reduced External Pressure.....	2.6-7
2.6.4	Increased External Pressure.....	2.6-8
2.6.4.1	Stress Calculations.....	2.6-8
2.6.4.2	Comparison with Allowable Stresses.....	2.6-9
2.6.4.3	Buckling Assessment of the Torispherical Heads.....	2.6-9
2.6.4.4	Buckling Assessment of the Cylindrical Shells.....	2.6-10
2.6.5	Vibration.....	2.6-11
2.6.5.1	Vibratory Loads Determination.....	2.6-12
2.6.5.2	Calculation of Alternating Stresses.....	2.6-12
2.6.5.3	Stress Limits and Results.....	2.6-13
2.6.6	Water Spray.....	2.6-14

2.6.7	Free Drop.....	2.6-14
2.6.8	Corner Drop.....	2.6-14
2.6.9	Compression.....	2.6-14
2.6.10	Penetration.....	2.6-14
2.7	Hypothetical Accident Conditions.....	2.7-1
2.7.1	Free Drop.....	2.7-2
2.7.1.1	Technical Basis for the Free Drop Tests.....	2.7-2
2.7.1.2	Test Sequence for the Selected Tests.....	2.7-3
2.7.1.3	Summary of Results from the Free Drop Tests.....	2.7-3
2.7.1.4	End Drop Bucking Evaluation.....	2.7-4
2.7.2	Crush.....	2.7-4
2.7.3	Puncture.....	2.7-5
2.7.3.1	Technical Basis for the Puncture Drop Tests.....	2.7-5
2.7.3.2	Test Sequence for the Selected Tests.....	2.7-6
2.7.3.3	Summary of Results from the Puncture Drop Tests.....	2.7-6
2.7.4	Thermal.....	2.7-7
2.7.4.1	Summary of Pressures and Temperatures.....	2.7-8
2.7.4.2	Differential Thermal Expansion.....	2.7-8
2.7.4.3	Stress Calculations.....	2.7-8
2.7.4.4	Comparison with Allowable Stresses.....	2.7-9
2.7.5	Immersion – Fissile Material.....	2.7-9
2.7.6	Immersion – All Packages.....	2.7-9
2.7.6.1	Buckling Assessment of the Torispherical Heads.....	2.7-9
2.7.6.2	Buckling Assessment of the Cylindrical Shells.....	2.7-10
2.7.7	Deep Water Immersion Test.....	2.7-12
2.7.8	Summary of Damage.....	2.7-12
2.8	Special Form.....	2.8-1
2.9	Fuel Rods.....	2.9-1
2.10	Appendices.....	2.10-1
2.10.1	Finite Element Analysis (FEA) Models.....	2.10.1-1
2.10.1.1	Outer Confinement Assembly (OCA) Structural Analysis.....	2.10.1-1
2.10.1.2	Inner Containment Vessel (ICV) Structural Analysis.....	2.10.1-5
2.10.2	Elastomer O-ring Seal Performance Tests.....	2.10.2-1
2.10.2.1	Introduction.....	2.10.2-1
2.10.2.2	Limits of O-ring Seal Compression and Temperature.....	2.10.2-1
2.10.2.3	Formulation Qualification Test Fixture and Procedure.....	2.10.2-6
2.10.2.4	Rainier Rubber R0405-70 Formulation Qualification Test Results .....	2.10.2-7
2.10.2.5	ASTM D2000 Standardized Batch Material Tests.....	2.10.2-8
2.10.3	Certification Tests.....	2.10.3-1
2.10.3.1	Introduction.....	2.10.3-1
2.10.3.2	Summary.....	2.10.3-1

2.10.3.3	Test Facilities .....	2.10.3-3
2.10.3.4	Description of the Certification Test Units .....	2.10.3-4
2.10.3.5	Technical Basis for Tests .....	2.10.3-10
2.10.3.6	Test Sequence for Selected Free Drop, Puncture Drop, and Fire Tests .....	2.10.3-14
2.10.3.7	Test Results .....	2.10.3-23
<b>3.0</b>	<b>THERMAL EVALUATION .....</b>	<b>3.1-1</b>
3.1	Discussion .....	3.1-1
3.1.1	Packaging .....	3.1-1
3.1.2	Payload Configuration.....	3.1-2
3.1.3	Boundary Conditions.....	3.1-3
3.1.4	Analysis Summary .....	3.1-4
3.2	Summary of Thermal Properties of Materials.....	3.2-1
3.3	Technical Specifications of Components.....	3.3-1
3.4	Thermal Evaluation for Normal Conditions of Transport.....	3.4-1
3.4.1	Thermal Model .....	3.4-1
3.4.1.1	Analytical Model.....	3.4-1
3.4.1.2	Test Model.....	3.4-3
3.4.2	Maximum Temperatures .....	3.4-3
3.4.3	Minimum Temperatures .....	3.4-3
3.4.4	Maximum Internal Pressure .....	3.4-3
3.4.4.1	Design Pressure .....	3.4-3
3.4.4.2	Maximum Pressure for Normal Conditions of Transport .....	3.4-3
3.4.4.3	Maximum Normal Operating Pressure.....	3.4-9
3.4.5	Maximum Thermal Stresses .....	3.4-10
3.4.6	Evaluation of Package Performance for Normal Conditions of Transport	3.4-11
3.5	Thermal Evaluation for Hypothetical Accident Conditions.....	3.5-1
3.5.1	Thermal Model .....	3.5-1
3.5.1.1	Analytical Model.....	3.5-1
3.5.1.2	Test Model.....	3.5-1
3.5.2	Package Conditions and Environment .....	3.5-2
3.5.2.1	CTU-1 Package Conditions and Environment .....	3.5-2
3.5.2.2	CTU-2 Package Conditions and Environment .....	3.5-3
3.5.3	Package Temperatures.....	3.5-3
3.5.4	Maximum Internal Pressure .....	3.5-3
3.5.5	Maximum Thermal Stresses .....	3.5-4
3.5.6	Evaluation of Package Performance for the Hypothetical Accident Thermal Conditions .....	3.5-4
3.6	Appendices .....	3.6-1

3.6.1	Computer Analysis Results .....	3.6.1-1
3.6.1.1	Fourteen 55-Gallon Drum Payload with 100 °F Ambient and Full Solar, Uniformly Distributed Decay Heat Load in All Drums (Case 1) .....	3.6.1-1
3.6.1.2	Fourteen 55-Gallon Drum Payload with 100 °F Ambient and Full Solar, Uniformly Distributed Decay Heat Load in Two Center Drums (Case 2).....	3.6.1-4
3.6.1.3	Fourteen 55-Gallon Drum Payload with 100 °F Ambient and Full Solar, Uniformly Distributed Decay Heat Load in Top Center Drum (Case 3).....	3.6.1-7
3.6.1.4	Two Standard Waste Box Payload with 100 °F Ambient and Full Solar, Uniformly Distributed Decay Heat Load in Both SWBs (Case 4).....	3.6.1-10
3.6.1.5	Two Standard Waste Box Payload with 100 °F Ambient and Full Solar, Uniformly Distributed Decay Heat Load in Top SWB (Case 5) .....	3.6.1-12
3.6.1.6	Fourteen 55-Gallon Drum Payload with 100 °F Ambient and No Solar, 40 Watts Uniform Decay Heat Load .....	3.6.1-14
3.6.1.7	Two Standard Waste Box Payload with 100 °F Ambient and No Solar, 40 Watts Uniform Decay Heat Load .....	3.6.1-16
3.6.2	Thermal Model Details.....	3.6.2-1
3.6.2.1	Convection Coefficient Calculation .....	3.6.2-1
3.6.2.2	Polyethylene Plastic Wrap Transmittance Calculation .....	3.6.2-2
<b>4.0</b>	<b>CONTAINMENT .....</b>	<b>4.1-1</b>
4.1	Containment Boundary.....	4.1-1
4.1.1	Containment Vessel.....	4.1-1
4.1.1.1	Outer Confinement Assembly (Secondary Confinement).....	4.1-1
4.1.1.2	Inner Containment Vessel (Primary Containment).....	4.1-1
4.1.2	Containment Penetrations.....	4.1-1
4.1.3	Seals and Welds.....	4.1-2
4.1.3.1	Seals.....	4.1-2
4.1.3.2	Welds.....	4.1-2
4.1.4	Closure.....	4.1-3
4.1.4.1	Outer Confinement Assembly (OCA) Closure .....	4.1-3
4.1.4.2	Inner Containment Vessel (ICV) Closure .....	4.1-3
4.2	Containment Requirements for Normal Conditions of Transport.....	4.2-1
4.2.1	Containment of Radioactive Material .....	4.2-1
4.2.2	Pressurization of Containment Vessel.....	4.2-1
4.2.3	Containment Criterion .....	4.2-1
4.3	Containment Requirements for Hypothetical Accident Conditions.....	4.3-1
4.3.1	Fission Gas Products .....	4.3-1
4.3.2	Containment of Radioactive Material .....	4.3-1

4.3.3	Containment Criterion .....	4.3-1
4.4	Special Requirements .....	4.4-1
4.4.1	Plutonium Shipments .....	4.4-1
4.4.2	Interchangeability .....	4.4-1
<b>5.0</b>	<b>SHIELDING EVALUATION .....</b>	<b>5.1-1</b>
5.1	Description of Shielding Design .....	5.1-2
5.1.1	Design Features .....	5.1-2
5.1.1.1	TRUPACT-II and HalfPACT .....	5.1-2
5.1.1.2	Generic .....	5.1-2
5.1.1.3	Criticality Control Overpack .....	5.1-3
5.1.1.4	6-in. Standard Pipe Overpack .....	5.1-3
5.1.1.5	12-in. Standard Pipe Overpack .....	5.1-3
5.1.1.6	Shielded Container Assembly .....	5.1-4
5.1.2	Summary Table of Maximum Radiation Levels .....	5.1-9
5.2	Source Specification .....	5.2-1
5.2.1	Gamma Source .....	5.2-1
5.2.2	Neutron Source .....	5.2-2
5.3	Shielding Model .....	5.3-1
5.3.1	Configuration of Source and Shielding .....	5.3-1
5.3.1.1	TRUPACT-II and HalfPACT .....	5.3-1
5.3.1.2	Generic .....	5.3-2
5.3.1.3	Criticality Control Overpack .....	5.3-2
5.3.1.4	6-in. Standard Pipe Overpack .....	5.3-3
5.3.1.5	12-in. Standard Pipe Overpack .....	5.3-3
5.3.1.6	Shielded Container Assembly .....	5.3-4
5.3.2	Material Properties .....	5.3-15
5.4	Shielding Evaluation .....	5.4-1
5.4.1	Methods .....	5.4-1
5.4.2	Input and Output Data .....	5.4-1
5.4.3	Flux-to-Dose Conversion .....	5.4-2
5.4.4	External Radiation Levels .....	5.4-3
5.4.4.1	Generic .....	5.4-4
5.4.4.2	Criticality Control Overpack .....	5.4-5
5.4.4.3	6-in. Standard Pipe Overpack .....	5.4-6
5.4.4.4	12-in. Standard Pipe Overpack .....	5.4-7
5.4.4.5	Shielded Container Assembly .....	5.4-7
5.4.4.6	Summary .....	5.4-8
5.5	Activity Limits .....	5.5-1
5.5.1	Generic .....	5.5-2
5.5.2	Criticality Control Overpack .....	5.5-10

5.5.3	6-in. Standard Pipe Overpack.....	5.5-17
5.5.4	12-in. Standard Pipe Overpack.....	5.5-21
5.5.5	Shielded Container Assembly .....	5.5-25
5.5.6	Determination of Acceptable Activity .....	5.5-29
5.5.6.1	Acceptable Activity Examples .....	5.5-30
5.6	Conclusions .....	5.6-1
5.7	Appendices .....	5.7-1
5.7.1	Sample MCNP Input Files .....	5.7.1-1
5.7.1.1	TRUPACT-II – Generic .....	5.7.1-1
5.7.1.2	HalfPACT – Generic .....	5.7.1-10
5.7.1.3	TRUPACT-II – Criticality Control Overpack.....	5.7.1-13
5.7.1.4	HalfPACT – Criticality Control Overpack.....	5.7.1-18
5.7.1.5	HalfPACT – 6-in. Standard Pipe Overpack .....	5.7.1-22
5.7.1.6	HalfPACT – 12-in. Standard Pipe Overpack .....	5.7.1-26
5.7.1.7	HalfPACT – Shielded Container Assembly .....	5.7.1-31
<b>6.0</b>	<b>CRITICALITY EVALUATION.....</b>	<b>6.1-1</b>
6.1	Discussion and Results .....	6.1-2
6.2	Package Contents .....	6.2-1
6.2.1	Applicability of Case A Limit .....	6.2-2
6.2.2	Applicability of Case B Limit .....	6.2-3
6.2.3	Applicability of Case C Limit .....	6.2-3
6.2.4	Applicability of Case D Limit .....	6.2-4
6.2.5	Applicability of Case E Limit .....	6.2-5
6.2.6	Applicability of Case F Limit.....	6.2-5
6.2.7	Applicability of Case I Limit.....	6.2-5
6.3	Model Specification .....	6.3-1
6.3.1	Contents Model .....	6.3-1
6.3.1.1	Case A Contents Model.....	6.3-1
6.3.1.2	Case B Contents Model.....	6.3-2
6.3.1.3	Case C Contents Model.....	6.3-2
6.3.1.4	Case D Contents Model.....	6.3-2
6.3.2	Packaging Model.....	6.3-3
6.3.3	Single-Unit Models .....	6.3-4
6.3.4	Array Models.....	6.3-5
6.3.5	Package Regional Densities .....	6.3-5
6.4	Criticality Calculations.....	6.4-1
6.4.1	Calculational or Experimental Method .....	6.4-1
6.4.2	Fuel Loading or Other Contents Loading Optimization .....	6.4-1
6.4.3	Criticality Results .....	6.4-2

6.4.3.1	Criticality Results for a Single TRUPACT-II Package.....	6.4-3
6.4.3.2	Criticality Results for Infinite Arrays of TRUPACT-II Packages.....	6.4-4
6.4.3.3	Special Reflectors in CH-TRU Waste.....	6.4-7
6.4.3.4	Machine Compacted CH-TRU Waste.....	6.4-8
6.4.3.5	Applicable Criticality Limits for CH-TRU Waste.....	6.4-9
6.5	Critical Benchmark Experiments.....	6.5-1
6.5.1	Benchmark Experiments and Applicability.....	6.5-1
6.5.2	Details of Benchmark Calculations.....	6.5-2
6.5.3	Results of Benchmark Calculations.....	6.5-2
<b>7.0</b>	<b>OPERATING PROCEDURES.....</b>	<b>7.1-1</b>
7.1	Procedures for Loading the Package.....	7.1-1
7.1.1	Removal of the TRUPACT-II Package from the Transport Trailer/Railcar.....	7.1-1
7.1.2	Outer Confinement Assembly (OCA) Lid Removal.....	7.1-1
7.1.3	Inner Containment Vessel (ICV) Lid Removal.....	7.1-2
7.1.4	Loading the Payload into the TRUPACT-II Package.....	7.1-2
7.1.5	Inner Containment Vessel (ICV) Lid Installation.....	7.1-3
7.1.6	Outer Confinement Assembly (OCA) Lid Installation.....	7.1-4
7.1.7	Final Package Preparations for Transport (Loaded).....	7.1-5
7.2	Procedures for Unloading the Package.....	7.2-1
7.2.1	Removal of the TRUPACT-II Package from the Transport Trailer/Railcar.....	7.2-1
7.2.2	Outer Confinement Assembly (OCA) Lid Removal.....	7.2-1
7.2.3	Inner Containment Vessel (ICV) Lid Removal.....	7.2-2
7.2.4	Unloading the Payload from the TRUPACT-II Package.....	7.2-2
7.2.5	Inner Containment Vessel (ICV) Lid Installation.....	7.2-2
7.2.6	Outer Confinement Assembly (OCA) Lid Installation.....	7.2-3
7.2.7	Final Package Preparations for Transport (Unloaded).....	7.2-4
7.3	Preparation of an Empty Package for Transport.....	7.3-1
7.4	Preshipment Leakage Rate Test.....	7.4-1
7.4.1	Gas Pressure Rise Leakage Rate Test Acceptance Criteria.....	7.4-1
7.4.2	Determining the Test Volume and Test Time.....	7.4-1
7.4.3	Performing the Gas Pressure Rise Leakage Rate Test.....	7.4-2
7.4.4	Optional Preshipment Leakage Rate Test.....	7.4-2
<b>8.0</b>	<b>ACCEPTANCE TESTS AND MAINTENANCE PROGRAM.....</b>	<b>8.1-1</b>
8.1	Acceptance Tests.....	8.1-1
8.1.1	Visual Inspection.....	8.1-1
8.1.2	Structural and Pressure Tests.....	8.1-1
8.1.2.1	Lifting Device Load Testing.....	8.1-1

8.1.2.2	Pressure Testing .....	8.1-2
8.1.3	Fabrication Leakage Rate Tests .....	8.1-2
8.1.3.1	Fabrication Leakage Rate Test Acceptance Criteria .....	8.1-3
8.1.3.2	Helium Leakage Rate Testing the ICV Structure Integrity .....	8.1-3
8.1.3.3	Helium Leakage Rate Testing the ICV Main O-ring Seal .....	8.1-3
8.1.3.4	Helium Leakage Rate Testing the ICV Outer Vent Port Plug O-ring Seal .....	8.1-4
8.1.3.5	Optional Helium Leakage Rate Testing the OCV Structure Integrity .....	8.1-5
8.1.3.6	Optional Helium Leakage Rate Testing the OCV Main O-ring Seal Integrity .....	8.1-5
8.1.3.7	Optional Helium Leakage Rate Testing the OCV Vent Port Plug O-ring Seal Integrity .....	8.1-6
8.1.4	Component Tests .....	8.1-7
8.1.4.1	Polyurethane Foam .....	8.1-7
8.1.5	Tests for Shielding Integrity .....	8.1-19
8.1.6	Thermal Acceptance Test .....	8.1-19
8.2	Maintenance Program .....	8.2-1
8.2.1	Structural and Pressure Tests .....	8.2-1
8.2.1.1	Pressure Testing .....	8.2-1
8.2.1.2	ICV Interior Surfaces Inspection .....	8.2-1
8.2.2	Maintenance/Periodic Leakage Rate Tests .....	8.2-1
8.2.2.1	Maintenance/Periodic Leakage Rate Test Acceptance Criteria .....	8.2-2
8.2.2.2	Helium Leakage Rate Testing the ICV Main O-ring Seal .....	8.2-2
8.2.2.3	Helium Leakage Rate Testing the ICV Outer Vent Port Plug O-ring Seal .....	8.2-3
8.2.3	Subsystems Maintenance .....	8.2-3
8.2.3.1	Fasteners .....	8.2-3
8.2.3.2	Locking Rings .....	8.2-3
8.2.3.3	Seal Areas and Grooves .....	8.2-4
8.2.4	Valves, Rupture Discs, and Gaskets .....	8.2-6
8.2.4.1	Valves .....	8.2-6
8.2.4.2	Rupture Discs .....	8.2-6
8.2.4.3	Gaskets .....	8.2-6
8.2.5	Shielding .....	8.2-7
8.2.6	Thermal .....	8.2-7
<b>9.0</b>	<b>QUALITY ASSURANCE .....</b>	<b>9.1-1</b>
9.1	Introduction .....	9.1-1
9.2	Quality Assurance Requirements .....	9.2-1
9.2.1	U.S. Nuclear Regulatory Commission .....	9.2-1
9.2.2	U.S. Department of Energy .....	9.2-1

9.2.3	Transportation to or from WIPP .....	9.2-1
9.3	Quality Assurance Program.....	9.3-1
9.3.1	NRC Regulatory Guide 7.10 .....	9.3-1
9.3.2	Design.....	9.3-1
9.3.3	Fabrication, Assembly, Testing, and Modification .....	9.3-1
9.3.4	Use.....	9.3-1
	9.3.4.1 DOE Shipments: To/From WIPP .....	9.3-1
	9.3.4.2 Other DOE Shipments: Non-WIPP .....	9.3-2
	9.3.4.3 Non-DOE Users of TRUPACT-II.....	9.3-2
9.3.5	Maintenance and Repair.....	9.3-2

## LIST OF TABLES

Table 2.1-1	– Containment Structure Allowable Stress Limits .....	2.1-7
Table 2.1-2	– Non-Containment Structure Allowable Stress Limits.....	2.1-7
Table 2.2-1	– TRUPACT-II Weight and Center of Gravity .....	2.2-6
Table 2.3-1	– Mechanical Properties of Type 304 Stainless Steel Components (for Analysis).....	2.3-5
Table 2.3-2	– Mechanical Properties of Polyurethane Foam (for Analysis) .....	2.3-7
Table 2.3-3	– Mechanical Properties of Metallic Materials (for Testing) .....	2.3-7
Table 2.6-1	– Summary of Stress Intensity Results for OCA Load Case 1 <sup>o</sup> .....	2.6-16
Table 2.6-2	– Summary of Stress Intensity Results for OCA Load Case 2 <sup>o</sup> .....	2.6-17
Table 2.6-3	– Summary of Stress Intensity Results for OCA Load Case 3 <sup>o</sup> .....	2.6-18
Table 2.6-4	– Summary of Stress Intensity Results for OCA Load Case 4 <sup>o</sup> .....	2.6-19
Table 2.6-5	– Summary of Stress Intensity Results for ICV Load Case 1 <sup>o</sup> .....	2.6-20
Table 2.6-6	– Summary of Stress Intensity Results for ICV Load Case 2 <sup>o</sup> .....	2.6-21
Table 2.6-7	– Buckling Geometry Parameters per Code Case N-284 .....	2.6-22
Table 2.6-8	– Stress Results for 14.7 psig External Pressure .....	2.6-23
Table 2.6-9	– Shell Buckling Summary for 14.7 psig External Pressure .....	2.6-23
Table 2.6-10	– Tie-Down Lug Weld Shear Stresses.....	2.6-24
Table 2.6-11	– OCA Outer Shell Compressive Membrane Stresses .....	2.6-24
Table 2.6-12	– OCA Tie-down Weldment Compressive Membrane Stresses.....	2.6-24
Table 2.6-13	– Maximum Unit Alternating Stress Intensities .....	2.6-24
Table 2.7-1	– Summary of Tests for TRUPACT-II CTU-1.....	2.7-13
Table 2.7-2	– Summary of Tests for TRUPACT-II CTU-2.....	2.7-14
Table 2.7-3	– Summary of Tests for TRUPACT-II CTU-3.....	2.7-15

Table 2.7-4 – Buckling Geometry Parameters for a 385g HAC End Drop .....	2.7-17
Table 2.7-5 – Shell Buckling Summary for a 385g HAC End Drop .....	2.7-18
Table 2.7-6 – Buckling Geometry Parameters per Code Case N-284 .....	2.7-19
Table 2.7-7 – Stress Results for 21 psig External Pressure .....	2.7-20
Table 2.7-8 – Shell Buckling Summary for 21 psig External Pressure .....	2.7-20
Table 2.10.1-1 – ANSYS® Input Listing for OCA Load Case 1 .....	2.10.1-7
Table 2.10.1-2 – ANSYS® Input Listing for OCA Load Case 2 .....	2.10.1-11
Table 2.10.1-3 – ANSYS® Input Listing for OCA Load Case 3 .....	2.10.1-15
Table 2.10.1-4 – ANSYS® Input Listing for OCA Load Case 4 .....	2.10.1-19
Table 2.10.1-5 – ANSYS® Input Listing for ICV Load Case 1 .....	2.10.1-23
Table 2.10.1-6 – ANSYS® Input Listing for ICV Load Case 2 .....	2.10.1-25
Table 2.10.2-1 – Formulation Qualification Test O-ring Seal Compression Parameters....	2.10.2-5
Table 2.10.2-2 – Rainier Rubber R0405-70 Formulation Qualification O-ring Seal Test Results .....	2.10.2-11
Table 2.10.3-1 – Summary of CTU-1 Test Results in Sequential Order .....	2.10.3-37
Table 2.10.3-2 – Summary of CTU-2 Test Results in Sequential Order .....	2.10.3-38
Table 2.10.3-3 – Summary of CTU-3 Test Results in Sequential Order .....	2.10.3-39
Table 2.10.3-4 – CTU-1 Temperature Indicating Label Locations and Results.....	2.10.3-41
Table 2.10.3-5 – CTU-2 Temperature Indicating Label Locations and Results.....	2.10.3-43
Table 3.1-1 – NCT Steady-State Temperatures with 40 Watts Decay Heat Load and Insolation; Fourteen 55-Gallon Drums .....	3.1-6
Table 3.1-2 – NCT Steady-State Temperatures with 40 Watts Decay Heat Load and No Insolation; Fourteen 55-Gallon Drums .....	3.1-7
Table 3.1-3 – NCT Steady-State Temperatures with 40 Watts Decay Heat Load and Insolation; Two Standard Waste Boxes .....	3.1-8
Table 3.1-4 – NCT Steady-State Temperatures with 40 Watts Decay Heat Load and No Insolation; Two Standard Waste Boxes .....	3.1-9
Table 3.2-1 – Thermal Properties of Materials .....	3.2-2
Table 3.2-2 – Thermal Properties of Air .....	3.2-2
Table 3.2-3 – Thermal Radiative Properties .....	3.2-3
Table 3.4-1 – NCT Steady-State Temperatures with Insolation, Payload Configuration 1 - Fourteen 55-Gallon Drums, Thermal Case 1 .....	3.4-12
Table 3.4-2 – NCT Steady-State Temperatures with Insolation, Payload Configuration 1 - Fourteen 55-Gallon Drums, Thermal Case 2 .....	3.4-13

Table 3.4-3 – NCT Steady-State Temperatures with Insolation, Payload Configuration 1 - Fourteen 55-Gallon Drums, Thermal Case 3 ..... 3.4-14

Table 3.4-4 – NCT Steady-State Temperatures with Insolation, Payload Configuration 2 - Two Standard Waste Boxes, Thermal Case 4 ..... 3.4-15

Table 3.4-5 – NCT Steady-State Temperatures with Insolation, Payload Configuration 2 - Two Standard Waste Boxes, Thermal Case 5 ..... 3.4-16

Table 3.4-6 – TRUPACT-II Pressure Increase with a 14-Drum Payload, 60-Day Duration\* 3.4-17

Table 3.4-7 – TRUPACT-II Pressure Increase with a 2 SWB Payload, 60-Day Duration\* ..... 3.4-17

Table 3.4-8 – TRUPACT-II Pressure Increase with 8 Drums Overpacked in 2 SWBs, 60-Day Duration\* ..... 3.4-17

Table 3.4-9 – TRUPACT-II Pressure Increase with 8 85-Gallon Drums or 8 55-Gallon Drums Overpacked in 8 85-Gallon Drums, 60-Day Duration\* ..... 3.4-18

Table 3.4-10 – TRUPACT-II Pressure Increase with 6 100-Gallon Drums, 60-Day Duration\* ... 3.4-18

Table 3.4-11 – TRUPACT-II Pressure Increase with a 1 TDOP Payload, 60-Day Duration\* ..... 3.4-18

Table 3.4-12 – TRUPACT-II Pressure Increase with 14 CCOs, 60-Day Duration\* ..... 3.4-19

Table 3.5-1 – HAC Pre-Fire Steady-State Temperatures with 40 Watts Decay Heat Load and No Insolation; Fourteen 55-Gallon Drums ..... 3.5-5

Table 3.5-2 – HAC Pre-Fire Steady-State Temperatures with 40 Watts Decay Heat Load and No Insolation; Two Standard Waste Boxes ..... 3.5-6

Table 3.5-3 – CTU-1 Temperature Indicating Label Locations and Results ..... 3.5-7

Table 3.5-4 – CTU-2 Temperature Indicating Label Locations and Results ..... 3.5-9

Table 3.5-5 – HAC Fire Temperature Readings; Fourteen 55-Gallon Drums ..... 3.5-11

Table 5.1-1 – TRUPACT-II with Generic Payload Summary of Maximum Dose Rates (mrem/hr) ..... 5.1-9

Table 5.1-2 – HalfPACT with Generic Payload Summary of Maximum Dose Rates (mrem/hr) ..... 5.1-9

Table 5.1-3 – TRUPACT-II with CCO Payload Summary of Maximum Dose Rates (mrem/hr) ..... 5.1-10

Table 5.1-4 – HalfPACT with CCO Payload Summary of Maximum Dose Rates (mrem/hr) ..... 5.1-10

Table 5.1-5 – HalfPACT with 6PO Payload Summary of Maximum Dose Rates (mrem/hr) 5.1-11

Table 5.1-6 – HalfPACT with 12PO Payload Summary of Maximum Dose Rates (mrem/hr) ..... 5.1-11

Table 5.1-7 – HalfPACT with SCA Payload Summary of Maximum Dose Rates (mrem/hr) 5.1-12

Table 5.3-1 – Summary of Shield Regional Densities ..... 5.3-15

Table 5.4-1 – Case Naming Conventions ..... 5.4-2

Table 5.4-2 – Neutron Flux-to-Dose Rate Conversion Factors from ANSI/ANS 6.1.1-1977..	5.4-2
Table 5.4-3 – Gamma Flux-to-Dose Rate Conversion Factors from ANSI/ANS 6.1.1-1977..	5.4-3
Table 5.4-4 – TRUPACT-II – Generic Dose Rates for 1 par/s Source.....	5.4-4
Table 5.4-5 – HalfPACT – Generic Dose Rates for 1 par/s Source .....	5.4-5
Table 5.4-6 – TRUPACT-II – CCO Dose Rates for 1 par/s Source .....	5.4-5
Table 5.4-7 – HalfPACT – CCO Dose Rates for 1 par/s Source .....	5.4-6
Table 5.4-8 – HalfPACT – 6PO Dose Rates for 1 par/s Source .....	5.4-6
Table 5.4-9 – HalfPACT – 12PO Dose Rates for 1 par/s Source .....	5.4-7
Table 5.4-10 – HalfPACT – SCA Dose Rates for 1 par/s Source .....	5.4-7
Table 5.5-1 – Discrete Gamma and Neutron Energies .....	5.5-2
Table 5.5-2 – TRUPACT-II – Generic Gamma Activity Limits.....	5.5-4
Table 5.5-3 – TRUPACT-II – Generic Neutron Activity Limits.....	5.5-5
Table 5.5-4 – HalfPACT – Generic Gamma Activity Limits.....	5.5-6
Table 5.5-5 – HalfPACT – Generic Neutron Activity Limits .....	5.5-7
Table 5.5-6 – TRUPACT-II – CCO Gamma Activity Limits .....	5.5-11
Table 5.5-7 – TRUPACT-II – CCO Neutron Activity Limits.....	5.5-12
Table 5.5-8 – HalfPACT – CCO Gamma Activity Limits .....	5.5-13
Table 5.5-9 – HalfPACT – CCO Neutron Activity Limits.....	5.5-14
Table 5.5-10 – HalfPACT – 6PO Gamma Activity Limits .....	5.5-18
Table 5.5-11 – HalfPACT – 6PO Neutron Activity Limits.....	5.5-19
Table 5.5-12 – HalfPACT – 12PO Gamma Activity Limits .....	5.5-22
Table 5.5-13 – HalfPACT – 12PO Neutron Activity Limits.....	5.5-23
Table 5.5-14 – HalfPACT – SCA Gamma Activity Limits.....	5.5-26
Table 5.5-15 – HalfPACT – SCA Neutron Activity Limits .....	5.5-27
Table 5.5-16 – Acceptable Activity Example #1 .....	5.5-30
Table 5.5-17 – Acceptable Activity Example #2.....	5.5-32
Table 5.5-18 – Acceptable Activity Example #3.....	5.5-34
Table 6.1-1 – Fissile Material Limit per Payload Container .....	6.1-4
Table 6.1-2 – Fissile Material Limit per TRUPACT-II Package.....	6.1-4
Table 6.1-3 – Summary of Criticality Analysis Results .....	6.1-5
Table 6.2-1 – Special Reflector Material Parameters that Achieve the Reactivity of a 25%/75% Polyethylene/Water Mixture Reflector .....	6.2-6
Table 6.3-1 – Description of Contents Displacement in Array Models .....	6.3-6

Table 6.3-2 – Fissile Contents Model Properties for Various H/Pu Ratios .....	6.3-7
Table 6.3-3 – Composition of Modeled Steels .....	6.3-8
Table 6.3-4 – Composition of the Polyethylene/Water/Beryllium Reflector .....	6.3-8
Table 6.4-1 – Single-Unit, NCT, Case A, 325 FGE; $k_s$ vs. H/Pu Ratio with Different Moderator and Reflector Compositions.....	6.4-11
Table 6.4-2 – Single Unit, NCT, Case A, 325 FGE; Variation of Reflector Volume Fraction (VF) at Near-Optimal H/Pu Ratio.....	6.4-12
Table 6.4-3 – Single-Unit, HAC, Case A, 325 FGE; $k_s$ vs. H/Pu at Maximum Reflection Conditions .....	6.4-12
Table 6.4-4 – Infinite Array Variation 0, HAC, Case A, 325 FGE; $k_s$ vs. H/Pu at Extremes of Reflection Conditions .....	6.4-13
Table 6.4-5 – Infinite Array Variation 0, HAC, Case A, 325 FGE; Variation of Reflector Volume Fraction at Near-Optimal H/Pu Ratios.....	6.4-14
Table 6.4-6 – Infinite Array Variation 1, HAC, Case A, 325 FGE; Variation of H/Pu Ratio at Extremes of Reflection Conditions.....	6.4-15
Table 6.4-7 – Infinite Array Variation 0, HAC, Case A; Variation of H/Pu Ratio for Various Gram Quantities of Pu-240 at Maximum Reflection Conditions .....	6.4-16
Table 6.4-8 – Infinite Array Variation 0, HAC, Case A, 5 g Pu-240, 340 FGE; $k_s$ vs. H/Pu for Various Combinations of U-235 and Pu-239 under Maximum Reflection Conditions..	6.4-17
Table 6.4-9 – Infinite Array Variation 0, HAC, Case B, 100 FGE; $k_s$ vs. H/Pu at Maximum Reflection Conditions .....	6.4-18
Table 6.4-10 – Infinite Array Variation 0, HAC, Case B, 100 FGE; $k_s$ vs. H/Pu for Various Moderator Volume Fractions of Beryllium under Maximum Reflection Conditions ....	6.4-19
Table 6.4-11 – Infinite Array Variation 0, HAC, Case B, 100 FGE; Variation of Reflector Volume Fraction at Near-Optimal H/Pu Ratio .....	6.4-20
Table 6.4-12 – Infinite Array Variation 1, HAC, Case B, 100 FGE; Variation of H/Pu Ratio at Reflector Volume Fraction to Maximize Interaction while Maintaining Beryllium Reflection.....	6.4-20
Table 6.4-13 – Infinite Array Variation 0, HAC, Case C, 250 FGE; $k_s$ vs. H/Pu at Maximum Reflection Conditions .....	6.4-21
Table 6.4-14 – Infinite Array Variation 0, HAC, Case C, 250 FGE; Variation of Reflector Volume Fraction at Near-Optimal H/Pu Ratio .....	6.4-21
Table 6.4-15 – Infinite Array Variation 1, HAC, Case C, 250 FGE; Variation of H/Pu Ratio at Reflector Volume Fraction to Maximize Interaction while Maintaining Reflection.....	6.4-22
Table 6.4-16 – Infinite Array Variation 0, HAC, Case D, 325 FGE; $k_s$ vs. H/Pu at Maximum Reflection Conditions .....	6.4-23
Table 6.4-17 – Infinite Array Variation 0, HAC, Case D, 325 FGE; Variation of Reflector Volume Fraction at Near-Optimal H/Pu Ratio .....	6.4-24

Table 6.4-18 – Infinite Array Variation 1, HAC, Case D, 325 FGE; Variation of H/Pu Ratio at Reflector Volume Fraction to Maximize Interaction while Maintaining Reflection.....	6.4-24
Table 6.5-1 – Benchmark Experiment Description with Experimental Uncertainties.....	6.5-4
Table 6.5-2 – Benchmark Case Parameters and Computed Results.....	6.5-5
Table 6.5-3 – Calculation of USL.....	6.5-13
Table 8.1-1 – Acceptable Compressive Stress Ranges for Foam (psi).....	8.1-19

## LIST OF FIGURES

Figure 1.1-1 – TRUPACT-II Package Assembly .....	1.1-3
Figure 1.1-2 – TRUPACT-II Packaging Closure/Seal Region Details.....	1.1-4
Figure 2.2-1 – TRUPACT-II Package Components.....	2.2-7
Figure 2.2-2 – Radial CG Shift for a 14 55-Gallon Drum Payload .....	2.2-8
Figure 2.2-3 – Radial Shift of CG for Eight 85-Gallon Drum Payload.....	2.2-9
Figure 2.2-4 – Radial Shift of CG for Six 100-Gallon Drum Payload .....	2.2-10
Figure 2.2-5 – Radial Shift of CG for SWB Payload .....	2.2-11
Figure 2.2-6 – Radial Shift of CG for TDOP Payload.....	2.2-12
Figure 2.5-1 – Tie-down Device Layout.....	2.5-12
Figure 2.5-2 – Tie-down Device Detail .....	2.5-13
Figure 2.5-3 – Tie-down Plan View and Reaction Force Diagram .....	2.5-14
Figure 2.5-4 – Tie-down Tensile/Shear Failure Modes .....	2.5-15
Figure 2.5-5 – Tie-down Lug Dimensions and Load Diagram.....	2.5-16
Figure 2.5-6 – Horizontal Doubler and Tripler Plate Details .....	2.5-17
Figure 2.6-1 – OCA Load Case 1, Overall Model.....	2.6-25
Figure 2.6-2 – OCA Load Case 1, Seal Region Detail .....	2.6-26
Figure 2.6-3 – OCA Load Case 2, Overall Model.....	2.6-27
Figure 2.6-4 – OCA Load Case 2, Seal Region Detail .....	2.6-28
Figure 2.6-5 – OCA Load Case 3, Overall Model.....	2.6-29
Figure 2.6-6 – OCA Load Case 3, Seal Region Detail .....	2.6-30
Figure 2.6-7 – OCA Load Case 4, Overall Model.....	2.6-31
Figure 2.6-8 – OCA Load Case 4, Seal Region Detail .....	2.6-32
Figure 2.6-9 – ICV Load Case 1, Overall Model .....	2.6-33
Figure 2.6-10 – ICV Load Case 1, Seal Region Detail.....	2.6-34
Figure 2.6-11 – ICV Load Case 2, Overall Model .....	2.6-35

Figure 2.6-12 – ICV Load Case 2, Seal Region Detail.....	2.6-36
Figure 2.7-1 – CTU-2 Free Drop Test No. 2 Accelerometer Data (Gage 1) .....	2.7-21
Figure 2.7-2 – CTU-2 Free Drop Test No. 2 Accelerometer Data (Gage 2) .....	2.7-21
Figure 2.7-3 – CTU-3 Free Drop Test No. 2 Accelerometer Data (Gage 1) .....	2.7-22
Figure 2.7-4 – CTU-3 Free Drop Test No. 2 Accelerometer Data (Gage 2) .....	2.7-22
Figure 2.10.1-1 – OCA Finite Element Analysis Model Element Plot .....	2.10.1-27
Figure 2.10.1-2 – ICV Finite Element Analysis Model Element Plot.....	2.10.1-28
Figure 2.10.2-1 – Configuration for Minimum ICV O-ring Seal Compression .....	2.10.2-13
Figure 2.10.2-2 – Test Fixture for O-ring Seal Performance Testing.....	2.10.2-14
Figure 2.10.3-1 – Drop Pad at the Coyote Canyon Aerial Cable Facility .....	2.10.3-45
Figure 2.10.3-2 – CTU OCV and ICV Pressurization Port Detail.....	2.10.3-46
Figure 2.10.3-3 – CTU Payload Representation (Concrete-Filled 55-Gallon Drums) .....	2.10.3-47
Figure 2.10.3-4 – Schematic of the CTU-1 Test Orientations.....	2.10.3-48
Figure 2.10.3-5 – Schematic of the CTU-2 Test Orientations.....	2.10.3-49
Figure 2.10.3-6 – Schematic of the CTU-3 Test Orientations.....	2.10.3-50
Figure 2.10.3-7 – CTU-1 and CTU-2 ICV Temperature Indicating Label Locations.....	2.10.3-51
Figure 2.10.3-8 – CTU-1 OCV Temperature Indicating Label Locations .....	2.10.3-52
Figure 2.10.3-9 – CTU-2 OCV Temperature Indicating Label Locations .....	2.10.3-53
Figure 2.10.3-10 – CTU-1 OCV Thermocouple Locations.....	2.10.3-54
Figure 2.10.3-11 – CTU-2 OCV Thermocouple Locations.....	2.10.3-55
Figure 2.10.3-12 – CTU-1 OCV Thermocouple Data (TH-1, TH-2, TH-3, TH-4).....	2.10.3-56
Figure 2.10.3-13 – CTU-1 OCV Thermocouple Data (TH-1A, TH-2A, TH-3A, TH-4A) .....	2.10.3-56
Figure 2.10.3-14 – CTU-1 OCV Thermocouple Data (TH-1C, TH-2C, TH-3C, TH-4C).....	2.10.3-57
Figure 2.10.3-15 – CTU-1 OCV Thermocouple Data (TH-1D, TH-2D, TH-3D, TH-4D).....	2.10.3-57
Figure 2.10.3-16 – CTU-2 OCV Thermocouple Data (TH-1, TH-2, TH-3, TH-4).....	2.10.3-58
Figure 2.10.3-17 – CTU-2 OCV Thermocouple Data (TH-1A, TH-2A, TH-3A, TH-4A) .....	2.10.3-58
Figure 2.10.3-18 – CTU-2 Free Drop Test No. 2 Accelerometer Data (Gage 1).....	2.10.3-59
Figure 2.10.3-19 – CTU-2 Free Drop Test No. 2 Accelerometer Data (Gage 2).....	2.10.3-59
Figure 2.10.3-20 – CTU-2 Free Drop Test No. 3 Accelerometer Data (Gage 1).....	2.10.3-60
Figure 2.10.3-21 – CTU-2 Free Drop Test No. 3 Accelerometer Data (Gage 2).....	2.10.3-60
Figure 2.10.3-22 – CTU-3 Free Drop Test No. 2 Accelerometer Data (Gage 1).....	2.10.3-61
Figure 2.10.3-23 – CTU-3 Free Drop Test No. 2 Accelerometer Data (Gage 2).....	2.10.3-61
Figure 2.10.3-24 – CTU-1 Pressure Transducer Data During Fire Test No. 10 .....	2.10.3-62

Figure 2.10.3-25 – CTU-2 Pressure Transducer Data During Fire Test No. 9 .....	2.10.3-62
Figure 2.10.3-26 – CTU-1 Free Drop No. 1; Initial Preparation for Testing .....	2.10.3-63
Figure 2.10.3-27 – CTU-1 Free Drop No. 1; Pre-Drop Positioning .....	2.10.3-63
Figure 2.10.3-28 – CTU-1 Free Drop No. 1; Post-Drop Damage at Top (Lid) .....	2.10.3-64
Figure 2.10.3-29 – CTU-1 Free Drop No. 1; Post-Drop Damage at Bottom (Body).....	2.10.3-64
Figure 2.10.3-30 – CTU-1 Free Drop No. 2; Pre-Drop Positioning .....	2.10.3-65
Figure 2.10.3-31 – CTU-1 Free Drop No. 2; Post-Drop Damage .....	2.10.3-65
Figure 2.10.3-32 – CTU-1 Free Drop No. 3; Pre-Drop Positioning .....	2.10.3-66
Figure 2.10.3-33 – CTU-1 Free Drop No. 3; Post-Drop Damage .....	2.10.3-66
Figure 2.10.3-34 – CTU-1 Free Drop No. 4; Pre-Drop Positioning .....	2.10.3-67
Figure 2.10.3-35 – CTU-1 Free Drop No. 4; Post-Drop Damage .....	2.10.3-67
Figure 2.10.3-36 – CTU-1 Puncture Drop No. 5; Pre-Drop Positioning .....	2.10.3-68
Figure 2.10.3-37 – CTU-1 Puncture Drop No. 5; Post-Drop Damage .....	2.10.3-68
Figure 2.10.3-38 – CTU-1 Puncture Drop No. 6; Pre-Drop Positioning .....	2.10.3-69
Figure 2.10.3-39 – CTU-1 Puncture Drop No. 6; Post-Drop Damage .....	2.10.3-69
Figure 2.10.3-40 – CTU-1 Puncture Drop No. 7; Pre-Drop Positioning .....	2.10.3-70
Figure 2.10.3-41 – CTU-1 Puncture Drop No. 7; Post-Drop Damage .....	2.10.3-70
Figure 2.10.3-42 – CTU-1 Puncture Drop No. 8; Pre-Drop Positioning .....	2.10.3-71
Figure 2.10.3-43 – CTU-1 Puncture Drop No. 8; Moment of Impact .....	2.10.3-71
Figure 2.10.3-44 – CTU-1 Puncture Drop No. 9; Pre-Drop Positioning .....	2.10.3-72
Figure 2.10.3-45 – CTU-1 Puncture Drop No. 9; Post-Drop Damage .....	2.10.3-72
Figure 2.10.3-46 – CTU-1 Fire No. 10; Pre-Fire Positioning, Side View .....	2.10.3-73
Figure 2.10.3-47 – CTU-1 Fire No. 10; Pre-Fire Positioning, Top End View .....	2.10.3-73
Figure 2.10.3-48 – CTU-1 Fire No. 10; Fully Engulfing Fire .....	2.10.3-74
Figure 2.10.3-49 – CTU-1 Fire No. 10; Post-Fire Cool-Down .....	2.10.3-74
Figure 2.10.3-50 – CTU-1 Disassembly; OCA Lid Unburned Foam.....	2.10.3-75
Figure 2.10.3-51 – CTU-1 Disassembly; OCA Lid Unburned Foam Thickness.....	2.10.3-75
Figure 2.10.3-52 – CTU-1 Disassembly; Payload Drum Removal .....	2.10.3-76
Figure 2.10.3-53 – CTU-1 Disassembly; Loose Debris on Pallet in ICV Body .....	2.10.3-76
Figure 2.10.3-54 – CTU-2 Free Drop No. 1; Initial Preparation for Testing .....	2.10.3-77
Figure 2.10.3-55 – CTU-2 Free Drop No. 1; Pre-Drop Positioning .....	2.10.3-77
Figure 2.10.3-56 – CTU-2 Free Drop No. 1; Post-Drop Damage .....	2.10.3-78
Figure 2.10.3-57 – CTU-2 Free Drop No. 1; Post-Drop Damage .....	2.10.3-78

Figure 2.10.3-58 – CTU-2 Free Drop No. 2; Pre-Drop Positioning .....	2.10.3-79
Figure 2.10.3-59 – CTU-2 Free Drop No. 2; Post-Drop Damage .....	2.10.3-79
Figure 2.10.3-60 – CTU-2 Free Drop No. 3; Pre-Drop Positioning .....	2.10.3-80
Figure 2.10.3-61 – CTU-2 Free Drop No. 3; Post-Drop Damage .....	2.10.3-80
Figure 2.10.3-62 – CTU-2 Puncture Drop No. R; Pre-Drop Positioning .....	2.10.3-81
Figure 2.10.3-63 – CTU-2 Puncture Drop R; Post-Drop Damage .....	2.10.3-81
Figure 2.10.3-64 – CTU-2 Puncture Drop No. 4; Pre-Drop Positioning .....	2.10.3-82
Figure 2.10.3-65 – CTU-2 Puncture Drop 4; Post-Drop Damage .....	2.10.3-82
Figure 2.10.3-66 – CTU-2 Puncture Drop No. 5; Pre-Drop Positioning .....	2.10.3-83
Figure 2.10.3-67 – CTU-2 Puncture Drop 5; Post-Drop Damage .....	2.10.3-83
Figure 2.10.3-68 – CTU-2 Puncture Drop No. 6; Pre-Drop Positioning .....	2.10.3-84
Figure 2.10.3-69 – CTU-2 Puncture Drop 6; Post-Drop Damage .....	2.10.3-84
Figure 2.10.3-70 – CTU-2 Puncture Drop No. 7; Pre-Drop Positioning .....	2.10.3-85
Figure 2.10.3-71 – CTU-2 Puncture Drop 7; Post-Drop Damage .....	2.10.3-85
Figure 2.10.3-72 – CTU-2 Puncture Drop No. 8; Pre-Drop Positioning .....	2.10.3-86
Figure 2.10.3-73 – CTU-2 Puncture Drop 8; Post-Drop Damage .....	2.10.3-86
Figure 2.10.3-74 – CTU-2 Fire No. 9; Pre-Fire Positioning .....	2.10.3-87
Figure 2.10.3-75 – CTU-2 Fire No. 9; Pre-Fire Positioning .....	2.10.3-87
Figure 2.10.3-76 – CTU-2 Fire No. 9; Starting Fire .....	2.10.3-88
Figure 2.10.3-77 – CTU-2 Fire No. 9; Post-Fire Cool-Down .....	2.10.3-88
Figure 2.10.3-78 – CTU-2 Disassembly; Loose Debris in ICV Lid .....	2.10.3-89
Figure 2.10.3-79 – CTU-2 Disassembly; Debris Contaminating the ICV Main O-ring Seals .....	2.10.3-89
Figure 2.10.3-80 – CTU-3 Free Drop No. 1; Pre-Drop Positioning .....	2.10.3-90
Figure 2.10.3-81 – CTU-3 Free Drop No. 1; Post-Drop Damage .....	2.10.3-90
Figure 2.10.3-82 – CTU-3 Free Drop No. 2; Pre-Drop Positioning .....	2.10.3-91
Figure 2.10.3-83 – CTU-3 Free Drop No. 2; Post-Drop Damage .....	2.10.3-91
Figure 2.10.3-84 – CTU-3 Free Drop No. 3; Pre-Drop Positioning .....	2.10.3-92
Figure 2.10.3-85 – CTU-3 Free Drop No. 3; Post-Drop Damage .....	2.10.3-92
Figure 2.10.3-86 – CTU-3 Puncture Drop No. 4; Pre-Drop Positioning .....	2.10.3-93
Figure 2.10.3-87 – CTU-3 Puncture Drop 4; Post-Drop Damage .....	2.10.3-93
Figure 2.10.3-88 – CTU-3 Puncture Drop No. 5; Pre-Drop Positioning .....	2.10.3-94
Figure 2.10.3-89 – CTU-3 Puncture Drop 5; Post-Drop Damage .....	2.10.3-94
Figure 2.10.3-90 – CTU-3 Puncture Drop No. 6; Pre-Drop Positioning .....	2.10.3-95

Figure 2.10.3-91 – CTU-3 Puncture Drop 6; Post-Drop Damage .....	2.10.3-95
Figure 2.10.3-92 – CTU-3 Puncture Drop No. 7; Pre-Drop Positioning .....	2.10.3-96
Figure 2.10.3-93 – CTU-3 Puncture Drop 7; Post-Drop Damage .....	2.10.3-96
Figure 2.10.3-94 – CTU-3 Puncture Drop No. 8; Pre-Drop Positioning .....	2.10.3-97
Figure 2.10.3-95 – CTU-3 Puncture Drop 8; Post-Drop Damage .....	2.10.3-97
Figure 2.10.3-96 – CTU-3 Disassembly; OCA Lid .....	2.10.3-98
Figure 2.10.3-97 – CTU-3 Disassembly; OCA Body .....	2.10.3-98
Figure 2.10.3-98 – CTU-3 Disassembly; ICV Lid Removal .....	2.10.3-99
Figure 2.10.3-99 – CTU-3 Disassembly; Loose Debris on Pallet in ICV Body .....	2.10.3-99
Figure 3.4-1 – TRUPACT-II Packaging Thermal Model Node Layout .....	3.4-21
Figure 3.4-2 – Seal Region Thermal Model Node Layout .....	3.4-22
Figure 3.4-3 – Fourteen 55-Gallon Drum Payload Thermal Node Layout .....	3.4-23
Figure 3.4-4 – Two Standard Waste Boxes Thermal Model Node Layout .....	3.4-24
Figure 3.5-1 – CTU-1 and CTU-2 ICV Temperature Indicating Label Locations .....	3.5-13
Figure 3.5-2 – CTU-1 OCV Temperature Indicating Label Locations .....	3.5-14
Figure 3.5-3 – CTU-2 OCV Temperature Indicating Label Locations .....	3.5-15
Figure 3.5-4 – CTU-1 OCV Thermocouple Locations .....	3.5-16
Figure 3.5-5 – CTU-2 OCV Thermocouple Locations .....	3.5-17
Figure 3.5-6 – CTU-1 OCV Thermocouple Data (TH-1, TH-2, TH-3, TH-4) .....	3.5-18
Figure 3.5-7 – CTU-1 OCV Thermocouple Data (TH-1A, TH-2A, TH-3A, TH-4A) .....	3.5-18
Figure 3.5-8 – CTU-1 OCV Thermocouple Data (TH-1B, TH-2B, TH-3B, TH-4B) .....	3.5-19
Figure 3.5-9 – CTU-1 OCV Thermocouple Data (TH-1C, TH-2C, TH-3C, TH-4C) .....	3.5-19
Figure 3.5-10 – CTU-2 OCV Thermocouple Data (TH-1, TH-2, TH-3, TH-4) .....	3.5-20
Figure 3.5-11 – CTU-2 OCV Thermocouple Data (TH-1A, TH-2A, TH-3A, TH-4A) .....	3.5-20
Figure 3.5-12 – CTU-1 Pressure Transducer Data During Fire Test No. 10 .....	3.5-21
Figure 3.5-13 – CTU-2 Pressure Transducer Data During Fire Test No. 9 .....	3.5-21
Figure 5.1-1 – Criticality Control Overpack .....	5.1-5
Figure 5.1-2 – 6-in. Standard Pipe Overpack .....	5.1-6
Figure 5.1-3 – 12-in. Standard Pipe Overpack .....	5.1-7
Figure 5.1-4 – Shielded Container Assembly .....	5.1-8
Figure 5.3-1 – TRUPACT-II Generic Payload MCNP Model for NCT .....	5.3-5
Figure 5.3-2 – HalfPACT Generic Payload MCNP Model for NCT .....	5.3-6
Figure 5.3-3 – TRUPACT-II Generic Payload MCNP Model for HAC .....	5.3-7

Figure 5.3-4 – HalfPACT Generic Payload MCNP Model for HAC .....	5.3-8
Figure 5.3-5 – TRUPACT-II CCO Payload MCNP Model for NCT .....	5.3-9
Figure 5.3-6 – HalfPACT CCO Payload MCNP Model for NCT .....	5.3-10
Figure 5.3-7 – TRUPACT-II CCO Payload MCNP Model for HAC.....	5.3-11
Figure 5.3-8 – HalfPACT CCO Payload MCNP Model for HAC .....	5.3-12
Figure 5.3-9 – HalfPACT SCA Payload MCNP Model for NCT .....	5.3-13
Figure 5.3-10 – HalfPACT SCA Payload MCNP Model for HAC.....	5.3-14
Figure 5.4-1 – Allowable Activity Comparison for Concentrated Sources.....	5.4-9
Figure 5.5-1 – TRUPACT-II & HalfPACT Generic Payload MCNP Models for Distributed Source at Unit Density .....	5.5-8
Figure 5.5-2 – TRUPACT-II Generic Payload DCF .....	5.5-9
Figure 5.5-3 – HalfPACT Generic Payload DCF .....	5.5-9
Figure 5.5-4 – TRUPACT-II & HalfPACT CCO Payload MCNP Models for Distributed Source at Unit Density .....	5.5-15
Figure 5.5-5 – TRUPACT-II CCO Payload DCF.....	5.5-16
Figure 5.5-6 – HalfPACT CCO Payload DCF.....	5.5-16
Figure 5.5-7 – HalfPACT 6PO Payload MCNP Model for Distributed Source at Unit Density .....	5.5-20
Figure 5.5-8 – HalfPACT 6PO Payload DCF.....	5.5-20
Figure 5.5-9 – HalfPACT 12PO Payload MCNP Model for Distributed Source at Unit Density .....	5.5-24
Figure 5.5-10 – HalfPACT 12PO Payload DCF.....	5.5-24
Figure 5.5-11 – HalfPACT SCA Payload MCNP Model for Distributed Source at Unit Density .....	5.5-28
Figure 5.5-12 – HalfPACT SCA Payload DCF .....	5.5-28
Figure 6.3-1 – Case A Contents Model .....	6.3-9
Figure 6.3-2 – Case B Contents Model.....	6.3-10
Figure 6.3-3 – Case C Contents Model.....	6.3-11
Figure 6.3-4 – Case D Contents Model .....	6.3-12
Figure 6.3-5 – NCT, Single-Unit Model; R-Z Slice .....	6.3-13
Figure 6.3-6 – HAC, Single-Unit Model; R-Z Slice.....	6.3-14
Figure 6.3-7 – Array Model Variation 0 (Reflective Boundary Conditions Imposed) .....	6.3-15
Figure 6.3-8 – Array Model Variation 1; X-Y Slice Through Top Axial Layer .....	6.3-16
Figure 7.4-1 – Pressure Rise Leakage Rate Test Schematic.....	7.4-2

Figure 8.2-1 – Method of Measuring Upper Seal Flange Groove Widths..... 8.2-8  
Figure 8.2-2 – Method of Measuring Lower Seal Flange Groove Widths ..... 8.2-9  
Figure 8.2-3 – Method of Measuring Upper Seal Flange Tab Widths ..... 8.2-10  
Figure 8.2-4 – Method of Measuring Lower Seal Flange Tab Widths ..... 8.2-11

This page intentionally left blank.

## 1.0 GENERAL INFORMATION

This chapter of the Safety Analysis Report (SAR) presents a general introduction and description of the TRUPACT-II contact-handled transuranic waste (CH-TRU) package. The major components comprising the TRUPACT-II package are presented as Figure 1.1-1 and Figure 1.1-2, where Figure 1.1-1 presents an exploded view of all major TRUPACT-II packaging components, and Figure 1.1-2 presents a detailed view of the closure and seal region. Detailed drawings presenting the TRUPACT-II packaging design are presented in Appendix 1.3.1, *Packaging General Arrangement Drawings*. All details relating to payloads and payload preparation for shipment in a TRUPACT-II package are presented in the *Contact-Handled Transuranic Waste Authorized Methods for Payload Control (CH-TRAMPAC)*<sup>1</sup>. Descriptions of the standard, S100, S200, and S300 pipe overpack payload configurations are provided in Appendices 4.1, 4.2, 4.3, and 4.4 respectively, of the *CH-TRU Payload Appendices*<sup>2</sup>. A description of the criticality control overpack payload configuration is provided in Appendix 4.6 of the *CH-TRU Payload Appendices*. Terminology and acronyms used throughout this document are presented as Appendix 1.3.2, *Glossary of Terms and Acronyms*.

### 1.1 Introduction

The model TRUPACT-II package has been developed for the U. S. Department of Energy (DOE) as a safe means for the transportation of CH-TRU materials and other authorized payloads.

The TRUPACT-II package is designed for truck transport. As many as three, loaded TRUPACT-II packages can be transported on a single semi-trailer. The rugged, lightweight design of the TRUPACT-II package allows the efficient transport of a maximum payload, thereby reducing the total number of radioactive shipments. The TRUPACT-II package is also suitable for rail transport. As many as seven loaded TRUPACT-II packages can be transported per railcar.

The goals of maintaining public safety while achieving a lightweight design are satisfied by use of a deformable sealing region that can absorb both normal conditions of transport (NCT) and hypothetical accident condition (HAC) deformations without loss of leaktight capability<sup>3</sup>. A variety of scaled and full-scale engineering development tests were included as part of the design process. Ultimately, three full-scale certification test units (CTUs) were subjected to a series of free drops and puncture drops. Following free drops and puncture tests, two CTUs were exposed to a fully engulfing pool fire test. These tests conclusively demonstrated containment integrity of the TRUPACT-II package.

The payload within each TRUPACT-II package will be within 55-gallon drums, 85-gallon drums, 100-gallon drums, standard waste boxes (SWBs), or a ten drum overpack (TDOP). Hereafter, the term "85-gallon drum" is used to refer to 75- to 88-gallon drums that may, with the appropriate

---

<sup>1</sup> U.S. Department of Energy (DOE), *Contact-Handled Transuranic Waste Authorized Methods for Payload Control (CH-TRAMPAC)*, U.S. Department of Energy, Carlsbad Field Office, Carlsbad, New Mexico.

<sup>2</sup> U.S. Department of Energy (DOE), *CH-TRU Payload Appendices*, U.S. Department of Energy, Carlsbad Field Office, Carlsbad, New Mexico.

<sup>3</sup> Leaktight is defined as  $1 \times 10^{-7}$  standard cubic centimeters per second (scc/s), or less, air leakage per the definition in ANSI N14.5-1997, *American National Standard for Radioactive Materials - Leakage Tests on Packages for Shipment*, American National Standards Institute, (ANSI), Inc.

dimensions, overpack a single 55-gallon drum. Pipe overpacks and criticality control overpacks (CCO) utilize 55-gallon drums as overpacks. A single TRUPACT-II package can transport fourteen 55-gallon drums (with or without pipe components or criticality control containers), eight 85-gallon drums, six 100-gallon drums, two SWBs, or one TDOP. Specifications for payload containers are provided in Section 2.0, *Container and Physical Properties Requirements*, of CH-TRAMPAC.

The TRUPACT-II packaging provides a single leakage rate testable level of containment for the payload during both normal conditions of transport (NCT) and hypothetical accident conditions (HAC). However, the TRUPACT-II package was originally designed, tested, and licensed prior to 2004 with two levels of containment. The 2004 NRC Rule change with regard to 10 CFR §71.63<sup>4,5</sup> eliminated the requirement for double containment in packages carrying in excess of 20 curies of plutonium in solid form. With only a single level of containment now required, the outer containment assembly (OCA) has been revised throughout this document to be the outer confinement assembly (still the OCA), and the outer containment vessel (OCV) has been revised throughout this document to be the outer confinement vessel (still the OCV). The use of O-ring seals (and corresponding pressure and leakage rate testing) is now optional for the OCV, and design and fabrication of the OCA (including the OCV) now falls under ASME Boiler and Pressure Vessel Code, Section III, Subsection NF<sup>6</sup>. For conservatism, structural calculations for the OCV presented in Chapter 2.0, *Structural Evaluation*, continue to use the requirements from ASME Boiler and Pressure Vessel Code, Section III, Subsection NB<sup>7</sup>.

Based on the shielding and criticality assessments provided in Chapter 5.0, *Shielding Evaluation*, and Chapter 6.0, *Criticality Evaluation*, the Criticality Safety Index (CSI) for the TRUPACT-II package is zero (0.0), and the shielding Transport Index (TI) is determined at the time of shipment.

Authorization is sought for shipment of the TRUPACT-II package by truck or railcar as a Type B(U)F-96 package per the definition delineated in 10 CFR §71.4<sup>4</sup>.

---

<sup>4</sup> Title 10, Code of Federal Regulations, Part 71 (10 CFR 71), *Packaging and Transportation of Radioactive Material*, 01-01-12 Edition.

<sup>5</sup> *Compatibility With IAEA Transportation Safety Standards (TS-R-1) and Other Transportation Safety Amendments*, Federal Register, 69 FR 3698, effective date October 1, 2004.

<sup>6</sup> American Society of Mechanical Engineers (ASME) Boiler and Pressure Vessel Code, Section III, *Rules for Construction of Nuclear Power Plant Components*, Subsection NF, *Supports*, 1986 Edition.

<sup>7</sup> American Society of Mechanical Engineers (ASME) Boiler and Pressure Vessel Code, Section III, *Rules for Construction of Nuclear Power Plant Components*, Subsection NB, *Class 1 Components*, 1986 Edition.

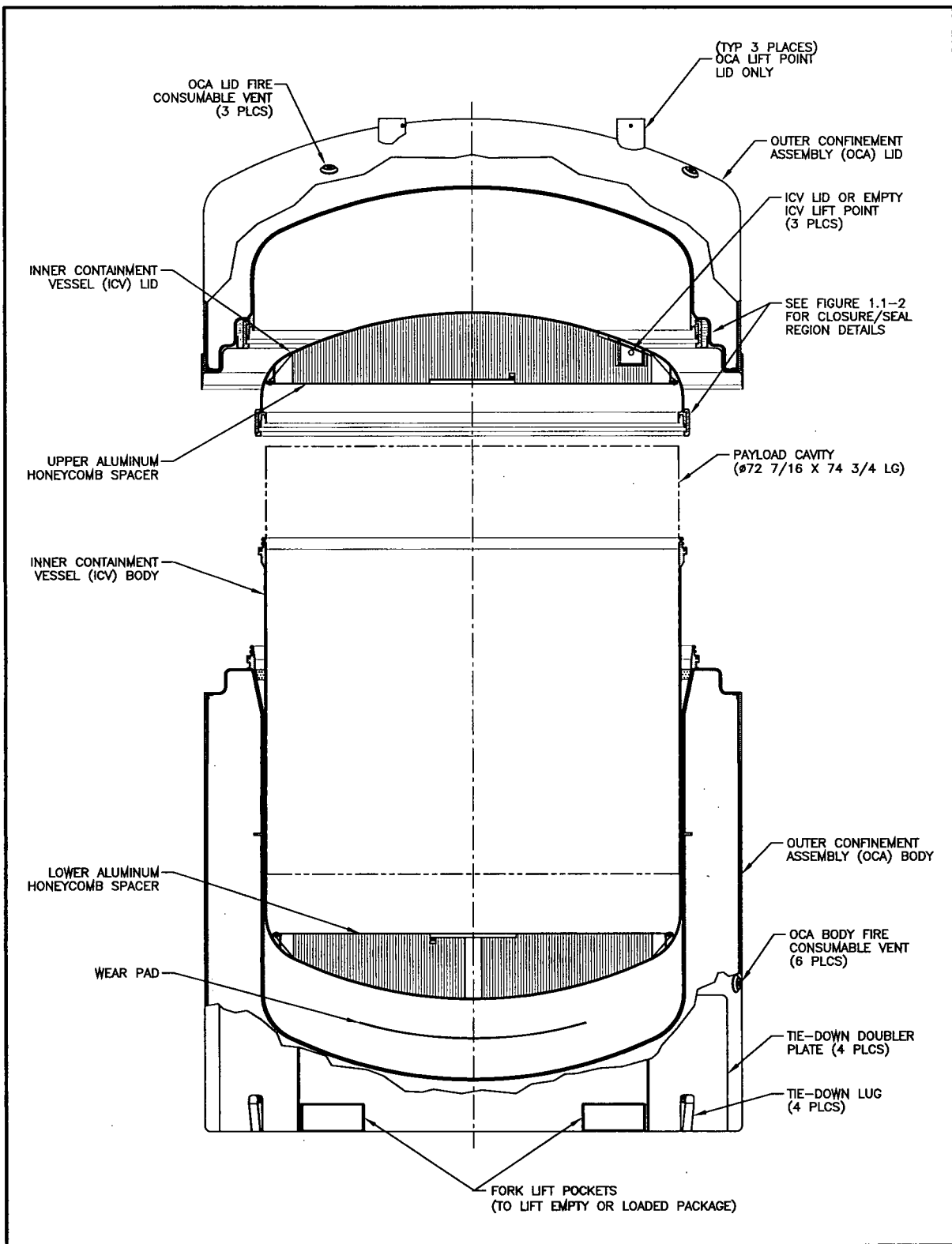


Figure 1.1-1 – TRUPACT-II Package Assembly

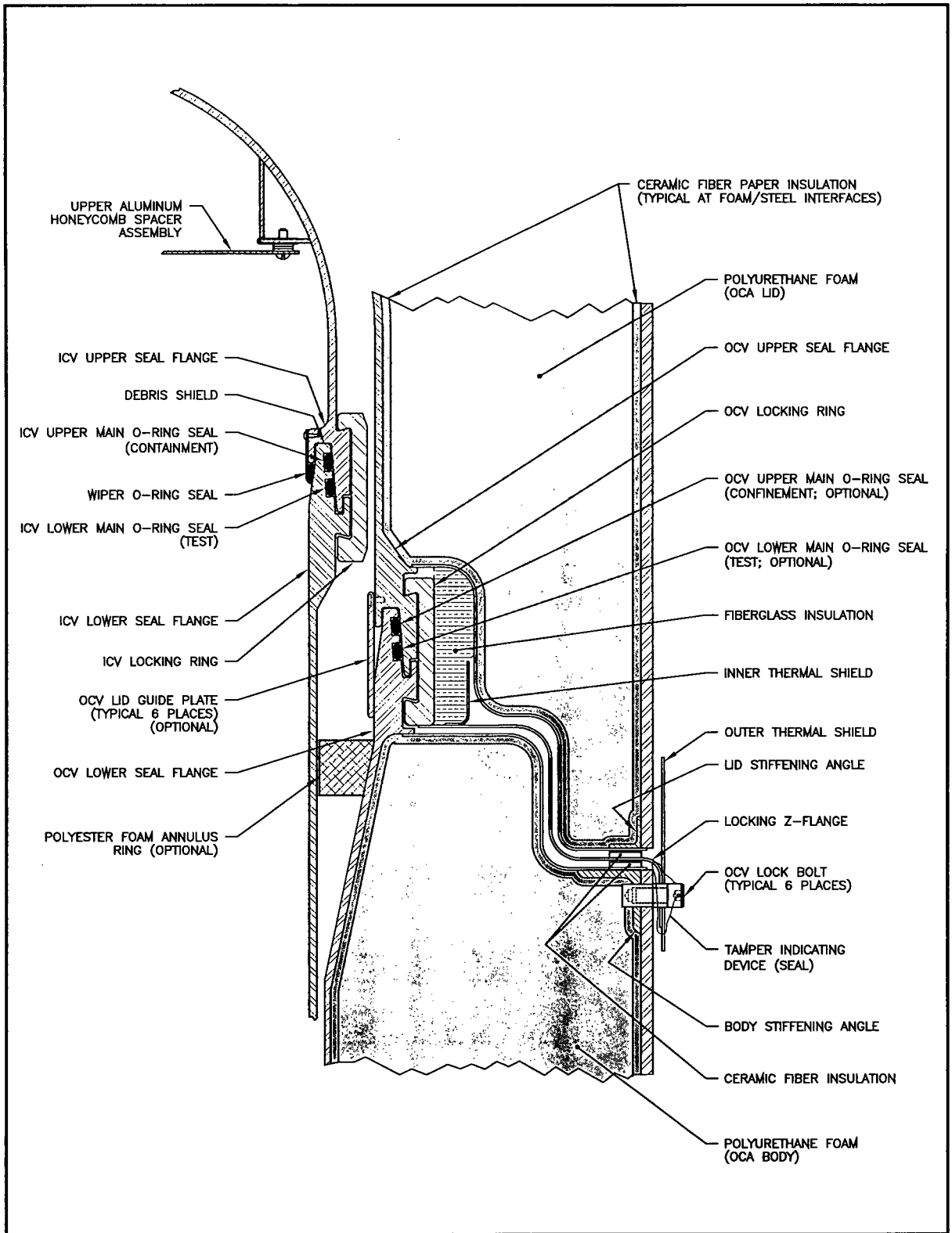


Figure 1.1-2 – TRUPACT-II Packaging Closure/Seal Region Details

## 1.2 Package Description

This section presents a basic description of the TRUPACT-II package. General arrangement drawings of the TRUPACT-II packaging are presented in Appendix 1.3.1, *Packaging General Arrangement Drawings*. Drawings illustrating payload assembly details are presented in the CH-TRAMPAC<sup>1</sup>.

### 1.2.1 Packaging

#### 1.2.1.1 Packaging Description

The TRUPACT-II packaging is comprised of an outer confinement assembly (OCA) that provides a secondary confinement boundary when its optional O-ring seals are utilized, and an inner containment vessel (ICV) that provides the primary containment boundary. Two aluminum honeycomb spacer assemblies are used within the ICV, one inside each ICV torispherical head. A silicone wear pad is utilized at the interface between the bottom exterior of the ICV and the bottom interior of the OCA. An optional polyester foam annulus ring may be used in the annulus between the ICV and OCV, just below the OCV lower seal flange, to prevent debris from becoming entrapped between the vessels.

Inside the ICV, the payload will be within 55-gallon drums, 85-gallon drums, 100-gallon drums, standard waste boxes (SWBs), or ten drum overpacks (TDOPs). The OCA, ICV, and the aluminum honeycomb spacer assemblies are fully described in the following subsections. The design details and overall arrangement of the TRUPACT-II packaging are presented in the Appendix 1.3.1, *Packaging General Arrangement Drawings*. Drawings illustrating payload assembly details are presented in the CH-TRAMPAC.

##### 1.2.1.1.1 Outer Confinement Assembly (OCA)

The OCA consists of an OCA lid and OCA body, each primarily comprised of an inner stainless steel shell structure, a relatively thick layer of rigid polyurethane foam, and an external stainless steel shell structure. The inner OCA shell structure comprises the outer confinement vessel (OCV).

Not considering the seal flange region, the OCA lid has a nominal external diameter of 94 $\frac{3}{8}$  inches and a nominal internal diameter of 76 $\frac{1}{16}$  inches. Likewise, not considering the seal flange region, the OCA body has a nominal external diameter of 94 $\frac{3}{8}$  inches and a nominal internal diameter of 73 $\frac{3}{8}$  inches, tapering outward to a nominal inside diameter of 76 $\frac{7}{8}$  inches at the OCV lower seal flange. The nominal external diameter of the OCV seal region is 95 inches, and the nominal internal diameter of the OCV seal region is 76 $\frac{1}{16}$  inches. With the OCA lid installed onto the OCA body, the OCA has a nominal external length of 121 $\frac{1}{2}$  inches, and a nominal internal height is 100 inches at the OCV cavity centerline.

The confinement boundary provided by the OCA consists of the inner stainless steel vessel formed by a mating lid and body, plus the uppermost of two optional main O-ring seals enclosed between an upper and lower seal flange. The main O-ring seals are polymer with a nominal

---

<sup>1</sup> U.S. Department of Energy (DOE), *Contact-Handled Transuranic Waste Authorized Methods for Payload Control (CH-TRAMPAC)*, U.S. Department of Energy, Carlsbad Field Office, Carlsbad, New Mexico.

3/8±1/8-inch diameter cross-section. The purpose of the lower main O-ring seal is for establishing a vacuum on the exterior side of the upper main O-ring seal for optional helium and/or pressure rise leakage rate testing.

A vent port feature in the OCV body's lower seal flange is the only other confinement boundary penetration. A vent port coupling, a seal welded threaded fitting, and an OCV vent port plug with an optional O-ring seal defines the confinement boundary at the OCV vent port penetration. Access to the OCV vent port is gained through an external penetration in the OCA outer shell once an outer 1½ NPT plug and a foam or ceramic fiber material plug is removed. The connecting tube is fabricated of non-thermally conductive fiberglass.

Optional leakage rate testing of the OCV's optional upper main O-ring seal (confinement seal) is performed through an OCV seal test port that is located in the OCA lid. Similar in design to the OCV vent port, access to the OCV seal test port is gained through an external penetration in the OCA outer shell once an outer 1½ NPT plug and a foam or ceramic fiber material plug is removed. The connecting tube is fabricated of thin-walled stainless steel.

The cylindrical portion of the OCV body is 3/16-inch nominal thickness, Type 304, stainless steel. All other shells comprising the OCV are 1/4-inch nominal thickness, Type 304, stainless steel, including the lower and upper torispherical heads. A single, 3/8-inch thick stiffening ring, extending radially out from the OCV shell, is included in the design. The OCA outer shell varies between 1/4- and 3/8-inch nominal thickness, Type 304, stainless steel. The 3/8-inch nominal thickness material is used adjacent to the closure interface to ensure protection from HAC puncture bar penetration near the sealing regions. All other shells comprising the OCA exterior are 1/4-inch nominal thickness, Type 304, stainless steel, including the lower flat head and upper torispherical head. As illustrated in Figure 1.1-2, the inner and outer shell structures for both the OCA lid and OCA body are connected together via 14-gauge (0.075-inch thick), Type 304, stainless steel Z-flanges. Secure attachment of the 14-gauge Z-flanges to the 3/8-inch thick OCA outer shell is assured by the use of rolled angle reinforcements (2 × 2 × 1/4 inches for the OCA body junction, and 1 × 1 × 1/8 inches for the OCA lid junction). A locking Z-flange between the upper and lower (i.e., OCA lid and OCA body) Z-flanges allows rotation of the OCV locking ring from the TRUPACT-II package exterior. The Z-flanges serve the purpose of precluding direct flame impingement on the OCV seal flanges during the hypothetical accident condition (HAC) thermal event (fire). To further preclude flame and hot gas entry into the Z-flange channel, inner and outer thermal shields are included as part of the locking Z-flange assembly.

The OCA lid is secured to the OCA body via the OCV locking ring located at the outer diameter of the OCV upper and lower seal flanges. Closure design and operation for the OCV is illustrated in Figure 1.2-1 (the OCV is similar). The lower end of the OCV locking ring has 18 tabs that mate with a corresponding set of 18 tabs on the OCV lower seal flange. To install the OCA lid, the OCV locking ring is rotated to the "unlocked" position, using alignment marks on the OCA exterior for reference. The unlocked position aligns the tabs on the OCV locking ring with the cutouts between the tabs on the OCV lower seal flange. Next, install the OCA lid onto the OCA body, optionally evacuating the OCV cavity through the OCV vent port sufficiently to allow free movement of the OCV locking ring. Positive closure is attained by rotating the OCV locking ring to the "locked" position, again using the alignment marks on the OCA exterior for reference. In order to allow rotation of the OCV locking ring from the TRUPACT-II packaging exterior, a locking Z-flange extends radially outward to the OCA exterior. Six, 1/2-inch diameter stainless

steel socket head cap screws secure the locking Z-flange in the locked position. A single, localized cutout in the OCV locking ring is provided for access to the OCV seal test port feature.

Within the annular void between the OCV and the OCA outer shell structure is a relatively thick layer of thermally insulating and energy absorbing, rigid, polyurethane foam. Surrounding the periphery of the polyurethane foam cavity is a layer of 1/4-inch nominal thickness, ceramic fiber paper capable of resisting temperatures in excess of 2,000 °F. The combination of OCA exterior shell, fire resistant polyurethane foam, and insulating ceramic fiber paper is sufficient to protect the confinement boundary from the consequences of all regulatory defined tests.

Two forklift pockets are incorporated into the base of the OCA body. These pockets provide the handling interface for lifting a TRUPACT-II package. Three sets of lifting straps are included in the OCA lid assembly for lifting of the OCA lid only, and are so appropriately identified. Four tie-down lugs with reinforcing doubler plates are also provided at the base of the OCA body.

Polymer materials used in the OCA include butyl, and ethylene propylene or neoprene, as applicable, for the main O-ring seals, silicone for the wear pad, and polyester foam for the optional annulus foam ring. Plastic is used for the polyurethane foam cavity, fire-consumable vent plugs, and optional guide plates. The OCA lid lift pockets, vent port access tube, and a portion of the seal test port access tube are made from fiberglass. Brass is used for the OCV vent and seal test port plugs. High alloy stainless steel is used for the OCV locking ring joint pins. Insulating materials such as ceramic fiber paper along the periphery of the polyurethane foam cavity, and fiberglass-type insulation for the inner thermal shield are also used. Finally, a variety of stainless steel fasteners, greases and lubricants, and adhesives are also utilized, as specified in Appendix 1.3.1, *Packaging General Arrangement Drawings*.

#### **1.2.1.1.2 Inner Containment Vessel (ICV) Assembly**

The inner containment vessel (ICV) assembly consists of an ICV lid and ICV body, each primarily comprised of a stainless steel shell structure. Not considering the seal flange region, the ICV lid has a nominal external diameter of  $74\frac{3}{8}$  inches and a nominal internal diameter of  $73\frac{7}{8}$  inches. Likewise, not considering the seal flange region, the ICV body has a nominal external diameter of  $73\frac{1}{8}$  inches and a nominal internal diameter of  $72\frac{5}{8}$  inches. The nominal external diameter of the ICV seal region is  $76\frac{5}{16}$  inches, and the nominal internal diameter of the ICV seal region is  $72\frac{1}{16}$  inches. With the ICV lid installed onto the ICV body, the ICV has a nominal external length of 99 inches, and a nominal internal height is  $98\frac{1}{2}$  inches at the ICV cavity centerline.

The containment boundary provided by the ICV consists of a stainless steel vessel formed by a mating lid and body, plus the uppermost of two main O-ring seals enclosed between an upper and lower seal flange. The upper main O-ring seal (containment) is butyl rubber with a nominal 0.400-inch diameter cross-section. The lower main O-ring seal (test) may be neoprene or ethylene propylene with a nominal 0.375-inch diameter cross-section. The purpose of the lower main O-ring seal is for establishing a vacuum on the exterior side of the upper main O-ring seal for helium and pressure rise leakage rate testing. To protect the main O-ring seals from debris that may be associated with some payloads, a wiper O-ring seal is used between the ICV upper and lower seal flanges. In addition to the wiper O-ring seal, a silicone debris shield, located at the top of the ICV lower seal flange, provides a secondary debris barrier to the upper main O-ring seal. To ensure that helium tracer gas reaches the region directly above the upper main O-ring seal (containment) during helium leakage rate testing, a helium fill port is integral to the

ICV vent port configuration (see Appendix 1.3.1, *Packaging General Arrangement Drawings*). In addition, to allow for pressure equalization across the silicone debris shield during ICV lid installation and removal, three, 1/8-inch nominal diameter holes are located in the top of the ICV lower seal flange.

A vent port feature in the ICV body's lower seal flange is the only other containment boundary penetration. A vent port insert and an outer ICV vent port plug with an O-ring seal define the containment boundary at the ICV vent port penetration.

Leakage rate testing of the ICV's upper main O-ring seal (containment seal) is performed through an ICV seal test port that is located in the ICV lid.

All shells comprising the ICV are 1/4-inch nominal thickness, Type 304, stainless steel, including the lower and upper torispherical heads.

The ICV lid is secured to the ICV body via the ICV locking ring located at the outer diameter of the ICV upper and lower seal flanges. Closure design and operation is illustrated in Figure 1.2-1. The lower end of the ICV locking ring has 18 tabs that mate with a corresponding set of 18 tabs on the ICV lower seal flange. To install the ICV lid, the ICV locking ring is rotated to the "unlocked" position, using alignment marks for reference. The unlocked position will align the tabs on the ICV locking ring with the cutouts between the tabs on the ICV lower seal flange. Next, the ICV lid is installed onto the ICV body, optionally evacuating the ICV cavity through the ICV vent port sufficiently to allow free movement of the ICV locking ring. Positive closure is attained by rotating the ICV locking ring to the "locked" position, using the alignment marks for reference. Three, 1/2-inch diameter stainless steel socket head cap screws secure the ICV locking ring in the locked position.

Three lift sockets, each containing a lift pin, are integrated into the ICV lid for lifting the ICV lid or an empty ICV assembly. Any lifting of the loaded ICV is performed using the OCA forklift pockets with the ICV located within the OCA.

Polymer materials used in the ICV include butyl, ethylene propylene, neoprene, buna-N, fluoro-silicone or fluoro-carbon, as applicable, for the main and wiper O-ring seals, and silicone for the debris shield. Brass is used for the ICV vent and seal test port plugs. High alloy stainless steel is used for the ICV locking ring joint pins. Finally, a variety of stainless steel fasteners, and greases and lubricants are also utilized, as specified in Appendix 1.3.1, *Packaging General Arrangement Drawings*.

#### **1.2.1.1.3 Aluminum Honeycomb Spacer Assemblies**

Aluminum honeycomb spacer assemblies are designed to fit within the torispherical heads at each end of the ICV cavity. Each aluminum honeycomb spacer assembly includes an optional, 18-inch nominal diameter by 1½-inch nominal depth pocket that may be used in the future to accommodate a catalyst assembly. The lower spacer assembly also includes a 3-inch nominal diameter hole at the center that serves as an inspection port to check for water accumulation in the ICV lower head. With the spacer assemblies in place, the nominal ICV cavity height becomes 74¾ inches.

### 1.2.1.2 Gross Weight

The gross shipping weight of a TRUPACT-II package is 19,250 pounds maximum. A summary of overall component weights is delineated in Table 2.2-1 of Section 2.2, *Weights and Centers of Gravity*.

### 1.2.1.3 Neutron Moderation and Absorption

The TRUPACT-II package does not require specific design features to provide neutron moderation and absorption for criticality control. Fissile materials in the payload are limited to amounts that ensure safely subcritical packages for both NCT and HAC. The fissile material limits for a single TRUPACT-II package are based on optimally moderated and reflected fissile material. The structural materials in the TRUPACT-II packaging are sufficient to maintain reactivity between the fissile material in an infinite array of damaged TRUPACT-II packages at an acceptable level. Further discussion of neutron moderation and absorption is provided in Chapter 6.0, *Criticality Evaluation*.

### 1.2.1.4 Receptacles, Valves, Testing, and Sampling Ports

There are no receptacles or valves used on the TRUPACT-II packaging, however, the OCV and ICV each have a seal test port and a vent port (see Appendix 1.3.1, *Packaging General Arrangement Drawings*). For each containment/confinement vessel, a seal test port provides access to the region between the upper and lower (containment/confinement and test) main O-ring seals between the upper and lower (lid and body) seal flanges. The seal test ports are used to leakage rate test the upper main ICV seal and, if used, the optional upper main OCV seal to verify proper assembly of the TRUPACT-II package prior to shipment.

The vent port is used during loading and unloading to facilitate lid installation and removal, and to allow blowdown of internal vacuum or pressure prior to opening a loaded package. As an option, a low vacuum may be applied to the vent port to fully seat the lid and assure free rotation of the locking ring.

Two separate penetrations through the polyurethane foam within the OCA are provided to access the seal test port and vent port plugs. The access ports are capped at the OCA exterior surface with 1½-inch pipe plugs (NPT) within 3-inch diameter couplings. Reinforcing doubler plates are also included on the inner surface of the OCA exterior shell, adjacent to the couplings. In addition, removable foam or ceramic fiber plugs fill the region within the access hole tubes to provide a level of thermal protection from the HAC thermal event. The vent port access tube is comprised of a non-metallic fiberglass, and a fiberglass link is included with the stainless steel, seal test port access tube as a lining to reduce radial thermal conductivity. When the OCA lid is removed, the ICV vent and seal test port plugs are readily accessible.

The OCV seal test port and both the ICV seal test and vent port plugs are accessed through localized cutouts in the corresponding vessel locking rings. An elongated cutout in the ICV locking ring is utilized at the ICV vent port location to allow locking ring rotation while an optional vacuum pump is installed. Smaller cutouts are provided in the ICV and OCV locking rings at the seal test port locations since these ports are only used with the locking rings in the locked position. The OCV vent port feature is located in the OCA body, therefore a cutout in the OCV locking ring is not necessary.

Detailed drawings of the test and vent port features and the associated local cutouts in the locking rings are provided in Appendix 1.3.1, *Packaging General Arrangement Drawings*.

#### **1.2.1.5 Heat Dissipation**

The TRUPACT-II package design capacity is 40 thermal watts maximum. The TRUPACT-II package dissipates this relatively low internal heat load entirely by passive heat transfer for both NCT and HAC. No special devices or features are needed or utilized to enhance the dissipation of heat. Features are included in the design to enhance thermal performance in the HAC thermal event. These include the use of a high temperature insulating material (ceramic fiber paper) at polyurethane foam-to-steel interfaces and the presence of an inner and outer thermal shield at the OCA lid-to-body interface. A more detailed discussion of the package thermal characteristics is provided in Chapter 3.0, *Thermal Evaluation*.

#### **1.2.1.6 Coolants**

Due to the passive design of the TRUPACT-II package with regard to heat transfer, there are no coolants utilized within the TRUPACT-II package.

#### **1.2.1.7 Protrusions**

The only significant protrusions on the TRUPACT-II package exterior are those associated with the lifting and tie-down features on the OCA exterior. The only significant external protrusions from the OCA lid are lift straps and corresponding guide pockets that extend from three equally spaced locations at the lid top. These lift features protrude above the OCA upper torispherical head, but are radially located such that they remain below torispherical head's crown and do not affect overall package height. The guide pockets are made of a fiberglass material that is designed to break away for lid-end impacts. The only significant external protrusions from the OCA body are the tie-down features at the bottom end of the package. Four tie-down lugs, with associated doubler plates, are used at locations corresponding with the main beams of the trailer. These tie-down protrusions extend a maximum of 2 $\frac{1}{8}$  inches radially from the OCA body exterior shell.

The only significant protrusion on the ICV exterior is the ICV locking ring. The ICV locking ring extends radially outward approximately one inch from the outside surface of the upper ICV torispherical head. With its 3 $\frac{7}{8}$ -inch axial length directly backed and supported by the OCV (the nominal radial gap is 1/4 inch), this external protrusion is of little consequence for the package. The only significant protrusions on the ICV interior are the three lift pockets that penetrate the upper ICV torispherical head. These lift pockets are equally spaced on a 56-inch diameter, extending into the ICV cavity a maximum of 4 $\frac{1}{2}$  inches from the inner surface of the upper ICV torispherical head. The ICV lift pockets are of little consequence as they are protected by the surrounding aluminum honeycomb spacer assembly. There are no significant internal or external protrusions associated with the ICV body.

#### **1.2.1.8 Lifting and Tie-down Devices**

Three sets of lift pins, lift straps and associated doubler plates used in the OCA lid are designed to handle the OCA lid only (including overcoming any resistance to lid removal associated with the presence of the main O-ring seals). The OCA lid lifting devices are not designed to lift a loaded package or empty OCA. Under excessive load, failure occurs in the region of the OCA lift pin locations (at the pin-to-strap welds), away from the OCA torispherical head. A loaded

TRUPACT-II package or any portion thereof can be lifted via the pair of forklift pockets that are located at the base of the OCA body. These pockets are sized to accommodate forks up to 10 inches wide and up to 4 inches thick. An overhead crane can also be used to lift the loaded package, utilizing lifting straps through the fork lift pockets.

Lifting of the ICV is via the three lift pockets inset into the upper ICV torispherical head. These lift pockets, with their associated lift pins and adjacent doubler plates, are sized to lift an empty ICV or handle the ICV lid (including overcoming any resistance to lid removal associated with the presence of the main O-ring seals). A loaded ICV must be fully supported with the OCA body and lifted via the OCA forklift pockets. Under excessive load, the ICV lift pins are designed to fail in shear prior to compromising the ICV containment boundary.

Both the OCA and ICV lifting points are appropriately labeled to limit their use to the intended manner.

Four tie-down lugs, with associated doubler plates, are used at locations corresponding with the main beams of the trailer. At each tie-down location, one doubler is used on the outside surface of the OCA side wall and one on the inside surface of the OCA lower flanged head. At each tie-down lug location, an internal gusset plate is also used between the inside of the OCA exterior shell and the doubler in the lower head to stiffen the tie-down regions. The doubler plates are sized to adequately distribute the regulatory-defined tie-down loads (10 gs longitudinal, 5 gs lateral, and 2 gs vertical, applied simultaneously) outwardly into the 1/4-inch thick OCA exterior shell. Each tie-down lug is welded directly to the adjacent side doubler plate. In an excessive load condition, these tie-down lug welds are sized to shear from the corresponding doubler plate.

A detailed discussion of lifting and tie-down designs, with corresponding structural analyses, is provided in Section 2.5, *Lifting and Tie-down Standards for All Packages*.

#### **1.2.1.9 Pressure Relief System**

There are no pressure relief systems included in the TRUPACT-II package design to relieve pressure from within the ICV or OCV. Fire-consumable vents in the form of plastic pipe plugs are employed on the exterior surface of the OCA. These vents are included to release any gases generated by charring polyurethane foam in the HAC thermal event (fire). During the HAC fire, the plastic pipe plugs melt allowing the release of gasses generated by the foam as it flashes to a char. Three vents are used on the OCA lid and six on the OCA body, located at the center of foam mass in each component. For optimum performance, the vents are located uniformly around the circumference of the OCA lid and body.

#### **1.2.1.10 Shielding**

Due to the nature of the contact-handled transuranic (CH-TRU) payload, no biological shielding is necessary or provided by the TRUPACT-II packaging.

### **1.2.2 Operational Features**

The TRUPACT-II package is not considered to be operationally complex. All operational features are readily apparent from an inspection of the drawings provided in Appendix 1.3.1, *Packaging General Arrangement Drawings*, and the previous discussions presented in Section 1.2.1, *Packaging*. Operational procedures and instructions for loading, unloading, and preparing

an empty TRUPACT-II package for transport are provided in Chapter 7.0. *Operating Procedures*.

### **1.2.3 Contents of Packaging**

The TRUPACT-II packaging is designed to transport contact-handled transuranic (CH-TRU) and other authorized payloads such as tritium-contaminated materials that do not exceed  $10^5$  A<sub>2</sub> quantities. The *Contact-Handled Transuranic Waste Authorized Methods for Payload Control (CH-TRAMPAC)*<sup>1</sup> is the governing document for shipments of solid or solidified CH-TRU and tritium-contaminated wastes in the TRUPACT-II package. All users of the TRUPACT-II package shall comply with all payload requirements outlined in the CH-TRAMPAC, using one or more of the methods described in that document.

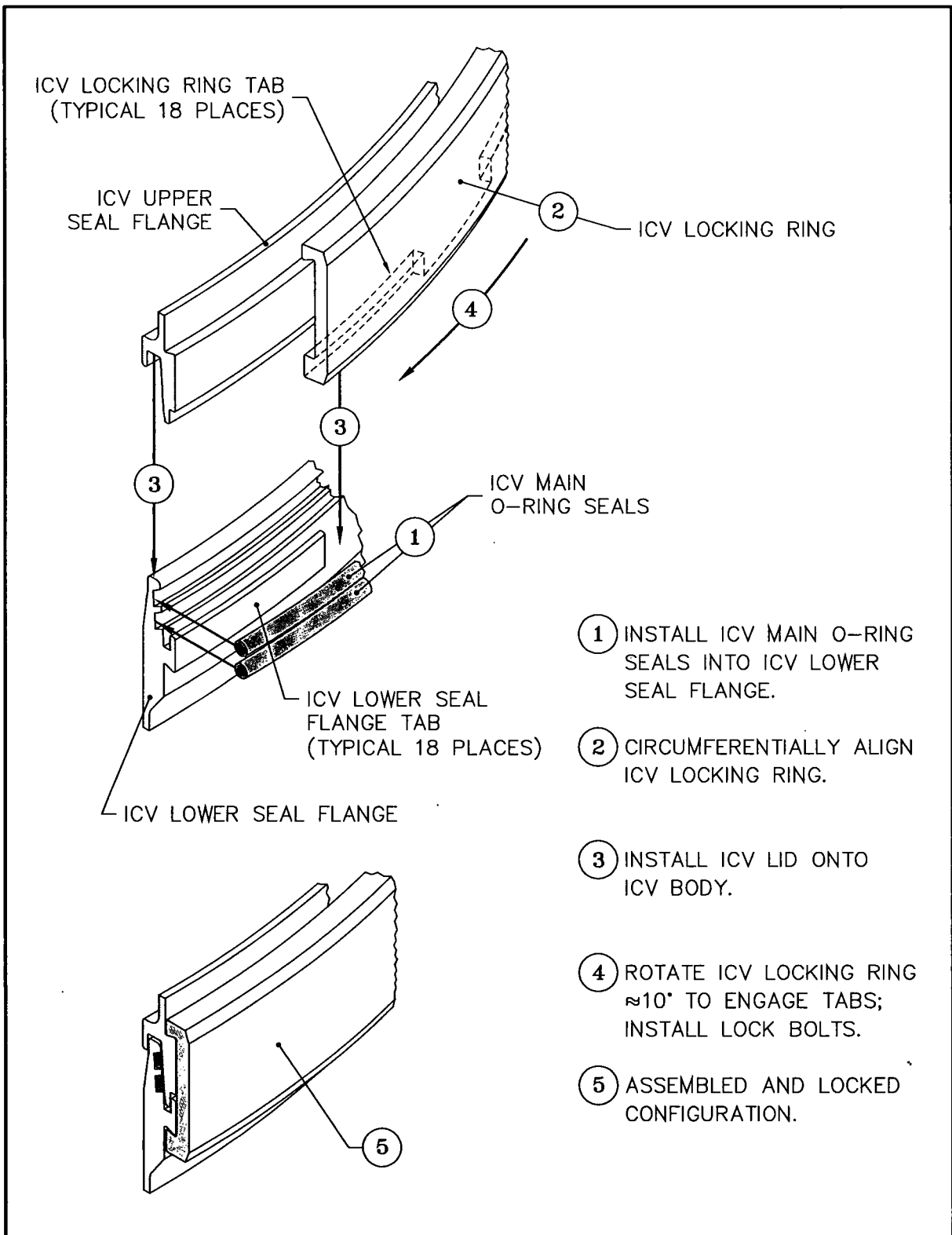


Figure 1.2-1 – ICV Closure Design (OCV closure is similar)

This page intentionally left blank.

### **1.3 Appendices**

- 1.3.1 *Packaging General Arrangement Drawings*
- 1.3.2 *Glossary of Terms and Acronyms*

This page intentionally left blank.

### 1.3.1 Packaging General Arrangement Drawings

This section presents the TRUPACT-II packaging general arrangement drawing<sup>1</sup>, consisting of 11 sheets entitled, *TRUPACT-II Packaging SAR Drawing, Drawing Number 2077-500SNP*. In addition, the standard pipe overpack general arrangement drawing, consisting of 3 sheets entitled, *Standard Pipe Overpack, Drawing Number 163-001*, is presented in this section. The S100 pipe overpack, the S200 pipe overpack, and the S300 pipe overpack are depicted in *Drawing Numbers 163-002, 163-003, and 163-004*, respectively. The 55-gallon, 85-gallon, and 100-gallon compacted puck drum spacers are depicted in *Drawing Number 163-006*. The criticality control overpack is depicted in *Drawing Number 163-009*.

Within the packaging general arrangement drawing, dimensions important to the packaging's safety are dimensioned and toleranced (e.g., structural shell thicknesses, polyurethane foam thicknesses, and the sealing regions on the seal flanges). All other dimensions are provided as a reference dimension, and are toleranced in accordance with the general tolerance block.

---

<sup>1</sup> The TRUPACT-II packaging, pipe overpack, and compacted puck drum spacer general arrangement drawings utilize the uniform standard practices of ASME/ANSI Y14.5M, *Dimensioning and Tolerancing*, American National Standards Institute, Inc. (ANSI).

This page intentionally left blank.

Figure Withheld Under 10 CFR 2.390

UNLESS OTHERWISE SPECIFIED

TOLERANCES					
FIN. DIMS.	FRACTIONS	1/16, 1/32	3/16, 1/2	1/2, 1	1, 2
0" - 1/4"	1/16	±0.005	±0.005	±0.005	
1/4" - 1/2"	1/16	±0.005	±0.005	±0.005	
1/2" - 1"	1/16	±0.005	±0.005	±0.005	
1" - 2"	1/16	±0.005	±0.005	±0.005	

DATE ANGLE PROJECTION

**ORIGINAL  
SIGNATURES  
ON FILE**

REVISION - AWS TRANSFER			
REV	DESCRIPTION	DATE	APPROVED
<b>Washington</b> TRU Solutions LLC TRUPACT-II PACKAGING SAR DRAWING			
0	PT01	2077-500SNP	Y

Figure Withheld Under 10 CFR 2.390

REV	2077-500SNP	REV	Y
-----	-------------	-----	---

<b>Washington</b> TRU Solutions LLC	REV	0	PT01	REV	2077-500SNP	REV	Y
	REV	NOTED FOR MARK	ADDEND	REV	2 OF 11		

8 7 6 5 4 3 1

2077-500SNP	REV	BY
	3	Y

Figure Withheld Under 10 CFR 2.390

D D

C C

B B

A A

8 7 6 5 4 3 2 1

Washington TRU Solutions LLC	REV	BY	DATE	REV
	D	PT01	2077-500SNP	Y
		REV	DATE	REV
		AutoCAD	REV	3 of 11

Figure Withheld Under 10 CFR 2.390

2077-500SNP	4	Y
-------------	---	---

<b>Washington</b> TRU Solutions LLC	D	PT01	2077-500SNP	Y
DATE	REVISED	REV	DATE	BY
			AutoCAD	
				4 OF 11

8 7 6 5 4 3 2 1

2077-500SNP 5 Y

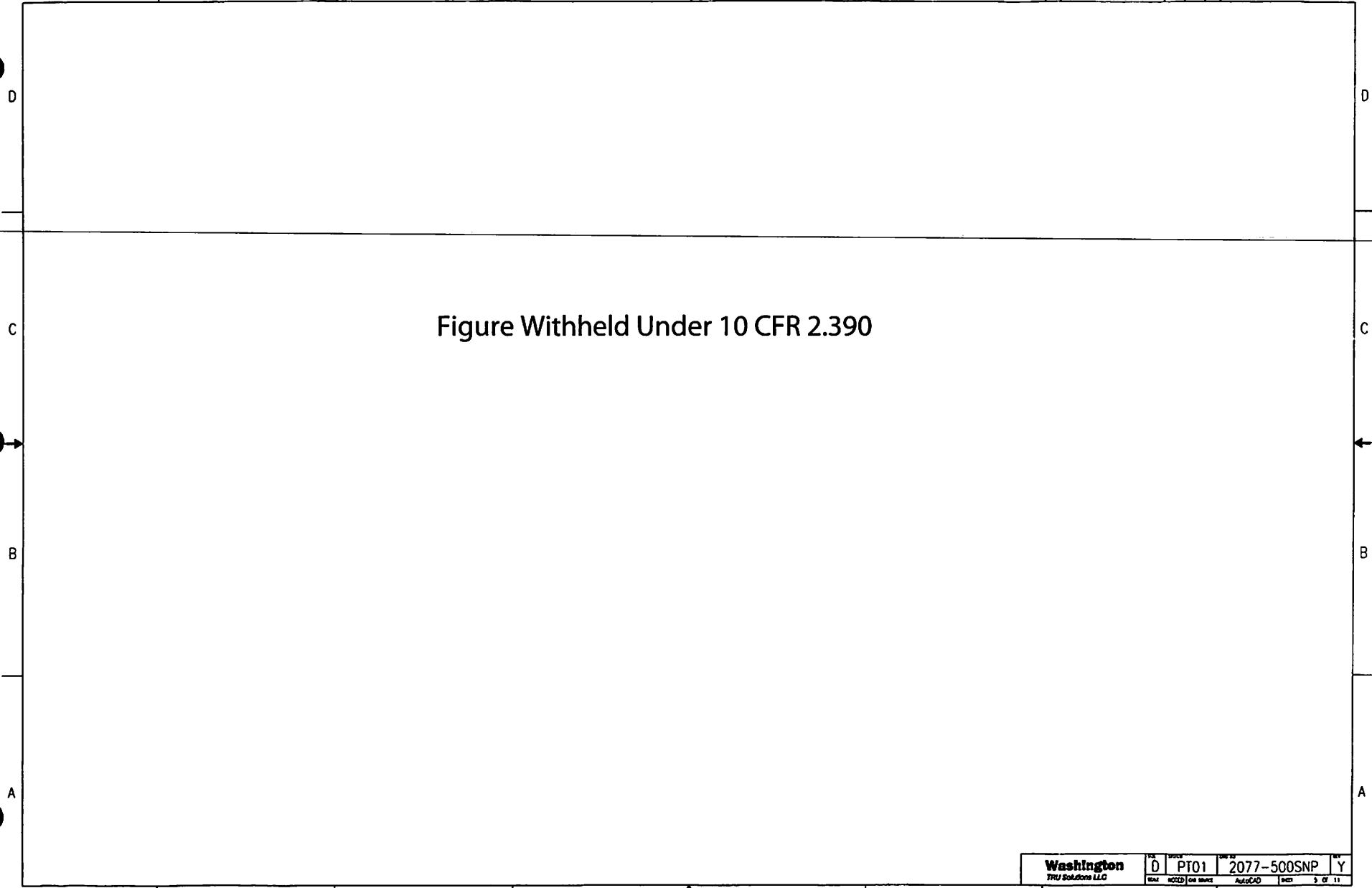


Figure Withheld Under 10 CFR 2.390

C B A

8 7 6 5 4 3 2 1

<b>Washington</b>	D	PT01	2077-500SNP	Y
<small>TRU Solutions LLC</small>	<small>DATE</small>	<small>NOCD</small>	<small>AutoCAD</small>	<small>DATE</small>

8 7 6 5 4 3 1

2077-500SNP 6 Y

Figure Withheld Under 10 CFR 2.390

D

D

C

C

B

B

A

A

8 7 6 5 4 3 2 1

<b>Washington</b>	DC	PT01	2077-500SNP	Y
<small>TRU Solutions LLC</small>	<small>DATE</small>	<small>REVISED</small>	<small>DATE</small>	<small>BY</small>

8 7 6 5 4 3 1

2077-500SNP 7 Y

Figure Withheld Under 10 CFR 2.390

C

C

B

B

A

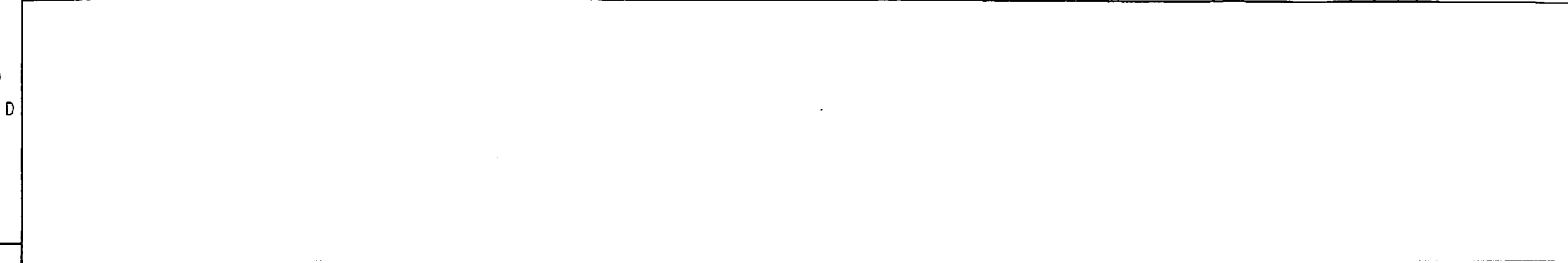
A

8 7 6 5 4 3 2 1

<b>Washington</b> TNU Solutions LLC	REV: D	TYPE: PT01	REV: 2077-500SNP	REV: Y
	DATE: 7/11	BY: A/JCAD	REV: 7	OF: 11

8 7 6 5 4 3 1

2077-500SNP 8 Y



C

Figure Withheld Under 10 CFR 2.390

C

B

B

A

A

8 7 6 5 4 3 2 1

Washington TRU Solutions LLC D PT01 2077-500SNP Y  
8 of 11



8 7 6 5 4 3 1

2077-500SNP

Figure Withheld Under 10 CFR 2.390

C

C

B

B

A

A

8 7 6 5 4 3 2 1

<b>Washington</b> TRU Solutions LLC	REV: D	THROW: PT01	REV: 2077-500SNP	REV: Y
	DATE: 10/20/20	DATE: 10/20/20	DATE: 10/20/20	DATE: 10/20/20

8 7 6 5 4 3 1

2077-500SNP 10 Y

Figure Withheld Under 10 CFR 2.390

D

D

C

C

B

B

A

A

8 7 6 5 4 3 2 1

<b>Washington</b>	REV	PT01	2077-500SNP	Y
TRU Substone LLC	DATE	2/1	AutoCAD	10 OF 11

8 7 6 5 4 3 1

Doc No	2077-500SNP	REV	Y
--------	-------------	-----	---



D

D

C

C



B

B



A

A

Figure Withheld Under 10 CFR 2.390

8 7 6 5 4 3 2 1

<b>Washington</b> TRU SubStore LLC	Doc ID	D	PI01	Doc No	2077-500SNP	REV	Y
	Doc	NOEY	Doc Name	AutoCAD	Doc	11	Of 11

8 7 6 5 4 3 163-001 1 7 1

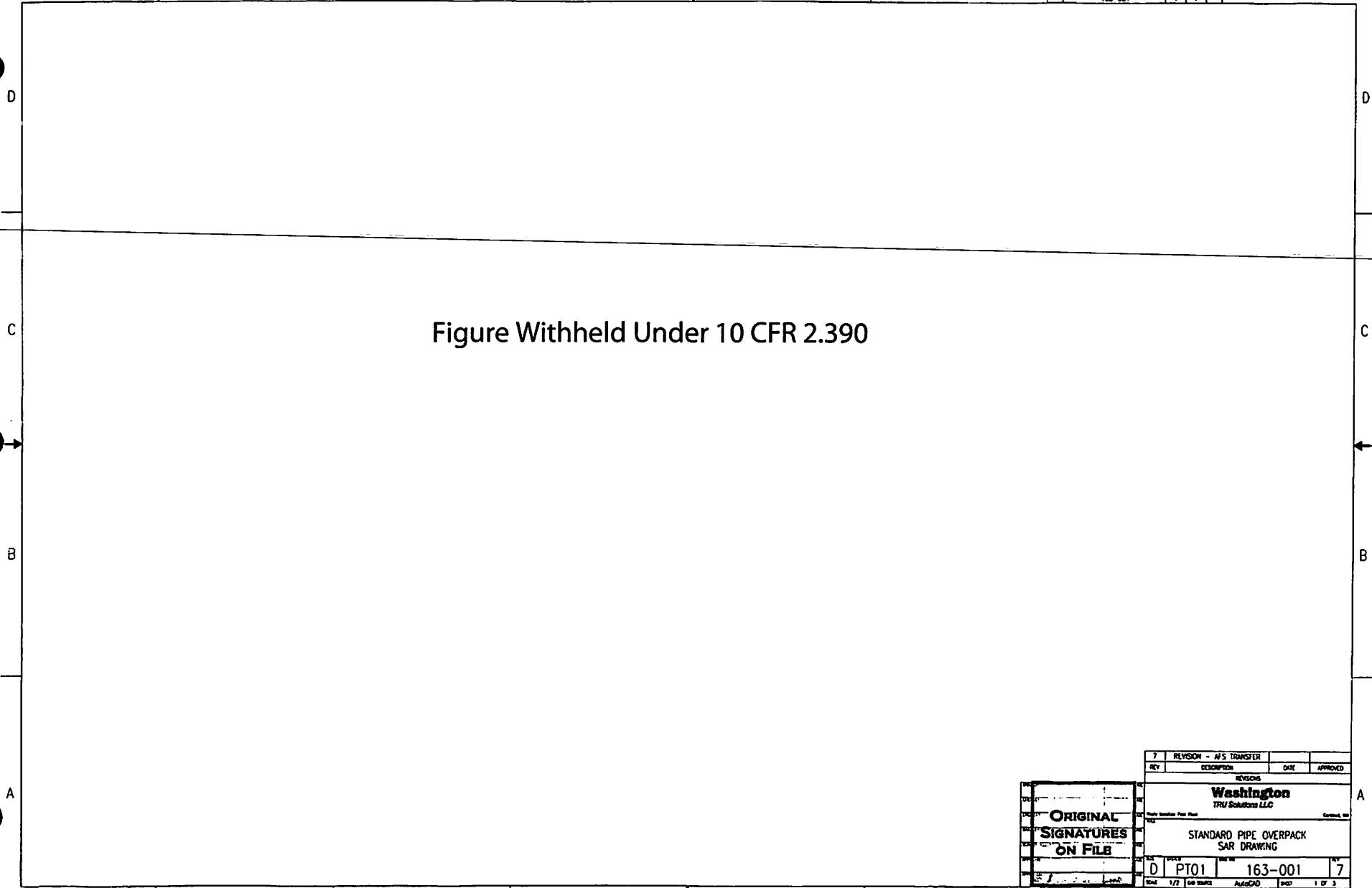


Figure Withheld Under 10 CFR 2.390

REV	DESCRIPTION	DATE	APPROVED
7	REVISION - AFS TRANSFER		
REVISIONS			
<b>Washington</b> TRU Solutions LLC			
STANDARD PIPE OVERPACK SAR DRAWING			
REV	DESCRIPTION	DATE	APPROVED
D	PT01	163-001	7
SHEET 1/2		OF 3	

8 7 6 5 4 3 2 1

8 7 6 5 4 3 1

163-001 2 7

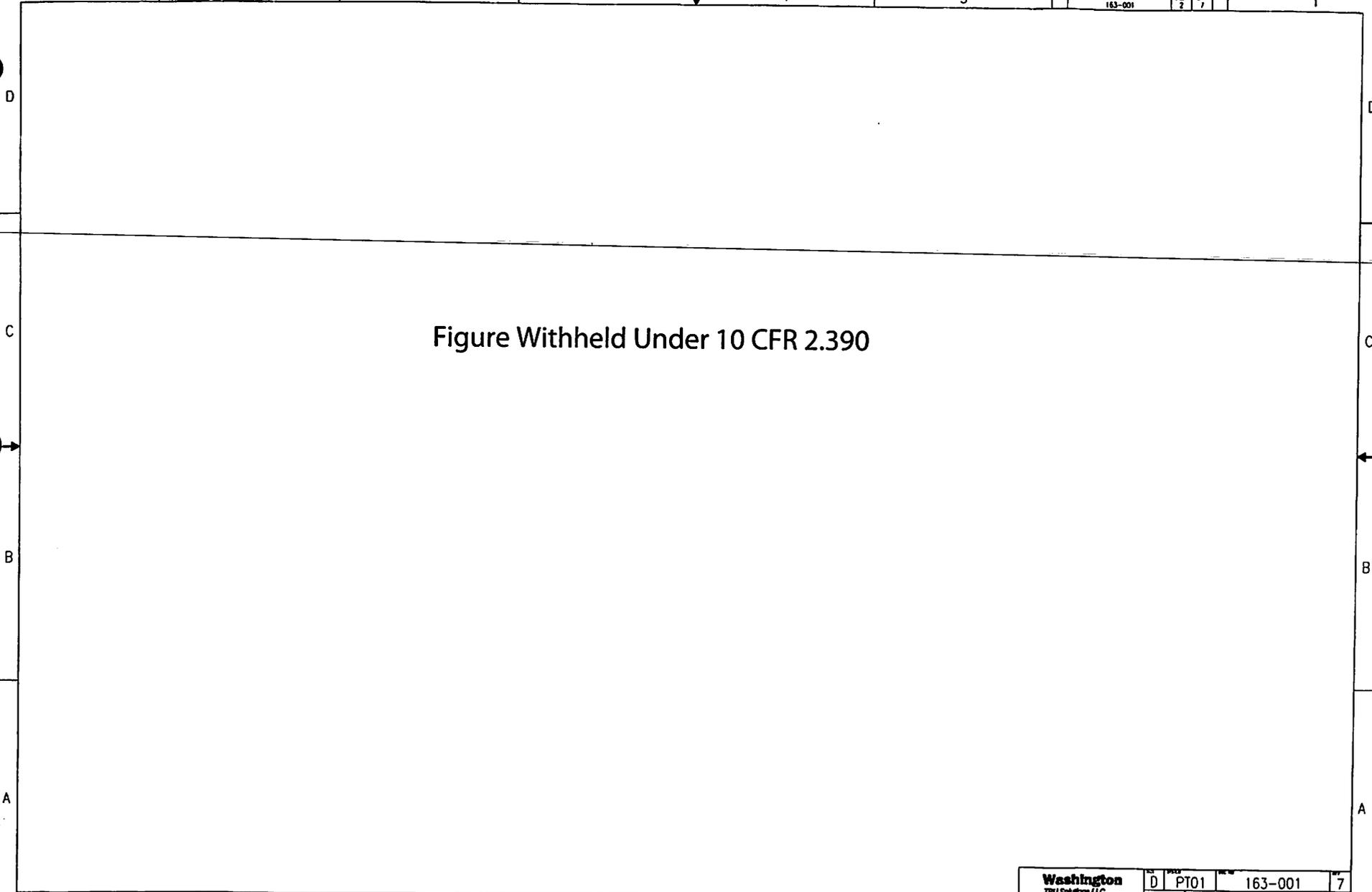


Figure Withheld Under 10 CFR 2.390

<b>Washington</b> TRU Software LLC	REV D	PROJ PT01	REV 163-001	REV 7
	DATE 1/12	BY GSK	APP AutoCAD	REV 2 OF 3

8 7 6 5 4 3 2 1

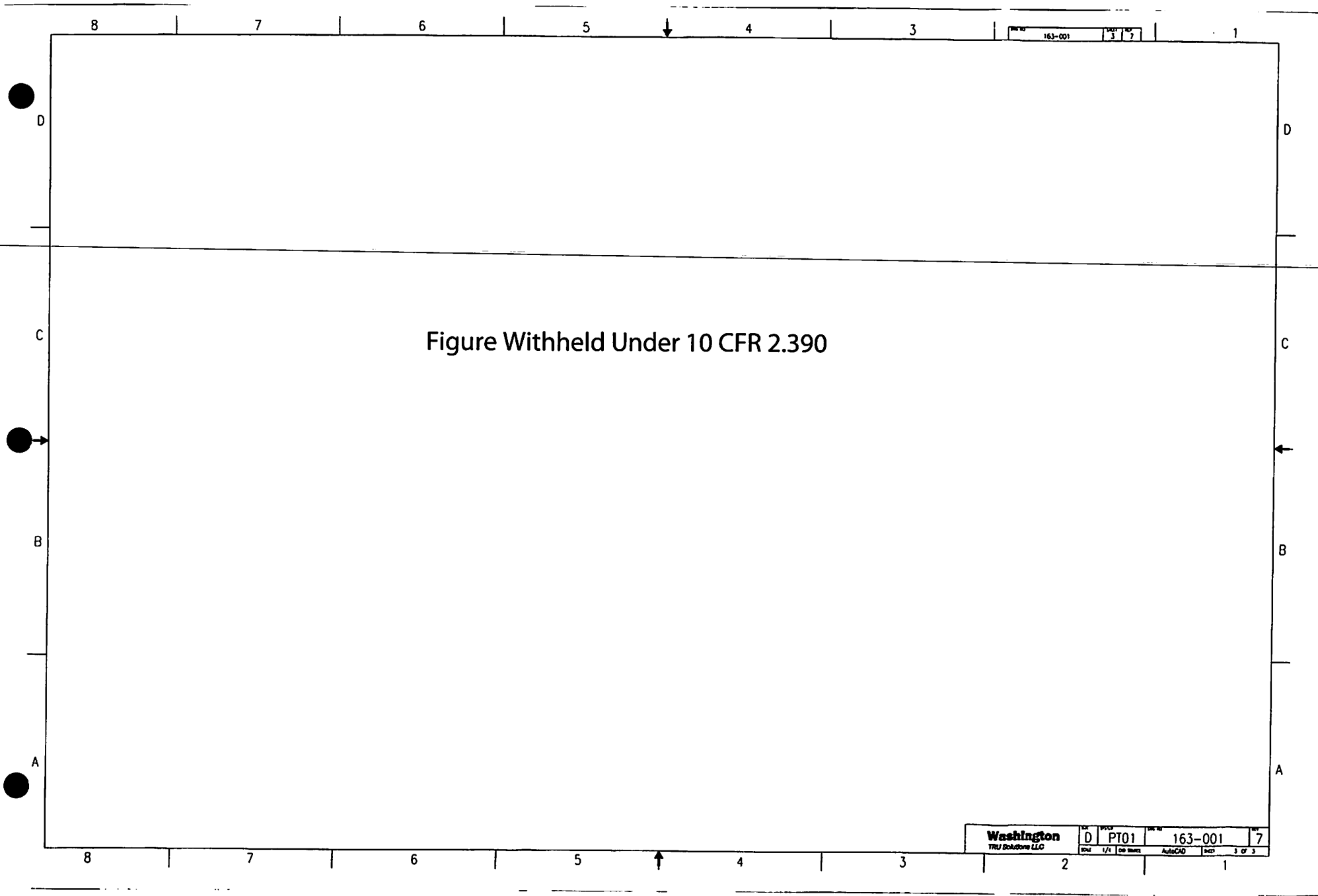


Figure Withheld Under 10 CFR 2.390

163-001	3	7
---------	---	---

<b>Washington</b> TRU Solutions LLC	DC	PT01	163-001	7
	1/1	20 items	AutoCAD	3 of 3

8 7 6 5 4 3 1

163-002 1 5

D

D

C

C

Figure Withheld Under 10 CFR 2.390

B

B

A

A

8 7 6 5 4 3 2 1

REV	5	REVISION - AFS TRANSFER		
		DESCRIPTION	DATE	APPROVED
<b>Washington</b> TRU Solutions LLC				
S100 PIPE OVERPACK SAR DRAWING				
D	PT01	163-002	5	
1 OF 2				

ORIGINAL SIGNATURES ON FILE

8 7 6 5 4 3 1

163-002 2 5

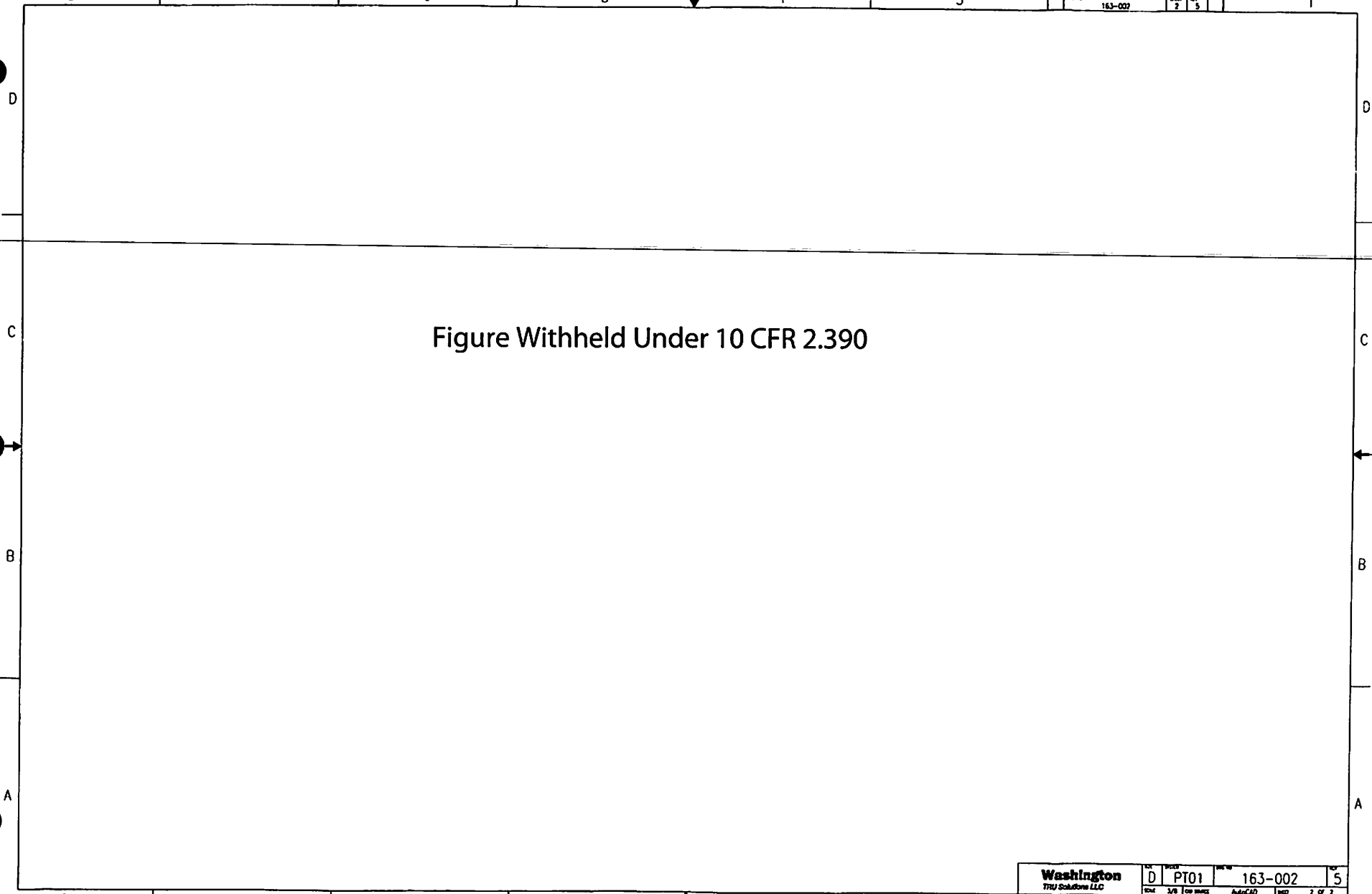


Figure Withheld Under 10 CFR 2.390

Washington  
TRU Solutions LLC  
D PT01  
163-002  
5  
2 1

8 7 6 5 4 3 2 1

8 7 6 5 4 3 1

163-003 1 4

Figure Withheld Under 10 CFR 2.390

D D

C C

B B

A A

4		REVISION - AFS TRANSFER			
REV	DESCRIPTION	DATE	APPROVED		
REVISIONS					
<b>Washington</b> TRU Solutions LLC					
S200 PIPE OVERPACK SAR DRAWING					
D	PT01	163-003	4		
1/2		AutoCAD	1 OF 2		

ORIGINAL SIGNATURES ON FILE

8 7 6 5 4 3 163-003 2 4 1

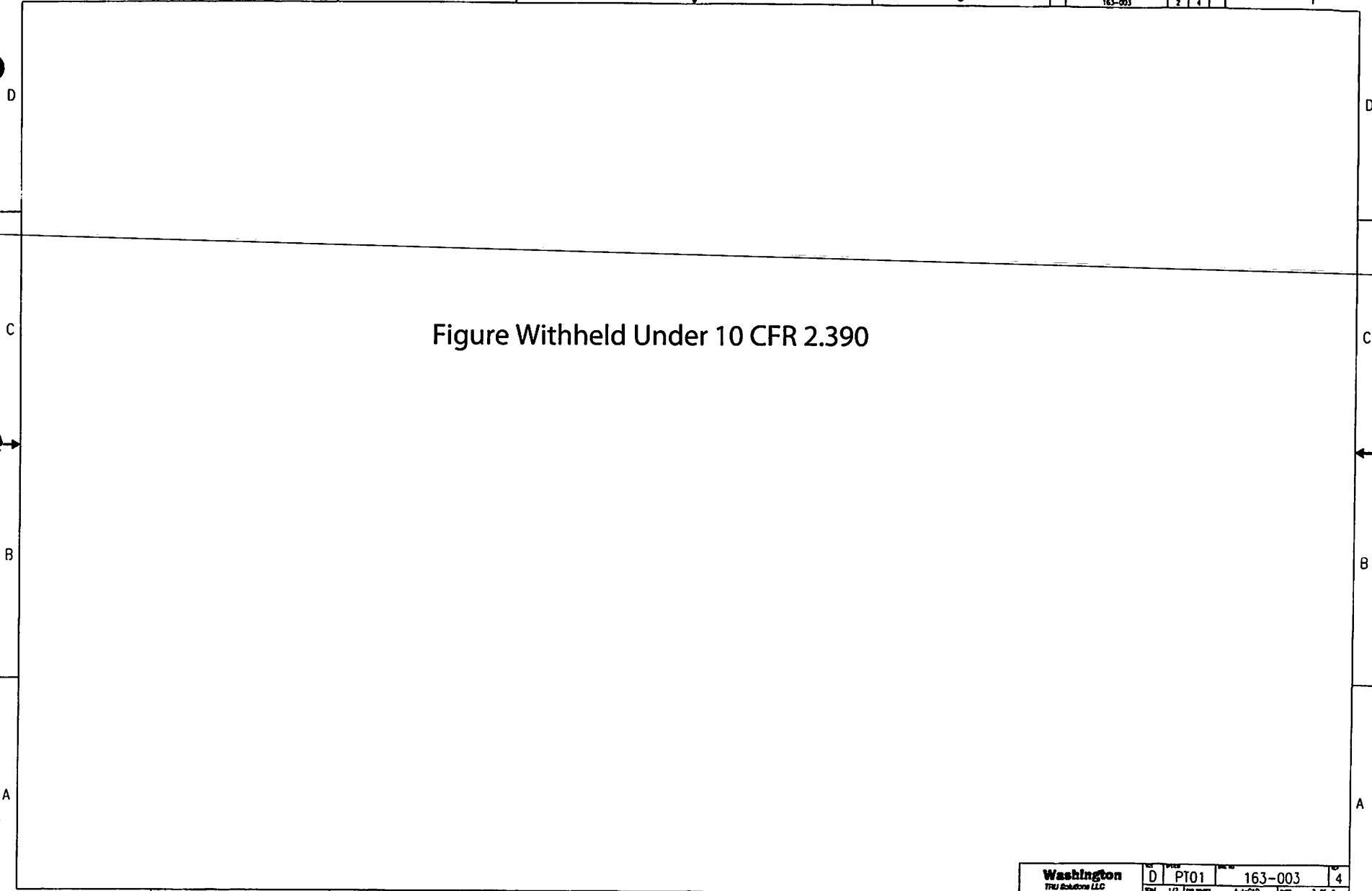


Figure Withheld Under 10 CFR 2.390

8 7 6 5 4 3 163-004 1 2 1

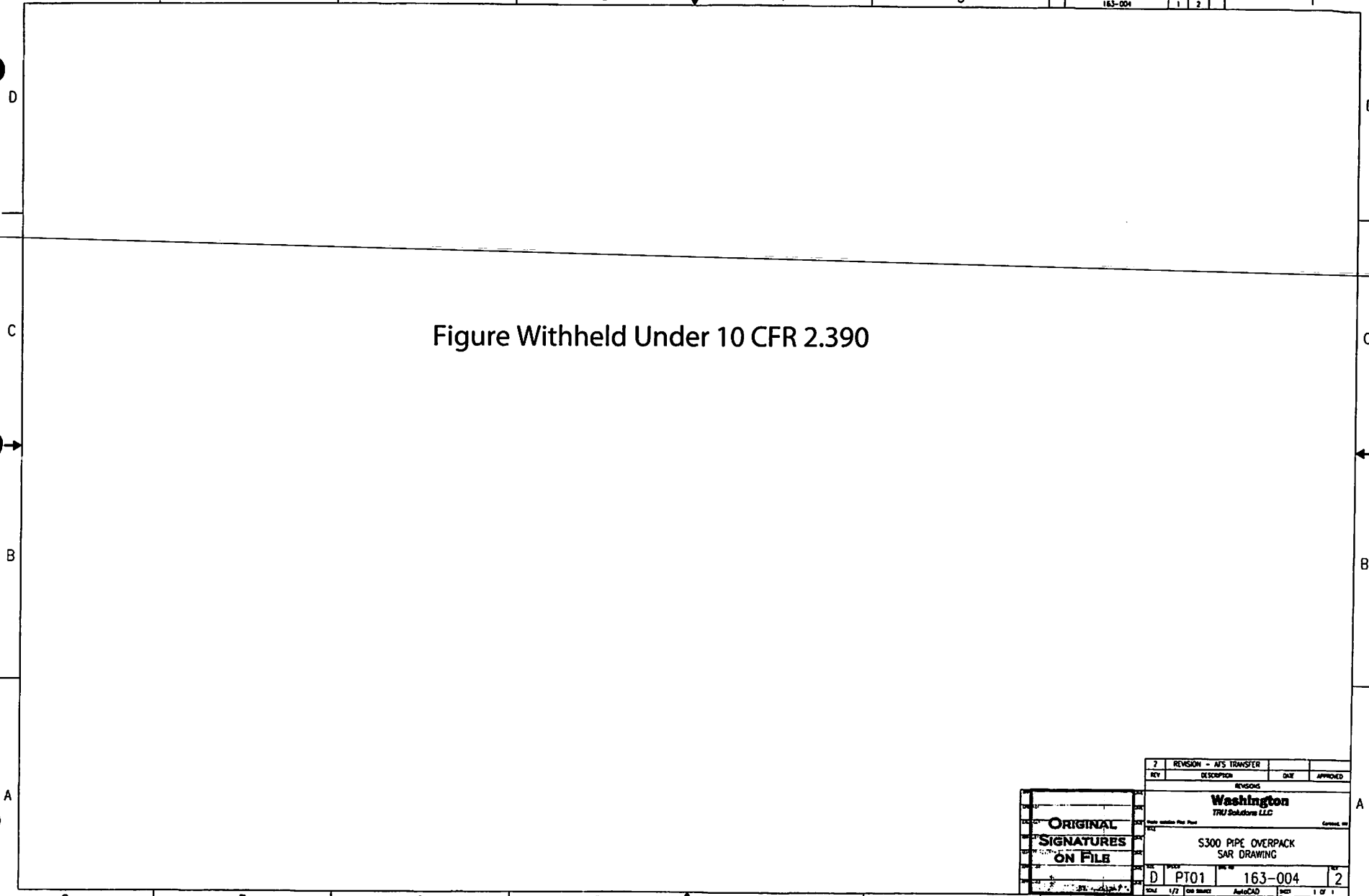


Figure Withheld Under 10 CFR 2.390

2		REVISION - AFS TRANSFER			
REV	DESCRIPTION	DATE	APPROVED		
REVISIONS					
<b>Washington</b>					
TRU Solutions LLC					
Title within the Plant		Contract No.			
S300 PIPE OVERPACK SAR DRAWING					
DESIGN	PT01	163-004		2	
TOTAL	1/2	FOR ISSUED	AutoCAD	1 OF 1	

ORIGINAL  
SIGNATURES  
ON FILE

8 7 6 5 4 3 2 1

8 7 6 5 4 3 1

163-006

Figure Withheld Under 10 CFR 2.390

D

D

C

C

B

B

A

A

8 7 6 5 4 3 2 1

1		REVISION - AFS TRANSFER	DATE	APPROVED
REV		DESCRIPTION	DATE	APPROVED
REVISIONS				
<b>Washington</b> TRU Solutions LLC				
COMPACTED PUCK DRUM SPACERS SAR DRAWING				
D	PT01	163-006	1	1
DATE		1/4	10/20/07	1 OF 1

ORIGINAL  
SIGNATURES  
ON FILE

Figure Withheld Under 10 CFR 2.390

163-009 SHEET 1 OF 0

UNLESS OTHERWISE SPECIFIED					
TOLERANCES					
FIN. NAME	FUNCTION	1 PL. DEC.	2 PL. DEC.	3 PL. DEC.	ANGLES
0"	-18"	0.010	0.012	0.015	0.010
0"	-24"	0.010	0.012	0.015	0.010
0"	-30"	0.012	0.015	0.020	0.010
0"	-36"	0.015	0.020	0.025	0.010

**ORIGINAL  
SIGNATURES  
ON FILE**

0	FIRST SUBMITTAL	DATE	APPROVED
REV.	DESCRIPTION		
REVISIONS			
<b>Washington</b>			
<b>TRU Solutions LLC</b>			
Scale Variation Print Price Contact, etc.			
CRITICALITY CONTROL OVERPACK SAR DRAWING			
DATE	ISSUE	NO.	REV.
D	PT01	163-009	0
DATE	1/4	DATE	PRO/ENGINEER
			SHEET 1 OF 2



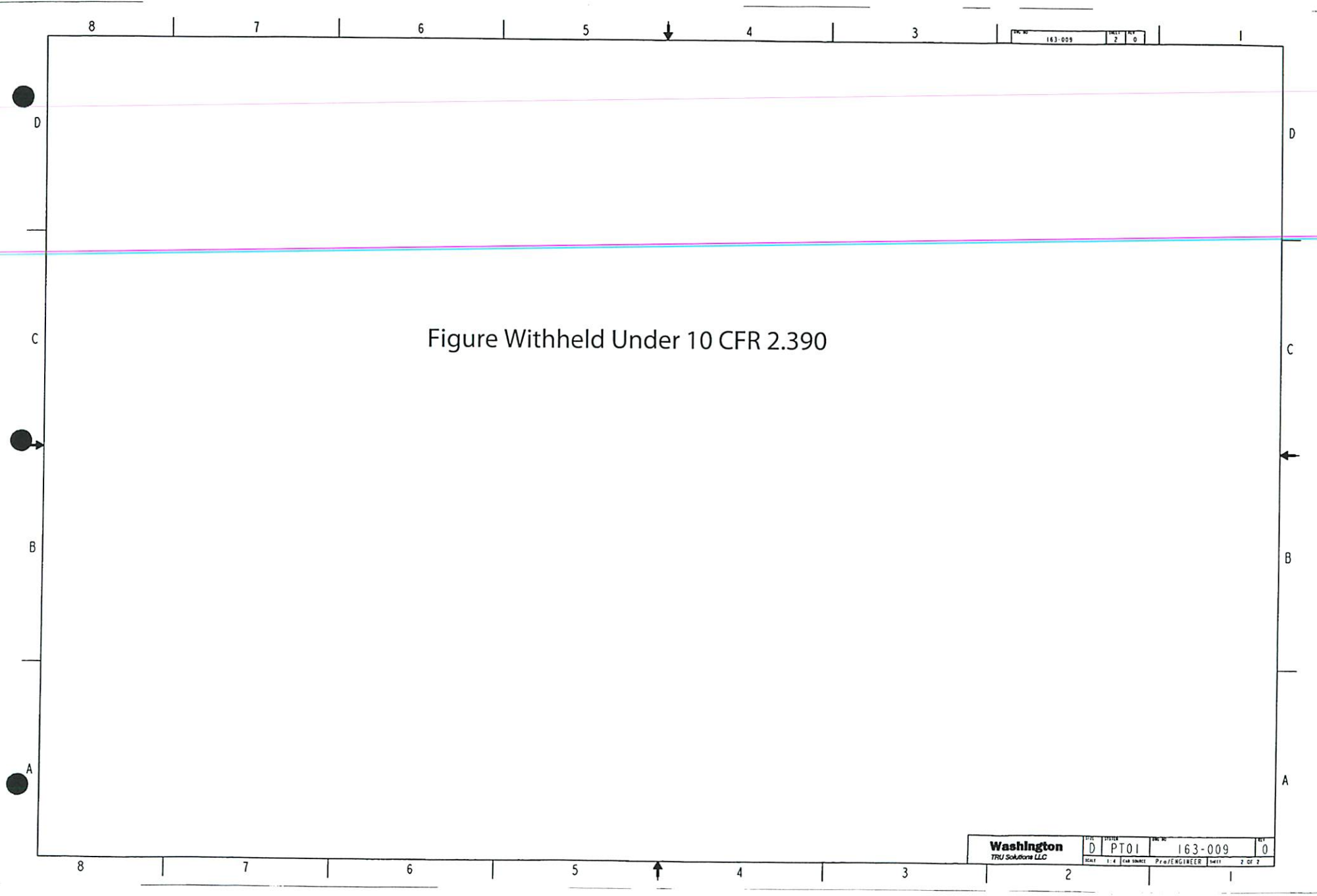


Figure Withheld Under 10 CFR 2.390

DC #	163-009	SHEET	2	OF	0
------	---------	-------	---	----	---

<b>Washington</b> TRU Solutions LLC	DC #	D	PT01	DC #	163-009	REV	0
	SHEET	1-4	OF SHEET	PRO/ENGINEER	SHEET	2	OF 2

### 1.3.2 Glossary of Terms and Acronyms

**55-Gallon Drum** – A payload container yielding 55 gallons.

**85-Gallon Drum** – A payload container with a range of dimensions yielding 75 to 88 gallons.

**85-Gallon Drum Overpacks** – A payload container consisting of a 55-gallon drum overpacked within an 85-gallon drum of the appropriate dimensions.

**100-Gallon Drum** – A payload container yielding 100 gallons.

**Aluminum Honeycomb Spacer Assembly** – An assembly that is located within each end of the ICV. The aluminum honeycomb spacer assembly supplements the ICV void volume to accommodate gas generated by the payload material, and acts as an energy-absorbing barrier between the payload and the ICV torispherical heads for axial loads.

**ASME** – American Society of Mechanical Engineers.

**ASME B&PVC** – ASME Boiler and Pressure Vessel Code.

**CCO** – Criticality Control Overpack

**CCC** – Criticality Control Container

**CTU** – Certification Test Unit.

**CH-TRAMPAC** – Contact-Handled Transuranic Waste Authorized Methods for Payload Control.

**CH-TRU Waste** – Contact-Handled Transuranic Waste.

**ICV** – Inner Containment Vessel.

**ICV Body** – The assembly consisting of the ICV lower seal flange, the cylindrical vessel, and the ICV lower torispherical head.

**ICV Inner Vent Port Plug** – The brass plug and accompanying O-ring seal that provides the pressure boundary in the ICV vent port penetration.

**ICV Lid** – The assembly consisting of the ICV upper seal flange, the ICV locking ring, a short section of cylindrical vessel, and the ICV upper torispherical head.

**ICV Lock Bolts** – The three 1/2-inch, socket head cap screws used to secure the ICV locking ring in the locked position.

**ICV Locking Ring** – The component that connects and locks the ICV upper seal flange to the ICV lower seal flange; included as an ICV lid component.

**ICV Lower Seal Flange** – The ICV body's sealing interface containing two O-ring grooves, the ICV vent port access, and the ICV test port.

**ICV Main O-ring Seal** – The upper elastomeric O-ring seal in the ICV lower seal flange; forms the containment boundary.

**ICV Main Test O-ring Seal** – The lower elastomeric O-ring seal in the ICV lower seal flange; forms the test boundary for leakage rate testing.

**ICV Outer Vent Port Plug** – The brass plug and accompanying O-ring seal that provides the containment boundary in the ICV vent port penetration.

**ICV Seal Test Port** – The radial penetration between the ICV main O-ring seal and ICV main test O-ring seal to allow leakage rate testing of the ICV main O-ring seal.

**ICV Seal Test Port Plug** – The brass plug and accompanying O-ring seal for the ICV seal test port.

**ICV Seal Test Port Insert** – A welded-in, replaceable component within the ICV lower seal flange that interfaces with the ICV seal test port plug.

**ICV Upper Seal Flange** – The ICV lid's sealing interface containing a mating sealing surface for the ICV lower seal flange and location for a wiper O-ring seal.

**ICV Vent Port** – The radial penetration into the ICV cavity that is located in the ICV lower seal flange.

**ICV Vent Port Cover** – The outer brass cover that directly protects the ICV vent port plugs.

**Inner Containment Vessel** – The assembly (comprised of an ICV lid and ICV body) providing the primary level of containment for the payload. Within each end of the inner containment vessel (ICV) is an aluminum honeycomb spacer assembly.

**Locking Z-Flange** – The z-shaped shell situated between the upper and lower Z-flanges that connects to the OCV locking ring; allows external operation of the OCV locking ring.

**Lower Z-Flange** – The z-shaped shell in the OCA body, connecting the OCA outer shell to the OCV lower seal flange.

**OCA** – Outer Confinement Assembly.

**OCA Body** – The assembly consisting of the OCV lower seal flange, the OCV cylindrical and conical shells (including stiffening ring), the OCV lower torispherical head, the lower Z-flange, the OCA cylindrical shell, the OCA lower flat head, corner reinforcing angles, tie-down structures, ceramic fiber paper, and polyurethane foam.

**OCA Inner Thermal Shield** – The L-shaped, 16-gauge (0.060-inch thick), inner shield that holds fiberglass insulating material against the OCV locking ring thereby preventing hot gasses and flames from directly impinging on the OCV sealing region in the event of a HAC fire.

**OCA Lid** – The assembly consisting of the OCV upper seal flange, the OCV locking ring, a short section of cylindrical vessel, the OCV upper torispherical head, the upper and locking Z-flanges, the inner and outer thermal shields, a short section of cylindrical shell, the OCA upper torispherical head, corner reinforcing angles, ceramic fiber paper, and polyurethane foam.

**OCA Lock Bolts** – The six 1/2-inch, socket head cap screws used to secure the OCV locking ring in the locked position.

**OCA Lower Head** – The lower ASME flat head comprising the OCA outer shell.

**OCA Outer Thermal Shield** – The 14-gauge (0.075-inch thick) × 6 1/8-inch wide outer shield surrounding the OCA lid-to-body joint that prevents hot gasses and flames from entering the joint in the event of a HAC fire.

**OCA Upper Head** – The upper ASME torispherical head comprising the OCA outer shell.

**OCV** – Outer Confinement Vessel.

**OCV Locking Ring** – The component that connects and locks the OCV upper seal flange to the OCV lower seal flange; included as an OCA lid component.

**OCV Lower Seal Flange** – The OCA body's sealing interface containing two O-ring grooves.

**OCV Main O-ring Seal** – The optional upper O-ring seal in the OCV lower seal flange; forms the confinement boundary.

**OCV Main Test O-ring Seal** – The optional lower O-ring seal in the OCV lower seal flange; forms the test boundary for optional leakage rate testing.

**OCV Seal Test Port** – The radial penetration between the OCV main O-ring seal and OCV main test O-ring seal to allow optional leakage rate testing of the OCV main O-ring seal.

**OCV Seal Test Port Access Plug** – The 1½-inch NPT plug located at the outside end of the OCV seal test port access tube (i.e., at the outside surface of the OCA lid outer shell).

**OCV Seal Test Port Insert** – A welded-in, replaceable component within the OCV lower seal flange that interfaces with the OCV seal test port plug.

**OCV Seal Test Port Plug** – The brass plug and accompanying optional O-ring seal for the OCV seal test port.

**OCV Seal Test Port Thermal Plug** – The foam or ceramic fiber plug located within the OCV seal test port access tube that thermally protects the OCV seal test port region.

**OCV Upper Seal Flange** – The OCA lid's sealing interface containing a mating sealing surface for the OCV lower seal flange.

**OCV Vent Port** – The radial penetration into the OCV cavity that is located in the OCV conical shell.

**OCV Vent Port Access Plug** – The 1½-inch NPT plug located at the outside end of the OCV vent port access tube (i.e., at the outside surface of the OCA body outer shell).

**OCV Vent Port Access Tube** – The fiberglass tube allowing external access to the OCV vent port.

**OCV Vent Port Cover** – The outer brass cover that directly protects the OCV vent port plug.

**OCV Vent Port Plug** – The brass plug and accompanying optional O-ring seal that provides the confinement boundary in the OCV vent port penetration.

**OCV Vent Port Thermal Plug** – The foam or ceramic fiber plug located within the OCV vent port access tube that thermally protects the OCV vent port region.

**Outer Confinement Assembly** – The assembly (comprised of an OCA lid and OCA body) providing a secondary level of confinement for the payload when its optional O-ring seals are utilized. The Outer Confinement Assembly (OCA) completely surrounds the Inner Containment Vessel and consists of an exterior stainless steel shell, a relatively thick layer of polyurethane foam and an inner stainless steel boundary that forms the Outer Confinement Vessel (OCV).

**Outer Confinement Vessel** – The innermost boundary of the Outer Confinement Assembly.

**Packaging** – The assembly of components necessary to ensure compliance with packaging requirements as defined in 10 CFR §71.4. Within this SAR, the packaging is denoted as the TRUPACT-II packaging.

**Package** – The packaging with its radioactive contents, or payload, as presented for transportation as defined in 10 CFR §71.4. Within this SAR, the package is denoted as the TRUPACT-II contact-handled transuranic waste package, or equivalently, the TRUPACT-II package.

**Payload** – Contact-handled transuranic (CH-TRU) waste or other authorized contents such as tritium-contaminated materials contained within approved payload containers. In this SAR, the payload includes a payload pallet for handling when drums are used. Any additional dunnage used that is external to the payload containers is also considered to be part of the payload. Payload requirements are defined by the CH-TRAMPAC.

**Payload Container** – Payload containers may be 55-gallon drums, pipe overpacks, criticality control overpacks (CCOs), 85-gallon drums (including overpacks), 100-gallon drums, standard waste boxes (SWBs), or ten drum overpacks (TDOPs).

**Payload Pallet** – A lightweight pallet, used for handling drum-type payload containers.

**Pipe Component** – A stainless steel container used for packaging specific waste forms within a 55-gallon drum. The pipe component is exclusively used as part of the pipe overpack.

**Pipe Overpack** – A payload container consisting of a pipe component positioned by dunnage within a 55-gallon drum with a rigid, polyethylene liner and lid. Fourteen pipe overpack assemblies will fit within the TRUPACT-II packaging.

**RTV** – Room Temperature Vulcanizing.

**SAR** – Safety Analysis Report (this document).

**Standard Waste Box** – A specialized payload container for use within the TRUPACT-II packaging.

**SWB** – Standard Waste Box.

**Ten Drum Overpack** – A specialized payload container for use within the TRUPACT-II packaging.

**TDOP** – Ten Drum Overpack.

**TRUPACT-II Package** – The package consisting of a TRUPACT-II packaging and the Payload.

**TRUPACT-II Packaging** – The packaging consisting of an outer confinement assembly (OCA), an inner containment vessel (ICV), and two aluminum honeycomb spacer assemblies.

**Upper Z-Flange** – The z-shaped shell in the OCA lid, connecting the OCA outer shell to the OCV upper seal flange.

## 2.0 STRUCTURAL EVALUATION

This section presents evaluations demonstrating that the TRUPACT-II package meets all applicable structural criteria. The TRUPACT-II packaging, consisting of an outer confinement assembly (OCA), with an integral outer confinement vessel (OCV), and an inner containment vessel (ICV), with aluminum honeycomb spacer assemblies, is evaluated and shown to provide adequate protection for the payload. Normal conditions of transport (NCT) and hypothetical accident condition (HAC) evaluations, using analytic and empirical techniques, are performed to address 10 CFR 71<sup>1</sup> performance requirements. Analytic demonstration techniques comply with the methodology presented in NRC Regulatory Guides 7.6<sup>2</sup> and 7.8<sup>3</sup>.

Numerous component and scale tests were successfully performed on the TRUPACT-II package during its development phase. Subsequent TRUPACT-II certification testing involved three, full-scale certification test units (CTUs). The TRUPACT-II CTUs were subjected to a series of free drop and puncture drop tests, and two of the three TRUPACT-II CTUs were subjected to fire testing. The TRUPACT-II CTUs remained leaktight<sup>4</sup> throughout certification testing. Details of the certification test program are provided in Appendix 2.10.3, *Certification Tests*.

### 2.1 Structural Design

#### 2.1.1 Discussion

A comprehensive discussion on the TRUPACT-II package design and configuration is provided in Section 1.2, *Package Description*. Specific discussions relating to the aspects important to demonstrating the structural configuration and performance to design criteria for the TRUPACT-II package are provided in the following sections. Standard fabrication methods are utilized to fabricate the TRUPACT-II packaging.

##### 2.1.1.1 Containment Vessel Structure (ICV)

The containment vessel cylindrical shell structure is fabricated in accordance with the tolerance requirements of the ASME Boiler and Pressure Vessel Code, Section III<sup>5</sup>, Division 1, Subsection NE, Article NE-4220, as delineated on the drawings in Appendix 1.3.1, *Packaging General Arrangement Drawings*. The containment vessel shell-to-shell joints are fabricated in accordance with the ASME Boiler and Pressure Vessel Code, Section III, Division 1, Subsection

---

<sup>1</sup> Title 10, Code of Federal Regulations, Part 71 (10 CFR 71), *Packaging and Transportation of Radioactive Material*, 01-01-12 Edition.

<sup>2</sup> U. S. Nuclear Regulatory Commission, Regulatory Guide 7.6, *Design Criteria for the Structural Analysis of Shipping Cask Containment Vessels*, Revision 1, March 1978.

<sup>3</sup> U. S. Nuclear Regulatory Commission, Regulatory Guide 7.8, *Load Combinations for the Structural Analysis of Shipping Casks for Radioactive Material*, Revision 1, March 1989.

<sup>4</sup> Leaktight is defined as leakage of  $1 \times 10^{-7}$  standard cubic centimeters per second (scc/s), air, or less per ANSI N14.5-1997, *American National Standard for Radioactive Materials – Leakage Tests on Packages for Shipment*, American National Standards Institute, Inc. (ANSI).

<sup>5</sup> American Society of Mechanical Engineers (ASME) Boiler and Pressure Vessel Code, Section III, *Rules for Construction of Nuclear Power Plant Components*, 1986 Edition.

NB, Article NB-4230, as delineated on the drawings in Appendix 1.3.1, *Packaging General Arrangement Drawings*.

All containment vessel heads are flanged torispherical heads, fabricated in accordance with the ASME Boiler and Pressure Vessel Code, Section VIII, Division 1<sup>6</sup>, as delineated on the drawings in Appendix 1.3.1, *Packaging General Arrangement Drawings*.

All seal flange material is ultrasonically or radiographically test inspected in accordance with the ASME Boiler and Pressure Vessel Code, Section III, Division 1, Subsection NB, Article NB-2500 and Section V<sup>7</sup>, Article 5 (ultrasonic) or Article 2 (radiograph), as delineated on the drawings in Appendix 1.3.1, *Packaging General Arrangement Drawings*.

Circumferential and longitudinal welds for the containment vessel shells, seal flanges, and locking rings are full penetration welds, subjected to visual and liquid penetrant examinations, and radiographically test inspected, as delineated on the drawings in Appendix 1.3.1, *Packaging General Arrangement Drawings*. Visual weld examinations are performed in accordance with AWS D1.6<sup>8</sup>. Liquid penetrant examinations are performed on the final pass in accordance with the ASME Boiler and Pressure Vessel Code, Section III, Division 1, Subsection NB, Article NB-5000 and Section V, Article 6. Radiograph test inspections are performed in accordance with the ASME Boiler and Pressure Vessel Code, Section III, Division 1, Subsection NB, Article NB-2500 and Section V, Article 2.

For the ICV vent port penetration and lifting sockets, liquid penetrant examinations are performed on the final pass for single pass welds and on the root and final passes for multipass welds in accordance with the ASME Boiler and Pressure Vessel Code, Section III, Division 1, Subsection NB, Article NB-5000 and Section V, Article 6, as delineated on the drawings in Appendix 1.3.1, *Packaging General Arrangement Drawings*.

The maximum weld reinforcement for containment vessel welds shall be 3/32 inch in accordance with the ASME Boiler and Pressure Vessel Code, Section III, Division 1, Subsection NB, Article NB-4426, Paragraph NB-4426.1, as delineated on the drawings in Appendix 1.3.1, *Packaging General Arrangement Drawings*.

#### **2.1.1.2 Non-Containment Vessel Structures (OCV and OCA)**

All non-containment vessel shell-to-shell joints and transitions in thickness, such as from the 1/4-inch thick OCV lower head to the 3/16-inch thick OCV shell and the 3/8-to-1/4-inch thick OCA outer shell transition, are fabricated in accordance with the ASME Boiler and Pressure Vessel Code, Section III, Division 1, Subsection NF, Article NF-4230, as delineated on the drawings in Appendix 1.3.1, *Packaging General Arrangement Drawings*.

The OCV has a top and bottom, flanged torispherical head, and the OCA outer shell has a top, flanged torispherical head and bottom, flanged flat head that are fabricated in accordance with the

<sup>6</sup> American Society of Mechanical Engineers (ASME) Boiler and Pressure Vessel Code, Section VIII, Division 1, *Rules for Construction of Pressure Vessels*, 1986 Edition.

<sup>7</sup> American Society of Mechanical Engineers (ASME) Boiler and Pressure Vessel Code, Section V, *Nondestructive Examination*, 1986 Edition.

<sup>8</sup> ANSI/AWS D1.6, *Structural Welding Code – Stainless Steel*, American Welding Society (AWS).

ASME Boiler and Pressure Vessel Code, Section VIII, Division 1, as delineated on the drawings in Appendix 1.3.1, *Packaging General Arrangement Drawings*.

Circumferential and longitudinal welds for the non-containment vessel shells are full penetration welds, subjected to visual and liquid penetrant examinations, as delineated on the drawings in Appendix 1.3.1, *Packaging General Arrangement Drawings*. Visual weld examinations are performed in accordance with AWS D1.6. Liquid penetrant examinations are performed on the final pass in accordance with the ASME Boiler and Pressure Vessel Code, Section III, Division 1, Subsection NF, Article NF-5000.

The maximum weld reinforcement for non-containment vessel welds shall be 3/32 inch in accordance with the ASME Boiler and Pressure Vessel Code, Section III, Division 1, Subsection NF, Article NF-4400, as delineated on the drawings in Appendix 1.3.1, *Packaging General Arrangement Drawings*.

## **2.1.2 Design Criteria**

Proof of performance for the TRUPACT-II package is achieved by a combination of analytic and empirical evaluations. The acceptance criteria for analytic assessments are in accordance with Regulatory Guide 7.6 and Section III of the ASME Boiler and Pressure Vessel Code. The acceptance criterion for empirical assessments is a demonstration that the containment boundary remains leaktight throughout NCT and HAC certification testing. Additionally, package deformations obtained from certification testing must be such that deformed geometry assumptions used in subsequent thermal, shielding, and criticality evaluations are validated.

The remainder of this section presents the detailed acceptance criteria used for all analytic structural assessments of the TRUPACT-II package.

### **2.1.2.1 Analytic Design Criteria (Allowable Stresses)**

This section defines the stress allowables for primary membrane, primary bending, secondary, shear, peak, and buckling stresses for containment and non-containment structures. These stress allowables are used for all analytic assessments of TRUPACT-II package structural performance. Regulatory Guide 7.6 is used in conjunction with Regulatory Guide 7.8 to evaluate the package integrity. Material yield strengths used in the analytic acceptance criteria,  $S_y$ , ultimate strengths,  $S_u$ , and design stress intensity values,  $S_m$ , are presented in Table 2.3-1 of Section 2.3, *Mechanical Properties of Materials*.

#### **2.1.2.1.1 Containment Structure (ICV)**

A summary of allowable stresses used for containment structures is presented in Table 2.1-1. These data are consistent with Regulatory Guide 7.6, and the ASME Boiler and Pressure Vessel Code, Section III, Subsection NB-3000 and Appendix F.

#### **2.1.2.1.2 Non-Containment Structures (OCV and OCA)**

A summary of allowable stresses used for non-containment structures is presented in Table 2.1-2. For conservatism, the allowable stresses applicable to containment structures presented in Table 2.1-1 are utilized for OCV evaluations.

For evaluation of lifting devices, the allowable stresses are limited to one-third of the material yield strength, consistent with the requirements of 10 CFR §71.45(a). For evaluation of tie-down devices, the allowable stresses are limited to the material yield strength, consistent with the requirements of 10 CFR §71.45(b).

For evaluations involving polyurethane foam, primary, load controlled compressive stresses are limited to two-thirds of the parallel-to-rise or perpendicular-to-rise compressive strength (as applicable) at 10% strain. Use of a two-thirds factor on compressive strength ensures elastic behavior of the polyurethane foam.

## **2.1.2.2 Miscellaneous Structural Failure Modes**

### **2.1.2.2.1 Brittle Fracture**

By avoiding the use of ferritic steels in the TRUPACT-II packaging, brittle fracture concerns are precluded. Specifically, most primary structural components are fabricated of Type 304 austenitic stainless steel. Since this material does not undergo a ductile-to-brittle transition in the temperature range of interest (down to -40 °F), it is safe from brittle fracture.

The lock bolts used to secure the ICV and OCV locking rings in the locked position are stainless steel, socket head cap screws ensuring that brittle fracture is not of concern. Other fasteners used in the TRUPACT-II packaging assembly, such as the 36, 1/4-inch screws attaching the locking Z-flange to the OCV locking ring, provide redundancy and are made from stainless steel, again eliminating brittle fracture concerns.

### **2.1.2.2.2 Fatigue Assessment**

#### **2.1.2.2.2.1 Normal Operating Cycles**

Normal operating cycles do not present a fatigue concern for the various TRUPACT-II packaging components. Most TRUPACT-II packaging components exhibit little-to-no stress concentrations, and by satisfying the allowable limit for range of primary plus secondary stress intensity for NCT ( $3.0S_m$ ), the allowable fatigue stress limit for the expected number of operating cycles is satisfied. For TRUPACT-II packaging components that do exhibit stress concentrations, stresses are low enough that allowable fatigue stress limits are again satisfied.

The maximum number of operating cycles reasonably expected for the TRUPACT-II package is 3,640, and is based on two round trips per week for 35 years. Conservatively, 5,000 cycles (or in excess of 1 cycle every 3 days) is used in the following calculations. A cycle is defined as the process of the internal pressure within the ICV increasing gradually from zero psig at the time of loading, to 50 psig (the maximum normal operating pressure, MNOP, per Section 3.4.4, *Maximum Internal Pressure*) during transport and then returning to 0 psig when the containment vessel is vented prior to unloading the payload. This scenario is conservative because most shipments will never generate pressure to the magnitude of the MNOP, and the system could never achieve MNOP in less than the assumed transportation cycle of 3 days.

From Figure I-9.2.1 and Table I-9.1 of the ASME Boiler and Pressure Vessel Code<sup>9</sup>, the fatigue allowable alternating stress intensity amplitude,  $S_a$ , for 5,000 cycles is 76,000 psi. This value, when multiplied by the ratio of elastic hot NCT modulus at 160 °F (the package wall temperature from Section 2.6.1, *Heat*) to a modulus at 70 °F,  $27.8(10)^6/28.3(10)^6$ , results in a fatigue allowable alternating stress intensity amplitude at 160 °F of 74,657 psi. The non-fatigue allowable stress intensity range, from the ASME Boiler and Pressure Vessel Code, Section III, Division 1, Subsection NB-3222.2, is 60,000 psi ( $3.0S_m$ , where  $S_m$  is 20,000 psi from Table 2.3-1 in Section 2.3, *Mechanical Properties of Materials*, at 160 °F). The alternating stress intensity is one-half of this range, or 30,000 psi. Thus, in the absence of stress concentrations, the fatigue allowable alternating stress intensity will not govern the TRUPACT-II packaging design.

Regions of stress concentrations for the package occur in the ICV and OCV seal flanges and locking rings. The maximum range of primary plus secondary stress intensity occurs between the case of maximum internal pressure under NCT hot conditions (see Section 2.6.1.3, *Stress Calculations*) and the vacuum case. For the seal flanges and locking rings, the maximum primary plus secondary stress intensity of  $30,810 + 2,688 = 33,498$  psi occurs in the upper seal flange (see Table 2.6-1 and Table 2.6-4 for OCA Load Cases 1 and 4, respectively). The stress range is therefore 33,498 psi.

In accordance with Paragraph C.3 of Regulatory Guide 7.6, a stress concentration factor of four will conservatively be applied to the value of maximum stress intensity from above. The resultant range of peak stress intensity, correcting the modulus of elasticity for temperature, becomes:

$$S_{\text{range}} = (33,498)(4) \left( \frac{28.3(10)^6}{27.8(10)^6} \right) = 136,400 \text{ psi}$$

where the modulus of elasticity at 70 °F is  $28.3(10)^6$  psi, and the modulus of elasticity at 160 °F is  $27.8(10)^6$  psi, both from Table 2.3-1 in Section 2.3, *Mechanical Properties of Materials*. The alternating stress intensity is one-half of this range, or:

$$S_{\text{alt}} = \left( \frac{1}{2} \right) 136,400 = 68,200 \text{ psi}$$

From Figure I-9.2.1 and Table I-9.1 of the ASME Boiler and Pressure Vessel Code, the allowable number of cycles for an alternating stress intensity amplitude of 68,200 psi is 7,740, or 55% more than the 5,000 cycles conservatively considered herein.

#### 2.1.2.2.2 Normal Vibration Over the Road

Fatigue associated with normal vibration over the road is addressed in Section 2.6.5, *Vibration*.

<sup>9</sup>American Society of Mechanical Engineers (ASME) Boiler and Pressure Vessel Code, Section III, *Rules for Construction of Nuclear Power Plant Components*, Appendix I, *Design Stress Intensity Values, Allowable Stresses, Material Properties, and Design Fatigue Curves*, 1986 Edition.

### 2.1.2.2.3 Extreme Total Stress Intensity Range

Per paragraph C.7 of Regulatory Guide 7.6:

The extreme total stress intensity range (including stress concentrations) between the initial state, the fabrication state, the normal operating conditions, and the accident conditions should be less than twice the adjusted value (adjusted to account for modulus of elasticity at the highest temperature) of  $S_a$  at 10 cycles given by the appropriate design fatigue curves.

Since the response of the TRUPACT-II package to accident conditions is typically evaluated empirically rather than analytically, the extreme total stress intensity range has not been quantified. However, full scale certification test units (see Appendix 2.10.3, *Certification Tests*) were tested at relatively low ambient temperatures during free drop and puncture testing, as well as exposure to fully engulfing pool fire events. The CTUs were also fabricated in accordance with the drawings in Appendix 1.3.1, *Packaging General Arrangement Drawings*, thus incurring prototypic fabrication induced stresses, increased internal pressure equal to 150% of MNOP during fabrication pressure testing, and reduced internal pressure (i.e., a full vacuum during leak testing) conditions as part of initial acceptance. Exposure to these extreme conditions while demonstrating leaktight containment resulting from certification testing satisfies the intent of the previously defined extreme total stress intensity range requirement.

### 2.1.2.2.3 Buckling Assessment

Buckling, per Regulatory Guide 7.6, is an unacceptable failure mode for the ICV. The intent of this provision is to preclude large deformations that would compromise the validity of linear analysis assumptions and quasi-linear stress allowables, as given in Paragraph C.6 of Regulatory Guide 7.6.

Buckling prevention criteria is applicable to the ICV containment boundary within the TRUPACT-II packaging. For conservatism, the criteria is also applied to the OCV confinement boundary. Shells for both vessels incorporate cylindrical midsections with torispherical heads at each end. The different geometric regions are considered separately to demonstrate that buckling will not occur for the two vessels. The methodology of ASME Boiler and Pressure Vessel Code Case N-284<sup>10</sup> is applied for the cylindrical regions of the containment and confinement vessels (buckling analysis details are provided in Section 2.7.6, *Immersion – All Packages*). The methodology of the ASME Boiler and Pressure Vessel Code, Section III, Subsection NE, is applied for the torispherical heads.

Consistent with Regulatory Guide 7.6 philosophy, factors of safety corresponding to ASME Boiler and Pressure Vessel Code, Level A and Level D service conditions are employed for NCT and HAC loadings, respectively, with factors of safety of 2.00 and 1.34, respectively.

It is also noted that 30-foot drop tests performed on full scale models with the package in various orientations produced no evidence of buckling of any of the ICV and OCV shells (see Appendix 2.10.3, *Certification Tests*). Certification testing does not provide a specific determination of the margin of safety against buckling, but is considered as evidence that buckling will not occur.

---

<sup>10</sup> American Society of Mechanical Engineers (ASME) Boiler and Pressure Vessel Code, Section III, *Rules for Construction of Nuclear Power Plant Components*, Division I, Class MC, Code Case N-284, *Metal Containment Shell Buckling Design Methods*, August 25, 1980 approval date.

**Table 2.1-1 – Containment Structure Allowable Stress Limits**

Stress Category	NCT	HAC
General Primary Membrane Stress Intensity	$S_m$	Lesser of: $2.4S_m$ $0.7S_u$
Local Primary Membrane Stress Intensity	$1.5S_m$	Lesser of: $3.6S_m$ $S_u$
Primary Membrane + Bending Stress Intensity	$1.5S_m$	Lesser of: $3.6S_m$ $S_u$
Range of Primary + Secondary Stress Intensity	$3.0S_m$	N/A
Pure Shear Stress	$0.6S_m$	$0.42S_u$
Peak	Per Section 2.1.2.2.2, <i>Fatigue Assessment</i>	
Buckling	Per Section 2.1.2.2.3, <i>Buckling Assessment</i>	

**Table 2.1-2 – Non-Containment Structure Allowable Stress Limits**

Stress Category	NCT	HAC
General Primary Membrane Stress Intensity	Greater of: $S_m$ $S_y$	$0.7S_u$
Local Primary Membrane Stress Intensity	Greater of: $1.5S_m$ $S_y$	$S_u$
Primary Membrane + Bending Stress Intensity	Greater of: $1.5S_m$ $S_y$	$S_u$
Range of Primary + Secondary Stress Intensity	Greater of: $3.0S_m$ $S_y$	N/A
Pure Shear Stress	Greater of: $0.6S_m$ $0.6S_y$	$0.42S_u$
Peak	Per Section 2.1.2.2.2, <i>Fatigue Assessment</i>	
Buckling	Per Section 2.1.2.2.3, <i>Buckling Assessment</i>	

This page intentionally left blank.

## 2.2 Weights and Centers of Gravity

The maximum gross weight of a TRUPACT-II package, including a maximum payload weight of 7,265 pounds, is 19,250 pounds. The maximum vertical center of gravity (CG) is located 59.0 inches above the bottom surface of the package for a fully loaded package. A conservative value of 60 inches is used in the lifting and tie-down calculations presented in Section 2.5, *Lifting and Tie-down Standards for All Packages*. These results are based on an assumption of a payload configuration consisting of uniformly loaded drums, standard waste boxes (SWBs), or a ten-drum overpack (TDOP). All other payload configurations result in a lower, package gross weight and CG than the uniformly loaded drum, SWB, or TDOP configurations. With reference to Figure 2.2-1, a detailed breakdown of the TRUPACT-II package component weights and CG is summarized in Table 2.2-1.

### 2.2.1 Effect of a Radial Payload Imbalance

A radial offset of the CG occurs when the individual payload containers do not have the same weight. The maximum offset of the radial CG is calculated in the following paragraphs.

#### Fourteen 55-Gallon Drum Payload Configuration:

The worst case CG offset occurs for an arrangement of four minimum weight (empty) 55-gallon drums, each having a weight of 60 pounds, together with three maximum weight (fully loaded) 55-gallon drums, each having a weight of 1,000 pounds, located in adjacent outside positions, as illustrated in Figure 2.2-2. A 55-gallon drum has a nominal outer diameter of 24 inches. For this case, the worst case radial location of the payload CG is:

$$\bar{r} = \frac{(24.0)(1,000) + 2(12.0)(1,000) + (0.0)(60) - 2(12.0)(60) - (24.0)(60)}{3(1,000) + 4(60)} = 13.93 \text{ inches}$$

The pipe overpack and criticality control overpack payload configurations, since they are enclosed and centered by dunnage within a 55-gallon drum, are enveloped by the foregoing considerations. For an empty package weight of 11,985 pounds, and a payload pallet weight of 350 pounds (see Table 2.2-1), the worst case radial offset of the CG of the entire TRUPACT-II package is:

$$\bar{R} = \frac{(13.93)(2)[3(1,000) + 4(60)]}{11,985 + 350 + 2[3(1,000) + 4(60)]} = 4.80 \text{ inches}$$

This radial offset equates to only 5.1% of the TRUPACT-II package's outer diameter of 94 $\frac{3}{8}$  inches. The effect of this relatively small radial offset may be neglected.

#### Eight 85-Gallon Drum Payload Configuration:

The term "85-gallon drum" refers to drum overpacks of 75 to 88 gallons, as discussed in Section 1.1, *Introduction*. The worst case CG offset occurs for an arrangement of two minimum weight (empty), tall 85-gallon drums, each having a weight of approximately 81 pounds, together with two maximum weight (fully loaded), tall 85-gallon drums, each having a weight of 1,000 pounds, located adjacent, as illustrated in Figure 2.2-3. A tall 85-gallon drum has a nominal outer diameter of 28 $\frac{5}{8}$  inches. For this case, the worst case radial location of the payload CG is:

$$\bar{r} = \frac{2(14.31)(1,000) - 2(14.31)(81)}{2(1,000) + 2(81)} = 12.17 \text{ inches}$$

For an empty package weight of 11,985 pounds, and a payload pallet weight of 350 pounds (see Table 2.2-1), the worst case radial offset of the CG of the entire TRUPACT-II package is:

$$\bar{R} = \frac{(12.17)(2)[2(1,000) + 2(81)]}{11,985 + 350 + 2[2(1,000) + 2(81)]} = 3.16 \text{ inches}$$

This radial offset equates to only 3.3% of the TRUPACT-II package's outer diameter of 94 $\frac{3}{8}$  inches. The effect of this relatively small radial offset may be neglected

#### **Six 100-Gallon Drum Payload Configuration:**

The worst case CG offset occurs for an arrangement of two minimum weight (empty), 100-gallon drums, each having a weight of 95 pounds, together with one maximum weight (fully loaded), 100-gallon drum of 1,000 pounds, as illustrated in Figure 2.2-4. A 100-gallon drum has a nominal outer diameter of 32 inches. For this case, the worst case radial location of the payload CG is:

$$\bar{r} = \frac{(18.48)(1,000) - 2(9.24)(95)}{1,000 + 2(95)} = 14.05 \text{ inches}$$

For an empty package weight of 11,985 pounds, and a payload pallet weight of 350 pounds (see Table 2.2-1), the worst case radial offset of the CG of the entire TRUPACT-II package is:

$$\bar{R} = \frac{(14.05)(2)[1,000 + 2(95)]}{11,985 + 350 + 2[1,000 + 2(95)]} = 2.27 \text{ inches}$$

This radial offset equates to only 2.4% of the TRUPACT-II package's outer diameter of 94 $\frac{3}{8}$  inches. The effect of this relatively small radial offset may be neglected.

#### **Two Standard Waste Box (SWB) Payload Configuration:**

For the maximum payload weight of 7,265 pounds, the maximum weight of a single loaded SWB is 7,265/2 = 3,633 pounds, where the weight of an empty SWB is 640 pounds. Therefore, the maximum weight of the contents is 3,633 - 640 = 2,993 pounds. The CG of the contents is conservatively located at a distance of 17.75 inches from the geometric center (i.e., one-quarter the SWB length), as illustrated in Figure 2.2-5. For this case, the worst case radial location of the payload CG is:

$$\bar{r} = \frac{(17.75)(2,993)}{3,633} = 14.6 \text{ inches}$$

For an empty package weight of 11,985 pounds (see Table 2.2-1), the worst case radial offset of the CG of the entire TRUPACT-II package is:

$$\bar{R} = \frac{(14.6)(7,265)}{11,985 + 7,265} = 5.51 \text{ inches}$$

This radial offset equates to only 5.8% of the TRUPACT-II package's outer diameter of 94 $\frac{3}{8}$  inches. As before, the effect of this relatively small radial offset may be neglected.

### One Ten-Drum Overpack (TDOP) Payload Configuration:

For the maximum payload weight of 6,700 pounds, the weight of an empty TDOP is 1,700 pounds. Therefore, the maximum weight of the contents is  $6,700 - 1,700 = 5,000$  pounds. Conservatively assume the CG of the contents is located at a distance of 18 inches from the geometric center (i.e., one-quarter the TDOP diameter), as illustrated in Figure 2.2-6. For this case, the worst-case radial location of the payload CG is:

$$\bar{r} = \frac{(18)(5,000)}{6,700} = 13.4 \text{ inches}$$

For an empty package weight of 11,985 pounds (see Table 2.2-1), the worst case radial offset of the CG of the entire TRUPACT-II package is:

$$\bar{R} = \frac{(13.4)(6,700)}{11,985 + 6,700} = 4.80 \text{ inches}$$

This radial offset equates to only 5.1% of the TRUPACT-II package's outer diameter of 94 $\frac{3}{8}$  inches. As before, the effect of this relatively small radial offset may be neglected.

### 2.2.2 Effect of an Axial Payload Imbalance

The maximum height of the package CG is associated with a uniformly loaded payload, where the CG of the payload containers is located at their mid-height. Due to a payload of non-uniform density or possible settling of the payload contents, the CG height of the payload containers may decrease somewhat. The fourteen 55-gallon drum payload configuration, since it is the heaviest payload, will result in greatest potential shift in axial CG. The greatest shift in location of the CG of an individual drum is bounded by one-quarter of the drum height, i.e., a shift from the drum mid-height to the quarter height. Thus, for a total 55-gallon drum height of 35 inches, the drum centerline is  $35/2 = 17.50$  inches below the nominal centerline for all 14 drums and the axial shift is  $35/4 = 8.75$  inches downward from the drum centerline. Since the empty weight of a 55-gallon drum is 60 pounds, the maximum contents weight for one drum is  $1,000 - 60 = 940$  pounds. The greatest downward shift in CG location of the TRUPACT-II packaging, assuming all seven drums in the upper layer are empty and the CG location of all seven maximally loaded drums in the lower layer is at one quarter of the drum height instead of at mid-height, is:

$$\bar{H} = \frac{7(17.50 + 8.75)(940)}{19,250} = 8.97 \text{ inches}$$

The axial offset amounts to only 7.4% of the total TRUPACT-II package height of 121 $\frac{1}{2}$  inches. The effect of this relatively small axial offset may be neglected. As an example, in the case of a hypothetical accident condition (HAC) puncture event where the puncture bar axis passes through the CG of the TRUPACT-II package, the variation in CG location of 9 inches is the same order of magnitude as the puncture bar diameter resulting in a variation of the puncture bar orientation of  $\text{TAN}^{-1}[59.00/1/2(94.375)] - \text{TAN}^{-1}[(59.00 - 8.97)/1/2(94.375)] = 4.7^\circ$ . In addition, vertical reduction of the CG would have no effect on lifting forces, and would serve to reduce tie-down forces. Therefore, the lifting and tie-down calculations, and the HAC free drop and puncture tests, are performed using a value that bounds the maximum CG height presented in Table 2.2-1, and the downward axial offset is conservatively neglected.

### 2.2.3 Significance of Package Center of Gravity Shifts

The 5.51-inch radial shift and 8.97-inch axial (downward) shift of the package CG associated with worst case non-uniform payload weight distributions are of little consequence for the TRUPACT-II package. The only load cases affected by such shifts are lifting, tie-down, vibration, free drop, and puncture. Each of these cases is discussed below.

#### 2.2.3.1 Lifting

A radial package CG shift will affect the lifting load by increasing the compressive stress in the polyurethane foam directly above the forklift pockets. Per Section 2.5.1, *Lifting Devices*, the compressive stress in the polyurethane foam was determined to be 60 psi with the overall package CG centered between the forklift pockets. With a 49½-inch spacing between the forklift pocket centerlines, a 5.51-inch radial shift in the package CG increases the maximum stress in the polyurethane foam by a factor of:

$$f = \frac{49.5/2 + 5.51}{49.5/2} = 1.22$$

Using the polyurethane foam allowable crush strength of 100 psi per Section 2.5.1, *Lifting Devices*, the design margin becomes:

$$\frac{100}{1.22(60)} - 1 = +0.37$$

An axial package CG shift will have no effect on the lifting load cases since all lifting loads are applied along the axis of the package.

#### 2.2.3.2 Tie-down

A radial package CG shift results in a slight increase in the vertical loads acting on the tie-down hardware since the four (4) tie-down locations no longer uniformly react the applied, vertical 2g tie-down load. With a 58.93-inch lateral distance between tie-down lugs, a 5.51-inch radial CG shift results in a maximum tie-down reaction load due to the vertical 2g tie-down load of:

$$F = \left(\frac{1}{2}\right) \left[ \frac{2(19,250)(58.93/2 + 5.51)}{58.93} \right] = 11,425 \text{ lb}$$

or 1,800 pounds greater than the 9,625 pounds previously calculated in Section 2.5.2.1, *Tie-down Forces*. When added to the combined lateral and longitudinal tie-down load of 84,906 pounds from Section 2.5.2.1, *Tie-down Forces*, the maximum vertical tensile force on any single tie-down lug is 84,906 + 11,425 = 96,331 pounds, again 1,800 pounds greater than the 94,531 pounds previously calculated. This 1.9% increase in the tie-down force reduces the minimum design margin from +0.31 to +0.29.

An axial package CG shift is always downward, thus reducing the overturning moment resulting from the lateral and longitudinal tie-down loads. A reduction in overturning moment has the beneficial effect of directly reducing the vertical loads acting on the tie-down hardware.

### 2.2.3.3 Vibration

The vibration evaluation per Section 2.6.5, *Vibration*, utilized results available from the tie-down analysis to arrive at peak vibratory stress magnitudes. Repeating the Section 2.6.5, *Vibration*, calculations with the 11,425 pound vertical load determined in Section 2.2.3.2, *Tie-down*, in place of the previously used 9,625 pound load results in a maximum alternating stress intensity of 745 psi (as compared to the previous value of 628 psi per Section 2.6.5.2, *Calculation of Alternating Stresses*). Thus, the maximum alternating stress becomes 12,662 psi (as compared to the previous value of 11,726 psi per Section 2.6.5.2, *Calculation of Alternating Stresses*). With an allowable of 13,360 psi per Section 2.6.5.3, *Stress Limits and Results*, and the margin of safety becomes:

$$MS = \frac{S_a}{S_{alt}} - 1 = \frac{13,360}{12,662} - 1 = +0.06$$

### 2.2.3.4 Free Drop and Puncture

The free drop and puncture load conditions have been addressed by an extensive test program that utilized four full-scale TRUPACT-II package prototypes. For all test units, the payload weight was uniformly distributed within the payload cavity to achieve the highest possible CG for the loaded package. The high CG was selected for testing so that maximum damage to the closure/seal regions would occur.

**Table 2.2-1 – TRUPACT-II Weight and Center of Gravity**

Item	Weight, pounds		Height to CG, inches <sup>Ⓣ</sup>	
	Component	Assembly	Component	Assembly
Outer Confinement Assembly (OCA)		9,365		58.8
• Lid	3,600		97.2	
• Body	5,765		34.8	
Inner Containment Vessel (ICV)		2,620		64.7
• Lid	795		96.4	
• Body	1,625		49.8	
• Aluminum Honeycomb Spacers	200		60.4	
Total Empty Package		11,985		60.1
Payload and Payload Components		7,265		57.3
• Payload (14 55-Gallon Drums)	6,915		59.1	
• Payload Pallet	350		22.5	
Total Loaded Package (Maximum)		19,250		59.0

Notes:

- ① The reference datum is the bottom of the TRUPACT-II package.

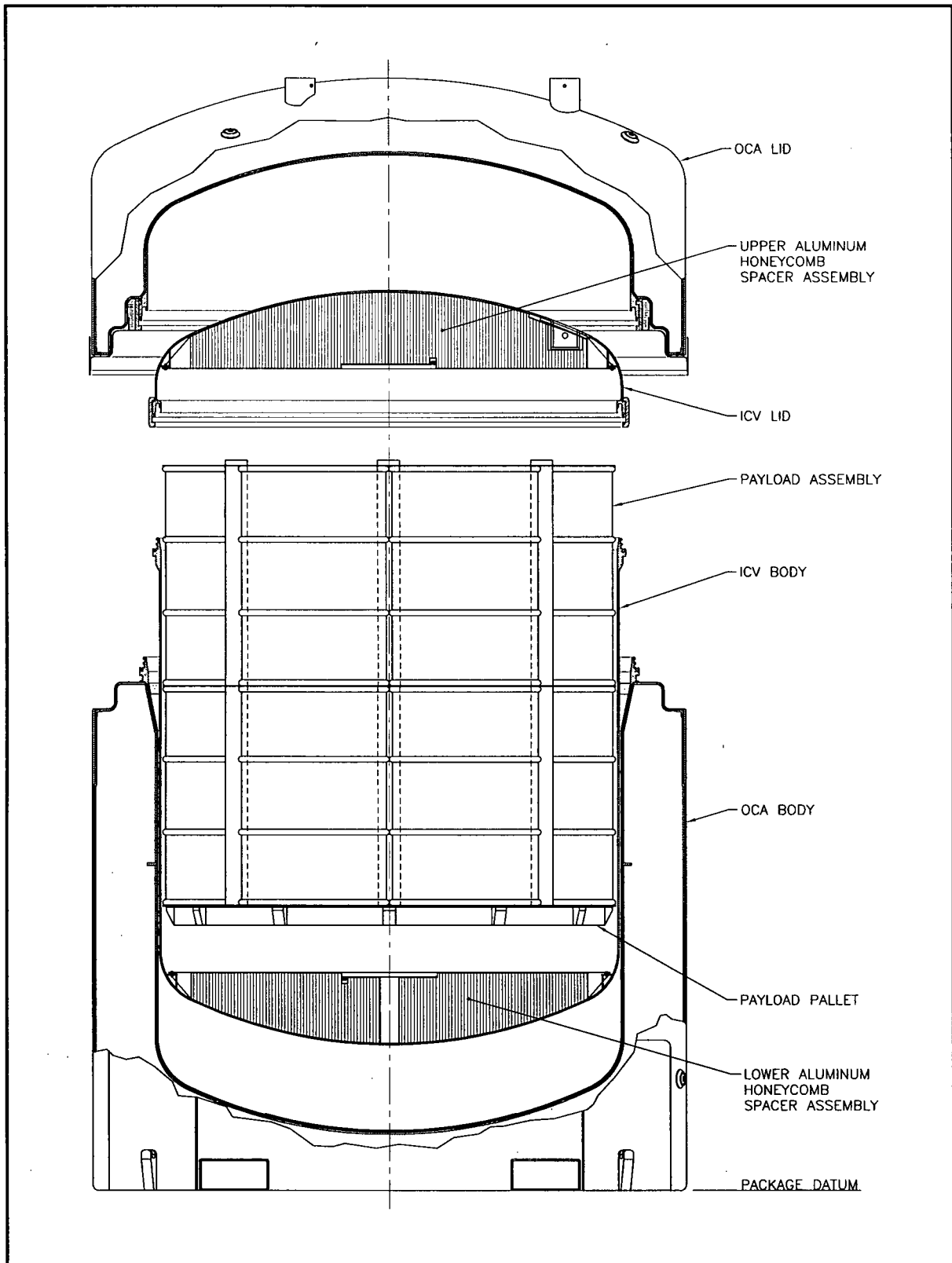


Figure 2.2-1 – TRUPACT-II Package Components

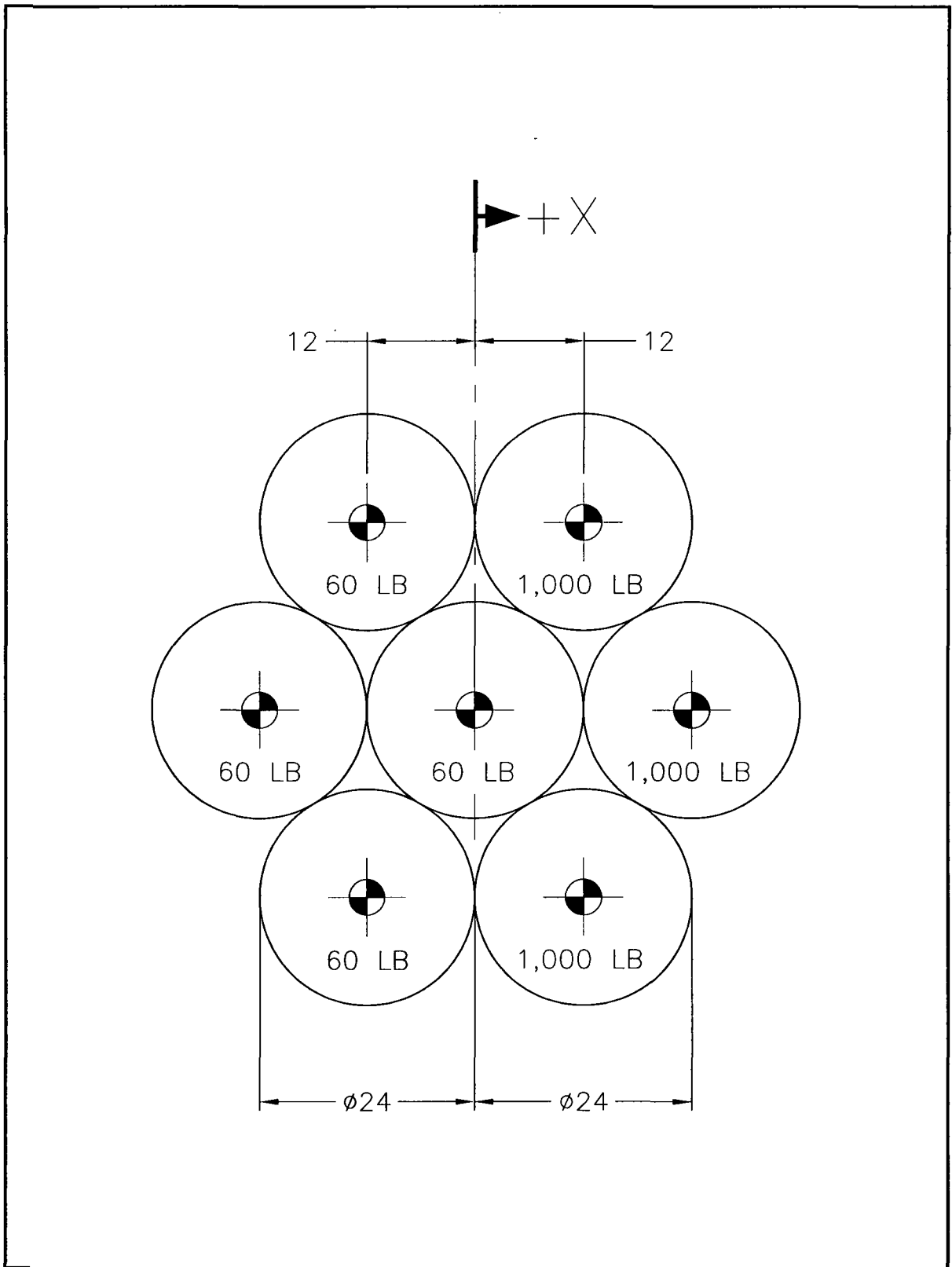


Figure 2.2-2 – Radial CG Shift for a 14 55-Gallon Drum Payload

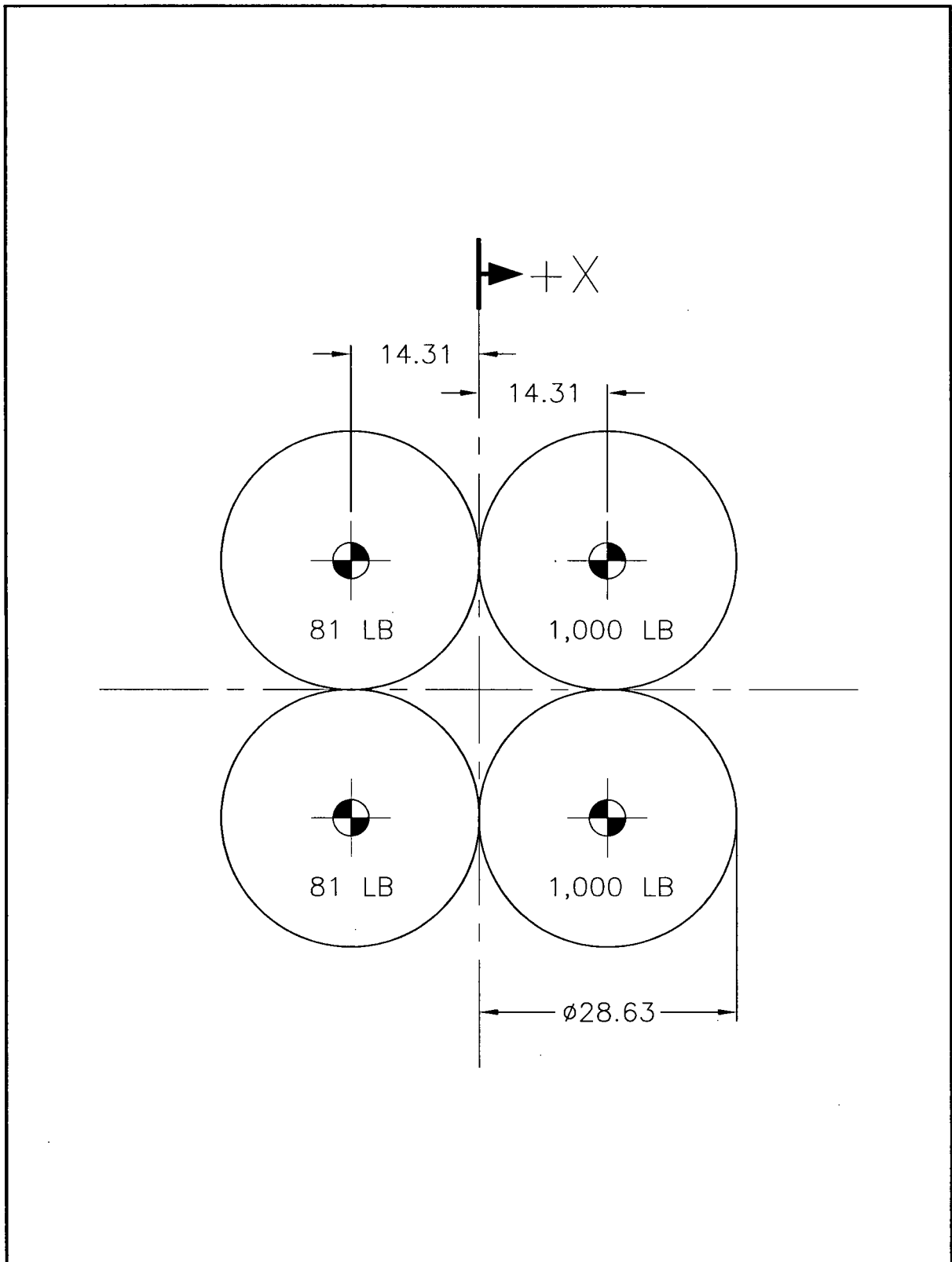


Figure 2.2-3 – Radial Shift of CG for Eight 85-Gallon Drum Payload

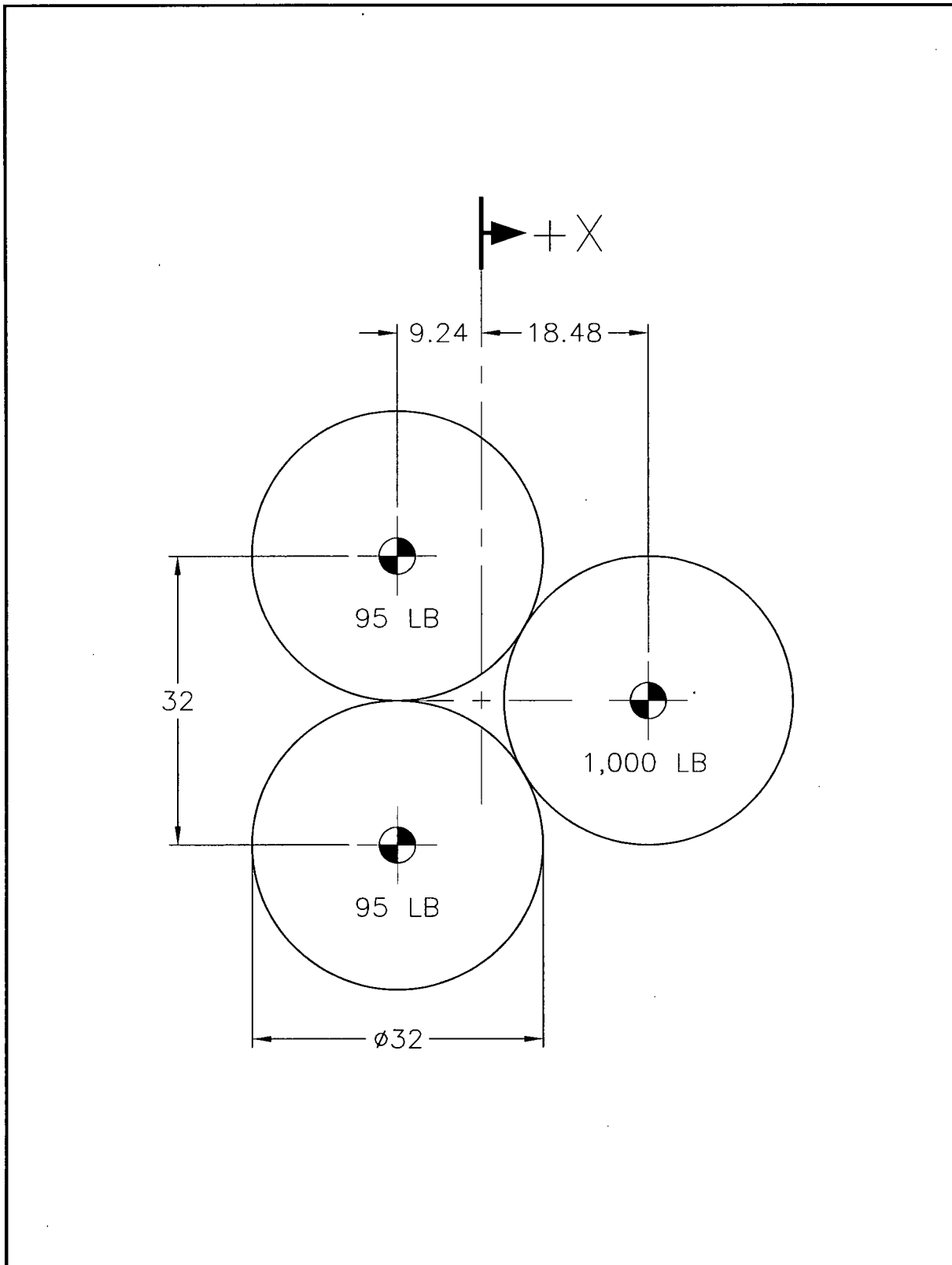


Figure 2.2-4 – Radial Shift of CG for Six 100-Gallon Drum Payload

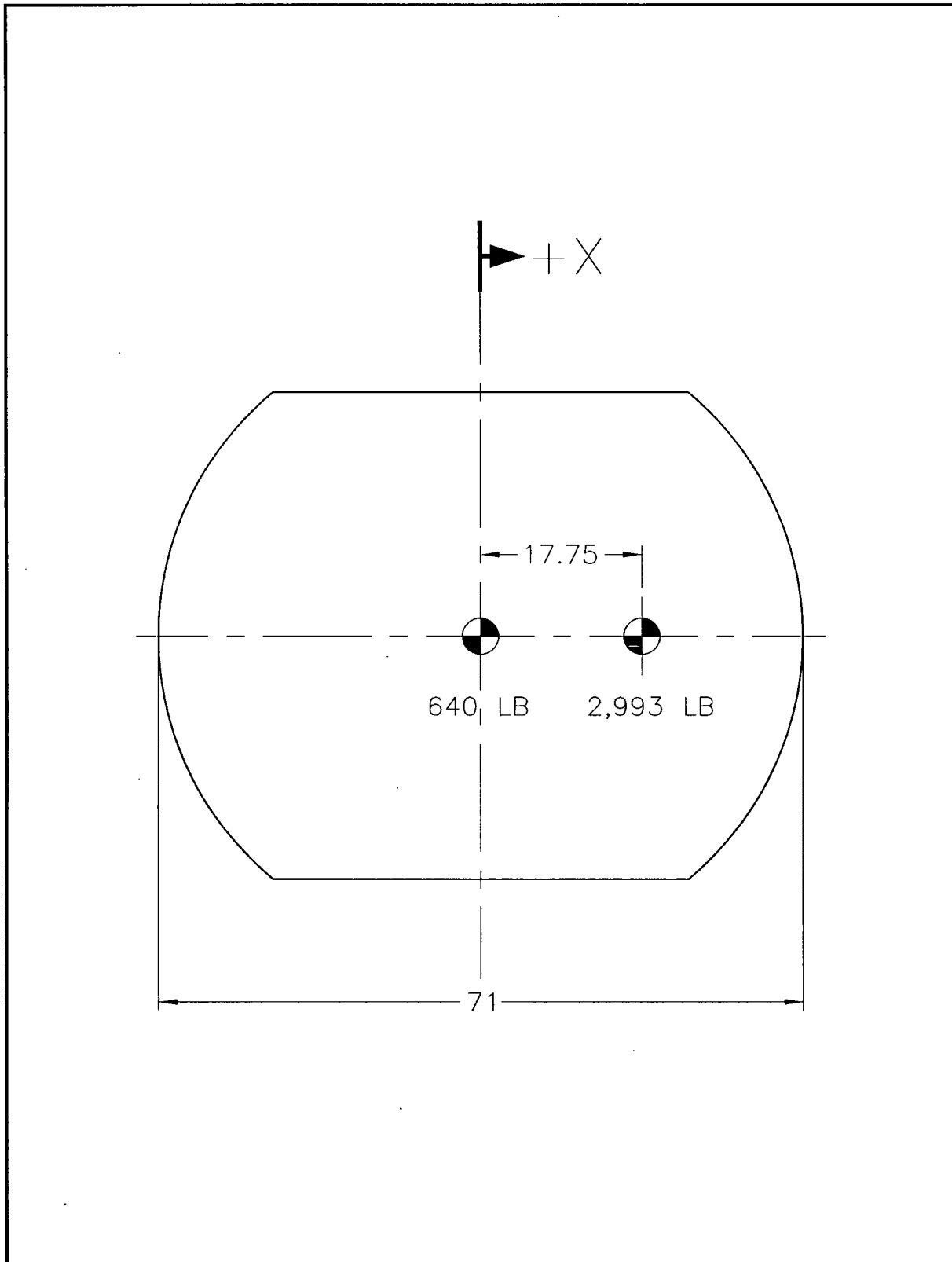


Figure 2.2-5 – Radial Shift of CG for SWB Payload

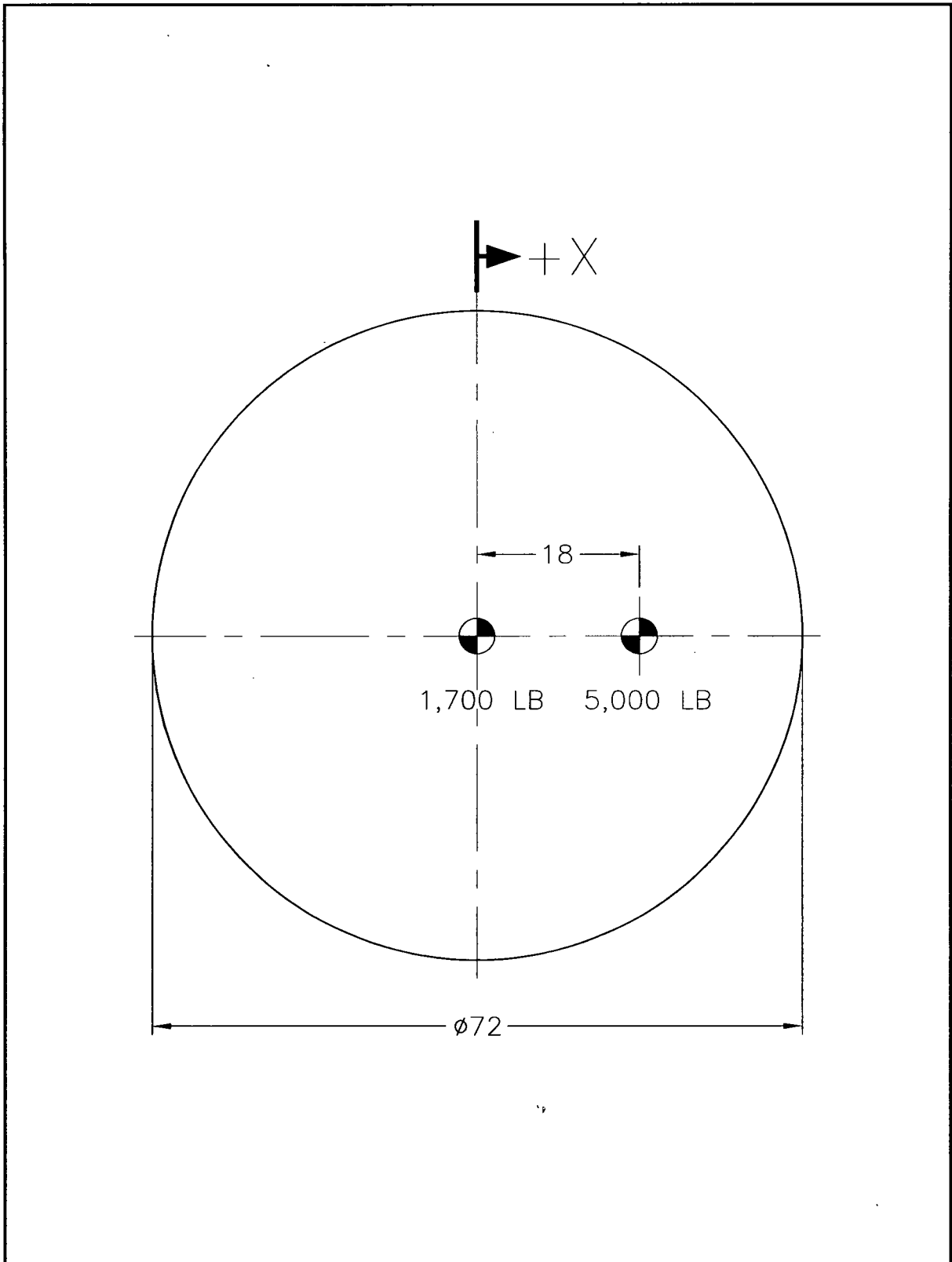


Figure 2.2-6 – Radial Shift of CG for TDOP Payload

## 2.3 Mechanical Properties of Materials

The major structural components, i.e., the outer confinement assembly (OCA) outer shells, outer confinement vessel (OCV), and inner containment vessel (ICV), of the TRUPACT-II packaging are fabricated of Type 304, austenitic stainless steel and  $8\frac{1}{4}$  lb/ft<sup>3</sup> (nominal density) polyurethane foam. Other materials performing a structural function are ASTM B16 brass (for the ICV and OCV vent port and seal test port plugs and covers), aluminum honeycomb (for the ICV aluminum honeycomb spacer assemblies), 300 series stainless steel (for the ICV and OCV locking ring lock bolts, and for attaching the locking Z-flange to the OCV locking ring), and ASTM A564, Type 630, stainless steel (joint pins for the OCV and ICV locking rings). Several varieties of non-structural materials are also utilized. Representative non-structural materials include butyl rubber and other elastomeric O-ring seals, a silicone wear pad, aluminum guide tubes for the OCA lid lift operation, ceramic fiber paper, fiberglass insulation, and plastic fire consumable foam cavity vent plugs. The drawings presented in Appendix 1.3.1, *Packaging General Arrangement Drawings*, delineate the specific material(s) used for each TRUPACT-II packaging component.

The remainder of this section presents and discusses pertinent mechanical properties for the materials that perform a structural function. Section 2.3.1, *Mechanical Properties Applied to Analytic Evaluations*, presents all properties used in analytic structural evaluations of the TRUPACT-II package. Most normal conditions of transport (NCT) tests are demonstrated analytically. Section 2.3.2, *Mechanical Properties Applied to Certification Testing*, presents the mechanical properties associated with components whose performance is demonstrated via certification testing. With the exception of immersion, all hypothetical accident condition (HAC) tests are demonstrated via certification testing.

### 2.3.1 Mechanical Properties Applied to Analytic Evaluations

Analytic evaluations are performed for the basic OCA, OCV, and ICV shells, seal flanges, and locking rings, comprised of Type 304 stainless steel. Table 2.3-1 presents the mechanical properties for the Type 304 stainless steel used in the TRUPACT-II packaging. Each of the mechanical properties of Type 304 stainless steel is taken from Section III of the ASME Boiler and Pressure Vessel Code<sup>1</sup>.

All analyses of the basic OCA, OCV, and ICV shells, seal flanges and locking rings utilize the properties presented for ASTM A240, Type 304, stainless steel. With the exception of elongation, which is not specifically used in the linear elastic analytic assessments, all materials presented in Table 2.3-1 exhibit equivalent or better properties than the ASTM A240 material. Minimum elongation values are important regarding testing and are therefore discussed in Section 2.3.2, *Mechanical Properties Applied to Certification Testing*. The density of stainless steel is taken as 0.29 lb/in<sup>3</sup>, and Poisson's Ratio is 0.3.

Unlike the other ASTM materials specified in Table 2.3-1, ASTM A276 material does not have an identical ASME material specification. However, structural use of ASTM A276 is as an option for the OCA rolled angles used at the lid-to-body interface, the OCV stiffening ring, and

---

<sup>1</sup> American Society of Mechanical Engineers (ASME) Boiler and Pressure Vessel Code, Section III, *Rules for Construction of Nuclear Power Plant Components*, 1986 Edition.

the OCA lid lifting straps. As these components are not part of the containment boundary, the use of ASTM A276, whose chemical and mechanical properties are identical to ASTM A479, is justified. Thus, material properties of ASTM A276 versus temperature are taken to be the same as for ASTM A479.

The analytic assessments of the polyurethane foam used in the TRUPACT-II packaging are limited to the NCT internal pressure, differential thermal expansion, and lifting load cases. The data summarized in Table 2.3-2 are established according to the procedures outlined in Section 8.1.4.1, *Polyurethane Foam*. Detailed stress-strain relationships for the polyurethane foam are not required for analysis since analytic assessments for the NCT or HAC free drop or puncture events are not performed. However, as discussed in Section 2.3.2, *Mechanical Properties Applied to Certification Testing*, since TRUPACT-II package performance is demonstrated by certification testing, and performance is a function of foam properties, compressive stress-strain characteristics and installation techniques are carefully controlled.

Material properties are linearly interpolated between, or, if necessary, extrapolated beyond the temperature values shown. For example, when a temperature outside a tabulated range is of interest (e.g., low temperature properties to -40 °F), data are extrapolated. When a particular analysis requires data extrapolation, it is identified within the applicable section of this chapter.

### 2.3.2 Mechanical Properties Applied to Certification Testing

The primary means of demonstrating the structural performance capabilities of the TRUPACT-II packaging under imposed NCT and HAC free drops, puncture, and thermal (fire) events is via certification testing. The overall response of the TRUPACT-II packaging to these events is dependent on the characteristics of several structural components. The characteristics of the polyurethane foam used in the OCA are of primary importance regarding TRUPACT-II package performance. For this reason, the method of installation of the foam material into the OCA, and the foam's compressive stress-strain characteristics are carefully controlled and monitored. Section 8.1.4.1, *Polyurethane Foam*, presents the details associated with foam installation and performance testing. Importantly, all TRUPACT-II packages will respond similarly to free drop, puncture, and thermal events. Thermal performance of the foam is discussed in Section 3.2. *Summary of Thermal Properties of Materials*.

At the time of polyurethane foam installation, test samples are retained from each foam pour, as discussed in Section 8.1.4.1, *Polyurethane Foam*. Using these samples, each foam pour is tested for compressive strength at strains of 10%, 40%, and 70%, both parallel and perpendicular to the direction of foam rise. To be acceptable, the average compressive strength of all tested samples from a single foamed component (i.e., the OCA lid or OCA body) for a particular rise direction is to fall within  $\pm 15\%$  of the corresponding nominal compressive stress. Additionally, the stress value of any single test specimen from a single pour is to fall within  $\pm 20\%$  of the corresponding nominal compressive stress.

In addition to controls on foam compressive stress, OCA foam thicknesses are controlled by the tolerances shown on the drawings provided in Appendix 1.3.1, *Packaging General Arrangement Drawings*. The foam thickness tolerance at the OCA top and sides is set at approximately  $\pm 5\%$  of the nominal thickness. In regions where foam strains are very small (e.g., bottom end), a slightly greater thickness tolerance (approximately  $\pm 8\%$ ) is allowed. The thickness tolerance is set at approximately one-third the magnitude of the compressive stress tolerance to minimize the

effect on package performance in the unlikely event that both tolerances are simultaneously at their extreme values in a given TRUPACT-II packaging assembly. Importantly, in the unlikely event that compressive stress and thickness tolerances are simultaneously at their worst case extremes, the net effect of combining the two tolerances is nearly identical to the compressive stress tolerance acting alone. This is directly attributable to the fact that a long portion of the compressive stress-strain curve for foam (at strains of ~50% or less) exhibits a relatively shallow slope (i.e., "plateau"). Consequently, although small changes in foam thickness directly affect foam strains, small changes in strain while on the plateau portion of the stress-strain curve do not significantly affect stress. As demonstrated by testing (documented in Appendix 2.10.3, *Certification Tests*), the TRUPACT-II packaging deformations due to 30-foot free drops were relatively small, demonstrating that resultant foam strains remained within the "plateau" portion of the compressive stress-strain curve.

In addition to the polyurethane foam, the performance of other primary TRUPACT-II packaging structural components is addressed by certification testing rather than by analysis. These components include the ASTM B16, Alloy 360, half-hard temper, brass vent port plugs, the ICV upper and lower aluminum honeycomb spacer assemblies, the 300 series stainless steel socket head cap screws used to secure the locking rings in the locked position, the ASTM A564, Type 630, Condition 1150, stainless steel pins used in the locking ring joints, and the 1/4-inch, 300 series stainless steel pan head screws used to attach the locking Z-flange to the OCV locking ring. As indicated above, and on the drawings provided in Appendix 1.3.1, *Packaging General Arrangement Drawings*, each of these components has a specific material callout thereby providing a specific control on its mechanical properties. The structurally significant mechanical properties for these materials are presented in Table 2.3-3.

With the exception of the aluminum honeycomb spacer assemblies, the 1/4-inch stainless steel pan head screws, and the OCV lock bolts, all of the above components remained intact during certification testing, and showed essentially no evidence of distress. By design, the aluminum honeycomb spacer assemblies were partially crushed as a result of the certification test program, but still provided adequate protection for the ICV torispherical heads from the simulated payload of fourteen, rigid, concrete-filled, 55-gallon drums.

Many of the 1/4-inch pan head screws that attach the locking Z-flange to the OCV locking ring (or, in some cases, the Z-flange's sheet metal adjacent to the screws) failed in each of the first two certification test units: 19 of 24 for CTU No. 1, and 20 of 24 for CTU No. 2; the number of failed screws was not noted for CTU No. 3. Although failure of these fasteners does not directly unlatch the 18 interlocking seal flange/locking ring tabs, 36 fasteners are used for TRUPACT-II packaging production units instead of the 24 that were used for each of the test units. Failure of the fasteners for a particular test unit is not likely attributed to a single accident sequence (i.e., a single 30-foot free drop followed by a single, 40-inch puncture event), but rather probably due to the multiple drops that were conservatively performed on each test unit.

The optional use of Type 304 stainless steel forgings or castings instead of ASTM A240 plate material for the OCV and ICV seal flanges and locking rings is stated on the drawings provided in Appendix 1.3.1, *Packaging General Arrangement Drawings*. As shown in Table 2.3-1, the ASTM A182 forging option and ASTM A351 casting option provide equivalent or improved strength, but a somewhat reduced elongation than does the ASTM A240. The reduced elongation values (30% for ASTM A182 and 35% for ASTM A351 versus 40% for ASTM A240 material) are acceptable based on the results of the certification testing program. Relatively little

permanent deformation was observed for the OCV or ICV seal flanges and locking rings as a result of certification testing, indicating that strains were well below the 30% minimum elongation provided by any of the specified materials. Any of the three material options are therefore acceptable for fabricating TRUPACT-II packagings.

**Table 2.3-1 – Mechanical Properties of Type 304 Stainless Steel Components (for Analysis)**

Material Specification	① Minimum Elongation (%)	Temperature (°F)	② Yield Strength, $S_y$ ( $\times 10^3$ psi)	③ Ultimate Strength, $S_u$ ( $\times 10^3$ psi)	④ Allowable Strength, $S_m$ ( $\times 10^3$ psi)	⑤ Elastic Modulus, $E$ ( $\times 10^6$ psi)	⑥⑦ Thermal Expansion Coefficient, $\alpha$ ( $\times 10^{-6}$ in/in/°F)
ASTM A213	35	70	30.0	75.0	20.0	28.3	8.46
ASTM A240	40	100	30.0	75.0	20.0	-----	8.55
ASTM A312	35	200	25.0	71.0	20.0	27.6	8.79
ASTM A376	35	300	22.5	66.0	20.0	27.0	9.00
ASTM A479	30	400	20.7	64.4	18.7	26.5	9.19
Type 304		500	19.4	63.5	17.5	25.8	9.37
ASTM A182 Type F304 (<5 inch thick)	30	70	30.0	75.0	20.0	28.3	8.46
		100	30.0	75.0	20.0	-----	8.55
		200	25.0	71.0	20.0	27.6	8.79
		300	22.5	66.0	20.0	27.0	9.00
		400	20.7	64.4	18.7	26.5	9.19
500	19.4	63.5	17.5	25.8	9.37		
ASTM A351 Grade CF8A	35	70	35.0	77.0	23.3	28.3	8.46
		100	35.0	77.0	23.3	-----	8.55
		200	29.1	72.8	23.3	27.6	8.79
		300	26.3	67.8	22.6	27.0	9.00
		400	24.2	66.1	21.8	26.5	9.19
500	22.8	65.2	20.5	25.8	9.37		
ASTM A276 <sup>ⓐ</sup>	30	70	30.0	75.0	20.0 <sup>ⓑ</sup>	28.3 <sup>ⓑ</sup>	8.46 <sup>ⓑ</sup>

Notes: ① ASME Code, Section III, Part A, 1986.

② ASME Code, Section III, Table I-2.2, 1986.

③ ASME Code, Section III, Table I-3.2, 1986.

④ ASME Code, Section III, Table I-1.2, 1986.

⑤ ASME Code, Section III, Table I-6.0, 1986.

⑥ ASME Code, Section III, Table I-5.0, 1986.

⑦ Mean from 70 °F.

ⓐ ASTM Standards, A276, Type 304, 1988.

ⓑ ASTM A479 material properties.

This page intentionally left blank.

**Table 2.3-2 – Mechanical Properties of Polyurethane Foam (for Analysis)**

Property	Direction	Nominal Room Temperature Value
Compressive Strength, S	Axial (Parallel-to-Rise)	235 psi
	Radial (Perpendicular-to-Rise)	195 psi
Compressive Modulus, E <sub>c</sub>	Axial (Parallel-to-Rise)	6,810 psi
	Radial (Perpendicular-to-Rise)	4,773 psi
Tensile Modulus, E <sub>t</sub>	Axial (Parallel-to-Rise)	10,767 psi
	Radial (Perpendicular-to-Rise)	6,935 psi
Shear Modulus, E <sub>s</sub>	Axial (Parallel-to-Rise)	1,921 psi
	Radial (Perpendicular-to-Rise)	2,553 psi
Thermal Expansion Coefficient, α	-----	$3.5 \times 10^{-5}$ in/in/°F
Poisson's Ratio, ν	-----	0.33
Density, ρ	-----	8.25 lb/ft <sup>3</sup>

**Table 2.3-3 – Mechanical Properties of Metallic Materials (for Testing)**

Material	Minimum Mechanical Properties (unless otherwise specified)	Notes
ASTM B16, Alloy 360 Brass, Half-Hard Temper	$\sigma_y = 25,000$ psi $\sigma_u = 55,000$ psi	-----
Hexcel ACG-3/8-.003-3.6P Aluminum Honeycomb	$\sigma_{bc} = 340$ psi $\pm 15\%$ (Bare Compressive Strength) $\sigma_c = 120$ psi $\pm 15\%$ (Crush Strength)	①
300 Series Stainless Steel Socket Head Cap Screws	$\sigma_y = 40,000$ psi $\sigma_u = 80,000$ psi	②
ASTM A564, Type 630, Condition 1150, Stainless Steel	$\sigma_y = 105,000$ psi $\sigma_u = 135,000$ psi	③
1/4-inch, 300 Series Stainless Steel Pan Head Screws	$\sigma_y = 30,000$ psi $\sigma_u = 75,000$ psi	④

Notes:

- ① *Mechanical Properties of Hexcel Honeycomb Materials*, TSB-120 (Technical Service Bulletin 120), Hexcel, 1992. The term "Bare Compressive Strength" is defined as the maximum strength that is exhibited by the honeycomb material at the onset of crushing. The term "Crush Strength" is defined as the average compressive strength that is sustained as the honeycomb material undergoes crushing.
- ② UNBRAKO Socket Screw Products Catalog, Copyright 1988, SPS Technologies.
- ③ ASME Boiler and Pressure Vessel Code, Section III, 1986 Edition.
- ④ Industrial Fasteners Institute, *Fastener Standard*, Fifth Edition.

This page intentionally left blank.

## 2.4 General Standards for All Packages

This section defines the general standards for all packages. The TRUPACT-II package, with an outer confinement vessel (OCV) that is integral to an outer confinement assembly (OCA), and an inner containment vessel (ICV) for primary containment, meets all requirements delineated for this section.

### 2.4.1 Minimum Package Size

The minimum transverse dimension (i.e., the diameter) of the TRUPACT-II package is 94 $\frac{3}{8}$  inches, and the minimum longitudinal dimension (i.e., the height) is 121 $\frac{1}{2}$  inches. Thus, the requirement of 10 CFR §71.43(a)<sup>1</sup> is satisfied.

### 2.4.2 Tamper-indicating Feature

Tamper-indicating seals are installed at one OCA lock bolt location and at the OCV vent port access plug, as delineated on the drawings in Appendix 1.3.1, *Packaging General Arrangement Drawings*. A lock wire device is used between two tie-points. For the OCV lock bolt, the tie-points are the bolt head and the locking Z-flange. The two tie-points for the OCV vent port access plug are the plug itself and a bolt tapped and welded to the OCA body outer shell. Failure of either tamper-indicating device provides evidence of possible unauthorized access. Thus, the requirement of 10 CFR §71.43(b) is satisfied.

### 2.4.3 Positive Closure

The TRUPACT-II package cannot be opened unintentionally. Both the OCA and ICV lids are attached to their respective bodies with locking rings. The OCV locking ring is secured with six, 1/2-13UNC, OCA lock bolts through the attached locking Z-flange. Similarly, the ICV locking ring is secured in the locked position with three, 1/2-13UNC, ICV lock bolts. For either lid, the presence of a single, lock bolt will prevent lid removal.

The OCV vent port has three levels of protection against inadvertent opening: 1) the OCV vent port access plug, 2) the OCV vent port cover, and 3) the OCV vent port plug. Each of these components are secured via threaded fittings. The ICV vent port has two levels of protection against inadvertent opening: 1) the ICV vent port cover, and 2) the ICV vent port plug. Thus, the requirements of 10 CFR §71.43(c) are satisfied.

### 2.4.4 Chemical and Galvanic Reactions

The major materials of construction of the TRUPACT-II packaging (i.e., austenitic stainless steel, aluminum, brass, polyurethane foam, ceramic fiber paper, fiberglass insulation, butyl rubber O-ring seals and other elastomeric materials) will not have significant chemical, galvanic or other reactions in air, inert gas or water environments, thereby satisfying the requirements of 10 CFR §71.43(d). These materials have been previously used, without incident, in radioactive material (RAM) packages for transport of similar payload materials. A successful RAM

---

<sup>1</sup> Title 10, Code of Federal Regulations, Part 71 (10 CFR 71), *Packaging and Transportation of Radioactive Material*, 01-01-12 Edition.

packaging history combined with successful use of these fabrication materials in similar industrial environments ensures that the integrity of the TRUPACT-II package will not be compromised by any chemical, galvanic or other reactions. The materials of construction and the payload are further evaluated below for potential reactions.

#### 2.4.4.1 Packaging Materials of Construction

The TRUPACT-II packaging is primarily constructed of Type 304 stainless steel. This material is highly corrosion resistant to most environments. The metallic structure of the TRUPACT-II packaging is composed entirely of this material and compatible 300 series weld material. The weld material and processes have been selected in accordance with the ASME Boiler and Pressure Vessel Code<sup>2</sup> to provide as good or better material properties, including corrosion resistance, as the base material. Since both the base and weld materials are 300 series materials, they have nearly identical electrochemical potential thereby minimizing any galvanic corrosion that could occur.

The stainless steel within the OCA foam cavity is lined with a ceramic fiber paper, composed of alumina silica. This material is nonreactive with either the polyurethane foam or the stainless steel, both dry or in water. The ceramic fiber paper and the silicone adhesive are very low in free chlorides to minimize the potential for stress corrosion of the OCA structure.

The polyurethane foam that is used in the OCA is essentially identical to previously licensed transportation packagings, such as the NuPac 125B (Docket 71-9200), the NuPac 10-142 (71-9208), and the NuPac PAS-1 (Docket 71-9184). All of these packagings have had a long and successful record of performance demonstrating that the polyurethane foam does not cause any adverse conditions with the packaging. The polyurethane foam in the OCA is a rigid, closed-cell (non-water absorbent) foam that is very low in free halogens and chlorides, as discussed in Section 8.1.4.1, *Polyurethane Foam*. The polyurethane foam material cavity is sealed with plastic pipe plugs to preclude the entrance of moisture.

Aluminum honeycomb is used in the TRUPACT-II packaging for the two, ICV aluminum honeycomb spacer assemblies in the upper and lower ICV torispherical heads. Aluminum honeycomb material is used for dunnage only, and is not used as any part of the TRUPACT-II packaging's containment boundary. The aluminum honeycomb is maintained at relatively low temperatures ensuring that no adverse reaction could occur at aluminum/steel interfaces that would compromise the packaging's containment integrity. Of final note, aluminum material is slightly anodic which serves to protect the stainless steel of the ICV.

The various brass fittings and plugs used in the TRUPACT-II packaging are very corrosion resistant. Like aluminum, brass material is slightly anodic to the stainless steel. Any damage that could occur to the brass is easily detectable since the fittings are all handled each time the TRUPACT-II package is loaded and unloaded.

The various elastomers (e.g., butyl rubber, polyester, silicone, etc.) that are used in the O-rings, annulus foam ring, debris shield, wear pad, etc., contain no corrosives that would react adversely affect the TRUPACT-II packaging. These materials are organic in nature and noncorrosive to the stainless steel containment boundary of the TRUPACT-II packaging.

---

<sup>2</sup> American Society of Mechanical Engineers (ASME) Boiler and Pressure Vessel Code, Section III, *Rules for Construction of Nuclear Power Plant Components*, 1986 Edition.

#### 2.4.4.2 Payload Interaction with Packaging Materials of Construction

The materials of construction of the TRUPACT-II packaging are checked for compatibility with the various payload chemistries when the payloads are evaluated for chemical compatibility. All payload materials are in approved payload containers delineated in the CH-TRAMPAC<sup>3</sup>.

The payload is typically further confined within multiple layers of plastic for radiological health purposes. This configuration ensures that the payload material has an insignificant level of contact with the TRUPACT-II packaging materials of construction. However, the evaluation of compatibility is based on complete interaction of payload materials with the packaging.

The design of the TRUPACT-II package is for transport of CH-TRU materials and other authorized payloads that are limited in form to solid or solidified material. Corrosive materials, pressurized containers, explosives, non-radioactive pyrophorics, and liquid volumes greater than 1% are prohibited. These restrictions ensure that the waste in the payload is in a non-reactive form for safe transport in the TRUPACT-II package. For a comprehensive discussion defining acceptable payload properties, see the CH-TRAMPAC.

#### 2.4.5 Valves

Neither the OCV nor the ICV have valves. However, beside their respective lids, the ICV and the OCV each have a vent port penetration into their containment and confinement cavities, respectively. These vent port penetrations are sealed using threaded vent port plugs comprised of brass material. Since the ICV is entirely contained within the OCV during transport, a tamper indicating device is not necessary. Access to the OCV vent port penetration is prevented by a lockwire that secures the OCV vent port access plug, as discussed in Section 2.4.2, *Tamper-indicating Feature*. Thus, the requirements of 10 CFR §71.43(e) are satisfied.

#### 2.4.6 Package Design

As shown in Chapter 2.0, *Structural Evaluation*, Chapter 3.0, *Thermal Evaluation*, Chapter 5.0, *Shielding Evaluation*, and Chapter 6.0, *Criticality Evaluation*, the structural, thermal, shielding, and criticality requirements, respectively, of 10 CFR §71.43(f) are satisfied for the TRUPACT-II package.

#### 2.4.7 External Temperatures

As shown in Table 3.5-1 and Table 3.5-2 from Section 3.5.3, *Package Temperatures*, the maximum accessible surface temperature with maximum internal decay heat load and no insolation is 102 °F. Since the maximum external temperature does not exceed 185 °F, the requirements of 10 CFR §71.43(g) are satisfied.

---

<sup>3</sup> U.S. Department of Energy (DOE), *Contact-Handled Transuranic Waste Authorized Methods for Payload Control* (CH-TRAMPAC), U.S. Department of Energy, Carlsbad Field Office, Carlsbad, New Mexico.

### **2.4.8 Venting**

The TRUPACT-II package does not include any features intended to allow continuous venting during transport. Thus, the requirements of 10 CFR §71.43(h) are satisfied.

## 2.5 Lifting and Tie-down Standards for All Packages

For analysis of the lifting and tie-down components of the TRUPACT-II packaging, material properties from Section 2.3, *Mechanical Properties of Materials*, are taken at a bounding temperature of 160 °F per Section 2.6.1.1, *Summary of Pressures and Temperatures*. The primary structural materials are Type 304 stainless steel, and polyurethane foam that is used in the outer confinement assembly (OCA).

A loaded TRUPACT-II package is only lifted by forklift pockets, located at the bottom of the OCA body. For this case, TRUPACT-II package lifting loads act parallel to the direction of foam rise. The nominal compressive strength of the polyurethane foam, as delineated in Table 2.3-2 from Section 2.3.1, *Mechanical Properties Applied to Analytic Evaluations*, is reduced by 15% to account for manufacturing tolerance; polyurethane foam manufacturing tolerances are discussed in Section 8.1.4.1.2.3.2, *Parallel-to-Rise Compressive Stress*. The nominal compressive strength of the polyurethane foam is further reduced by 25% to account for elevated temperature effects, as discussed in Section 2.6.1.1, *Summary of Pressures and Temperatures*.

Properties of Type 304 stainless steel and polyurethane foam, parallel to the direction of foam rise accounting for manufacturing tolerances and elevated temperature, are summarized below.

Material Property	Value	Reference
<b>Type 304 Stainless Steel at 160 °F</b>		
Elastic Modulus, E	$27.8 \times 10^6$ psi	Table 2.3-1
Yield Strength, $\sigma_y$	27,000 psi	
Shear Stress, equal to $(0.6)\sigma_y$	16,200 psi	
<b>Polyurethane Foam (parallel-to-rise) at 160 °F</b>		
Minimum compressive strength, $\sigma_c$	150 psi	Table 2.3-2
Bearing stress, assumed equal to $(2/3)\sigma_c$	100 psi	

### 2.5.1 Lifting Devices

This section demonstrates that the forklift pockets, the only attachments designed to lift the TRUPACT-II package, are designed with a minimum safety factor of three against yielding, per the requirements of 10 CFR §71.45(a). The lifting devices in the OCA lid are restricted to only lifting the OCA lid, and the lifting devices in the ICV lid are restricted to only lifting an ICV lid or empty ICV. Although these lifting devices are designed with a minimum safety factor of three against yielding, detailed analyses are not specifically included herein since these lifting devices are not intended for lifting a TRUPACT-II package.

When lifting the entire package, the applied lift force without yielding is simply three times the total package weight of 19,250 pounds, as given in Section 2.2, *Weights and Centers of Gravity*.

$$F_L = (3)(19,250) = 57,750 \text{ pounds}$$

The entire package is lifted via two forklift pockets located at the bottom of the OCA. Loads are considered to be concentrated at the forklift pocket interfaces and act parallel to the direction of foam rise. For the purposes of this analysis, the minimum assumed fork width is 8 inches, and the minimum assumed engagement length is 60 inches. The total bearing area for two forks is:

$$A = (2)(8)(60) = 960 \text{ in}^2$$

Assuming the entire lifted load is carried directly into the polyurethane foam, thereby ignoring any beneficial load carrying associated with the presence of the relatively stiff stainless steel forklift pocket and OCA outer shell, the compressive stress is:

$$\sigma_c = \frac{F_L}{A} = \frac{57,750}{960} = 60 \text{ psi}$$

The allowable compressive stress for the polyurethane foam is 100 psi. Therefore, the margin of safety is:

$$MS = \frac{100}{60} - 1 = +0.67$$

## 2.5.2 Tie-down Devices

The TRUPACT-II package is secured to its dedicated semi-trailer at four points, two on each trailer main beam. For railcar shipments, the TRUPACT-II package is secured to an adapter that mimics the trailer's four attachment points. Subsequent use of the term "trailer" or "trailer main beam(s)" encompass the railcar adapter and railcar frame. The attachment is made using trailer tie-down devices that pass over the tie-down lugs located at the bottom of the OCA body. The semi-trailer is also fitted with kick plates at the four tie-down points to provide horizontal restraint (blocking). The tie-down scheme utilized for the TRUPACT-II package is illustrated in Figure 2.5-1 and Figure 2.5-2.

Inertial loads of 10g longitudinally, 5g laterally, and 2g vertically, per 10 CFR §71.45(b)(1), are applied through the TRUPACT-II package center of gravity, conservatively assumed to be 60 inches above the package's base. The horizontal loads of 10g longitudinally and 5g laterally are reacted in compression against the kick plates. The resultant overturning moment is reacted in compression on a trailer main beam and in tension by the four tie-down lugs. The vertical load applied to the center of gravity (2g) is evenly reacted at the four tie-down points, and is assumed to act in the direction (up or down) that maximizes the total tie-down load (i.e., down for the compressive reaction point and up for the tensile reaction points).

### 2.5.2.1 Tie-down Forces

Tensile tie-down points are on a 48.4-inch radius circle (to the center of the tie-down lugs, in line with the tie-down fixture). The compressive reaction point is at the trailer main beam, occurring at the edge of the tie-down lug's doubler plate, a radius of 47.56 inches. A plan view of the tie-down geometry is depicted in Figure 2.5-3, including a corresponding free-body force diagram. If the TRUPACT-II package is treated as a rigid body, the reaction forces may be determined from the following set of equations:

$$F_1L_1 + F_2L_2 + F_3L_3 + F_4L_4 = HF_g$$

$$\frac{F_1}{L_1} = \frac{F_2}{L_2} = \frac{F_3}{L_3} = \frac{F_4}{L_4} = k$$

$$F_1 + F_2 + F_3 + F_4 = F_c$$

where, the height of the package center of gravity above its base,  $H = 60$  inches, the horizontal inertia force,  $F_g = 19,250 \times (10^2 + 5^2)^{1/2} = 215,222$  pounds, and the tie-down lug reaction lengths,  $L_1 = 47.56 - 47.52 = 0.04$  inches,  $L_2 = 47.56 - 21.16 = 26.40$  inches,  $L_3 = 47.56 + 21.16 = 68.72$  inches, and  $L_4 = 47.56 + 47.52 = 95.08$  inches. Solving for  $k$ :

$$k = \frac{HF_g}{L_1^2 + L_2^2 + L_3^2 + L_4^2} = \frac{(60)(215,222)}{(0.04)^2 + (26.40)^2 + (68.72)^2 + (95.08)^2} = 893 \text{ lb/in}$$

Therefore,  $F_1 = k \times L_1 = 36$  pounds,  $F_2 = k \times L_2 = 23,575$  pounds,  $F_3 = k \times L_3 = 61,367$  pounds,  $F_4 = k \times L_4 = 84,906$  pounds, and  $F_c = 169,884$  pounds. The maximum vertical tensile force on any single tie-down lug, including the contribution of the vertical load of  $2g$ , is then found as:

$$F_{t-\max} = 84,906 + \frac{(2g)(19,250)}{4 \text{ lugs}} = 94,531 \text{ pounds}$$

Similarly, the maximum compressive force is found as:

$$F_{c-\max} = 169,884 + \frac{(2g)(19,250)}{4 \text{ lugs}} = 179,509 \text{ pounds}$$

Since the line of action of the combined  $10g$  longitudinal and the  $5g$  lateral accelerations pass almost exactly over the centerline of the kickplate ( $27.6^\circ$  for the kickplate centerline versus  $26.6^\circ$  for the line of action of the force), the total horizontal reaction force is conservatively assumed to be reacted against a single kickplate. This force is given by:

$$F_h = F_g = 215,222 \text{ pounds}$$

### 2.5.2.2 Tie-down Stress Due to a Vertical Tensile Load

Several failure modes are considered for the vertical tensile force on the tie-down lug. Shear failure of the tie-down lug itself is not an issue because the shear area of the lug is much greater than the lug attachment welds. The remaining failure modes, as illustrated in Figure 2.5-4, are:

- (a) Shear and bending failure of the tie-down lug welds (shear + bending loads),
- (b) Tearout of the tie-down lug doubler plate at the lug weld outline,
- (c) Shear failure of the welds attaching the lug doubler plate to the OCA outer shell, and
- (d) Tearout of the OCA outer shell at the doubler outline.

#### 2.5.2.2.1 Failure of the Tie-down Lug Welds Due to Shear and Bending Loads

Figure 2.5-5 presents dimensional details of the tie-down, including an appropriate free-body diagram. The length of the tie-down lug weld along the two sides is 5.49 inches. The arc length of the weld across the top of the lug is 3.38 inches. The groove weld at the bottom is 2.38 inches long. On three sides, the weld is a  $3/8$ -inch fillet over a  $3/8$  inch-groove. The minimum throat

length for this weld is  $0.375/(\sin 45^\circ) = 0.53$  inches. For the 3/8-inch groove weld at the bottom, the minimum throat length is 0.375 inches. Thus, the total shear area for the weld is:

$$A_s = [(2)(5.49) + 3.38](0.53) + (2.38)(0.375) = 8.50 \text{ in}^2$$

The maximum shearing force,  $V$ , is the maximum tensile force,  $F_{t-\max} = 94,531$  pounds from Section 2.5.2.1, *Tie-down Forces*, resulting in a corresponding shear stress of:

$$\tau_v = \frac{V}{A_s} = \frac{94,531}{8.50} = 11,121 \text{ psi}$$

The maximum weld shear stress due to bending is found using the standard beam bending formula, but by treating the weld as a line<sup>1</sup>, or:

$$\tau_B = \frac{Mc}{I}$$

where  $M$  is the moment on weld group,  $c$  is the maximum weld distance from the weld group centroid, and  $I$  is the moment of inertia of weld group. The weld group centroid, relative to the bottom edge of the tie-down lug, is:

$$\bar{y} = \frac{(0.53)(3.38)(6.00) + 2(0.53)(5.49)(5.49/2)}{(0.53)(3.38) + 2(0.53)(5.49) + (0.375)(2.38)} = 3.143 \text{ inches}$$

where the centroid of the arc formed by the weld at the top of the tie-down lug is located 6.00 inches above the base of the lug. For the sides, the contribution to the moment of inertia is:

$$I_s = 2 \left[ \frac{tL^3}{12} + Ad^2 \right] = 2 \left[ \frac{(0.53)(5.49)^3}{12} + (0.53)(5.49) \left( 3.143 - \frac{5.49}{2} \right)^2 \right] = 15.54 \text{ in}^4$$

For the top (arc-shaped) weld, conservatively ignoring the moment of inertia about its own centroid, the contribution to the moment of inertia is:

$$I_t = Ad^2 = (0.53)(3.38)(6.00 - 3.143)^2 = 14.62 \text{ in}^4$$

For the bottom weld, the contribution to the moment of inertia is:

$$I_b = Ad^2 = (0.375)(2.38)(3.143)^2 = 8.82 \text{ in}^4$$

Summing the contributions from each part of the weld group, the total moment of inertia of the weld group, treated as a line, is:

$$I = I_s + I_t + I_b = 15.54 + 14.62 + 8.82 = 38.98 \text{ in}^4$$

The distance from the centroid of the weld group to the extreme fiber is  $c = 3.143$  inches. The line of action for the vertical force is 0.7 inches from the side of the tie-down doubler plate, as illustrated in Figure 2.5-5. Therefore, the shear stress on the weld group due to bending is:

<sup>1</sup> Shigley, *Mechanical Engineering Design*, Third Edition, McGraw-Hill, Inc., 1977, Section 7-4, *Bending in Welded Joints*.

$$\tau_B = \frac{Mc}{I} = \frac{(94,531)(0.7)(3.143)}{38.98} = 5,335 \text{ psi}$$

The maximum shear stress in the tie-down lug weld due to the shear and bending loads is:

$$\tau = \sqrt{\tau_v^2 + \tau_B^2} = \sqrt{(11,121)^2 + (5,335)^2} = 12,334 \text{ psi}$$

The allowable shear stress for the tie-down lug welds is 16,200 psi. Therefore, the margin of safety is:

$$MS = \frac{16,200}{12,334} - 1 = +0.31$$

### 2.5.2.2.2 Tearout of the Tie-down Doubler Plate at the Tie-Down Lug Weld Outline

Assume that a rectangular region equal to  $2.88 + 2 \times 0.375 = 3.63$  inches wide by  $(6.25 + 0.375) = 6.63$  inches high, tears out from the 3/8-inch thick doubler plate. Under the direct shear load of 94,531 pounds, the top edge will be in direct tension while the sides and bottom will be in direct shear. Conservatively assuming the top and sides are all in direct shear, the shear area in the 3/8-inch thick, tie-down doubler plate is:

$$A_p = [3.63 + 2(6.63)](0.375) = 6.33 \text{ in}^2$$

The shear area of the 1.0-inch groove weld attaching the bottom of the doubler plate to the OCA body flat head is:

$$A_w = (3.63)(1.0) = 3.63 \text{ in}^2$$

Thus, the total shear area is:

$$A_s = A_p + A_w = 6.33 + 3.63 = 9.96 \text{ in}^2$$

The maximum shearing force,  $V$ , is the maximum tensile force,  $F_{t-\max} = 94,531$  pounds from Section 2.5.2.1, *Tie-down Forces*, resulting in a corresponding shear stress of:

$$\tau_v = \frac{V}{A_s} = \frac{94,531}{9.96} = 9,491 \text{ psi}$$

The maximum weld shear stress due to bending is found using the standard beam bending formula, but by treating the weld as a line, or:

$$\tau_B = \frac{Mc}{I}$$

where  $M$  is the moment on weld group,  $c$  is the maximum weld distance from the weld group centroid, and  $I$  is the moment of inertia of weld group. The weld group centroid, relative to the bottom edge of the tie-down lug, is:

$$\bar{y} = \frac{(0.375)(3.63)(6.63) + 2(0.375)(6.63)(6.63/2) + (1.0)(3.63)(1.0/2)}{(0.375)(3.63) + 2(0.375)(6.63) + (1.0)(3.63)} = 2.742 \text{ inches}$$

For the sides of the rectangular region, the contribution to the moment of inertia is:

$$I_s = 2 \left[ \frac{L^3 t}{12} + Ad^2 \right] = 2 \left[ \frac{(6.63)^3 (0.375)}{12} + (0.375)(6.63) \left( 2.742 - \frac{6.63}{2} \right)^2 \right] = 19.85 \text{ in}^4$$

For the top of the rectangular region, the contribution to the moment of inertia is:

$$I_t = \frac{Lt^3}{12} + Ad^2 = \frac{(3.63)(0.375)^3}{12} + (0.375)(3.63)(6.63 - 2.742)^2 = 20.59 \text{ in}^4$$

For the bottom groove weld, the contribution to the moment of inertia is:

$$I_b = \frac{Lt^3}{12} + Ad^2 = \frac{(3.63)(1.0)^3}{12} + (1.0)(3.63) \left( 2.742 - \frac{1.0}{2} \right)^2 = 18.55 \text{ in}^4$$

Summing the contributions from each part of the rectangular region, the total moment of inertia of the weld group, treated as a line, is:

$$I = I_s + I_t + I_b = 19.85 + 20.59 + 18.55 = 58.99 \text{ in}^4$$

The distance from the centroid of the rectangular region to the extreme fiber is  $c = 6.63 - 2.742 = 3.888$  inches. The line of action for the vertical force is  $0.7 + 0.375/2 = 0.89$  inches from the center of the tie-down doubler plate. Therefore, the shear stress due to bending is:

$$\tau_B = \frac{Mc}{I} = \frac{(94,531)(0.89)(3.888)}{58.99} = 5,545 \text{ psi}$$

The maximum shear stress in the tie-down doubler plate due to the shear and bending loads is:

$$\tau = \sqrt{\tau_v^2 + \tau_B^2} = \sqrt{(9,491)^2 + (5,545)^2} = 10,992 \text{ psi}$$

The allowable shear stress for the tie-down doubler plate is 16,200 psi. Therefore, the margin of safety is:

$$MS = \frac{16,200}{10,992} - 1 = +0.47$$

### 2.5.2.2.3 Shear Failure of the Tie-down Lug Doubler Plate to OCA Outer Shell Welds

The tie-down lug doubler plate is 24 inches square, and welded to the OCA outer shell on its top and sides with 1/4-inch fillet welds. Although the bottom weld is a groove weld, conservatively assume it acts as a 1/4-inch fillet weld, resulting in a total weld length of 96 inches. In addition, 30, 1½-inch diameter, 1/4-inch fillet welds supplement the peripheral fillet welds, providing an additional  $30 \times \pi(1.5) = 141$  inches of weld. Thus, the total weld length is 237 inches, resulting in a weld shear area of:

$$A_s = (0.25)(\sin 45^\circ)(237) = 41.9 \text{ in}^2$$

The weld shear area is much greater than determined in both previous cases (i.e.,  $A_s = 8.50 \text{ in}^2$  for Section 2.5.2.2.1, *Failure of the Tie-down Lug Welds Due to Shear and Bending Loads*, and  $A_s = 9.96 \text{ in}^2$  for Section 2.5.2.2.2, *Tearout of the Tie-down Doubler Plate at the Tie-Down Lug Weld Outline*). Thus, the weld shear stress for the same vertical load will be correspondingly less. Similarly, a much larger moment of inertia will be determined for a nearly identical bending moment, thereby resulting in a substantially reduced bending stress. In conclusion, by inspection the resulting margin of safety will correspondingly be much greater and does not need to be explicitly determined.

#### 2.5.2.2.4 Tearout of the OCA Outer Shell at the Tie-Down Lug Doubler Plate Outline

A potential failure mode for the tie-down hardware is tearout of the 1/4-inch thick OCA outer shell just outboard of the 24.0 inch square doubler plate. The downward acting force puts the OCA shell adjacent to the top edge of the doubler plate in direct tension. The OCA outer shell immediately adjacent to the sides and bottom edge of the doubler plate is in direct shear.

Assume that the 24- × 24-inch tie-down lug doubler plate tears out from 1/4-inch thick OCA outer shell. Under the direct shear load of 94,531 pounds, the top edge will be in direct tension while the sides and bottom will be in direct shear. Conservatively assuming that all sides are all in direct shear, the shear area in the 1/4-inch thick OCA outer shell is:

$$A_s = 4(24)(0.25) = 24.0 \text{ in}^2$$

Once again, the shell shear area is much greater than determined in both previous cases (i.e.,  $A_s = 8.50 \text{ in}^2$  for Section 2.5.2.2.1, *Failure of the Tie-down Lug Welds Due to Shear and Bending Loads*, and  $A_s = 9.96 \text{ in}^2$  for Section 2.5.2.2.2, *Tearout of the Tie-down Doubler Plate at the Tie-Down Lug Weld Outline*). Thus, the weld shear stress for the same vertical load will be correspondingly less. As before, a much larger moment of inertia will be determined for a nearly identical bending moment, thereby resulting in a substantially reduced bending stress. In conclusion, by inspection the resulting margin of safety will correspondingly be much greater and does not need to be explicitly determined.

#### 2.5.2.3 Tie-down Stress Due to a Vertical Compressive Load

The stresses in the TRUPACT-II package due to a vertical compressive load may be analyzed by two bounding cases. First, the combination of overturning and vertical, 2g inertial compressive loads carried through the OCA outer shell and tie-down lug doubler plate, and second, the 2g inertial compressive load carried entirely by the polyurethane foam.

##### 2.5.2.3.1 Bearing Stress in the OCA Outer Shell and Tie-down Lug Doubler Plate

The vertical compressive tie-down load is carried in bearing against the semi-trailer main beams. Conservatively assume that this load is carried only by the cylindrical portion of the OCA outer shell and doubler that is directly over the trailer main beams and tie-down support structure. With reference to Figure 2.5-3, the arc length,  $s$ , of the OCA that spans the trailer main beams is:

$$s = R \left( \frac{\pi}{180} \right) (\phi_1 - \phi_2) = (47.56) \left( \frac{\pi}{180} \right) \left[ \sin^{-1} \left( \frac{32}{47.56} \right) - \sin^{-1} \left( \frac{18}{47.56} \right) \right] = 16.64 \text{ inches}$$

For an OCA outer shell thickness of 1/4 inch, and a tie-down lug doubler plate thickness of 3/8 inch, the area is:

$$A = (16.64)(0.25 + 0.375) = 10.40 \text{ in}^2$$

Thus, from Section 2.5.2.1, *Tie-down Forces*, the maximum compressive force,  $F_{c-\max} = 179,509$  pounds, and the corresponding compressive stress is:

$$\sigma_c = \frac{F_{c-\max}}{A} = \frac{179,509}{10.40} = 17,260 \text{ psi}$$

The allowable stress for the OCA outer shell and tie-down lug doubler plate is 27,000 psi. Therefore, the margin of safety is:

$$MS = \frac{27,000}{17,260} - 1 = +0.56$$

### 2.5.2.3.2 Compressive Stress in the Polyurethane Foam

The TRUPACT-II package is supported on the two main trailer beams during transport. With reference to Figure 2.5-3, the length,  $L$ , under the OCA that spans the trailer main beams is:

$$L = 2\sqrt{(47.56)^2 - (22)^2} = 84.3 \text{ inches}$$

For two, 8-inch wide trailer main beams, the total compressive area is:

$$A = 2(8)(84.3) = 1,349 \text{ in}^2$$

Conservatively ignoring the load carrying capacity of the OCA outer shell and forklift pockets, the compressive stress in the polyurethane foam due to a 2g vertical (downward) inertial force is:

$$\sigma_c = \frac{2(19,250)}{A} = \frac{38,500}{1,349} = 29 \text{ psi}$$

The allowable stress for the polyurethane foam is 100 psi. Therefore, the margin of safety is:

$$MS = \frac{100}{29} - 1 = +2.45$$

### 2.5.2.4 Tie-down Stresses Due to a Horizontal Compressive Load

The horizontal load,  $F_h = 215,222$  pounds, determined in Section 2.5.2.1, *Tie-down Forces*, is reacted by a single tie-down weldment. The following sections consider the bearing stress in the tie-down weldment, and the shear stresses in the welds holding the horizontal tripler plate to the doubler plate, and the doubler plate to the lower OCA flat head. Based on their relative thicknesses, assume that one-quarter the horizontal load is carried through the 1/4-inch thick OCA flat head, one-quarter is carried through the 1/4-inch thick doubler plate, and one-half is carried through the 1/2-inch thick tripler plate.

### 2.5.2.4.1 Bearing Stress in the Tie-down Weldment

The horizontal load,  $F_h = 215,222$  pounds, is carried from the 8.0-inch wide trailer kickplate through the horizontal doubler and tripler plates welded inside the lower OCA flat head, as illustrated in Figure 2.5-3. For a kickplate length,  $L = 8$  inches, a bottom shell thickness,  $t_s = 1/4$  inch, a doubler plate thickness,  $t_d = 1/4$  inch, and a tripler plate thickness,  $t_t = 1/2$  inch, the area available to carry the horizontal compressive load at the kickplate interface is:

$$A = L(t_s + t_d + t_t) = (8.0)(0.25 + 0.25 + 0.5) = 8.0 \text{ in}^2$$

The corresponding compressive (bearing) stress is:

$$\sigma_c = \frac{F_h}{A} = \frac{215,222}{8.0} = 26,903 \text{ psi}$$

The allowable bearing stress for the OCA outer shell, including the horizontal doubler and tripler plates, is 27,000 psi. Therefore, the margin of safety is:

$$MS = \frac{27,000}{26,903} - 1 = +0.004$$

### 2.5.2.4.2 Shear Stress in the Tripler Plate Welds

Based on the assumed load distribution in Section 2.5.2.4, *Tie-down Stresses Due to a Horizontal Compressive Load*, the force on the welds attaching the tripler plate to the doubler plate is then one-half of 215,222 pounds, or 107,611 pounds. The tripler plate is welded with 3/8-inch fillet welds along three of its edges, and a 1/2-inch groove weld along the outer edge. The two side welds are approximately 8 inches long, and the back weld is 7 inches long, for a total, 3/8-inch fillet weld length of 23 inches. Four, 1/2-inch diameter, 3/8 inch fillet welds supplement the peripheral 3/8-inch fillet welds, providing an additional  $4 \times \pi(1.5) = 18.85$  inches of 3/8-inch fillet weld. Thus, the total 3/8-inch fillet weld length is 41.85 inches. In addition, the 10-inch long outer edge is welded with a 1/2-inch groove weld. The resulting weld shear area is:

$$A_s = (0.375)(\sin 45^\circ)(41.85) + (0.5)(10) = 16.1 \text{ in}^2$$

Thus, the shear stress in the tripler plate fillet welds is:

$$\tau = \frac{107,611}{16.1} = 6,684 \text{ psi}$$

The allowable shear stress for the tripler plate welds is 16,200 psi. Therefore, the margin of safety is:

$$MS = \frac{16,200}{6,684} - 1 = +1.42$$

As an option, the tripler plate may be one inch thick and welded into a cutout through the 1/4-inch thick lower OCA flat head and 1/4-inch thick doubler plate in the same orientation and location as shown in Figure 2.5-6. Full penetration groove welds are used around the periphery of the tripler plate (i.e., a one inch groove weld along the outside, 10-inch long edge, and 1/2-inch groove welds along the remaining three edges). The two side welds are approximately 8

inches long, and the back weld is 7 inches long, for a total weld length of 23 inches. The resulting weld shear area is:

$$A = (0.5)(23) + (1.0)(10) = 21.5 \text{ in}^2$$

Thus, the shear stress in the tripler plate groove welds is:

$$\tau = \frac{215,222}{21.5} = 10,010 \text{ psi}$$

The allowable shear stress for the tripler plate welds is 16,200 psi. Therefore, the margin of safety is:

$$MS = \frac{16,200}{10,010} - 1 = +0.62$$

#### 2.5.2.4.3 Shear Stress in the Doubler Plate Welds

Based on the assumed load distribution in Section 2.5.2.4, *Tie-down Stresses Due to a Horizontal Compressive Load*, the force on the welds attaching the doubler plate to the OCA flat head is then one-half plus one-quarter of 215,222 pounds, or 161,417 pounds. The doubler plate is welded with 1/4-inch fillet welds along its four inner edges, for a total 1/4-inch fillet weld length of approximately 35 inches. Eighteen, 1-inch diameter, 1/4-inch fillet welds supplement the peripheral 1/4-inch fillet welds, providing an additional  $18 \times \pi(1.0) = 56$  inches of 1/4-inch fillet weld. Thus, the total 1/4-inch fillet weld length is 91 inches. In addition, the 20-inch long outer edge is welded with a 1/4-inch groove weld. The resulting weld shear area is:

$$A_s = (0.25)(\sin 45^\circ)(91) + (0.25)(20) = 21.1 \text{ in}^2$$

Thus, the shear stress in the doubler plate fillet welds is:

$$\tau = \frac{161,417}{21.1} = 7,650 \text{ psi}$$

The allowable shear stress for the doubler plate welds is 16,200 psi. Therefore, the margin of safety is:

$$MS = \frac{16,200}{7,650} - 1 = +1.12$$

#### 2.5.2.5 Response of the Package if Treated as a Fixed Cantilever Beam

The preceding sections considered stresses in a localized region in and around the tie-down components. This section demonstrates that a more global response of the TRUPACT-II package to tie-down loads is also acceptable. For this assessment, the TRUPACT-II package is treated as a cantilever beam, fixed at its base. The 1/4 inch thick, OCA outer shell is conservatively assumed to be the only structural member resisting the applied 10g, 5g and 2g inertia loads. Stress intensity, SI, in the OCA outer shell is determined as follows:

$$SI = 2 \sqrt{\left(\frac{\sigma}{2}\right)^2 + \tau^2} = \sqrt{\left(\frac{P}{A} + \frac{Mc}{I}\right)^2 + \left(\frac{2V}{A}\right)^2}$$

where for 2g vertically, the axial force,  $P = (2)(19,250) = 38,500$  pounds, the bending moment from Section 2.5.2.1, *Tie-down Forces*,  $M = HF_g = (60)(215,222) = 12,913,320$  in-lbs, the extreme fiber distance,  $c = \frac{1}{2}(94\frac{3}{8}) = 47.2$  inches, the horizontal shear force,  $V = F_g = 215,222$  pounds, the OCA outer shell cross-sectional area,  $A = (\pi/4)[(94.375)^2 - (93.875)^2] = 74$  in<sup>2</sup>, and the OCA outer shell moment of inertia,  $I = (\pi/64)[(94.375)^4 - (93.875)^4] = 81,869$  in<sup>4</sup>. The resulting stress intensity is:

$$SI = \sqrt{\left(\frac{38,500}{74} + \frac{(12,913,320)(47.2)}{81,869}\right)^2 + \left(\frac{2(215,222)}{74}\right)^2} = 9,863 \text{ psi}$$

The allowable stress intensity for the OCA outer shell is 27,000 psi. Therefore, the margin of safety is:

$$MS = \frac{27,000}{9,863} - 1 = +1.74$$

### 2.5.2.6 Summary

All margins of safety for tie-down loads, per 10 CFR §71.45(b)(1), are positive. The smallest tensile or shear margin of safety,  $MS = +0.31$ , is for failure of the welds attaching the tie-down lug to the doubler plate, indicating that this will be the mode of failure for the tie-downs under an excessive load condition. Note that compressive modes of failure are not considered relevant in the excessive load evaluation. In accordance with 10 CFR §71.45(b)(3), this failure mode does not compromise the performance capabilities of the TRUPACT-II package since no main shell is breached. Finally, it is noted that the forklift pockets and OCA lifting sockets are not intended to be used as tie-down devices, and are appropriately disabled to prevent inadvertent use. The forklift pockets and OCA lifting sockets are disabled by affixing a plate over each pocket and a cover over the each socket respectively (see the drawings in Appendix 1.3.1, *Packaging General Arrangement Drawings*).

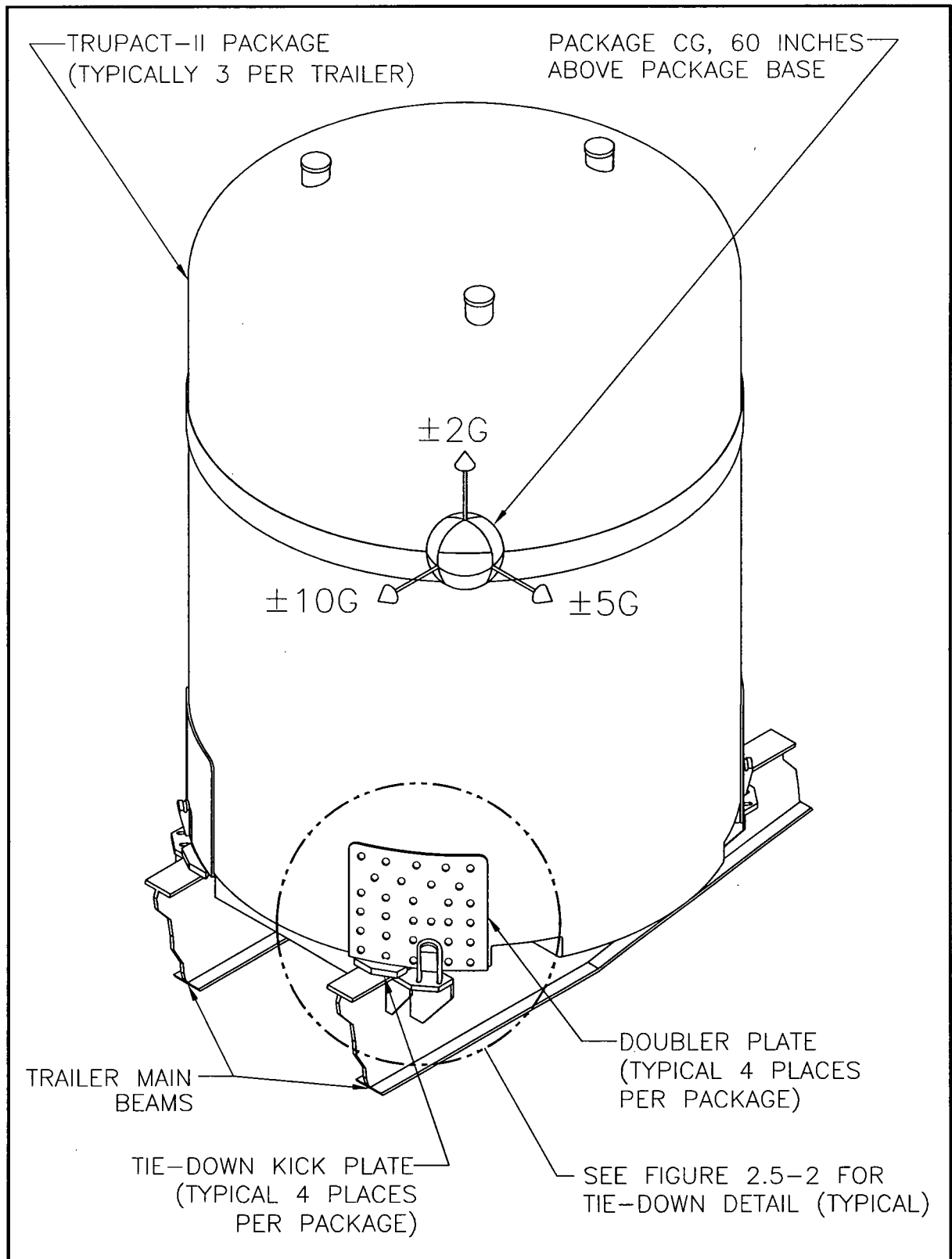


Figure 2.5-1 – Tie-down Device Layout

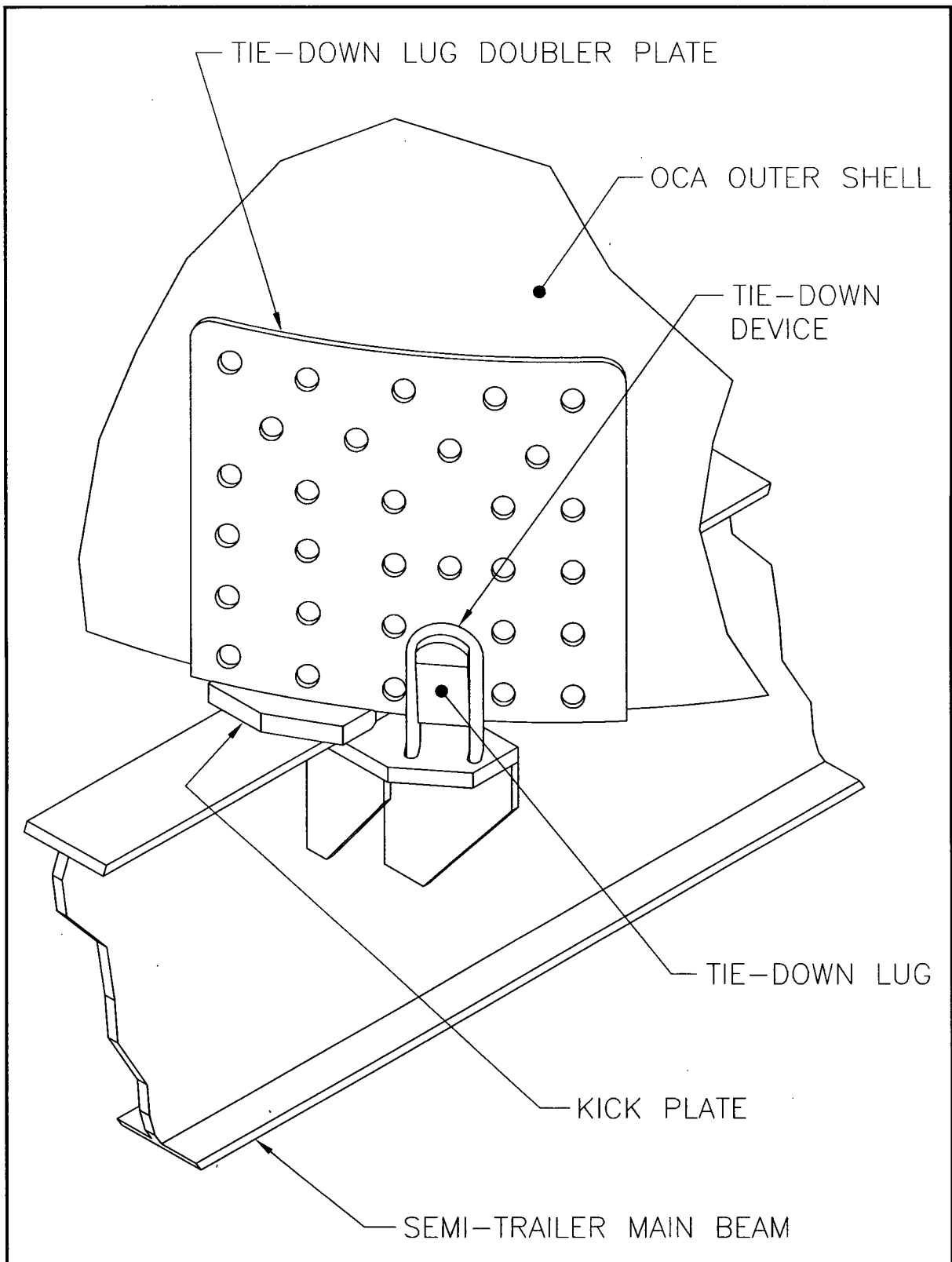


Figure 2.5-2 – Tie-down Device Detail

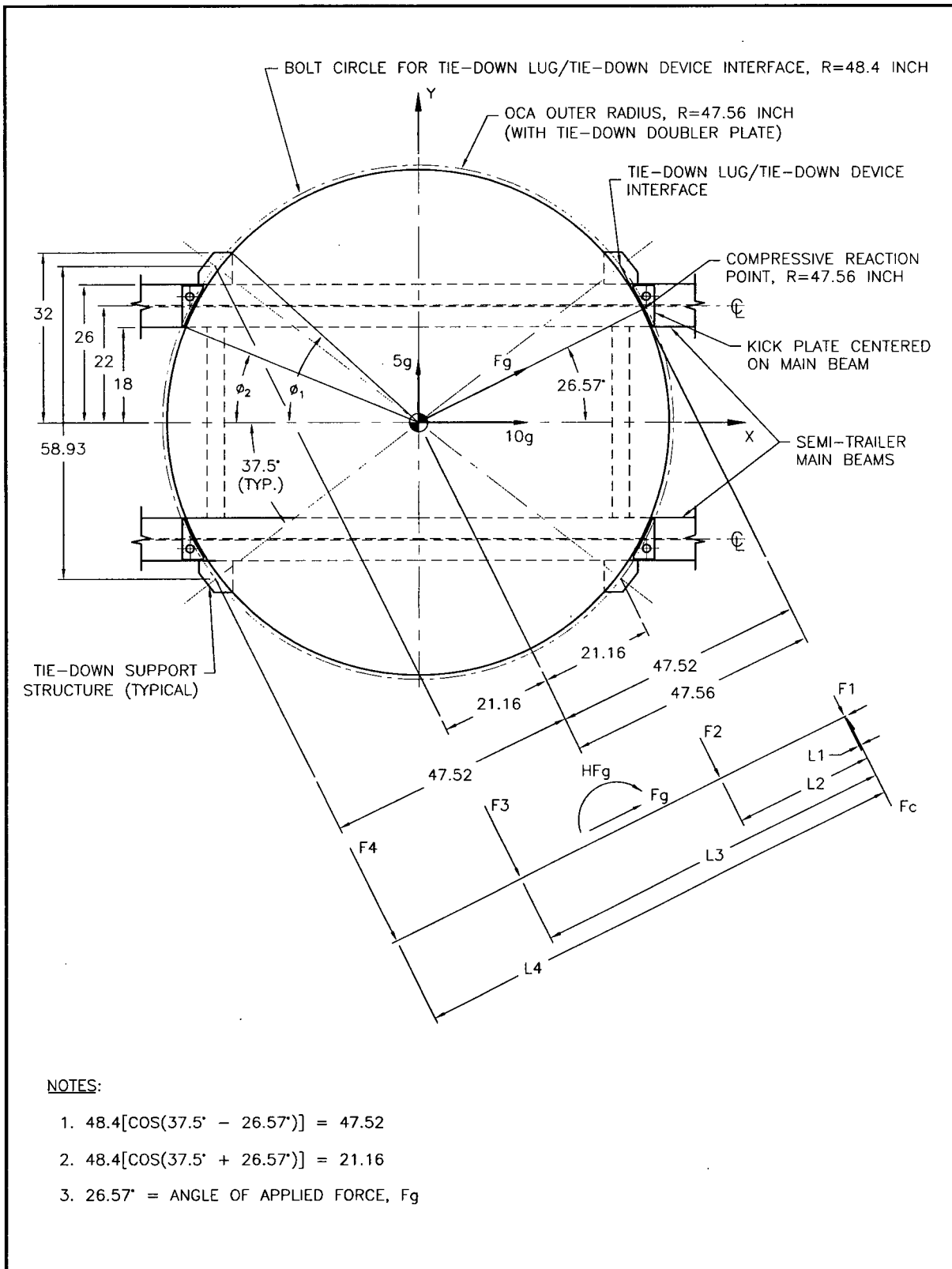


Figure 2.5-3 – Tie-down Plan View and Reaction Force Diagram

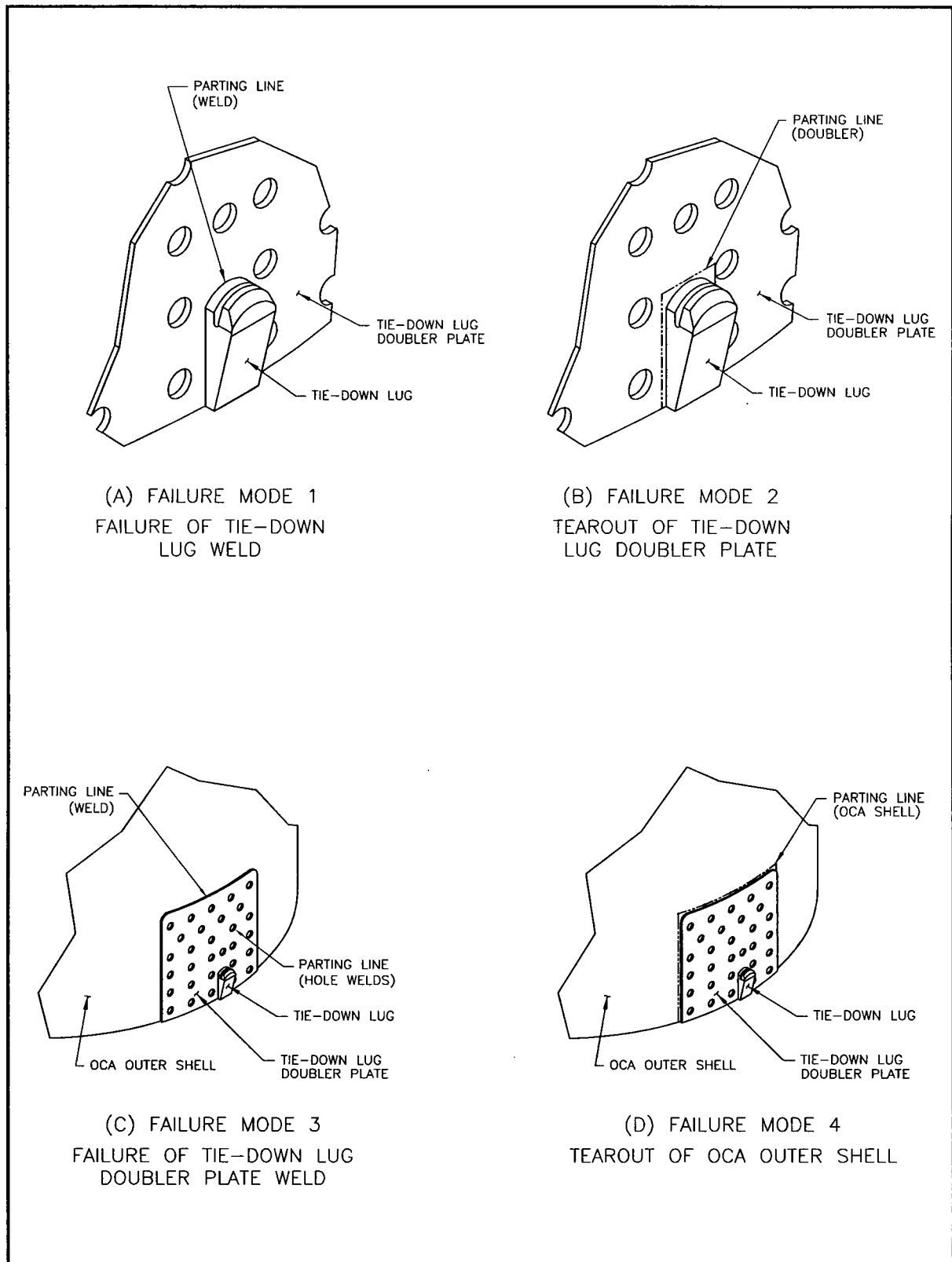


Figure 2.5-4 – Tie-down Tensile/Shear Failure Modes

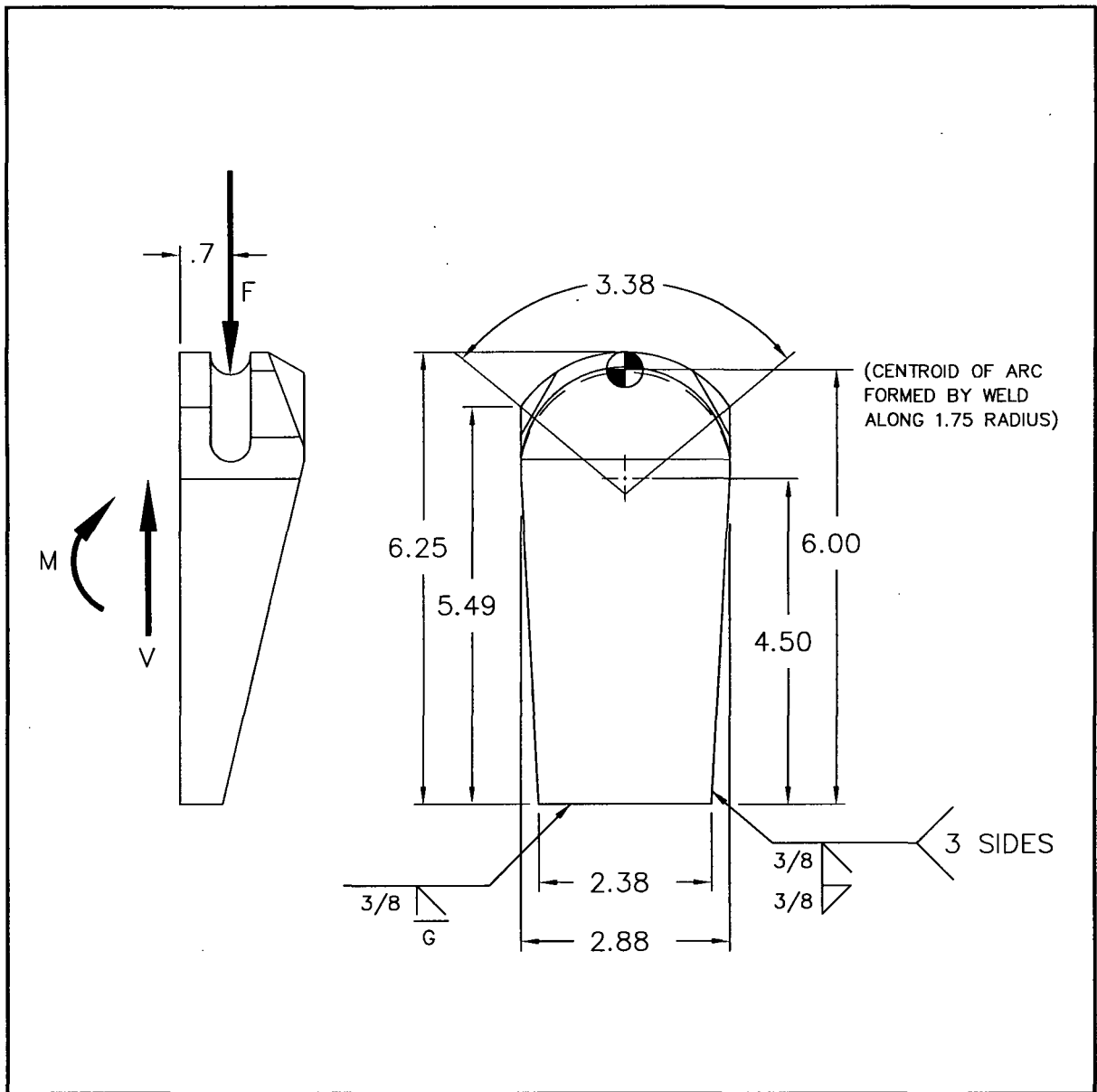


Figure 2.5-5 – Tie-down Lug Dimensions and Load Diagram

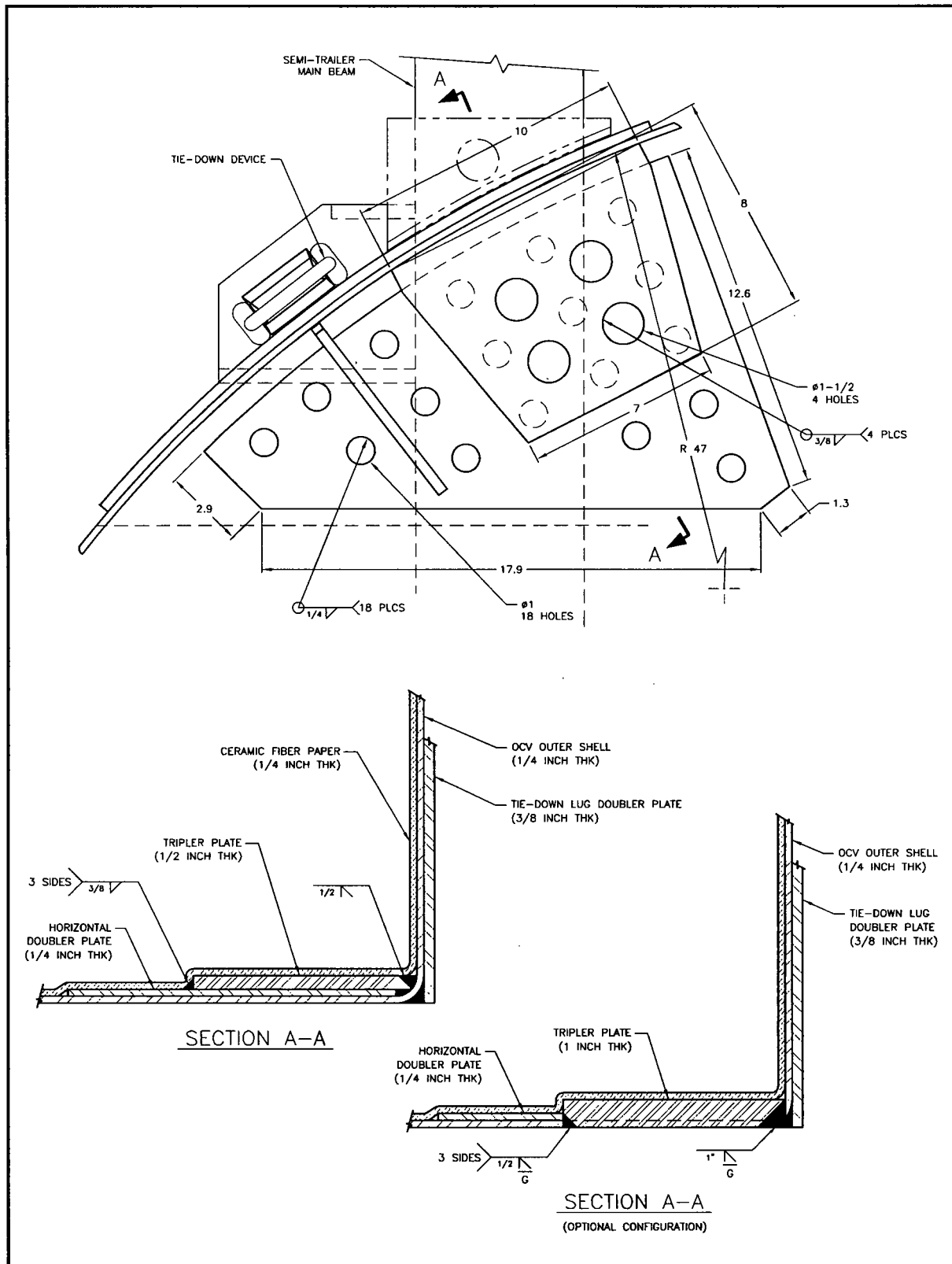


Figure 2.5-6 – Horizontal Doubler and Tripler Plate Details

This page intentionally left blank.

## 2.6 Normal Conditions of Transport

The TRUPACT-II package, when subjected to the normal conditions of transport (NCT) specified in 10 CFR §71.71<sup>1</sup>, is shown to meet the performance requirements specified in Subpart E of 10 CFR 71. As discussed in the introduction to this chapter, with the exception of the NCT free drop, the primary proof of NCT performance is via analytic methods. Regulatory Guide 7.6<sup>2</sup> criteria are demonstrated as acceptable for all NCT analytic evaluations presented in this section. Specific discussions regarding brittle fracture and fatigue are presented in Section 2.1.2.2, *Miscellaneous Structural Failure Modes*, and are shown not to be limiting cases for the TRUPACT-II package design. The ability of the butyl O-ring containment seals to remain leaktight is documented in Appendix 2.10.2, *Elastomer O-ring Seal Performance Tests*.

With the exception of the NCT free drop evaluation, analyses for heat, cold, reduced external pressure, increased external pressure, and vibration are performed in this section. Allowable stress limits are consistent with Table 2.1-1 and Table 2.1-2 in Section 2.1.2.1, *Analytic Design Criteria (Allowable Stresses)*, using temperature-adjusted material properties taken from Table 2.3-1 from Section 2.3.1, *Mechanical Properties Applied to Analytic Evaluations*.

For the analytic assessments performed within this section, properties for Type 304 stainless steel are based on data in Table 2.3-1 from Section 2.3.1, *Mechanical Properties Applied to Analytic Evaluations*. Similarly, the bounding values for polyurethane foam compressive strength are based on data in Table 2.3-2 from Section 2.3.1, *Mechanical Properties Applied to Analytic Evaluations*. Polyurethane foam compressive strength is further adjusted  $\pm 15\%$  to account for manufacturing tolerance. At elevated NCT temperatures (i.e., 160 °F), the nominal compressive strength is reduced 25% for elevated temperature effects and reduced 15% for manufacturing tolerance. At reduced NCT temperatures (i.e., -40 °F), the nominal compressive strength is increased 50% for reduced temperature effects and increased 15% for manufacturing tolerance.

Properties of Type 304 stainless steel and polyurethane foam are summarized below.

Material Property	Material Property Value (psi)			Reference
	-40 °F	70 °F	160 °F	
<b>Type 304 Stainless Steel</b>				
Elastic Modulus, E	$28.8 \times 10^6$	$28.3 \times 10^6$	$27.8 \times 10^6$	Table 2.3-1
Design Stress Intensity, $S_m$	20,000	20,000	20,000	
Yield Strength, $S_m$	N/A	30,000	27,000	
<b>Polyurethane Foam Compressive Strength</b>				
Parallel-to-Rise Direction, $\sigma_c$	405	235	150	Table 2.3-2
Perpendicular-to-Rise Direction, $\sigma_c$	336	195	124	

<sup>1</sup> Title 10, Code of Federal Regulations, Part 71 (10 CFR 71), *Packaging and Transportation of Radioactive Material*, 01-01-12 Edition.

<sup>2</sup> U. S. Nuclear Regulatory Commission, Regulatory Guide 7.6, *Design Criteria for the Structural Analysis of Shipping Cask Containment Vessels*, Revision 1, March 1978.

Finite element analysis methods are utilized to determine stresses in the TRUPACT-II packaging structure at various temperature extremes, including the effects of differential thermal expansion, when appropriate, and internal (I) and external (E) pressure combinations, as summarized below.

Load Case Number	Reference Section	Differential Expansion?	Pressure Differential	Temperature		Table Number	Figure Numbers
				Uniform	Reference		
OCA Case 1	§2.6.1	No	61.2 psig (I)	160 °F	160 °F	2.6-1	2.6-1/-2
OCA Case 2	§2.6.1	Yes	61.2 psig (I)	160 °F	70 °F	2.6-2	2.6-3/-4
OCA Case 3	§2.6.2	Yes	0 psig	-40 °F	70 °F	2.6-3	2.6-5/-6
OCA Case 4	§2.6.4	No	14.7 psig (E)	70 °F	70 °F	2.6-4	2.6-7/-8
ICV Case 1	§2.6.1	No	61.2 psig (I)	160 °F	160 °F	2.6-5	2.6-9/-10
ICV Case 2	§2.6.4	No	14.7 psig (E)	70 °F	70 °F	2.6-6	2.6-11/-12

For the NCT free drop evaluation, a certification test program was undertaken using three TRUPACT-II certification test units (CTUs). Results from certification testing demonstrated that under NCT free drop conditions, two leaktight levels of containment were maintained. NCT certification testing also demonstrated the TRUPACT-II package's ability to survive subsequent HAC, 30-foot free drop, puncture, and fire tests was not compromised. Analyses are performed, when appropriate, to supplement or expand on the available test results. This combination of analytic and test, structural evaluations provides an initial configuration for NCT thermal, shielding and criticality performance. In accordance with 10 CFR §71.43(f), the evaluations performed herein successfully demonstrate that under NCT tests the TRUPACT-II package experiences "no substantial reduction in the effectiveness of the packaging". Summaries of the more significant aspects of the full scale free drop testing are included in Section 2.6.7, *Free Drop*, with details presented in Appendix 2.10.3, *Certification Tests*.

## 2.6.1 Heat

The NCT thermal analyses presented in Section 3.4, *Thermal Evaluation for Normal Conditions of Transport*, consists of exposing the TRUPACT-II package to direct sunlight and 100 °F still air per the requirements of 10 CFR §71.71(b). Although the actual internal heat load is a function of the particular payload configuration being transported, this section utilizes the maximum internal heat allowed within a TRUPACT-II package, or 40 thermal watts. The 40-thermal watt case results in maximum temperature gradients throughout the TRUPACT-II package.

### 2.6.1.1 Summary of Pressures and Temperatures

The maximum normal operating pressure (MNOP) is 50 psig, as determined in Section 3.4.4, *Maximum Internal Pressure*. The pressure stress analyses within this section combine the internal pressure of 50 psig due to MNOP with a reduced external pressure, per 10 CFR §71.71(c)(3), of 3.5 psia (11.2 psig). The net resulting internal pressure utilized in all NCT structural analyses considering internal pressure is therefore 61.2 psig.

The NCT heat input results in modest temperatures and temperature gradients throughout the TRUPACT-II package. Maximum temperatures for the major packaging components are

summarized in Table 3.4-1 from Section 3.4.2, *Maximum Temperatures*. As shown in Table 3.4-1, all packaging temperatures remain at or below 156 °F. For conservatism, structural analyses of the OCA and ICV utilize a uniform bounding temperature of 160 °F. Use of a uniform bounding temperature is also conservative since material strengths are lowest at the highest temperatures. In addition, in the case of the OCA, the main contributor to thermal stress is the result of differential expansion of the polyurethane foam and the surrounding stainless steel. Also shown by the temperatures presented in Table 3.4-1, temperature gradients are modest for the NCT heat condition. Thus, temperature gradients are reasonably ignored in the analyses herein.

### 2.6.1.2 Differential Thermal Expansion

With NCT temperatures throughout the packaging being relatively uniform, (i.e., no significant temperature gradients), the concern with differential expansions is limited to regions of the TRUPACT-II packaging that employ adjacent materials with sufficiently different coefficients of thermal expansion. The OCA is a double-wall, composite construction of polyurethane foam between inner and outer shells of stainless steel. The polyurethane foam expands and contracts to a much greater degree than the surrounding stainless steel shells resulting in stresses due to differential thermal expansion. Finite element analyses presented in the following sections quantify these differential thermal expansion stresses. Differential thermal expansion stresses are negligible in the ICV for three reasons: 1) the temperature distribution throughout the entire ICV is relatively uniform, 2) the ICV is fabricated from only one type of structural material, and 3) the ICV is not radially or axially constrained within a tight-fitting structure (i.e., the OCV).

### 2.6.1.3 Stress Calculations

A finite element model of the OCA is used to determine the stresses due to the combined effects of pressure loads, and temperature loads due to differential thermal expansion. The details of this model are presented in Appendix 2.10.1.1, *Outer Confinement Assembly (OCA) Structural Analysis*. The ICV is also analyzed for the combined effects of pressure and temperature using a finite element model that is described in Appendix 2.10.1.2, *Inner Containment Vessel (ICV) Structural Analysis*. For the NCT heat condition, evaluations include two load cases for the OCA and one load case for the ICV.

Maximum stress intensities are determined for each component, and classified according to primary or secondary, membrane or bending. Classification of stress intensities is per Table NB-3217-1 of the ASME Boiler and Pressure Vessel Code<sup>3</sup>. Maximum stress intensities are presented for the maximum general primary membrane stress intensity,  $P_m$ , the maximum local primary membrane stress intensity,  $P_L$ , the maximum primary membrane (general or local) plus primary bending stress intensity,  $P_m + P_b$  or  $P_L + P_b$ , and the maximum primary plus secondary stress intensity,  $P_m + P_b + Q$  or  $P_L + P_b + Q$ .

**OCA Load Case 1** (see Table 2.6-1, and Figure 2.6-1 and Figure 2.6-2): This analysis is performed at a uniform temperature of 160 °F, but with the reference temperature also set to 160 °F thereby eliminating any differential thermal expansion stresses. The internal pressure considers the effects of a maximum normal operating pressure (MNOP) of 50 psig, internal,

<sup>3</sup> American Society of Mechanical Engineers (ASME) Boiler and Pressure Vessel Code, Section III, *Rules for Construction of Nuclear Power Plant Components*, 1986 Edition.

coupled with a reduced external pressure of 3.5 psia (i.e., 11.2 psig, internal). The net result is an internal pressure of  $50.0 + 11.2 = 61.2$  psig.

$P_m = 16,170$  psi, located in the OCV shell at the cylindrical/conical transition,

$P_L = 27,990$  psi, located in the knuckle region of the upper OCV torispherical head,

$P_L + P_b = 30,810$  psi, located in the upper OCV seal flange/shell transition, and

$P_L + P_b + Q = 37,978$  psi, located in the knuckle region of the upper OCV torispherical head.

**OCA Load Case 2** (see Table 2.6-2, and Figure 2.6-3 and Figure 2.6-4): This analysis is performed at a uniform temperature of 160 °F, but with the reference temperature set to 70 °F thereby including any differential thermal expansion stresses. As with OCA Load Case 1, the MNOP is coupled with the reduced external pressure for a net internal pressure of 61.2 psig. The use of these two cases allows primary stress intensities (from pressure loads) to be considered independently of secondary stress intensities (from differential thermal expansion loads).

$P_L + P_b + Q = 39,520$  psi, located in the knuckle region of the lower OCV torispherical head.

**ICV Load Case 1** (see Table 2.6-5, and Figure 2.6-9 and Figure 2.6-10): This analysis is performed at a uniform temperature of 160 °F, but with the reference temperature also set to 160 °F thereby eliminating any differential thermal expansion stresses. As with OCA Load Cases 1 and 2, the MNOP is coupled with the reduced external pressure for a net internal pressure of 61.2 psig.

$P_m = 15,236$  psi, located in the crown region of the upper ICV torispherical head,

$P_L = 26,935$  psi, located in the knuckle region of the upper ICV torispherical head.

$P_L + P_b = 31,310$  psi, located in the upper ICV seal flange/shell transition, and

$P_L + P_b + Q = 38,280$  psi, located in the knuckle region of the upper ICV torispherical head.

Polyurethane foam stress intensities are insignificant for OCA Load Case 1 (maximum stress intensity is 16 psi) and reach a maximum value of 197 psi for OCA Load Case 2. This highly localized, secondary stress intensity results primarily from a compressive stress parallel to the direction of foam rise and occurs where the lower Z-flange joins the OCA body outer 3/8-inch thick shell. Adjacent nodes 528, 530, and 531 have stress intensities in the range 149 - 190 psi whereas stress intensity levels at all other nodes are less than 70 psi.

For the polyurethane foam at 160 °F, the parallel-to-rise compressive strength is 150 psi and the perpendicular-to-rise compressive strength is 124 psi. Since the calculated compressive stress in the foam exceeds its crush strength, a minor amount of highly localized permanent crushing of the foam will occur. Such localized crushing will relieve the deformation controlled polyurethane foam stresses and will not affect the overall performance of the package. In addition, a beneficial effect results because stresses are also relieved in the adjacent stainless steel shell structures.

#### 2.6.1.4 Comparison with Allowable Stresses

Section 2.1.2, *Design Criteria*, presents the design criteria for structural evaluation of the TRUPACT-II packaging. The containment vessel design criteria for NCT analyses are in accordance with Regulatory Guide 7.6, which uses as a basis the criteria defined for Level A

service limits in Section III of the ASME Boiler and Pressure Vessel Code<sup>4</sup>. Load combinations follow the guidelines of Regulatory Guide 7.8<sup>5</sup>.

From Table 2.3-1 in Section 2.3.1, *Mechanical Properties Applied to Analytic Evaluations*, the design stress intensity for Type 304 stainless steel used in the ICV and OCV is  $S_m = 20,000$  psi at 160 °F. From Table 2.1-1 in Section 2.1.2.1.1, *Containment Structure (ICV)*, the allowable stress intensities for the NCT hot condition is  $S_m$  for general primary membrane stress intensity ( $P_m$ ),  $1.5S_m$  for local primary membrane stress intensity ( $P_L$ ),  $1.5S_m$  for primary membrane (general or local) plus primary bending stress intensity ( $P_m + P_b$  or  $P_L + P_b$ ), and  $3.0S_m$  for the range of primary plus secondary stress intensity ( $P_m + P_b + Q$  or  $P_L + P_b + Q$ ).

Maximum stress intensity, allowable stress intensity, and minimum margins of safety for each stress category and each load case are presented in Table 2.6-1, Table 2.6-2, and Table 2.6-5 for each of the cases discussed above. Since all margins of safety are positive, the design criteria are satisfied.

### 2.6.1.5 Range of Primary Plus Secondary Stress Intensities

Per Paragraph C.4 of Regulatory Guide 7.6, the maximum range of primary plus secondary stress intensity for NCT must be less than  $3.0S_m$ . This limitation on stress intensity range applies to the entire history of NCT loadings and not only to the stresses from each individual load transient.

#### 2.6.1.5.1 Range of Primary Plus Secondary Stress Intensities for the OCA

The extreme ends of the stress range are determined from OCA Load Case 2 (from Section 2.6.1, *Heat*) and OCA Load Case 4 (from Section 2.6.4, *Increased External Pressure*). One extreme, OCA Load Case 2 represents the case of maximum internal pressure coupled with reduced external pressure, plus the effect of differential thermal expansion associated with heat-up from 70 °F to 160 °F. The other extreme, OCA Load Case 4, considers the effect of a minimum internal pressure at 70 °F. Note that combinations of other OCA load cases such as increased external pressure (20 psia, 5.3 psig) plus cool-down from 70 °F to -20 °F were also considered and found not to be bounding for the stress intensity range calculation.

The maximum range of primary plus secondary stress intensity occurs in the knuckle region of the lower OCV torispherical head (element 320). The extreme values of stress intensity are 39,520 psi and 9,219 psi from Table 2.6-2 and Table 2.6-4 for OCA Load Cases 2 and 4, respectively. Since OCA Load Cases 2 and 4 have opposite loads, the maximum range of primary plus secondary stress intensity is simply  $39,520 + 9,219 = 48,739$  psi. The allowable stress intensity is  $3.0S_m$ , where  $S_m = 20,000$  psi for Type 304 stainless steel at 160 °F. The margin of safety is:

$$MS = \frac{3(20,000)}{48,739} - 1 = +0.23$$

The positive margin of safety indicates that the design criterion is satisfied.

<sup>4</sup> American Society of Mechanical Engineers (ASME) Boiler and Pressure Vessel Code, Section III, *Rules for Construction of Nuclear Power Plant Components*, 1986 Edition.

<sup>5</sup> U. S. Nuclear Regulatory Commission, Regulatory Guide 7.8, *Load Combinations for the Structural Analysis of Shipping Casks for Radioactive Material*, Revision 1, March 1989.

### 2.6.1.5.2 Range of Primary Plus Secondary Stress Intensities for the ICV

The extreme ends of the stress range are determined from ICV Load Case 1 (from Section 2.6.1, *Heat*) and ICV Load Case 2 (from Section 2.6.4, *Increased External Pressure*). One extreme, ICV Load Case 1 represents the case of maximum internal pressure coupled with reduced external pressure, plus the effect of differential thermal expansion associated with heat-up from 70 °F to 160 °F. The other extreme, ICV Load Case 2, considers the effect of a minimum internal pressure at 70 °F.

The extreme values of stress intensity are 38,280 psi and 9,105 psi from Table 2.6-5 and Table 2.6-6 for ICV Load Cases 1 and 2, respectively, conservatively ignoring the fact that the extreme values occur at locations remote from each other. Since ICV Load Cases 1 and 2 have opposite loads, the maximum range of primary plus secondary stress intensity is simply  $38,280 + 9,105 = 47,385$  psi. The allowable stress intensity is  $3.0S_m$ , where  $S_m = 20,000$  psi for Type 304 stainless steel at 160 °F. The margin of safety is:

$$MS = \frac{3(20,000)}{47,385} - 1 = +0.27$$

The positive margin of safety indicates that the design criterion is satisfied.

## 2.6.2 Cold

The NCT cold condition consists of exposing the TRUPACT-II packaging to a steady-state ambient temperature of -40 °F. Insolation and payload internal decay heat are assumed to be zero. These conditions will result in a uniform temperature throughout the package of -40 °F. With no internal heat load (i.e., no contents to produce heat and, therefore, pressure), the net pressure differential is assumed to be zero (14.7 psia internal, 14.7 psia external).

For the OCA, the principal structural concern due to the NCT cold condition is the effect of the differential expansion of the polyurethane foam relative to the surrounding stainless steel shells. During the cool-down from 70 °F to -40 °F, the foam material shrinks onto the OCV because thermal expansion coefficient for foam is greater than stainless steel. The resulting stresses are discussed in Section 2.6.2.1, *Stress Calculations*.

Differential thermal expansion stresses are negligible in the ICV for three reasons: 1) the temperature distribution throughout the entire ICV is relatively uniform, 2) the ICV is fabricated from only one type of structural material, and 3) the ICV is not radially or axially constrained within a tight-fitting structure (i.e., the OCV).

Brittle fracture at -40 °F is addressed in Section 2.1.2.2.1, *Brittle Fracture*. Performance of the O-ring seals at -40 °F is discussed in Appendix 2.10.2, *Elastomer O-ring Seal Performance Tests*.

### 2.6.2.1 Stress Calculations

A finite element model of the OCA is used to determine the stresses due to the combined effects of pressure loads, and temperature loads due to differential thermal expansion. The details of this model are presented in Appendix 2.10.1.1, *Outer Confinement Assembly (OCA) Structural Analysis*. For the NCT cold condition, evaluations include one load case for the OCA.

Maximum stress intensities are determined for each component, and classified according to primary or secondary, membrane or bending. Classification of stress intensities is per Table NB-3217-1 of

the ASME Boiler and Pressure Vessel Code. Membrane and membrane plus bending stresses due to differential thermal expansion are classified as secondary stresses (Q). Since there are no pressure loads, primary stresses ( $P_m$ ,  $P_L$ , and  $P_m + P_b$  or  $P_L + P_b$ ) are equal to zero.

**OCA Load Case 3** (see Table 2.6-3, and Figure 2.6-5 and Figure 2.6-6): This analysis is performed at a uniform temperature of  $-40^\circ\text{F}$ , but with the reference temperature set to  $70^\circ\text{F}$  thereby including differential thermal expansion stresses. For a uniform temperature cold case at  $-40^\circ\text{F}$ , both payload decay heat and solar heat are assumed to be zero. These conditions result in an internal pressure of 14.7 psia balanced with an external pressure of 14.7 psia, for a net pressure differential of zero.

$P_L + P_b + Q = 14,746$  psi, located in the lower OCV shell near the stiffening ring.

Polyurethane foam stress intensities are well below the allowable crush strength for OCA Load Case 3 (maximum stress intensity is 69 psi). For the polyurethane foam at  $-40^\circ\text{F}$  (+50%) and applying the manufacturing tolerance (-15%), the minimum parallel-to-rise compressive strength is 300 psi and the minimum perpendicular-to-rise compressive strength is 249 psi.

### 2.6.2.2 Comparison with Allowable Stresses

Section 2.1.2, *Design Criteria*, presents the design criteria for structural evaluation of the TRUPACT-II packaging. The containment vessel design criteria for NCT analyses are in accordance with Regulatory Guide 7.6, which uses as a basis the criteria defined for Level A service limits in Section III of the ASME Boiler and Pressure Vessel Code. Load combinations follow the guidelines of Regulatory Guide 7.8.

In Table 2.3-1 from Section 2.3.1, *Mechanical Properties Applied to Analytic Evaluations*, the design stress intensity for Type 304 stainless steel used in the ICV and OCV is  $S_m = 20,000$  psi at  $-40^\circ\text{F}$ . In Table 2.1-1 from Section 2.1.2.1.1, *Containment Structure (ICV)*, the allowable stress intensity for the NCT cold condition is  $3.0S_m$  for the range of primary plus secondary stress intensity ( $P_m + P_b + Q$  or  $P_L + P_b + Q$ ).

Maximum stress intensity, allowable stress intensity, and minimum margins of safety for each stress category and each load case are presented in Table 2.6-3 for OCA Load Case 3. Since all margins of safety are positive, the design criteria are satisfied.

Since the NCT cold condition results in shrinking of the polyurethane foam onto the OCV shell, compressive stresses develop in the OCV shell. The buckling evaluation within Section 2.6.4, *Increased External Pressure*, demonstrates that the compressive stresses due to increased external pressure do not exceed the NCT allowable stresses. The compressive stresses generated during the NCT cold condition are bounded by the NCT increased external pressure condition, therefore no explicit buckling evaluation is required for the NCT cold condition.

### 2.6.3 Reduced External Pressure

The effect of a reduced external pressure of 3.5 psia (11.2 psig internal pressure), per 10 CFR §71.71(c)(3), is negligible for the TRUPACT-II packaging. This conclusion is based on the analyses presented in Section 2.6.1, *Heat*, addressing the ability of both the ICV and OCV to independently withstand a maximum normal operating pressure (MNOP) of 50 psig, combined with a reduced external pressure of 3.5 psia, for a net effective internal pressure of 61.2 psig.

## 2.6.4 Increased External Pressure

The effect of an increased external pressure of 20 psia (5.3 psig external pressure), per 10 CFR §71.71(c)(4), is negligible for the TRUPACT-II packaging. Both the ICV and OCV are designed to withstand a full vacuum equivalent to 14.7 psi external pressure during acceptance leakage rate testing of the TRUPACT-II package, as described in Section 8.1.3, *Fabrication Leakage Rate Tests*. Therefore, the worst case NCT external pressure loading is 14.7 psig.

The external pressure induces small compressive stresses in the ICV and OCV that are limited by stability (buckling) requirements. Buckling assessments are performed for the OCV and ICV in Section 2.6.4.3, *Buckling Assessment of the Torispherical Heads*, and Section 2.6.4.4, *Buckling Assessment of the Cylindrical Shells*.

### 2.6.4.1 Stress Calculations

A finite element model of the OCA is used to determine the stresses due to the effect of a pressure load. The details of this model are presented in Appendix 2.10.1.1, *Outer Confinement Assembly (OCA) Structural Analysis*. The ICV is also analyzed for the effects of a pressure using a finite element model that is described in Appendix 2.10.1.2, *Inner Containment Vessel (ICV) Structural Analysis*. For the NCT increased external pressure condition, evaluations include one load case for the OCA and one load case for the ICV.

Maximum stress intensities are determined for each component, and classified according to primary or secondary, membrane or bending. Classification of stress intensities is per Table NB-3217-1 of the ASME Boiler and Pressure Vessel Code. Maximum stress intensities are presented for the maximum general primary membrane stress intensity,  $P_m$ , the maximum local primary membrane stress intensity,  $P_L$ , the maximum primary membrane (general or local) plus primary bending stress intensity,  $P_m + P_b$  or  $P_L + P_b$ , and the maximum primary plus secondary stress intensity,  $P_m + P_b + Q$  or  $P_L + P_b + Q$ .

**OCA Load Case 4** (see Table 2.6-4, and Figure 2.6-7 and Figure 2.6-8): This analysis is performed at a uniform temperature of 70 °F, and the reference temperature also set to 70 °F thereby eliminating any differential thermal expansion stresses. The external pressure is 14.7 psig.

$P_m = 4,621$  psi, located in the OCV shell at the cylindrical/conical transition,

$P_L = 6,843$  psi, located in the knuckle region of the upper OCV torispherical head,

$P_L + P_b = 4,880$  psi, located in the OCV shell at the cylindrical/conical transition, and

$P_L + P_b + Q = 9,322$  psi, located in the knuckle region of the upper OCV torispherical head.

**ICV Load Case 2** (see Table 2.6-6, and Figure 2.6-11 and Figure 2.6-12): This analysis is performed at a uniform temperature of 70 °F, but with the reference temperature also set to 70 °F thereby eliminating any differential thermal expansion stresses. As with OCA Load Case 4, the external pressure is 14.7 psig.

$P_m = 3,636$  psi, located in the crown region of the upper ICV torispherical head,

$P_L = 6,382$  psi, located in the knuckle region of the upper ICV torispherical head,

$P_L + P_b = 4,650$  psi, located in the crown region of the upper ICV torispherical head, and

$P_L + P_b + Q = 9,105$  psi, located in the knuckle region of the upper ICV torispherical head.

Polyurethane foam stress intensities are insignificant for OCA Load Case 4.

### 2.6.4.2 Comparison with Allowable Stresses

Section 2.1.2, *Design Criteria*, presents the design criteria for structural evaluation of the TRUPACT-II packaging. The containment vessel design criteria for NCT analyses are in accordance with Regulatory Guide 7.6, which uses as a basis the criteria defined for Level A service limits in Section III of the ASME Boiler and Pressure Vessel Code. Load combinations follow the guidelines of Regulatory Guide 7.8.

In Table 2.3-1 from Section 2.3.1, *Mechanical Properties Applied to Analytic Evaluations*, the design stress intensity for Type 304 stainless steel used in the ICV and OCV is  $S_m = 20,000$  psi at 160 °F. In Table 2.1-1 from Section 2.1.2.1.1, *Containment Structure (ICV)*, the allowable stress intensities for the NCT increased external pressure condition is  $S_m$  for general primary membrane stress intensity ( $P_m$ ),  $1.5S_m$  for local primary membrane stress intensity ( $P_L$ ),  $1.5S_m$  for primary membrane (general or local) plus primary bending stress intensity ( $P_m + P_b$  or  $P_L + P_b$ ), and  $3.0S_m$  for the range of primary plus secondary stress intensity ( $P_m + P_b + Q$  or  $P_L + P_b + Q$ ).

Maximum stress intensity, allowable stress intensity, and minimum margins of safety for each stress category and each load case are presented in Table 2.6-4 and Table 2.6-6 for each of the cases discussed above. Since all margins of safety are positive, the design criteria are satisfied.

### 2.6.4.3 Buckling Assessment of the Torispherical Heads

The buckling analysis of the torispherical heads is based on the methodology outlined in Paragraph NE-3133.4(e), *Torispherical Heads*, of the ASME Boiler and Pressure Vessel Code, Section III, Subsection NE. The results from following this methodology are summarized below.

Parameter	OCV Torispherical Head		ICV Torispherical Head	
	Upper	Lower	Upper	Lower
R	77.3125	74.1250	74.3750	73.1250
T	0.25	0.25	0.25	0.25
$A = \frac{0.125}{(R/T)}$	0.00040	0.00042	0.00042	0.00043
$B^6$	5,600	5,800	5,800	5,900
$P_a = \frac{B}{(R/T)}$	18.1	19.6	19.5	20.2

The smallest allowable pressure,  $P_a$ , is 18.1 psig for the OCV upper head. For an applied external pressure of 14.7 psig, the corresponding buckling margin of safety is:

<sup>6</sup> Factor B is found from American Society of Mechanical Engineers (ASME) Boiler and Pressure Vessel Code, Section III, *Rules for Construction of Nuclear Power Plant Components*, Figure VII-1102-4, *Chart for Determining Shell Thickness of Cylindrical and Spherical Components Under External Pressure When Constructed of Austenitic Steel (18Cr-8Ni, Type 304)*, 1986 Edition. The 100 °F temperature curve is used for each case.

$$MS = \frac{18.1}{14.7} - 1 = +0.23$$

Since the margin of safety in the worst case is positive, it is concluded that none of the OCV or ICV torispherical heads will buckle for an external pressure of 14.7 psig.

#### 2.6.4.4 Buckling Assessment of the Cylindrical Shells

The cylindrical portions of the OCV and ICV are evaluated using ASME Boiler and Pressure Vessel Code Case N-284<sup>7</sup>. Consistent with Regulatory Guide 7.6 philosophy, a factor of safety of 2.0 is applied for NCT buckling evaluations per ASME Code Case N-284, corresponding to ASME Code, Service Level A conditions.

Buckling analysis geometry parameters are summarized in Table 2.6-7, and loading parameters are summarized in Table 2.6-8. The cylindrical shell buckling analysis utilizes an OCV and ICV temperature of 70 °F. The stresses are determined using an external pressure of 14.7 psig. The hoop stress,  $\sigma_{\theta}$ , and axial stress,  $\sigma_{\phi}$ , are found from:

$$\sigma_{\theta} = \frac{Pr}{t} \quad \sigma_{\phi} = \frac{Pr}{2t}$$

where P is the applied external pressure of 14.7 psi, r is the mean radius, and t is the cylindrical shell thickness. As shown in Table 2.6-9, since all interaction check parameters are less than 1.0, as required, the design criteria are satisfied.

The OCV length is conservatively measured from the ring stiffener to an assumed support point located one-third of the depth of the lower OCV torispherical head below the head-to-shell interface (i.e., 32.67 inches).

#### OCV Shell Ring Stiffener Axial Compression Check:

Per Paragraph -1714.1(a) of ASME Boiler and Pressure Vessel Code Case N-284, the required ring stiffener cross-section area is the larger of:

$$A_{\theta} \geq \left( \frac{0.334}{M_s^{0.6}} - 0.063 \right) \ell_{s\phi} t = 0.076 \text{ in}^2 \quad \text{or} \quad A_{\theta} \geq (0.06) \ell_{s\phi} t = 0.350 \text{ in}^2$$

where, from Table 2.6-7, R = 36.91 inches and t = 0.188 inches, and  $M_s = \ell_{si}/(Rt)^{1/2} = 11.77$ , and the length,  $\ell_{s\phi}$ , is the average of the distance from the stiffening ring to the lower head (32.67 inches) and the distance from the stiffening ring to the upper seal flange (29.33 inches), or  $\ell_{s\phi} = \ell_{si} = 1/2(32.67 + 29.33) = 31.00$  inches.

The cross-section area of the stiffening ring is  $A = 0.375 \times 1.5 = 0.563 \text{ in}^2$ . Since  $A = 0.563 \text{ in}^2 > 0.350 \text{ in}^2 = A_{\theta}$ , the size of the stiffening ring for axial compression is acceptable.

<sup>7</sup> American Society of Mechanical Engineers (ASME) Boiler and Pressure Vessel Code, Section III, *Rules for Construction of Nuclear Power Plant Components*, Division I, Class MC, Code Case N-284, *Metal Containment Shell Buckling Design Methods*, August 25, 1980, approval date.

**OCV Shell Ring Stiffener Hoop Compression Check:**

Per Paragraph –1714.1(b)(1) of ASME Boiler and Pressure Vessel Code Case N-284, the required moment of inertia for an intermediate stiffening ring to resist hoop compression is:

$$I_{E0} = \frac{(1.2)\sigma_{\theta eL}\ell_{s\phi}R_c^2t}{E(n^2 - 1)} = 0.264 \text{ in}^4$$

where  $\sigma_{\theta eL} = 11,273$  psi (Table 2.6-9),  $\ell_{s\phi} = 31.00$  inches,  $R_c = 36.91 + 0.356 = 37.27$  inches,  $t = 0.188$  inches,  $E = 28.3(10)^6$  psi at 70 °F, and  $n^2$  is:

$$n^2 = \frac{(1.875)R^{\frac{3}{2}}}{L_B t^{\frac{3}{2}}} = 15.64$$

where  $R = 36.91$  inches (Table 2.6-7), the effective length of the OCV shell between “bulkheads” is  $L_B = 62.0$  inches, and  $t = 0.188$  inches (Table 2.6-7).

The effective stiffness of the ring stiffener also includes a portion of the adjacent cylindrical shell whose length is determined from Paragraph –1200 of ASME Code Case N-284 as follows:

$$\ell_{ci} = 1.56\sqrt{Rt} = 4.11 \text{ in}$$

where, from Table 2.6-7,  $R = 36.91$  inches and  $t = 0.188$  inches.

The distance to the composite stiffening ring neutral axis,  $\bar{X}$ , is:

$$\bar{X} = \frac{(0.375)(1.5)(0.188 + 1.5)}{2[(0.188)(4.11) + (0.375)(1.5)]} = 0.356 \text{ in}$$

Knowing the distance to the neutral axis of the composite stiffening ring, the ring stiffener in-plane moment of inertia is:

$$I_r = \frac{(0.375)(1.5)^3}{12} + (0.375)(1.5)\left(\frac{0.188 + 1.5}{2} - 0.356\right)^2 = 0.239 \text{ in}^4$$

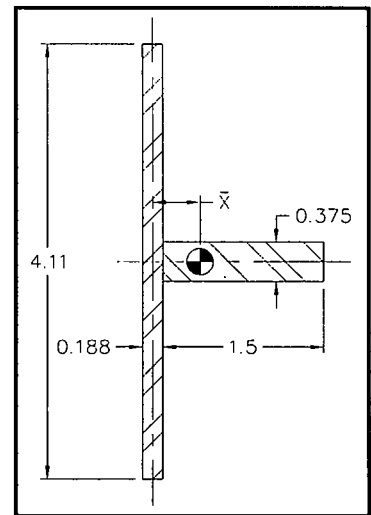
Similarly, the shell out-of-plane moment of inertia is:

$$I_s = \frac{(4.11)(0.188)^3}{12} + (0.188)(4.11)(0.356)^2 = 0.100 \text{ in}^4$$

Combining both results, the effective moment of inertia is  $I_E = 0.239 + 0.100 = 0.339 \text{ in}^4$ . Since  $I_E = 0.339 \text{ in}^4 > 0.264 \text{ in}^4 = I_{E0}$ , the size of the stiffening ring for hoop compression is acceptable.

**2.6.5 Vibration**

By comparing the alternating stresses arising during NCT with the established endurance limits of the TRUPACT-II packaging materials of construction, the effects of vibration normally incident to transport are shown to be acceptable. These comparisons apply the methodology and limits of NRC Regulatory Guide 7.6. By conservatively comparing NCT stresses with endurance stress



limits for an infinite service life, the development of accurate vibratory loading cycles is not required. The vibration evaluation is comprehensively addressed in the following sections.

### 2.6.5.1 Vibratory Loads Determination

ANSI N14.23<sup>8</sup> provides a basis for estimating peak truck trailer vibration inputs. A summary of peak vibratory accelerations for a truck semi-trailer bed with light loads (less than 15 tons) is provided in Table 2 of ANSI N14.23. The component accelerations are given in Table 2 as 1.3g longitudinally, 0.5g laterally, and 2.0g vertically. Three fully loaded TRUPACT-II packages on a single trailer will exceed the light load limit, but acceleration magnitudes associated with light loads are conservative for heavy loads per Table 2 of ANSI N14.23. The commentary provided within Section 4.2, *Package Response*, of ANSI N14.23 states that recent “tests conducted by Sandia National Laboratories have shown that the *truck bed* accelerations provide an upper bound on *cask* (response) accelerations.” Based upon these data, conservatively assume the peak acceleration values from Table 2 are applied to the TRUPACT-II package in a continuously cycling fashion.

The compressive stress in the polyurethane foam for a 2g vertical acceleration is determined by conservatively ignoring the contributory effect of the OCA outer shell and dividing a maximum weight TRUPACT-II package (19,250 pounds) by the projected area of the package’s bottom. The projected area of a TRUPACT-II package is simply  $(\pi/4)(94.375)^2 = 6,995 \text{ in}^2$ . Therefore, the compressive stress is  $(2)(19,250)/6,995 = 6 \text{ psi}$ . This stress is negligible compared to the parallel-to-rise compressive strength of 150 psi for polyurethane foam at 160 °F, as discussed in Section 2.6.1, *Heat*. Therefore, the remainder of the NCT vibration evaluation addresses only the structural steel portions of the TRUPACT-II packaging.

### 2.6.5.2 Calculation of Alternating Stresses

The TRUPACT-II package is a compact right circular cylinder. As such, the stresses developed as a result of transportation vibration become significant only where concentrated in the vicinity of the tie-downs and package interfaces with the transport vehicle. This fact allows the stress analyses of Section 2.5.2, *Tie-down Devices*, to serve as the basis for derivation of alternating stress estimates.

The analyses of Section 2.5.2, *Tie-down Devices*, identify three maximum stress locations of importance in the immediate vicinity of the tie-down lugs:

- 1. Tie-down lug weld shear stresses due to tensile tie-down forces.** Under a combined set of tie-down forces (i.e., 10g longitudinally, 5g laterally, and 2g vertically), the tie-down lug vertical tensile force is  $F_{t\text{-max}} = 94,531$  pounds. The corresponding tie-down lug weld shear stress is  $\tau = 12,334$  psi, from Section 2.5.2.2.1, *Failure of the Tie-down Lug Welds Due to Shear and Bending Loads*. Weld shear stresses associated with unit accelerations (i.e., 1g) are derived from these values, as presented in Table 2.6-10. Under unit horizontal and vertical accelerations, the maximum weld shear stresses are 991 psi and 628 psi, respectively, as shown in Table 2.6-10.

---

<sup>8</sup> ANSI N14.23, *Design Basis for Resistance to Shock and Vibration of Radioactive Material Packages Greater than One Ton in Truck Transport* (Draft), 1980, American National Standards Institute, Inc. (ANSI).

**2. OCA outer shell compressive membrane stresses due to vertical compressive loads.**

Under a combined set of tie-down forces (i.e., 10g longitudinally, 5g laterally, and 2g vertically), the OCA outer shell and tie-down lug doubler plate vertical compressive load is  $F_{c-max} = 179,509$  pounds. The corresponding compressive membrane stress is  $\sigma_c = 17,260$  psi, from Section 2.5.2.3.1, *Bearing Stress in the OCA Outer Shell and Tie-down Lug Doubler Plate*. Compressive membrane stresses associated with unit accelerations (i.e., 1g) are derived from these values, as presented in Table 2.6-11. Under unit horizontal and vertical accelerations, the maximum membrane compression stresses are 1,461 psi and 463 psi, respectively, as shown in Table 2.6-11.

**3. OCA tie-down weldment compressive membrane stresses due to horizontal compressive loads.**

Under a combined set of tie-down forces (i.e., 10g longitudinally, 5g laterally, and 2g vertically), the OCA tie-down weldment horizontal compressive load is  $F_h = 215,222$  pounds. The corresponding compressive membrane stress is  $\sigma_c = 26,903$  psi, from Section 2.5.2.4.1, *Bearing Stress in the Tie-down Weldment*. Compressive membrane stresses associated with unit accelerations (i.e., 1g) are derived from these values, as presented in Table 2.6-12. Under unit horizontal accelerations, the maximum membrane compression stress is 2,406 psi, as shown in Table 2.6-12.

Alternating stress intensities,  $S_{alt}$ , due to 1g unit accelerations, are calculated directly from the above values since there are no other measurable stresses acting on the package at the locations considered. Unit alternating stress intensities at the three evaluated locations are found as shown in Table 2.6-13, making use of the definition of alternating stress intensity as one-half of the range of stress intensity at the location of interest, and the definition of stress intensity as twice the shear stress.

These maximum alternating stress intensity unit values correspond to the bearing stress in the tie-down weldment (horizontal component) and shear stress in the tie-down lug weld (vertical component). A stress concentration factor of four is conservatively applied in accordance with Paragraph C.3.d of Regulatory Guide 7.6. Normalizing the unit values to the peak acceleration estimates given in Section 2.6.5.1, *Vibratory Loads Determination*, and including the stress concentration factor of four and assuming these worst cases occur at the same location, results in the following conservative estimates of alternating stress intensity associated with the vibratory environments.

For the maximum horizontal alternating stress intensity of 1,203 psi from Table 2.6-13:

$$S_{alt} = 4(1,203)\sqrt{(1.3)^2 + (0.5)^2} = 6,702 \text{ psi}$$

and for the maximum vertical alternating stress intensity of 628 psi from Table 2.6-13:

$$S_{alt} = 4(628)(2.0) = 5,024 \text{ psi}$$

Assuming a simultaneous application of the above alternating stress intensities associated with horizontal and vertical loads yields a maximum alternating stress of  $6,702 + 5,024 = 11,726$  psi.

### 2.6.5.3 Stress Limits and Results

The permissible alternating stress intensity,  $S_a$ , is given by conservatively using the minimum asymptotic value from the design fatigue curves in Table I-9.2.2 of the ASME Boiler and

Pressure Vessel Code<sup>9</sup>. For design fatigue curve C at  $10^{11}$  cycles,  $S_a = 13,600$  psi, based on an elastic modulus of  $28.3(10)^6$  psi. This value, when multiplied by the ratio of the elastic modulus at 160 °F of  $27.8(10)^6$  psi to an elastic modulus at 70 °F of  $28.3(10)^6$  psi results in an allowable alternating stress intensity amplitude at 160 °F of:

$$S_a = 13,600 \left( \frac{27.8}{28.3} \right) = 13,360 \text{ psi}$$

Finally, a conservative estimate of the margin of safety for vibratory effects becomes:

$$MS = \frac{S_a}{S_{alt}} - 1 = \frac{13,360}{11,726} - 1 = +0.14$$

### 2.6.6 Water Spray

The materials of construction utilized for the TRUPACT-II package are such that the water spray test identified in 10 CFR §71.71(c)(6) will have a negligible effect on the package.

### 2.6.7 Free Drop

Since the maximum gross weight of the TRUPACT-II package is 19,250 pounds, a 3-foot free drop is required per 10 CFR §71.71(c)(7). As discussed in Appendix 2.10.3, *Certification Tests*, a NCT, 3-foot side drop, aligned over the OCV vent port, was performed on a TRUPACT-II package certification test unit (CTU) as an initial condition for subsequent hypothetical accident condition (HAC) tests. Leakage rate testing following certification testing demonstrated the ability of the TRUPACT-II package to maintain leaktight (i.e.,  $1.0 \times 10^{-7}$  standard cubic centimeters per second (scc/sec), air) sealing integrity. Therefore, the requirements of 10 CFR §71.71(c)(7) are met.

### 2.6.8 Corner Drop

This test does not apply, since the package weight is in excess of 100 kg (220 pounds), and the materials do not include wood or fiberboard, as delineated in 10 CFR §71.71(c)(8).

### 2.6.9 Compression

This test does not apply, since the package weight is in excess of 5,000 kg (11,000 pounds), as delineated in 10 CFR §71.71(c)(9).

### 2.6.10 Penetration

The one-meter (40-inch) drop of a 13-pound, hemispherically-headed, 1¼-inch diameter, steel cylinder, as delineated in 10 CFR §71.71(c)(10), is of negligible consequence to the TRUPACT-II package. This is due to the fact that the TRUPACT-II package is designed to minimize the consequences associated with the much more limiting case of a 40-inch drop of the entire package

<sup>9</sup> American Society of Mechanical Engineers (ASME) Boiler and Pressure Vessel Code, Section III, *Rules for Construction of Nuclear Power Plant Components*, Appendix I, *Design Stress Intensity Values, Allowable Stresses, Material Properties, and Design Fatigue Curves*, 1986 Edition.

onto a puncture bar as discussed in Section 2.7.3, *Puncture*. The 1/4-inch minimum thickness, OCA outer shell, the tie-down lugs and doubler plates, and the vent port and seal test port penetrations are not damaged by the penetration event.

**Table 2.6-1 – Summary of Stress Intensity Results for OCA Load Case 1<sup>①</sup>**

Component	Location	Stress Intensity (psi)			
		General Primary Membrane ( $P_m$ )	Local Primary Membrane ( $P_L$ )	Primary Membrane + Bending ( $P_{m/L} + P_b$ )	Primary Plus Secondary ( $P_{m/L} + P_b + Q$ )
OCV Shells	Cylindrical and Conical Shells	16,170 (Element 336)	----	17,338 (Element 340)	----
OCV Lower Torispherical Head	Crown	10,971 (Element 318)	----	15,300 (Element 317)	----
	Knuckle	----	24,769 (Element 320)	----	35,850 (Element 320)
OCV Upper Torispherical Head	Crown	13,360 (Element 347)	----	18,672 (Element 348)	----
	Knuckle	----	27,990 (Element 345)	----	37,978 (Element 345)
OCV Upper and Lower Seal Flanges	Shell side of the thickness transition	----	----	30,810 (Node 2010)	----
	Flange side of the thickness transition	----	----	18,460 (Node 2016)	----
OCV Locking Ring	Any location	----	----	23,040 (Node 3050)	----
OCA Outer Shell and Z-flanges	Any location	7,986 (Element 414)	----	13,642 (Element 414)	----
Maximum Stress Intensity		16,170	27,990	30,810	37,978
Allowable Stress Intensity		20,000 ( $S_m$ )	30,000 ( $1.5S_m$ )	30,000 ( $1.5S_m$ )	60,000 ( $3.0S_m$ )
Minimum Design Margin		+0.24	+0.07	-0.03 <sup>②</sup>	+0.58

**Notes:**

- ① 64.7 psia internal pressure, 3.5 psia external pressure; without differential thermal expansion (i.e., the uniform temperature is 160 °F and the reference temperature is 160 °F).
- ② Although slightly above the allowable stress intensity, this result is within the accuracy of the ANSYS<sup>®</sup> finite element model which itself is affected by element mesh size and element aspect ratio. In addition, actual pressure testing to 150% of the design pressure of 50 psig (75 psig) during the certification test program resulted in an acceptable nondestructive examination and no permanent dimensional changes to the OCV structure.

**Table 2.6-2 – Summary of Stress Intensity Results for OCA Load Case 2<sup>①</sup>**

Component	Location	Stress Intensity (psi)			
		General Primary Membrane ( $P_m$ )	Local Primary Membrane ( $P_L$ )	Primary Membrane + Bending ( $P_{m/L} + P_b$ )	Primary Plus Secondary ( $P_{m/L} + P_b + Q$ )
OCV Shells	Cylindrical and Conical Shells	----	----	----	14,954 (Element 324)
OCV Lower Torispherical Head	Crown	----	----	----	18,000 (Element 317)
	Knuckle	----	----	----	39,520 (Element 320)
OCV Upper Torispherical Head	Crown	----	----	----	18,514 (Element 348)
	Knuckle	----	----	----	37,490 (Element 345)
OCV Upper and Lower Seal Flanges	Shell side of the thickness transition	----	----	----	27,650 (Node 2010)
	Flange side of the thickness transition	----	----	----	17,130 (Node 1025)
OCV Locking Ring	Any location	----	----	----	22,740 (Node 3050)
OCA Outer Shell and Z-flanges	Any location	----	----	----	20,581 (Element 406)
Maximum Stress Intensity		----	----	----	39,520
Allowable Stress Intensity		20,000 ( $S_m$ )	30,000 ( $1.5S_m$ )	30,000 ( $1.5S_m$ )	60,000 ( $3.0S_m$ )
Minimum Design Margin		----	----	----	+0.52

**Notes:**

- ① 64.7 psia internal pressure, 3.5 psia external pressure; with differential thermal expansion (i.e., the uniform temperature is 160 °F and the reference temperature is 70 °F).

**Table 2.6-3 – Summary of Stress Intensity Results for OCA Load Case 3<sup>ⓐ</sup>**

Component	Location	Stress Intensity (psi)			
		General Primary Membrane ( $P_m$ )	Local Primary Membrane ( $P_L$ )	Primary Membrane + Bending ( $P_{m/L} + P_b$ )	Primary Plus Secondary ( $P_{m/L} + P_b + Q$ )
OCV Shells	Cylindrical and Conical Shells	-----	-----	-----	14,746 (Element 331)
OCV Lower Torispherical Head	Crown	-----	-----	-----	3,048 (Element 317)
	Knuckle	-----	-----	-----	2,587 (Element 323)
OCV Upper Torispherical Head	Crown	-----	-----	-----	580 (Element 354)
	Knuckle	-----	-----	-----	3,677 (Element 342)
OCV Upper and Lower Seal Flanges	Shell side of the thickness transition	-----	-----	-----	682 (Node 2005)
	Flange side of the thickness transition	-----	-----	-----	543 (Node 2121)
OCV Locking Ring	Any location	-----	-----	-----	7 (Node 3006)
OCA Outer Shell and Z-flanges	Any location	-----	-----	-----	2,969 (Element 414)
Maximum Stress Intensity		-----	-----	-----	14,746
Allowable Stress Intensity		20,000 ( $S_m$ )	30,000 ( $1.5S_m$ )	30,000 ( $1.5S_m$ )	60,000 ( $3.0S_m$ )
Minimum Design Margin		-----	-----	-----	+3.07

Notes:

- ⓐ 14.7 psia internal pressure, 14.7 psia external pressure; with differential thermal expansion (i.e., the uniform temperature is -40 °F and the reference temperature is 70 °F).

**Table 2.6-4 – Summary of Stress Intensity Results for OCA Load Case 4<sup>①</sup>**

Component	Location	Stress Intensity (psi)			
		General Primary Membrane ( $P_m$ )	Local Primary Membrane ( $P_L$ )	Primary Membrane + Bending ( $P_{m/L} + P_b$ )	Primary Plus Secondary ( $P_{m/L} + P_b + Q$ )
OCV Shells	Cylindrical and Conical Shells	4,621 (Element 336)	-----	4,880 (Element 336)	-----
OCV Lower Torispherical Head	Crown	2,780 (Element 318)	-----	4,283 (Element 317)	-----
	Knuckle	-----	6,330 (Element 320)	-----	9,219 (Element 320)
OCV Upper Torispherical Head	Crown	3,328 (Element 347)	-----	4,565 (Element 348)	-----
	Knuckle	-----	6,843 (Element 345)	-----	9,322 (Element 345)
OCV Upper and Lower Seal Flanges	Shell side of the thickness transition	-----	-----	-----	3,534 (Node 1016)
	Flange side of the thickness transition	-----	-----	4,103 (Node 1164)	-----
OCV Locking Ring	Any location	-----	-----	51 (Node 3148)	-----
OCA Outer Shell and Z-flanges	Any location	860 (Element 414)	-----	1,343 (Element 414)	-----
Maximum Stress Intensity		4,621	6,843	4,880	9,322
Allowable Stress Intensity		20,000 ( $S_m$ )	30,000 ( $1.5S_m$ )	30,000 ( $1.5S_m$ )	60,000 ( $3.0S_m$ )
Minimum Design Margin		+3.33	+3.38	+5.15	+5.44

Notes:

- ① 0.0 psia internal pressure, 14.7 psia external pressure; without differential thermal expansion (i.e., the uniform temperature is 70 °F and the reference temperature is 70 °F).

**Table 2.6-5 – Summary of Stress Intensity Results for ICV Load Case 1<sup>①</sup>**

Component	Location	Stress Intensity (psi)			
		General Primary Membrane ( $P_m$ )	Local Primary Membrane ( $P_L$ )	Primary Membrane + Bending ( $P_{m/L} + P_b$ )	Primary Plus Secondary ( $P_{m/L} + P_b + Q$ )
ICV Shells	Cylindrical Shells	14,827 (Element 364)	-----	21,441 (Element 365)	-----
ICV Lower Torispherical Head	Crown	14,712 (Element 299)	-----	18,910 (Element 298)	-----
	Knuckle	-----	25,853 (Element 302)	-----	36,741 (Element 301)
ICV Upper Torispherical Head	Crown	15,236 (Element 376)	-----	19,483 (Element 377)	-----
	Knuckle	-----	26,935 (Element 373)	-----	38,280 (Element 374)
ICV Upper and Lower Seal Flanges	Shell side of the thickness transition	-----	-----	31,310 (Node 2058)	-----
	Flange side of the thickness transition	-----	-----	25,930 (Node 2053)	-----
ICV Locking Ring	Any location	-----	-----	21,030 (Node 3046)	-----
Maximum Stress Intensity		15,236	26,935	31,310	38,280
Allowable Stress Intensity		20,000 ( $S_m$ )	30,000 ( $1.5S_m$ )	30,000 ( $1.5S_m$ )	60,000 ( $3.0S_m$ )
Minimum Design Margin		+0.31	+0.11	-0.04 <sup>②</sup>	+0.57

**Notes:**

- ① 64.7 psia internal pressure, 3.5 psia external pressure; without differential thermal expansion (i.e., the uniform temperature is 160 °F and the reference temperature is 160 °F).
- ② Although slightly above the allowable stress intensity, this result is within the accuracy of the ANSYS<sup>®</sup> finite element model which itself is affected by element mesh size and element aspect ratio. In addition, actual pressure testing to 150% of the design pressure of 50 psig (75 psig) during the certification test program resulted in an acceptable nondestructive examination and no permanent dimensional changes to the ICV structure.

**Table 2.6-6 – Summary of Stress Intensity Results for ICV Load Case 2<sup>①</sup>**

Component	Location	Stress Intensity (psi)			
		General Primary Membrane ( $P_m$ )	Local Primary Membrane ( $P_L$ )	Primary Membrane + Bending ( $P_{m/L} + P_b$ )	Primary Plus Secondary ( $P_{m/L} + P_b + Q$ )
ICV Shells	Cylindrical Shells	2,354 (Element 363)	-----	2,532 (Element 364)	-----
ICV Lower Torispherical Head	Crown	3,534 (Element 299)	-----	4,542 (Element 298)	-----
	Knuckle	-----	6,210 (Element 302)	-----	8,825 (Element 301)
ICV Upper Torispherical Head	Crown	3,636 (Element 376)	-----	4,650 (Element 377)	-----
	Knuckle	-----	6,382 (Element 373)	-----	9,105 (Element 374)
ICV Upper and Lower Seal Flanges	Shell side of the thickness transition	-----	-----	-----	2,577 (Node 2054)
	Flange side of the thickness transition	-----	-----	3,561 (Node 1129)	-----
ICV Locking Ring	Any location	-----	-----	10 (Node 3141)	-----
Maximum Stress Intensity		3,636	6,382	4,650	9,105
Allowable Stress Intensity		20,000 ( $S_m$ )	30,000 ( $1.5S_m$ )	30,000 ( $1.5S_m$ )	60,000 ( $3.0S_m$ )
Minimum Design Margin		+4.50	+3.70	+5.45	+5.59

**Notes:**

- ① 0.0 psia internal pressure, 14.7 psia external pressure; without differential thermal expansion (i.e., the uniform temperature is 70 °F and the reference temperature is 70 °F).

**Table 2.6-7 – Buckling Geometry Parameters per Code Case N-284**

<b>Geometry and Material Input</b>		
	<b>ICV</b>	<b>OCV</b>
Mean Radius, inch	36.44	36.91
Shell Thickness, inch	0.25	0.188
Length, inch	65.70 <sup>①</sup>	32.67 <sup>②</sup>
<b>Geometry Output (nomenclature consistent with ASME Code Case N-284)</b>		
R =	36.44	36.91
t =	0.25	0.188
$(Rt)^{1/2} =$	3.018	2.634
$\ell_{\phi} =$	65.70	32.67
$\ell_{\theta} =$	229.0	231.9
$M_{\phi} =$	21.77	12.40
$M_{\theta} =$	75.87	88.03
M =	21.77	12.40

Notes:

- ① The ICV length is conservatively measured from five inches below the top of the lower ICV seal flange (at the beginning of the 1/4-inch wall thickness) to an assumed support point located one-third of the depth of the lower ICV torispherical head below the head-to-shell interface.
- ② The OCV length is conservatively measured from the ring stiffener to an assumed support point located one-third of the depth of the lower OCV torispherical head below the head-to-shell interface. This length assumes that the ring stiffener is sized per the requirements in Paragraphs -1714.1(a) and -1714.1(b)(1) of ASME Code Case N-284.

**Table 2.6-8 – Stress Results for 14.7 psig External Pressure**

ICV		OCV	
Axial Stress, $\sigma_\phi$	1,071	Axial Stress, $\sigma_\phi$	1,443
Hoop Stress, $\sigma_\theta$	2,143	Hoop Stress, $\sigma_\theta$	2,886

**Table 2.6-9 – Shell Buckling Summary for 14.7 psig External Pressure**

Condition	ICV	OCV	Remarks
<b>Capacity Reduction Factors (-1511)</b>			
$\alpha_{\phi L} =$	0.2670	0.2670	
$\alpha_{\theta L} =$	0.8000	0.8000	
<b>Plasticity Reduction Factors (-1610)</b>			
$\eta_\phi =$	1.0000	1.0000	
$\eta_\theta =$	1.0000	1.0000	
<b>Theoretical Buckling Values (-1712.1.1)</b>			
$C_\phi =$	0.6050	0.6050	
$\sigma_{\phi eL} =$	117,464 psi	87,208 psi	
$C_{\theta h} =$	0.0435	0.0782	
$\sigma_{\theta eL} = \sigma_{heL} =$	8,452 psi	11,273 psi	
<b>Elastic Interaction Equations (-1713.1.1)</b>			
$\sigma_{\phi s} =$	8,022 psi	10,809 psi	
$\sigma_{\theta s} =$	5,358 psi	7,215 psi	
Axial + Hoop $\Rightarrow$ Check (a):	N/A	N/A	
Axial + Hoop $\Rightarrow$ Check (b):	0.435	0.473	<1.0 OK

**Table 2.6-10 – Tie-Down Lug Weld Shear Stresses**

Case and Orientation	Load Factors (gs)	Load (pounds)	Shear Stress (psi)
Combined	10(x), 5(y), 2(z)	94,531	12,334
Horizontal	$[10^2 + 5^2]^{1/2} = 11.18$ (unit horizontal of 1g)	84,906 (7,594)	11,079 (991)
Vertical	2.00 (unit vertical of 1g)	9,625 (4,813)	1,255 (628)

**Table 2.6-11 – OCA Outer Shell Compressive Membrane Stresses**

Case and Orientation	Load Factors (gs)	Load (pounds)	Membrane Stress (psi)
Combined	10(x), 5(y), 2(z)	179,509	17,260
Horizontal	$[10^2 + 5^2]^{1/2} = 11.18$ (unit horizontal of 1g)	169,884 (15,195)	16,334 (1,461)
Vertical	2.00 (unit vertical of 1g)	9,625 (4,813)	925 (463)

**Table 2.6-12 – OCA Tie-down Weldment Compressive Membrane Stresses**

Case and Orientation	Load Factors (gs)	Load (pounds)	Membrane Stress (psi)
Horizontal	$[10^2 + 5^2]^{1/2} = 11.18$ (unit horizontal of 1g)	215,222 (19,250)	26,903 (2,406)

**Table 2.6-13 – Maximum Unit Alternating Stress Intensities**

Case and Orientation	Alternating Stress Intensity
Lug Weld Shear	$S_{alt} = \frac{2\tau_{max}}{2} = 991 \text{ psi, Horizontal}$ $= 628 \text{ psi, Vertical}$
OCA Shell Compression	$S_{alt} = \frac{\sigma_{max}}{2} = 731 \text{ psi, Horizontal}$ $= 232 \text{ psi, Vertical}$
OCA Base Compression	$S_{alt} = \frac{\sigma_{max}}{2} = 1,203 \text{ psi, Horizontal}$
Maximum Unit Values	$= 1,203 \text{ psi, Horizontal}$ $= 628 \text{ psi, Vertical}$

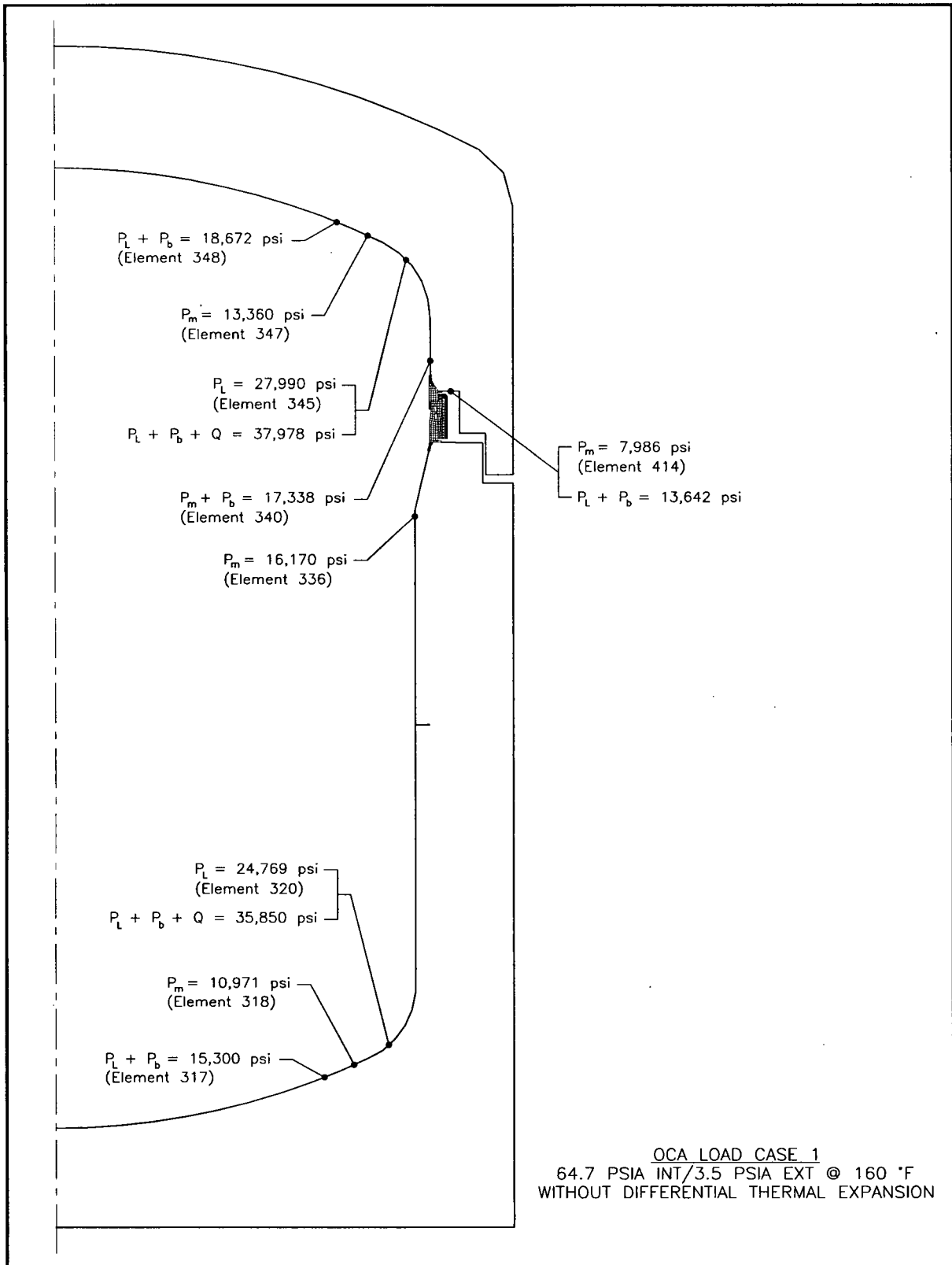
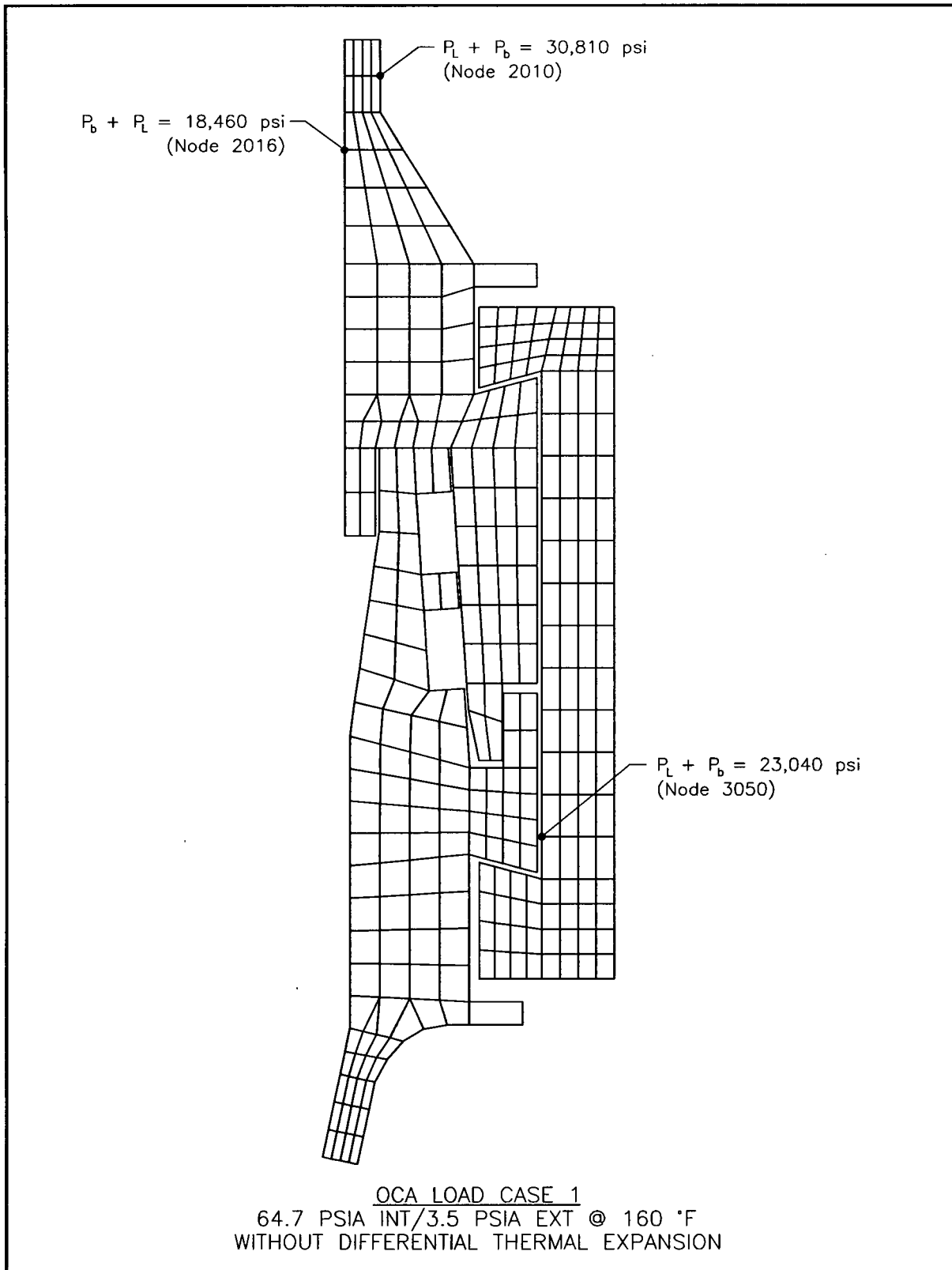


Figure 2.6-1 – OCA Load Case 1, Overall Model



**Figure 2.6-2 – OCA Load Case 1, Seal Region Detail**

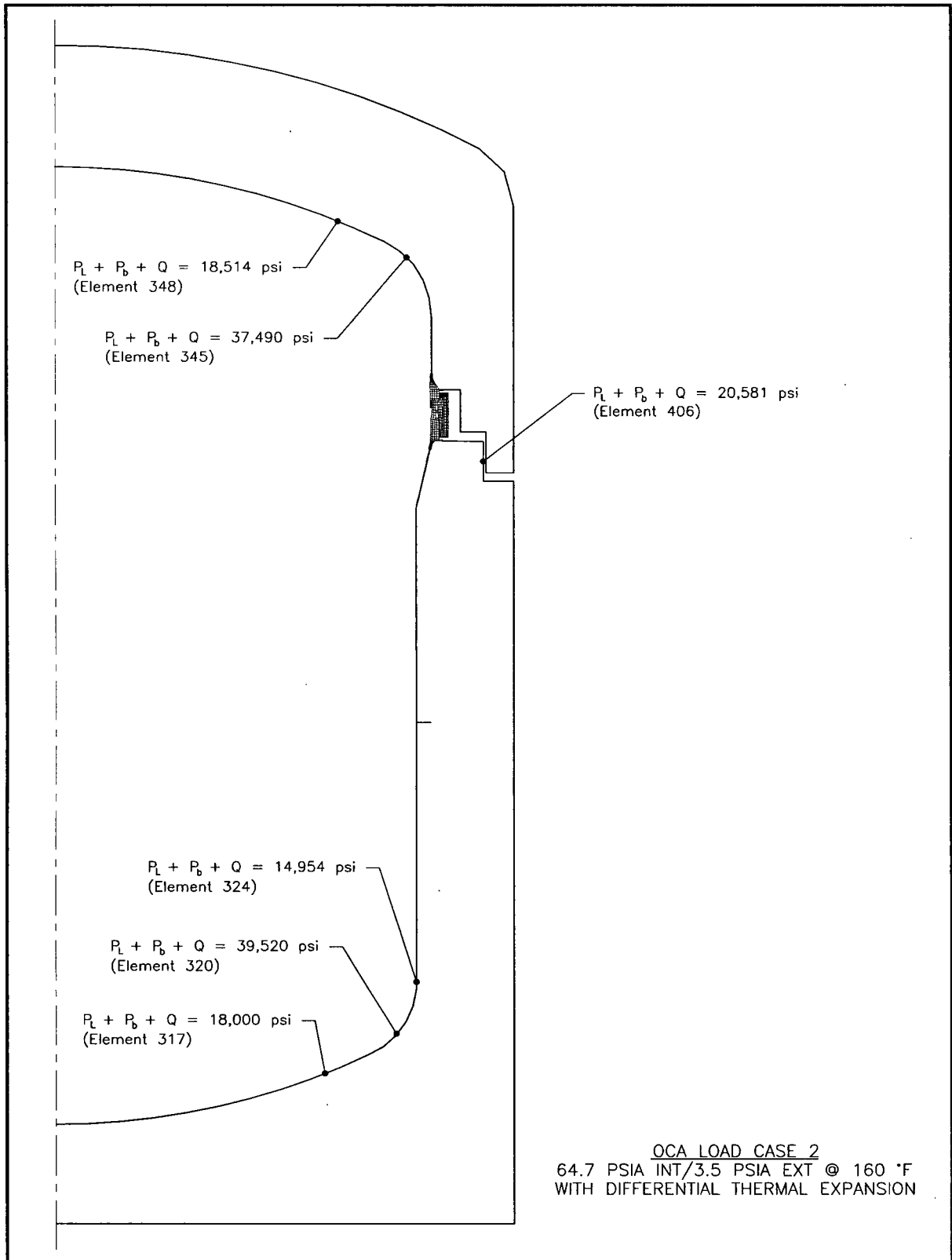


Figure 2.6-3 – OCA Load Case 2, Overall Model

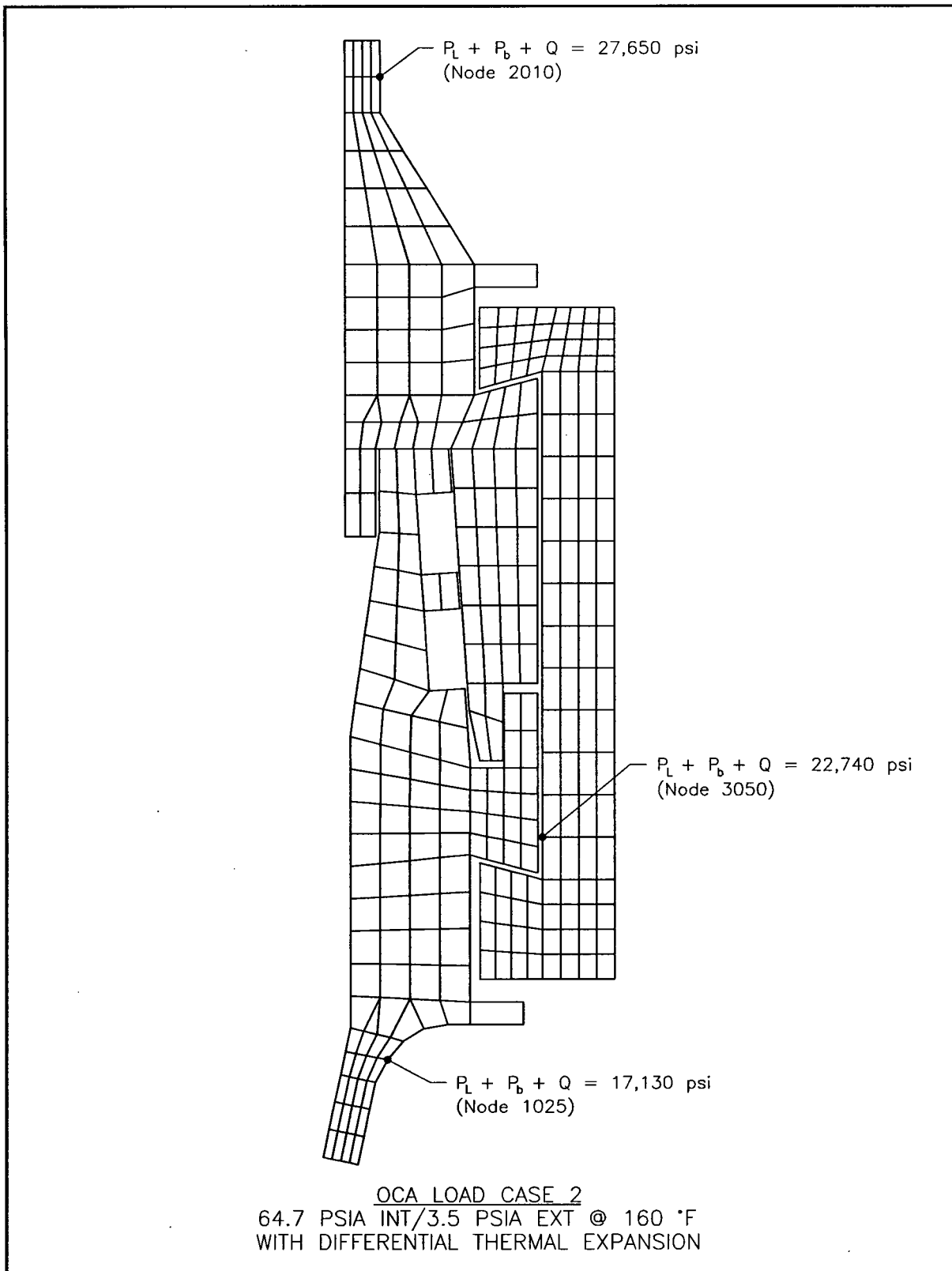


Figure 2.6-4 – OCA Load Case 2, Seal Region Detail

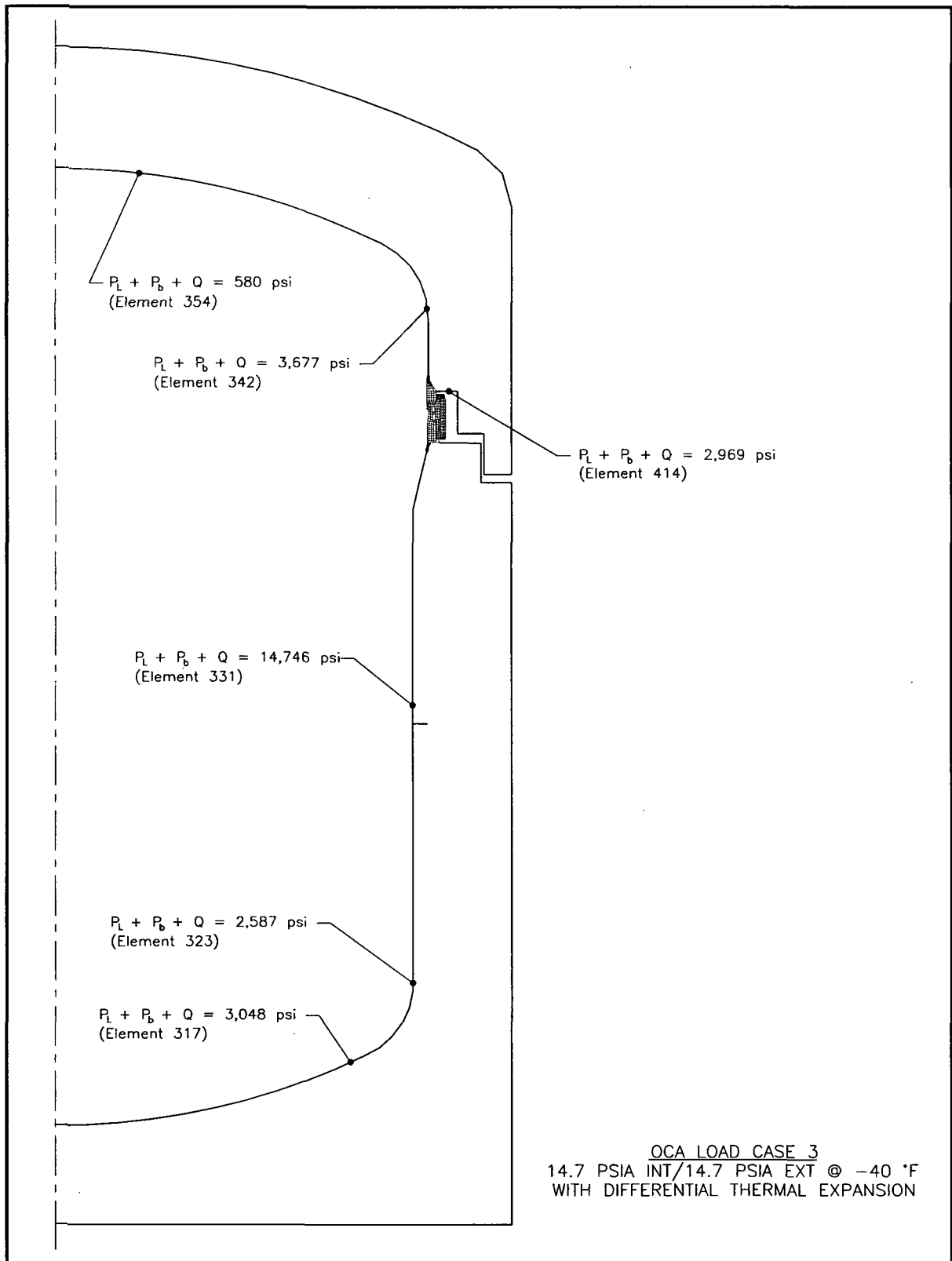


Figure 2.6-5 – OCA Load Case 3, Overall Model

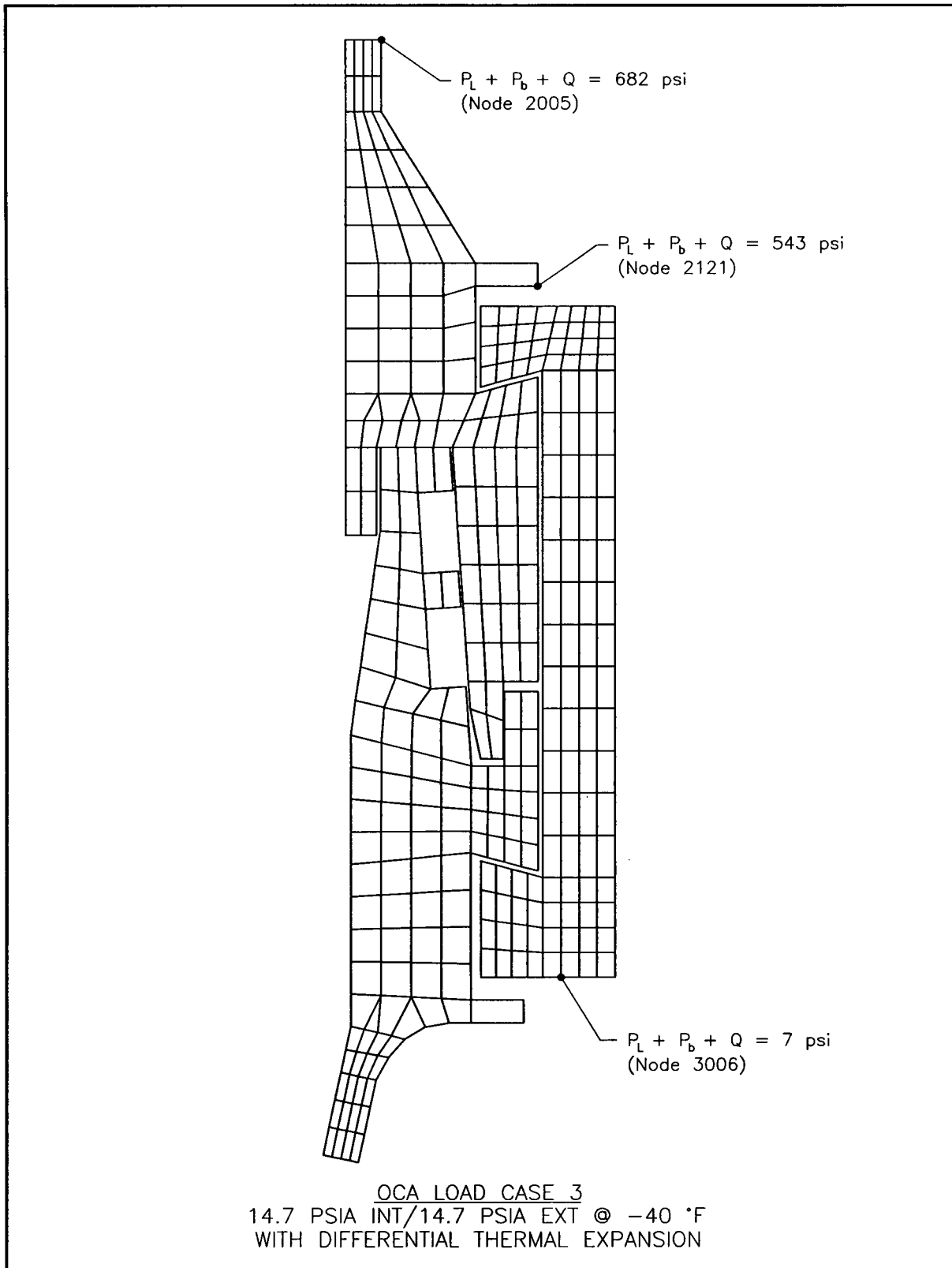


Figure 2.6-6 – OCA Load Case 3, Seal Region Detail

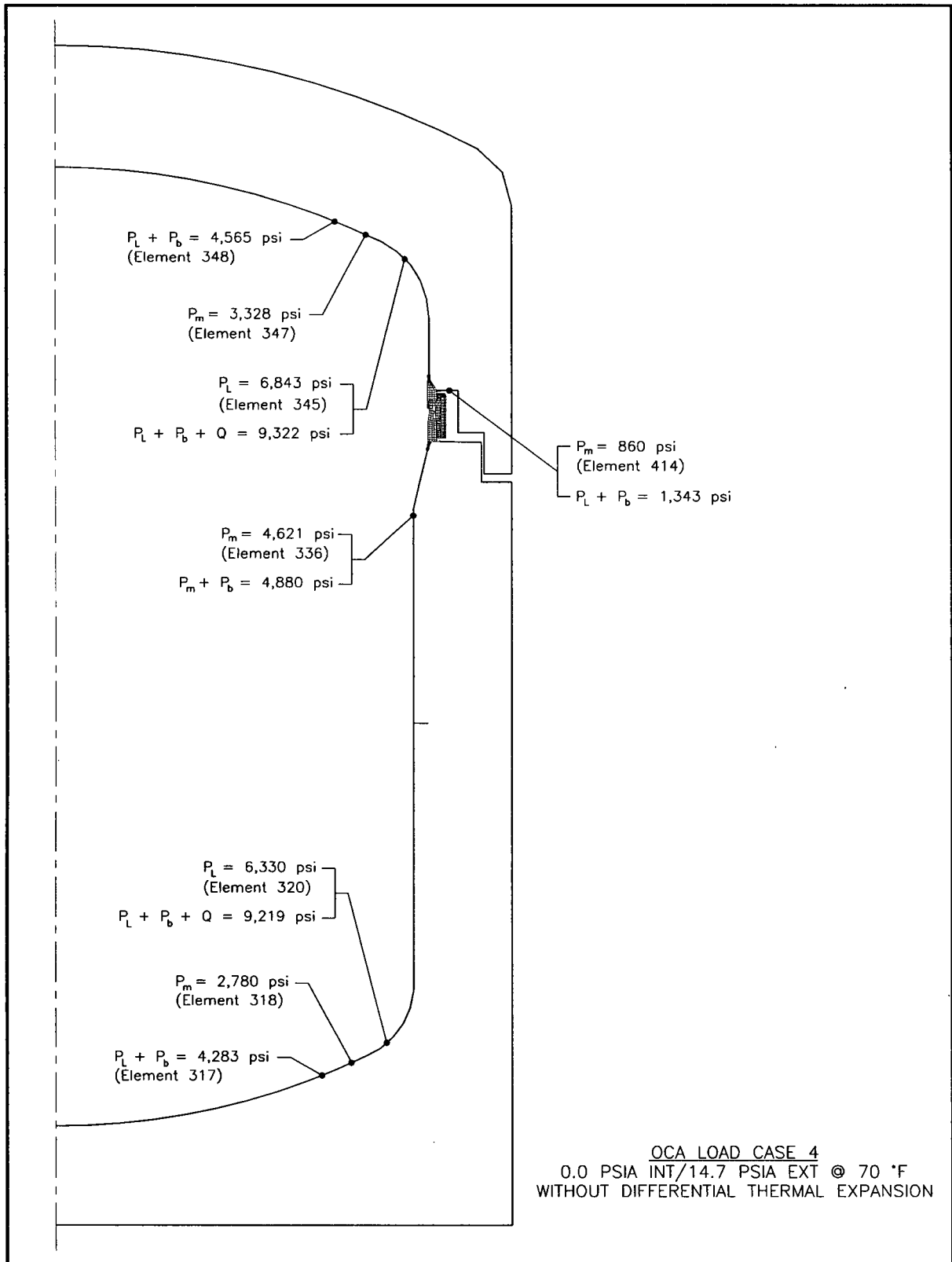
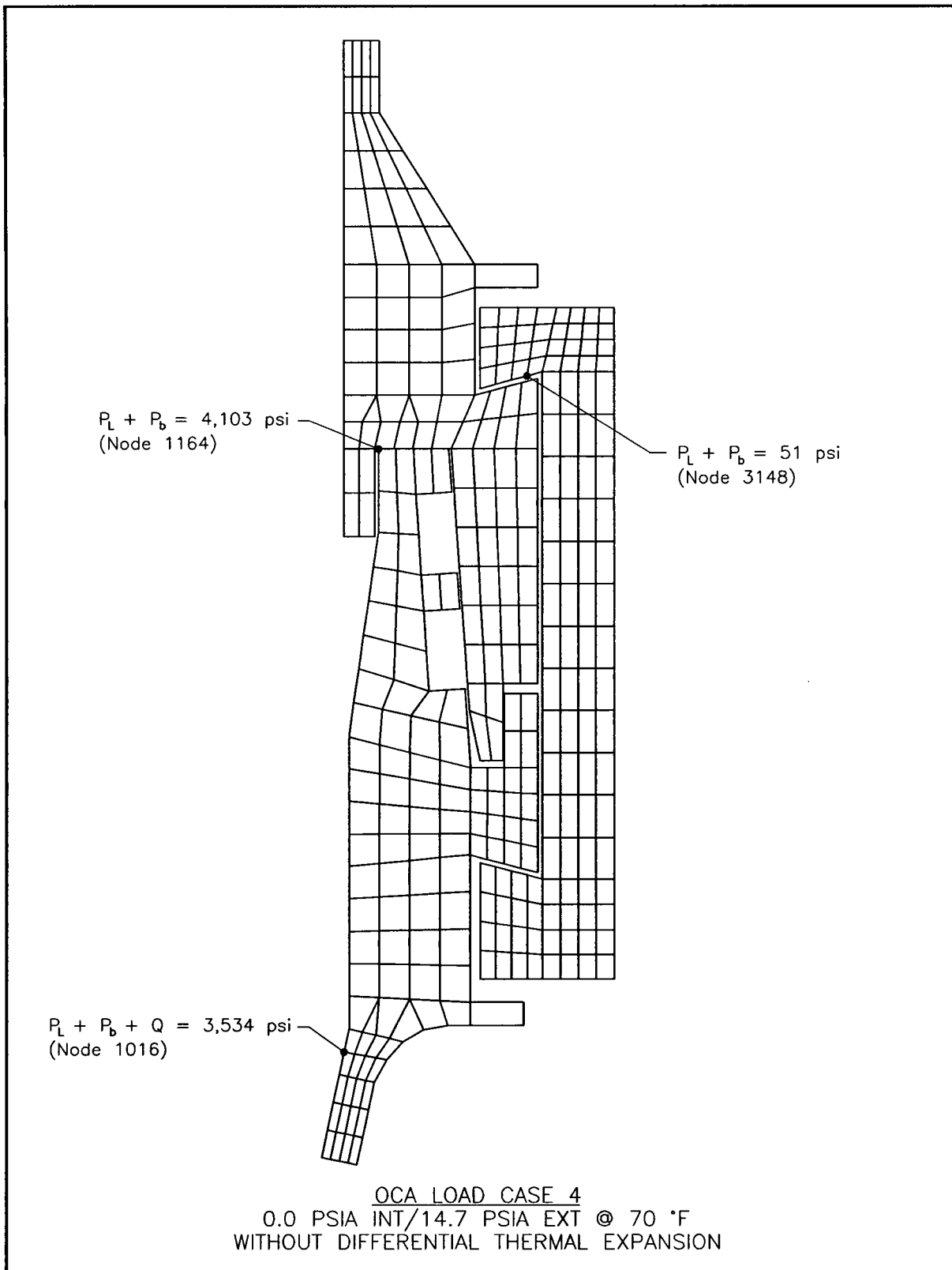


Figure 2.6-7 – OCA Load Case 4, Overall Model



**Figure 2.6-8 – OCA Load Case 4, Seal Region Detail**

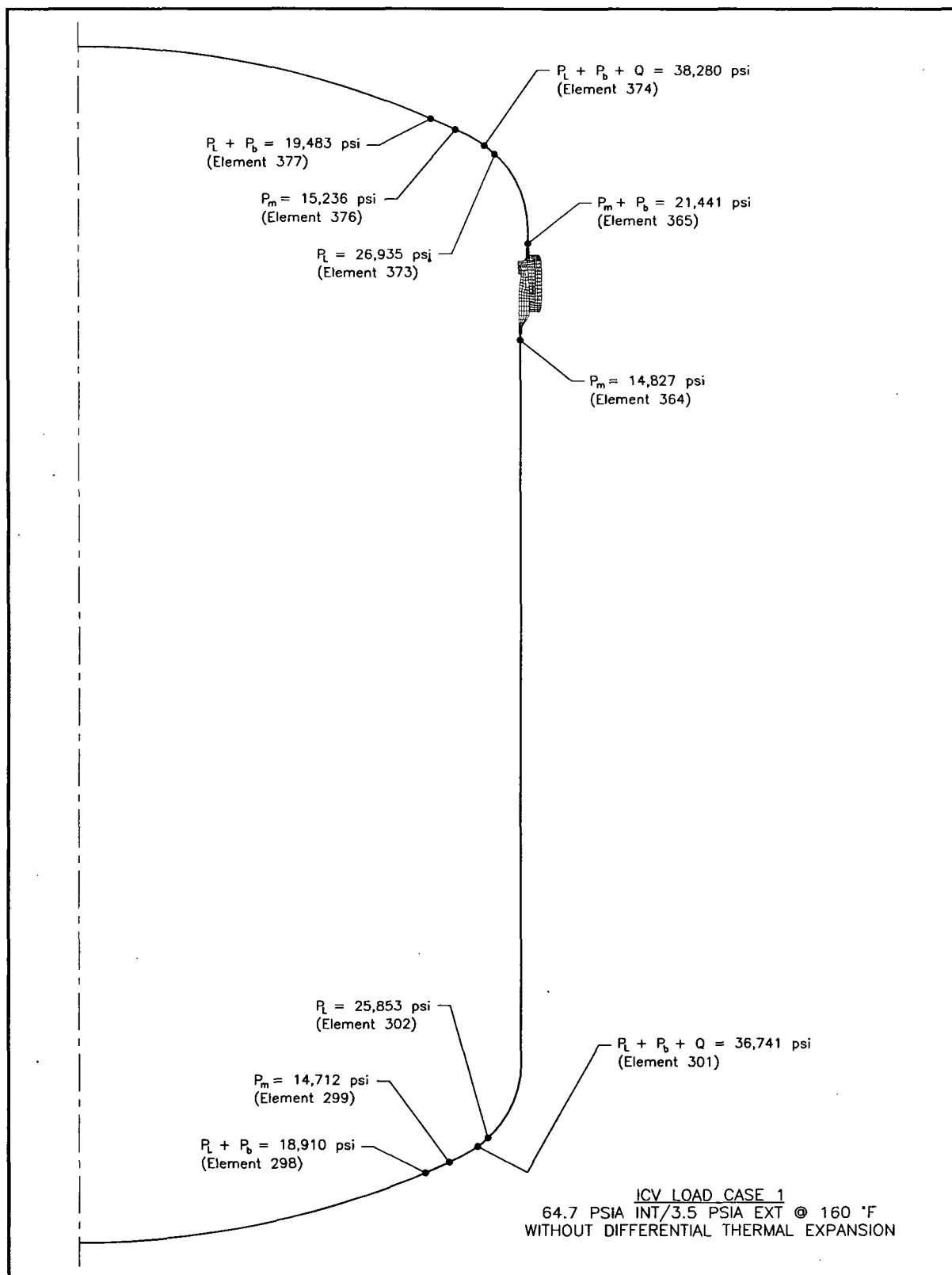
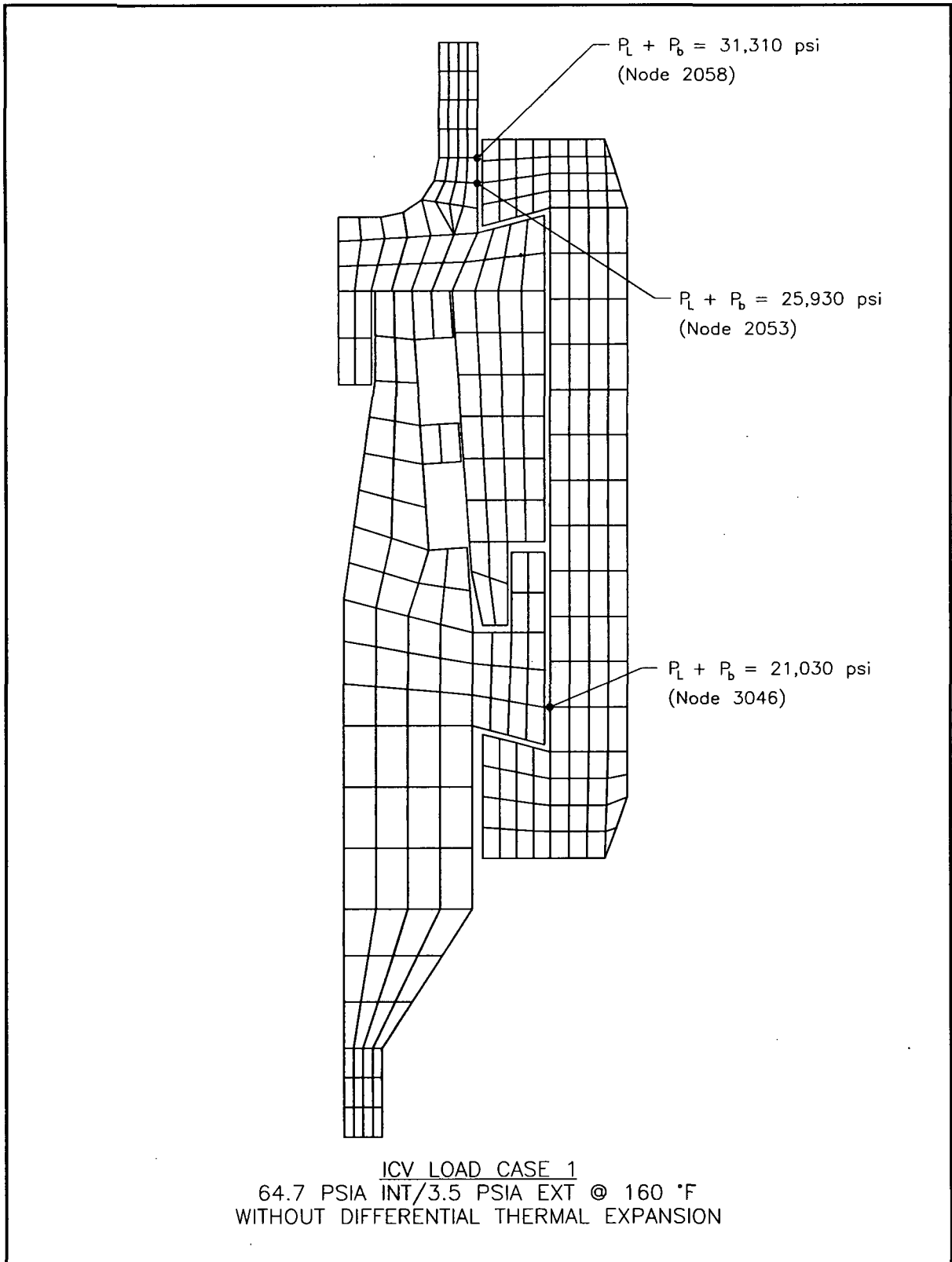


Figure 2.6-9 – ICV Load Case 1, Overall Model



**Figure 2.6-10 – ICV Load Case 1, Seal Region Detail**

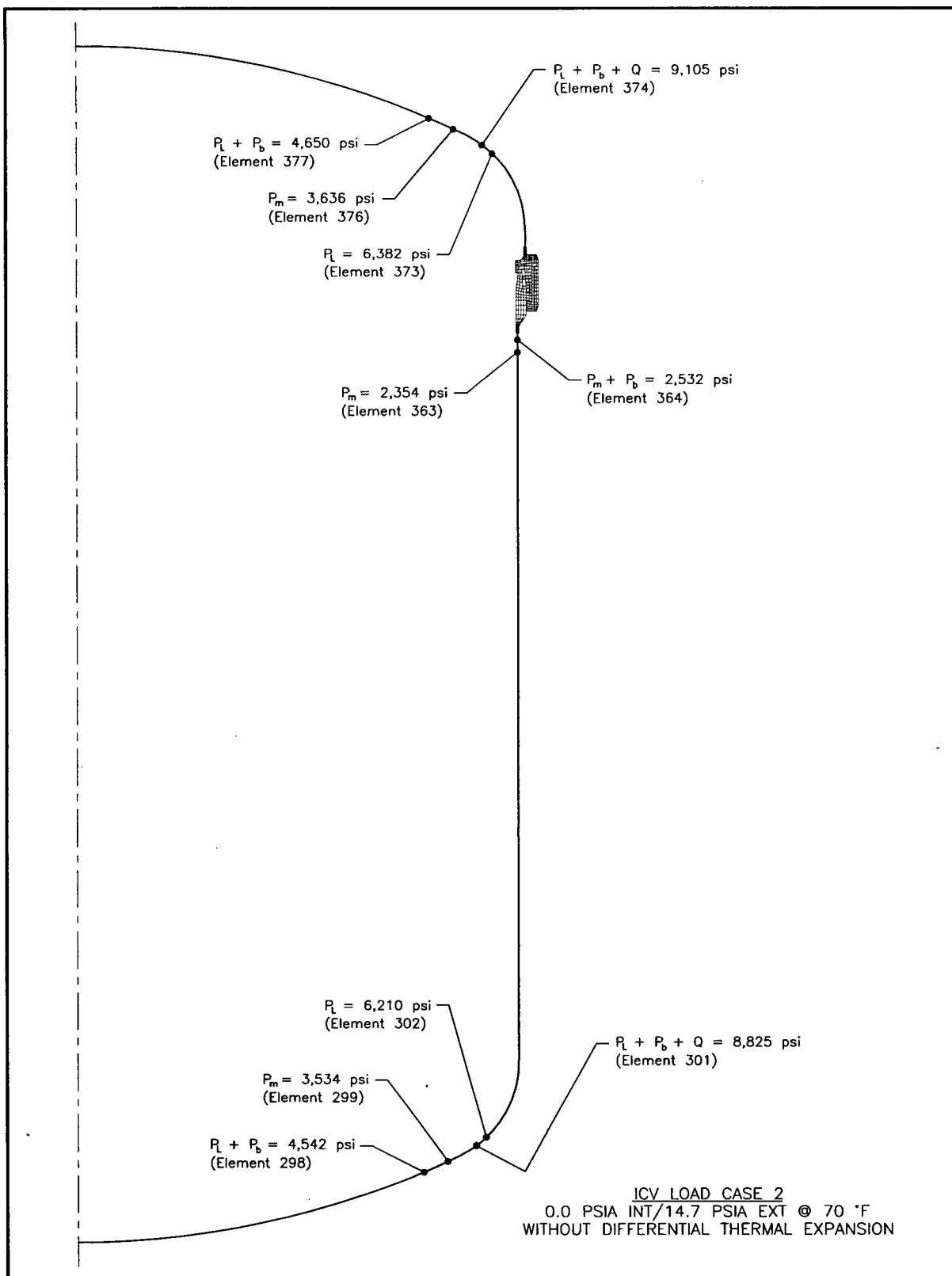


Figure 2.6-11 – ICV Load Case 2, Overall Model

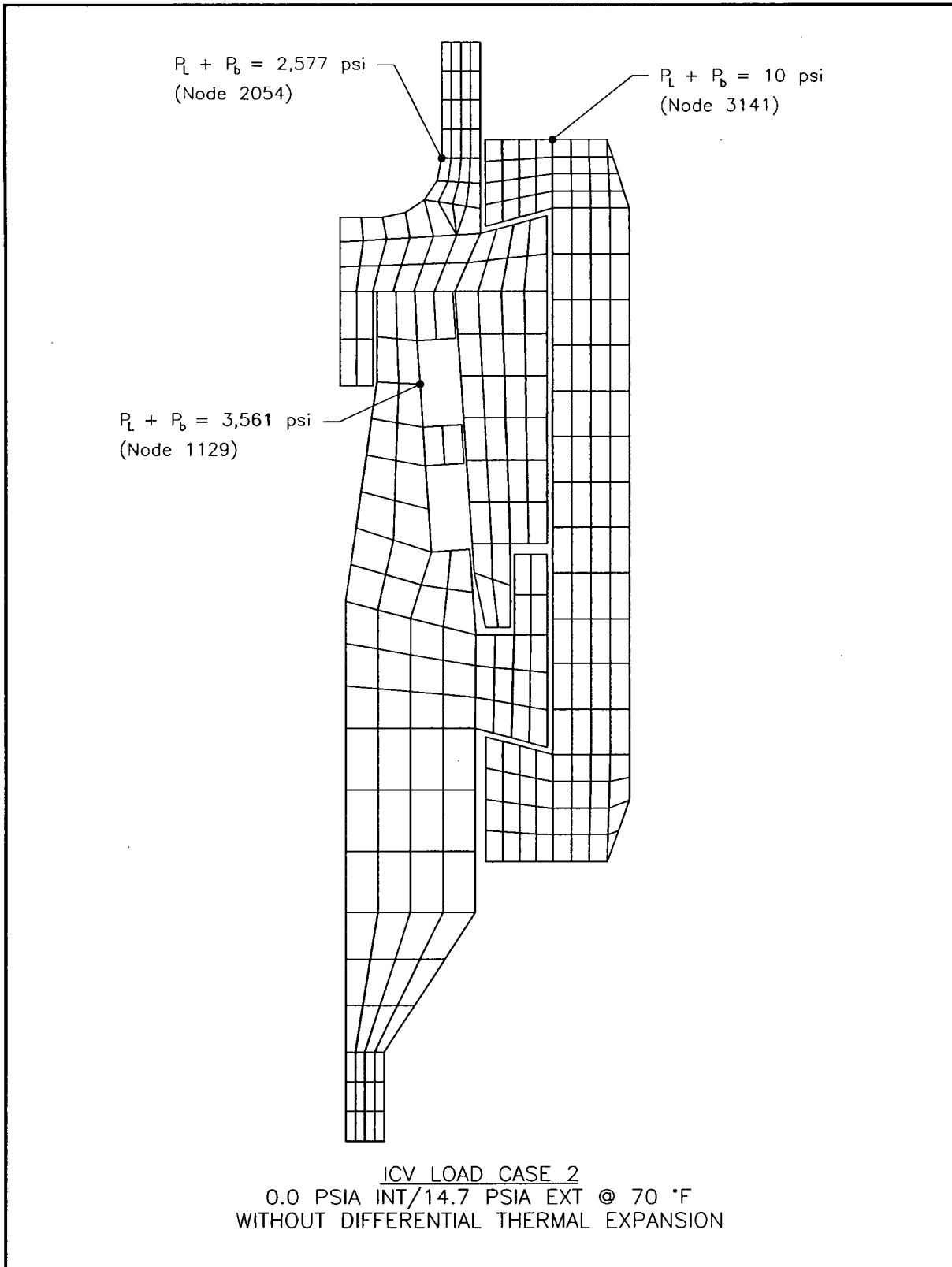


Figure 2.6-12 – ICV Load Case 2, Seal Region Detail

## 2.7 Hypothetical Accident Conditions

The TRUPACT-II package, when subjected to the sequence of hypothetical accident condition (HAC) tests specified in 10 CFR §71.73<sup>1</sup>, subsequent to the sequence of normal conditions of transport (NCT) tests specified in 10 CFR §71.71, is shown to meet the performance requirements specified in Subpart E of 10 CFR 71. As discussed in the introduction to Chapter 2.0, *Structural Evaluation*, with the exception of the immersion test, the primary proof of performance for the HAC tests is via the use of full-scale testing. Three certification test units (CTUs) were free drop, puncture, and fire tested (fire testing was not performed on the last CTU) to confirm that both the inner containment vessel (ICV) and outer containment (now confinement) vessel (OCV) boundaries remained leaktight after a worst-case HAC sequence. Observations from CTU testing confirm the conservative nature of the deformed geometry assumptions used in the criticality assessment provided in Chapter 6.0, *Criticality Evaluation*.

Test results are summarized in Section 2.7.8, *Summary of Damage*, with details provided in Appendix 2.10.3, *Certification Tests*. Immersion is addressed by analysis, employing acceptance criteria consistent with NRC Regulatory Guide 7.6<sup>2</sup>.

For the analytic assessments performed within this section, properties for Type 304 stainless steel are based on data in Table 2.3-1 from Section 2.3.1, *Mechanical Properties Applied to Analytic Evaluations*. Similarly, the bounding values for the compressive strength of polyurethane foam are based on data in Table 2.3-2 from Section 2.3.1, *Mechanical Properties Applied to Analytic Evaluations*. Polyurethane foam compressive strength is further adjusted  $\pm 15\%$  to account for manufacturing tolerance. At elevated HAC temperatures (i.e., 160 °F), the nominal compressive strength is reduced 25% for elevated temperature effects and reduced 15% for manufacturing tolerance. At reduced HAC temperatures (i.e., -20 °F), the nominal compressive strength is increased 40% for reduced temperature effects and increased 15% for manufacturing tolerance.

Properties of Type 304 stainless steel and polyurethane foam, as applied to analytic assessments within this section, are summarized below.

Material Property	Material Property Value (psi)			Reference
	-20 °F	70 °F	160 °F	
<b>Type 304 Stainless Steel</b>				
Elastic Modulus, E	$28.72 \times 10^6$	$28.3 \times 10^6$	$27.8 \times 10^6$	Table 2.3-1
Design Stress Intensity, $S_m$	20,000	20,000	20,000	
Yield Strength, $S_m$	35,000	30,000	27,000	
<b>Polyurethane Foam Compressive Strength</b>				
Parallel-to-Rise Direction, $\sigma_c$	378	235	150	Table 2.3-2
Perpendicular-to-Rise Direction, $\sigma_c$	314	195	124	

<sup>1</sup> Title 10, Code of Federal Regulations, Part 71 (10 CFR 71), *Packaging and Transportation of Radioactive Material*, 01-01-12 Edition.

<sup>2</sup> U. S. Nuclear Regulatory Commission, Regulatory Guide 7.6, *Design Criteria for the Structural Analysis of Shipping Cask Containment Vessels*, Revision 1, March 1978.

## 2.7.1 Free Drop

Subpart F of 10 CFR 71 requires performing a free drop test in accordance with the requirements of 10 CFR §71.73(c)(1). The free drop test involves performing a 30-foot HAC free drop onto a flat, essentially unyielding, horizontal surface, with the package striking the surface in a position (orientation) for which maximum damage is expected. The ability of the TRUPACT-II package to adequately withstand this specified free drop condition is demonstrated via testing of three full-scale, TRUPACT-II CTUs.

### 2.7.1.1 Technical Basis for the Free Drop Tests

To properly select a worst-case package orientation for the 30-foot free drop event, items that could potentially compromise containment integrity, shielding integrity, and/or criticality safety of the TRUPACT-II package must be clearly identified. For the TRUPACT-II package design, the foremost item to be addressed is the ability of the containment seals to remain leaktight. Shielding integrity is not a controlling case for the reasons described in Chapter 5.0, *Shielding Evaluation*. Criticality safety is conservatively evaluated based on measured physical damage to the outer containment (now confinement) assembly (OCA) shells and polyurethane foam from certification testing, as described in Chapter 6.0, *Criticality Evaluation*.

The leaktight capability of the containment seals may be compromised by two methods: 1) as a result of excessive sealing surface deformation leading to reduced seal compression, and/or 2) as a result of thermal degradation of the seal material itself in a subsequent fire event. Importantly, these methods require significant impact damage to the surrounding polyurethane foam. In other words, a significant reduction in polyurethane foam thickness or a gross exposure of the foam through splits or punctures in the OCA outer shell would have to occur near the main O-ring seal or vent port seal region.

Additional items for consideration include the possibility of separating the OCA lid from the OCA body (or significantly opening up the nominal 1/2-inch gap which exists between the upper and lower Z-flanges at the lid to body interface), and buckling of the OCV or ICV from a bottom end drop.

For the above reasons, testing must include impact orientations that affect the upper end of the TRUPACT-II package, with particularly emphasis in the closure region. Loads and resultant deformations occurring over the lower half of the package do not present a worst case regarding the leaktight capability of the seals or the separation of the OCA lid from the OCA body. However, as discussed above, a bottom end drop is of interest regarding the possibility of shell buckling because of the high axial acceleration forces imparted to the package.

In addition to package orientation, initial test conditions such as temperatures and pressures must be selected to complete the definition of the conditions existing at the time of a HAC free drop. In general, higher temperatures at the time of a drop test result in greater deformations and lesser acceleration loads than do lower temperatures. This is due primarily to the modest temperature sensitivity of the energy absorbing polyurethane foam used within the TRUPACT-II OCA.

Appendix 2.10.3, *Certification Tests*, provides a comprehensive report of the certification test process and results. Discussions specific to the configuration of the test units are provided in Appendix 2.10.3.4, *Description of the Certification Test Units*. Discussions specific to CTU test orientations for free drop, puncture, and fire tests, including initial test conditions, are provided

in Appendix 2.10.3.5, *Technical Basis for Tests*. Discussions specific to CTU test sequences for selected tests are provided in Appendix 2.10.3.6, *Test Sequence for Selected Free Drop, Puncture Drop, and Fire Tests*.

### 2.7.1.2 Test Sequence for the Selected Tests

Based on the above general discussions, the three CTUs were tested for various HAC 30-foot free drops. Although only a single “worst-case” 30-foot free drop is required by 10 CFR §71.73(c)(1), multiple 30-foot free drop tests were performed at different orientations to ensure that the most vulnerable package features were subjected to “worst-case” loads and deformations. The specific conditions selected for CTU free drop testing are summarized in Table 2.7-1, Table 2.7-2, and Table 2.7-3.

### 2.7.1.3 Summary of Results from the Free Drop Tests

Successful HAC free drop testing of the CTUs indicates that the various TRUPACT-II packaging design features are adequately designed to withstand the HAC 30-foot free drop event. The most important result of the testing program was the demonstrated ability of the OCV and ICV to remain leaktight<sup>3</sup>. Significant results of HAC free drop testing common to all test units are as follows:

- Buckling was not observed for either the ICV or OCV shells. Additionally, accelerometers mounted directly on the OCV shell were utilized to determine the axial acceleration resulting from a 30-foot bottom end drop events on CTU Nos. 2 and 3 (see Section 2.7.1.4, *End Drop Bucking Evaluation*).
- No excessive distortion of the seal flange regions occurred for either the ICV or OCV, although some permanent deformation was noted.
- All three (3) ICV and all six (6) OCV locking ring lock bolts remained intact and locking ring and lower seal flange tabs remained fully interlocked during and following the drop tests. Some OCA locking Z-flange-to-locking ring fasteners failed during the testing, but a sufficient number remained intact to securely retain the locking ring in the locked position. Additionally, for test purposes, only 24 fasteners were used whereas 36 are specified for the design.
- The ICV and OCV were shown to be capable of maintaining pressure before, during, and after each 30-foot drop test. At the instant of impact, internal pressures in both the ICV and OCV would typically increase slightly (a few psi) for a moment and then return, within the accuracy of the instrumentation, to their initial, pre-drop test values.
- The aluminum honeycomb spacer assemblies used in the ICV upper and lower torispherical heads were shown to adequately protect the heads from damaging payload interactions.
- Rupture was not observed for the 3/8-inch thick, OCA outer shell.
- Internal pressures increased during the drops, but returned to pre-drop pressures afterward.
- Observed permanent deformations of the TRUPACT-II packaging were less than those assumed for the criticality evaluation.

<sup>3</sup> “Leaktight” is a leak rate not exceeding  $1 \times 10^{-7}$  standard cubic centimeters per second (scc/sec), air, as defined in ANSI N14.5-1997, *American National Standard for Radioactive Materials – Leakage Tests on Packages for Shipment*, American National Standards Institute, Inc. (ANSI).

A comprehensive summary of free drop test results is provided in Appendix 2.10.3.7, *Test Results*.

#### 2.7.1.4 End Drop Bucking Evaluation

Figure 2.7-1 and Figure 2.7-2 present the axial acceleration time histories (filtered at 500 Hz) obtained from two axially oriented accelerometers located 180° apart on the OCV shell during bottom end drop event (Free Drop Test No. 2) for CTU-2. From Figure 2.7-1, a maximum acceleration of 385 gs results. The bottom end drop accelerations measured for CTU-3 are presented in Figure 2.7-3 and Figure 2.7-4, and show a lesser maximum impact acceleration of 335 gs. The CTU-2 value of 385 gs is therefore selected for analysis.

Although the ICV shell is slightly thicker than the OCV shell (1/4 inch versus 3/16 inch), it is the more buckling sensitive component. The OCV shell is less sensitive to buckling because it is surrounded by polyurethane foam and is reinforced by a stiffening ring located approximately at its mid-length. Under the action of 385 gs acceleration, the compressive stress in the 1/4-inch ICV shell at a location just above the lower torispherical head is:

$$\sigma_{\phi} = (385) \left( \frac{2,110}{2\pi(36.44)(0.25)} \right) = 14,192 \text{ psi}$$

where the axial ICV stress,  $\sigma_{\phi}$ , is determined using a weight of 2,110 pounds consisting of the upper torispherical head (with honeycomb spacer), seal flanges and locking ring, and cylindrical shell. The ICV shell's cross-sectional area is  $2\pi Rt$ , where  $R = 36.44$  inches, and  $t = 0.25$  inches. Note that the hoop stress,  $\sigma_{\theta}$ , and in-plane shear stress,  $\sigma_{\phi\theta}$ , are zero.

The cylindrical portion of the ICV is evaluated using ASME Boiler and Pressure Vessel Code Case N-284<sup>4</sup>. Consistent with Regulatory Guide 7.6 philosophy, a factor of safety of 1.34 is applied for HAC buckling evaluations per ASME Code Case N-284, corresponding to ASME Code, Service Level D conditions.

Buckling analysis geometry parameters are summarized in Table 2.7-4. The cylindrical shell buckling analysis utilizes an ICV temperature of -20 °F, consistent with the temperature of the shells during the drop tests. At the -20 °F temperature, the material's yield strength and elastic modulus are extrapolated from Table 2.3-1 in Section 2.3.1, *Mechanical Properties Applied to Analytic Evaluations*, and found to be 35,000 psi and 28.72(10)<sup>6</sup> psi, respectively.

As shown in Table 2.7-5, since all interaction check parameters are less than 1.0, as required, the design criteria are satisfied.

### 2.7.2 Crush

Subpart F of 10 CFR 71 requires performing a dynamic crush test in accordance with the requirements of 10 CFR §71.73(c)(2). Since the TRUPACT-II package weight exceeds 1,100 pounds, the dynamic crush test is not required.

<sup>4</sup> American Society of Mechanical Engineers (ASME) Boiler and Pressure Vessel Code, Section III, *Rules for Construction of Nuclear Power Plant Components*, Division I, Class MC, Code Case N-284, *Metal Containment Shell Buckling Design Methods*, August 25, 1980, approval date.

### 2.7.3 Puncture

Subpart F of 10 CFR 71 requires performing a puncture test in accordance with the requirements of 10 CFR §71.73(c)(3). The puncture test involves a 40-inch free drop of a package onto the upper end of a solid, vertical, cylindrical, mild steel bar mounted on an essentially unyielding, horizontal surface. The bar must be 6 inches in diameter, with the top surface horizontal and its edge rounded to a radius of not more than 1/4 inch. The package is to be oriented in a position for which maximum damage will occur. The minimum length of the bar is to be 8 inches. The ability of the TRUPACT-II package to adequately withstand this specified puncture drop condition is demonstrated via testing of three full-scale, TRUPACT-II CTUs.

#### 2.7.3.1 Technical Basis for the Puncture Drop Tests

To properly select a worst-case package orientation for the puncture drop event, items that could potentially compromise containment integrity, shielding integrity, and/or criticality safety of the TRUPACT-II package must be clearly identified. For the TRUPACT-II package design, the foremost item to be addressed is the ability of the containment seals to remain leaktight. Shielding integrity is not a controlling case for the reasons described in Chapter 5.0, *Shielding Evaluation*. Criticality safety is conservatively evaluated based on measured physical damage to the OCA shells and polyurethane foam from certification testing, as described in Chapter 6.0, *Criticality Evaluation*.

The leaktight capability of the O-ring seals would be most easily compromised by imposing gross deformations in the sealing region. These types of deformations are of concern from a mechanical viewpoint (i.e., leakage caused by excessive relative movement of the sealing surfaces). In addition, such deformations are of concern from a thermal viewpoint (i.e., leakage caused by thermal degradation of the butyl O-ring seals in a subsequent fire). Importantly, for mechanical damage to occur in the seal regions, the puncture event would have to result in a gross rupturing of the OCA outer shell near the O-ring seals. This could allow the puncture bar to reach and directly impact the OCA seal flanges or locking ring. Similarly, for thermal degradation of the butyl O-ring seals to occur in a subsequent fire, damage to the OCA outer shell near the O-ring seals would again have to occur as a result of the puncture event. Another item associated with the puncture event is the possibility of the puncture bar penetrating the OCA outer shell and rupturing the OCV. Puncture is most likely to occur if the center of gravity of the package is directly in-line with the puncture bar, and the surface of the package is oriented at an angle to the bar axis. If the center of gravity of the package is not in-line with the puncture bar, puncture is less likely since package potential energy is transformed into rotational kinetic energy. Puncture is also more likely if the puncture bar impacts the package surface adjacent to a package shell weld seam. Observations from prior testing indicate that impacts with the package surface, normal to the axis of the puncture bar, will not lead to penetration of the OCA exterior shell. This is the primary reason for utilizing a torispherical head for the OCA lid. The torispherical head results in the puncture bar being oriented normal to the package surface when the center of gravity of the package is directly over the puncture bar. Further, a 3/8-inch thick OCA outer shell is used near the closure region to ensure that no puncture will occur in this region, regardless of impact angle.

In addition to package orientation, initial test conditions such as temperatures and pressures must be selected to complete the definition of the conditions existing at the time of a HAC puncture drop. In general, higher temperatures at the time of a puncture test result in greater deformations

and lesser acceleration loads than do lower temperatures. This is due primarily to the modest temperature sensitivity of the polyurethane foam used within the TRUPACT-II OCA.

Appendix 2.10.3, *Certification Tests*, provides a comprehensive report of the certification test process and results. Discussions specific to the configuration of the test units are provided in Appendix 2.10.3.4, *Description of the Certification Test Units*. Discussions specific to orientations of the test units for free drop, puncture, and fire tests, including initial test conditions, are provided in Appendix 2.10.3.5, *Technical Basis for Tests*. Discussions specific to test sequences for selected tests for the test units is provided in Appendix 2.10.3.6, *Test Sequence for Selected Free Drop, Puncture Drop, and Fire Tests*.

### 2.7.3.2 Test Sequence for the Selected Tests

Based on the above general discussions, the three CTUs were tested for various HAC puncture drops. Although only a single “worst-case” puncture drop is required by 10 CFR §71.73(c)(3), multiple puncture drop tests were performed at different orientations to ensure that the most vulnerable package features were subjected to “worst-case” loads and deformations. The specific conditions selected for CTU puncture drop testing are summarized in Table 2.7-1, Table 2.7-2, and Table 2.7-3.

### 2.7.3.3 Summary of Results from the Puncture Drop Tests

Successful HAC puncture drop testing of the CTUs indicates that the various TRUPACT-II packaging design features are adequately designed to withstand the HAC puncture drop event. As with the free drop test, the most important result of the testing program was the demonstrated ability of the OCV and ICV to remain leaktight. Significant results of puncture drop testing common to all test units are as follows:

- With one exception, permanent deformations of the containment boundary are not attributed to the puncture event. The single exception occurred for a puncture impact onto the 1/4-inch thick OCA outer shell at a location 40 inches above the base of the package (Test No. 7 for CTU No. 1, and Test No. R for CTU No. 2). This puncture event resulted in a hole through the OCA outer shell. The permanent damage to the OCV and ICV shells was an inward bulge of approximately 1½ inches to the OCV and ICV sidewalls. Importantly, permanent deformations were limited to the cylindrical shell portions of the OCV and ICV lower bodies, with no significant deformation near the seal flanges.
- Rupture was not observed for the 3/8-inch thick OCA outer shell. Penetrations of the OCA outer shell closest to the seal regions were 22 inches above and 37 inches below the closure interface. Minor tearing of the Z-flange-to-3/8-inch thick OCA interfaces was observed for some test orientations. These regions are covered by the outer thermal shield; therefore, such tears are of little consequence.
- Tearing of the OCA outer shell occurred at the 3/8-to-1/4-inch thick, OCA body outer shell transition (weld) during testing of CTU-2 and CTU-3 (Test 4).
- In the regions where a significant amount of polyurethane foam was exposed by a puncture event (i.e., 40 inches above the package base and near the OCA top knuckle), the intumescent (i.e., self-extinguishing) characteristics of the polyurethane foam were sufficient to provide effective insulation from the effects of the subsequent HAC fire. Additional discussion regarding HAC fire testing is provided in Section 2.7.4, *Thermal*.

A comprehensive summary of test results is provided in Appendix 2.10.3.7. *Test Results*.

## 2.7.4 Thermal

Subpart F of 10 CFR 71 requires performing a thermal test in accordance with the requirements of 10 CFR §71.73(c)(4). To demonstrate the performance capabilities of the TRUPACT-II package when subjected to the HAC thermal test specified in 10 CFR §71.73(c)(4), two full-scale TRUPACT-II CTUs were burned in two, separate, fully engulfing pool fires. Each test unit was subjected to a variety of HAC, 30-foot free drop and puncture tests prior to being burned, as discussed in Section 2.7.1, *Free Drop*, and Section 2.7.3, *Puncture*, respectively. Active and passive temperature instrumentation was employed during CTU fire testing.

As discussed further in Appendix 2.10.3, *Certification Tests*, each CTU was oriented horizontally in a test stand a distance one-meter above the fuel per the requirements of 10 CFR §71.73(c)(4). The CTU was oriented circumferentially to position the worst-case damage from the various 30-foot free drops and puncture drops 1/2-meter above the lowest part of the package while on the stand (i.e., 1½ meters above the fuel<sup>5</sup>). This particular arrangement placed the maximum drop damage in the hottest section of the fire. Prior to fire testing, each CTU was preheated to the worst-case NCT steady-state temperature (i.e., 100 °F still air without insulation).

Successful HAC fire testing of the CTUs indicates that the various TRUPACT-II packaging design features are adequately designed to withstand the HAC fire event. As with the free drop and puncture tests, the most important result of the testing program was the demonstrated ability of the OCV and ICV to remain leaktight. Significant results of fire testing common to both test units are as follows:

- The intumescent (i.e., self-extinguishing) characteristic of the polyurethane foam was sufficient to provide insulation from the effects of the HAC fire even in regions where the most significant amounts of foam were exposed.
- The maximum measured temperatures for the OCV and ICV elastomeric (butyl) O-ring seals were 260 °F (thermocouple reading during the fire, 250 °F by passive temperature indicating label) and 200 °F, respectively. The maximum measured temperatures for the OCV and ICV structural components were 439 °F and 270 °F, respectively. The 270 °F ICV temperature was most likely a result of the preheat operation used to heat the vessels prior to the fire test, rather than a result of the fire test itself. Air was pumped into the OCV/ICV annulus at 40 psi and 350 °F, and within close proximity of the particular temperature indicating label that measured the 270 °F temperature. The next highest ICV temperature reading was 220 °F.
- Both the ICV and OCV demonstrated the capability of maintaining pressure before, during, and after the fire event. Note that pressure was lost in the CTU No. 1 OCV during fire

---

<sup>5</sup> M. E. Schneider and L. A. Kent, *Measurements of Gas Velocities and Temperatures in a Large Open Pool Fire*, Sandia National Laboratories (reprinted from *Heat and Mass Transfer in Fire*, A. K. Kulkarni and Y. Jaluria, Editors, HTD-Vol. 73 (Book No. H00392), American Society of Mechanical Engineers). Figure 3 shows that maximum temperatures occur at an elevation approximately 2.3 meters above the pool floor. The pool was initially filled with water and fuel to a level of 0.814 meters. The maximum temperatures therefore occur approximately 1½ meters above the level of the fuel, i.e., 1/2 meter above the lowest part of the package when set one meter above the fuel source per the requirements of 10 CFR §71.73(c)(4).

testing. However, the loss of pressure was due to failure of a test-related pressure fitting, not to a packaging design feature. Post-test repair of the fitting and re-pressurization of the OCV indicated that the pressure retention capabilities of the OCV had not been compromised by the fire test.

- Following fire testing, disassembly of the OCA demonstrated that, except for the local area damaged by the puncture impacts 40 inches above the base of the package, a layer of unburned polyurethane foam remained around the entire OCV. For both CTUs, the average thickness of the layer was approximately 5 to 6 inches along the cylindrical sides and lower head of the OCV, and even greater adjacent to the OCV upper dished head. This residual polyurethane foam thickness is consistent with the shielding evaluation provided in Chapter 5.0, *Shielding Evaluation*, and the criticality evaluation presented in Chapter 6.0, *Criticality Evaluation*.

A comprehensive summary of test results is provided in Appendix 2.10.3.7, *Test Results*.

#### **2.7.4.1 Summary of Pressures and Temperatures**

Package pressures and temperatures due to the HAC fire test are presented in Appendix 2.10.3, *Certification Tests*. Detailed discussions regarding measured temperatures are provided in Section 3.5.3, *Package Temperatures*. Detailed discussions regarding calculated pressures are provided in Section 3.5.4, *Maximum Internal Pressure*.

##### **2.7.4.1.1 Summary of Temperatures**

Both active and passive temperature measuring devices were employed prior to, during, and following the HAC fire tests. As discussed in Section 2.7.4, *Thermal*, the maximum measured temperatures for the OCV and ICV O-ring seals were 260 °F and 200 °F, respectively.

##### **2.7.4.1.2 Summary of Pressures**

Even considering the test anomaly associated with CTU No. 1, the maximum measured internal pressures occurred for CTU No. 2. The maximum measured ICV pressure was 65.7 psia (53.7 psig internal pressure, plus 12 psia atmospheric pressure), with a 63.1 psia (51.1 psig) starting pressure. The maximum measured OCV pressure was 66.6 psia (54.6 psig), with a 62 psia (50 psig) starting pressure.

#### **2.7.4.2 Differential Thermal Expansion**

Fire testing of two, full scale TRUPACT-II prototypes indicate that the effects associated with differential thermal expansion of the various packaging components are negligible. Subsequent to all NCT and HAC free drop, puncture drop, and fire tests, comprehensive helium leak testing of both the ICV and OCV demonstrated that differential thermal expansion does not affect the capability to remain leaktight.

#### **2.7.4.3 Stress Calculations**

As shown in Section 2.7.4.1.2, *Summary of Pressures*, the measured internal pressure within the ICV increases 2.6 psig (+5%), and within the OCV increases 4.6 psig (+9%) due to the HAC fire test. Pressure stresses due to the HAC fire test correspondingly increase a maximum of 9%. With reference to Table 2.1-1 from Section 2.1.2.1.1, *Containment Structure (ICV)*, the HAC

allowable stress intensity for general primary membrane stresses (applicable to pressure loads) is 240% of the NCT allowable stress intensity. Therefore, a HAC pressure stress increase of 9% will not exceed the HAC allowable stresses. Further, the pressure stresses in conjunction with stresses associated with differential thermal expansion are limited to an acceptable level since both the ICV and OCV were shown to be leaktight after all NCT and HAC free drop, puncture drop, and fire tests (see Appendix 2.10.3.7, *Test Results*).

#### **2.7.4.4 Comparison with Allowable Stresses**

As discussed in Section 2.7.4.3, *Stress Calculations*, further quantification of stresses in the various TRUPACT-II package components is not required.

#### **2.7.5 Immersion – Fissile Material**

Subpart F of 10 CFR 71 requires performing an immersion test for fissile material packages in accordance with the requirements of 10 CFR §71.73(c)(5). The criticality evaluation presented in Chapter 6.0, *Criticality Evaluation*, assumes optimum hydrogenous moderation of the contents, thereby conservatively addressing the effects and consequences of water in-leakage.

#### **2.7.6 Immersion – All Packages**

Subpart F of 10 CFR 71 requires performing an immersion test for all packages in accordance with the requirements of 10 CFR §71.73(c)(6). For the TRUPACT-II package design, the effect of a 21 psig external pressure due to immersion in 50 feet of water is applied to the ICV and OCV.

The external pressure induces small compressive stresses in the ICV and OCV that are limited by stability (buckling) requirements. Buckling assessments are performed for the OCV and ICV in Section 2.7.6.1, *Buckling Assessment of the Torispherical Heads*, and Section 2.7.6.2, *Buckling Assessment of the Cylindrical Shells*.

##### **2.7.6.1 Buckling Assessment of the Torispherical Heads**

The buckling analysis of the torispherical heads is based on the methodology outlined in Paragraph NE-3133.4(e), *Torispherical Heads*, of the ASME Boiler and Pressure Vessel Code, Section III<sup>6</sup>, Subsection NE. Since the external pressure loading due to immersion may be classified as Level D, the allowable buckling stress and, therefore, the allowable pressure, can be increased by 150% per paragraph NE-3222.2. The results from following this methodology are summarized below.

---

<sup>6</sup> American Society of Mechanical Engineers (ASME) Boiler and Pressure Vessel Code, Section III, *Rules for Construction of Nuclear Power Plant Components*, 1986 Edition.

Parameter	OCV Torispherical Head		ICV Torispherical Head	
	Upper	Lower	Upper	Lower
R	77.3125	74.1250	74.3750	73.1250
T	0.25	0.25	0.25	0.25
$A = \frac{0.125}{(R/T)}$	0.00040	0.00042	0.00042	0.00043
$B^7$	5,600	5,800	5,800	5,900
$P_a = \frac{(1.5)B}{(R/T)}$	27.2	29.3	29.2	30.3

The smallest allowable pressure,  $P_a$ , is 27.2 psig for the OCV upper head. For an applied external pressure of 21 psig, the corresponding buckling margin of safety is:

$$MS = \frac{27.2}{21} - 1 = +0.30$$

Since the margin of safety in the worst case is positive, it is concluded that none of the OCV or ICV torispherical heads will buckle for an external pressure of 21 psig.

#### 2.7.6.2 Buckling Assessment of the Cylindrical Shells

The cylindrical portions of the OCV and ICV are evaluated using ASME Boiler and Pressure Vessel Code Case N-284. Consistent with Regulatory Guide 7.6 philosophy, a factor of safety of 1.34 is applied for HAC buckling evaluations per ASME Code Case N-284, corresponding to ASME Code, Service Level D conditions.

Buckling analysis geometry parameters are summarized in Table 2.7-6, and loading parameters are summarized in Table 2.7-7. The cylindrical shell buckling analysis utilizes an OCV and ICV temperature of 70 °F. The stresses are determined using an external pressure of 21.0 psig. The hoop stress,  $\sigma_\theta$ , and axial stress,  $\sigma_\phi$ , are found from:

$$\sigma_\theta = \frac{Pr}{t} \quad \sigma_\phi = \frac{Pr}{2t}$$

where P is the applied external pressure of 21.0 psi, r is the mean radius, and t is the cylindrical shell thickness. As shown in Table 2.7-8, since all interaction check parameters are less than 1.0, as required, the design criteria are satisfied.

The OCV length is conservatively measured from the ring stiffener to an assumed support point located one-third of the depth of the lower OCV torispherical head below the head-to-shell interface (i.e., 32.67 inches).

<sup>7</sup> Factor B is found from American Society of Mechanical Engineers (ASME) Boiler and Pressure Vessel Code, Section III, *Rules for Construction of Nuclear Power Plant Components*, Figure VII-1102-4, *Chart for Determining Shell Thickness of Cylindrical and Spherical Components Under External Pressure When Constructed of Austenitic Steel (18Cr-8Ni, Type 304)*, 1986 Edition. The 100 °F temperature curve is used for each case.

**OCV Shell Ring Stiffener Axial Compression Check:**

Per Paragraph –1714.1(a) of ASME Boiler and Pressure Vessel Code Case N-284, the required ring stiffener cross-section area is the larger of:

$$A_0 \geq \left( \frac{0.334}{M_s^{0.6}} - 0.063 \right) \ell_{s\phi} t = 0.076 \text{ in}^2 \quad \text{or} \quad A_0 \geq (0.06) \ell_{s\phi} t = 0.350 \text{ in}^2$$

where, from Table 2.7-6.  $R = 36.91$  inches and  $t = 0.188$  inches, and  $M_s = \ell_{si}/(Rt)^{1/2} = 11.77$ , and the length,  $\ell_{s\phi}$ , is the average of the distance from the stiffening ring to the lower head (32.67 inches) and the distance from the stiffening ring to the upper seal flange (29.33 inches), or  $\ell_{s\phi} = \ell_{si} = 1/2(32.67 + 29.33) = 31.00$  inches.

The cross-section area of the stiffening ring is  $A = 0.375 \times 1.5 = 0.563 \text{ in}^2$ . Since  $A = 0.563 \text{ in}^2 > 0.350 \text{ in}^2 = A_0$ , the size of the stiffening ring for axial compression is acceptable.

**OCV Shell Ring Stiffener Hoop Compression Check:**

Per Paragraph –1714.1(b)(1) of ASME Boiler and Pressure Vessel Code Case N-284, the required moment of inertia for an intermediate stiffening ring to resist hoop compression is:

$$I_{E0} = \frac{(1.2)\sigma_{\theta eL} \ell_{s\phi} R_c^2 t}{E(n^2 - 1)} = 0.264 \text{ in}^4$$

where  $\sigma_{\theta eL} = 11,273$  psi (Table 2.7-8),  $\ell_{s\phi} = 31.00$  inches,  $R_c = 36.91 + 0.356 = 37.27$  inches,  $t = 0.188$  inches,  $E = 28.3(10)^6$  psi at 70 °F, and  $n^2$  is:

$$n^2 = \frac{(1.875)R^{3/2}}{L_B t^{1/2}} = 15.64$$

where  $R = 36.91$  inches (Table 2.7-6), the effective length of the OCV shell between “bulkheads” is  $L_B = 62.0$  inches, and  $t = 0.188$  inches (Table 2.7-6).

The effective stiffness of the ring stiffener also includes a portion of the adjacent cylindrical shell whose length is determined from Paragraph –1200 of ASME Code Case N-284 as follows:

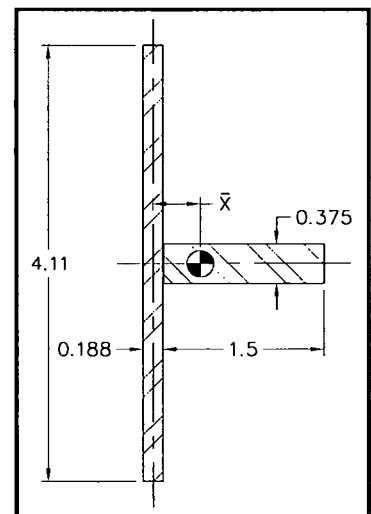
$$\ell_{ei} = 1.56\sqrt{Rt} = 4.11 \text{ in}$$

where, from Table 2.7-6,  $R = 36.91$  inches and  $t = 0.188$  inches.

The distance to the composite stiffening ring neutral axis,  $\bar{X}$ , is:

$$\bar{X} = \frac{(0.375)(1.5)(0.188 + 1.5)}{2[(0.188)(4.11) + (0.375)(1.5)]} = 0.356 \text{ in}$$

Knowing the distance to the neutral axis of the composite stiffening ring, the ring stiffener in-plane moment of inertia is:



$$I_r = \frac{(0.375)(1.5)^3}{12} + (0.375)(1.5) \left( \frac{0.188 + 1.5}{2} - 0.356 \right)^2 = 0.239 \text{ in}^4$$

Similarly, the shell out-of-plane moment of inertia is:

$$I_s = \frac{(4.11)(0.188)^3}{12} + (0.188)(4.11)(0.356)^2 = 0.100 \text{ in}^4$$

Combining both results, the effective moment of inertia is  $I_E = 0.239 + 0.100 = 0.339 \text{ in}^4$ . Since  $I_E = 0.339 \text{ in}^4 > 0.264 \text{ in}^4 = I_{E0}$ , the size of the stiffening ring for hoop compression is acceptable.

### 2.7.7 Deep Water Immersion Test

Subpart E of 10 CFR 71 requires performing a deep water immersion test in accordance with 10 CFR §71.61. Since the TRUPACT-II does not transport payloads with an activity of greater than  $10^5 A_2$ , this requirement does not apply.

### 2.7.8 Summary of Damage

As discussed in the previous sections, the cumulative damaging effects of free drop, puncture drop, and fire tests were satisfactorily withstood by the TRUPACT-II packaging during certification testing. Subsequent helium leak testing confirmed that containment integrity was maintained throughout the test series. Therefore, the requirements of 10 CFR §71.73 have been adequately met.

**Table 2.7-1 – Summary of Tests for TRUPACT-II CTU-1**

Test No.	Test Description	Test Unit Angular Orientation		Pressure (psig)		CTU Temperature	Remarks
		Axial <sup>①</sup>	Circumferential <sup>②</sup>	ICV	OCV		
1	NCT, 3-foot side drop onto OCV vent port	0°	110°	50	50	Ambient	Impact in region expected to produce worst-case cumulative damage to package.
2	HAC, 30-foot side drop onto OCV vent port	0°	110°	50	0	Ambient	Impact in region expected to produce worst-case cumulative damage to package.
3	HAC, 30-foot CG onto OCA lid knuckle near OCA lid lift pocket	-47°	-100°	50	50	Ambient	Payload drums centered over OCA lid lift pocket to produce maximum cumulative damage to lids.
4	HAC, 30-foot top drop	-90°	N/A	50	50	Ambient	Impact to produce maximum cumulative internal damage to lids.
5	HAC, puncture drop on OCA vent port fitting	-15°	110°	50	50	Ambient	Puncture in region expected to produce worst-case cumulative damage to package.
6	HAC, puncture drop onto OCA body below 1/4-to-3/8 shell weld	-3°	110°	50	50	Ambient	Puncture in region expected to produce worst-case cumulative damage to package.
7	HAC, puncture drop 40 inches above package bottom	28°	110°	50	0	Ambient	Puncture in region expected to produce worst-case cumulative damage to package.
8	HAC, puncture drop onto damaged OCA lid knuckle	-54°	110°	50	0	Ambient	Puncture in region expected to produce worst-case cumulative damage to package.
9	HAC, puncture drop on OCA seal test port fitting	-24°	20°	50	50	Ambient	Puncture in thinnest region of the package sidewall.
10	HAC, fire test	0°	145°	50	50	At HAC pre-fire temperature	Circumferential orientation places damage from most drop tests in hottest part of fire.

Notes:

- ① Axial angle,  $\theta$ , is relative to horizontal (i.e., side drop orientation).
- ② Circumferential angle,  $\phi$ , is relative to the forklift pockets when parallel to the ground.

**Table 2.7-2 – Summary of Tests for TRUPACT-II CTU-2**

Test No.	Test Description	Test Unit Angular Orientation		Pressure (psig)		CTU Temperature	Remarks
		Axial <sup>①</sup>	Circumferential <sup>②</sup>	ICV	OCV		
1	HAC, 30-foot top slapdown drop; initial impact on OCA lid knuckle	-20°	-5°	33	0	-20 °F	Slapdown onto locking ring joints.
2	HAC, 30-foot bottom drop	90°	N/A	33	33	-20 °F	Drop producing maximum axial acceleration.
3	HAC, 30-foot slapdown drop; initial impact on tie-down lug	18°	143°	50	50	Ambient	Slapdown in region expected to produce worst-case cumulative damage to package.
R	HAC, puncture drop 40 inches above package bottom	23°	143°	50	0	Ambient	Impact in region expected to produce worst-case cumulative damage to package; repeat of Test No. 7 for CTU-1.
4	HAC, puncture drop at the 1/4-to-3/8 lid shell interface	-42°	143°	50	50	Ambient	Puncture in region expected to produce worst-case cumulative damage to package.
5	HAC, puncture drop onto package bottom adjacent to forklift pocket	55°	-110°	50	0	Ambient	HAC impact at location not tested during previous TRUPACT-II certification tests.
6	HAC, puncture drop onto outer thermal shield	-67°	-67°	0	0	Ambient	Attempt to tear outer thermal shield away from OCA.
7	HAC, puncture drop onto OCA body at closure; 40° from OCA vent port fitting	-15°	110°	50	50	Ambient	Puncture at closure region at same elevation as OCA vent port fitting.
8	HAC, puncture drop onto OCA lid at closure; 180° from OCA seal test port fitting	-22°	-145°	50	50	Ambient	Puncture at closure region at same elevation as OCA seal test port fitting; thinnest region of the package sidewall.
9	HAC, fire test	0°	200°	50	50	At HAC pre-fire temperature	Circumferential orientation places damage from Tests 3, R, and 4 in hottest part of fire.

**Notes:**

- ① Axial angle,  $\theta$ , is relative to horizontal (i.e., side drop orientation).
- ② Circumferential angle,  $\phi$ , is relative to the forklift pockets when parallel to the ground.

**Table 2.7-3 – Summary of Tests for TRUPACT-II CTU-3**

Test No.	Test Description	Test Unit Angular Orientation		Pressure (psig)		CTU Temperature	Remarks
		Axial <sup>①</sup>	Circumferential <sup>②</sup>	ICV	OCV		
1	HAC, 30-foot top slapdown drop; initial impact on OCA lid knuckle	-20°	-5°	33	0	-20 °F	Slapdown onto locking ring joints.
2	HAC, 30-foot bottom drop	90°	N/A	33	33	-20 °F	Drop producing maximum axial acceleration.
3	HAC, 30-foot slapdown drop; initial impact on tie-down lug	18°	143°	50	50	Ambient	Slapdown in region expected to produce worst-case cumulative damage to package.
4	HAC, puncture drop at the 1/4-to-3/8 lid shell interface	-42°	143°	50	50	Ambient	Puncture in region expected to produce worst-case cumulative damage to package.
5	HAC, puncture drop onto package bottom adjacent to forklift pocket	55°	-110°	50	0	Ambient	HAC impact at location not tested during previous TRUPACT-II certification tests.
6	HAC, puncture drop onto outer thermal shield	-67°	-67°	0	0	Ambient	Attempt to tear outer thermal shield away from OCA.
7	HAC, puncture drop onto OCA body at closure; 40° from OCA vent port fitting	-15°	110°	50	50	Ambient	Puncture at closure region at same elevation as OCA vent port fitting.
8	HAC, puncture drop onto OCA lid at closure; 180° from OCA seal test port fitting	-22°	-145°	50	50	Ambient	Puncture at closure region at same elevation as OCA seal test port fitting; thinnest region of the package sidewall.

Notes:

- ① Axial angle,  $\theta$ , is relative to horizontal (i.e., side drop orientation).  
 ② Circumferential angle,  $\phi$ , is relative to the forklift pockets when parallel to the ground.

This page intentionally left blank.

**Table 2.7-4 – Buckling Geometry Parameters for a 385g HAC End Drop**

<b>Geometry and Material Input</b>	
	<b>ICV</b>
Mean Radius, inch	36.44
Shell Thickness, inch	0.25
Length, inch	65.70 <sup>①</sup>
<b>Geometry Output (nomenclature consistent with ASME Code Case N-284)</b>	
R =	36.44
t =	0.25
$(Rt)^{1/2} =$	3.018
$l_{\phi} =$	65.70
$l_{\theta} =$	229.0
$M_{\phi} =$	21.77
$M_{\theta} =$	75.87
M =	21.77

Notes:

- ① The ICV length is conservatively measured from five inches below the top of the lower ICV seal flange (at the beginning of the 1/4-inch wall thickness) to an assumed support point located one-third of the depth of the lower ICV torispherical head below the head-to-shell interface.

**Table 2.7-5 – Shell Buckling Summary for a 385g HAC End Drop**

Condition	ICV	Remarks
<b>Capacity Reduction Factors (-1511)</b>		
$\alpha_{\phi L} =$	0.3170	
$\alpha_{\theta L} =$	0.8000	
<b>Plasticity Reduction Factors (-1610)</b>		
$\eta_{\phi} =$	1.0000	
$\eta_{\theta} =$	1.0000	
<b>Theoretical Buckling Values (-1712.1.1)</b>		
$C_{\phi} =$	0.6050	
$\sigma_{\phi eL} =$	119,207 psi	
$C_{\theta h} =$	0.0435	
$\sigma_{\theta eL} = \sigma_{heL} =$	8,577 psi	
<b>Elastic Interaction Equations (-1713.1.1)</b>		
$\sigma_{\phi s} =$	59,991 psi	
$\sigma_{\theta s} =$	0 psi	
Axial + Hoop $\Rightarrow$ Check (a):	N/A	
Axial + Hoop $\Rightarrow$ Check (b):	0.485	<1.0 OK

**Table 2.7-6 – Buckling Geometry Parameters per Code Case N-284**

<b>Geometry and Material Input</b>		
	<b>ICV</b>	<b>OCV</b>
Mean Radius, inch	36.44	36.91
Shell Thickness, inch	0.25	0.188
Length, inch	65.70 <sup>①</sup>	32.67 <sup>②</sup>
<b>Geometry Output (nomenclature consistent with ASME Code Case N-284)</b>		
R =	36.44	36.91
t =	0.25	0.188
$(Rt)^{1/2} =$	3.018	2.634
$\ell_{\phi} =$	65.70	32.67
$\ell_{\theta} =$	229.0	231.9
$M_{\phi} =$	21.77	12.40
$M_{\theta} =$	75.87	88.03
M =	21.77	12.40

Notes:

- ① The ICV length is conservatively measured from five inches below the top of the lower ICV seal flange (at the beginning of the 1/4-inch wall thickness) to an assumed support point located one-third of the depth of the lower ICV torispherical head below the head-to-shell interface.
- ② The OCV length is conservatively measured from the ring stiffener to an assumed support point located one-third of the depth of the lower OCV torispherical head below the head-to-shell interface. This length assumes that the ring stiffener is sized per the requirements in Paragraphs -1714.1(a) and -1714.1(b)(1) of ASME Code Case N-284.

**Table 2.7-7 – Stress Results for 21 psig External Pressure**

ICV		OCV	
Axial Stress, $\sigma_\phi$	1,530	Axial Stress, $\sigma_\phi$	2,061
Hoop Stress, $\sigma_\theta$	3,061	Hoop Stress, $\sigma_\theta$	4,123

**Table 2.7-8 – Shell Buckling Summary for 21 psig External Pressure**

Condition	ICV	OCV	Remarks
<b>Capacity Reduction Factors (-1511)</b>			
$\alpha_{\phi L} =$	0.2670	0.2670	
$\alpha_{\theta L} =$	0.8000	0.8000	
<b>Plasticity Reduction Factors (-1610)</b>			
$\eta_\phi =$	1.0000	1.0000	
$\eta_\theta =$	1.0000	1.0000	
<b>Theoretical Buckling Values (-1712.1.1)</b>			
$C_\phi =$	0.6050	0.6050	
$\sigma_{\phi eL} =$	117,464 psi	87,208 psi	
$C_{\theta h} =$	0.0435	0.0782	
$\sigma_{\theta eL} = \sigma_{heL} =$	8,452 psi	11,273 psi	
<b>Elastic Interaction Equations (-1713.1.1)</b>			
$\sigma_{\phi s} =$	7,679 psi	10,344 psi	
$\sigma_{\theta s} =$	5,127 psi	6,906 psi	
Axial + Hoop $\Rightarrow$ Check (a):	N/A	N/A	
Axial + Hoop $\Rightarrow$ Check (b):	0.398	0.433	<1.0 OK

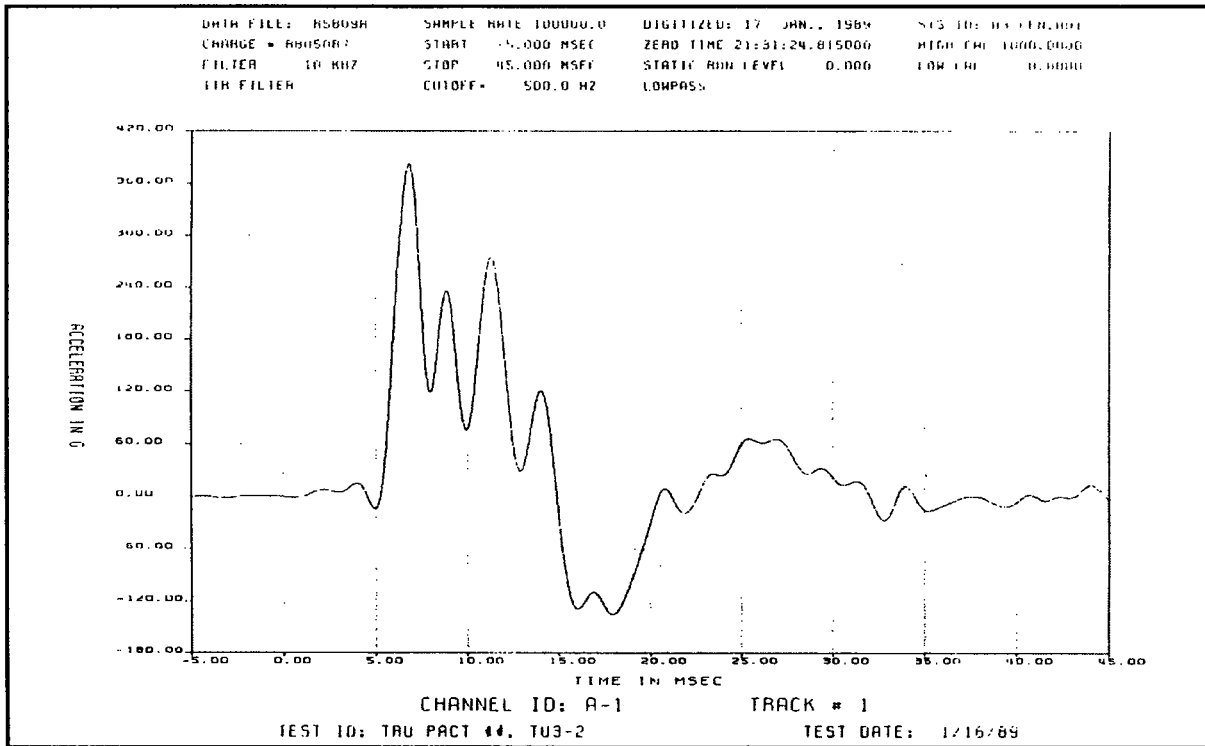


Figure 2.7-1 – CTU-2 Free Drop Test No. 2 Accelerometer Data (Gage 1)

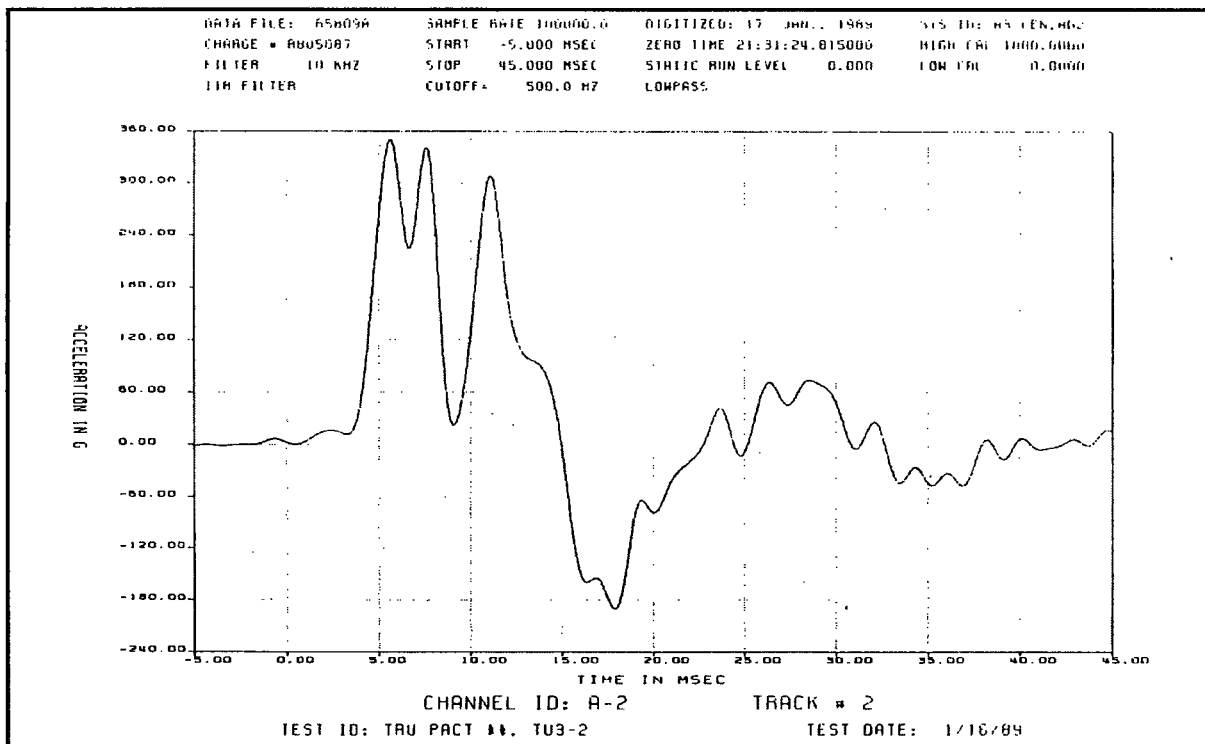


Figure 2.7-2 – CTU-2 Free Drop Test No. 2 Accelerometer Data (Gage 2)

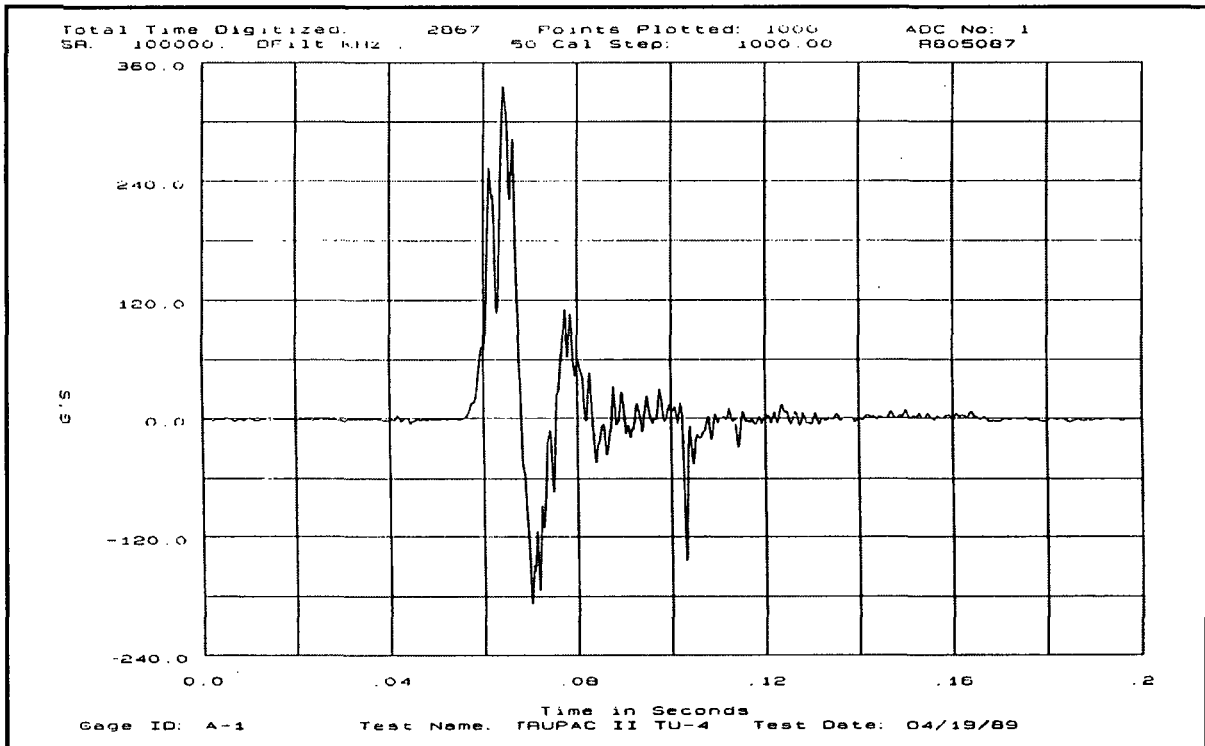


Figure 2.7-3 – CTU-3 Free Drop Test No. 2 Accelerometer Data (Gage 1)

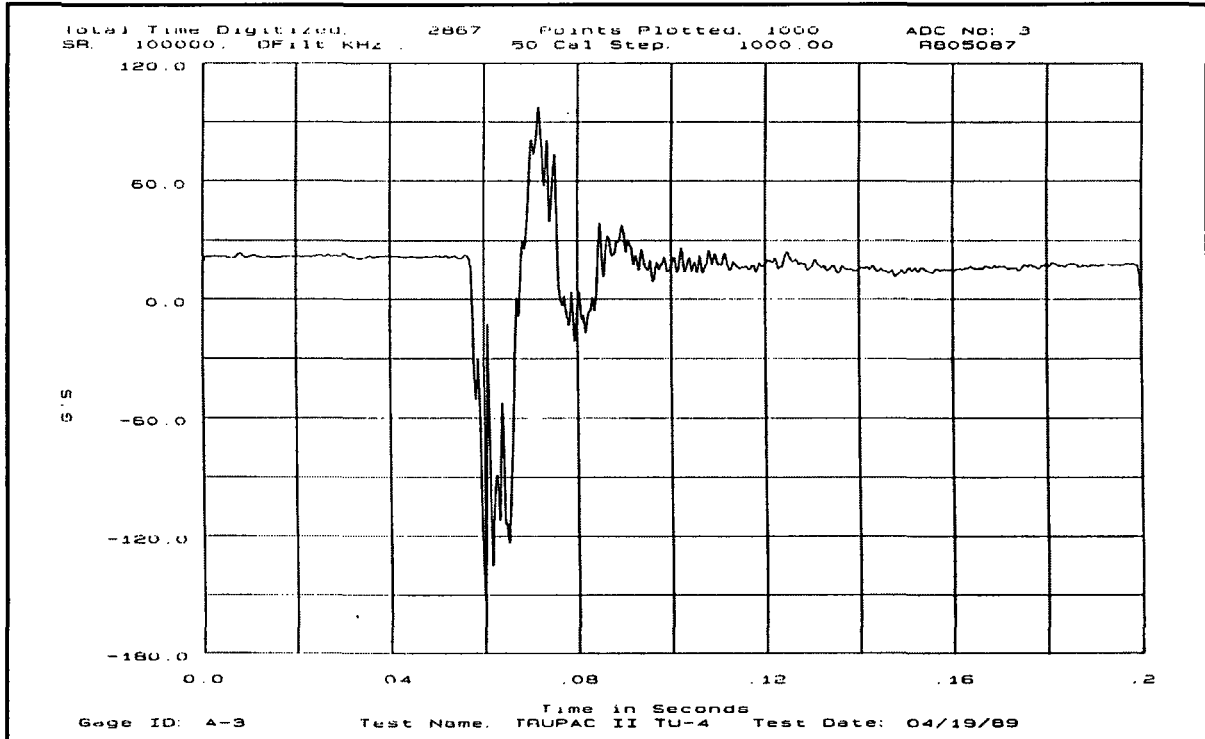


Figure 2.7-4 – CTU-3 Free Drop Test No. 2 Accelerometer Data (Gage 2)

## **2.8 Special Form**

This section does not apply for the TRUPACT-II package, since special form is not claimed.

This page intentionally left blank.

## **2.9 Fuel Rods**

This section does not apply for the TRUPACT-II package, since fuel rods are not included as an approved payload configuration.

This page intentionally left blank.

## **2.10 Appendices**

2.10.1 *Finite Element Analysis (FEA) Models*

2.10.2 *Elastomer O-ring Seal Performance Tests*

2.10.3 *Certification Tests*

This page intentionally left blank.

## 2.10.1 Finite Element Analysis (FEA) Models

### 2.10.1.1 Outer Confinement Assembly (OCA) Structural Analysis

Finite element analyses (FEA) are performed on the OCA structure to determine the stress states of the various components under normal conditions of transport (NCT) loads. The FEA analyses are performed using ANSYS<sup>®</sup> 4.3A2<sup>1</sup>. The OCA FEA model is comprised of six separate major structural components, modeled as shown in :

- upper OCV seal flange
- lower OCV seal flange
- OCV locking ring
- OCV shells
- OCA shells and z-flanges
- polyurethane foam

The lower and upper seal flanges, locking ring and polyurethane foam are modeled using 2-D, isoparametric solid elements (PLANE42). The quadrilateral elements are defined by four nodal points (a triangular element may be formed by defining duplicate the 3<sup>rd</sup> and 4<sup>th</sup> node numbers), each having two degrees of freedom: translations in the nodal x-direction (radial) and y-direction (axial).

The upper and lower OCA shells (OCA lid and body shells, respectively) are modeled using 2-D, axisymmetric conical shell elements (SHELL51). The lineal elements are defined by two nodal points, each having three degrees of freedom: translations in the nodal x-direction (radial) and y-direction (axial), and rotation about the nodal z-axis (hoop). In addition, the axisymmetric conical shell element is biaxial, with membrane and bending capabilities. The OCA inner shell defines the outer confinement vessel (OCV).

Relatively stiff, 2-D elastic beams (BEAM3) are utilized to maintain bending continuity between the three degree of freedom conical shell elements and two degree of freedom, isoparametric solid elements. Specifically, for both the lower and upper OCV seal flanges, four stiff beams are placed at each junction between the shell elements and the solid elements of the seal flanges. These elements are included to transmit the moment (i.e., to maintain slope continuity) between the shell and flange portions of the model, and have a negligible effect on the stress results.

Three sets of 2-D interface elements (CONTAC12) are utilized to connect the lower and upper OCV seal flanges to each other and to the OCV locking ring. The interface element is capable of supporting a load only in the direction normal to the surfaces, and is frictionless in the tangential direction. The interface element has two degrees of freedom at each node: translations in the nodal x-direction (radial) and y-direction (axial). A stiffness of  $2 \times 10^{10}$  lb/in is chosen to reflect the relatively high contact stiffness when closed. Three sets of interface elements are used in these analyses: 1) between the lower OCV seal flange and the OCV locking ring, 2) between the upper OCV seal flange and the OCV locking ring, and 3) between the lower OCV seal flange and the upper OCV seal flange.

Interface elements are also located along the entire shell-to-foam periphery to allow relative motion between the steel shells and the polyurethane foam. This approach effectively models the ceramic fiber paper by allowing compression-only forces, and assumes no shear continuity or tension effects. A contact stiffness of  $2 \times 10^{10}$  lb/in is chosen to reflect the stiffness between the

---

<sup>1</sup> ANSYS<sup>®</sup>, Inc., *ANSYS Engineering Analysis System User's Manual for ANSYS<sup>®</sup> Revision 4.3A2*, Houston, PA.

shells, ceramic fiber paper, and polyurethane foam. Stress results in the package shells and OCV seal flanges exhibit a negligible dependence on the actual magnitude of the gap contact stiffness.

To account for the tangential (hoop) direction slotting for the lower OCV seal flange and OCV locking ring in the axisymmetric model, the material properties in the directly affected regions are modified. Specifically, material properties for the shaded elements in the lower OCV seal flange and OCV locking ring, illustrated in Figure 2.10.1-1, are modified to reflect only one-half the stainless steel being present for strength purposes. Specifically, the elastic modulus in the x- and y-directions is reduced to one-half their normal value (since only approximately one-half the material remains in the slotted regions), and the elastic modulus in the z-direction is set to a very low value to eliminate virtually all tangential (hoop) stiffness in the slotted regions. In addition, Poisson's ratio is set at the normal value of 0.3 for the x-y plane, but is set to zero in the x-z and y-z planes. In these ways, the analyses accurately depict the stress levels in all regions.

The global origin of the nodal coordinate system is located at the bottom center of the OCA body, as shown in Figure 2.10.1-1. As such, the nodal x-axis corresponds to the radial direction, the nodal y-axis corresponds to the axial direction, and the nodal z-axis corresponds to the tangential (or hoop) direction. The model is constrained from translating in the radial direction and rotating about the hoop axis at the y-z symmetry plane at x equal zero. The model is also constrained from translating in the axial direction at a single node on the OCV locking ring.

#### 2.10.1.1.1 OCA Structural Analysis – Load Case 1

For OCA Load Case 1, the OCA structural analysis uses a 50 psig (64.7 psia) internal pressure, corresponding to the maximum normal operating pressure (MNOP) from Section 3.4.4, *Maximum Internal Pressure*, coupled with a reduced external pressure of 3.5 psia (equivalently an 11.2 psig internal pressure), per Section 2.6.3, *Reduced External Pressure*, and 10 CFR §71.51(c)(3)<sup>2</sup>. The net internal pressure for this case is 61.2 psig, applied throughout the inner periphery of the model. Relative to the upper and lower OCV seal flanges, the internal pressure does not extend beyond (below) the top of the upper main O-ring seal groove.

A uniform temperature of 160 °F, per Section 2.6.1.1, *Summary of Pressures and Temperatures*, is utilized to determine the temperature-dependent, material property values. The only material properties affected by a temperature of 160 °F are the elastic modulus and the thermal expansion coefficient for the stainless steel. Consistent with Table 2.3-1 from Section 2.3.1, *Mechanical Properties Applied to Analytic Evaluations*, the elastic modulus and thermal expansion coefficient for Type 304 stainless steel are  $27.8(10)^6$  psi and  $8.694(10)^{-6}$  inches/inch/°F, respectively, at a temperature of 160 °F.

The material properties for the polyurethane foam are consistent with those specified within Table 2.3-2 from Section 2.3.1, *Mechanical Properties Applied to Analytic Evaluations*. The elastic modulus in the x- (radial) and z- (hoop) directions is based on the average of the tensile and compressive, perpendicular-to-rise elastic modulus, or 5,854 psi. The elastic modulus in the y- (axial) direction is based on the average of the tensile and compressive, parallel-to-rise elastic modulus, or 8,789 psi. In addition, Poisson's ratio is 0.33, and the thermal expansion coefficient is  $4.9(10)^{-5}$  inches/inch/°F. Due to the relatively low stiffness of the polyurethane foam

---

<sup>2</sup> Title 10, Code of Federal Regulations, Part 71 (10 CFR 71), *Packaging and Transportation of Radioactive Material*, 01-01-12 Edition.

compared with the surrounding stainless steel structures, temperature adjusting the foam's elastic modulus will have a negligible effect on component stresses.

Both the reference and uniform temperature are set to 160 °F, thereby excluding the effects of differential thermal expansion for this case. The effects of differential thermal expansion are considered in Section 2.10.1.1.2, *OCA Structural Analysis – Load Case 2*.

For analysis model review, the ANSYS® input file is listed in Table 2.10.1-1.

#### **2.10.1.1.2 OCA Structural Analysis – Load Case 2**

For OCA Load Case 2, the OCA structural analysis uses a 50 psig (64.7 psia) internal pressure, corresponding to the maximum normal operating pressure (MNOP) from Section 3.4.4, *Maximum Internal Pressure*, coupled with a reduced external pressure of 3.5 psia (equivalently an 11.2 psig internal pressure), per Section 2.6.3, *Reduced External Pressure*, and 10 CFR §71.51(c)(3). The net internal pressure for this case is 61.2 psig, applied throughout the inner periphery of the model. Relative to the upper and lower OCV seal flanges, the internal pressure does not extend beyond (below) the top of the upper main O-ring seal groove.

A uniform temperature of 160 °F, per Section 2.6.1.1, *Summary of Pressures and Temperatures*, is utilized to determine the temperature-dependent, material property values. The only material properties affected by a temperature of 160 °F are the elastic modulus and the thermal expansion coefficient for the stainless steel. Consistent with Table 2.3-1 from Section 2.3.1, *Mechanical Properties Applied to Analytic Evaluations*, the elastic modulus and thermal expansion coefficient for Type 304 stainless steel are  $27.8(10)^6$  psi and  $8.694(10)^{-6}$  inches/inch/°F, respectively, at a temperature of 160 °F.

The material properties for the polyurethane foam are consistent with those specified within Table 2.3-2 from Section 2.3.1, *Mechanical Properties Applied to Analytic Evaluations*. The elastic modulus in the x- (radial) and z- (hoop) directions is based on the average of the tensile and compressive, perpendicular-to-rise elastic modulus, or 5,854 psi. The elastic modulus in the y- (axial) direction is based on the average of the tensile and compressive, parallel-to-rise elastic modulus, or 8,789 psi. In addition, Poisson's ratio is 0.33, and the thermal expansion coefficient is  $4.9(10)^{-5}$  inches/inch/°F. Due to the relatively low stiffness of the polyurethane foam compared with the surrounding stainless steel structures, temperature adjusting the foam's elastic modulus will have a negligible effect on component stresses.

The reference temperature is set to 70 °F, and the uniform temperature is set to 160 °F, thereby including the effects of differential thermal expansion for this case.

For analysis model review, the ANSYS® input file is listed in Table 2.10.1-2.

#### **2.10.1.1.3 OCA Structural Analysis – Load Case 3**

For OCA Load Case 3, the OCA structural analysis uses a 0.0 psig (14.7 psia) internal pressure coupled with an external pressure of 0.0 psig (14.7 psia) for a net pressure differential of 0.0 psig.

A uniform temperature of -40 °F, per Section 2.6.2, *Cold*, is utilized to determine the temperature-dependent, material property values. The only material properties affected by a temperature of -40 °F are the elastic modulus and the thermal expansion coefficient for the stainless steel. Consistent with Table 2.3-1 from Section 2.3.1, *Mechanical Properties Applied to Analytic Evaluations*, the

elastic modulus and thermal expansion coefficient for Type 304 stainless steel are  $28.8(10)^6$  psi and  $8.08(10)^{-6}$  inches/inch/°F, respectively, at a temperature of -40 °F.

The material properties for the polyurethane foam are consistent with those specified within Table 2.3-2 from Section 2.3.1, *Mechanical Properties Applied to Analytic Evaluations*. The elastic modulus in the x- (radial) and z- (hoop) directions is based on the average of the tensile and compressive, perpendicular-to-rise elastic modulus, or 5,854 psi. The elastic modulus in the y- (axial) direction is based on the average of the tensile and compressive, parallel-to-rise elastic modulus, or 8,789 psi. In addition, Poisson's ratio is 0.33, and the thermal expansion coefficient is  $4.3(10)^{-5}$  inches/inch/°F. Due to the relatively low stiffness of the polyurethane foam compared with the surrounding stainless steel structures, temperature adjusting the foam's elastic modulus will have a negligible effect on component stresses.

The reference temperature is set to 70 °F, and the uniform temperature is set to -40 °F, thereby including the effects of differential thermal expansion for this case.

For analysis model review, the ANSYS® input file is listed in Table 2.10.1-3.

#### **2.10.1.1.4 OCA Structural Analysis – Load Case 4**

For OCA Load Case 4, the OCA structural analysis uses a -14.7 psig (0.0 psia) internal pressure (i.e., full vacuum) coupled with an increased external pressure of 0.0 psig (14.7 psia), per Section 2.6.4, *Increased External Pressure*. The net external pressure for this case is 14.7 psig, applied throughout the inner periphery of the model. Relative to the upper and lower OCV seal flanges, the internal pressure does not extend beyond (below) the top of the upper main O-ring seal groove.

A uniform temperature of 70 °F is utilized to determine the temperature-dependent, material property values. The only material properties affected by a temperature of 70 °F are the elastic modulus and the thermal expansion coefficient for the stainless steel. Consistent with Table 2.3-1 from Section 2.3.1, *Mechanical Properties Applied to Analytic Evaluations*, the elastic modulus and thermal expansion coefficient for Type 304 stainless steel are  $28.3(10)^6$  psi and  $8.46(10)^{-6}$  inches/inch/°F, respectively, at a temperature of 70 °F.

The material properties for the polyurethane foam are consistent with those specified within Table 2.3-2 from Section 2.3.1, *Mechanical Properties Applied to Analytic Evaluations*. The elastic modulus in the x- (radial) and z- (hoop) directions is based on the average of the tensile and compressive, perpendicular-to-rise elastic modulus, or 5,854 psi. The elastic modulus in the y- (axial) direction is based on the average of the tensile and compressive, parallel-to-rise elastic modulus, or 8,789 psi. In addition, Poisson's ratio is 0.33, and the thermal expansion coefficient is  $4.6(10)^{-5}$  inches/inch/°F.

Both the reference and uniform temperature are set to 70 °F, thereby excluding the effects of differential thermal expansion for this case.

For analysis model review, the ANSYS® input file is listed in Table 2.10.1-4.

### 2.10.1.2 Inner Containment Vessel (ICV) Structural Analysis

Finite element analyses (FEA) are performed on the ICV structure to determine the stress states of the various components under normal conditions of transport (NCT) loads. The FEA analyses are performed using ANSYS® 4.3A2. The ICV FEA model is comprised of four separate major structural components, modeled as shown in Figure 2.10.1-2:

- upper ICV seal flange
- lower ICV seal flange
- ICV locking ring
- ICV shells

The lower and upper seal flanges, and locking ring are modeled using 2-D, isoparametric solid elements (PLANE42). The quadrilateral elements are defined by four nodal points (a triangular element may be formed by defining duplicate the 3<sup>rd</sup> and 4<sup>th</sup> node numbers), each having two degrees of freedom: translations in the nodal x-direction (radial) and y-direction (axial).

The upper and lower ICV shells (ICV lid and body shells, respectively) are modeled using 2-D, axisymmetric conical shell elements (SHELL51). The lineal elements are defined by two nodal points, each having three degrees of freedom: translations in the nodal x-direction (radial) and y-direction (axial), and rotation about the nodal z-axis (hoop). In addition, the axisymmetric conical shell element is biaxial, with membrane and bending capabilities.

Relatively stiff, 2-D elastic beams (BEAM3) are utilized to maintain bending continuity between the three degree of freedom conical shell elements and two degree of freedom, isoparametric solid elements. Specifically, for both the lower and upper ICV seal flanges, four stiff beams are placed at each junction between the shell elements and the solid elements of the seal flanges. These elements are included to transmit the moment (i.e., to maintain slope continuity) between the shell and flange portions of the model, and have a negligible effect on the stress results.

Three sets of 2-D gap elements (CONTAC12) are utilized to connect the lower and upper ICV seal flanges to each other and to the ICV locking ring. The gap element is capable of supporting a load only in the direction normal to the surfaces, and is frictionless in the tangential direction. The gap element has two degrees of freedom at each node: translations in the nodal x-direction (radial) and y-direction (axial). A stiffness of  $2 \times 10^{10}$  lb/in is chosen to reflect the relatively high contact stiffness when closed. Three sets of gap elements are used in these analyses: 1) between the lower ICV seal flange and the ICV locking ring, 2) between the upper ICV seal flange and the ICV locking ring, and 3) between the lower ICV seal flange and the upper ICV seal flange.

To account for the tangential (hoop) direction slotting for the lower ICV seal flange and ICV locking ring in the axisymmetric model, the material properties in the directly affected regions are modified. Specifically, material properties for the shaded elements in the lower ICV seal flange and ICV locking ring, illustrated in Figure 2.10.1-2, are modified to reflect only one-half the stainless steel being present for strength purposes. Specifically, the elastic modulus in the x- and y-directions is reduced to one-half their normal value (since only approximately one-half the material remains in the slotted regions), and the elastic modulus in the z-direction is set to a very low value to eliminate virtually all tangential (hoop) stiffness in the slotted regions. In addition, Poisson's ratio is set at the normal value of 0.3 for the x-y plane, but is set to zero in the y-z and x-z planes. In these ways, the analyses accurately depict the stress levels in all regions.

The global origin of the nodal coordinate system is located at the bottom center of the ICV body, as shown in Figure 2.10.1-2. As such, the nodal x-axis corresponds to the radial direction, the

nodal y-axis corresponds to the axial direction, and the nodal z-axis corresponds to the tangential (or hoop) direction. The model is constrained from translating in the radial direction and rotating about the hoop axis at the y-z symmetry plane at x equal zero. The model is also constrained from translating in the axial direction at a single node on the ICV locking ring.

#### 2.10.1.2.1 ICV Structural Analysis – Load Case 1

For ICV Load Case 1, the ICV structural analysis uses a 50 psig (64.7 psia) internal pressure, corresponding to the maximum normal operating pressure (MNOP) from Section 3.4.4, *Maximum Internal Pressure*, coupled with a reduced external pressure of 3.5 psia (equivalently an 11.2 psig internal pressure), per Section 2.6.3, *Reduced External Pressure*, and 10 CFR §71.51(c)(3). The net internal pressure for this case is 61.2 psig, applied throughout the inner periphery of the model. Relative to the upper and lower ICV seal flanges, the internal pressure does not extend beyond (below) the top of the upper main O-ring seal groove.

A uniform temperature of 160 °F, per Section 2.6.1.1, *Summary of Pressures and Temperatures*, is utilized to determine the temperature-dependent, material property values. The only material properties affected by a temperature of 160 °F are the elastic modulus and the thermal expansion coefficient for the stainless steel. Consistent with Table 2.3-1 from Section 2.3.1, *Mechanical Properties Applied to Analytic Evaluations*, the elastic modulus and thermal expansion coefficient for Type 304 stainless steel are  $27.8(10)^6$  psi and  $8.694(10)^{-6}$  inches/inch/°F, respectively, at a temperature of 160 °F.

Both the reference and uniform temperature are set to 160 °F, thereby excluding the effects of differential thermal expansion for this case.

For analysis model review, the ANSYS® input file is listed in Table 2.10.1-5.

#### 2.10.1.2.2 ICV Structural Analysis – Load Case 2

For ICV Load Case 2, the ICV structural analysis uses a -14.7 psig (0.0 psia) internal pressure (i.e., full vacuum) coupled with an increased external pressure of 0.0 psig (14.7 psia), per Section 2.6.4, *Increased External Pressure*. The net external pressure for this case is 14.7 psig, applied throughout the inner periphery of the model. Relative to the upper and lower ICV seal flanges, the internal pressure does not extend beyond (below) the top of the upper main O-ring seal groove.

A uniform temperature of 70 °F is utilized to determine the temperature-dependent, material property values. The only material properties affected by a temperature of 70 °F are the elastic modulus and the thermal expansion coefficient for the stainless steel. Consistent with Table 2.3-1 from Section 2.3.1, *Mechanical Properties Applied to Analytic Evaluations*, the elastic modulus and thermal expansion coefficient for Type 304 stainless steel are  $28.3(10)^6$  psi and  $8.46(10)^{-6}$  inches/inch/°F, respectively, at a temperature of 70 °F.

Both the reference and uniform temperature are set to 70 °F, thereby excluding the effects of differential thermal expansion for this case.

For analysis model review, the ANSYS® input file is listed in Table 2.10.1-6.

Table 2.10.1-1 – ANSYS® Input Listing for OCA Load Case 1

```

/TITLE, OCV: PRES=64.7/3.5 PSIA; TEMP=160/160 DEG-F
C*** Define the element types
ET,1,42,,,1
ET,2,51
ET,3,42,,,1
ET,4,12,,,1
ET,5,12
ET,6,3
C*** Define the reference and uniform temperatures
TREF,160
TUNIF,160
C*** Define the material properties for non-slotted
steel regions
EX,1,27.8E+06
NUXY,1,.3
DENS,1,7.505E-04
ALPX,1,8.694E-06
C*** Define the material properties for slotted
steel regions
EX,2,13.9E+06
EY,2,13.9E+06
EZ,2,1
NUXY,2,.3
NUXZ,2,0
NUYZ,2,0
DENS,2,3.7525E-04
ALPX,2,8.694E-06
ALPY,2,8.694E-06
ALPZ,2,8.694E-06
C*** Define the material properties for the
polyurethane foam
EX,3,5854
EY,3,8789
EZ,3,5854
GXY,3,2553
GXZ,3,1921
GYZ,3,2553
NUXY,3,.33
DENS,3,1.198E-05
ALPX,3,4.9E-05
C*** Define the material properties for the rigid
coupling elements (STIF3 beams)
EX,4,27.8E+06
NUXY,4,.3
DENS,4,0
ALPX,4,8.694E-06
C*** Define the element real constants
R,1,.25
R,2,.1875
R,3,.375
R,4,.075
R,5,2E+10,,1
R,6,-15,2E+10,-.036
R,7,15,2E+10,-.036
R,8,0,2E+10,,1
R,9,1,1,1
R,101,-180.000,2E+10,,1
R,102,-177.444,2E+10,,1
R,103,-174.888,2E+10,,1
R,104,-172.333,2E+10,,1
R,105,-169.777,2E+10,,1
R,106,-167.221,2E+10,,1
R,107,-164.665,2E+10,,1
R,108,-162.109,2E+10,,1
R,109,-159.553,2E+10,,1
R,110,-156.998,2E+10,,1
R,111,-154.442,2E+10,,1
R,112,-141.553,2E+10,,1
R,113,-128.665,2E+10,,1
R,114,-115.777,2E+10,,1
R,115,-102.888,2E+10,,1
R,116,-90.0000,2E+10,,1
R,130,-102.000,2E+10,,1
R,136,-77.1520,2E+10,,1
R,137,-64.3041,2E+10,,1
R,138,-51.4561,2E+10,,1
R,139,-38.6081,2E+10,,1
R,140,-25.7602,2E+10,,1
R,141,-23.1841,2E+10,,1
R,142,-20.6081,2E+10,,1
R,143,-18.0321,2E+10,,1
R,144,-15.4561,2E+10,,1
R,145,-12.8801,2E+10,,1
R,146,-10.3041,2E+10,,1
R,147,-7.72805,2E+10,,1
R,148,-5.15203,2E+10,,1
R,149,-2.57602,2E+10,,1
R,150,,2E+10,,1
R,639,-58.7238,2E+10,,1
R,640,-27.4476,2E+10,,1
R,641,-24.7029,2E+10,,1
R,642,-21.9581,2E+10,,1
R,643,-19.2133,2E+10,,1
R,644,-16.4686,2E+10,,1
R,645,-13.7238,2E+10,,1
R,646,-10.9790,2E+10,,1
R,647,-8.23429,2E+10,,1
R,648,-5.48952,2E+10,,1
R,649,-2.74476,2E+10,,1
C*** Define the nodes for the lower seal flange
LOCAL,11,,38.24941495,80.051977923,,-12
N,1001
N,1005,.25
FILL
N,1016,,.58677836
N,1020,.25,.58677836
FILL
FILL,1001,1016,2,1006,5,5,1
N,1026,,.896632635
LOCAL,12,,38.505,80
MOVE,1026,11,0,999,0,12,-.065,999,0
FILL,1016,1026,1,1021
LOCAL,11,1,39.12699808,80.47
N,1025,.5,148.5
N,1030,.5,129
N,1031,.5,109.5
N,1032,.5,90
CSYS,12
FILL,1021,1025,3,1022,1,2,5
N,1033,.775,.97
N,1034,1,145,.97
N,1076,-.065,2.98
FILL,1026,1076,8,1035,5
FILL,1035,1076,7,1041,5
N,1060,.775,2.15593612
NGEN,2,6,1033,1034,1,,.16
FILL,1039,1060,3,1045,5
FILL,1035,1039
FILL,1041,1045,3,1042,1,4,5
N,1064,1,245,2.03
FILL,1060,1064
N,1092,-.065,2.98
N,1096,.77960172,2.76
FILL
N,1100,1,245,2.76
FILL,1096,1100
FILL,1056,1092,3,1065,9,9,1
NGEN,3,9,1098,1100,1,,.26
N,1146,.14020351,4.4
FILL,1092,1146,5,1101,9
N,1164,.14020351,4.98
FILL,1146,1164,1,1155
LOCAL,11,,39.13520351,84.98,,-86.15
N,1168
N,1159,.3
NGEN,3,-1,1159,1159,,-.125
N,1148,.58,-.25
NGEN,2,-18,1157,1159,1,.56
NGEN,2,-9,1139,1141,1,.25
NGEN,2,-27,1148,1148,,.81
NGEN,2,-18,1130,1132,1,.56
FILL,1096,1114,1,1105
CSYS,12
FILL,1101,1105
FILL,1110,1112,1,1111,,6,9
FILL,1164,1168

```

C\*\*\* Define the nodes for the upper seal flange

LOCAL,11,,38.405,82.81  
 N,2001,,5  
 N,2005,,25,5  
 FILL  
 NGEN,3,5,2001,2005,1,,-.25  
 N,2031,,3.45  
 N,2035,,91,3.45  
 FILL  
 FILL,2011,2031,3,2016,5,5,1  
 N,2051,,2.543442101  
 N,2055,,91,2.543442101  
 FILL  
 FILL,2031,2051,3,2036,5,4,1  
 N,2040,,91,3.29  
 FILL,2040,2055,2,2045,5  
 N,2059,1.345,2.66  
 FILL,2055,2059  
 N,2071,,2.17  
 N,2073,,21504507,2.17  
 FILL  
 N,2077,,74504507,2.17  
 FILL,2073,2077  
 FILL,2051,2071,1,2060  
 FILL,2054,2076,1,2065  
 FILL,2060,2065  
 N,2081,1.345,2.17  
 FILL,2077,2081  
 FILL,2055,2077,1,2066,,5,1  
 N,2107,,85759646,,54  
 N,2109,1.10488343,,54  
 FILL  
 N,2111,1.345,,54  
 FILL,2109,2111  
 FILL,2077,2107,5,2082,5,5,1  
 N,2117,,94488343  
 N,2119,1.10488343  
 FILL  
 FILL,2109,2119,1,2114  
 N,2112,,870715847,,35  
 FILL,2112,2114  
 N,2120,1.345,3.45  
 N,2121,1.345,3.29  
 NGEN,2,51,2071,2073,1,,-.305  
 NGEN,2,3,2122,2124,1,,-.305

C\*\*\* Define the nodes for the locking ring

LOCAL,11,,39.35,81.29  
 N,3001  
 N,3005,,435  
 FILL  
 N,3009,,935  
 FILL,3005,3009  
 N,3037,,81  
 N,3041,,435,,693442101  
 FILL  
 N,3045,,935,,693442101  
 FILL,3041,3045  
 FILL,3001,3037,3,3010,9,9,1  
 N,3145,,4.11  
 N,3149,,435,4.226557899  
 FILL  
 N,3153,,935,4.226557899  
 FILL,3149,3153  
 FILL,3041,3149,11,3050,9,5,1  
 N,3181,,4.67  
 N,3185,,535,4.67  
 FILL  
 N,3189,,935,4.67  
 FILL,3185,3189  
 FILL,3145,3181,3,3154,9,9,1

C\*\*\* Define the nodes for the OCA inner shell (OCV)

LOCAL,11,1,,84.5  
 N,101,74.25,-90  
 N,111,74.25,-64.44174492  
 FILL  
 LOCAL,12,1,28.3125,24.29659664  
 N,116,8.625  
 FILL,111,116  
 CSYS  
 N,117,36.9375,25.79659664  
 N,123,36.9375,51.79659664  
 FILL  
 N,129,36.9375,73.95292590

FILL,123,129  
 NGEN,2,-872,1003,1003  
 FILL,129,131  
 NGEN,2,-1870,2003,2003  
 N,135,38.53,93.78649751  
 FILL,133,135  
 LOCAL,13,1,29.905,93.78649751  
 N,140,8.625,64.23984399  
 FILL,135,140  
 LOCAL,14,1,,31.8125  
 N,150,77.4375,90  
 FILL,140,150

C\*\*\* Define the nodes for the OCA outer shell

CSYS  
 N,601  
 N,613,47.0625  
 FILL  
 N,626,47.0625,64.7775  
 FILL,613,626  
 N,629,47.0625,76.7775  
 FILL,626,629  
 N,630,47.0625,77.6325  
 N,638,47.0625,105.3440689  
 FILL,630,638  
 LOCAL,15,1,40.5625,105.3440689  
 N,640,6.5,62.55238078  
 FILL,638,640  
 LOCAL,16,1,,27.25  
 N,650,94.5,90  
 FILL,640,650

C\*\*\* Define the nodes for the polyurethane foam inner surface

CSYS  
 NGEN,2,100,101,150,1  
 N,132,38.58338729,80.97  
 N,232,38.53,86.26

C\*\*\* Define the nodes for the polyurethane foam outer surface

NGEN,2,-100,601,650,1

C\*\*\* Define the intermediate polyurethane foam nodes

FILL,201,501,2,301,100,29,1  
 N,300,43.9375,80.9  
 N,331,41.5375,81.8825  
 N,332,41.5375,86.26  
 N,429,43.9375,76.7775  
 N,430,44.2375,77.6375  
 N,431,44.2375,81.8825  
 FILL,229,429,1,329,100,2,1  
 FILL,230,300,1,330  
 FILL,332,532,1,432  
 FILL,233,533,2,333,100,18,1  
 N,323,38.4375,51.79659664

C\*\*\* Define the nodes for the Z-flanges

NGEN,2,272,429,429,0  
 NGEN,2,402,300,300,0  
 NGEN,2,273,430,430,0  
 RP2,,1,1  
 NGEN,2,374,331,331,0  
 RP2,,1,1

C\*\*\* Define the elements for the lower seal flange

TYPE,1  
 MAT,1  
 REAL,1  
 E,1001,1002,1007,1006  
 RP4,1,1,1,1  
 EGEN,5,5,1,4,1  
 E,1026,1027,1036,1035  
 E,1027,1028,1036  
 E,1028,1029,1037,1036  
 E,1029,1030,1031,1037  
 E,1031,1032,1038,1037  
 RP3,1,1,1,1  
 E,1035,1036,1042,1041  
 RP4,1,1,1,1  
 E,1041,1042,1047,1046  
 RP4,1,1,1,1  
 EGEN,3,5,32,35,1  
 E,1056,1057,1066,1065  
 RP4,1,1,1,1  
 EGEN,4,9,44,47,1

```

MAT,2
E,1060,1061,1070,1069
RP4,1,1,1,1
EGEN,4,9,60,63,1
EGEN,3,9,74,75,1
EGEN,3,9,56,59,1
EGEN,7,9,84,85,1
EGEN,3,1,99,99
EGEN,3,1,93,93
C*** Define the elements for the upper seal flange
TYPE,1
MAT,1
REAL,1
E,2006,2007,2002,2001
RP4,1,1,1,1
EGEN,10,5,104,107,1
E,2040,2121,2120,2035
E,2060,2061,2052,2051
E,2061,2062,2052
E,2062,2063,2053,2052
E,2063,2064,2053
E,2064,2065,2054,2053
RP6,1,1,1,1
E,2071,2072,2061,2060
RP10,1,1,1,1
E,2122,2123,2072,2071
RP2,1,1,1,1
E,2125,2126,2123,2122
RP2,1,1,1,1
E,2082,2083,2078,2077
RP4,1,1,1,1
EGEN,6,5,169,172,1
EGEN,3,5,189,190,1
C*** Define the elements for the locking ring
TYPE,1
MAT,2
REAL,1
E,3001,3002,3011,3010
RP4,1,1,1,1
EGEN,4,9,197,200,1
MAT,1
E,3005,3006,3015,3014
RP4,1,1,1,1
EGEN,20,9,213,216,1
E,3145,3146,3155,3154
RP4,1,1,1,1
EGEN,4,9,293,296,1
C*** Define the elements for the OCA inner shell
(OVCV)
TYPE,2
MAT,1
REAL,1
E,101,102
RP16,1,1
REAL,2
E,117,118
RP12,1,1
REAL,3
E,123,323
REAL,1
E,129,130
E,130,1003
E,2003,134
E,134,135
RP16,1,1
C*** Define the elements for the OCA outer shell
REAL,1
E,601,602
RP25,1,1
REAL,3
E,626,627
RP3,1,1
E,630,631
RP8,1,1
REAL,1
E,638,639
RP12,1,1
C*** Define the elements for the Z-flanges
REAL,4
E,629,701
E,701,702
E,702,1034
E,1034,1033
E,630,703
E,703,704
RP3,1,1
E,706,2120
E,2120,2035
C*** Define the polyurethane foam elements
TYPE,3
MAT,3
REAL,1
E,201,301,302,202
RP29,1,1,1,1
E,231,230,330
E,301,401,402,302
RP28,1,1,1,1
E,329,429,300,330
E,300,132,231,330
E,401,501,502,402
RP28,1,1,1,1
E,333,233,232,332
E,233,333,334,234
RP17,1,1,1,1
E,331,431,432,332
RP19,1,1,1,1
E,430,530,531,431
RP20,1,1,1,1
C*** Define the interface elements between the steel
shells and the polyurethane foam
TYPE,5
MAT,1
REAL,101
E,101,201
REAL,102
E,102,202
REAL,103
E,103,203
REAL,104
E,104,204
REAL,105
E,105,205
REAL,106
E,106,206
REAL,107
E,107,207
REAL,108
E,108,208
REAL,109
E,109,209
REAL,110
E,110,210
REAL,111
E,111,211
REAL,112
E,112,212
REAL,113
E,113,213
REAL,114
E,114,214
REAL,115
E,115,215
REAL,116
E,116,216
RP7,1,1
E,124,224
RP6,1,1
REAL,130
E,129,229
RP2,1,1
E,1003,231
REAL,101
E,702,300
E,701,429
E,622,529
REAL,150
E,706,332
E,705,331
E,704,431
E,703,430
E,630,530
REAL,116
E,300,702
E,429,701
E,706,332

```

```

E,705,331
E,704,431
E,703,430
E,2003,233
E,134,234
RP2,1,1
REAL,136
E,136,236
REAL,137
E,137,237
REAL,138
E,138,238
REAL,139
E,139,239
REAL,140
E,140,240
REAL,141
E,141,241
REAL,142
E,142,242
REAL,143
E,143,243
REAL,144
E,144,244
REAL,145
E,145,245
REAL,146
E,146,246
REAL,147
E,147,247
REAL,148
E,148,248
REAL,149
E,149,249
REAL,150
E,150,250
REAL,101
E,501,601
RPL3,1,1
REAL,116
E,513,613
RP26,1,1
REAL,639
E,539,639
REAL,640
E,540,640
REAL,641
E,541,641
REAL,642
E,542,642
REAL,643
E,543,643
REAL,644
E,544,644
REAL,645
E,545,645
REAL,646
E,546,646
REAL,647
E,547,647
REAL,648
E,548,648
REAL,649
E,549,649
REAL,150
E,550,650

C*** Define the interface elements between the lower
seal flange and the locking ring
TYPE,4
MAT,1
REAL,6
E,3038,1061
RP3,1,1

```

```

C*** Define the interface elements between the upper
seal flange and the locking ring
TYPE,4
MAT,1
REAL,7
E,2056,3146
RP3,1,1

C*** Define the interface elements between the lower
seal flange and the upper seal flange
TYPE,5
MAT,1
REAL,8
E,1164,2073
RP5,1,1

C*** Couple the lower shell to the lower seal flange
TYPE,6
MAT,4
REAL,9
E,1001,1002
RP4,1,1

C*** Couple the upper shell to the upper seal flange
TYPE,6
MAT,4
REAL,9
E,2001,2002
RP4,1,1

C*** Define the displacement constraints
D,101,UX,0,,601,500,ROTZ
D,201,UX,0,,501,100
D,150,UX,0,,650,500,ROTZ
D,250,UX,0,,550,100
D,3099,UY,0

C*** Define the pressure loads
P,101,102,61.2,,129,1
P,130,1003,61.2
P,1001,1006,61.2,,1021,5
P,1026,1035,61.2
P,1035,1041,61.2
P,1041,1046,61.2,,1051,5
P,1056,1065,61.2,,1155,9
P,1164,1165,61.2,,1167,1
P,1168,1159,61.2
P,2077,2082,61.2
P,2073,2074,61.2,,2076,1
P,2127,2124,61.2
P,2124,2073,61.2
P,2125,2126,61.2,,2126,1
P,2122,2125,61.2
P,2071,2122,61.2
P,2001,2002,61.2,,2002,1
P,2001,2006,61.2,,2046,5
P,2051,2060,61.2
P,2060,2071,61.2
P,2003,134,61.2
P,134,135,61.2,,149,1

C*** Re-order the elements to reduce execution time
WSTART,101,601,100
WSTART,150,650,100
WSTART,1003
WSTART,1034
WSTART,2120
WSTART,2003
WAVES

C*** Set convergence criteria, write a solution
file, and exit
ITER,-20,20
AFWRITE
FINISH

```

Table 2.10.1-2 – ANSYS® Input Listing for OCA Load Case 2

```

/TITLE, OCV: PRES=64.7/3.5 PSIA; TEMP=70/160 DEG-F
C*** Define the element types
ET,1,42,,,1
ET,2,51
ET,3,42,,,1
ET,4,12,,,1
ET,5,12
ET,6,3
C*** Define the reference and uniform temperatures
TREF,70
TUNIF,160
C*** Define the material properties for non-slotted
steel regions
EX,1,27.8E+06
NUXY,1,.3
DENS,1,7.505E-04
ALPX,1,8.694E-06
C*** Define the material properties for slotted
steel regions
EX,2,13.9E+06
EY,2,13.9E+06
EZ,2,1
NUXY,2,.3
NUXZ,2,0
NUYZ,2,0
DENS,2,3.7525E-04
ALPX,2,8.694E-06
ALPY,2,8.694E-06
ALPZ,2,8.694E-06
C*** Define the material properties for the
polyurethane foam
EX,3,5854
EY,3,8789
EZ,3,5854
GXZ,3,2553
GYZ,3,1921
NUXY,3,.33
DENS,3,1.198E-05
ALPX,3,4.9E-05
C*** Define the material properties for the rigid
coupling elements (STIF3 beams)
EX,4,27.8E+06
NUXY,4,.3
DENS,4,0
ALPX,4,8.694E-06
C*** Define the element real constants
R,1,.25
R,2,.1875
R,3,.375
R,4,.075
R,5,,2E+10,,1
R,6,-15,2E+10,-.036
R,7,15,2E+10,-.036
R,8,0,2E+10,,1
R,9,1,1,1
R,101,-180.000,2E+10,,1
R,102,-177.444,2E+10,,1
R,103,-174.888,2E+10,,1
R,104,-172.333,2E+10,,1
R,105,-169.777,2E+10,,1
R,106,-167.221,2E+10,,1
R,107,-164.665,2E+10,,1
R,108,-162.109,2E+10,,1
R,109,-159.553,2E+10,,1
R,110,-156.998,2E+10,,1
R,111,-154.442,2E+10,,1
R,112,-141.553,2E+10,,1
R,113,-128.665,2E+10,,1
R,114,-115.777,2E+10,,1
R,115,-102.888,2E+10,,1
R,116,-90.0000,2E+10,,1
R,130,-102.000,2E+10,,1
R,136,-77.1520,2E+10,,1
R,137,-64.3041,2E+10,,1
R,138,-51.4561,2E+10,,1
R,139,-38.6081,2E+10,,1
R,140,-25.7602,2E+10,,1
R,141,-23.1841,2E+10,,1
R,142,-20.6081,2E+10,,1
R,143,-18.0321,2E+10,,1
R,144,-15.4561,2E+10,,1
R,145,-12.8801,2E+10,,1
R,146,-10.3041,2E+10,,1
R,147,-7.72805,2E+10,,1
R,148,-5.15203,2E+10,,1
R,149,-2.57602,2E+10,,1
R,150,,2E+10,,1
R,639,-58.7238,2E+10,,1
R,640,-27.4476,2E+10,,1
R,641,-24.7029,2E+10,,1
R,642,-21.9581,2E+10,,1
R,643,-19.2133,2E+10,,1
R,644,-16.4686,2E+10,,1
R,645,-13.7238,2E+10,,1
R,646,-10.9790,2E+10,,1
R,647,-8.23429,2E+10,,1
R,648,-5.48952,2E+10,,1
R,649,-2.74476,2E+10,,1
C*** Define the nodes for the lower seal flange
LOCAL,11,,38.24941495,80.051977923,,-12
N,1001
N,1005,,25
FILL
N,1016,,.58677836
N,1020,,25,.58677836
FILL
FILL,1001,1016,2,1006,5,5,1
N,1026,,.896632635
LOCAL,12,,38.505,80
MOVE,1026,11,0,999,0,12,-.065,999,0
FILL,1016,1026,1,1021
LOCAL,11,1,39.12699808,80.47
N,1025,,.5,148.5
N,1030,,.5,129
N,1031,,.5,109.5
N,1032,,.5,90
CSYS,12
FILL,1021,1025,3,1022,1,2,5
N,1033,,.775,.97
N,1034,1,145,.97
N,1076,-.065,2.98
FILL,1026,1076,8,1035,5
FILL,1035,1076,7,1041,5
N,1060,,.775,2.15593612
NGEN,2,6,1033,1034,1,,.16
FILL,1039,1060,3,1045,5
FILL,1035,1039
FILL,1041,1045,3,1042,1,4,5
N,1064,1,245,2.03
FILL,1060,1064
N,1092,-.065,2.98
N,1096,,.77960172,2.76
FILL
N,1100,1,245,2.76
FILL,1096,1100
FILL,1056,1092,3,1065,9,9,1
NGEN,3,9,1098,1100,1,,.26
N,1146,.14020351,4.4
FILL,1092,1146,5,1101,9
N,1164,.14020351,4.98
FILL,1146,1164,1,1155
LOCAL,11,,39.13520351,84.98,,-86.15
N,1168
N,1159,.3
NGEN,3,-1,1159,1159,,-.125
N,1148,.58,-.25
NGEN,2,-18,1157,1159,1,.56
NGEN,2,-9,1139,1141,1,.25
NGEN,2,-27,1148,1148,1,.81
NGEN,2,-18,1130,1132,1,.56
FILL,1096,1114,1,1105
CSYS,12
FILL,1101,1105
FILL,1110,1112,1,1111,,6,9
FILL,1164,1168

```

C\*\*\* Define the nodes for the upper seal flange

LOCAL,11,,38.405,82.81  
 N,2001,,5  
 N,2005,,25,5  
 FILL  
 NGEN,3,5,2001,2005,1,,-.25  
 N,2031,,3.45  
 N,2035,,.91,3.45  
 FILL  
 FILL,2011,2031,3,2016,5,5,1  
 N,2051,,2.543442101  
 N,2055,,.91,2.543442101  
 FILL  
 FILL,2031,2051,3,2036,5,4,1  
 N,2040,,.91,3.29  
 FILL,2040,2055,2,2045,5  
 N,2059,1.345,2.66  
 FILL,2055,2059  
 N,2071,,2.17  
 N,2073,,.21504507,2.17  
 FILL  
 N,2077,,.74504507,2.17  
 FILL,2073,2077  
 FILL,2051,2071,1,2060  
 FILL,2054,2076,1,2065  
 FILL,2060,2065  
 N,2081,1.345,2.17  
 FILL,2077,2081  
 FILL,2055,2077,1,2066,,5,1  
 N,2107,,.85759646,.54  
 N,2109,1.10488343,.54  
 FILL  
 N,2111,1.345,.54  
 FILL,2109,2111  
 FILL,2077,2107,5,2082,5,5,1  
 N,2117,,.94488343  
 N,2119,1.10488343  
 FILL  
 FILL,2109,2119,1,2114  
 N,2112,,.870715847,.35  
 FILL,2112,2114  
 N,2120,1.345,3.45  
 N,2121,1.345,3.29  
 NGEN,2,51,2071,2073,1,,-.305  
 NGEN,2,3,2122,2124,1,,-.305

C\*\*\* Define the nodes for the locking ring

LOCAL,11,,39.35,81.29  
 N,3001  
 N,3005,,.435  
 FILL  
 N,3009,,.935  
 FILL,3005,3009  
 N,3037,,.81  
 N,3041,,.435,.693442101  
 FILL  
 N,3045,,.935,.693442101  
 FILL,3041,3045  
 FILL,3001,3037,3,3010,9,9,1  
 N,3145,,4.11  
 N,3149,,.435,4.226557899  
 FILL  
 N,3153,,.935,4.226557899  
 FILL,3149,3153  
 FILL,3041,3149,11,3050,9,5,1  
 N,3181,,4.67  
 N,3185,,.535,4.67  
 FILL  
 N,3189,,.935,4.67  
 FILL,3185,3189  
 FILL,3145,3181,3,3154,9,9,1

C\*\*\* Define the nodes for the OCA inner shell (OCV)

LOCAL,11,1,,84.5  
 N,101,74.25,-90  
 N,111,74.25,-64.44174492  
 FILL  
 LOCAL,12,1,28.3125,24.29659664  
 N,116,8.625  
 FILL,111,116  
 CSYS  
 N,117,36.9375,25.79659664  
 N,123,36.9375,51.79659664  
 FILL  
 N,129,36.9375,73.95292590

FILL,123,129  
 NGEN,2,-872,1003,1003  
 FILL,129,131  
 NGEN,2,-1870,2003,2003  
 N,135,38.53,93.78649751  
 FILL,133,135  
 LOCAL,13,1,29.905,93.78649751  
 N,140,8.625,64.23984399  
 FILL,135,140  
 LOCAL,14,1,,31.8125  
 N,150,77.4375,90  
 FILL,140,150

C\*\*\* Define the nodes for the OCA outer shell

CSYS  
 N,601  
 N,613,47.0625  
 FILL  
 N,626,47.0625,64.7775  
 FILL,613,626  
 N,629,47.0625,76.7775  
 FILL,626,629  
 N,630,47.0625,77.6325  
 N,638,47.0625,105.3440689  
 FILL,630,638  
 LOCAL,15,1,40.5625,105.3440689  
 N,640,6.5,62.55238078  
 FILL,638,640  
 LOCAL,16,1,,27.25  
 N,650,94.5,90  
 FILL,640,650

C\*\*\* Define the nodes for the polyurethane foam inner surface

CSYS  
 NGEN,2,100,101,150,1  
 N,132,38.58338729,80.97  
 N,232,38.53,86.26

C\*\*\* Define the nodes for the polyurethane foam outer surface

NGEN,2,-100,601,650,1

C\*\*\* Define the intermediate polyurethane foam nodes

FILL,201,501,2,301,100,29,1  
 N,300,43.9375,80.9  
 N,331,41.5375,81.8825  
 N,332,41.5375,86.26  
 N,429,43.9375,76.7775  
 N,430,44.2375,77.6375  
 N,431,44.2375,81.8825  
 FILL,229,429,1,329,100,2,1  
 FILL,230,300,1,330  
 FILL,332,532,1,432  
 FILL,233,533,2,333,100,18,1  
 N,323,38.4375,51.79659664

C\*\*\* Define the nodes for the Z-flanges

NGEN,2,272,429,429,0  
 NGEN,2,402,300,300,0  
 NGEN,2,273,430,430,0  
 RP2,,1,1  
 NGEN,2,374,331,331,0  
 RP2,,1,1

C\*\*\* Define the elements for the lower seal flange

TYPE,1  
 MAT,1  
 REAL,1  
 E,1001,1002,1007,1006  
 RP4,1,1,1,1  
 EGEN,5,5,1,4,1  
 E,1026,1027,1036,1035  
 E,1027,1028,1036  
 E,1028,1029,1037,1036  
 E,1029,1030,1031,1037  
 E,1031,1032,1038,1037  
 RP3,1,1,1,1  
 E,1035,1036,1042,1041  
 RP4,1,1,1,1  
 E,1041,1042,1047,1046  
 RP4,1,1,1,1  
 EGEN,3,5,32,35,1  
 E,1056,1057,1066,1065  
 RP4,1,1,1,1  
 EGEN,4,9,44,47,1

```

MAT,2
E,1060,1061,1070,1069
RP4,1,1,1,1
EGEN,4,9,60,63,1
EGEN,3,9,74,75,1
EGEN,3,9,56,59,1
EGEN,7,9,84,85,1
EGEN,3,1,99,99
EGEN,3,1,93,93
C*** Define the elements for the upper seal flange
TYPE,1
MAT,1
REAL,1
E,2006,2007,2002,2001
RP4,1,1,1,1
EGEN,10,5,104,107,1
E,2040,2121,2120,2035
E,2060,2061,2052,2051
E,2061,2062,2052
E,2062,2063,2053,2052
E,2063,2064,2053
E,2064,2065,2054,2053
RP6,1,1,1,1
E,2071,2072,2061,2060
RP10,1,1,1,1
E,2122,2123,2072,2071
RP2,1,1,1,1
E,2125,2126,2123,2122
RP2,1,1,1,1
E,2082,2083,2078,2077
RP4,1,1,1,1
EGEN,6,5,169,172,1
EGEN,3,5,189,190,1
C*** Define the elements for the locking ring
TYPE,1
MAT,2
REAL,1
E,3001,3002,3011,3010
RP4,1,1,1,1
EGEN,4,9,197,200,1
MAT,1
E,3005,3006,3015,3014
RP4,1,1,1,1
EGEN,20,9,213,216,1
E,3145,3146,3155,3154
RP4,1,1,1,1
EGEN,4,9,293,296,1
C*** Define the elements for the OCA inner shell
(OCV)
TYPE,2
MAT,1
REAL,1
E,101,102
RP16,1,1
REAL,2
E,117,118
RP12,1,1
REAL,3
E,123,323
REAL,1
E,129,130
E,130,1003
E,2003,134
E,134,135
RP16,1,1
C*** Define the elements for the OCA outer shell
REAL,1
E,601,602
RP25,1,1
REAL,3
E,626,627
RP3,1,1
E,630,631
RP8,1,1
REAL,1
E,638,639
RP12,1,1
C*** Define the elements for the Z-flanges
REAL,4
E,629,701
E,701,702
E,702,1034
E,1034,1033
E,630,703
E,703,704
RP3,1,1
E,706,2120
E,2120,2035
C*** Define the polyurethane foam elements
TYPE,3
MAT,3
REAL,1
E,201,301,302,202
RP29,1,1,1,1
E,231,230,330
E,301,401,402,302
RP28,1,1,1,1
E,329,429,300,330
E,300,132,231,330
E,401,501,502,402
RP28,1,1,1,1
E,333,233,232,332
E,233,333,334,234
RP17,1,1,1,1
E,331,431,432,332
RP19,1,1,1,1
E,430,530,531,431
RP20,1,1,1,1
C*** Define the interface elements between the steel
shells and the polyurethane foam
TYPE,5
MAT,1
REAL,101
E,101,201
REAL,102
E,102,202
REAL,103
E,103,203
REAL,104
E,104,204
REAL,105
E,105,205
REAL,106
E,106,206
REAL,107
E,107,207
REAL,108
E,108,208
REAL,109
E,109,209
REAL,110
E,110,210
REAL,111
E,111,211
REAL,112
E,112,212
REAL,113
E,113,213
REAL,114
E,114,214
REAL,115
E,115,215
REAL,116
E,116,216
RP7,1,1
E,124,224
RP6,1,1
REAL,130
E,129,229
RP2,1,1
E,1003,231
REAL,101
E,702,300
E,701,429
E,622,529
REAL,150
E,706,332
E,705,331
E,704,431
E,703,430
E,630,530
REAL,116
E,300,702
E,429,701
E,706,332

```

```

E,705,331
E,704,431
E,703,430
E,2003,233
E,134,234
RP2,1,1
REAL,136
E,136,236
REAL,137
E,137,237
REAL,138
E,138,238
REAL,139
E,139,239
REAL,140
E,140,240
REAL,141
E,141,241
REAL,142
E,142,242
REAL,143
E,143,243
REAL,144
E,144,244
REAL,145
E,145,245
REAL,146
E,146,246
REAL,147
E,147,247
REAL,148
E,148,248
REAL,149
E,149,249
REAL,150
E,150,250
REAL,101
E,501,601
RP13,1,1
REAL,116
E,513,613
RP26,1,1
REAL,639
E,539,639
REAL,640
E,540,640
REAL,641
E,541,641
REAL,642
E,542,642
REAL,643
E,543,643
REAL,644
E,544,644
REAL,645
E,545,645
REAL,646
E,546,646
REAL,647
E,547,647
REAL,648
E,548,648
REAL,649
E,549,649
REAL,150
E,550,650

C*** Define the interface elements between the lower
seal flange and the locking ring

TYPE,4
MAT,1
REAL,6
E,3038,1061
RP3,1,1

```

```

C*** Define the interface elements between the upper
seal flange and the locking ring

TYPE,4
MAT,1
REAL,7
E,2056,3146
RP3,1,1

C*** Define the interface elements between the lower
seal flange and the upper seal flange

TYPE,5
MAT,1
REAL,8
E,1164,2073
RP5,1,1

C*** Couple the lower shell to the lower seal flange

TYPE,6
MAT,4
REAL,9
E,1001,1002
RP4,1,1

C*** Couple the upper shell to the upper seal flange

TYPE,6
MAT,4
REAL,9
E,2001,2002
RP4,1,1

C*** Define the displacement constraints

D,101,UX,0,,601,500,ROTZ
D,201,UX,0,,501,100
D,150,UX,0,,650,500,ROTZ
D,250,UX,0,,550,100
D,3099,UY,0

C*** Define the pressure loads

P,101,102,61.2,,129,1
P,130,1003,61.2
P,1001,1006,61.2,,1021,5
P,1026,1035,61.2
P,1035,1041,61.2
P,1041,1046,61.2,,1051,5
P,1056,1065,61.2,,1155,9
P,1164,1165,61.2,,1167,1
P,1168,1159,61.2
P,2077,2082,61.2
P,2073,2074,61.2,,2076,1
P,2127,2124,61.2
P,2124,2073,61.2
P,2125,2126,61.2,,2126,1
P,2122,2125,61.2
P,2071,2122,61.2
P,2001,2002,61.2,,2002,1
P,2001,2006,61.2,,2046,5
P,2051,2060,61.2
P,2060,2071,61.2
P,2003,134,61.2
P,134,135,61.2,,149,1

C*** Re-order the elements to reduce execution time

WSTART,101,601,100
WSTART,150,650,100
WSTART,1003
WSTART,1034
WSTART,2120
WSTART,2003
WAVES

C*** Set convergence criteria, write a solution
file, and exit

ITER,-20,20
AFWRITE
FINISH

```

Table 2.10.1-3 – ANSYS® Input Listing for OCA Load Case 3

```

/TITLE, OCV: PRES=14.7/14.7 PSIA; TEMP=70/-40 DEG-F
C*** Define the element types
ET,1,42,,,1
ET,2,51
ET,3,42,,,1
ET,4,12,,,1
ET,5,12
ET,6,3
C*** Define the reference and uniform temperatures
TREF,70
TUNIF,-40
C*** Define the material properties for non-slotted
steel regions
EX,1,28.8E+06
NUXY,1,.3
DENS,1,7.505E-04
ALPX,1,8.080E-06
C*** Define the material properties for slotted
steel regions
EX,2,14.4E+06
EY,2,14.4E+06
EZ,2,1
NUXY,2,.3
NUXZ,2,0
NUYZ,2,0
DENS,2,3.7525E-04
ALPX,2,8.080E-06
ALPY,2,8.080E-06
ALPZ,2,8.080E-06
C*** Define the material properties for the
polyurethane foam
EX,3,5854
EY,3,8789
EZ,3,5854
GXY,3,2553
GXZ,3,1921
GYZ,3,2553
NUXY,3,.33
DENS,3,1.198E-05
ALPX,3,4.3E-05
C*** Define the material properties for the rigid
coupling elements (STIF3 beams)
EX,4,28.8E+06
NUXY,4,.3
DENS,4,0
ALPX,4,8.080E-06
C*** Define the element real constants
R,1,.25
R,2,.1875
R,3,.375
R,4,.075
R,5,2E+10,,1
R,6,-15,2E+10,-.036
R,7,15,2E+10,-.036
R,8,0,2E+10,,1
R,9,1,1,1
R,101,-180.000,2E+10,,1
R,102,-177.444,2E+10,,1
R,103,-174.888,2E+10,,1
R,104,-172.333,2E+10,,1
R,105,-169.777,2E+10,,1
R,106,-167.221,2E+10,,1
R,107,-164.665,2E+10,,1
R,108,-162.109,2E+10,,1
R,109,-159.553,2E+10,,1
R,110,-156.998,2E+10,,1
R,111,-154.442,2E+10,,1
R,112,-141.553,2E+10,,1
R,113,-128.665,2E+10,,1
R,114,-115.777,2E+10,,1
R,115,-102.888,2E+10,,1
R,116,-90.0000,2E+10,,1
R,130,-102.000,2E+10,,1
R,136,-77.1520,2E+10,,1
R,137,-64.3041,2E+10,,1
R,138,-51.4561,2E+10,,1
R,139,-38.6081,2E+10,,1
R,140,-25.7602,2E+10,,1
R,141,-23.1841,2E+10,,1
R,142,-20.6081,2E+10,,1
R,143,-18.0321,2E+10,,1
R,144,-15.4561,2E+10,,1
R,145,-12.8801,2E+10,,1
R,146,-10.3041,2E+10,,1
R,147,-7.72805,2E+10,,1
R,148,-5.15203,2E+10,,1
R,149,-2.57602,2E+10,,1
R,150,2E+10,,1
R,639,-58.7238,2E+10,,1
R,640,-27.4476,2E+10,,1
R,641,-24.7029,2E+10,,1
R,642,-21.9581,2E+10,,1
R,643,-19.2133,2E+10,,1
R,644,-16.4686,2E+10,,1
R,645,-13.7238,2E+10,,1
R,646,-10.9790,2E+10,,1
R,647,-8.23429,2E+10,,1
R,648,-5.48952,2E+10,,1
R,649,-2.74476,2E+10,,1
C*** Define the nodes for the lower seal flange
LOCAL,11,,38.24941495,80.051977923,,-12
N,1001
N,1005,.25
FILL
N,1016,.58677836
N,1020,.25,.58677836
FILL
FILL,1001,1016,2,1006,5,5,1
N,1026,.896632635
LOCAL,12,,38.505,80
MOVE,1026,11,0,999,0,12,-.065,999,0
FILL,1016,1026,1,1021
LOCAL,11,1,39.12699808,80.47
N,1025,.5,148.5
N,1030,.5,129
N,1031,.5,109.5
N,1032,.5,90
CSYS,12
FILL,1021,1025,3,1022,1,2,5
N,1033,.775,.97
N,1034,1,145,.97
N,1076,-.065,2.98
FILL,1026,1076,8,1035,5
FILL,1035,1076,7,1041,5
N,1060,.775,2.15593612
NGEN,2,6,1033,1034,1,16
FILL,1039,1060,3,1045,5
FILL,1035,1039
FILL,1041,1045,3,1042,1,4,5
N,1064,1,245,2,03
FILL,1060,1064
N,1092,-.065,2.98
N,1096,.77960172,2.76
FILL
N,1100,1,245,2,76
FILL,1096,1100
FILL,1056,1092,3,1065,9,9,1
NGEN,3,9,1098,1100,1,26
N,1146,.14020351,4.4
FILL,1092,1146,5,1101,9
N,1164,.14020351,4.98
FILL,1146,1164,1,1155
LOCAL,11,,39.13520351,84.98,,-86.15
N,1168
N,1159,.3
NGEN,3,-1,1159,1159,,-.125
N,1148,.58,-.25
NGEN,2,-18,1157,1159,1,.56
NGEN,2,-9,1139,1141,1,.25
NGEN,2,-27,1148,1148,1,.81
NGEN,2,-18,1130,1132,1,.56
FILL,1096,1114,1,1105
CSYS,12
FILL,1101,1105
FILL,1110,1112,1,1111,6,9
FILL,1164,1168

```

C\*\*\* Define the nodes for the upper seal flange

LOCAL,11,,38.405,82.81  
 N,2001,,5  
 N,2005,.25,5  
 FILL  
 NGEN,3,5,2001,2005,1,,-.25  
 N,2031,,3.45  
 N,2035,.91,3.45  
 FILL  
 FILL,2011,2031,3,2016,5,5,1  
 N,2051,,2.543442101  
 N,2055,.91,2.543442101  
 FILL  
 FILL,2031,2051,3,2036,5,4,1  
 N,2040,.91,3.29  
 FILL,2040,2055,2,2045,5  
 N,2059,1.345,2.66  
 FILL,2055,2059  
 N,2071,,2.17  
 N,2073,.21504507,2.17  
 FILL  
 N,2077,.74504507,2.17  
 FILL,2073,2077  
 FILL,2051,2071,1,2060  
 FILL,2054,2076,1,2065  
 FILL,2060,2065  
 N,2081,1.345,2.17  
 FILL,2077,2081  
 FILL,2055,2077,1,2066,,5,1  
 N,2107,.85759646,.54  
 N,2109,1.10488343,.54  
 FILL  
 N,2111,1.345,.54  
 FILL,2109,2111  
 FILL,2077,2107,5,2082,5,5,1  
 N,2117,.94488343  
 N,2119,1.10488343  
 FILL  
 FILL,2109,2119,1,2114  
 N,2112,.870715847,.35  
 FILL,2112,2114  
 N,2120,1.345,3.45  
 N,2121,1.345,3.29  
 NGEN,2,51,2071,2073,1,,-.305  
 NGEN,2,3,2122,2124,1,,-.305

C\*\*\* Define the nodes for the locking ring

LOCAL,11,,39.35,81.29  
 N,3001  
 N,3005,.435  
 FILL  
 N,3009,.935  
 FILL,3005,3009  
 N,3037,,.81  
 N,3041,.435,.693442101  
 FILL  
 N,3045,.935,.693442101  
 FILL,3041,3045  
 FILL,3001,3037,3,3010,9,9,1  
 N,3145,,4.11  
 N,3149,.435,4.226557899  
 FILL  
 N,3153,.935,4.226557899  
 FILL,3149,3153  
 FILL,3041,3149,11,3050,9,5,1  
 N,3181,,4.67  
 N,3185,.535,4.67  
 FILL  
 N,3189,.935,4.67  
 FILL,3185,3189  
 FILL,3145,3181,3,3154,9,9,1

C\*\*\* Define the nodes for the OCA inner shell (OCV)

LOCAL,11,1,,84.5  
 N,101,74.25,-90  
 N,111,74.25,-64.44174492  
 FILL  
 LOCAL,12,1,28.3125,24.29659664  
 N,116,8.625  
 FILL,111,116  
 CSYS  
 N,117,36.9375,25.79659664  
 N,123,36.9375,51.79659664  
 FILL  
 N,129,36.9375,73.95292590

FILL,123,129  
 NGEN,2,-872,1003,1003  
 FILL,129,131  
 NGEN,2,-1870,2003,2003  
 N,135,38.53,93.78649751  
 FILL,133,135  
 LOCAL,13,1,29.905,93.78649751  
 N,140,8.625,64.23984399  
 FILL,135,140  
 LOCAL,14,1,,31.8125  
 N,150,77.4375,90  
 FILL,140,150

C\*\*\* Define the nodes for the OCA outer shell

CSYS  
 N,601  
 N,613,47.0625  
 FILL  
 N,626,47.0625,64.7775  
 FILL,613,626  
 N,629,47.0625,76.7775  
 FILL,626,629  
 N,630,47.0625,77.6325  
 N,638,47.0625,105.3440689  
 FILL,630,638  
 LOCAL,15,1,40.5625,105.3440689  
 N,640,6.5,62.55238078  
 FILL,638,640  
 LOCAL,16,1,,27.25  
 N,650,94.5,90  
 FILL,640,650

C\*\*\* Define the nodes for the polyurethane foam inner surface

CSYS  
 NGEN,2,100,101,150,1  
 N,132,38.58338729,80.97  
 N,232,38.53,86.26

C\*\*\* Define the nodes for the polyurethane foam outer surface

NGEN,2,-100,601,650,1

C\*\*\* Define the intermediate polyurethane foam nodes

FILL,201,501,2,301,100,29,1  
 N,300,43.9375,80.9  
 N,331,41.5375,81.8825  
 N,332,41.5375,86.26  
 N,429,43.9375,76.7775  
 N,430,44.2375,77.6375  
 N,431,44.2375,81.8825  
 FILL,229,429,1,329,100,2,1  
 FILL,230,300,1,330  
 FILL,332,532,1,432  
 FILL,233,533,2,333,100,18,1  
 N,323,38.4375,51.79659664

C\*\*\* Define the nodes for the Z-flanges

NGEN,2,272,429,429,0  
 NGEN,2,402,300,300,0  
 NGEN,2,273,430,430,0  
 RP2,,1,1  
 NGEN,2,374,331,331,0  
 RP2,,1,1

C\*\*\* Define the elements for the lower seal flange

TYPE,1  
 MAT,1  
 REAL,1  
 E,1001,1002,1007,1006  
 RP4,1,1,1,1  
 EGEN,5,5,1,4,1  
 E,1026,1027,1036,1035  
 E,1027,1028,1036  
 E,1028,1029,1037,1036  
 E,1029,1030,1031,1037  
 E,1031,1032,1038,1037  
 RP3,1,1,1,1  
 E,1035,1036,1042,1041  
 RP4,1,1,1,1  
 E,1041,1042,1047,1046  
 RP4,1,1,1,1  
 EGEN,3,5,32,35,1  
 E,1056,1057,1066,1065  
 RP4,1,1,1,1  
 EGEN,4,9,44,47,1

```

MAT,2
E,1060,1061,1070,1069
RP4,1,1,1,1
EGEN,4,9,60,63,1
EGEN,3,9,74,75,1
EGEN,3,9,56,59,1
EGEN,7,9,84,85,1
EGEN,3,1,99,99
EGEN,3,1,93,93
C*** Define the elements for the upper seal flange
TYPE,1
MAT,1
REAL,1
E,2006,2007,2002,2001
RP4,1,1,1,1
EGEN,10,5,104,107,1
E,2040,2121,2120,2035
E,2060,2061,2052,2051
E,2061,2062,2052
E,2062,2063,2053,2052
E,2063,2064,2053
E,2064,2065,2054,2053
RP6,1,1,1,1
E,2071,2072,2061,2060
RP10,1,1,1,1
E,2122,2123,2072,2071
RP2,1,1,1,1
E,2125,2126,2123,2122
RP2,1,1,1,1
E,2082,2083,2078,2077
RP4,1,1,1,1
EGEN,6,5,169,172,1
EGEN,3,5,189,190,1
C*** Define the elements for the locking ring
TYPE,1
MAT,2
REAL,1
E,3001,3002,3011,3010
RP4,1,1,1,1
EGEN,4,9,197,200,1
MAT,1
E,3005,3006,3015,3014
RP4,1,1,1,1
EGEN,20,9,213,216,1
E,3145,3146,3155,3154
RP4,1,1,1,1
EGEN,4,9,293,296,1
C*** Define the elements for the OCA inner shell
(OCV)
TYPE,2
MAT,1
REAL,1
E,101,102
RP16,1,1
REAL,2
E,117,118
RP12,1,1
REAL,3
E,123,323
REAL,1
E,129,130
E,130,1003
E,2003,134
E,134,135
RP16,1,1
C*** Define the elements for the OCA outer shell
REAL,1
E,601,602
RP25,1,1
REAL,3
E,626,627
RP3,1,1
E,630,631
RP8,1,1
REAL,1
E,638,639
RP12,1,1
C*** Define the elements for the Z-flanges
REAL,4
E,629,701
E,701,702
E,702,1034
E,1034,1033
E,630,703
E,703,704
RP3,1,1
E,706,2120
E,2120,2035
C*** Define the polyurethane foam elements
TYPE,3
MAT,3
REAL,1
E,201,301,302,202
RP29,1,1,1,1
E,231,230,330
E,301,401,402,302
RP28,1,1,1,1
E,329,429,300,330
E,300,132,231,330
E,401,501,502,402
RP28,1,1,1,1
E,333,233,232,332
E,233,333,334,234
RP17,1,1,1,1
E,331,431,432,332
RP19,1,1,1,1
E,430,530,531,431
RP20,1,1,1,1
C*** Define the interface elements between the steel
shells and the polyurethane foam
TYPE,5
MAT,1
REAL,101
E,101,201
REAL,102
E,102,202
REAL,103
E,103,203
REAL,104
E,104,204
REAL,105
E,105,205
REAL,106
E,106,206
REAL,107
E,107,207
REAL,108
E,108,208
REAL,109
E,109,209
REAL,110
E,110,210
REAL,111
E,111,211
REAL,112
E,112,212
REAL,113
E,113,213
REAL,114
E,114,214
REAL,115
E,115,215
REAL,116
E,116,216
RP7,1,1
E,124,224
RP6,1,1
REAL,130
E,129,229
RP2,1,1
E,1003,231
REAL,101
E,702,300
E,701,429
E,622,529
REAL,150
E,706,332
E,705,331
E,704,431
E,703,430
E,630,530
REAL,116
E,300,702
E,429,701
E,706,332

```

```

E,705,331
E,704,431
E,703,430
E,2003,233
E,134,234
RP2,1,1
REAL,136
E,136,236
REAL,137
E,137,237
REAL,138
E,138,238
REAL,139
E,139,239
REAL,140
E,140,240
REAL,141
E,141,241
REAL,142
E,142,242
REAL,143
E,143,243
REAL,144
E,144,244
REAL,145
E,145,245
REAL,146
E,146,246
REAL,147
E,147,247
REAL,148
E,148,248
REAL,149
E,149,249
REAL,150
E,150,250
REAL,101
E,501,601
RP13,1,1
REAL,116
E,513,613
RP26,1,1
REAL,639
E,539,639
REAL,640
E,540,640
REAL,641
E,541,641
REAL,642
E,542,642
REAL,643
E,543,643
REAL,644
E,544,644
REAL,645
E,545,645
REAL,646
E,546,646
REAL,647
E,547,647
REAL,648
E,548,648
REAL,649
E,549,649

```

```

REAL,150
E,550,650
C*** Define the interface elements between the lower
seal flange and the locking ring
TYPE,4
MAT,1
REAL,6
E,3038,1061
RP3,1,1
C*** Define the interface elements between the upper
seal flange and the locking ring
TYPE,4
MAT,1
REAL,7
E,2056,3146
RP3,1,1
C*** Define the interface elements between the lower
seal flange and the upper seal flange
TYPE,5
MAT,1
REAL,8
E,1164,2073
RP5,1,1
C*** Couple the lower shell to the lower seal flange
TYPE,6
MAT,4
REAL,9
E,1001,1002
RP4,1,1
C*** Couple the upper shell to the upper seal flange
TYPE,6
MAT,4
REAL,9
E,2001,2002
RP4,1,1
C*** Define the displacement constraints
D,101,UX,0,,601,500,ROTZ
D,201,UX,0,,501,100
D,150,UX,0,,650,500,ROTZ
D,250,UX,0,,550,100
D,3099,UY,0
C*** Re-order the elements to reduce execution time
WSTART,101,601,100
WSTART,150,650,100
WSTART,1003
WSTART,1034
WSTART,2120
WSTART,2003
WAVES
C*** Set convergence criteria, write a solution
file, and exit
ITER,-20,20
AFWRITE
FINISH

```

Table 2.10.1-4 – ANSYS® Input Listing for OCA Load Case 4

```

/TITLE, OCV: PRES=0/14.7 PSIA; TEMP=70/70 DEG-F
C*** Define the element types
ET,1,42,,,1
ET,2,51
ET,3,42,,,1
ET,4,12,,,1
ET,5,12
ET,6,3
C*** Define the reference and uniform temperatures
TREF,70
TUNIF,70
C*** Define the material properties for non-slotted
steel regions
EX,1,28.3E+06
NUXY,1,.3
DENS,1,7.505E-04
ALPX,1,8.460E-06
C*** Define the material properties for slotted
steel regions
EX,2,14.15E+06
EY,2,14.15E+06
EZ,2,1
NUXY,2,.3
NUXZ,2,0
NUYZ,2,0
DENS,2,3.7525E-04
ALPX,2,8.460E-06
ALPY,2,8.460E-06
ALPZ,2,8.460E-06
C*** Define the material properties for the
polyurethane foam
EX,3,5854
EY,3,8789
EZ,3,5854
GXZ,3,2553
GYZ,3,1921
GYZ,3,2553
NUXY,3,.33
DENS,3,1.198E-05
ALPX,3,4.6E-05
C*** Define the material properties for the rigid
coupling elements (STIF3 beams)
EX,4,28.3E+06
NUXY,4,.3
DENS,4,0
ALPX,4,8.460E-06
C*** Define the element real constants
R,1,.25
R,2,.1875
R,3,.375
R,4,.075
R,5,2E+10,,1
R,6,-15,2E+10,-.036
R,7,15,2E+10,-.036
R,8,0,2E+10,,1
R,9,1,1,1
R,101,-180.000,2E+10,,1
R,102,-177.444,2E+10,,1
R,103,-174.888,2E+10,,1
R,104,-172.333,2E+10,,1
R,105,-169.777,2E+10,,1
R,106,-167.221,2E+10,,1
R,107,-164.665,2E+10,,1
R,108,-162.109,2E+10,,1
R,109,-159.553,2E+10,,1
R,110,-156.998,2E+10,,1
R,111,-154.442,2E+10,,1
R,112,-141.553,2E+10,,1
R,113,-128.665,2E+10,,1
R,114,-115.777,2E+10,,1
R,115,-102.888,2E+10,,1
R,116,-90.0000,2E+10,,1
R,130,-102.000,2E+10,,1
R,136,-77.1520,2E+10,,1
R,137,-64.3041,2E+10,,1
R,138,-51.4561,2E+10,,1
R,139,-38.6081,2E+10,,1
R,140,-25.7602,2E+10,,1
R,141,-23.1841,2E+10,,1
R,142,-20.6081,2E+10,,1
R,143,-18.0321,2E+10,,1
R,144,-15.4561,2E+10,,1
R,145,-12.8801,2E+10,,1
R,146,-10.3041,2E+10,,1
R,147,-7.72805,2E+10,,1
R,148,-5.15203,2E+10,,1
R,149,-2.57602,2E+10,,1
R,150,2E+10,,1
R,639,-58.7238,2E+10,,1
R,640,-27.4476,2E+10,,1
R,641,-24.7029,2E+10,,1
R,642,-21.9581,2E+10,,1
R,643,-19.2133,2E+10,,1
R,644,-16.4686,2E+10,,1
R,645,-13.7238,2E+10,,1
R,646,-10.9790,2E+10,,1
R,647,-8.23429,2E+10,,1
R,648,-5.48952,2E+10,,1
R,649,-2.74476,2E+10,,1
C*** Define the nodes for the lower seal flange
LOCAL,11,,38.24941495,80.051977923,,-12
N,1001
N,1005,,.25
FILL
N,1016,,.58677836
N,1020,,.25,.58677836
FILL
FILL,1001,1016,2,1006,5,5,1
N,1026,,.896632635
LOCAL,12,,38.505,80
MOVE,1026,11,0,999,0,12,-.065,999,0
FILL,1016,1026,1,1021
LOCAL,11,1,39.12699808,80.47
N,1025,,5,148.5
N,1030,,5,129
N,1031,,5,109.5
N,1032,,5,90
CSYS,12
FILL,1021,1025,3,1022,1,2,5
N,1033,,775,.97
N,1034,1,145,.97
N,1076,-.065,2.98
FILL,1026,1076,8,1035,5
FILL,1035,1076,7,1041,5
N,1060,,775,2.15593612
NGEN,2,6,1033,1034,1,,.16
FILL,1039,1060,3,1045,5
FILL,1035,1039
FILL,1041,1045,3,1042,1,4,5
N,1064,1,245,2.03
FILL,1060,1064
N,1092,-.065,2.98
N,1096,.77960172,2.76
FILL
N,1100,1,245,2.76
FILL,1096,1100
FILL,1056,1092,3,1065,9,9,1
NGEN,3,9,1098,1100,1,,.26
N,1146,.14020351,4.4
FILL,1092,1146,5,1101,9
N,1164,.14020351,4.98
FILL,1146,1164,1,1155
LOCAL,11,,39.13520351,84.98,,-86.15
N,1168
N,1159,.3
NGEN,3,-1,1159,1159,,-.125
N,1148,.58,-.25
NGEN,2,-18,1157,1159,1,.56
NGEN,2,-9,1139,1141,1,.25
NGEN,2,-27,1148,1148,1,.81
NGEN,2,-18,1130,1132,1,.56
FILL,1096,1114,1,1105
CSYS,12
FILL,1101,1105
FILL,1110,1112,1,1111,,6,9
FILL,1164,1168

```

C\*\*\* Define the nodes for the upper seal flange

LOCAL,11,,38.405,82.81  
 N,2001,,5  
 N,2005,,25,5  
 FILL  
 NGEN,3,5,2001,2005,1,,-.25  
 N,2031,,3.45  
 N,2035,,91,3.45  
 FILL  
 FILL,2011,2031,3,2016,5,5,1  
 N,2051,,2.543442101  
 N,2055,,91,2.543442101  
 FILL  
 FILL,2031,2051,3,2036,5,4,1  
 N,2040,,91,3.29  
 FILL,2040,2055,2,2045,5  
 N,2059,1.345,2.66  
 FILL,2055,2059  
 N,2071,,2.17  
 N,2073,,21504507,2.17  
 FILL  
 N,2077,,74504507,2.17  
 FILL,2073,2077  
 FILL,2051,2071,1,2060  
 FILL,2054,2076,1,2065  
 FILL,2060,2065  
 N,2081,1.345,2.17  
 FILL,2077,2081  
 FILL,2055,2077,1,2066,,5,1  
 N,2107,,85759646,.54  
 N,2109,1.10488343,.54  
 FILL  
 N,2111,1.345,.54  
 FILL,2109,2111  
 FILL,2077,2107,5,2082,5,5,1  
 N,2117,,94488343  
 N,2119,1.10488343  
 FILL  
 FILL,2109,2119,1,2114  
 N,2112,,870715847,.35  
 FILL,2112,2114  
 N,2120,1.345,3.45  
 N,2121,1.345,3.29  
 NGEN,2,51,2071,2073,1,,-.305  
 NGEN,2,3,2122,2124,1,,-.305

C\*\*\* Define the nodes for the locking ring

LOCAL,11,,39.35,81.29  
 N,3001  
 N,3005,,435  
 FILL  
 N,3009,,935  
 FILL,3005,3009  
 N,3037,,.81  
 N,3041,,435,.693442101  
 FILL  
 N,3045,,935,.693442101  
 FILL,3041,3045  
 FILL,3001,3037,3,3010,9,9,1  
 N,3145,,4.11  
 N,3149,,435,4.226557899  
 FILL  
 N,3153,,935,4.226557899  
 FILL,3149,3153  
 FILL,3041,3149,11,3050,9,5,1  
 N,3181,,4.67  
 N,3185,,535,4.67  
 FILL  
 N,3189,,935,4.67  
 FILL,3185,3189  
 FILL,3145,3181,3,3154,9,9,1

C\*\*\* Define the nodes for the OCA inner shell (OCV)

LOCAL,11,1,,84.5  
 N,101,74.25,-90  
 N,111,74.25,-64.44174492  
 FILL  
 LOCAL,12,1,28.3125,24.29659664  
 N,116,8.625  
 FILL,111,116  
 CSYS  
 N,117,36.9375,25.79659664  
 N,123,36.9375,51.79659664  
 FILL  
 N,129,36.9375,73.95292590

FILL,123,129  
 NGEN,2,-872,1003,1003  
 FILL,129,131  
 NGEN,2,-1870,2003,2003  
 N,135,38.53,93.78649751  
 FILL,133,135  
 LOCAL,13,1,29.905,93.78649751  
 N,140,8.625,64.23984399  
 FILL,135,140  
 LOCAL,14,1,,31.8125  
 N,150,77.4375,90  
 FILL,140,150

C\*\*\* Define the nodes for the OCA outer shell

CSYS  
 N,601  
 N,613,47.0625  
 FILL  
 N,626,47.0625,64.7775  
 FILL,613,626  
 N,629,47.0625,76.7775  
 FILL,626,629  
 N,630,47.0625,77.6325  
 N,638,47.0625,105.3440689  
 FILL,630,638  
 LOCAL,15,1,40.5625,105.3440689  
 N,640,6.5,62.55238078  
 FILL,638,640  
 LOCAL,16,1,,27.25  
 N,650,94.5,90  
 FILL,640,650

C\*\*\* Define the nodes for the polyurethane foam inner surface

CSYS  
 NGEN,2,100,101,150,1  
 N,132,38.58338729,80.97  
 N,232,38.53,86.26

C\*\*\* Define the nodes for the polyurethane foam outer surface

NGEN,2,-100,601,650,1

C\*\*\* Define the intermediate polyurethane foam nodes

FILL,201,501,2,301,100,29,1  
 N,300,43.9375,80.9  
 N,331,41.5375,81.8825  
 N,332,41.5375,86.26  
 N,429,43.9375,76.7775  
 N,430,44.2375,77.6375  
 N,431,44.2375,81.8825  
 FILL,229,429,1,329,100,2,1  
 FILL,230,300,1,330  
 FILL,332,532,1,432  
 FILL,233,533,2,333,100,18,1  
 N,323,38.4375,51.79659664

C\*\*\* Define the nodes for the Z-flanges

NGEN,2,272,429,429,0  
 NGEN,2,402,300,300,0  
 NGEN,2,273,430,430,0  
 RP2,,1,1  
 NGEN,2,374,331,331,0  
 RP2,,1,1

C\*\*\* Define the elements for the lower seal flange

TYPE,1  
 MAT,1  
 REAL,1  
 E,1001,1002,1007,1006  
 RP4,1,1,1,1  
 EGEN,5,5,1,4,1  
 E,1026,1027,1036,1035  
 E,1027,1028,1036  
 E,1028,1029,1037,1036  
 E,1029,1030,1031,1037  
 E,1031,1032,1038,1037  
 RP3,1,1,1,1  
 E,1035,1036,1042,1041  
 RP4,1,1,1,1  
 E,1041,1042,1047,1046  
 RP4,1,1,1,1  
 EGEN,3,5,32,35,1  
 E,1056,1057,1066,1065  
 RP4,1,1,1,1  
 EGEN,4,9,44,47,1

```

MAT,2
E,1060,1061,1070,1069
RP4,1,1,1,1
EGEN,4,9,60,63,1
EGEN,3,9,74,75,1
EGEN,3,9,56,59,1
EGEN,7,9,84,85,1
EGEN,3,1,99,99
EGEN,3,1,93,93

C*** Define the elements for the upper seal flange
TYPE,1
MAT,1
REAL,1
E,2006,2007,2002,2001
RP4,1,1,1,1
EGEN,10,5,104,107,1
E,2040,2121,2120,2035
E,2060,2061,2052,2051
E,2061,2062,2052
E,2062,2063,2053,2052
E,2063,2064,2053
E,2064,2065,2054,2053
RP6,1,1,1,1
E,2071,2072,2061,2060
RP10,1,1,1,1
E,2122,2123,2072,2071
RP2,1,1,1,1
E,2125,2126,2123,2122
RP2,1,1,1,1
E,2082,2083,2078,2077
RP4,1,1,1,1
EGEN,6,5,169,172,1
EGEN,3,5,189,190,1

C*** Define the elements for the locking ring
TYPE,1
MAT,2
REAL,1
E,3001,3002,3011,3010
RP4,1,1,1,1
EGEN,4,9,197,200,1
MAT,1
E,3005,3006,3015,3014
RP4,1,1,1,1
EGEN,20,9,213,216,1
E,3145,3146,3155,3154
RP4,1,1,1,1
EGEN,4,9,293,296,1

C*** Define the elements for the OCA inner shell
(OCV)
TYPE,2
MAT,1
REAL,1
E,101,102
RP16,1,1
REAL,2
E,117,118
RP12,1,1
REAL,3
E,123,323
REAL,1
E,129,130
E,130,1003
E,2003,134
E,134,135
RP16,1,1

C*** Define the elements for the OCA outer shell
REAL,1
E,601,602
RP25,1,1
REAL,3
E,626,627
RP3,1,1
E,630,631
RP8,1,1
REAL,1
E,638,639
RP12,1,1

C*** Define the elements for the Z-flanges
REAL,4
E,629,701
E,701,702
E,702,1034
E,1034,1033
E,630,703
E,703,704
RP3,1,1
E,706,2120
E,2120,2035

C*** Define the polyurethane foam elements
TYPE,3
MAT,3
REAL,1
E,201,301,302,202
RP29,1,1,1,1
E,231,230,330
E,301,401,402,302
RP28,1,1,1,1
E,329,429,300,330
E,300,132,231,330
E,401,501,502,402
RP28,1,1,1,1
E,333,233,232,332
E,233,333,334,234
RP17,1,1,1,1
E,331,431,432,332
RP19,1,1,1,1
E,430,530,531,431
RP20,1,1,1,1

C*** Define the interface elements between the steel
shells and the polyurethane foam
TYPE,5
MAT,1
REAL,101
E,101,201
REAL,102
E,102,202
REAL,103
E,103,203
REAL,104
E,104,204
REAL,105
E,105,205
REAL,106
E,106,206
REAL,107
E,107,207
REAL,108
E,108,208
REAL,109
E,109,209
REAL,110
E,110,210
REAL,111
E,111,211
REAL,112
E,112,212
REAL,113
E,113,213
REAL,114
E,114,214
REAL,115
E,115,215
REAL,116
E,116,216
RP7,1,1
E,124,224
RP6,1,1
REAL,130
E,129,229
RP2,1,1
E,1003,231
REAL,101
E,702,300
E,701,429
E,622,529
REAL,150
E,706,332
E,705,331
E,704,431
E,703,430
E,630,530
REAL,116
E,300,702
E,429,701
E,706,332

```

```

E,705,331
E,704,431
E,703,430
E,2003,233
E,134,234
RP2,1,1
REAL,136
E,136,236
REAL,137
E,137,237
REAL,138
E,138,238
REAL,139
E,139,239
REAL,140
E,140,240
REAL,141
E,141,241
REAL,142
E,142,242
REAL,143
E,143,243
REAL,144
E,144,244
REAL,145
E,145,245
REAL,146
E,146,246
REAL,147
E,147,247
REAL,148
E,148,248
REAL,149
E,149,249
REAL,150
E,150,250
REAL,101
E,501,601
RP13,1,1
REAL,116
E,513,613
RP26,1,1
REAL,639
E,539,639
REAL,640
E,540,640
REAL,641
E,541,641
REAL,642
E,542,642
REAL,643
E,543,643
REAL,644
E,544,644
REAL,645
E,545,645
REAL,646
E,546,646
REAL,647
E,547,647
REAL,648
E,548,648
REAL,649
E,549,649
REAL,150
E,550,650

C*** Define the interface elements between the lower
seal flange and the locking ring
TYPE,4
MAT,1
REAL,6
E,3038,1061
RP3,1,1

C*** Define the interface elements between the upper
seal flange and the locking ring
TYPE,4
MAT,1
REAL,7
E,2056,3146
RP3,1,1

C*** Define the interface elements between the lower
seal flange and the upper seal flange
TYPE,5
MAT,1
REAL,8
E,1164,2073
RP5,1,1

C*** Couple the lower shell to the lower seal flange
TYPE,6
MAT,4
REAL,9
E,1001,1002
RP4,1,1

C*** Couple the upper shell to the upper seal flange
TYPE,6
MAT,4
REAL,9
E,2001,2002
RP4,1,1

C*** Define the displacement constraints
D,101,UX,0,,601,500,ROTZ
D,201,UX,0,,501,100
D,150,UX,0,,650,500,ROTZ
D,250,UX,0,,550,100
D,3099,UY,0

C*** Define the pressure loads
P,101,102,-14.7,,129,1
P,130,1003,-14.7
P,1001,1006,-14.7,,1021,5
P,1026,1035,-14.7
P,1035,1041,-14.7
P,1041,1046,-14.7,,1051,5
P,1056,1065,-14.7,,1155,9
P,1164,1165,-14.7,,1167,1
P,1168,1159,-14.7
P,2077,2082,-14.7
P,2073,2074,-14.7,,2076,1
P,2127,2124,-14.7
P,2124,2073,-14.7
P,2125,2126,-14.7,,2126,1
P,2122,2125,-14.7
P,2071,2122,-14.7
P,2001,2002,-14.7,,2002,1
P,2001,2006,-14.7,,2046,5
P,2051,2060,-14.7
P,2060,2071,-14.7
P,2003,134,-14.7
P,134,135,-14.7,,149,1

C*** Re-order the elements to reduce execution time
WSTART,101,601,100
WSTART,150,650,100
WSTART,1003
WSTART,1034
WSTART,2120
WSTART,2003
WAVES

C*** Set convergence criteria, write a solution
file, and exit
ITER,-20,20
AFWRITE
FINISH

```

Table 2.10.1-5 – ANSYS® Input Listing for ICV Load Case 1

```

/TITLE, ICV: PRES=64.7/3.5 PSIA; TEMP=160/160 DEG-F
C*** Define the element types
ET,1,42,,,1
ET,2,51
ET,3,12,,,1
ET,4,12
ET,5,3
C*** Define the reference and uniform temperatures
TREF,160
TUNIF,160
C*** Define the material properties for non-slotted
steel regions
EX,1,27.8E+06
NUXY,1,.3
DENS,1,7.505E-04
ALPX,1,8.694E-06
C*** Define the material properties for slotted
steel regions
EX,2,13.9E+06
EY,2,13.9E+06
EZ,2,1
NUXY,2,.3
NUYZ,2,0
NUXZ,2,0
DENS,2,3.7525E-04
ALPX,2,8.694E-06
ALPY,2,8.694E-06
ALPZ,2,8.694E-06
C*** Define the material properties for the rigid
coupling elements
EX,3,27.8E+06
NUXY,3,.3
DENS,3,0
ALPX,3,8.694E-06
C*** Define the element real constants
R,1,.25
R,2,-15,2E+10,-.036
R,3,15,2E+10,-.036
R,4,0,2E+10,-.01
R,5,1,1,1
C*** Define the nodes for the lower seal ring
LOCAL,11,0,36.315,75.08954245
N,1001
N,1005,.25
FILL
N,1016,,.575
N,1020,.25,.575
FILL
FILL,1001,1016,2,1006,5,5,1
N,1031,.148
N,1035,.84,1.48
FILL
FILL,1016,1031,2,1021,5,5,1
N,1046,.2.6759361
N,1050,.84,2.67593612
FILL
FILL,1031,1046,2,1036,5,5,1
N,1054,1.31,2.55
FILL,1050,1054
N,1073,.3.5
N,1077,.844601720,3.28
FILL
N,1079,1.095,3.28
FILL,1077,1079
N,1081,1.31,3.28
FILL,1079,1081
FILL,1046,1073,2,1055,9,9,1
N,1127,.205,4.92
FILL,1073,1127,5,1082,9
LOCAL,12,,37.01020351,80.58954246,-86.15
N,1140,.3
N,1138,.3,-.25
FILL
N,1122,.86
N,1120,.86,-.25
FILL
N,1113,1.11
N,1111,1.11,-.25
FILL
N,1095,1.67
N,1093,1.67,-.25
FILL
CSYS,11
N,1145,.205,5.5
FILL,1127,1145,1,1136
N,1149,.695,5.5
FILL,1145,1149
FILL,1120,1138,1,1129
FILL,1093,1111,1,1102
FILL,1077,1095,1,1086
FILL,1091,1093,,,6,9
FILL,1073,1091,1,1082,,5,1
NGEN,3,9,1079,1081,1,,.26
C*** Define the nodes for the upper seal ring
N,2001,-.035,4.89
N,2003,.180045070,4.89
FILL
N,2007,-0.035,5.5
N,2009,.180045070,5.5
FILL
FILL,2001,2007,1,2004,,3,1
N,2013,.710045070,5.5
FILL,2009,2013
N,2017,1.31,5.5
FILL,2013,2017
N,2040,-0.035,5.98
FILL,2007,2040,2,2018,11
N,2035,0.875,5.873442101
FILL,2029,2035
N,2039,1.31,5.99
FILL,2035,2039
FILL,2008,2030,1,2019,,10,1
N,2042,.245,5.98
FILL,2040,2042
N,2043,.390419704,6.008925778
N,2044,.513700577,6.091299423
N,2049,.596074222,6.214580296
N,2054,.625,6.36
N,2058,.875,6.36
FILL
FILL,2035,2058,2,2048,5
FILL,2044,2048
FILL,2049,2053
NGEN,5,5,2054,2058,1,,.1875
N,2104,.822596460,3.87
N,2106,1.07,3.87
FILL
N,2116,1.07,3.33
FILL,2106,2116,1,2111
N,2108,1.31,3.87
FILL,2106,2108
FILL,2013,2104,5,2079,5,5,1
N,2109,.835715950,3.68
FILL,2109,2111
N,2114,.909883430,3.33
FILL,2114,2116
C*** Define the nodes for the locking ring
LOCAL,13,0,37.225,76.89954245
N,3001
N,3005,.435
FILL
N,3008,.789412
FILL,3005,3008
N,3037,.81
N,3041,.435,.693442101
FILL
N,3045,.935,.693442101
FILL,3041,3045
FILL,3001,3037,3,3010,9,8,1
N,3027,.935,.4
FILL,3008,3027,1,3018
FILL,3027,3045,1,3036
N,3101,.4.11
N,3105,.435,4.226557898
FILL
N,3109,.935,4.226557899
FILL,3105,3109
FILL,3041,3105,11,3046,5,5,1
N,3137,.4.67
N,3141,.435,4.67
FILL
N,3144,.789412,4.67
FILL,3141,3144
FILL,3101,3137,3,3110,9,8,1
FILL,3109,3144,3,3118,9

```

```

C*** Define the nodes for the lower shell
LOCAL,14,1,,73.25
N,4001,73.25,-90
N,4016,73.25,-64.50665929
FILL
LOCAL,15,1,27.815,14.9171927
N,4025,8.625
FILL,4016,4025
CSYS,0
N,4081,36.44,75.08954245
FILL,4025,4081
N,4001,0,0
C*** Define the nodes for the upper shell
LOCAL,16,1,,24.25
N,5001,74.5,90
N,5016,74.5,64.42280563
FILL
LOCAL,17,1,28.44,83.66954245
N,5025,8.625
FILL,5016,5025
CSYS,0
N,5027,37.065,82.16954245
FILL,5025,5027
N,5001,0,98.75
C*** Define the elements for the lower seal ring
TYPE,1
MAT,1
REAL,1
E,1001,1002,1007,1006
RP4,1,1,1,1
EGEN,9,5,1,4,1
E,1046,1047,1056,1055
RP4,1,1,1,1
EGEN,5,9,37,40,1
EGEN,7,9,53,54,1
EGEN,3,27,55,56,1
MAT,2
E,1050,1051,1060,1059
RP4,1,1,1,1
EGEN,3,9,73,76,1
EGEN,3,9,83,84,1
C*** Define the elements for the upper seal ring
TYPE,1
MAT,1
REAL,1
E,2001,2002,2005,2004
RP2,1,1,1,1
EGEN,2,3,89,90,1
E,2007,2008,2019,2018
RP10,1,1,1,1
EGEN,2,11,93,102,1
EGEN,2,11,103,107,1
E,2046,2045,2034
RP2,1,1,0
E,2034,2035,2048,2047
E,2044,2045,2050,2049
RP4,1,1,1,1
EGEN,6,5,121,124,1
E,2079,2080,2014,2013
RP4,1,1,1,1
E,2084,2085,2080,2079
RP4,1,1,1,1
EGEN,5,5,149,152,1
EGEN,3,5,165,166,1
C*** Define the elements for the locking ring
TYPE,1
MAT,2
REAL,1
E,3001,3002,3011,3010
RP4,1,1,1,1
EGEN,4,9,173,176,1
MAT,1
E,3005,3006,3015,3014
RP3,1,1,1,1
E,3018,3017,3008
E,3014,3015,3024,3023
RP4,1,1,1,1
EGEN,3,9,193,196,1
E,3041,3042,3047,3046
RP4,1,1,1,1
EGEN,11,5,205,208,1
E,3096,3097,3106,3105
RP4,1,1,1,1
E,3101,3102,3111,3110
RP8,1,1,1,1
EGEN,4,9,253,259,1
E,3117,3118,3127,3126
E,3126,3127,3136,3135
E,3135,3136,3144,3144
C*** Define the elements for the lower shell
TYPE,2
MAT,1
REAL,1
E,4001,4002
RP79,1,1
E,4080,1003
C*** Define the elements for the upper shell
TYPE,2
MAT,1
REAL,1
E,2076,5026
E,5026,5025
RP25,-1,-1
C*** Define the interface elements between the lower
seal flange and the locking ring
TYPE,3
MAT,1
REAL,2
E,3038,1051
RP3,1,1
C*** Define the interface elements between the upper
seal flange and the locking ring
TYPE,3
MAT,1
REAL,3
E,2036,3102
RP3,1,1
C*** Define the interface elements between the lower
seal flange and the upper seal flange
TYPE,4
MAT,1
REAL,4
E,1145,2009
RP5,1,1
C*** Couple the lower shell to the lower seal flange
TYPE,5
MAT,3
REAL,5
E,1001,1002
RP4,1,1
C*** Couple the upper shell to the upper seal flange
TYPE,5
MAT,3
REAL,5
E,2074,2075
RP4,1,1
C*** Define the displacement constraints
D,4001,UX,0,,5001,1000,ROTX
D,3075,UY,0
C*** Define the pressure loads
P,4001,4002,61.2,,4079,1
P,4080,1003,61.2
P,1001,1006,61.2,,1041,5
P,1046,1055,61.2,,1136,9
P,1145,1146,61.2,,1148,9
P,1140,1149,61.2
P,2001,2002,61.2,,2002,1
P,2003,2006,61.2,,2006,3
P,2009,2010,61.2,,2012,1
P,2013,2079,61.2
P,2001,2004,61.2,,2004,3
P,2007,2018,61.2,,2029,11
P,2040,2041,61.2,,2043,1
P,2044,2049,61.2,,2069,5
P,5001,5002,61.2,,5025,1
P,5026,2076,61.2
C*** Re-order the elements to reduce execution time
WSTART,4001
WAVES
C*** Set convergence criteria, write a solution
file, and exit
ITER,-10,10
AFWRITE
FINISH

```

Table 2.10.1-6 – ANSYS® Input Listing for ICV Load Case 2

```

/TITLE, ICV: PRES=0/14.7 PSIA; TEMP=70/70 DEG-F
C*** Define the element types
ET,1,42,,,1
ET,2,51
ET,3,12,,,1
ET,4,12
ET,5,3
C*** Define the reference and uniform temperatures
TREF,70
TUNIF,70
C*** Define the material properties for non-slotted
steel regions
EX,1,28.3E+06
DENS,1,7.505E-04
NUXY,1,.3
ALPX,1,8.46E-06
C*** Define the material properties for slotted
steel regions
EX,2,14.15E+06
EY,2,14.15E+06
EZ,2,1
NUXY,2,.3
NUYZ,2,0
NUXZ,2,0
DENS,1,3.7525E-04
ALPX,2,8.46E-6
ALPY,2,8.46E-6
ALPZ,2,8.46E-6
C*** Define the material properties for the rigid
coupling elements
EX,3,28.3E+06
NUXY,3,.3
DENS,3,0
ALPX,3,8.46E-6
C*** Define the element real constants
R,1,.25
R,2,-15.2E+10,-.036
R,3,15.2E+10,-.036
R,4,0,2E+10,-.01
R,5,1,1,1
C*** Define the nodes for the lower seal ring
LOCAL,11,0,36.315,75.08954245
N,1001
N,1005,.25
FILL
N,1016,,.575
N,1020,.25,.575
FILL
FILL,1001,1016,2,1006,5,5,1
N,1031,.1.48
N,1035,.84,1.48
FILL
FILL,1016,1031,2,1021,5,5,1
N,1046,.2.6759361
N,1050,.84,2.67593612
FILL
FILL,1031,1046,2,1036,5,5,1
N,1054,1.31,2.55
FILL,1050,1054
N,1073,.3.5
N,1077,.844601720,3.28
FILL
N,1079,1.095,3.28
FILL,1077,1079
N,1081,1.31,3.28
FILL,1079,1081
FILL,1046,1073,2,1055,9,9,1
N,1127,.205,4.92
FILL,1073,1127,5,1082,9
LOCAL,12,,37.01020351,80.58954246,, -86.15
N,1140,.3
N,1138,.3,-.25
FILL
N,1122,.86
N,1120,.86,-.25
FILL
N,1113,1.11
N,1111,1.11,-.25
FILL
N,1095,1.67
N,1093,1.67,-.25
FILL
CSYS,11
N,1145,.205,5.5
FILL,1127,1145,1,1136
N,1149,.695,5.5
FILL,1145,1149
FILL,1120,1138,1,1129
FILL,1093,1111,1,1102
FILL,1077,1095,1,1086
FILL,1091,1093,,,6,9
FILL,1073,1091,1,1082,,5,1
NGEN,3,9,1079,1081,1,,.26
C*** Define the nodes for the upper seal ring
N,2001,-.035,4.89
N,2003,.180045070,4.89
FILL
N,2007,-0.035,5.5
N,2009,.180045070,5.5
FILL
FILL,2001,2007,1,2004,,3,1
N,2013,.710045070,5.5
FILL,2009,2013
N,2017,1.31,5.5
FILL,2013,2017
N,2040,-0.035,5.98
FILL,2007,2040,2,2018,11
N,2035,0.875,5.873442101
FILL,2029,2035
N,2039,1.31,5.99
FILL,2035,2039
FILL,2008,2030,1,2019,,10,1
N,2042,.245,5.98
FILL,2040,2042
N,2043,.390419704,6.008925778
N,2044,.513700577,6.091299423
N,2049,.596074222,6.214580296
N,2054,.625,6.36
N,2058,.875,6.36
FILL
FILL,2035,2058,2,2048,5
FILL,2044,2048
FILL,2049,2053
NGEN,5,5,2054,2058,1,,.1875
N,2104,.822596460,3.87
N,2106,1.07,3.87
FILL
N,2116,1.07,3.33
FILL,2106,2116,1,2111
N,2108,1.31,3.87
FILL,2106,2108
FILL,2013,2104,5,2079,5,5,1
N,2109,.835715950,3.68
FILL,2109,2111
N,2114,.909883430,3.33
FILL,2114,2116
C*** Define the nodes for the locking ring
LOCAL,13,0,37.225,76.89954245
N,3001
N,3005,.435
FILL
N,3008,.789412
FILL,3005,3008
N,3037,,.81
N,3041,.435,.693442101
FILL
N,3045,.935,.693442101
FILL,3041,3045
FILL,3001,3037,3,3010,9,8,1
N,3027,.935,.4
FILL,3008,3027,1,3018
FILL,3027,3045,1,3036
N,3101,,4.11
N,3105,.435,4.226557898
FILL
N,3109,.935,4.226557899
FILL,3105,3109
FILL,3041,3105,11,3046,5,5,1
N,3137,,4.67
N,3141,.435,4.67
FILL
N,3144,.789412,4.67
FILL,3141,3144
FILL,3101,3137,3,3110,9,8,1
FILL,3109,3144,3,3118,9

```

```

C*** Define the nodes for the lower shell
LOCAL,14,1,,73.25
N,4001,73.25,-90
N,4016,73.25,-64.50665929
FILL
LOCAL,15,1,27.815,14.9171927
N,4025,8.625
FILL,4016,4025
CSYS,0
N,4081,36.44,75.08954245
FILL,4025,4081
N,4001,0,0

C*** Define the nodes for the upper shell
LOCAL,16,1,,24.25
N,5001,74.5,90
N,5016,74.5,64.42280563
FILL
LOCAL,17,1,28.44,83.66954245
N,5025,8.625
FILL,5016,5025
CSYS,0
N,5027,37.065,82.16954245
FILL,5025,5027
N,5001,0,98.75

C*** Define the elements for the lower seal ring
TYPE,1
MAT,1
REAL,1
E,1001,1002,1007,1006
RP4,1,1,1,1
EGEN,9,5,1,4,1
E,1046,1047,1056,1055
RP4,1,1,1,1
EGEN,5,9,37,40,1
EGEN,7,9,53,54,1
EGEN,3,27,55,56,1
MAT,2
E,1050,1051,1060,1059
RP4,1,1,1,1
EGEN,3,9,73,76,1
EGEN,3,9,83,84,1

C*** Define the elements for the upper seal ring
TYPE,1
MAT,1
REAL,1
E,2001,2002,2005,2004
RP2,1,1,1,1
EGEN,2,3,89,90,1
E,2007,2008,2019,2018
RP10,1,1,1,1
EGEN,2,11,93,102,1
EGEN,2,11,103,107,1
E,2046,2045,2034
RP2,1,1,0
E,2034,2035,2048,2047
E,2044,2045,2050,2049
RP4,1,1,1,1
EGEN,6,5,121,124,1
E,2079,2080,2014,2013
RP4,1,1,1,1
E,2084,2085,2080,2079
RP4,1,1,1,1
EGEN,5,5,149,152,1
EGEN,3,5,165,166,1

C*** Define the elements for the locking ring
TYPE,1
MAT,2
REAL,1
E,3001,3002,3011,3010
RP4,1,1,1,1
EGEN,4,9,173,176,1
MAT,1
E,3005,3006,3015,3014
RP3,1,1,1,1
E,3018,3017,3008
E,3014,3015,3024,3023
RP4,1,1,1,1
EGEN,3,9,193,196,1
E,3041,3042,3047,3046
RP4,1,1,1,1
EGEN,11,5,205,208,1
E,3096,3097,3106,3105
RP4,1,1,1,1
E,3101,3102,3111,3110
RP8,1,1,1,1
EGEN,4,9,253,259,1
E,3117,3118,3127,3126

E,3126,3127,3136,3135
E,3135,3136,3144,3144

C*** Define the elements for the lower shell
TYPE,2
MAT,1
REAL,1
E,4001,4002
RP79,1,1
E,4080,1003

C*** Define the elements for the upper shell
TYPE,2
MAT,1
REAL,1
E,2076,5026
E,5026,5025
RP25,-1,-1

C*** Define the interface elements between the lower
seal flange and the locking ring
TYPE,3
MAT,1
REAL,2
E,3038,1051
RP3,1,1

C*** Define the interface elements between the upper
seal flange and the locking ring
TYPE,3
MAT,1
REAL,3
E,2036,3102
RP3,1,1

C*** Define the interface elements between the lower
seal flange and the upper seal flange
TYPE,4
MAT,1
REAL,4
E,1145,2009
RP5,1,1

C*** Couple the lower shell to the lower seal flange
TYPE,5
MAT,3
REAL,5
E,1001,1002
RP4,1,1

C*** Couple the upper shell to the upper seal flange
TYPE,5
MAT,3
REAL,5
E,2074,2075
RP4,1,1

C*** Define the displacement constraints
D,4001,UX,0,,5001,1000,ROTZ
D,3075,UY,0

C*** Define the pressure loads
P,4001,4002,-14.7,,4079,1
P,4080,1003,-14.7
P,1001,1006,-14.7,,1041,5
P,1046,1055,-14.7,,1136,9
P,1145,1146,-14.7,,1148,9
P,1140,1149,-14.7
P,2001,2002,-14.7,,2002,1
P,2003,2006,-14.7,,2006,3
P,2009,2010,-14.7,,2012,1
P,2013,2079,-14.7
P,2001,2004,-14.7,,2004,3
P,2007,2018,-14.7,,2029,11
P,2040,2041,-14.7,,2043,1
P,2044,2049,-14.7,,2069,5
P,5001,5002,-14.7,,5025,1
P,5026,2076,-14.7

C*** Re-order the elements to reduce execution time
WSTART,4001
WAVES

C*** Set convergence criteria, write a solution
file, and exit
ITER,-10,10
AFWRITE
FINISH

```

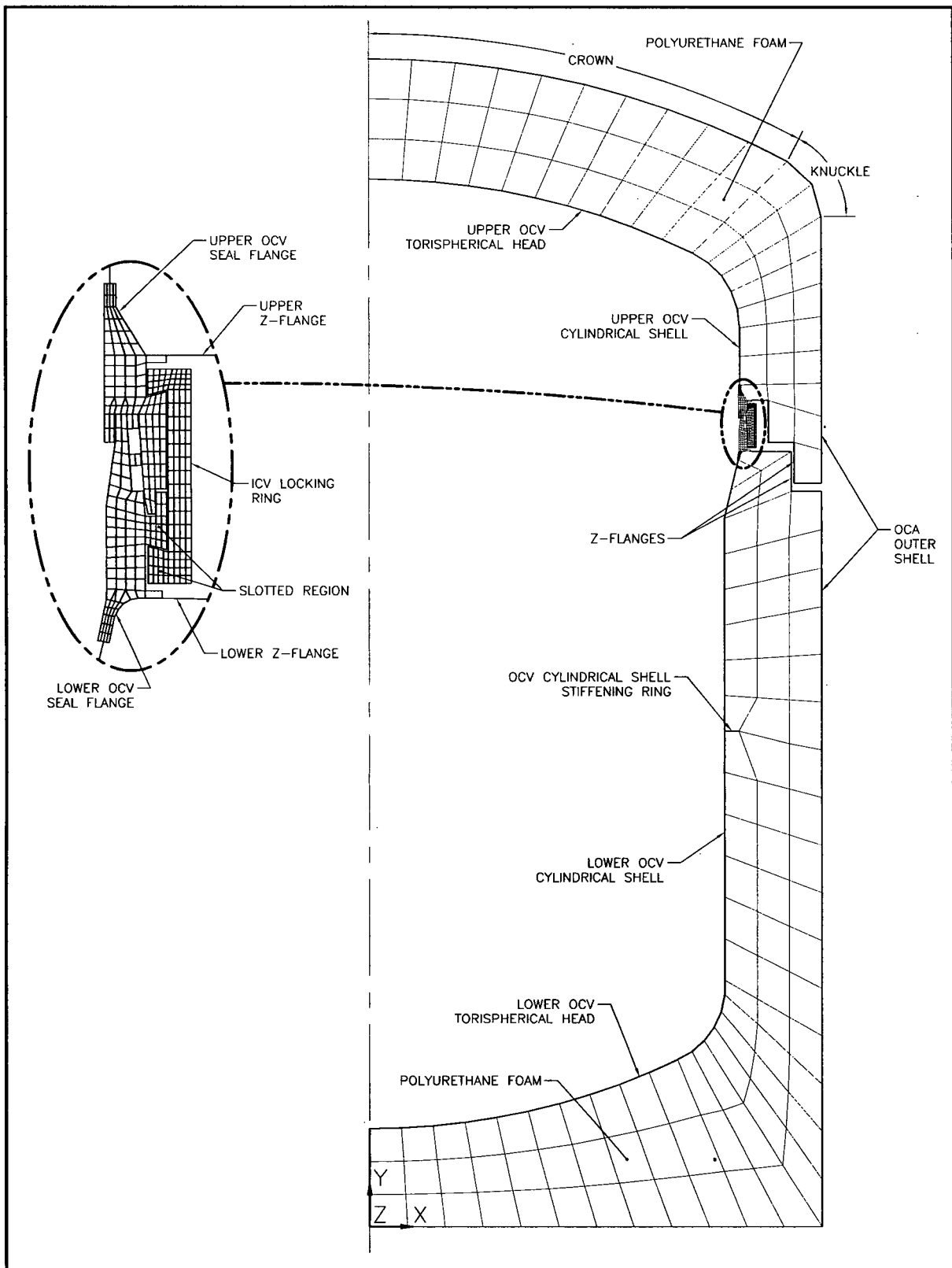


Figure 2.10.1-1 – OCA Finite Element Analysis Model Element Plot

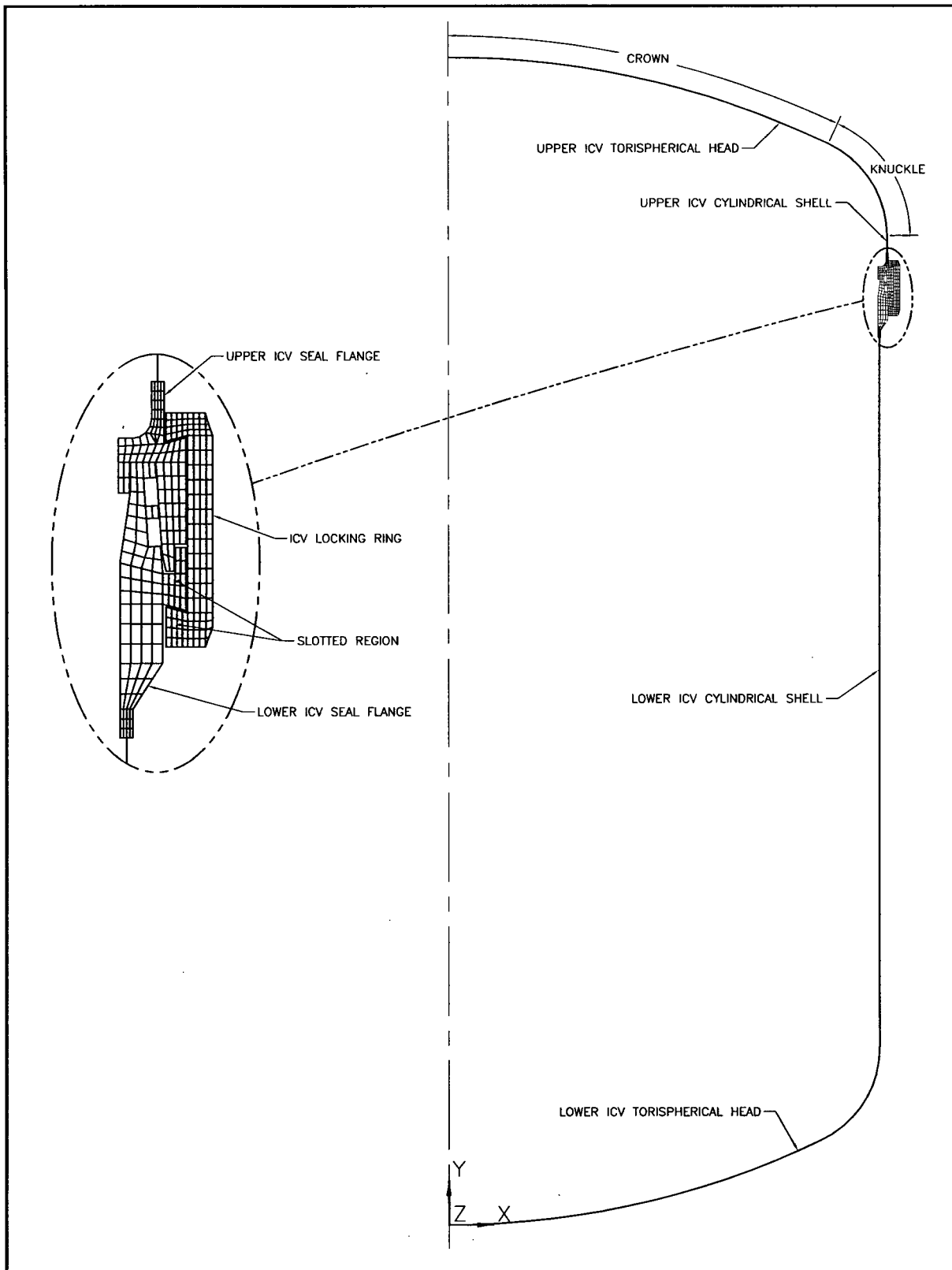


Figure 2.10.1-2 – ICV Finite Element Analysis Model Element Plot

## 2.10.2 Elastomer O-ring Seal Performance Tests

### 2.10.2.1 Introduction

Each containment O-ring seal material formulation shall be initially qualified for use in the TRUPACT-II packaging through the application of performance tests that demonstrate the material's ability to achieve and maintain a leaktight<sup>1</sup> seal at or beyond extremes for temperature, duration, minimum seal compression, and maximum seal compression change in a prototypical test fixture. The basis for formulation qualification test conditions applicable to the TRUPACT-II packaging is provided in Section 2.10.2.2, *Limits of O-ring Seal Compression and Temperature*. Section 2.10.2.3, *Formulation Qualification Test Fixture and Procedure*, defines the test fixture and test procedure for O-ring seal material qualification tests. Section 2.10.2.4, *Rainier Rubber R0405-70 Formulation Qualification Test Results*, summarizes the results of qualification testing successfully performed on Rainier Rubber<sup>2</sup> butyl rubber compound R0405-70.

Each batch of containment O-ring seal material shall additionally be required to satisfy the requirements of ASTM D2000<sup>3</sup> M4AA710 A13 B13 F17 F48 Z Trace Element. Section 2.10.2.5, *ASTM D2000 Standardized Batch Material Tests*, summarizes the industry standardized batch tests and correlates the ASTM D2000 designator to specific O-ring performance characteristics.

Additional information regarding past containment O-ring seal testing is presented in the report *Design Development and Certification Testing of the TRUPACT-II Package*<sup>4</sup>.

### 2.10.2.2 Limits of O-ring Seal Compression and Temperature

#### 2.10.2.2.1 Inner Containment Vessel Containment O-ring Seal Compression

The inner containment vessel (ICV) closure seal configuration consists of two O-ring seals, each located on a slightly different diameter in the ICV lid due to the tapered bore (see Appendix 1.3.1, *Packaging General Arrangement Drawings*, Sheets 4 and 7 of 11, for dimensional details). The upper O-ring seal is defined as the containment boundary, and the lower O-ring seal provides an annulus in which to establish a vacuum for leak testing.

In order to determine the minimum compression that may occur for the ICV containment O-ring seal, the worst-case tolerance stack-up on the lid flange, body flange, locking ring, and O-ring seal dimensions are utilized with the upper and lower seal flanges offset relative to each other. Figure 2.10.2-1 depicts the O-ring seal flange geometry for minimum ICV containment O-ring seal compression (note the reference datum for calculations).

<sup>1</sup> Leaktight is defined as leakage of  $1 \times 10^{-7}$  standard cubic centimeters per second (scc/sec), air, or less, per Section 5.4(3), *Reference Air Leakage Rate*, of ANSI N14.5-1997, *American National Standard for Radioactive Materials – Leakage Tests on Packages for Shipment*. American National Standards Institute, Inc. (ANSI).

<sup>2</sup> Rainier Rubber Company, Seattle, WA.

<sup>3</sup> ASTM D2000-08, *Standard Classification System for Rubber Products in Automotive Applications*. American Society for Testing and Materials, Philadelphia, PA, Volume 09.02, 2008.

<sup>4</sup> S. A. Porter, et al, *Design Development and Certification Testing of the TRUPACT-II Package*, 016-03-09, Portemus Engineering, Inc., Puyallup, Washington.

With reference to Figure 2.10.2-1, the following dimensions define the worst-case configuration for determining the minimum ICV containment O-ring seal compression:

- $a = 0.153$  inches (maximum vertical gap; see Section 8.2.3.3.2.3, *Axial Play*)
- $b = 0.493$  inches (minimum tab width; see Section 8.2.3.3.2.2, *Tab Widths*)
- $c = 0.561$  inches (maximum groove width; see Section 8.2.3.3.2.1, *Groove Widths*)
- $d_L = 0.251$  inches (maximum vertical offset (gage depth); see Figure 8.2-4)
- $d_U = 0.249$  inches (minimum vertical offset (ball diameter); see Figure 8.2-1)
- $e = 0.330$  inches (maximum seal groove offset; based on  $0.300 \pm 0.030$ )
- $f = 0.000$  inches (minimum horizontal gap between upper and lower seal flange; closed)
- $r = 0.125$  inches (nominal lower seal flange tab edge radius)
- $h = 0.253$  inches (maximum O-ring seal groove depth; based on  $0.250 \pm 0.003$ )
- $w = 0.563$  inches (maximum O-ring seal groove width; based on  $0.560 \pm 0.003$ )
- $\alpha = 3.60^\circ$  (minimum lower flange tab angle; based on  $3.85^\circ \pm 0.25^\circ$ )
- $\beta = 4.20^\circ$  (maximum upper flange seal surface angle; based on  $3.95^\circ \pm 0.25^\circ$ )
- $\theta = 3.60^\circ$  (contact surfaces angle based on the average of angles  $\alpha$  and  $\beta$ )
- $\gamma = 5.00^\circ$  (maximum O-ring seal groove angle; based on  $0^\circ - 5^\circ$ )

### 1. Worst-Case Location for the Center-Bottom of the O-ring Seal Groove

With reference to Figure 2.10.2-1, the worst-case location for the center-bottom of the O-ring seal groove is determined by finding the horizontal and vertical distance from the datum to the O-ring seal contact point on the lower seal flange,  $x_i$  and  $y_i$ , respectively:

$$x_i = f + b + \left[ \left( e - \frac{d_L}{\cos(\alpha)} \right) + (h) \tan(\gamma) + \frac{w}{2} \right] \sin(\alpha) - (h) \cos(\alpha) = 0.264494 \text{ inches}$$

$$y_i = a + d_L + \left[ \left( e - \frac{d_L}{\cos(\alpha)} \right) + (h) \tan(\gamma) + \frac{w}{2} \right] \cos(\alpha) + (h) \sin(\alpha) = 0.801270 \text{ inches}$$

### 2. Worst-Case Location for O-ring Seal Contact on the Upper Flange Sealing Surface

With reference to Figure 2.10.2-1, the worst-case location for O-ring seal contact on the upper seal flange sealing surface is determined by finding the horizontal and vertical distance from the datum to the O-ring seal contact point on the upper seal flange,  $x_o$  and  $y_o$ , respectively:

$$x_o = \frac{y_i + (x_i) \tan(\theta) + \frac{c}{\tan(\beta)} - d_U}{\frac{1}{\tan(\beta)} + \tan(\theta)} = 0.599877 \text{ inches}$$

$$y_o = d_U + \frac{x_o - c}{\tan(\beta)} = 0.778404 \text{ inches}$$

### 3. Maximum O-ring Seal Groove-to-Contact Surface Gap

The maximum O-ring seal groove-to-contact surface gap is determined by using the distance formula in two-dimensional Cartesian space:

$$g = \sqrt{(x_o - x_i)^2 + (y_o - y_i)^2} = 0.336162 \text{ inches}$$

### 4. Minimum O-ring Seal Cross-Sectional Diameter Due to Stretch

The minimum reduced O-ring seal cross-sectional diameter,  $d_{csr}$ , is determined by finding the maximum ICV containment O-ring seal groove diameter,  $D_g$ , calculating the O-ring seal stretch,  $s$ , and calculating the corresponding maximum reduction in O-ring seal cross-sectional diameter,  $r_{cs}$ , using worst-case dimensions.

Given a maximum lower seal flange control diameter,  $D_L = 74.185$  inches (based on  $74.155 \pm 0.030$ ), and a minimum lower seal flange control height,  $H_L = 0.970$  inches (based on  $1.000 \pm 0.030$ ), the maximum ICV containment O-ring seal groove diameter,  $D_g$ , is:

$$D_g = D_L - 2 \left\{ \left[ H_L - \left( e + (h) \tan(\gamma) + \frac{w}{2} \right) \cos(\alpha) \right] \tan(\alpha) - (h) \cos(\alpha) \right\} = 73.637517 \text{ inches}$$

Given a minimum ICV containment O-ring seal inside diameter,  $D_i = 70.070$  inches (based on  $71.500 \pm 2\%$ ), the maximum ICV containment O-ring stretch,  $s$ , is

$$s = \frac{D_g - D_i}{D_i} = 5.09\%$$

The maximum reduction in O-ring seal cross-sectional diameter,  $r_{cs}$ , due to stretch (from Figure 3-3 of the *Parker O-ring Handbook*<sup>5</sup>) is calculated with the stretch,  $s = 5.09$ :

$$r_{cs} = 0.56 + 0.59s - 0.0046s^2 = 3.44\%$$

Given a minimum ICV containment O-ring seal cross-sectional diameter,  $d_s = 0.390$  inches (based on  $0.400 \pm 0.010$ ), the resulting reduced O-ring seal cross-sectional diameter,  $d_{csr}$ , is:

$$d_{csr} = d_s (1 - r_{cs}) = 0.376584 \text{ inches}$$

### 5. Minimum O-ring Seal Compression with an Offset Lid

The minimum ICV containment O-ring seal compression,  $\xi$ , is:

$$\xi = \frac{d_{csr} - g}{d_{csr}} = 10.73\%$$

The minimum O-ring seal compression is 10.73% with an offset lid. This is the worst case possible as a result of the HAC free drop.

<sup>5</sup> ORD 5700, *Parker O-ring Handbook*, 2007, Parker Hannifin Corporation, Cleveland, OH.

## 6. Minimum O-ring Seal Compression with a Centered Lid

With reference to Figure 2.10.2-1, the “centered” position for the lower seal flange relative to the upper seal flange occurs when point ① on the lower seal flange is moved to the midpoint between points ① and ②. Calculate the x-locations for points ① and ②:

$$x_1 = b - (d_L - r[1 - \sin(\alpha)])\tan(\alpha) = 0.484579 \text{ inches}$$

$$x_2 = c + (a + r[1 - \sin(\alpha)] - d_U)\tan(\beta) = 0.562553 \text{ inches}$$

Half the difference between the  $x_1$  and  $x_2$  values centers the lower seal flange tab within the upper seal flange groove (i.e., the ICV lid is centered in the ICV body). The “centered” horizontal offset,  $f_c$ , is:

$$f_c = \frac{x_1 - x_2}{2} = 0.038987 \text{ inches}$$

Recalculate the O-ring seal gap,  $g_c$ , based on the lid centered relative to the body:

$$x_{ci} = f_c + b + \left[ \left( e - \frac{d_L}{\cos(\alpha)} \right) + (h)\tan(\gamma) + \frac{w}{2} \right] \sin(\alpha) - (h)\cos(\alpha) = 0.303481 \text{ inches}$$

$$y_{ci} = a + d_L + \left[ \left( e - \frac{d_L}{\cos(\alpha)} \right) + (h)\tan(\gamma) + \frac{w}{2} \right] \cos(\alpha) + (h)\sin(\alpha) = 0.801270 \text{ inches}$$

$$x_{co} = \frac{y_{ci} + (x_{ci})\tan(\theta) + \frac{c}{\tan(\beta)} - d_U}{\frac{1}{\tan(\beta)} + \tan(\theta)} = 0.6000071 \text{ inches}$$

$$y_{co} = d_U + \frac{x_{co} - c}{\tan(\beta)} = 0.781046 \text{ inches}$$

$$g_c = \sqrt{(x_{co} - x_{ci})^2 + (y_{co} - y_{ci})^2} = 0.297279 \text{ inches}$$

Knowing that the ICV containment O-ring seal groove diameter,  $D_g$ , and correspondingly the O-ring seal stretch,  $s$ , and the reduced O-ring seal cross-sectional diameter,  $d_{csr}$ , are the same, the minimum ICV containment O-ring seal compression,  $\xi_c$ :

$$\xi_c = \frac{d_{csr} - g_c}{d_{csr}} = 21.06\%$$

The minimum O-ring seal compression is 21.06% with a centered lid. This is the normal, as-installed configuration, since the presence of the O-ring seal will inherently self-center the lid.

### 7. Maximum Change in O-ring Seal Compression from a Centered Lid to an Offset Lid

The maximum resulting change in compression,  $\Delta$ , resulting in a minimally compressed ICV containment O-ring seal is:

$$\Delta = \xi_c - \xi = 10.33\%$$

This is the maximum change in compression of the O-ring seal as a result of the HAC free drop.

#### 2.10.2.2.2 Containment O-ring Seal Qualification Temperature

Per Section 3.4.3, *Minimum Temperatures*, the minimum ICV containment O-ring seal temperature is -40 °F for normal conditions of transport (NCT) and -20 °F for hypothetical accident conditions (HAC). Per Table 3.4-1 through Table 3.4-5 in Section 3.4.2, *Maximum Temperatures*, the maximum ICV O-ring seal temperature for NCT is 150 °F. The duration of O-ring seal material exposure to elevated temperatures under NCT can conservatively be assumed as one year based on the replacement frequency of the O-ring seals. Per Table 3.5-5 in Section 3.5.3, *Package Temperatures*, the maximum ICV O-ring seal temperature for HAC is 200 °F. Evaluating the time-history of OCV O-ring seal temperatures provided in Figure 3.5-6 for Certification Test Unit 1 (CTU-1) and Figure 3.5-10 for Certification Test Unit 2 (CTU-2), the duration of ICV O-ring seal material exposure to elevated temperatures within 90% of the reported 260 °F maximum is conservatively estimated to be less than 12 hours.

An Arrhenius correlation for butyl material with an activation energy of 80 kJ/mol for butyl rubber has been developed to account for diffusion limited oxidation effects.<sup>6</sup> Use of the Arrhenius correlation allows the effects of both NCT and HAC elevated temperature/duration conditions identified above to be conservatively enveloped by a single, 360 °F, 8-hour test.

Based on the above evaluations, the minimum O-ring seal qualification test parameters required for initial formulation testing of ICV containment O-ring seal materials is summarized in Table 2.10.2-1.

**Table 2.10.2-1 – Formulation Qualification Test O-ring Seal Compression Parameters**

Simulated Condition	Required Compression (%)	Required Compression Change (%)	Required Temperature (°F)	Required Temperature Duration (hours)
NCT Cold	≤21.06	N/A	≤-40	N/A
HAC Free Drop	≤10.73	≥10.33	≤-20	N/A
HAC Fire		N/A	≥360	≥8

<sup>6</sup> K. T. Gillen, C. Mathias, and M. R. Keenan, *Methods for Predicting More Confident Lifetimes of Seals in Air Environments*, SAND99-0553J, Sandia National Laboratories, March 1999.

### 2.10.2.3 Formulation Qualification Test Fixture and Procedure

A bore-type test fixture shall be used to test the containment O-ring seal, representative of the bore seal configuration of the TRUPACT-II packaging. The fixture shall include an inner disk containing two, side-by-side O-ring seal grooves. An O-ring seal of prototypic cross-section for the ICV and butyl material, as delineated on the drawings in Appendix 1.3.1, *Packaging General Arrangement Drawings*, shall be placed into each seal groove, and the assembly then placed within a mating bore component. The test fixture shall employ jacking screws or equivalent devices to displace the disk radially relative to the bore, affecting the required O-ring compression on one side of the test fixture. Figure 2.10.2-2 conceptually illustrates the O-ring seal test fixture.

The sizes of all sealing components and O-ring seals utilized in the test fixture, including the amount of O-ring seal stretch, may be adjusted along with the amount of radial displacement to ensure that the parameters in Table 2.10.2-1 can be achieved. The test fixture's overall diameter may be reduced relative to a full-scale TRUPACT-II package to achieve a practical size for testing. A reduction in relative diameter is acceptable since the O-ring seal compression, compression change, and temperature are the parameters of primary importance relative to evaluating an O-ring material's ability to maintain a leaktight seal.

All test specimens may be coated lightly with vacuum grease prior to installation into the test fixture. The fully assembled test fixture shall be placed within an environmental test chamber for both heating and cooling with thermocouples attached to the fixture used to confirm the O-ring seal temperature.

The region between the two O-ring seals constitutes a test volume. To perform a leak test, the test volume shall be connected to a helium mass spectrometer leak detector, then evacuated to an appropriate level of vacuum and the outside of the test fixture surrounded with a contained and highly concentrated environment of helium gas, consistent with the guidelines of Appendix A, Section A.5.3, *Gas Filled Envelope – Gas Detector*, of ANSI N14.5<sup>7</sup>. An O-ring seal test shall be successful if the leakage between the seals is  $1 \times 10^{-7}$  standard cubic centimeters per second (scc/sec), air, or less (i.e., "leaktight").

Test conditions shall be selected to simulate temperature/duration and minimum compression for the prototypic O-ring seals under NCT and HAC conditions. Each set of two test O-ring seals shall be subjected to an initial test at NCT Cold conditions with the inner disk offset as necessary to achieve the NCT required compression, to a second test at HAC Free Drop conditions with the inner disk initially positioned and then radially offset as necessary to achieve the HAC required compression and compression change magnitudes, to a third test at HAC Fire conditions after the required soak duration with the inner disk remaining offset, and to a fourth test at HAC Cold conditions with the inner disk remaining offset (see Table 2.10.2-1).

Helium leakage rate tests shall be performed at each cold temperature test configuration, either at -40 °F for the NCT Cold condition case, or at -20 °F for all other cases. Helium leakage rate testing is not practical at hot condition temperatures due to the rapid permeation and saturation of helium gas through the elastomeric material at high temperatures; a fully saturated O-ring seal test specimen results in a measured leakage in excess of  $1 \times 10^{-7}$  scc/sec, air. In lieu of leakage rate testing at the hot temperature test configuration, the ability to establish a rapid, hard vacuum

---

<sup>7</sup> ANSI N14.5-1997, *American National Standard for Radioactive Materials – Leakage Tests on Packages for Shipment*, American National Standards Institute, Inc. (ANSI).

between the O-ring seals shall be used as the basis for acceptance at elevated temperatures, with leaktightness proven subsequent to the elevated temperature phase by the final leakage rate test at -20 °F. The duration of each of the cold temperature phases of the test shall be defined by the time required to achieve the requisite cold temperatures whereas the duration of the hot phase shall be defined by the required elevated temperature and associated temperature duration given in Table 2.10.2-1.

#### **2.10.2.3.1 Formulation Qualification Test Procedure**

The process of formulation qualification leak testing O-ring seal material is given below.

1. Assemble the test fixture with two test O-ring seals.
2. Radially shift the disk inside the bore to establish reduced O-ring seal compression on one side of the test fixture, ensuring the NCT Cold compression requirements are met per Table 2.10.2-1.
3. Cool the test fixture to  $\leq -40$  °F, continuing to restrain the disk in the NCT offset position relative to the bore.
4. Perform a helium leakage rate test with the test fixture temperature at  $\leq -40$  °F.
5. Reposition the disk inside the bore to establish an appropriate starting position for the HAC Free Drop test with the test fixture temperature at  $\leq -20$  °F.
6. Radially shift the disk inside the bore to establish a reduced O-ring seal compression on one side of the test fixture, ensuring the HAC Cold compression and compression change requirements are met per Table 2.10.2-1.
7. Perform a helium leakage rate test with the test fixture temperature at  $\leq -20$  °F.
8. Warm the test fixture to the elevated test temperature (i.e., HAC Fire temperature per Table 2.10.2-1), continuing to restrain the disk in the HAC offset position relative to the bore.
9. Maintain the elevated temperature for  $\geq 8$ -hour duration.
10. At the end of the elevated temperature duration, confirm that a rapid, hard vacuum can be achieved and maintained in the test volume between the two, test O-ring seals at the elevated temperature.
11. Cool the test fixture to  $\leq -20$  °F, continuing to restrain the disk in the HAC offset position relative to the bore.
12. Perform a helium leakage rate test with the test fixture temperature at  $\leq -20$  °F.

#### **2.10.2.4 Rainier Rubber R0405-70 Formulation Qualification Test Results**

Test results are summarized in Table 2.10.2-2, as referenced from GEN-REP-0001.<sup>8</sup> As shown in the table, the Rainier Rubber compound R0405-70 butyl rubber material is capable of maintaining a leaktight seal when subjected to worst-case seal compressions beyond the range of NCT and HAC cold and hot temperatures applicable to the TRUPACT-II package. For

---

<sup>8</sup> *Formulation Qualification Testing of Rainier Rubber Butyl Compound RR0405-70*, GEN-REP-0001, Rev. 0, Washington TRU Solutions, February 2010.

comparison, the minimum O-ring seal compression applicable for the NCT Cold condition (see Table 2.10.2-1) is 21.06% for the ICV. The NCT Cold tests summarized in Table 2.10.2-2 were conservatively performed with the disk in its full offset position, thus showing leaktight capability at NCT Cold conditions to as low as 10.38%. For the remaining tests, the applicable minimum compression is 10.73% for the ICV whereas the tests were all performed in the full offset position, thus showing leaktight capability to as low as 10.38%. For the HAC Free Drop test, the disk was initially centered and then shifted as much as 10.74%, which enveloped the applicable worst-case shift of 10.33% for the ICV. For the HAC Fire test, again per Table 2.10.2-1, a test temperature of at least 360 °F for at least 8 hours is applicable, whereas the actual test was conservatively performed at 400 °F for 8 hours, as noted in Table 2.10.2-2. Therefore, formulation qualification testing of Rainier Rubber compound R0405-70 bounds the minimum O-ring seal compressions for the TRUPACT-II package.

### 2.10.2.5 ASTM D2000 Standardized Batch Material Tests

Based on successfully demonstrating the ability to remain leaktight when subject to the formulation qualification tests, Rainier Rubber R0405-70 butyl rubber compound was selected to benchmark material performance parameters that can be evaluated using available industry standardized tests. Correlation of the R0405-70 butyl rubber compound performance to industry standard performance specifications establishes a standard quality and performance benchmark that is suitable for use in material batch testing. Note that a “formulation” represents a controlled chemical recipe and production process as defined by the material supplier, a “batch” represents the chemical compounding of a production quantity of material before vulcanizing, and a “lot” refers to the quantity of finished product made at any one time.

Qualification testing identified certain key parameters that are important to seal performance. Of these, two important parameters for this application are resistance to helium permeation and acceptable resiliency at cold temperatures. Butyl rubber performs very well resisting helium permeation, and the TR-10 test in ASTM D1329<sup>9</sup> provides an acceptable method for determining cold temperature material resiliency, with the properties of the R0405-70 acting as a baseline for the required resiliency.

The ability of the compound to withstand elevated temperatures while not having significant reduction in material properties is also required to maintain seal integrity after the hypothetical accident condition thermal event. Material properties in elastomers are reduced through the process of de-polymerization, an aging phenomenon. Elastomer aging can be accelerated by the application of energy (heat). The effect of aging can be quantified by measuring the reduction of physical properties after maintaining the seal material at an elevated temperature for a specific length of time. For the same amount of reduction in properties, a shorter time can be used at a higher temperature, or a longer time can be used at a lower temperature. ASTM D573<sup>10</sup> provides an acceptable method for determining the effects of temperature aging on elastomeric compounds.

<sup>9</sup> ASTM D1329-88 (re-approved 1998), *Standard Test Method for Evaluating Rubber Property – Retraction at Lower Temperatures (TR Test)*, American Society for Testing and Materials, Philadelphia, PA, Volume 09.01, 2001.

<sup>10</sup> ASTM D573-99, *Standard Test Method for Rubber – Deterioration in an Air Oven*, American Society for Testing and Materials, Philadelphia, PA, Volume 09.01, 2001.

ASTM D395<sup>11</sup> provides an acceptable method for determining the effects of compression set. R0405-70 butyl rubber compound uses an acceptance criteria of less than 25% compression set for 22 hours at an elevated temperature of 70 °C.

ASTM D2137<sup>12</sup> provides an acceptable method for determining an elastomeric material's ability to withstand cold temperatures and remain pliable. Although the TR-10 test in ASTM D1329 demonstrates the seal material's resiliency at a much lower temperature, this test verifies the seal material's lack of brittleness at the minimum regulatory temperature of -40 °C.

Hardness or durometer along with tensile strength and elongation are defined and checked to ensure durability of the seal material during operation. ASTM D2240<sup>13</sup> provides an acceptable method for determining the required 70 ±5 durometer, and ASTM D412<sup>14</sup> provides an acceptable method for determining the required minimum 10 MPa (1,450 psi) tensile strength and minimum 250% elongation, with the properties of the R0405-70 acting as a baseline for the required hardness, tensile strength, and elongation.

For proprietary seal materials that have fairly demanding requirements such as the R0405-70 butyl rubber compound, the compound is commonly specified by a company designator and subsequently checked against exacting performance standards. Specifying an elastomeric compound by its chemistry alone is difficult considering the sheer number of parameters that affect seal performance. However, by applying the above nationally recognized standards to a material batch, the important parameters are defined for verifying the performance of the seal material.

ASTM D1414<sup>15</sup> is the standard method for testing O-ring seals, and covers most, but not all, of the required testing delineated above. However, due to the overall size of the O-ring seals and the additional testing specified, ASTM D2000<sup>3</sup> provides a better standard classification system.

Using the ASTM D2000 designator, O-ring seals with properties equivalent to R0405-70 butyl rubber material are classified as follows and summarized in the table below:

M4AA710 A13 B13 F17 F48 Z Trace Element

---

<sup>11</sup> ASTM D395-01, *Standard Test Methods for Rubber Property – Compression Set*, American Society for Testing and Materials, Philadelphia, PA, Volume 09.01, 2001.

<sup>12</sup> ASTM D2137-94 (re-approved 2000), *Standard Test Methods for Rubber Property – Brittleness Point of Flexible Polymers and Coated Fabrics*, American Society for Testing and Materials, Philadelphia, PA, Volume 09.02, 2001.

<sup>13</sup> ASTM D2240-00, *Standard Test Method for Rubber Property – Durometer Hardness*, American Society for Testing and Materials, Philadelphia, PA, Volume 09.01, 2002.

<sup>14</sup> ASTM D412-98a, *Standard Test Methods for Vulcanized Rubber and Thermoplastic Rubbers and Thermoplastic Elastomers – Tension*, American Society for Testing and Materials, Philadelphia, PA, Volume 09.01, 2001.

<sup>15</sup> ASTM D1414-94 (re-approved 1999), *Standard Test Methods for Rubber O-Rings*, American Society for Testing and Materials, Philadelphia, PA, Volume 09.02, 2001.

Designator	Condition
M	Metric units designator (default condition)
4	Grade 4 acceptance criteria for the tests specified
AA	Butyl rubber compound
7	70 Shore A durometer hardness per ASTM D2240
10	Tensile strength and elongation per ASTM D 412; acceptance criteria are a minimum 10 MPa (1,450 psi) tensile strength and a minimum 250% elongation
A13	Heat resistance test per ASTM D573; the acceptance criteria are a maximum 10 Shore A durometer hardness increase, a maximum reduction in tensile strength of 25%, and a maximum reduction in ultimate elongation of 25% at 70 °C
B13	Compression set per Method B of ASTM D395; acceptance criterion is a maximum 25% compression set after 22 hours at 70 °C
F17	Cold temperature resistance specifying low temperature brittleness per Method A, 9.3.2, of ASTM D2137; non-brittle after 3 minutes at -40 °C
F48	Cold temperature resiliency, where F is for cold temperature resistance, and 4 specifies testing to the TR-10 test of ASTM D1329; 8 indicates a TR-10 temperature of -50 °C (-58 °F), or less
Z Trace Element	Z designator allows specific notes to be added; "Z Trace Element" allows trace elements to be added to the elastomeric compound to meet the seal material requirements

**Table 2.10.2-2 – Rainier Rubber R0405-70 Formulation Qualification O-ring Seal Test Results**

Test Number <sup>ⓐ</sup>	O-ring Seal Number <sup>ⓐ</sup>	O-ring Seal Inside Diameter, D <sub>s</sub> (in)	O-ring Seal Cross-Sectional Diameter, d <sub>cs</sub> (in)		O-ring Seal Stretch, S (%) <sup>ⓐ</sup>	O-ring Seal Reduction in Cross-Sectional Diameter, R (%) <sup>ⓐ</sup>	Minimum O-ring Seal Cross-Sectional Diameter, d <sub>csr</sub> (in) <sup>ⓐ</sup>	O-ring Seal Compression (%) <sup>ⓐ</sup>			Temperature for "Leaktight" Leak Test (≤ 8.8 × 10 <sup>-8</sup> scc/sec, He) <sup>ⓐ</sup>			
			Max	Min				Center Disk	Offset Disk	Change	-40 °F	-20 °F	400 °F <sup>ⓐ</sup>	-20 °F
			1	1				11.368	0.396	0.394	6.80	4.36	0.377	21.12
	4	11.500	0.396	0.392	5.58	3.71	0.377	21.12	10.38	10.74	Yes	Yes	Yes	Yes
2	2	11.417	0.396	0.395	6.34	4.12	0.379	21.54	10.85	10.69	Yes	Yes	Yes	Yes
	3	11.465	0.395	0.394	5.90	3.88	0.379	21.54	10.85	10.69	Yes	Yes	Yes	Yes

Notes:

- ① The test fixture's pertinent dimensions are taken in line with the direction of offset, which is also the position where the minimum cross-sectional diameter of the O-ring seals are placed: bore inside diameter, D<sub>i</sub> = 12.736 inches; disk outside diameter, D<sub>o</sub> = 12.655 inches; and the O-ring seal groove diameter, D<sub>g</sub> = 12.14125 inches (based on the average of fixture measurements taken along the axis of offset). All tests are performed using WTS Test Fixture No. 4.
- ② Material for all O-ring seal test specimens is butyl rubber compound R0405-70, Rainier Rubber Co., Seattle, WA.
- ③ Given the O-ring seal inside diameter, D<sub>s</sub>, the percent of O-ring seal stretch, S = 100 × (D<sub>g</sub> - D<sub>s</sub>)/D<sub>s</sub>.
- ④ From Figure 3-3 of the *Parker O-ring Handbook*<sup>5</sup> and based on the O-ring seal cross-sectional diameter, d<sub>cs</sub>, the percent reduction in O-ring seal cross-sectional diameter, R = -0.005 + 1.19S - 0.19S<sup>2</sup> - 0.001S<sup>3</sup> + 0.008S<sup>4</sup> for 0 ≤ S ≤ 3%, and R = 0.56 + 0.59S - 0.0046S<sup>2</sup> for 3% < S ≤ 25%.
- ⑤ The reduced O-ring seal cross-sectional diameter, d<sub>csr</sub> = d<sub>cs</sub>(1 - R/100).
- ⑥ The percent O-ring seal compression with the disk *centered* is 100 × [d<sub>csr</sub> - ½(D<sub>i</sub> - D<sub>g</sub>)]/d<sub>csr</sub>.
- ⑦ The percent O-ring seal compression with the disk *offset* is 100 × [d<sub>csr</sub> - (D<sub>i</sub> - D<sub>o</sub>) - ½(D<sub>o</sub> - D<sub>g</sub>)]/d<sub>csr</sub>.
- ⑧ A "Yes" response indicates that helium leakage testing demonstrated that the leakage rate was ≤ 1.0 × 10<sup>-7</sup> scc/sec, air (i.e., "leaktight" per ANSI N14.5). In all cases, measured leakage rates were ≤ 8.8 × 10<sup>-8</sup> scc/sec, helium, for tests with a "Yes" response.
- ⑨ No helium leak tests were performed at elevated temperatures due to O-ring seal permeation and saturation by helium gas. The ability of the test fixture to establish a rapid, hard vacuum between the O-ring seals was used as the basis for leak test acceptance at elevated temperatures. A "Yes" response indicates that all tests rapidly developed a hard vacuum.

This page intentionally left blank.

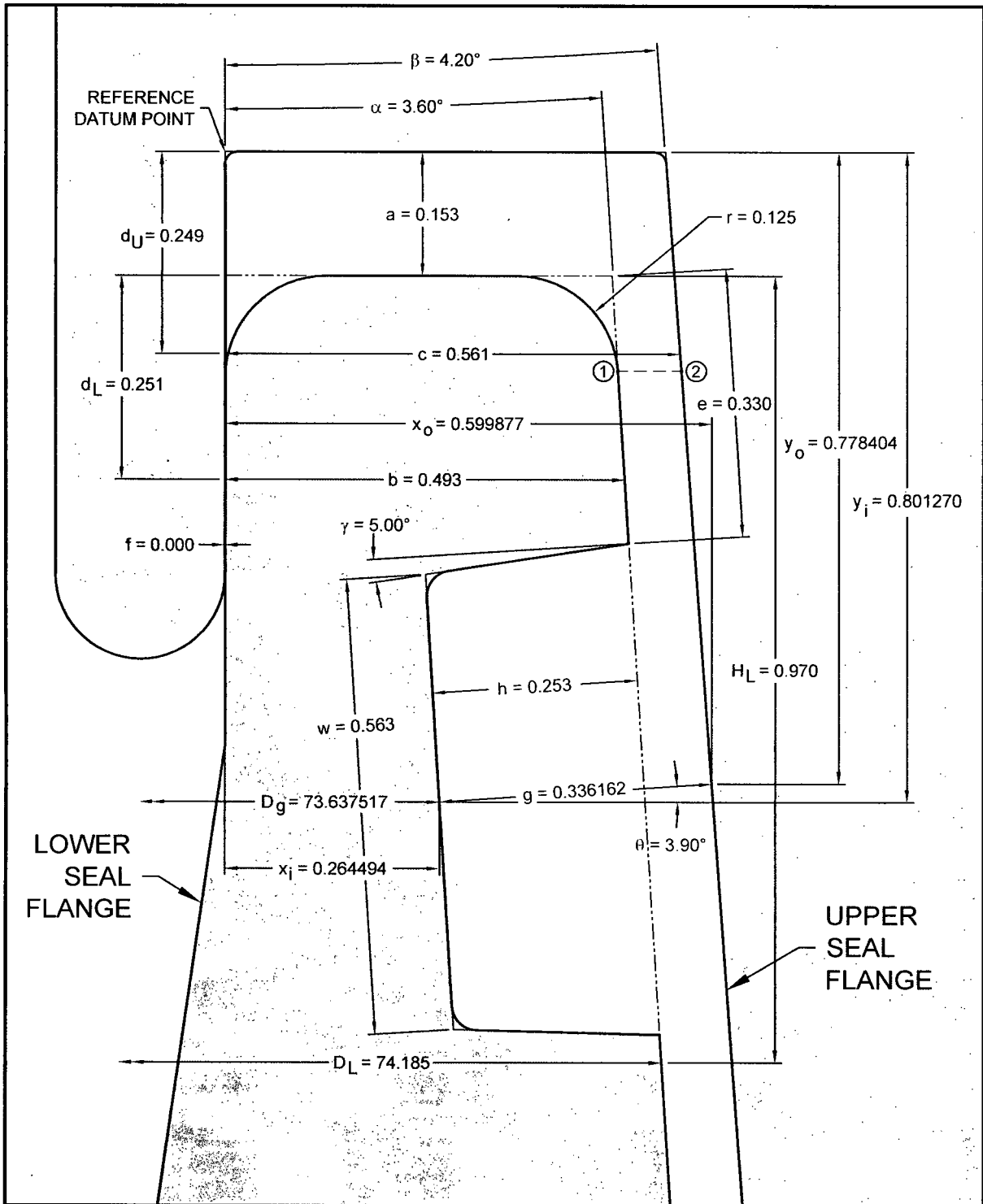


Figure 2.10.2-1 – Configuration for Minimum ICV O-ring Seal Compression

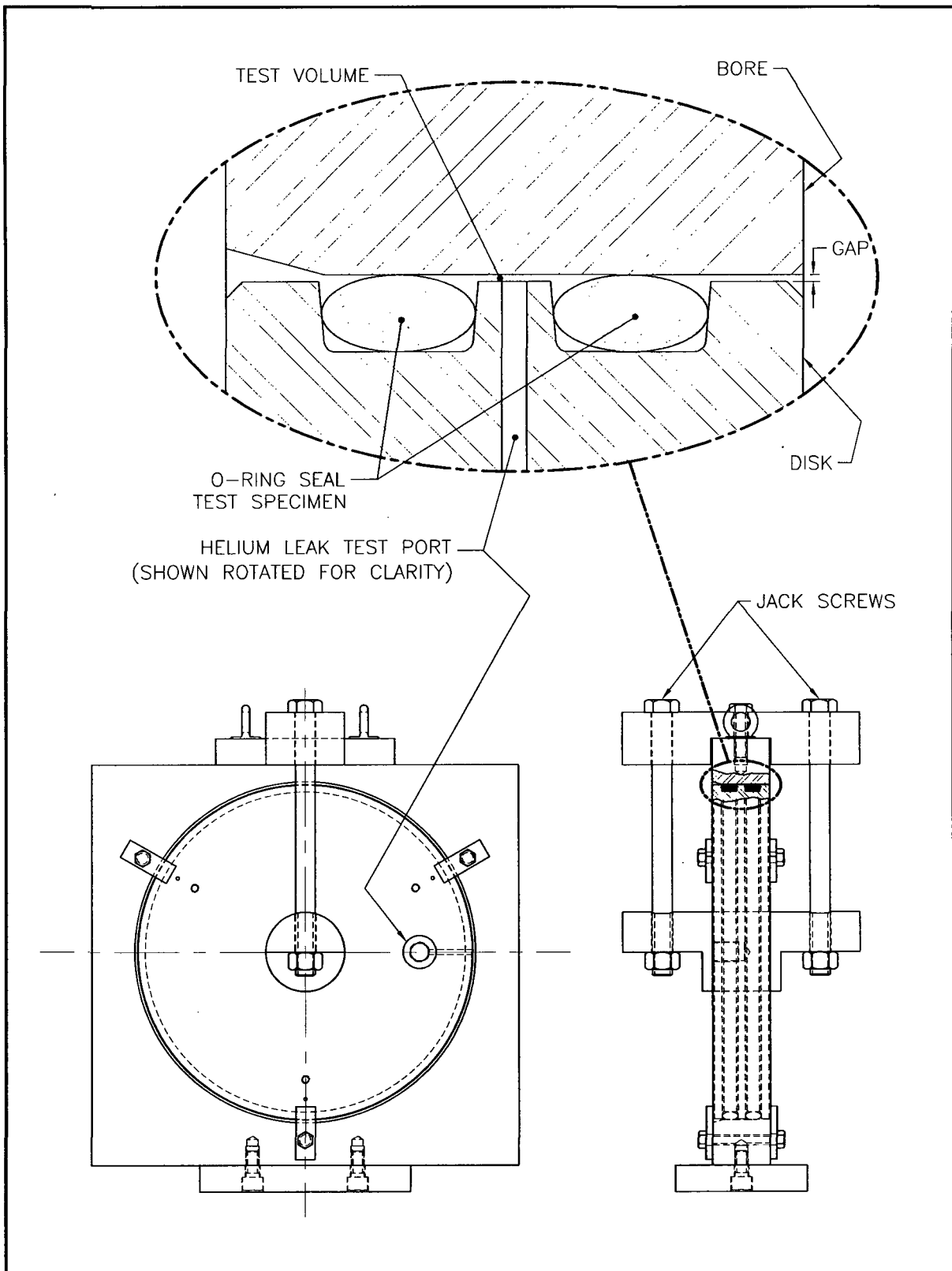


Figure 2.10.2-2 – Test Fixture for O-ring Seal Performance Testing

### 2.10.3 Certification Tests

Presented herein are the results of normal conditions of transport (NCT) and hypothetical accident condition (HAC) tests that address the free drop, puncture, and fire test performance requirements of 10 CFR 71<sup>1</sup>. This appendix summarizes the information presented in the report *Design Development and Certification Testing of the TRUPACT-II Package*<sup>2</sup>. The test units discussed in this section were configured for testing with two independent containment boundaries. All test results and conclusions with respect to the inner containment vessel (ICV) remain unchanged with the outer containment (now confinement) vessel (OCV) configured as secondary confinement boundary when its optional O-ring seals are utilized. The leaktight capability of the ICV and the structural response and ability of the outer containment (now confinement) assembly (OCA) to protect the ICV are unaffected by the OCV configuration using optional O-ring seals.

#### 2.10.3.1 Introduction

The TRUPACT-II package, when subjected to the sequence of hypothetical accident condition (HAC) tests specified in 10 CFR §71.73, subsequent to the sequence of normal conditions of transport (NCT) tests specified in 10 CFR §71.71, is shown to meet the performance requirements specified in Subpart E of 10 CFR 71. As indicated in the introduction to Chapter 2.0, *Structural Evaluation*, with the exception of the immersion test, the primary proof of performance for the HAC tests is via the use of full-scale testing. In particular, free drop, puncture, and fire testing of three TRUPACT-II certification test units (CTUs) confirmed that the ICV and OCV remained leaktight after a worst case HAC sequence. Observations from testing of the CTUs also confirm the conservative nature of deformed geometry assumptions used in the criticality assessment provided in Chapter 6.0, *Criticality Evaluation*.

#### 2.10.3.2 Summary

Three CTUs (hereafter referred to as CTU-1, CTU-2, and CTU-3) were used to demonstrate compliance with the HAC structural and thermal requirements of 10 CFR 71. CTU-1 was subjected to ten tests: one NCT 3-foot free drop, three HAC 30-foot free drops, five HAC 40-inch puncture drops, and one HAC 30-minute fire. CTU-2 was subjected to nine separate tests and one repeat test: three HAC 30-foot free drops, six HAC 40-inch puncture drops (one being a repeat test for CTU-1), and one HAC 30-minute fire. CTU-3, using the same ICV and OCV as CTU-2 but modified to prevent debris encroachment into the ICV seals, was subjected to eight repeat tests for CTU-2: three HAC 30-foot free drops and five HAC 40-inch puncture drops; the HAC 30-minute fire test was not repeated.

As seen in the figures presented in Section 2.10.3.6.3, *Test Sequence for Selected Free Drop, Puncture Drop, and Fire Tests*, successful testing of the CTUs indicates that the various TRUPACT-II packaging design features are adequately designed to withstand the HAC tests

---

<sup>1</sup> Title 10, Code of Federal Regulations, Part 71 (10 CFR 71), *Packaging and Transportation of Radioactive Material*, 01-01-12 Edition.

<sup>2</sup> S. A. Porter, et al, *Design Development and Certification Testing of the TRUPACT-II Package*, 016-03-09, Portemus Engineering, Inc., Puyallup, Washington.

specified in 10 CFR §71.73. The most important result of the testing program was the demonstrated ability of the OCV and ICV to remain leaktight<sup>3</sup>.

Significant results of HAC free drop testing common to all CTUs are as follows:

- Buckling was not observed for either containment boundary shell. Additionally, accelerometers mounted directly on the OCV shell were utilized to determine the axial acceleration resulting from a 30-foot bottom end drop events on CTU-2 and CTU-3.
- No excessive distortion of the seal flange regions occurred for either containment vessel, although some permanent deformation was noted.
- All three (3) ICV and all six (6) OCV locking ring lock bolts remained intact and locking ring and lower seal flange tabs remained fully interlocked during and following the drop tests. Some OCA locking Z-flange-to-locking ring fasteners failed during the testing, but a sufficient number remained intact to securely retain the locking ring in the locked position. Additionally, for test purposes, only 24 fasteners were used whereas 36 are specified for the design.
- The containment boundaries were shown to be capable of maintaining pressure before, during, and after each 30-foot drop test. At the instant of impact, internal pressures in both the ICV and OCV would typically increase slightly (a few psi) for a moment and then return, within the accuracy of the instrumentation, to their initial, pre-drop test values.
- The aluminum honeycomb spacer assemblies used in the ICV upper and lower torispherical heads were shown to adequately protect the heads from damaging payload interactions.
- Rupture was not observed for the 3/8-inch thick, OCA outer shell.
- Internal pressures increased during the drops, but returned to pre-drop pressures afterward.
- Observed permanent deformations of the TRUPACT-II packaging were less than those assumed for the criticality evaluation.

Significant results of puncture drop testing common to all CTUs are as follows:

- With one exception, permanent deformations of the containment boundary are not attributed to the puncture event. The single exception occurred for a puncture impact onto the 1/4-inch thick OCA outer shell at a location 40 inches above the base of the package (Test No. 7 for CTU-1, and Test No. R for CTU-2). This puncture event resulted in a hole through the OCA outer shell. The permanent damage to the OCV and ICV shells was an inward bulge of approximately 1½ inches to the OCV and ICV sidewalls. Importantly, permanent deformations were limited to the cylindrical shell portions of the OCV and ICV lower bodies, with no significant deformation near the seal flanges.
- Rupture was not observed for the 3/8-inch thick, OCA outer shell. Penetrations of the OCA outer shell closest to the seal regions were 22 inches above and 37 inches below the closure interface. Minor tearing of the Z-flange-to-3/8-inch thick OCA interfaces was observed for some test orientations. These regions are covered by the outer thermal shield; therefore, such tears are of little consequence.
- Tearing of the OCA outer shell occurred at the 3/8-to-1/4-inch thick, OCA body outer shell transition (weld) during testing of CTU-2 and CTU-3 (Test 4).

---

<sup>3</sup> "Leaktight" is a leak rate not exceeding  $1 \times 10^{-7}$  standard cubic centimeters per second (scc/sec), air, as defined in ANSI N14.5-1997, *American National Standard for Radioactive Materials – Leakage Tests on Packages for Shipment*, American National Standards Institute, Inc. (ANSI).

- In the regions where a significant amount of polyurethane foam was exposed by a puncture event (i.e., 40 inches above the package base and near the OCA top knuckle), the intumescent (i.e., self-extinguishing) characteristics of the polyurethane foam were sufficient to provide effective insulation from the effects of the subsequent HAC fire.

Significant results of fire testing common to the first two CTUs are as follows:

- The intumescent (i.e., self-extinguishing) characteristic of the polyurethane foam was sufficient to provide insulation from the effects of the HAC fire even in regions where the most significant amounts of foam were exposed.
- The maximum measured temperatures for the OCV and ICV elastomeric (butyl) O-ring seals were 260 °F (thermocouple reading during the fire, 250 °F by passive temperature indicating label) and 200 °F, respectively. The maximum measured temperatures for the OCV and ICV structural components were 439 °F and 270 °F, respectively. The 270 °F ICV temperature was most likely a result of the preheat operation used to heat the vessels prior to the fire test, rather than a result of the fire test itself. Air was pumped into the OCV/ICV annulus at 40 psi and 350 °F, and within close proximity of the corresponding temperature indicating label that measured the 270 °F temperature. The next highest ICV temperature reading was 220 °F.
- Both containment boundaries demonstrated the capability of maintaining pressure before, during, and after the fire event. Note that pressure was lost in the CTU-1 OCV during fire testing. However, the loss of pressure was due to failure of a test-related pressure fitting, not to a packaging design feature. Post-test repair of the fitting and re-pressurization of the OCV indicated that the pressure retention capabilities of the OCV had not been compromised by the fire test.
- Following fire testing, disassembly of the OCA demonstrated that, except for the local area damaged by the puncture impacts 40 inches above the base of the package, a layer of unburned polyurethane foam remained around the entire OCV. For both CTUs, the average thickness of the layer was approximately 5 to 6 inches along the cylindrical sides and lower head of the OCV, and even greater adjacent to the OCV upper dished head. This residual polyurethane foam thickness is consistent with the shielding evaluation provided in Chapter 5.0, *Shielding Evaluation*, and the criticality evaluation presented in Chapter 6.0, *Criticality Evaluation*.

### 2.10.3.3 Test Facilities

Drop testing of the TRUPACT-II package prototype test unit was performed at Sandia National Laboratories' Coyote Canyon Aerial Cable Facility in Albuquerque, New Mexico. The drop test facility utilizes free fall and, if needed, rocket power to attain closely controlled impact velocities as defined by a particular testing program. The drop test facility consists of a 5,000-foot long wire cable suspended across a mountain canyon. The cable can support proportionally heavier package weights at lower elevations, with a package weight in excess of 50,000 pounds for the regulatory defined, hypothetical accident condition 30-foot free drop test. The "unyielding" target consists of a highly reinforced, armor steel plated concrete block as illustrated in Figure 2.10.3-1. The target is designed to accommodate test packages weighing up to 100 tons.

In accordance with the requirements of 10 CFR §71.73(c)(3), the puncture bar was fabricated from solid, 6.0-inch diameter mild steel, and of sufficient length to perform the necessary test. The puncture bar was welded perpendicularly to a 1½-inch thick, mild steel plate having an outside

diameter of approximately 24 inches. The top edge of the puncture bar was finished to a 1/4-inch radius. When utilized, the puncture bar was securely welded (mounted) to the impact surface.

Fire testing of the TRUPACT-II package prototype test unit was performed at Sandia National Laboratories' Lurance Canyon Burn Site in Albuquerque, New Mexico. The open pool fire facility can be adjusted to a maximum size of 30-by-60 feet for performing free-burning fires for a duration of 2 hours, maximum. Packages weighing up to 149 tons can be supported at heights up to a few meters above the pool surface. During fire testing, thermocouples and calorimeters that are strategically placed measure and record fire temperatures and heat flux, respectively.

#### **2.10.3.4 Description of the Certification Test Units**

Three prototypic TRUPACT-II packages were built for certification testing, using prototypic fabrication processes and inspection techniques. Each CTU was built according to the design requirements delineated in Appendix 1.3.1, *Packaging General Arrangement Drawings*, with additions, omissions, differences from the general arrangement drawing requirements, measured as-built configurations, and selection of component options are described as follows. Payload representation is also described.

##### **2.10.3.4.1 Additions, Omissions, Differences from Drawing Requirements, As-Built Configurations, and Component Options**

###### **2.10.3.4.1.1 Additions**

- Painted external reference grid for photographic documentation; red for CTU-1, blue for CTU-2, and orange for CTU-3.
- External lifting devices for lifting and handling during certification testing.
- Internal lifting cables for lifting and handling the payload within the ICV.
- Secondary test vent port located circumferentially 180° from the prototypic vent port.
- Thermocouples (16 internal and 10 external for CTU-1, 8 internal and 8 external for CTU-2, and 5 internal for CTU-3).
- Temperature indicating labels.
- Axial-only accelerometers (two for CTU-2, and four for CTU-3).
- Remote pressurization port through the OCA/OCV/ICV bottom (see Figure 2.10.3-2)

###### **2.10.3.4.1.2 Omissions**

- Tapered lead-ins on the OCV and ICV upper seal flanges.
- Tamper-indicating devices.
- Warning/informational stenciling.
- OCV and ICV lock ring stop plates.
- OCA lid lift pocket fiberglass guide tubes (removed for tests 1 and 2 on CTU-1; removed for all tests on CTU-3).
- ICV lid lift pin diameter reduction grooves.
- Nameplates.

### 2.10.3.4.1.3 Differences from Drawing Requirements

- The OCV was fabricated to the requirements of the ASME Boiler and Pressure Vessel Code, Section III, Division 1, Subsection NB (rather than Subsection NF).
- The relative locations of the OCA seal test port, vent port, and locking ring joint are different than delineated in Appendix 1.3.1, *Packaging General Arrangement Drawings*; fabrication of the CTUs occurred before operational considerations defined the final locations.
- The relative locations of the OCA lid lifting pockets are different than delineated in Appendix 1.3.1, *Packaging General Arrangement Drawings*; fabrication of the CTUs occurred before operational considerations defined the final locations.
- A 10-inch inside diameter (rather than a 3-inch inside diameter) was used for the silicone wear pad to prevent interference with the bottom test pressurization port.
- A 10-inch width (rather than the optional 18-inch width) was used for the neoprene weather seal for CTU-1.
- The OCV locking Z-flange was secured to the OCV lock ring via 24 (rather than 36), 1/4-20 UNC screws.
- The thickness of the ceramic fiber industrial textile (woven tape) between the upper/lower Z-flanges and the locking Z-flange was 1/4 inch thick (rather than 1/8 inch thick) for CTU-1 and CTU-2.
- The OCV lock bolt attachments in the OCA outer shell used inset Rivnuts with a 0.34-inch lock bolt thread engagement (rather than internal thread inserts inside cylindrical blocks with a 0.59-inch lock bolt thread engagement).
- The OCA lid top centerline thickness was 12½ inches (rather than 12¼ inches).
- The OCA body bottom centerline thickness was 9½ inches (rather than 9¼ inches).
- The outer thermal shield is located 3/8 inch above the location shown in Appendix 1.3.1, *Packaging General Arrangement Drawings*; the outer thermal shield was located 3/8 inch downward to enhance interchangeability of lids and bodies between different TRUPACT-II packages; a 3/4-inch × 10½-inch relief, not present in the CTUs, was added along the bottom edge of the outer thermal shield for OCA vent port tool clearance.
- The ICV vent port configuration included a polyurethane filter in the inner vent port plug to facilitate post-test helium leak testing (rather than a solid inner vent port plug).
- An ICV wiper O-ring seal and holder were not included for CTU-1 or CTU-2.
- ICV lid guide plates were used to facilitate assembly for CTU-1 and CTU-2; the addition of the ICV wiper O-ring seal configuration eliminated the need for the ICV lid guide plates.
- Some detailed dimensions for the tie-down lugs are slightly different from those delineated in Appendix 1.3.1, *Packaging General Arrangement Drawings*; fabrication of the CTUs occurred before operational considerations defined the final dimensions.
- The cross-sectional diameter of the lower main ICV and OCV O-ring seals was 0.393 inches and the material was butyl rubber (rather than a cross-section diameter of 0.375 inches and a material of either neoprene or ethylene propylene); these are non-containment seals.
- The CTUs were fabricated with a minimum main containment O-ring seal compression of 15%, whereas a minimum main containment O-ring seal compression of 10.73% is attainable by the dimensions delineated in Appendix 1.3.1, *Packaging General Arrangement Drawings*.

Additional bench testing was performed after fabrication and testing of the CTUs that demonstrated the acceptability of the lower compression.

- The maximum reinforcement for the OCA external welds was 1/32 inch for the CTUs; a maximum reinforcement of 3/32 inch is delineated in Appendix 1.3.1, *Packaging General Arrangement Drawings*.
- The CTUs used an ICV silicone sponge debris shield with a nominally 1/4-inch thickness; a minimum 1/8-inch thickness is delineated in Appendix 1.3.1, *Packaging General Arrangement Drawings*.
- Some detailed dimensions for the recesses in the ICV and OCV seal test port plugs, ICV inner and outer vent port plugs, and the ICV vent port cover are slightly different from those delineated in Appendix 1.3.1, *Packaging General Arrangement Drawings*.
- Some detailed dimensions for the OCV seal flanges, locking ring, and OCV upper main O-ring seal are slightly different from those delineated in Appendix 1.3.1, *Packaging General Arrangement Drawings*.

### 2.10.3.4.1.4 As-Built Measurements

#### 2.10.3.4.1.4.1 Component Weights

The following table summarizes the major component weights for the three CTUs, and includes the calculated weights from Section 2.2, *Weights and Centers of Gravity*, for comparison:

Packaging Component	CTU-1	CTU-2	CTU-3	Calculated
<b>Empty Package:</b>				
• ICV Lid (without Spacer)	750	890	760	795
• ICV Body (without Spacer)	1,650	1,718	1,620	1,625
• ICV Upper Honeycomb Spacer	105	83	95	100
• ICV Lower Honeycomb Spacer	109	82	95	100
• OCA Lid	3,550	3,600	3,466	3,600
• OCA Body	5,900	5,800	5,730	5,765
• <i>Total</i>	12,064	12,173	11,766	11,985
<b>Payload:</b>				
• Drums	7,000	7,000	7,000	6,915
• Pallet	156	130	187	200
• Guide Tubes	20	21	20	20
• Slipsheets, Plates, and Cables	139	118	108	130
• <i>Total</i>	7,315	7,269	7,375 <sup>ⓐ</sup>	7,265
<b>Package Total:</b>				
• Summing Above Components	19,379	19,442	19,141	19,250
• Truck Scale	19,360	19,260	---	---

Notes:

- ⓐ Assembled payload weight using a Sandia National Laboratory load cell, and does not equal the sum of the individual components.

#### 2.10.3.4.1.4.2 Polyurethane Foam Properties

The average parallel-to-rise and perpendicular-to-rise compressive strengths for the polyurethane foam in the OCA lids and bodies, including the nominal  $\pm 15\%$  limits that are defined in Table 8.1-1 from Section 8.1.4.1, *Polyurethane Foam*, are summarized in the following table:

Compressive Strength (psi)	Parallel-to-Rise at Strain, $\epsilon_{\parallel}$			Perpendicular-to-Rise at Strain, $\epsilon_{\perp}$		
	$\epsilon=10\%$	$\epsilon=40\%$	$\epsilon=70\%$	$\epsilon=10\%$	$\epsilon=40\%$	$\epsilon=70\%$
<i>Nominal +15%</i>	270	311	782	224	270	771
• CTU-1, Lid	231	266	667	190	234	667
• CTU-1, Body	233	267	674	194	239	670
• CTU-2, Lid	249	289	739	214	265	745
• CTU-2, Body	242	276	709	207	254	716
• CTU-3, Lid	222	258	666	194	237	678
• CTU-3, Body	230	261	673	201	245	676
<i>Nominal -15%</i>	200	230	578	166	200	570

In addition to the polyurethane foam compressive strength properties, the measured thicknesses of the OCA, including the minimum and maximum thicknesses specified in Appendix 1.3.1, *Packaging General Arrangement Drawings*, are summarized in the following table:

Polyurethane Foam Thickness (inches)	OCA Lid		OCA Body	
	Top	Side	Side	Bottom
Maximum Thickness	12 $\frac{7}{8}$	9 $\frac{3}{16}$	11	10
CTUs	12 $\frac{1}{2}$	8 $\frac{3}{4}$	10 $\frac{1}{16}$	9 $\frac{1}{2}$
Minimum Thickness	11 $\frac{5}{8}$	8 $\frac{5}{16}$	9 $\frac{7}{8}$	8 $\frac{1}{2}$

#### 2.10.3.4.1.4.3 Upper Main O-ring Seal Compression (Containment)

The range of percent compression in the upper main O-ring seals is calculated via a set of direct measurements (O-ring seal cross-section, O-ring seal inside diameter, upper groove depth, upper groove inside diameter, and initial perpendicular gap between the lower and upper seal flanges at the upper groove). The following table summarizes the maximum and minimum percent O-ring compression for a "production" package based on the dimensions specified in Appendix 1.3.1, *Packaging General Arrangement Drawings*, and measurements taken for each CTU:

Percent O-ring Compression	Production		CTU-1		CTU-2		CTU-3	
	ICV	OCV	ICV	OCV	ICV	OCV	ICV	OCV
Maximum	31.5	31.5	18.0	17.5	17.1	18.0	18.3	17.5
Minimum	16.8	16.8	13.6	14.1	12.8	15.3	12.6	13.6

#### 2.10.3.4.1.5 Component Options

- Z-flanges may be a welded construction of discs and cylinders or a spun construction; CTU-1 and CTU-2 used the welded option whereas CTU-3 used the spun option.
- Upper seal flanges, lower seal flanges, and locking rings may be fabricated using rolled and welded plate, forgings, or castings; all CTUs used the rolled and welded plate option.
- Attachment of the inner thermal shield to the locking Z-flange may be via pop rivets or spot welds; CTU-1 used the rivet option whereas CTU-2 and CTU-3 used the spot weld option.
- Vacuum grease may be applied to the seal flanges as well as the O-ring seals; only the O-ring seals were greased for CTU-1, whereas CTU-2 and CTU-3 used grease on the seal flanges as well.
- Vacuum grease may be applied to the vent port plug O-ring seals and covers; the CTU vent port plug O-ring seals and covers were greased.
- The upper inside taper on the ICV lower seal flange may have a length of 2.0 or 2.2 inches; all CTUs used a length of 2.0 inches.
- The wiper O-ring seal holder may be integrated into the ICV upper seal flange or fabricated from rolled sheet metal and attached with drive screws; CTU-3 used the rolled sheet metal/drive screw option.
- The 55-gallon drums used in the payload representation may be steel banded or wrapped with stretch plastic; all CTUs used the steel banding option.
- The 14-gauge aluminum sheet used for the aluminum honeycomb spacer assembly may be fabricated using a single sheet or two sheets with a full-penetration weld; all CTU spacers used a single sheet.
- The OCA outer shell welds may be inspected on the final pass using the liquid penetrant method; all CTU outer shell welds were inspected using the radiograph method.
- The exposed surfaces of the OCA may be unpainted or painted with a low-halogen paint; with the exception of painting colored reference grids, all CTUs were unpainted.
- Ceramic fiber paper is used on the inner surfaces of the OCA and OCV; all CTUs used Lytherm ceramic fiber paper.
- The wear pad may be plain or self-adhesive for securing to the bottom of the lower OCV torispherical head; all CTU wear pads were adhered to the lower OCV torispherical head.
- The maximum reinforcement for the OCA shell welds is 3/32 inch; the maximum reinforcement for the OCA shell welds for all CTUs was 1/32 inch.
- The ICV and OCV locking rings may be unplated or electroless nickel plated; all CTU locking rings were unplated.
- The ICV upper and lower spacer assembly bracket configurations may be a cantilever bracket or angle section; all CTUs used cantilever brackets.
- The insulating material for OCV vent and seal test port access plugs may be fabricated using polyurethane foam or ceramic fiber material; all CTUs used polyurethane foam plugs.
- The round tubing for the OCA lid lifting covers may be equivalent material to fiberglass; all CTUs used round fiberglass tubing.
- The OCA fire consumable vent plugs may use any plastic material; all CTUs used ABS plastic plugs.

- The OCA thread inserts may use an equivalent to Tridair inserts; all CTUs used Tridair KeenSerts.
- Generic polymer may be used for the optional OCV containment (now confinement), test, and OCV vent port plug O-ring seals; all CTUs utilized butyl rubber for these seals.
- Butyl, neoprene, or ethylene propylene elastomers may be used for the ICV inner vent port plug O-ring seal, and the ICV seal test port plug O-ring seal; all CTUs used butyl rubber for these seals.
- Generic polymer may be used for the optional OCV vent port plug and cover handling O-ring seals, the OCV vent port cover O-ring seal, and the OCV seal test port plug O-ring seal; all CTUs used butyl rubber for these seals.
- The OCA lock bolts may use either the OCA or OCA/ICV lock bolt configuration; all CTUs used the OCA lock bolt configuration.
- The material for the ICV inner and outer vent port plugs and cover may be ASTM B10 or B16 brass; all CTUs used ASTM B10 brass for the ICV inner and outer vent port plugs and cover.
- The ICV vent port insert has an optional configuration; all CTUs used the non-optional ICV vent port insert.
- The OCV and ICV seal test port inserts may be a threaded or slip-in configuration; all CTUs used the threaded configuration for the OCV and ICV seal test port inserts.
- Generic polymer may be used for the optional OCV guide plates; all CTUs used stainless steel for these plates.
- Aluminum honeycomb spacers may be constructed with one or two top sheet layers of aluminum; all CTUs used one top sheet layer.

#### **2.10.3.4.2 Payload Representation**

Payloads for the all CTUs are essentially identical. Fourteen concrete filled 55-gallon drums are used to represent the worst-case payload configuration since they place the highest concentrated loading on the ICV. For conservatism, a 12-inch diameter tube was centered within each drum and the annulus filled with concrete to a weight near, but not over 500 pounds. Sand-filled bags were used to provide the remaining weight for precisely meeting the weight limit of 500 pounds. Figure 2.10.3-3 illustrates the payload representation.

In addition to the 500-pound 55-gallon drums, approximately nine (9) pounds of Portland cement and sand were added to the ICV cavity to represent loose debris that could move freely within the ICV and contaminate the sealing regions.

#### **2.10.3.5 Technical Basis for Tests**

The following sections supply the technical basis for the chosen test orientations and sequences for the TRUPACT-II CTUs as presented in Section 2.10.3.6, *Test Sequence for Selected Free Drop, Puncture Drop, and Fire Tests*.

### 2.10.3.5.1 Initial Test Conditions

#### 2.10.3.5.1.1 Internal Pressure

The maximum normal operating pressure as well as the design pressure for both the ICV and the OCV is 50 psig. This pressure corresponds to a normal operating average ICV air temperature of 148 °F (from Table 3.1-1 in Section 3.1, *Discussion*). Because of a constant internal volume, the corresponding pressure at -20 °F is 33 psig, as found using Ideal Gas Law equations as follows:

$$P_{-20} = (50 + 12) \left( \frac{-20 + 460}{148 + 460} \right) = 45 \text{ psia} = 33 \text{ psig}$$

where the ambient pressure at the Sandia National Laboratory test site is 12 psia.

For drop test purposes, pressurizing the ICV to its maximum pressure consistent with the temperature selected for the particular drop is reasonable. The OCV may be either unpressurized or pressurized to its maximum design pressure consistent with the temperature selected for the drop. Note that with the exception of a slight pressure change associated with normal heat-up of the ICV/OCV annulus air or due to barometric changes, an unpressurized OCV is the expected condition during transport since the OCV can only become pressurized if the ICV fails. By pressurizing the OCV in some tests and not in others, pressure can be eliminated as a primary factor in demonstrating the package's ability to meet the applicable regulatory performance requirements. This conclusion is proven by showing that at the instant of impact, pressures within the vessels only increase by a few psig and immediately return to their initial values, and subsequent leak testing demonstrated containment integrity.

#### 2.10.3.5.1.2 Temperature

In general, higher temperatures result in greater deformations and lesser acceleration loads than lower temperatures. This result is due primarily to the temperature sensitivity of the energy absorbing polyurethane foam used within the TRUPACT-II OCA. Linearly interpolating the polyurethane foam data shown in Section 2.6, *Normal Conditions of Transport*, the compressive strength at -20 °F is approximately 40% greater than the compressive strength at 70 °F, and the compressive strength at 160 °F is approximately 25% less than the compressive strength at 70 °F. The strength of the Type 304 stainless steel used in the TRUPACT-II packaging similarly varies as a function of temperature, but to a much lesser extent (e.g., yield strength decreases from 30,000 psi at 70 °F to 27,000 psi at 160 °F, per Table 2.3-1 in Section 2.3.1, *Mechanical Properties Applied to Analytic Evaluations*). Thus, for drop orientations where stresses in structural steel members are of concern (e.g., containment shell buckling), the worst-case temperature is -20 °F, since this temperature results in the greatest ratio of the impact induced acceleration load-to-steel strength.

In contrast, for drop orientations where deformations are of concern, a higher temperature would result in a worst-case condition. Free drop tests at maximum temperatures are not necessary; parametric analyses<sup>2</sup> demonstrate an increase in polyurethane foam permanent deformation of 1/2 inches to 1 1/8 inches, depending on the particular orientation. For this reason, free and puncture drops are performed at the prevailing ambient temperature at the time of the test.

### 2.10.3.5.2 Free Drop Tests

Properly selecting a worst-case TRUPACT-II package orientation for the 30-foot free drop event requires investigating parameters that may compromise package integrity. For the TRUPACT-II packaging design, the primary regulatory requirement is demonstration of containment integrity (i.e., the containment boundary remaining leaktight).

For the 30-foot free drop event, leaktightness of the O-ring seals may be compromised due to mechanical degradation caused by relative movement of the sealing surfaces (resulting in reduced O-ring seal compression), or thermal degradation of the butyl rubber material from the hypothetical accident condition fire event. Importantly, for mechanical or thermal degradation to occur, significant reduction in polyurethane foam thickness or significant direct exposure of the polyurethane foam to the fire would have to occur in the vicinity of the O-ring seals due to a 30-foot free drop event.

Another possibility is separation of the OCA lid from the OCA body (or significantly opening up the nominal 1/2-inch gap that exists between the upper and lower Z-flanges at the OCA lid-to-body interface), and buckling of the ICV or OCV in a bottom end drop orientation. Separation of the OCA lid from the OCA body is most likely to occur from a drop that imposes a significant lateral load on the knuckle portion of the OCA exterior torispherical head. Therefore, free drop testing includes impact orientations that affect the upper end of the package in general and the seal/closure area in particular. Loads and resultant deformations occurring over the lower half of the package do not present a worst-case regarding separation of the OCA lid from the OCA body.

As discussed earlier, a bottom end drop orientation is of interest because of the possibility of containment shell buckling due to the high acceleration forces imparted to the package in this orientation. These potential failure modes are worst when the ratio of applied load-to-steel strength is at its maximum value. Therefore, these free drop cases will be the worst-case if performed at cold temperatures.

### 2.10.3.5.3 Puncture Drop Tests

Properly selecting a worst-case TRUPACT-II package orientation for the puncture drop event requires investigating parameters that may compromise package integrity. For the TRUPACT-II packaging design, the primary regulatory requirement is demonstration of containment integrity (i.e., the containment boundary remaining leaktight).

For the puncture drop event, leaktightness of the O-ring seals may be compromised due to mechanical degradation caused by relative movement of the sealing surfaces (resulting in reduced O-ring seal compression), gross deformations of the sealing region, or thermal degradation of the butyl rubber material from the hypothetical accident condition fire event. Importantly, for mechanical degradation to occur, the puncture event would require gross rupturing of the OCA outer shell near the O-ring seals, thereby allowing the puncture bar to impact directly on the OCV seal flanges or locking ring. Similarly, for thermal degradation to occur, the puncture event would require gross rupturing of the OCA outer shell near the O-ring seals, thereby allowing direct flame impingement on the underlying polyurethane foam. For these reasons, puncture events are mostly directed at the seal regions.

Another possibility is the puncture bar penetrating the OCA outer shell and breaching the OCV containment boundary in a region removed from the seal regions. Based on the results of 1/2-

and 3/4-scale design development testing and the full-scale engineering development testing, the puncture events most likely to lead to a penetration of the OCA exterior shell are those that have the package center of gravity directly above the puncture bar and, importantly, have the surface of the package at the point of contact with the puncture bar at an oblique angle with respect to the puncture bar. Specifically, if the impacting package surface is at an angle equal to or greater than approximately 20° relative to the top horizontal surface of the puncture bar, penetration is much more likely than if the package surface is normal to the axis of the puncture bar. The following table summarizes observations from the aforementioned development test programs. These results tested the package with the center of gravity directly over the puncture bar. If the center of gravity is not directly over the puncture bar, penetration becomes less likely since some of the available impact energy is transformed into rotational kinetic energy.

Full Scale Shell Thickness (in)	Orientation Relative to Puncture Bar	
	0° (normal)	≥20°
3/16	no penetration	penetration
1/4	no penetration	penetration
3/8	no penetration	no penetration

Observations from testing concluded that impacting the puncture bar with the package surface normal to the axis of the puncture bar will not lead to penetration of the OCA exterior shell. This was the primary reason for utilizing a torispherical (dished) upper head for the OCA lid. With a dished head, orientations with the package center of gravity directly over the puncture bar tend to be such that the package surface is also normal to the axis of the bar. Furthermore, observations concluded that a 3/8-inch thick shell could not be penetrated by the puncture bar, even under the worst-case conditions described earlier. Thus, 3/8-inch thick material was selected for use adjacent to the OCA closure joint (sealing regions) and as backup to the OCA vent and seal test ports to prevent puncture bar encroachment under all conditions.

Puncture drop tests were also selected to investigate regions containing stiffness discontinuities: 1/4- to-3/8-inch outer shell transitions, vent port and seal test port penetrations, and the forklift pocket structure. Finally, discontinuities in the OCA outer shell such as at the lid-to-body interface were tested to firmly establish the puncture resistant capability of that region.

Puncture drop events that do not significantly penetrate the OCA outer shell to expose significant amounts of foam are not of concern as packaging deformations and resultant acceleration loads associated with these events will be much less significant than the deformations and acceleration loads associated with the preceding 30-foot free drop tests. Additionally, differing temperatures and pressures during puncture drop testing will not significantly affect performance of the package. For this reason, although a variety of initial pressure conditions were included in the drop sequences, all puncture tests were performed at the prevailing ambient temperature.

#### 2.10.3.5.4 Fire Test

At the conclusion of free drop and puncture drop testing, the CTU-1 and CTU-2 were subjected to a fully engulfing pool fire test in accordance with 10 CFR §71.73(c)(4). The package was oriented horizontally in the flames and minimally supported to least impede the heat flow into

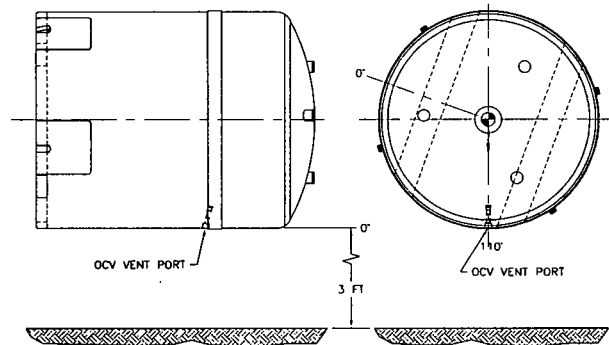
the package. The combined worst-case damage due to the drop tests was located in the hottest portion of the fire, i.e., 1½ meters above the fuel surface and 1/2 meter above the lowest part of the package<sup>4</sup>. Prior to fire testing, each CTU was preheated to the worst-case NCT steady-state temperature (i.e., 100 °F still air without insolation).

### 2.10.3.6 Test Sequence for Selected Free Drop, Puncture Drop, and Fire Tests

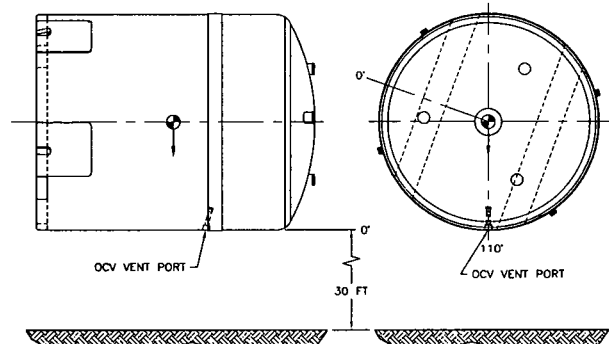
The following sections establish the selected free drop, puncture drop, and fire test sequence for the TRUPACT-II CTUs based on the discussions provided in Section 2.10.3.5, *Technical Basis for Tests*. Test sequences are summarized in Table 2.10.3-2, Table 2.10.3-3, and Table 2.10.3-3, and correspondingly illustrated in Figure 2.10.3-4, Figure 2.10.3-5, and Figure 2.10.3-6, for CTU-1, CTU-2, and CTU-3, respectively.

#### 2.10.3.6.1 Test Sequence for CTU-1

**CTU-1 Free Drop No. 1** is an NCT free drop from a height of 3 feet, impacting horizontally on the CTU side, aligned with the OCV vent port. The 3-foot free drop height is based on the requirements of 10 CFR §71.71(c)(7). The purpose of this test is to demonstrate that the NCT free drop does not compromise the ability of the TRUPACT-II package to successfully sustain subsequent HAC test events in the same or other orientations.

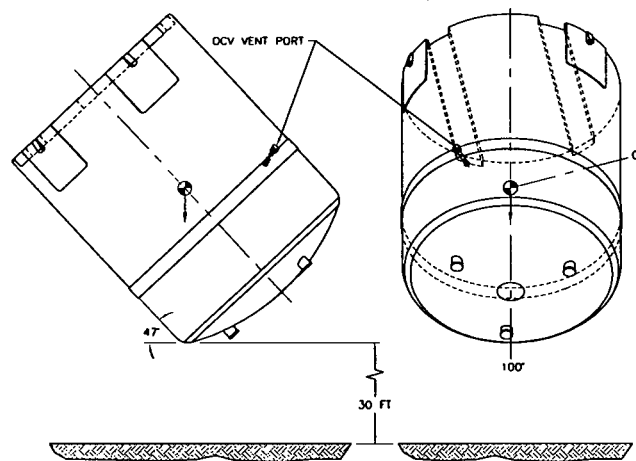


**CTU-1 Free Drop No. 2** is a HAC free drop from a height of 30 feet, impacting horizontally on the CTU side, aligned with the OCV vent port. The 30-foot drop height is based on the requirements of 10 CFR §71.73(c)(1). The purpose of Free Drop Nos. 1 and 2, combined with Puncture Drop Nos. 5, 6, 7, and 8, is to create the greatest possible cumulative damage (i.e., the greatest reduction in foam thickness) in a region punctured through the OCA outer shell.

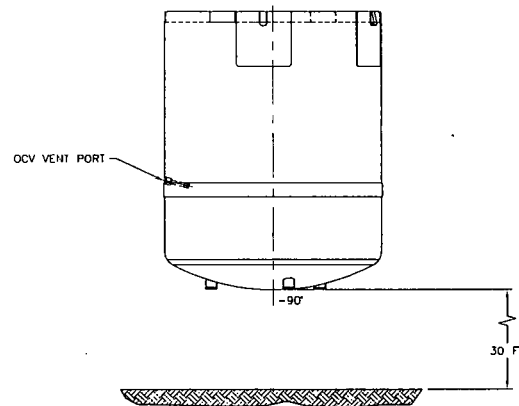


<sup>4</sup> M. E. Schneider and L. A. Kent, *Measurements of Gas Velocities and Temperatures in a Large Open Pool Fire*, Sandia National Laboratories (reprinted from *Heat and Mass Transfer in Fire*, A. K. Kulkarni and Y. Jaluria, Editors, HTD-Vol. 73 (Book No. H00392), American Society of Mechanical Engineers). Figure 3 shows that maximum temperatures occur at an elevation approximately 2.3 meters above the pool floor. The pool was initially filled with water and fuel to a level of 0.814 meters. The maximum temperatures therefore occur approximately 1½ meters above the level of the fuel, i.e., 1/2 meter above the lowest part of the package when set one meter above the fuel source per the requirements of 10 CFR §71.73(c)(4).

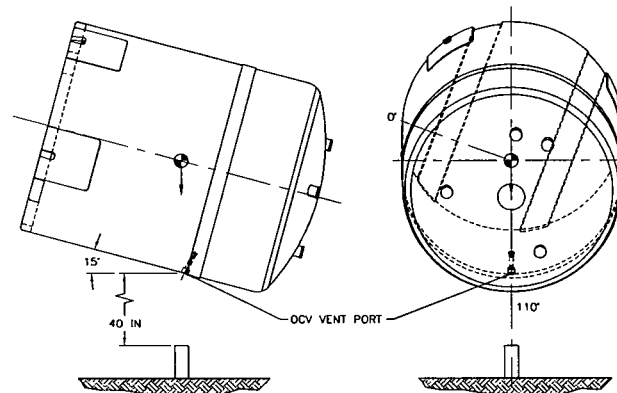
**CTU-1 Free Drop No. 3** is a HAC free drop from a height of 30 feet, impacting near an OCA lid lift pocket and almost opposite the cumulative damage created by Free Drop Nos. 1 and 2, and Puncture Drop Nos. 5, 6, 7, and 8. The 30-foot drop height is based on the requirements of 10 CFR §71.73(c)(1). This drop orientation aligns the centerline of the 55-gallon drums with the point of impact. The purpose of this test is to produce maximum concentrated damage to the OCA lid.



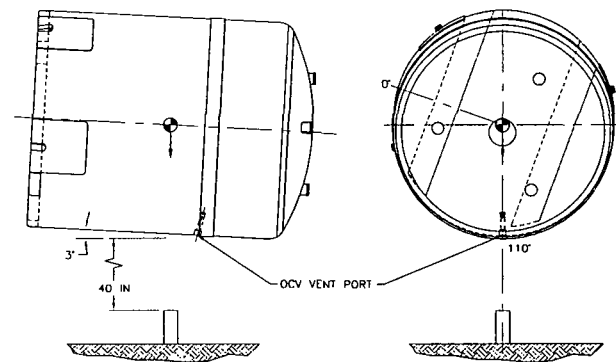
**CTU-1 Free Drop No. 4** is a HAC free drop from a height of 30 feet, impacting vertically on the CTU top. The 30-foot drop height is based on the requirements of 10 CFR §71.73(c)(1). This top-down drop aligns the 55-gallon drums directly over the three lift pockets. The purpose of this test is to create the greatest possible damage (i.e., the greatest reduction in foam thickness) to the OCA lid top, and to drive the OCA lift pocket steel straps inward against the OCV lid's torispherical (i.e., dished) head.



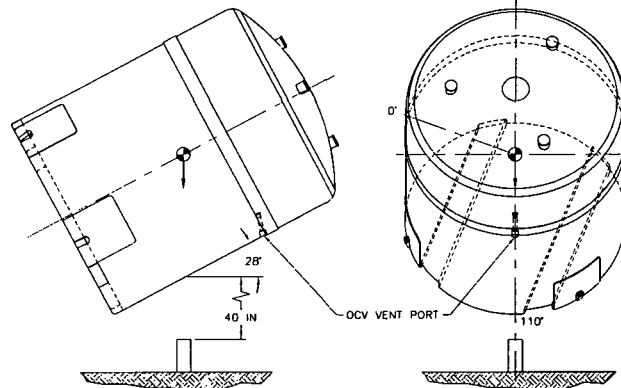
**CTU-1 Puncture Drop No. 5** impacts directly onto the OCV vent port fitting, compounding the cumulative damage created by Free Drop Nos. 1 and 2. The puncture drop height is based on the requirements of 10 CFR §71.73(c)(3). The purpose of this test is to create the greatest cumulative damage (i.e., greatest reduction in foam thickness) over the OCV vent port region. Cumulative testing of this package region demonstrates that containment integrity is maintained.



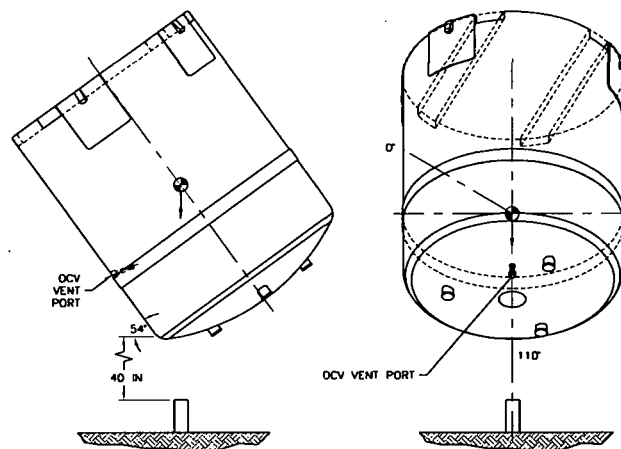
**CTU-1 Puncture Drop No. 6** impacts directly onto the damage created by Free Drop Nos. 1 and 2, and onto the 3/8-to-1/4-inch OCA body's outer shell transition. The puncture drop height is based on the requirements of 10 CFR §71.73(c)(3). The purpose of this test is to penetrate the outer shell. Cumulative testing of this package region demonstrates that containment integrity is maintained.



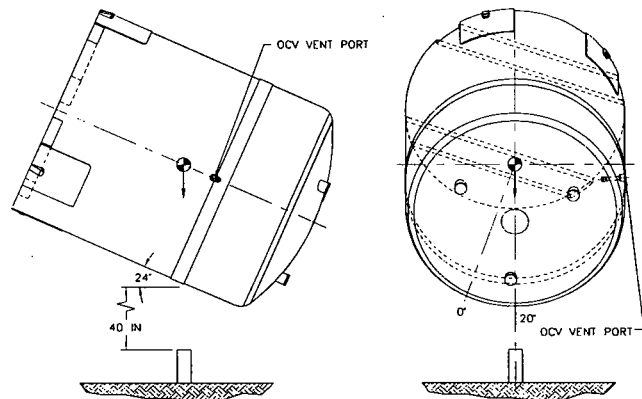
**CTU-1 Puncture Drop No. 7** impacts directly onto the damage created by Free Drop Nos. 1 and 2, at a distance 40 inches above the package bottom. The puncture drop height is based on the requirements of 10 CFR §71.73(c)(3). The purpose of this test is to penetrate the 1/4-inch thick OCA body outer shell; this impact angle will ensure penetration occurs. Cumulative testing of this package region demonstrates that containment integrity is maintained.



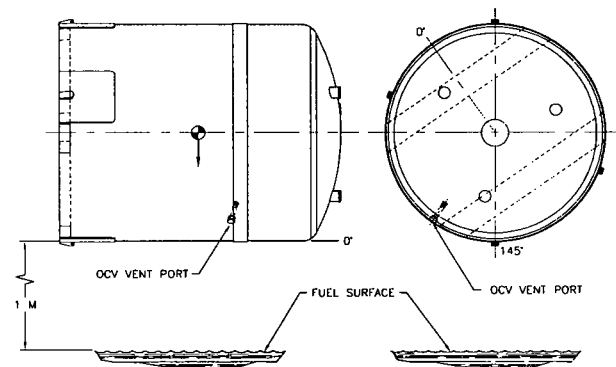
**CTU-1 Puncture Drop No. 8** impacts directly onto the OCA's torispherical (i.e., dished) head, compounding the cumulative damage created by Free Drop Nos. 1 and 2. The puncture drop height is based on the requirements of 10 CFR §71.73(c)(3). The purpose of this test is to penetrate the region most weakened by Free Drop Nos. 1 and 2 (i.e., side drops). Cumulative testing of this package region demonstrates that containment integrity is maintained.



**CTU-1 Puncture Drop No. 9** impacts directly onto the OCV seal test port fitting. The puncture drop height is based on the requirements of 10 CFR §71.73(c)(3). The purpose of this test is to create the greatest cumulative damage (i.e., greatest reduction in foam thickness) over the OCV seal test port region, and to demonstrate reliability of the underlying doubler support structure. Testing of this package region demonstrates that containment integrity is maintained.

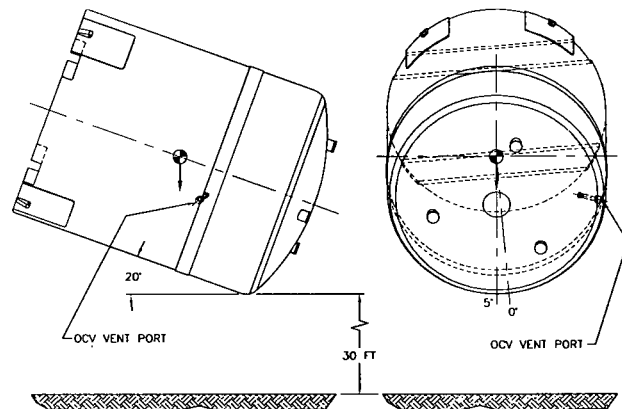


**CTU-1 Fire No. 10** is performed by orienting the cumulative damage from Free Drop Nos. 1 and 2, and Puncture Drop Nos. 5, 6, 7, and 8 at the hottest location in the fire (i.e., 1½ meters above the fuel surface). The purpose of this test is to demonstrate that the reduction in sidewall thickness and puncture drop damage do not inhibit the package's containment integrity.



**2.10.3.6.2 Test Sequence for CTU-2**

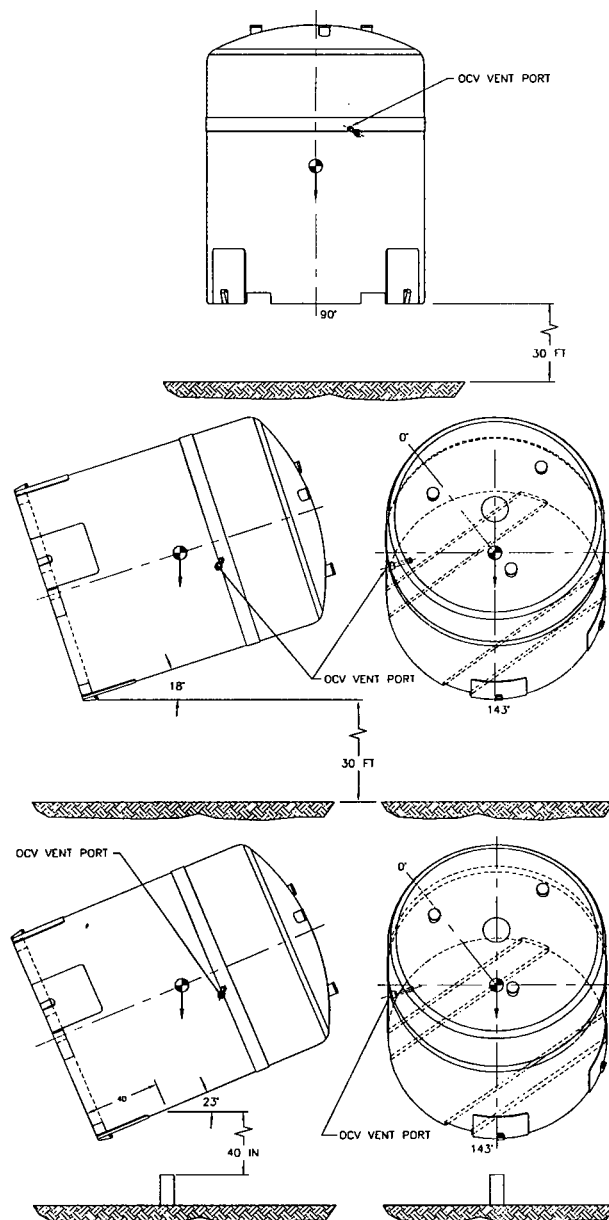
**CTU-2 Free Drop No. 1** is a HAC free drop from a height of 30 feet. This slapdown drop initially impacts on the OCA top knuckle. The 30-foot drop height is based on the requirements of 10 CFR §71.73(c)(1). The impact point is aligned with both the ICV and OCV pinned locking ring joints and underlying 55-gallon drum payload. The purpose of Free Drop No. 1 is to cause the most damage to the locking rings.



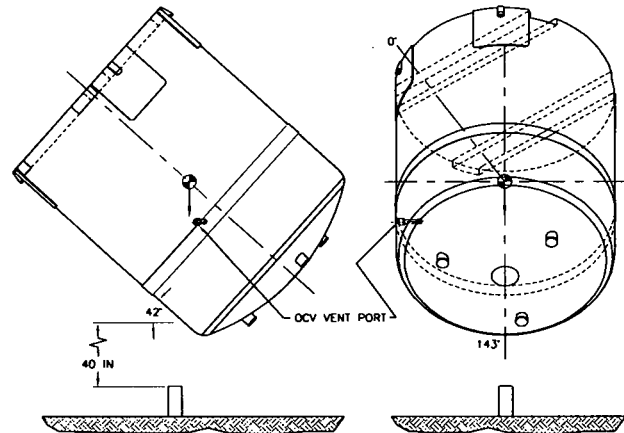
**CTU-2 Free Drop No. 2** is a HAC free drop from a height of 30 feet, impacting vertically on the CTU bottom. The 30-foot drop height is based on the requirements of 10 CFR §71.73(c)(1). The purpose of this test is to create the greatest axial acceleration on the cylindrical containment vessels. This test will demonstrate that both the ICV and OCV cylindrical shells will not buckle or collapse.

**CTU-2 Free Drop No. 3** is a HAC free drop from a height of 30 feet. This slapdown drop initially impacts on the tie-down lug and its relatively rigid underlying structure, with secondary impact on the OCA top knuckle. The 30-foot drop height is based on the requirements of 10 CFR §71.73(c)(1). The purpose of this test is to create the maximum bending moment in the closure region by maximizing the slapdown drop accelerations.

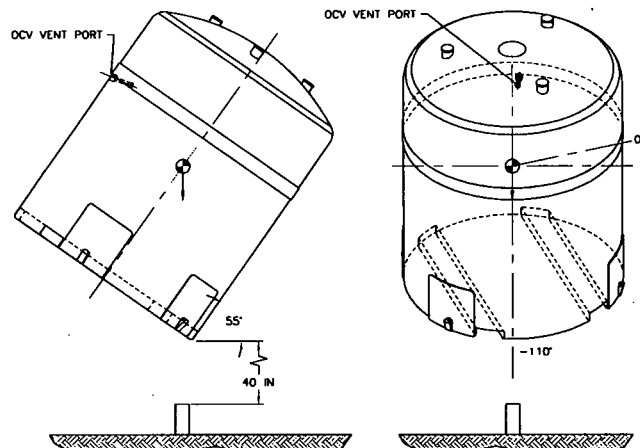
**CTU-2 Puncture Drop No. R** impacts at a distance 40 inches above the package bottom; this puncture drop test repeats Puncture Drop No. 7 on CTU-1. The puncture drop height is based on the requirements of 10 CFR §71.73(c)(3). The purpose of this test is to penetrate the 1/4-inch thick OCA body outer shell; this impact angle will assure that penetration occurs.



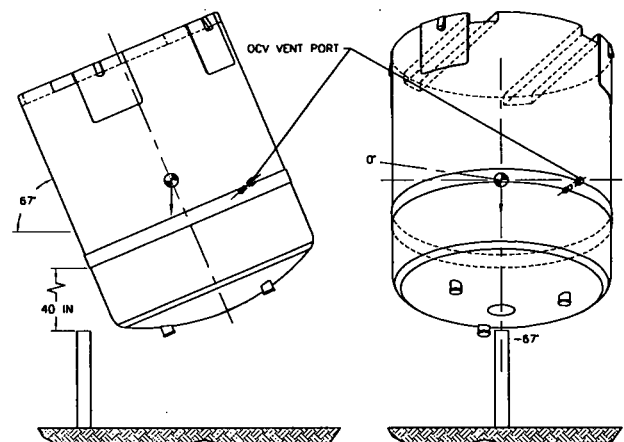
**CTU-2 Puncture Drop No. 4** impacts directly onto the damage created by Free Drop No. 3, and onto the 3/8-to-1/4-inch, OCA lid's outer shell transition. The puncture drop height is based on the requirements of 10 CFR §71.73(c)(3). The purpose of this test is to attempt to penetrate the outer shell at the 3/8-to-1/4-inch transition between the OCA lid cylindrical shell and the relatively stiff upper torispherical (i.e., dished) head's knuckle. Cumulative testing of this package region demonstrates that containment integrity is maintained.



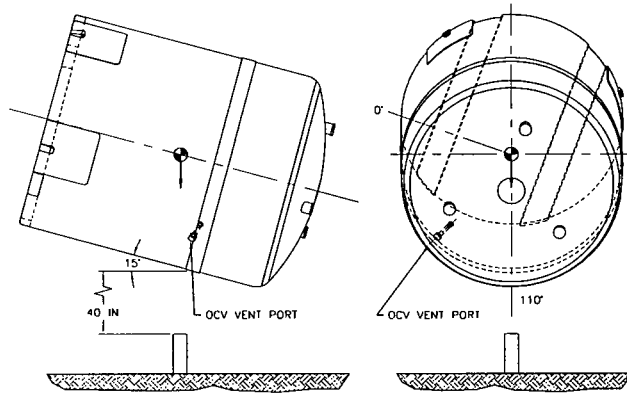
**CTU-2 Puncture Drop No. 5** impacts directly onto the package bottom corner, adjacent to a forklift pocket. The puncture drop height is based on the requirements of 10 CFR §71.73(c)(3). The purpose of this test is to penetrate the 1/4-inch thick OCA flat bottom at a location where structural discontinuities will more easily induce tearing. Should tearing occur, this location could create a possible "chimney" for the HAC fire test by allowing free flow of air from the penetration due to Puncture Drop No. R.



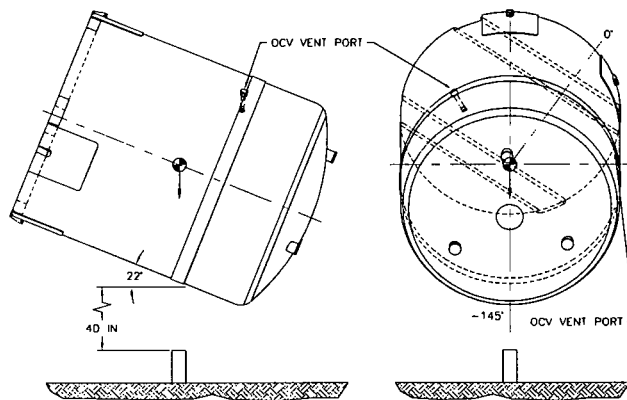
**CTU-2 Puncture Drop No. 6** impacts directly onto the inverted package's OCA lid side, adjacent to the outer thermal shield. The puncture drop height is based on the requirements of 10 CFR §71.73(c)(3). The purpose of this test is to attempt a tearing dislocation of the outer thermal shield by getting the pin to slide into and "snag" the protruding sheet metal. Sufficient removal of the outer thermal shield could expose the OCA closure joint gap to direct flame impingement during the HAC fire test.



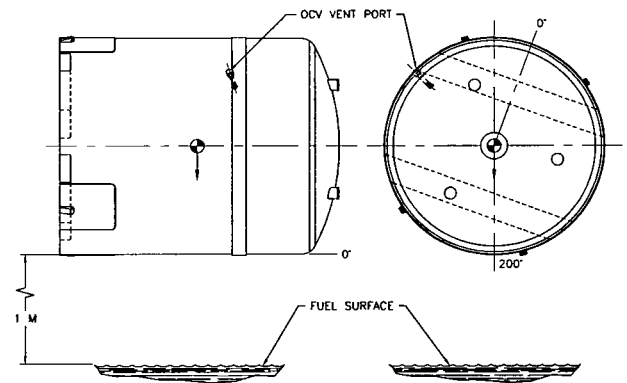
**CTU-2 Puncture Drop No. 7** impacts directly onto the OCA body at the same elevation as the OCV vent port fitting. The puncture drop height is based on the requirements of 10 CFR §71.73(c)(3). The purpose of this test is to demonstrate that the 3/8-inch thick OCA body cylindrical shell adjacent to the closure will not deform inward to the extent that the HAC fire test damages the O-ring seal region.



**CTU-2 Puncture Drop No. 8** impacts directly onto the OCA body at the same elevation as the OCV seal test port fitting. The puncture drop height is based on the requirements of 10 CFR §71.73(c)(3). The purpose of this test is to demonstrate that the 3/8-inch thick OCA lid cylindrical shell adjacent to the closure will not deform inward to the extent that the HAC fire test damages the O-ring seal region.



**CTU-2 Fire No. 9** is performed by orienting the cumulative damage from Free Drop No. 3, and Puncture Drop Nos. 4, R, and 5 at the hottest location in the fire (i.e., 1½ meters above the fuel surface). The purpose of this test is to demonstrate that the reduction in sidewall thickness and puncture drop damage do not inhibit the package's containment integrity.

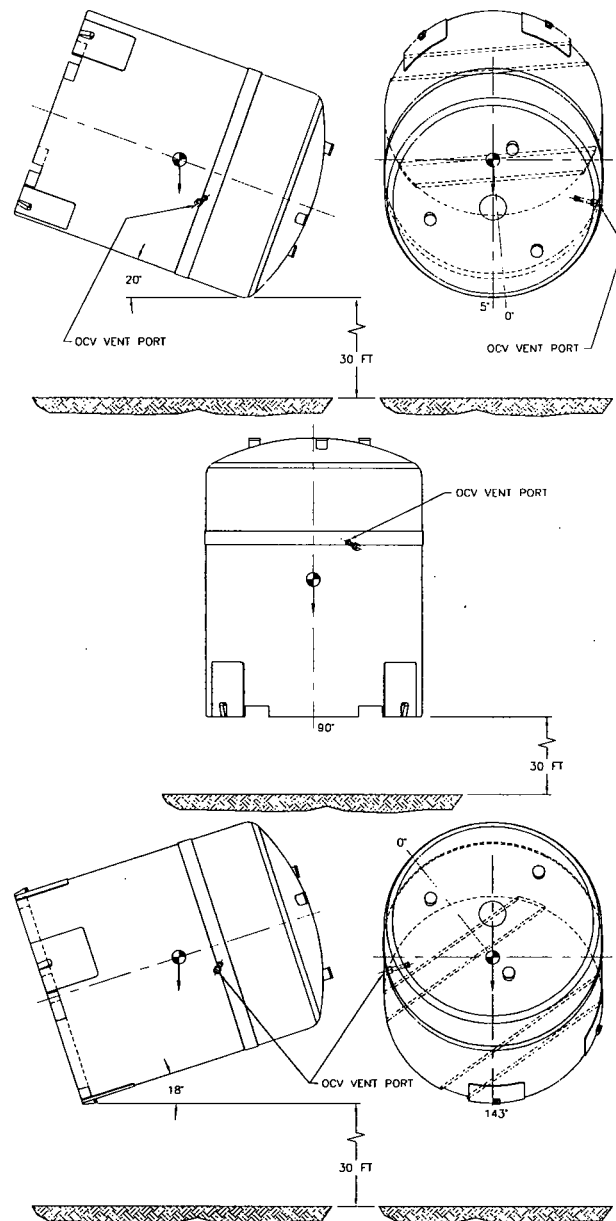


### 2.10.3.6.3 Test Sequence for CTU-3

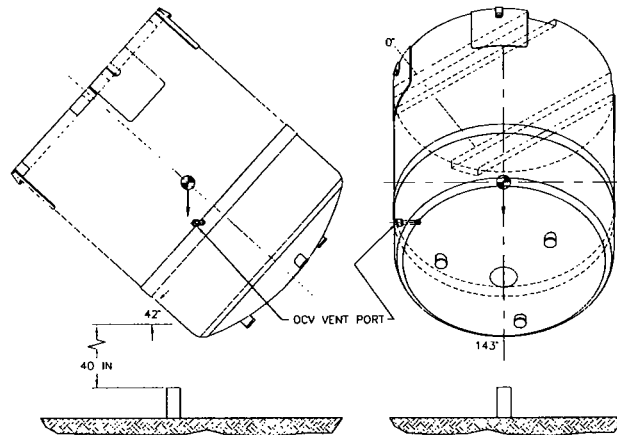
**CTU-3 Free Drop No. 1** is a HAC free drop from a height of 30 feet. This slapdown drop initially impacts on the OCA top knuckle. The 30-foot drop height is based on the requirements of 10 CFR §71.73(c)(1). The impact point is aligned with both the ICV and OCV pinned locking ring joints and underlying 55-gallon drum payload. The purpose of Free Drop No. 1 is to cause the most damage to the locking rings.

**CTU-3 Free Drop No. 2** is a HAC free drop from a height of 30 feet, impacting vertically on the CTU bottom. The 30-foot drop height is based on the requirements of 10 CFR §71.73(c)(1). The purpose of this test is to create the greatest axial acceleration on the cylindrical containment vessels. This test will demonstrate that both the ICV and OCV cylindrical shells will not buckle or collapse.

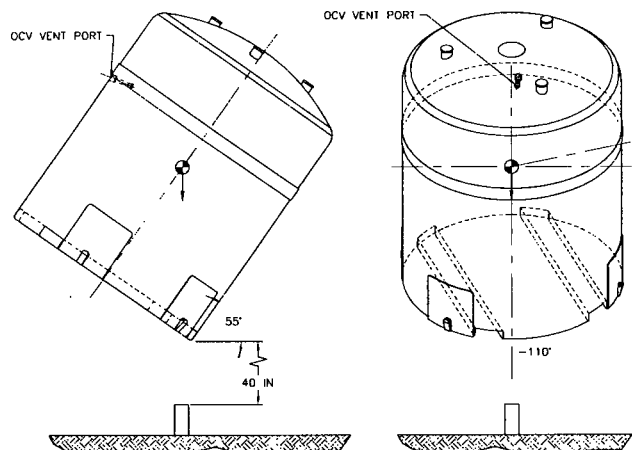
**CTU-3 Free Drop No. 3** is a HAC free drop from a height of 30 feet. This slapdown drop initially impacts on the tie-down lug and its relatively rigid underlying structure, with secondary impact on the OCA top knuckle. The 30-foot drop height is based on the requirements of 10 CFR §71.73(c)(1). The purpose of this test is to create the maximum bending moment in the closure region by maximizing the slapdown drop accelerations.



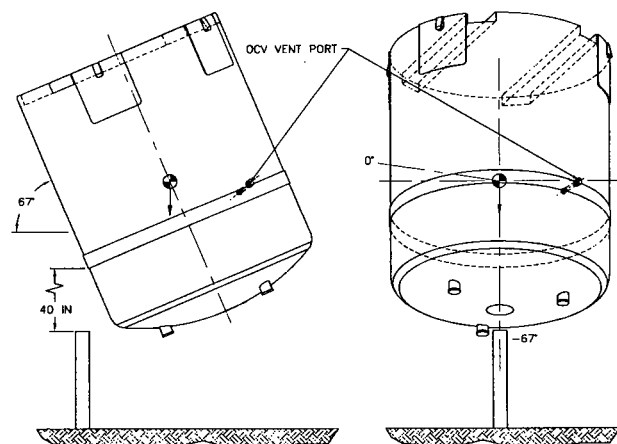
**CTU-3 Puncture Drop No. 4** impacts directly onto the damage created by Free Drop No. 3, and onto the 3/8-to-1/4-inch OCA lid's outer shell transition. The puncture drop height is based on the requirements of 10 CFR §71.73(c)(3). The purpose of this test is to attempt to penetrate the outer shell at the 3/8-to-1/4-inch transition between the OCA lid cylindrical shell and the relatively stiff upper torispherical (i.e., dished) head's knuckle. Cumulative testing of this package region demonstrates that containment integrity is maintained.



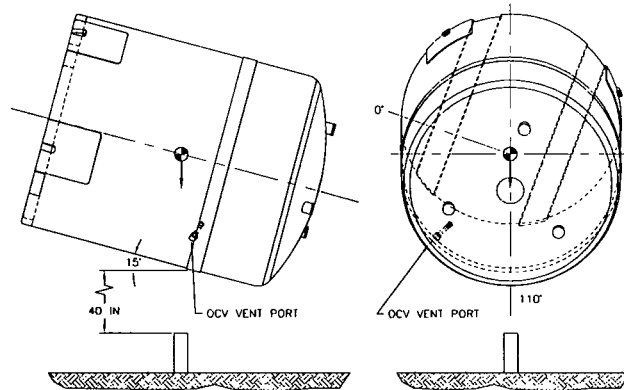
**CTU-3 Puncture Drop No. 5** impacts directly onto the package bottom corner, adjacent to a forklift pocket. The puncture drop height is based on the requirements of 10 CFR §71.73(c)(3). The purpose of this test is to penetrate the 1/4-inch thick OCA flat bottom at a location where structural discontinuities will more easily induce tearing. Should tearing occur, this location could create a possible "chimney" for a subsequent HAC fire test. Alternating the axial impact direction also verifies the effectiveness of the wiper O-ring seal design by attempting to drive more debris into the ICV sealing region.



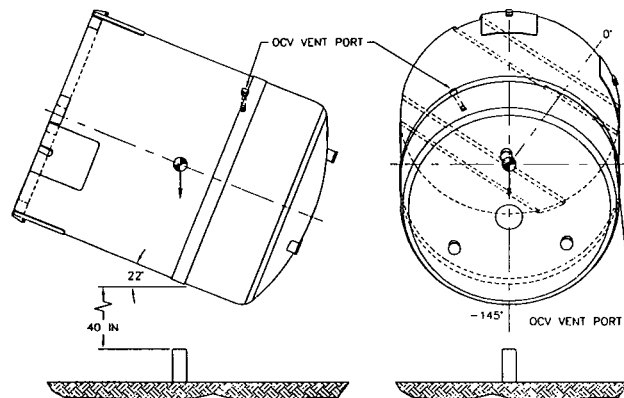
**CTU-3 Puncture Drop No. 6** impacts directly onto the inverted package's OCA lid side, adjacent to the outer thermal shield. The puncture drop height is based on the requirements of 10 CFR §71.73(c)(3). The purpose of this test is to attempt a tearing dislocation of the outer thermal shield by getting the pin to "snag" the protruding sheet metal. Sufficient outer thermal shield damage could expose the closure joint gap to direct flame impingement during the HAC fire test. Alternating the axial impact direction also verifies the effectiveness of the wiper O-ring seal design by attempting to drive more debris into the ICV sealing region.



**CTU-3 Puncture Drop No. 7** impacts directly onto the OCA body at the same elevation as the OCV vent port fitting. The puncture drop height is based on the requirements of 10 CFR §71.73(c)(3). The purpose of this test is to demonstrate that the 3/8-inch thick OCA body cylindrical shell adjacent to the closure will not deform inward to the extent that the HAC fire test damages the O-ring seal region.



**CTU-3 Puncture Drop No. 8** impacts directly onto the OCA body at the same elevation as the OCV seal test port fitting. The puncture drop height is based on the requirements of 10 CFR §71.73(c)(3). The purpose of this test is to demonstrate that the 3/8-inch thick OCA lid cylindrical shell adjacent to the closure will not deform inward to the extent that the HAC fire test damages the O-ring seal region.



### 2.10.3.7 Test Results

The following sections report the results of free drop, puncture drop, and fire tests following the sequence provided in Section 2.10.3.6, *Test Sequence for Selected Free Drop, Puncture Drop, and Fire Tests*. Results are summarized in Table 2.10.3-2, Table 2.10.3-3, and Table 2.10.3-3, and correspondingly illustrated in Figure 2.10.3-4, Figure 2.10.3-5, and Figure 2.10.3-6 for CTU-1, CTU-2, and CTU-3, respectively.

Figure 2.10.3-26 through Figure 2.10.3-53 sequentially photo-document the certification testing process for the CTU-1, Figure 2.10.3-54 through Figure 2.10.3-79 sequentially photo-document the certification testing process for the CTU-2, and Figure 2.10.3-80 through Figure 2.10.3-99 sequentially photo-document the certification testing process for the CTU-3.

#### 2.10.3.7.1 Test Results for CTU-1

##### 2.10.3.7.1.1 CTU-1 Free Drop No. 1

Free Drop No. 1 was an NCT free drop from a height of 3 feet, impacting onto the OCA vent port. As shown in Figure 2.10.3-4, CTU-1 was oriented horizontal to the impact surface (axial angle (i.e., pitch) = 0°), and circumferentially aligned to impact onto the OCA vent port (110° from the forklift pocket reference). At the time of the test, the measured ICV and OCV temperatures were 58 °F and 48 °F, respectively. The test was conducted on 12/04/88.

The measured permanent deformations for CTU-1 were flats 18 inches wide at the top (OCA lid), and 18 inches wide at the bottom (OCA body), each corresponding to a crush depth of approximately 7/8 inches. The ICV and OCV internal pressures did not change.

#### **2.10.3.7.1.2 CTU-1 Free Drop No. 2**

Free Drop No. 2 was a HAC free drop from a height of 30 feet, impacting onto the OCA vent port. As shown in Figure 2.10.3-4, CTU-1 was oriented horizontal to the impact surface (axial angle (i.e., pitch) = 0°), and circumferentially aligned to impact onto the OCA vent port (110° from the forklift pocket reference). At the time of the test, the measured OCV temperature was 53 °F. The test was conducted on 12/04/88.

The measured permanent deformations for CTU-1 were flats 37 inches wide at the top (OCA lid), and 35 inches wide at the bottom (OCA body), corresponding to a crush depth of approximately 3 5/8 inches. The ICV and OCV internal pressures did not change.

#### **2.10.3.7.1.3 CTU-1 Free Drop No. 3**

Free Drop No. 3 was a HAC free drop from a height of 30 feet, impacting onto the CTU lid knuckle near an OCA lid lifting pocket. As shown in Figure 2.10.3-4, CTU-1 was oriented -47° from horizontal (axial angle (i.e., pitch) = 47° top down), and circumferentially aligned to impact nearly opposite the OCA vent port (-100° from the forklift pocket reference). At the time of the test, the measured OCV temperature was 50 °F. The test was conducted on 12/05/88.

The measured permanent deformation for CTU-1 was a flat 30 inches wide and 53 inches long on the OCA lid, corresponding to a crush depth of approximately 3 3/4 inches. The ICV and OCV internal pressures were not measured due to test damage to the pressurization lines.

#### **2.10.3.7.1.4 CTU-1 Free Drop No. 4**

Free Drop No. 4 was a HAC free drop from a height of 30 feet, impacting vertically onto the CTU lid (i.e., top-down orientation), as shown in Figure 2.10.3-4. At the time of the test, the measured OCV temperature was 47 °F. The test was conducted on 12/06/88.

The measured permanent deformation for CTU-1 was a 53-inch diameter flat on the OCA lid, corresponding to a crush depth of approximately 3 7/8 inches. The ICV internal pressure did not change; however, the OCV internal pressure dropped 1.3 psig.

#### **2.10.3.7.1.5 CTU-1 Puncture Drop No. 5**

Puncture Drop No. 5 was a HAC puncture drop from a height of 40 inches, impacting onto the OCA vent port. As shown in Figure 2.10.3-4, CTU-1 was oriented -15° from horizontal (axial angle (i.e., pitch) = 15° top down) through the package's center of gravity, and circumferentially aligned to impact onto the OCA vent port (110° from the forklift pocket reference). At the time of the test, the measured OCV temperature was 32 °F. The test was conducted on 12/07/88.

The measured permanent deformation for CTU-1 was a dent approximately 3 inches deep, and a 16-inch long tear at the shell-to-angle (Z-flange) interface. The ICV and OCV internal pressures did not change.

**2.10.3.7.1.6 CTU-1 Puncture Drop No. 6**

Puncture Drop No. 6 was a HAC puncture drop from a height of 40 inches, impacting onto the OCA body at the 1/4-to-3/8-inch thickness outer shell transition. As shown in Figure 2.10.3-4, CTU-1 was oriented  $-3^\circ$  from horizontal (axial angle (i.e., pitch) =  $3^\circ$  top down) through the package's center of gravity, and circumferentially aligned with the OCA vent port ( $110^\circ$  from the forklift pocket reference). At the time of the test, the measured OCV temperature was  $30^\circ\text{F}$ . The test was conducted on 12/07/88.

The measured permanent deformation for CTU-1 was a dent approximately 3/4 inches deep. The ICV internal pressure did not change; however, the OCV internal pressure dropped 0.3 psig.

**2.10.3.7.1.7 CTU-1 Puncture Drop No. 7**

Puncture Drop No. 7 was a HAC puncture drop from a height of 40 inches, impacting onto the OCA body at a location 40 inches above the package bottom. As shown in Figure 2.10.3-4, CTU-1 was oriented  $28^\circ$  from horizontal (axial angle (i.e., pitch) =  $28^\circ$  top up) through the package's center of gravity, and circumferentially aligned with the OCA vent port ( $110^\circ$  from the forklift pocket reference). At the time of the test, the measured OCV temperature was  $25^\circ\text{F}$ . The test was conducted on 12/08/88.

The measured permanent deformation for CTU-1 was an 8-inch wide, 11-inch long, and 8½-inch deep hole through the OCA outer shell. The ICV and OCV internal pressures did not change.

**2.10.3.7.1.8 CTU-1 Puncture Drop No. 8**

Puncture Drop No. 8 was a HAC puncture drop from a height of 40 inches, impacting onto the OCA lid's knuckle at the location of side drop damage from Free Drop Nos. 1 and 2. As shown in Figure 2.10.3-4, CTU-1 was oriented  $-54^\circ$  from horizontal (axial angle (i.e., pitch) =  $54^\circ$  top down) through the package's center of gravity, and circumferentially aligned with the OCA vent port ( $110^\circ$  from the forklift pocket reference). At the time of the test, the measured OCV temperature was  $37^\circ\text{F}$ . The test was conducted on 12/09/88.

The measured permanent deformation for CTU-1 was some additional denting of the OCA lid's knuckle. The ICV and OCV internal pressures did not change.

**2.10.3.7.1.9 CTU-1 Puncture Drop No. 9**

Puncture Drop No. 9 was a HAC puncture drop from a height of 40 inches, impacting onto the OCA seal test port. As shown in Figure 2.10.3-4, CTU-1 was oriented  $-24^\circ$  from horizontal (axial angle (i.e., pitch) =  $24^\circ$  top down) through the package's center of gravity, and circumferentially aligned with the OCA seal test port ( $20^\circ$  from the forklift pocket reference). At the time of the test, the measured OCV temperature was  $36^\circ\text{F}$ . The test was conducted on 12/10/88.

The measured permanent deformation for CTU-1 was a dent approximately 3 inches deep, and a 7-inch wide tear in the outer thermal shield. The ICV internal pressure did not change; however, the OCV internal pressure dropped 0.5 psig.

### 2.10.3.7.1.10 CTU-1 Fire No. 10

Fire No. 10 was performed to demonstrate packaging compliance with the requirements of 10 CFR §71.73(c)(4) and the guidelines set forth in IAEA Safety Series No. 37<sup>5</sup>. The following list summarizes the test parameters:

- CTU-1 was oriented on an insulated test stand with the most severe damage approximately 1½ meters above the fuel surface. With a circumferential orientation of 145° (see Figure 2.10.3-4), the most severe damage was determined to be from the cumulative effects of Free Drop Nos. 1 and 2, and Puncture Drop Nos. 5 and 7 located 1½ meters above the fuel surface.
- Consistent with 10 CFR §71.73(c)(4), CTU-1 was installed onto an insulated test stand at an elevation to place the lowest part of the package one meter above the fuel surface. CTU-1 was oriented horizontally on the test stand to maximize heat input.
- Consistent with 10 CFR §71.73(c)(4), requiring the test pool to extend 1 to 3 meters beyond the package edges, the test pool size extended approximately 1½ meters beyond each side of CTU-1.
- Consistent with Paragraph A-628.5 of IAEA Safety Series No. 37, requiring wind speeds not to exceed 2 m/s (4.5 mph), the average wind speed was measured to be 1.97 m/s (4.4 mph).
- Consistent with 10 CFR §71.73(c)(4), a JP4-type fuel was used for the fire test, and the amount of fuel was controlled to ensure the fire duration exceeded 30 minutes. The fuel was floated on a pool of water approximately 1/2 meter deep to ensure even distribution during burning. The fire test lasted approximately 32 minutes, and burning continued for approximately 64 minutes after the end of the fire.
- The test pool was instrumented to measure fire temperatures and heat fluxes at various locations around CTU-1. Temperatures were monitored before, during, and following the fire test until magnitudes stabilized back to ambient conditions. The average OCA surface temperature, based on thermocouple traces, was between 1,500 °F and 1,750 °F.
- The CTU-1 containment O-ring seals were leak tested following performance testing to verify containment integrity, as discussed in Section 2.10.3.7.1.12, *CTU-1 Post-Test Disassembly*.
- The average OCV thermocouple pre-heat temperature was 127 °F at the time of the test (compared to the analytically determined HAC initial temperature of 120 °F).
- The test was conducted on 12/14/88.

The maximum ICV seal flange temperature was 170 °F (via temperature indicating labels), and the maximum OCV seal flange temperature was 260 °F (via thermocouples; 250 °F via temperature indicating labels). The temperature indicating label locations and results are provided in Table 2.10.3-4, and Figure 2.10.3-7 and Figure 2.10.3-8. The thermocouple locations are provided in Figure 2.10.3-10, and the results are provided in Figure 2.10.3-12, Figure 2.10.3-13, Figure 2.10.3-14, and Figure 2.10.3-15. The ICV internal pressure increased 1.9 psig, and the OCV internal pressure increased 1.6 psig (see Figure 2.10.3-24).

---

<sup>5</sup> IAEA Safety Series No. 37, *Advisory Material for the IAEA Regulations for the Safe Transport of Radioactive Material (1985 Edition)*, Third Edition (As Amended 1990), International Atomic Energy Agency, Vienna, 1990.

### 2.10.3.7.1.11 CTU-1 Testing Anomalies

As can be expected with any test program, a certain number of test-related anomalies occurred during CTU-1 testing. The following paragraphs summarize each anomaly and its significance.

- The secondary impact from Free Drop No. 3 resulted in the ICV and OCV pressurization lines being cut (however, pressure was maintained throughout the primary impact; post-test re-pressurization of the ICV and OCV demonstrated containment integrity was maintained).
- Pressure rise leak testing of the OCV was planned between each free drop and puncture test; shifting of the OCV relative to the seal leak test port, pump oil contamination (used to pump hot, pre-heat air into the ICV and OCV), and expediting testing were the reasons that pressure rise leak testing was not always performed.
- Puncture Drop No. 7 was not considered a valid test, and was repeated as Puncture Drop No. R on CTU-2; CTU-1 contacted the ground prior to expending all of its kinetic energy on the puncture bar.
- Pressure within the OCV was lost during post-fire test cool-down; the pressure loss was traced to a non-prototypic test gasket (see "FLAT GASKET" in Figure 2.10.3-2).
- During post-test helium leak testing of the ICV, the bottom port to be used for helium injection had frozen closed; a new port was drilled in the ICV lid's torispherical head (in an undamaged region on the crown).

### 2.10.3.7.1.12 CTU-1 Post-Test Disassembly

Post-test disassembly of CTU-1 was performed following Fire No. 10. Both abrasive cutting and gas plasma cutting methods were utilized, depending on their potential effect on subsequent post-test seal testing, to enable destructive disassembly of CTU-1.

Upon removal of the OCA lid and body outer shells, the presence of several inches of very light density foam char showed the intumescent behavior of the polyurethane foam. Except for the local area damaged by the puncture impact 40 inches above the bottom of the OCA body, a layer of unburned polyurethane foam remained around the entire OCV. The average thickness of the layer was approximately 5 to 6 inches along the cylindrical sides and bottom, and 10 inches on top.

Demonstration of containment vessel leaktightness was accomplished by performing helium mass spectrometer leakage rate testing on each containment vessel's main O-ring seal, vent port O-ring seal, and metallic boundary. The main and vent port O-ring seals were tested when cooled to an average measured temperature below -20 °F; the metallic boundary was tested at ambient temperature. Results of successful mass spectrometer helium leakage rate testing are summarized in the following table:

Sealing Component	OCV	ICV
Main O-ring Seal	$<2.0 \times 10^{-8}$ cc/s, helium	$3.0 \times 10^{-8}$ cc/s, helium
Vent Port Plug O-ring Seal	$<2.0 \times 10^{-8}$ cc/s, helium	$6.4 \times 10^{-8}$ cc/s, helium
Metallic Boundary	$2.0 \times 10^{-8}$ cc/s, helium	$7.0 \times 10^{-8}$ cc/s, helium

When accounting for the conversion between air leakage (per ANSI N14.5) and helium leakage, a 2.6 factor applies for standard temperatures and pressures. Thus, a reported helium leakage

rate of  $1.3 \times 10^{-7}$  cc/s, helium, is equivalently  $5 \times 10^{-8}$  cc/s, air, a magnitude well below the "leaktight" criterion of  $1 \times 10^{-7}$  cc/s, air, per ANSI N14.5.

In conclusion, the test series performed on CTU-1 demonstrates the TRUPACT-II package's ability to meet the normal conditions of transport and hypothetical accident conditions regulatory requirements as defined in 10 CFR §71.71 and §71.73, respectively.

### **2.10.3.7.2 Test Results for CTU-2**

#### **2.10.3.7.2.1 CTU-2 Free Drop No. 1**

Free Drop No. 1 was a HAC free drop from a height of 30 feet. The primary impact for this slapdown drop occurred onto the OCA lid knuckle, with the secondary impact onto the OCA body's bottom edge, approximately midway between tie-down lugs. As shown in Figure 2.10.3-5, CTU-2 was oriented  $-20^\circ$  from horizontal (axial angle (i.e., pitch) =  $20^\circ$  top down), and circumferentially aligned to impact the ICV and OCV locking ring pinned joints and coincident payload drums to produce maximum damage ( $-5^\circ$  from the forklift pocket reference). At the time of the test, the measured OCV temperature was  $-26^\circ\text{F}$ . The test was conducted on 01/14/89.

The measured permanent deformations for CTU-2 were flats 45 inches wide at the top (OCA lid), and 21 inches wide at the bottom (OCA body). The OCV internal pressure did not change; however, the ICV internal pressure dropped 0.5 psig, and was most likely due to disconnecting and reconnecting the pressure monitoring device.

#### **2.10.3.7.2.2 CTU-2 Free Drop No. 2**

Free Drop No. 2 was a HAC free drop from a height of 30 feet, impacting vertically onto the CTU bottom, as shown in Figure 2.10.3-5. At the time of the test, the measured OCV temperature was  $-26^\circ\text{F}$ . The test was conducted on 01/16/89.

The permanent deformation for CTU-2 was negligible. The ICV and OCV internal pressures were lost due to damaged pressure test fittings from the free drop test. The maximum axial acceleration was 385 gs (filtered at 500 Hz; see Figure 2.10.3-18 and Figure 2.10.3-19).

#### **2.10.3.7.2.3 CTU-2 Free Drop No. 3**

Free Drop No. 3 was a HAC free drop from a height of 30 feet. The primary impact for this slapdown drop occurred onto a tie-down lug, with the secondary impact onto the OCA lid. As shown in Figure 2.10.3-5, CTU-2 was oriented  $18^\circ$  from horizontal (axial angle (i.e., pitch) =  $18^\circ$  top up), and circumferentially aligned with the tie-down lug ( $143^\circ$  from the forklift pocket reference). The test was conducted on 01/17/89.

The measured permanent deformations for CTU-2 were flats 15 inches wide at the top (OCA lid), and 45 inches wide at the bottom (OCA body). The ICV and OCV internal pressures did not change. The maximum axial acceleration was 44 gs (filtered at 500 Hz; see Figure 2.10.3-20 and Figure 2.10.3-21).

#### **2.10.3.7.2.4 CTU-2 Puncture Drop No. R**

Puncture Drop No. R was a HAC puncture drop from a height of 40 inches, impacting onto the OCA body at a location 40 inches above the package bottom. As shown in Figure 2.10.3-5,

CTU-2 was oriented 23° from horizontal (axial angle (i.e., pitch) = 23° top up) through the package's center of gravity, and circumferentially aligned with the tie-down lug (143° from the forklift pocket reference). The test was conducted on 01/17/89.

The measured permanent deformation for CTU-2 was a 10-inch wide, 11-inch long, and 9-inch deep hole through the OCA outer shell. The ICV and OCV internal pressures did not change.

#### **2.10.3.7.2.5 CTU-2 Puncture Drop No. 4**

Puncture Drop No. 4 was a HAC puncture drop from a height of 40 inches, impacting onto the OCA body at the 1/4-to-3/8-inch thickness outer shell transition. As shown in Figure 2.10.3-5, CTU-2 was oriented -42° from horizontal (axial angle (i.e., pitch) = 42° top down) through the package's center of gravity, and circumferentially aligned with the tie-down lug (143° from the forklift pocket reference). The test was conducted on 01/18/89.

The measured permanent deformation for CTU-2 was an 8-inch wide, 10-inch long, and 7-inch deep hole through the OCA outer shell. The ICV internal pressure did not change; however, the OCV internal pressure dropped 1.0 psig.

#### **2.10.3.7.2.6 CTU-2 Puncture Drop No. 5**

Puncture Drop No. 5 was a HAC puncture drop from a height of 40 inches, impacting onto the OCA bottom edge, adjacent to a forklift pocket. As shown in Figure 2.10.3-5, CTU-2 was oriented 55° from horizontal (axial angle (i.e., pitch) = 55° top up) through the package's center of gravity, and circumferentially -110° from the forklift pocket reference. The test was conducted on 01/19/89.

The measured permanent deformation for CTU-2 was a dent approximately 5 inches deep. The ICV and OCV internal pressures did not change.

#### **2.10.3.7.2.7 CTU-2 Puncture Drop No. 6**

Puncture Drop No. 6 was a HAC puncture drop from a height of 40 inches, impacting glancingly onto the OCA lid adjacent to the outer thermal shield. As shown in Figure 2.10.3-5, CTU-2 was oriented -67° from horizontal (axial angle (i.e., pitch) = 67° top down), and circumferentially -67° from the forklift pocket reference. The test was conducted on 01/20/89.

The measured permanent deformation for CTU-2 was a 24-inch long dent approximately 1 inch deep. The ICV and OCV internal pressures did not change.

#### **2.10.3.7.2.8 CTU-2 Puncture Drop No. 7**

Puncture Drop No. 7 was a HAC puncture drop from a height of 40 inches, impacting onto the OCA body at the closure joint. As shown in Figure 2.10.3-5, CTU-2 was oriented -15° from horizontal (axial angle (i.e., pitch) = 15° top down) through the package's center of gravity, and circumferentially 110° from the forklift pocket reference. The test was conducted on 01/20/89.

The measured permanent deformation for CTU-2 was a 4-inch deep dent and a 3-inch long tear in the outer shell-to-Z-flange angle interface. The ICV and OCV internal pressures did not change.

### 2.10.3.7.2.9 CTU-2 Puncture Drop No. 8

Puncture Drop No. 8 was a HAC puncture drop from a height of 40 inches, impacting onto the OCA lid at the closure joint. As shown in Figure 2.10.3-5, CTU-2 was oriented  $-22^\circ$  from horizontal (axial angle (i.e., pitch) =  $22^\circ$  top down) through the package's center of gravity, and circumferentially  $-145^\circ$  from the forklift pocket reference. The test was conducted on 01/21/89.

The measured permanent deformation for CTU-2 was a 4-inch deep dent. The ICV and OCV internal pressures did not change.

### 2.10.3.7.2.10 CTU-2 Fire No. 9

Fire No. 9 was performed to demonstrate packaging compliance with the requirements of 10 CFR §71.73(c)(4) and the guidelines set forth in IAEA Safety Series No. 37. The following list summarizes the test parameters:

- CTU-2 was oriented on an insulated test stand with the most severe damage approximately  $1\frac{1}{2}$  meters above the fuel surface. With a circumferential orientation of  $200^\circ$  (see Figure 2.10.3-5), the most severe damage was determined to be from the cumulative effects of Free Drop No. 3, and Puncture Drop Nos. R and 4 located  $1\frac{1}{2}$  meters above the fuel surface.
- Consistent with 10 CFR §71.73(c)(4), CTU-2 was installed onto an insulated test stand at an elevation to place the lowest part of the package one meter above the fuel surface. CTU-2 was oriented horizontally on the test stand to maximize heat input.
- Consistent with 10 CFR §71.73(c)(4), requiring the test pool to extend 1 to 3 meters beyond the package edges, the test pool size extended approximately  $1\frac{1}{2}$  meters beyond each side of CTU-2.
- Consistent with Paragraph A-628.5 of IAEA Safety Series No. 37, requiring wind speeds not to exceed 2 m/s (4.5 mph), the average wind speed was measured to be 1.9 m/s (4.2 mph).
- Consistent with 10 CFR §71.73(c)(4), a JP4-type fuel was used for the fire test, and the amount of fuel was controlled to ensure the fire duration exceeded 30 minutes. The fuel was floated on a pool of water approximately  $\frac{1}{2}$  meter deep to ensure even distribution during burning. The fire test lasted approximately 31 minutes, and burning continued for approximately 70 minutes after the end of the fire.
- The test pool was instrumented to measure fire temperatures and heat fluxes at various locations around CTU-2. Temperatures were monitored before, during, and following the fire test until magnitudes stabilized back to ambient conditions. The average OCA surface temperature, based on thermocouple traces, was between  $1,500^\circ\text{F}$  and  $1,750^\circ\text{F}$ .
- The CTU-2 containment O-ring seals were leakage rate tested following performance testing to verify containment integrity, as discussed in Section 2.10.3.7.2.12, *CTU-2 Post-Test Disassembly*.
- The average OCV thermocouple pre-heat temperature was  $127^\circ\text{F}$  at the time of the test (compared to the analytically determined HAC initial temperature of  $120^\circ\text{F}$ ).
- The test was conducted on 01/30/89.

The maximum ICV seal flange temperature was  $200^\circ\text{F}$  (via temperature indicating labels), and the maximum OCV seal flange temperature was  $253^\circ\text{F}$  (via thermocouples;  $250^\circ\text{F}$  via temperature indicating labels). Temperature indicating label locations and results are provided in Table 2.10.3-5, and Figure 2.10.3-7 and Figure 2.10.3-9. Thermocouple locations are provided in Figure

2.10.3-11, and the results are provided in Figure 2.10.3-16 and Figure 2.10.3-17. The ICV internal pressure increased 2.6 psig, and the OCV internal pressure increased 4.6 psig (see Figure 2.10.3-25).

#### **2.10.3.7.2.11 CTU-2 Testing Anomalies**

As can be expected with any test program, a certain number of test-related anomalies occurred during CTU-2 testing. The following paragraphs summarize each anomaly and its significance.

- The impact from Free Drop No. 2 caused the neoprene weather seal to slide downward and break the OCV pressurization line, the break occurring just after the impact event and, therefore, not compromising the test; post-test re-pressurization of the OCV demonstrated containment integrity was maintained.
- Following impact from Puncture Drop No. 4, CTU-2 rolled off the puncture bar and damaged the OCV and ICV pressurization fittings; the 1.0 psig OCV pressure loss was attributed to this post-test condition.
- Pressure rise leak testing of the OCV was planned between each free drop and puncture test; shifting of the OCV relative to the seal leak test port and expediting testing were the reasons that pressure rise leak testing was not always performed.
- The ICV main O-ring seal could not be made to pass the post-test helium leakage rate test; however, the lower (non-containment) O-ring seal was leakage rate tested and shown to remain leaktight at -20 °F. The cause of debris getting past the debris shield was determined to be water condensate from the concrete-filled payload drums collecting on the open-cell foam rubber and freezing, thereby losing enough resiliency to prevent debris from getting into the main O-ring seal (see Figure 2.10.3-79). A wiper O-ring seal was added to the ICV design to prevent debris from contaminating the main O-ring seals for all temperature and moisture ranges.

#### **2.10.3.7.2.12 CTU-2 Post-Test Disassembly**

Post-test disassembly of CTU-2 was performed following Fire No. 9. Both abrasive cutting and gas plasma cutting methods were utilized, depending on their potential effect on subsequent post-test seal testing, to enable destructive disassembly of CTU-2.

As with CTU-1, upon removal of the OCA lid and body outer shells, the presence of several inches of very light density foam char showed the intumescent behavior of the polyurethane foam. Except for the local area damaged by the puncture impact 40 inches above the bottom of the OCA body and in the OCA lid, a layer of unburned polyurethane foam remained around the entire OCV. The average thickness of the layer was approximately 5 to 6 inches along the cylindrical sides and bottom, and 10 inches on top.

Demonstration of containment vessel leaktightness was accomplished by performing helium mass spectrometer leakage rate testing on each containment vessel's main O-ring seal, vent port O-ring seal, and metallic boundary. The main and vent port O-ring seals were tested when cooled to an average measured temperature below -20 °F; the metallic boundary was tested at ambient temperature. Results of successful mass spectrometer helium leakage rate testing for all components of each containment boundary, except the ICV main O-ring seal, are summarized in the following table:

Sealing Component	OCV	ICV
Main O-ring Seal	$4.5 \times 10^{-8}$ cc/s, helium	- - -
Vent Port Plug O-ring Seal	$<2.0 \times 10^{-8}$ cc/s, helium	$<2.0 \times 10^{-8}$ cc/s, helium
Metallic Boundary	$6.0 \times 10^{-8}$ cc/s, helium	$<2.0 \times 10^{-8}$ cc/s, helium

Subsequent testing of the main ICV non-containment (test) O-ring seal showed it to be leaktight. When accounting for the conversion between air leakage (per ANSI N14.5) and helium leakage, a 2.6 factor applies for standard temperatures and pressures. Thus, a reported helium leakage rate of  $1.3 \times 10^{-7}$  cc/s, helium, is equivalently  $5 \times 10^{-8}$  cc/s, air, a magnitude well below the "leaktight" criterion of  $1 \times 10^{-7}$  cc/s, air, per ANSI N14.5.

### 2.10.3.7.3 Test Results for CTU-3

#### 2.10.3.7.3.1 CTU-3 Free Drop No. 1

Free Drop No. 1 was a HAC free drop from a height of 30 feet. The primary impact for this slapdown drop occurred onto the OCA lid knuckle, with the secondary impact onto the OCA body's bottom edge, approximately midway between tie-down lugs. As shown in Figure 2.10.3-6, CTU-3 was oriented  $-20^\circ$  from horizontal (axial angle (i.e., pitch) =  $20^\circ$  top down), and circumferentially aligned to impact the ICV and OCV locking ring pinned joints and coincident payload drums to produce maximum damage ( $-5^\circ$  from the forklift pocket reference). At the time of the test, the measured OCV temperature was  $-26^\circ\text{F}$ . The test was conducted on 04/19/89.

The measured permanent deformations for CTU-3 were flats 48 inches wide at the top (OCA lid), and 23 inches wide at the bottom (OCA body). The ICV and OCV internal pressures did not change.

#### 2.10.3.7.3.2 CTU-3 Free Drop No. 2

Free Drop No. 2 was a HAC free drop from a height of 30 feet, impacting vertically onto the CTU bottom, as shown in Figure 2.10.3-6. At the time of the test, the measured OCV temperature was  $-22^\circ\text{F}$ . The test was conducted on 04/19/89.

The permanent deformation for CTU-3 was negligible. The ICV internal pressure did not change; however, the OCV internal pressure dropped 0.5 psig. The maximum axial acceleration was 335 gs (filtered at 500 Hz; see Figure 2.10.3-22 and Figure 2.10.3-23).

#### 2.10.3.7.3.3 CTU-3 Free Drop No. 3

Free Drop No. 3 was a HAC free drop from a height of 30 feet. The primary impact for this slapdown drop occurred onto a tie-down lug, with the secondary impact onto the OCA lid. As shown in Figure 2.10.3-6, CTU-3 was oriented  $18^\circ$  from horizontal (axial angle (i.e., pitch) =  $18^\circ$  top up), and circumferentially aligned with the tie-down lug ( $143^\circ$  from the forklift pocket reference). The test was conducted on 04/19/89.

The measured permanent deformations for CTU-3 were flats 13 inches wide at the top (OCA lid), and 40 inches wide at the bottom (OCA body). The ICV internal pressure did not change; however, the OCV internal pressure dropped 1.0 psig.

#### **2.10.3.7.3.4 CTU-3 Puncture Drop No. 4**

Puncture Drop No. 4 was a HAC puncture drop from a height of 40 inches, impacting onto the OCA body at the 1/4-to-3/8-inch thickness outer shell transition. As shown in Figure 2.10.3-6, CTU-3 was oriented  $-42^\circ$  from horizontal (axial angle (i.e., pitch) =  $42^\circ$  top down) through the package's center of gravity, and circumferentially aligned with the tie-down lug ( $143^\circ$  from the forklift pocket reference). The test was conducted on 04/19/89.

The measured permanent deformation for CTU-3 was an 8-inch wide, 10-inch long, and 8-inch deep hole through the OCA outer shell. The ICV internal pressure did not change; however, the OCV internal pressure dropped 0.5 psig.

#### **2.10.3.7.3.5 CTU-3 Puncture Drop No. 5**

Puncture Drop No. 5 was a HAC puncture drop from a height of 40 inches, impacting onto the OCA bottom edge, adjacent to a forklift pocket. As shown in Figure 2.10.3-6, CTU-3 was oriented  $55^\circ$  from horizontal (axial angle (i.e., pitch) =  $55^\circ$  top up) through the package's center of gravity, and circumferentially  $-110^\circ$  from the forklift pocket reference. The test was conducted on 04/20/89.

The measured permanent deformation for CTU-3 was a hole approximately 8 inches deep. The ICV and OCV internal pressures did not change.

#### **2.10.3.7.3.6 CTU-3 Puncture Drop No. 6**

Puncture Drop No. 6 was a HAC puncture drop from a height of 40 inches, impacting glancingly onto the OCA lid adjacent to the outer thermal shield. As shown in Figure 2.10.3-6, CTU-3 was oriented  $-67^\circ$  from horizontal (axial angle (i.e., pitch) =  $67^\circ$  top down), and circumferentially  $-67^\circ$  from the forklift pocket reference. The test was conducted on 04/21/89.

The measured permanent deformation for CTU-3 was a dent approximately 2 inches deep. The ICV and OCV internal pressures did not change.

#### **2.10.3.7.3.7 CTU-3 Puncture Drop No. 7**

Puncture Drop No. 7 was a HAC puncture drop from a height of 40 inches, impacting onto the OCA body at the closure joint. As shown in Figure 2.10.3-6, CTU-3 was oriented  $-15^\circ$  from horizontal (axial angle (i.e., pitch) =  $15^\circ$  top down) through the package's center of gravity, and circumferentially  $110^\circ$  from the forklift pocket reference. The test was conducted on 04/21/89.

The measured permanent deformation for CTU-3 was a 4-inch deep dent. The ICV and OCV internal pressures did not change.

#### **2.10.3.7.3.8 CTU-3 Puncture Drop No. 8**

Puncture Drop No. 8 was a HAC puncture drop from a height of 40 inches, impacting onto the OCA lid at the closure joint. As shown in Figure 2.10.3-6, CTU-3 was oriented  $-22^\circ$  from

horizontal (axial angle (i.e., pitch) = 22° top down) through the package's center of gravity, and circumferentially -145° from the forklift pocket reference. The test was conducted on 04/21/89.

The measured permanent deformation for CTU-3 was a 4-inch deep dent. The ICV and OCV internal pressures did not change.

#### 2.10.3.7.3.9 CTU-3 Testing Anomalies

As can be expected with any test program, a certain number of test related anomalies occurred during CTU-3 testing. The following paragraphs summarize each anomaly and its significance.

- Pressure rise leak testing of the OCV was planned between each free drop and puncture test; shifting of the OCV relative to the seal leak test port and expediting testing were the reasons that pressure rise leak testing was not always performed.
- One of the four OCV seal region thermocouples failed early in testing; reported temperatures are the average of the remaining three thermocouples.
- Pressure drops in the OCV were noted for Free Drop Nos. 2 and 3, and Puncture Drop No. 4; a momentary increase in pressure occurred at the moment of CTU impact, followed by a reduction below the original value, was most likely due to the gauge "sticking" because of the pressure pulse.
- Because the ICV main O-ring seal could not be made to pass the post-test helium leakage rate test for CTU-2, a wiper O-ring seal was added to the ICV design for CTU-3 to prevent debris from contaminating the main O-ring seal for all temperature and moisture ranges. The wiper O-ring seal holder was fabricated from rolled sheet and attached via 114 drive screws. Of the 114 original drive screws, 16 were damaged (sheared head); nevertheless, the seal holder remained in position and prevented debris from contaminating the main O-ring seal.

#### 2.10.3.7.3.10 CTU-3 Post-Test Disassembly

Post-test disassembly of CTU-3 was performed following Puncture Drop No. 8. Both abrasive cutting and gas plasma cutting methods were utilized, depending on their potential effect on subsequent post-test seal testing, to enable destructive disassembly of CTU-3.

Demonstration of containment vessel leaktightness was accomplished by performing helium mass spectrometer leakage rate testing on each containment vessel's main O-ring seal, vent port O-ring seal, and metallic boundary. The ICV main and ICV vent port O-ring seals were tested when cooled to an average measured temperature below -20 °F; the metallic boundary was tested at ambient temperature. The OCV main and OCV vent port O-ring seals, and metallic boundary were tested at ambient temperature. Results of successful mass spectrometer helium leakage rate testing are summarized in the following table:

Sealing Component	OCV	ICV
Main O-ring Seal	$<2.0 \times 10^{-8}$ cc/s, helium	$<2.0 \times 10^{-8}$ cc/s, helium
Vent Port Plug O-ring Seal	$<2.0 \times 10^{-8}$ cc/s, helium	$<2.0 \times 10^{-8}$ cc/s, helium
Metallic Boundary	$<2.0 \times 10^{-8}$ cc/s, helium	$<9.2 \times 10^{-8}$ cc/s, helium

When accounting for the conversion between air leakage (per ANSI N14.5) and helium leakage, a 2.6 factor applies for standard temperatures and pressures. Thus, a reported helium leakage rate of  $1.3 \times 10^{-7}$  cc/s, helium, is equivalently  $5 \times 10^{-8}$  cc/s, air, a magnitude well below the "leaktight" criterion of  $1 \times 10^{-7}$  cc/s, air, per ANSI N14.5.

In conclusion, the test series performed on CTU-3 demonstrates the TRUPACT-II package's ability to meet the normal conditions of transport and hypothetical accident conditions regulatory requirements as defined in 10 CFR §71.71 and §71.73, respectively, and demonstrates that the wiper O-ring seal retrofit prevents debris from contaminating the ICV main O-ring seal.

This page intentionally left blank.

**Table 2.10.3-1 – Summary of CTU-1 Test Results in Sequential Order**

Test No.	Test Description	Test Unit Angular Orientation		Pressure (psig)		CTU Temperature	Observations and Results
		Axial <sup>①</sup>	Circumferential <sup>②</sup>	ICV	OCV		
1	NCT, 3-foot side drop onto OCV vent port	0°	110°	50	50	Ambient	18" wide flat at top (OCA lid) × 18" wide flat at bottom (OCA body) × ~7/8" deep
2	HAC, 30-foot side drop onto OCV vent port	0°	110°	50	0	Ambient	37" wide flat at top (OCA lid) × 35" wide flat at bottom (OCA body) × ~3 3/8" deep
3	HAC, 30-foot CG onto OCA lid knuckle near OCA lid lift pocket	-47°	-100°	50	50	Ambient	30" wide × 53" long flat at top (OCA lid) × ~3 3/4" deep
4	HAC, 30-foot top drop	-90°	N/A	50	50	Ambient	53" diameter flat at top (OCA lid) × ~3 3/8" deep
5	HAC, puncture drop on OCA vent port fitting	-15°	110°	50	50	Ambient	16" long tear at shell-to-angle interface on OCA body at vent port × ~3" deep
6	HAC, puncture drop onto OCA body below 1/4-to-3/8 shell weld	-3°	110°	50	50	Ambient	~3/4" deep dent
7	HAC, puncture drop 40 inches above package bottom	28°	110°	50	0	Ambient	8" wide × 11" long × ~8 1/2" deep hole through OCA outer shell; CTU-1 may have hit ground; repeated as CTU-2, Test No. R
8	HAC, puncture drop onto damaged OCA lid knuckle	-54°	110°	50	0	Ambient	Some additional denting; no penetration
9	HAC, puncture drop on OCA seal test port fitting	-24°	20°	50	50	Ambient	~3" deep dent; ~7" wide tear of outer thermal shield
10	HAC, fire test	0°	145°	50	50	At HAC pre-fire temperature	~32 minute fire; maximum 170 °F and 260 °F ICV and OCV seal flange temperature, and maximum 1.9 psig and 1.4 psig ICV and OCV pressure rise, respectively

**Notes:**

- ① Axial angle,  $\theta$ , is relative to horizontal (i.e., side drop orientation).
- ② Circumferential angle,  $\phi$ , is relative to the forklift pockets when parallel to the ground.

**Table 2.10.3-2 – Summary of CTU-2 Test Results in Sequential Order**

Test No.	Test Description	Test Unit Angular Orientation		Pressure (psig)		CTU Temperature	Observations and Results
		Axial <sup>①</sup>	Circumferential <sup>②</sup>	ICV	OCV		
1	HAC, 30-foot top slapdown drop; initial impact on OCA lid knuckle	-20°	-5°	33	0	-20 °F	45" wide flat at top (OCA lid) × 21" wide flat at bottom (OCA body)
2	HAC, 30-foot bottom drop	90°	N/A	33	33	-20 °F	negligible visible damage
3	HAC, 30-foot slapdown drop; initial impact on tie-down lug	18°	143°	50	50	Ambient	15" wide flat at top (OCA lid) × 45" wide flat at bottom (OCA body)
R	HAC, puncture drop 40 inches above package bottom	23°	143°	50	0	Ambient	10" wide × 11" long hole; ~9" deep hole; minor denting of OCV and ICV shells
4	HAC, puncture drop at the 1/4-to-3/8 lid shell interface	-42°	143°	50	50	Ambient	8" wide × 10" long hole; ~7" deep hole
5	HAC, puncture drop onto package bottom adjacent to forklift pocket	55°	-110°	50	0	Ambient	~5" deep dent
6	HAC, puncture drop onto outer thermal shield	-67°	-67°	0	0	Ambient	~24" long × ~1" deep dent
7	HAC, puncture drop onto OCA body at closure; 40° from OCA vent port fitting	-15°	110°	50	50	Ambient	3" long tear at shell-to-angle interface on OCA body × ~4" deep dent
8	HAC, puncture drop onto OCA lid at closure; 180° from OCA seal test port fitting	-22°	-145°	50	50	Ambient	~4" deep dent
9	HAC, fire test	0°	200°	50	50	At HAC pre-fire temperature	~31 minute fire; maximum 200 °F and 250 °F ICV and OCV seal flange temperature, and maximum 2.7 psig and 4.5 psig ICV and OCV pressure rise, respectively

Notes:

- ① Axial angle,  $\theta$ , is relative to horizontal (i.e., side drop orientation).
- ② Circumferential angle,  $\phi$ , is relative to the forklift pockets when parallel to the ground.

**Table 2.10.3-3 – Summary of CTU-3 Test Results in Sequential Order**

Test No.	Test Description	Test Unit Angular Orientation		Pressure (psig)		CTU Temperature	Observations and Results
		Axial <sup>①</sup>	Circumferential <sup>②</sup>	ICV	OCV		
1	HAC, 30-foot top slapdown drop; initial impact on OCA lid knuckle	-20°	-5°	33	0	-20 °F	48" wide flat at top (OCA lid) × 23" wide flat at bottom (OCA body)
2	HAC, 30-foot bottom drop	90°	N/A	33	33	-20 °F	negligible visible damage
3	HAC, 30-foot slapdown drop; initial impact on tie-down lug	18°	143°	50	50	Ambient	13" wide flat at top (OCA lid) × 40" wide flat at bottom (OCA body)
4	HAC, puncture drop at the 1/4-to-3/8 lid shell interface	-42°	143°	50	50	Ambient	8" wide × 10" long hole; ~8" deep hole
5	HAC, puncture drop onto package bottom adjacent to forklift pocket	55°	-110°	50	0	Ambient	~8" deep hole
6	HAC, puncture drop onto outer thermal shield	-67°	-67°	0	0	Ambient	~2" deep dent
7	HAC, puncture drop onto OCA body at closure; 40° from OCA vent port fitting	-15°	110°	50	50	Ambient	~4" deep dent
8	HAC, puncture drop onto OCA lid at closure; 180° from OCA seal test port fitting	-22°	-145°	50	50	Ambient	~4" deep dent

Notes:

- ① Axial angle,  $\theta$ , is relative to horizontal (i.e., side drop orientation).  
 ② Circumferential angle,  $\phi$ , is relative to the forklift pockets when parallel to the ground.

This page intentionally left blank.

**Table 2.10.3-4 – CTU-1 Temperature Indicating Label Locations and Results**

Label Identifier	Location		Indicated Temperature	Remarks
	Y (in)	C (deg)		
TI-1	0.0	0.0	160 °F	Payload pallet; top center
TI-2	19.0	85.0	130 °F	Drum #1; side toward payload center
TI-3	19.0	12.0	140 °F	Drum #4 (bottom center drum); side
TI-4	34.0	0.0	130 °F	Drum #4 (bottom center drum); top center
TI-5	53.0	85.0	130 °F	Drum #8; side toward payload center
TI-6	53.0	12.0	130 °F	Drum #11 (top center drum); side
TI-7	69.0	0.0	130 °F	Drum #11 (top center drum); top
TI-8	62.0	49.0	150 °F	ICV body; inner lower seal flange surface
TI-9	62.0	13.5	170 °F	ICV body; inner lower seal flange surface
TI-10	62.0	205.0	170 °F	ICV body; inner lower seal flange surface
TI-11	62.0	166.0	150 °F	ICV body; inner lower seal flange surface
TI-12	62.0	128.0	140 °F	ICV body; inner lower seal flange surface
TI-13	62.0	88.5	150 °F	ICV body; inner lower seal flange surface
TI-14	29.5	49.0	160 °F	ICV body; inner shell surface
TI-15	29.5	13.5	170 °F	ICV body; inner shell surface
TI-16	29.5	205.0	160 °F	ICV body; inner shell surface
TI-17	29.5	166.0	140 °F	ICV body; inner shell surface
TI-18	29.5	128.0	140 °F	ICV body; inner shell surface
TI-19	29.5	88.5	160 °F	ICV body; inner shell surface
TI-20	1.5	49.0	150 °F	ICV body; shell-to-lower torispherical head weld
TI-21	1.5	13.5	170 °F	ICV body; shell-to-lower torispherical head weld
TI-22	1.5	205.0	190 °F	ICV body; shell-to-lower torispherical head weld
TI-23	1.5	166.0	140 °F	ICV body; shell-to-lower torispherical head weld
TI-24	1.5	128.0	150 °F	ICV body; shell-to-lower torispherical head weld
TI-25	1.5	88.5	180 °F	ICV body; shell-to-lower torispherical head weld
TI-26	Bottom Center		270 °F	ICV body; lower torispherical head
TI-27	1.5	90.0	160 °F	ICV lid; shell-to-upper torispherical head weld
TI-28	1.5	210.0	160 °F	ICV lid; shell-to-upper torispherical head weld
TI-29	1.5	330.0	130 °F	ICV lid; shell-to-upper torispherical head weld
TI-30	Top Center		150 °F	ICV lid; upper torispherical head
TI-31	Near TI-29		140 °F	Upper aluminum honeycomb spacer; lower face
TI-32	57.5	30.0	220 °F	OCV body; inner lower seal flange surface
TI-33	57.5	64.0	230 °F	OCV body; inner lower seal flange surface
TI-34	57.5	74.0	250 °F	OCV body; inner lower seal flange surface
TI-35	57.5	101.0	220 °F	OCV body; inner lower seal flange surface
TI-36	57.5	138.0	190 °F	OCV body; inner lower seal flange surface
TI-37	57.5	183.0	190 °F	OCV body; inner lower seal flange surface
TI-38	57.5	201.0	210 °F	OCV body; inner lower seal flange surface

Label Identifier	Location		Indicated Temperature	Remarks
	Y (in)	C (deg)		
TI-39	57.5	236.0	200 °F	OCV body; inner lower seal flange surface
TI-40	50.5	30.0	190 °F	OCV body; inner conical shell surface
TI-41	50.5	74.0	240 °F	OCV body; inner conical shell surface
TI-42	50.5	101.0	180 °F	OCV body; inner conical shell surface
TI-43	50.5	138.0	160 °F	OCV body; inner conical shell surface
TI-44	50.5	183.0	170 °F	OCV body; inner conical shell surface
TI-45	50.5	201.0	170 °F	OCV body; inner conical shell surface
TI-46	50.5	236.0	170 °F	OCV body; inner conical shell surface
TI-47	26.5	30.0	310 °F	OCV body; inner shell surface near stiffening ring
TI-48	26.5	74.0	340 °F	OCV body; inner shell surface near stiffening ring
TI-49	26.5	101.0	290 °F	OCV body; inner shell surface near stiffening ring
TI-50	26.5	138.0	220 °F	OCV body; inner shell surface near stiffening ring
TI-51	26.5	183.0	170 °F	OCV body; inner shell surface near stiffening ring
TI-52	26.5	201.0	160 °F	OCV body; inner shell surface near stiffening ring
TI-53	26.5	236.0	170 °F	OCV body; inner shell surface near stiffening ring
TI-54	1.5	30.0	160 °F	OCV body; shell-to-lower torispherical head weld
TI-55	1.5	74.0	340 °F	OCV body; shell-to-lower torispherical head weld
TI-56	1.5	101.0	270 °F	OCV body; shell-to-lower torispherical head weld
TI-57	1.5	138.0	170 °F	OCV body; shell-to-lower torispherical head weld
TI-58	1.5	183.0	150 °F	OCV body; shell-to-lower torispherical head weld
TI-59	1.5	201.0	170 °F	OCV body; shell-to-lower torispherical head weld
TI-60	1.5	236.0	200 °F	OCV body; shell-to-lower torispherical head weld
TI-61	-16.6	30.0	210 °F	OCV body; lower torispherical head
TI-62	-16.6	74.0	200 °F	OCV body; lower torispherical head
TI-63	-16.6	160.0	200 °F	OCV body; lower torispherical head
TI-64	-16.6	201.0	230 °F	OCV body; lower torispherical head
TI-65	1.0	90.5	220 °F	OCV lid; shell-to-upper torispherical head weld
TI-66	1.0	131.5	220 °F	OCV lid; shell-to-upper torispherical head weld
TI-67	1.0	171.5	230 °F	OCV lid; shell-to-upper torispherical head weld
TI-68	1.0	211.5	190 °F	OCV lid; shell-to-upper torispherical head weld
TI-69	1.0	251.5	200 °F	OCV lid; shell-to-upper torispherical head weld
TI-70	1.0	291.5	210 °F	OCV lid; shell-to-upper torispherical head weld
TI-71	18.0	90.5	160 °F	OCV lid; upper torispherical head
TI-72	18.0	131.5	260 °F	OCV lid; upper torispherical head
TI-73	18.0	171.5	300 °F	OCV lid; upper torispherical head
TI-74	18.0	211.5	170 °F	OCV lid; upper torispherical head
TI-75	18.0	251.5	340 °F	OCV lid; upper torispherical head
TI-76	18.0	291.5	170 °F	OCV lid; upper torispherical head
TI-77	Top Center		Damaged	OCV lid; upper torispherical head

**Table 2.10.3-5 – CTU-2 Temperature Indicating Label Locations and Results**

Label Identifier	Location		Indicated Temperature	Remarks
	Y (in)	C (deg)		
TI-1	Top Center		160 °F	Payload pallet; top center
TI-2	19.0	27.0	140 °F	Drum #1 (bottom center drum); side
TI-3	19.0	210.0	150 °F	Drum #3; side
TI-4	Top Center		150 °F	Drum #1 (bottom center drum); top center
TI-5	19.0	180.0	Damaged	Drum #3; side (outside edge of payload)
TI-6	19.0	250.0	150 °F	Drum #5; side (outside edge of payload)
TI-7	19.0	120.0	170 °F	Drum #7; side (outside edge of payload)
TI-8	54.0	90.0	160 °F	Drum #8 (top center drum); side
TI-9	Top Center		150 °F	Drum #8 (top center drum); top center
TI-10	56.0	120.0	150 °F	Drum #10; side (outside edge of payload)
TI-11	6.0	0.0	Damaged	OCV lid; shell surface
TI-12	6.0	90.0	200 °F	OCV lid; shell surface
TI-13	6.0	180.0	170 °F	OCV lid; shell surface
TI-14	6.0	270.0	190 °F	OCV lid; shell surface
TI-15	25.0	0.0	340 °F	OCV lid; upper torispherical head
TI-16	25.0	90.0	250 °F	OCV lid; upper torispherical head
TI-17	25.0	180.0	170 °F	OCV lid; upper torispherical head
TI-18	25.0	270.0	220 °F	OCV lid; upper torispherical head
TI-19	18.0	143.0	270 °F	OCV lid; upper torispherical head
TI-20	Top Center		290 °F	OCV lid; upper torispherical head
TI-21	6.0	135.0	220 °F	OCV lid; upper torispherical head
TI-22	6.0	225.0	280 °F	OCV lid; upper torispherical head
TI-23	57.0	0.0	250 °F	OCV body; inner lower seal flange surface
TI-24	57.0	90.0	220 °F	OCV body; inner lower seal flange surface
TI-25	57.0	180.0	220 °F	OCV body; inner lower seal flange surface
TI-26	57.0	215.0	230 °F	OCV body; inner lower seal flange surface
TI-27	57.0	270.0	200 °F	OCV body; inner lower seal flange surface
TI-28	49.0	0.0	220 °F	OCV body; inner conical shell surface
TI-29	49.0	90.0	190 °F	OCV body; inner conical shell surface
TI-30	49.0	180.0	210 °F	OCV body; inner conical shell surface
TI-31	49.0	215.0	170 °F	OCV body; inner conical shell surface
TI-32	49.0	270.0	170 °F	OCV body; inner conical shell surface
TI-33	26.0	0.0	Damaged	OCV body; inner shell surface near stiffening ring
TI-34	26.0	90.0	170 °F	OCV body; inner shell surface near stiffening ring
TI-35	26.0	180.0	190 °F	OCV body; inner shell surface near stiffening ring
TI-36	26.0	270.0	170 °F	OCV body; inner shell surface near stiffening ring
TI-37	1.0	0.0	Damaged	OCV body; shell-to-lower torispherical head weld
TI-38	1.0	90.0	Damaged	OCV body; shell-to-lower torispherical head weld
TI-39	1.0	135.0	220 °F	OCV body; shell-to-lower torispherical head weld
TI-40	1.0	180.0	Damaged	OCV body; shell-to-lower torispherical head weld

Label Identifier	Location		Indicated Temperature	Remarks
	Y (in)	C (deg)		
TI-41	1.0	225.0	190 °F	OCV body; shell-to-lower torispherical head weld
TI-42	1.0	270.0	Damaged	OCV body; shell-to-lower torispherical head weld
TI-43	-18.0	0.0	350 °F	OCV body; lower torispherical head
TI-44	-18.0	90.0	250 °F	OCV body; lower torispherical head
TI-45	-18.0	180.0	250 °F	OCV body; lower torispherical head
TI-46	-11.0	250.0	250 °F	OCV body; lower torispherical head
TI-47	-18.0	270.0	260 °F	OCV body; lower torispherical head
TI-48	66.5	0.0	200 °F	ICV body; inner lower seal flange surface
TI-49	Seal Test Port		170 °F	ICV body; inner lower seal flange surface
TI-50	Vent Port		170 °F	ICV body; inner lower seal flange surface
TI-51	66.5	270.0	170 °F	ICV body; inner lower seal flange surface
TI-52	66.5	180.0	170 °F	ICV body; inner lower seal flange surface
TI-53	66.5	90.0	180 °F	ICV body; inner lower seal flange surface
TI-54	45.5	0.0	200 °F	ICV body; inner shell surface
TI-55	45.5	90.0	170 °F	ICV body; inner shell surface
TI-56	45.5	180.0	Damaged	ICV body; inner shell surface
TI-57	45.5	270.0	160 °F	ICV body; inner shell surface
TI-58	-14.5	270.0	190 °F	ICV body; lower torispherical head
TI-59	21.5	0.0	210 °F	ICV body; inner shell surface
TI-60	21.5	90.0	170 °F	ICV body; inner shell surface
TI-61	21.5	180.0	180 °F	ICV body; inner shell surface
TI-62	21.5	270.0	160 °F	ICV body; inner shell surface
TI-63	3.5	0.0	220 °F	ICV body; shell-to-lower torispherical head weld
TI-64	3.5	90.0	170 °F	ICV body; shell-to-lower torispherical head weld
TI-65	3.5	180.0	Damaged	ICV body; shell-to-lower torispherical head weld
TI-66	3.5	270.0	180 °F	ICV body; shell-to-lower torispherical head weld
TI-67	-14.5	0.0	Damaged	ICV body; lower torispherical head
TI-68	-14.5	90.0	200 °F	ICV body; lower torispherical head
TI-69	-14.5	180.0	190 °F	ICV body; lower torispherical head
TI-70	Near Test Ports		250 °F	ICV body; lower torispherical head
TI-71	4.0	0.0	200 °F	ICV lid; shell-to-upper torispherical head weld
TI-72	4.0	90.0	Damaged	ICV lid; shell-to-upper torispherical head weld
TI-73	4.0	180.0	210 °F	ICV lid; shell-to-upper torispherical head weld
TI-74	4.0	270.0	180 °F	ICV lid; shell-to-upper torispherical head weld
TI-75	24.0	0.0	190 °F	ICV lid; upper torispherical head
TI-76	24.0	90.0	170 °F	ICV lid; upper torispherical head
TI-77	24.0	180.0	200 °F	ICV lid; upper torispherical head
TI-78	24.0	270.0	190 °F	ICV lid; upper torispherical head
TI-79	N/A	120.0	180 °F	ICV lid; inner lift pocket surface
TI-80	N/A	240.0	190 °F	ICV lid; inner lift pocket surface

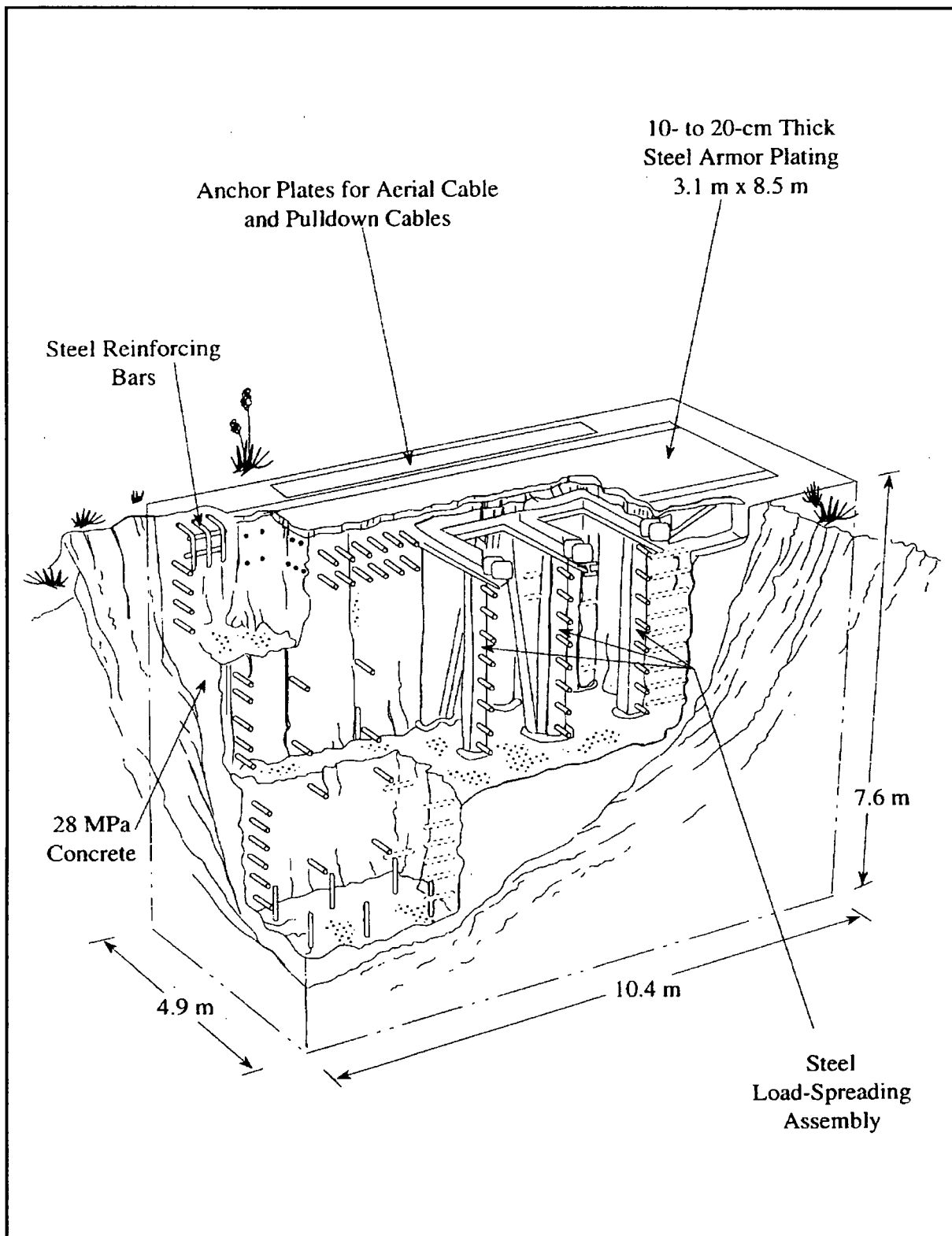


Figure 2.10.3-1 – Drop Pad at the Coyote Canyon Aerial Cable Facility

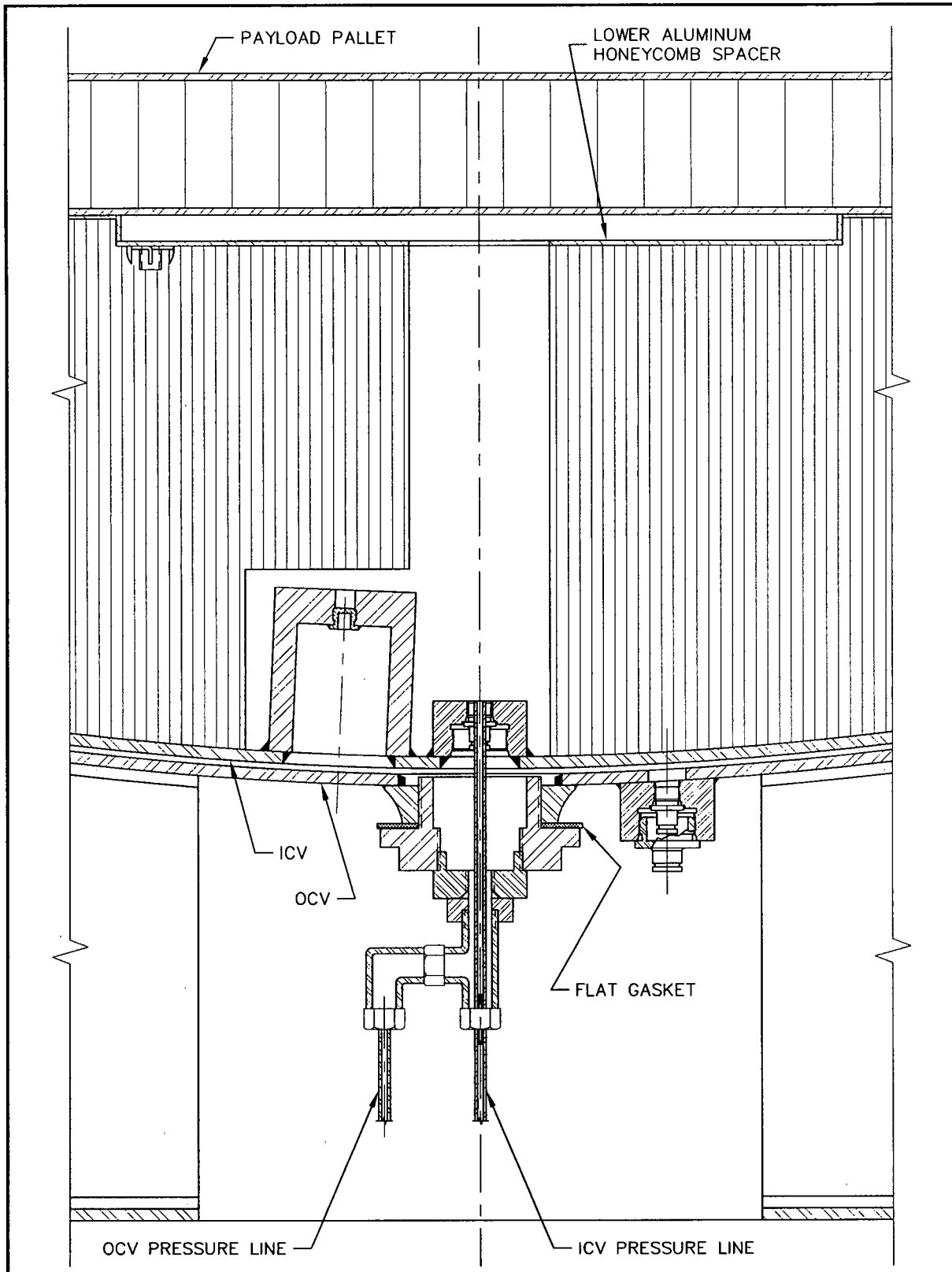


Figure 2.10.3-2 – CTU OCV and ICV Pressurization Port Detail

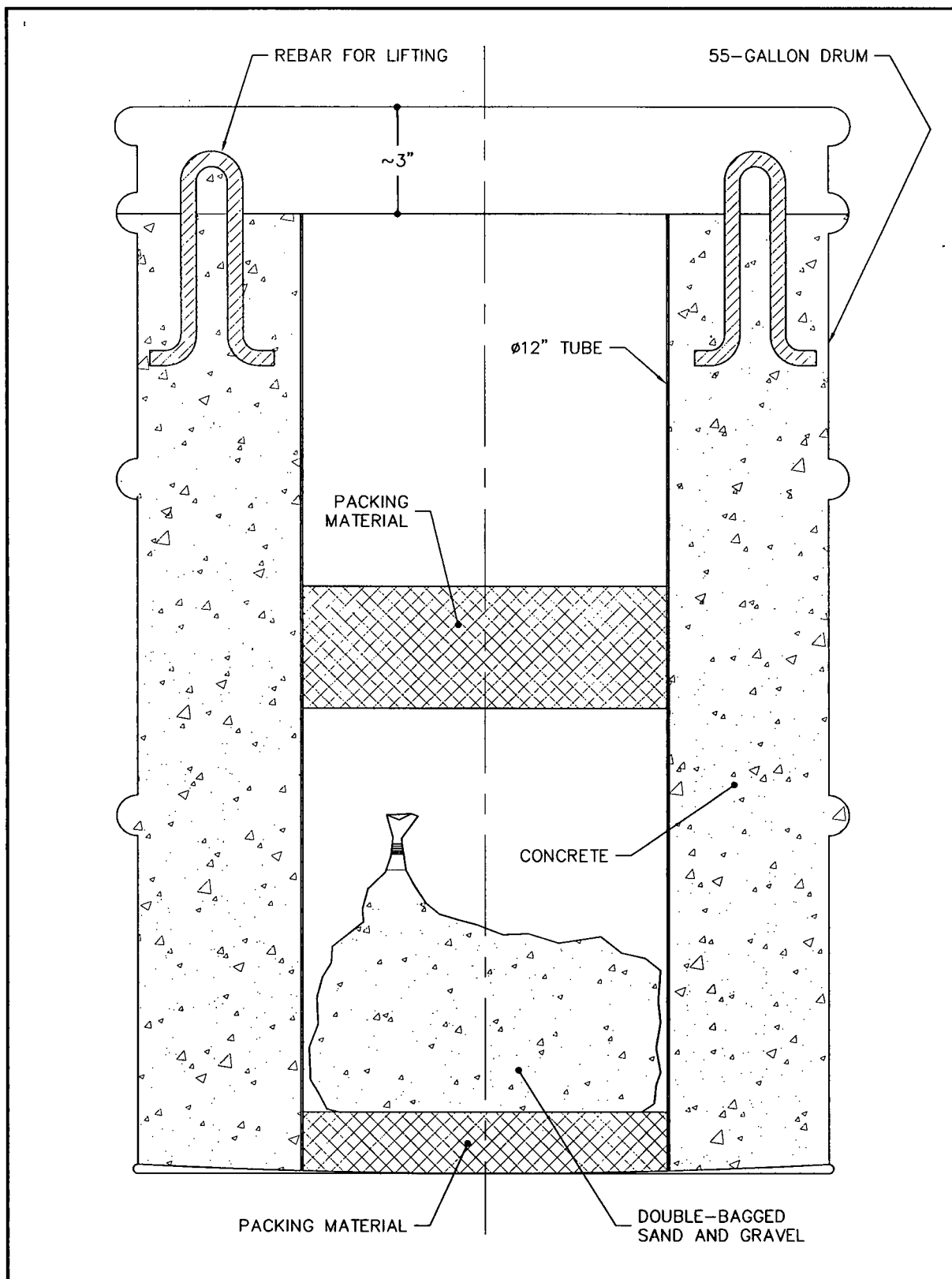


Figure 2.10.3-3 – CTU Payload Representation (Concrete-Filled 55-Gallon Drums)

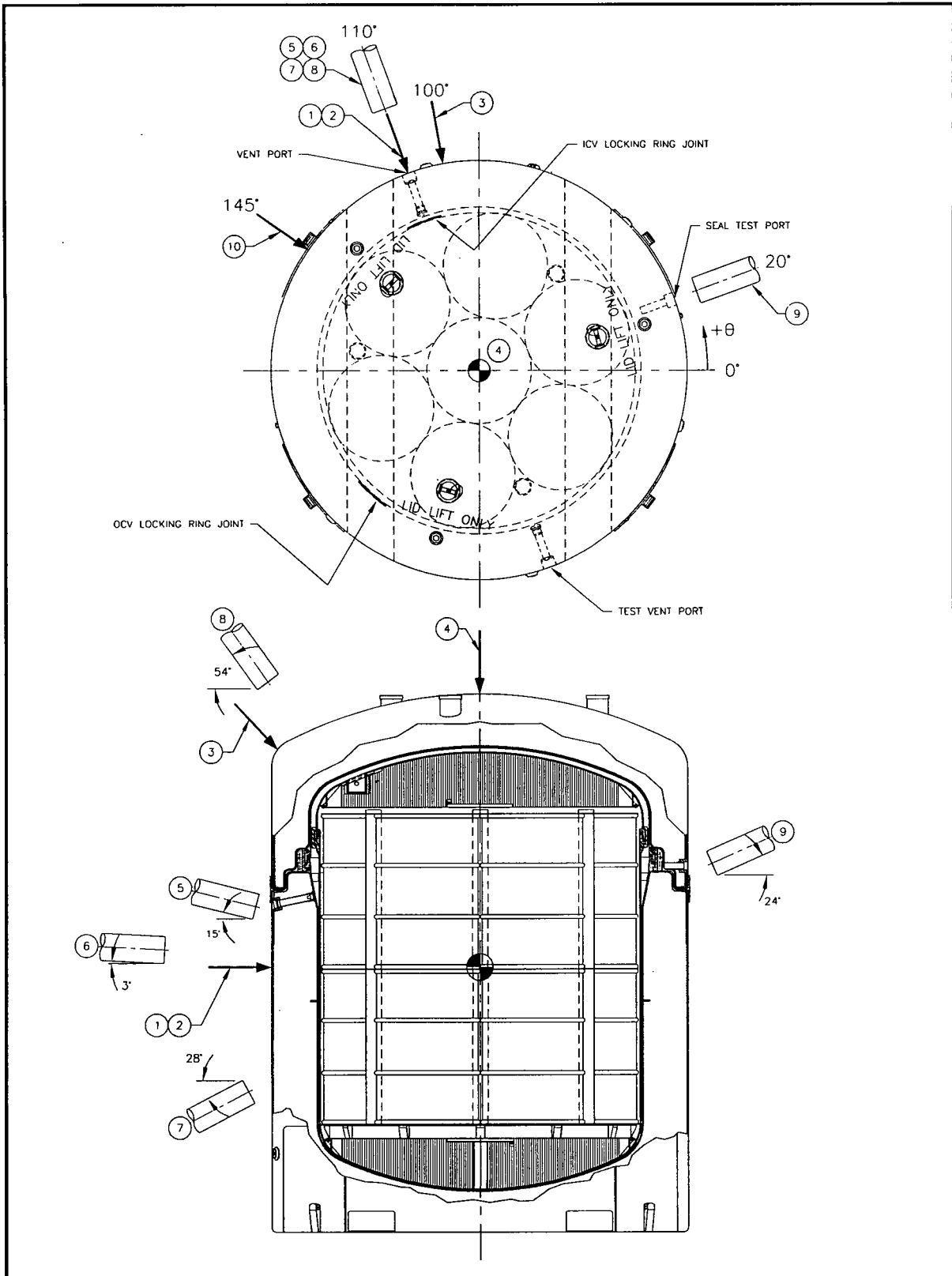


Figure 2.10.3-4 – Schematic of the CTU-1 Test Orientations

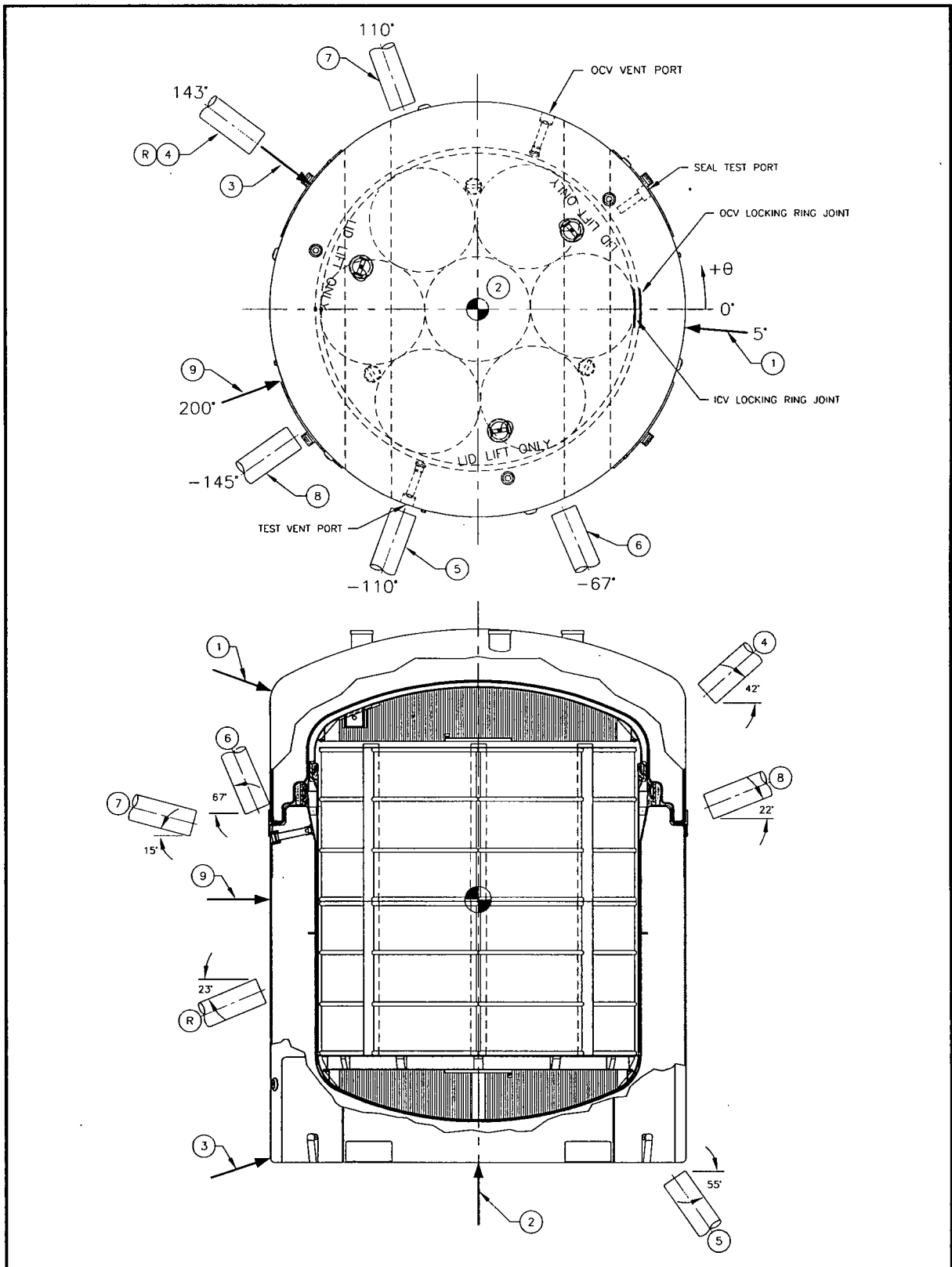


Figure 2.10.3-5 – Schematic of the CTU-2 Test Orientations

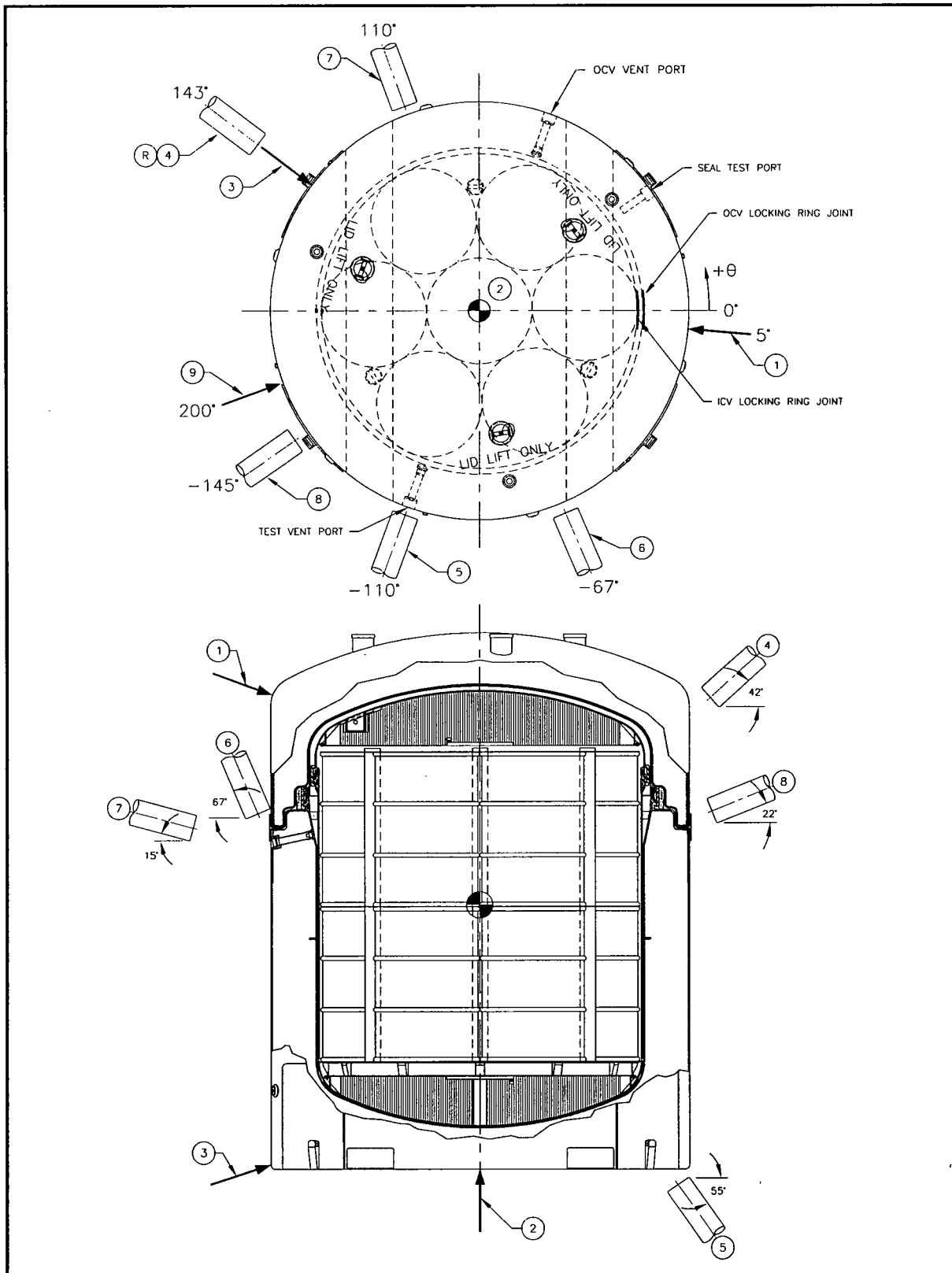


Figure 2.10.3-6 – Schematic of the CTU-3 Test Orientations

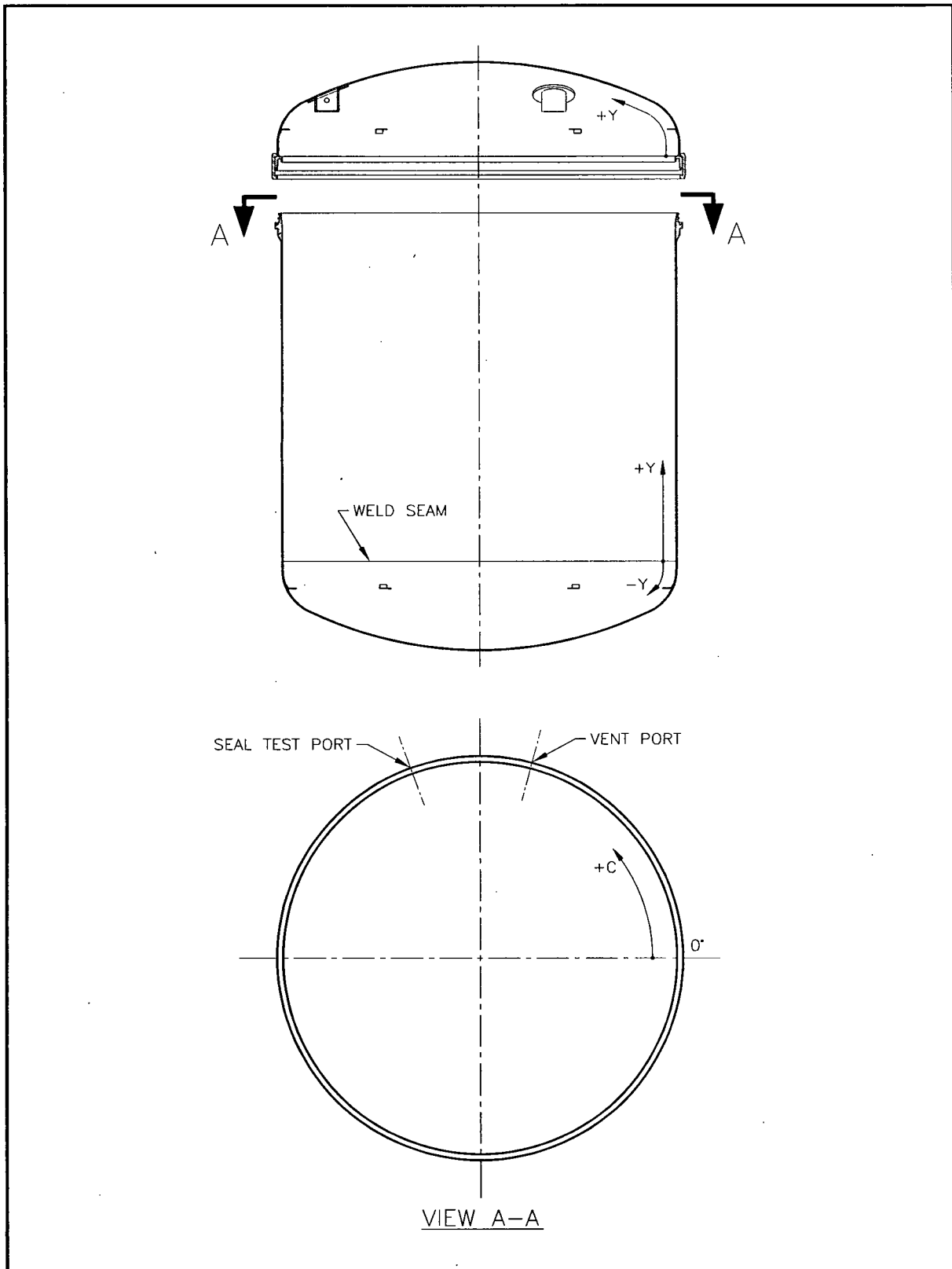


Figure 2.10.3-7 – CTU-1 and CTU-2 ICV Temperature Indicating Label Locations

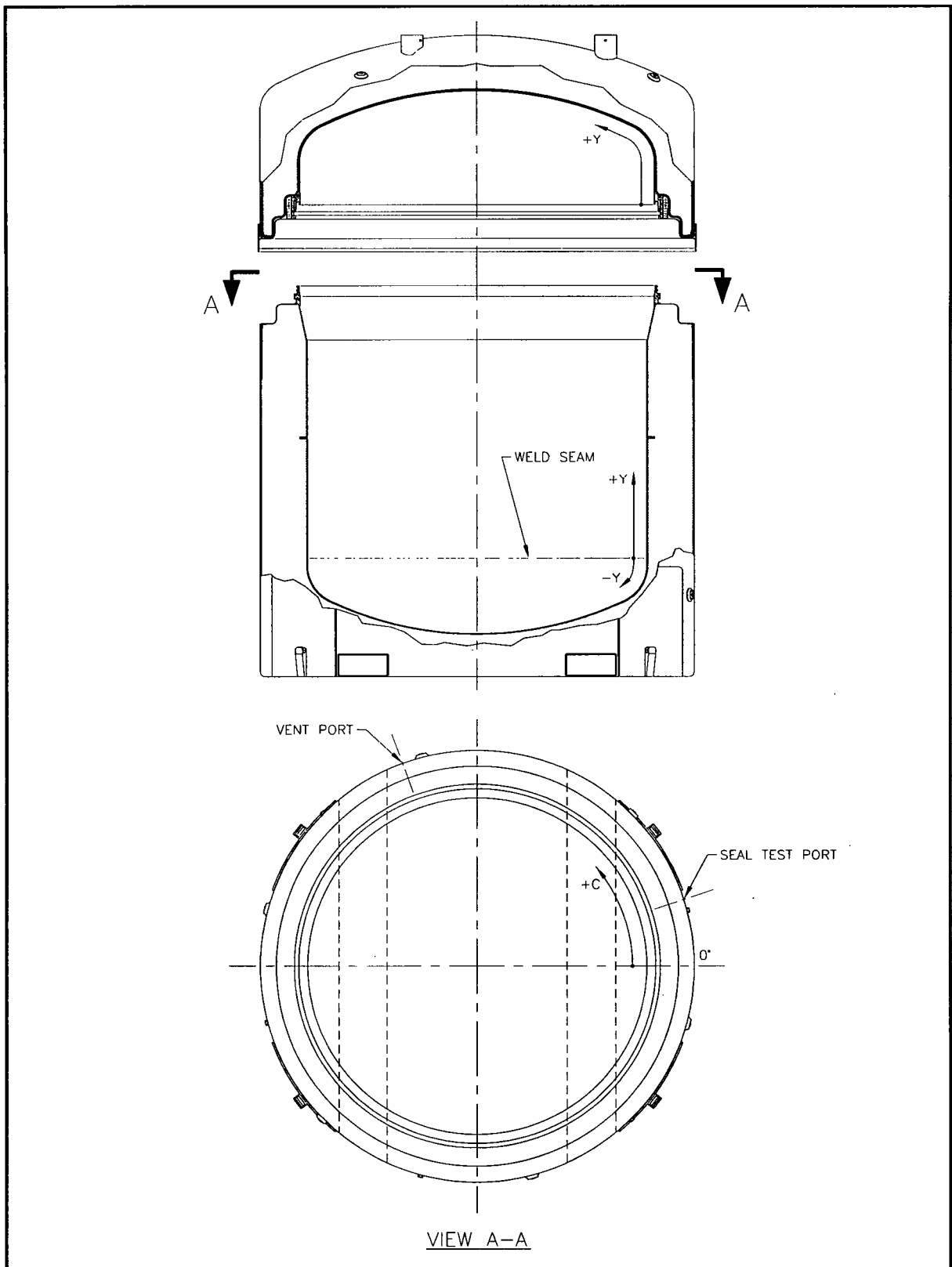


Figure 2.10.3-8 – CTU-1 OCV Temperature Indicating Label Locations

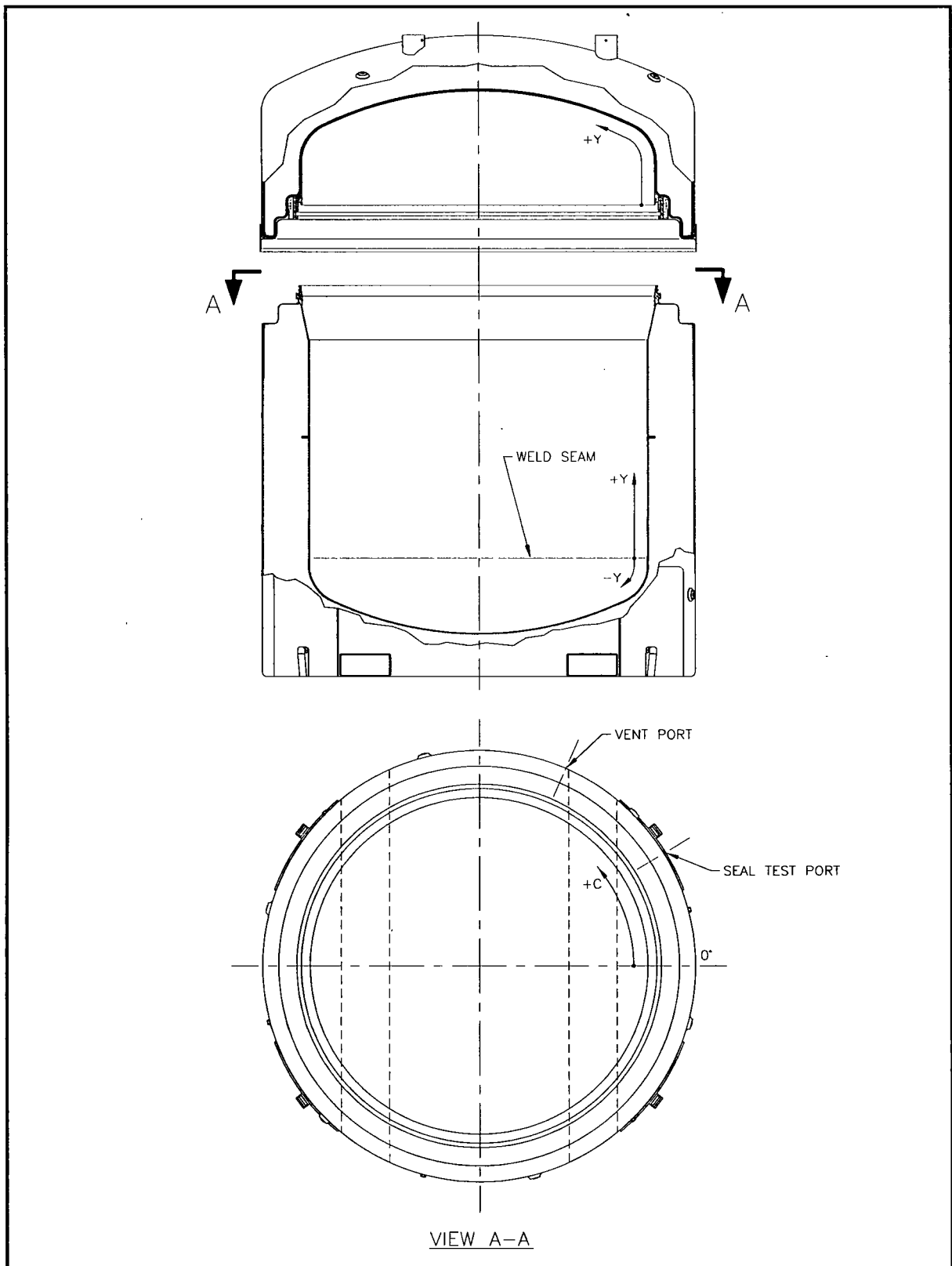


Figure 2.10.3-9 – CTU-2 OCV Temperature Indicating Label Locations

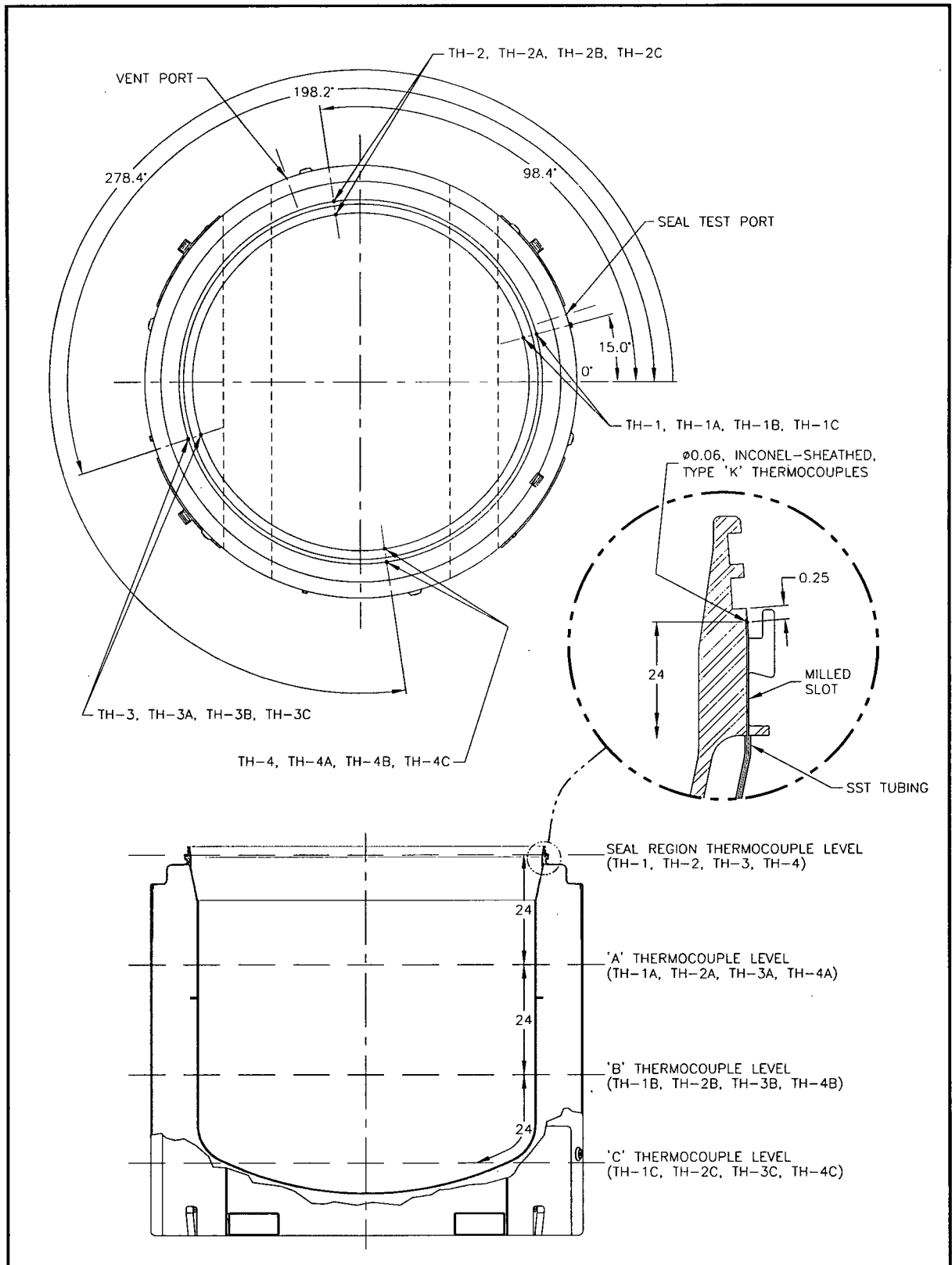


Figure 2.10.3-10 – CTU-1 OCV Thermocouple Locations

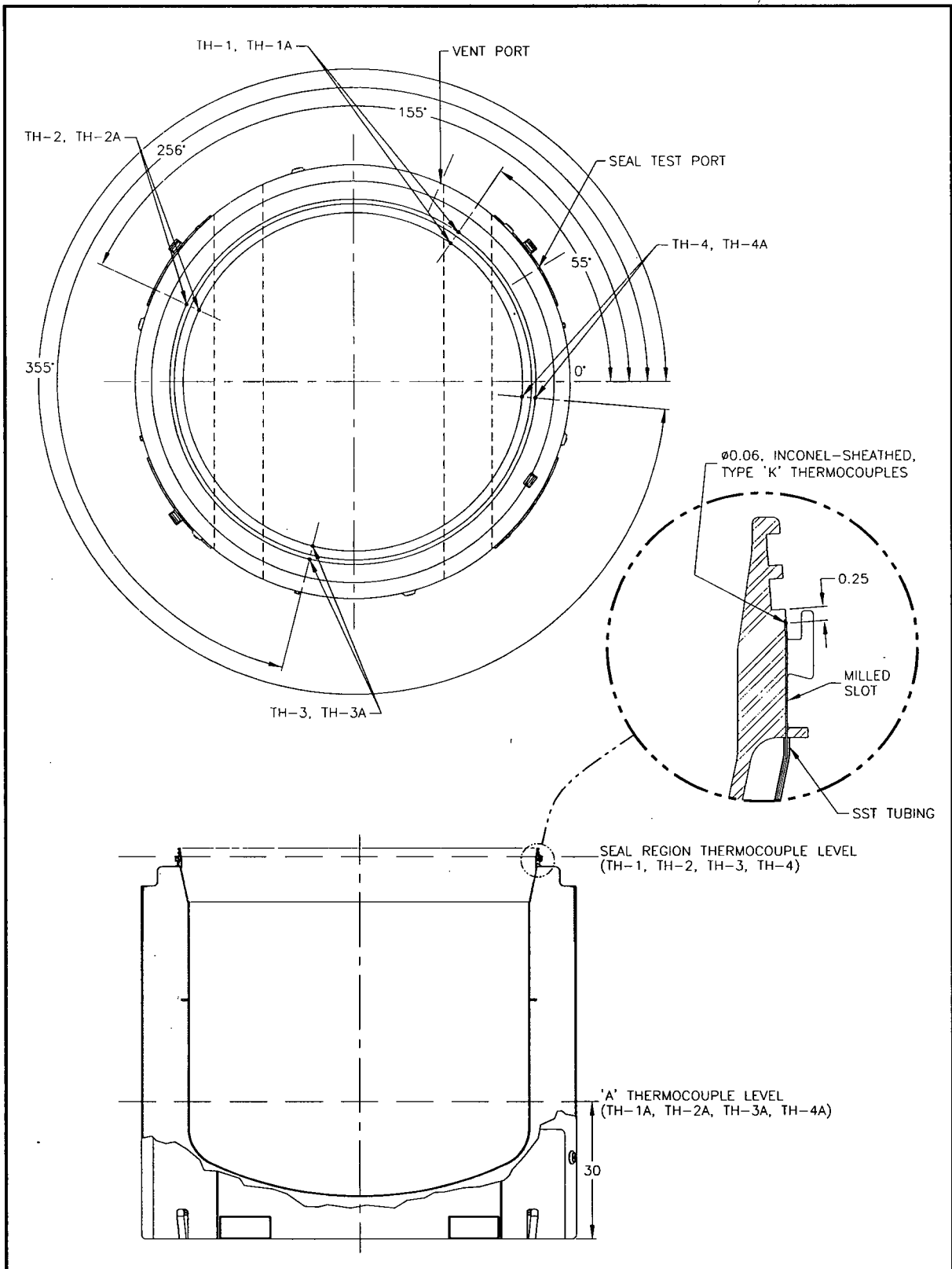


Figure 2.10.3-11 – CTU-2 OCV Thermocouple Locations

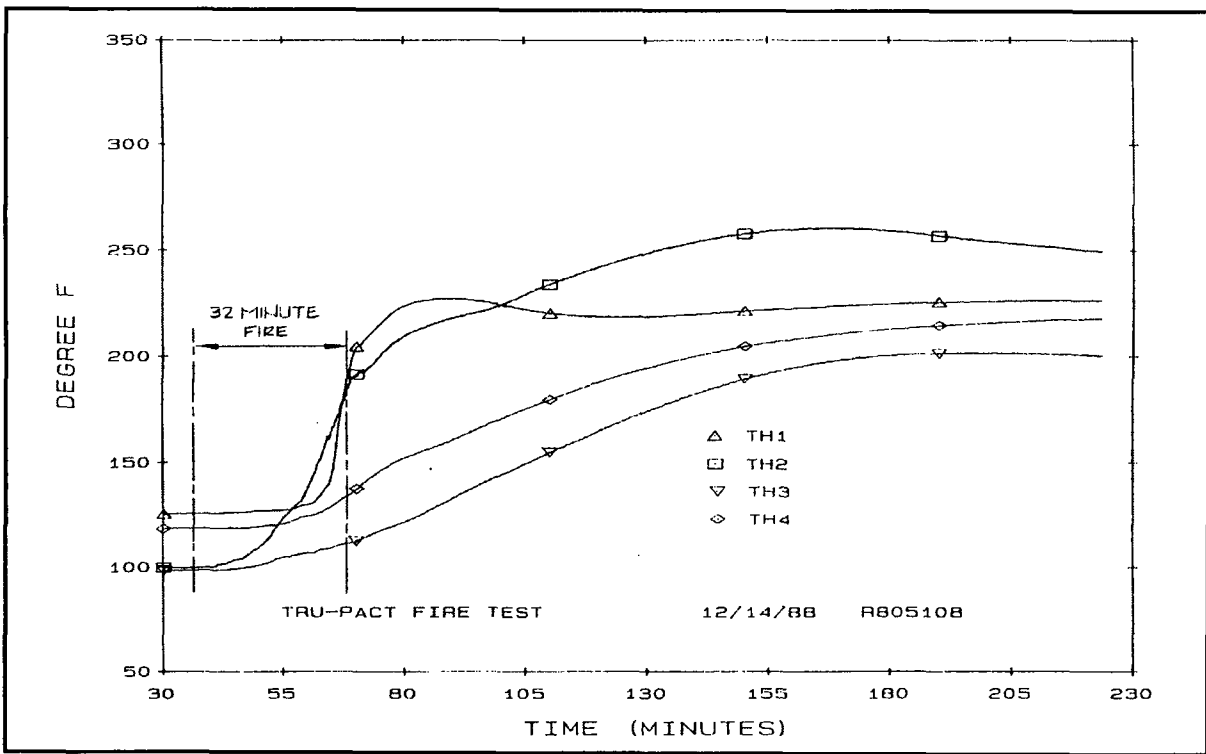


Figure 2.10.3-12 - CTU-1 OCV Thermocouple Data (TH-1, TH-2, TH-3, TH-4)

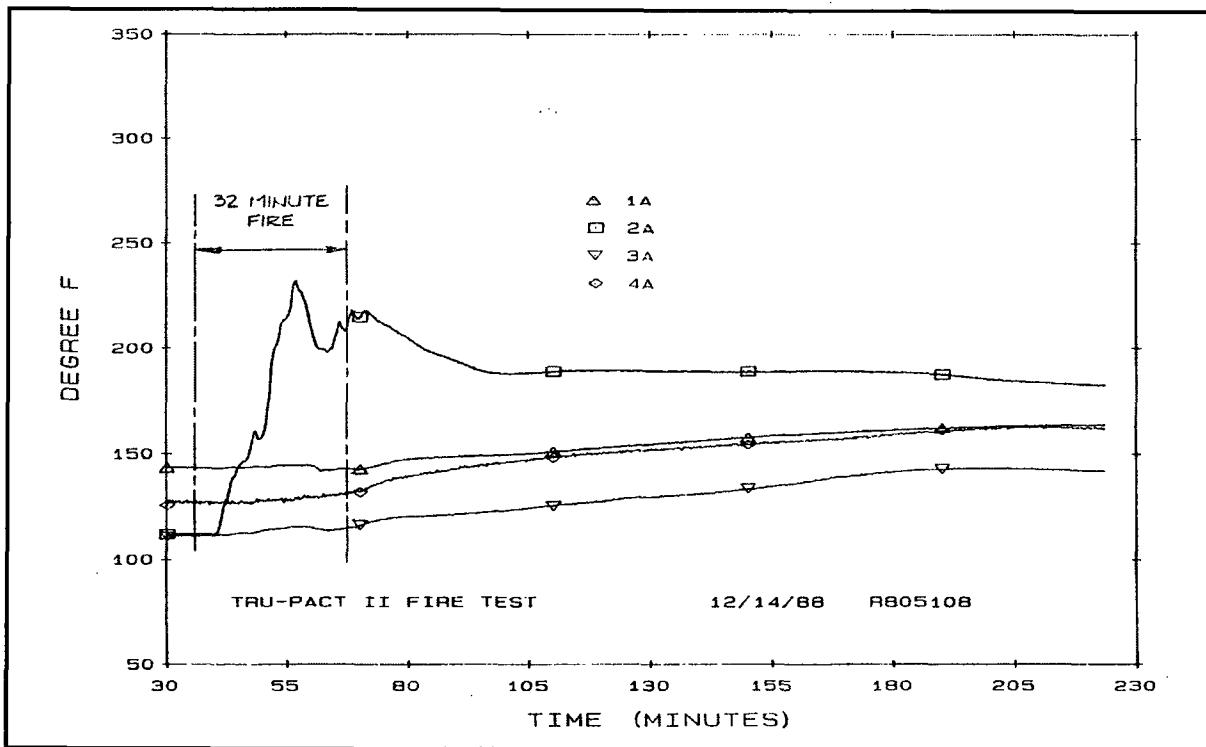


Figure 2.10.3-13 - CTU-1 OCV Thermocouple Data (TH-1A, TH-2A, TH-3A, TH-4A)

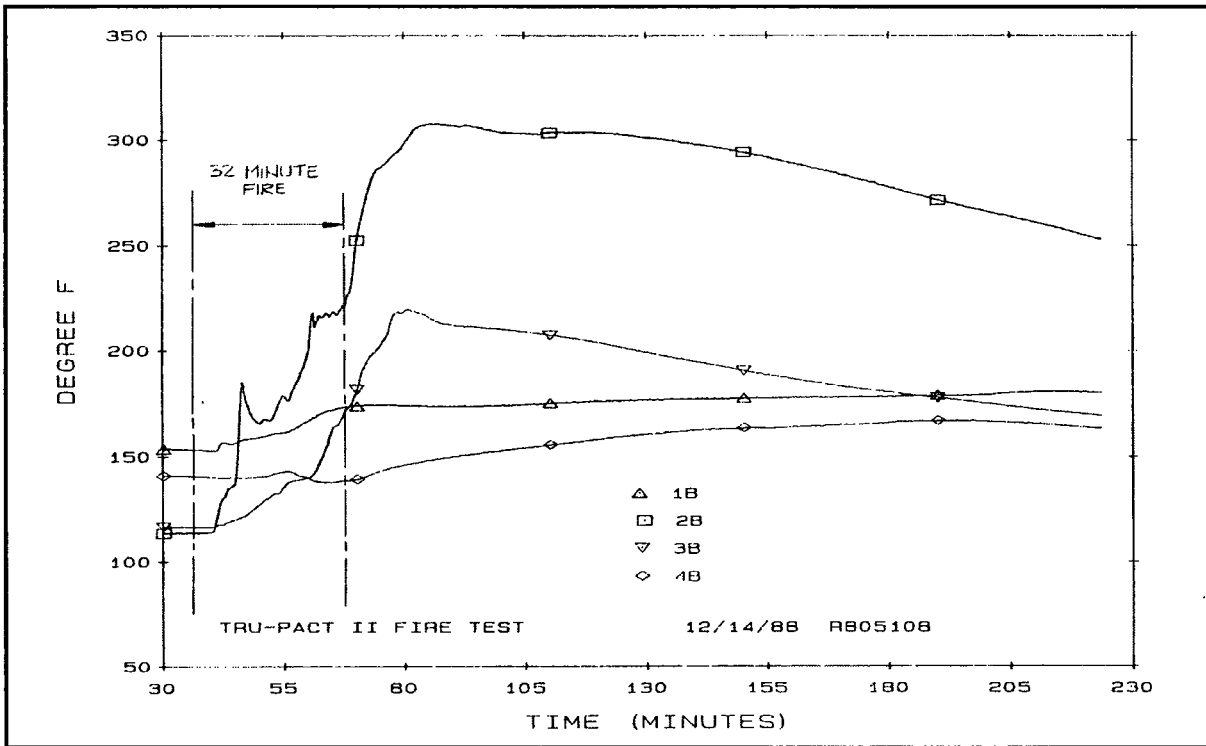


Figure 2.10.3-14 – CTU-1 OCV Thermocouple Data (TH-1C, TH-2C, TH-3C, TH-4C)

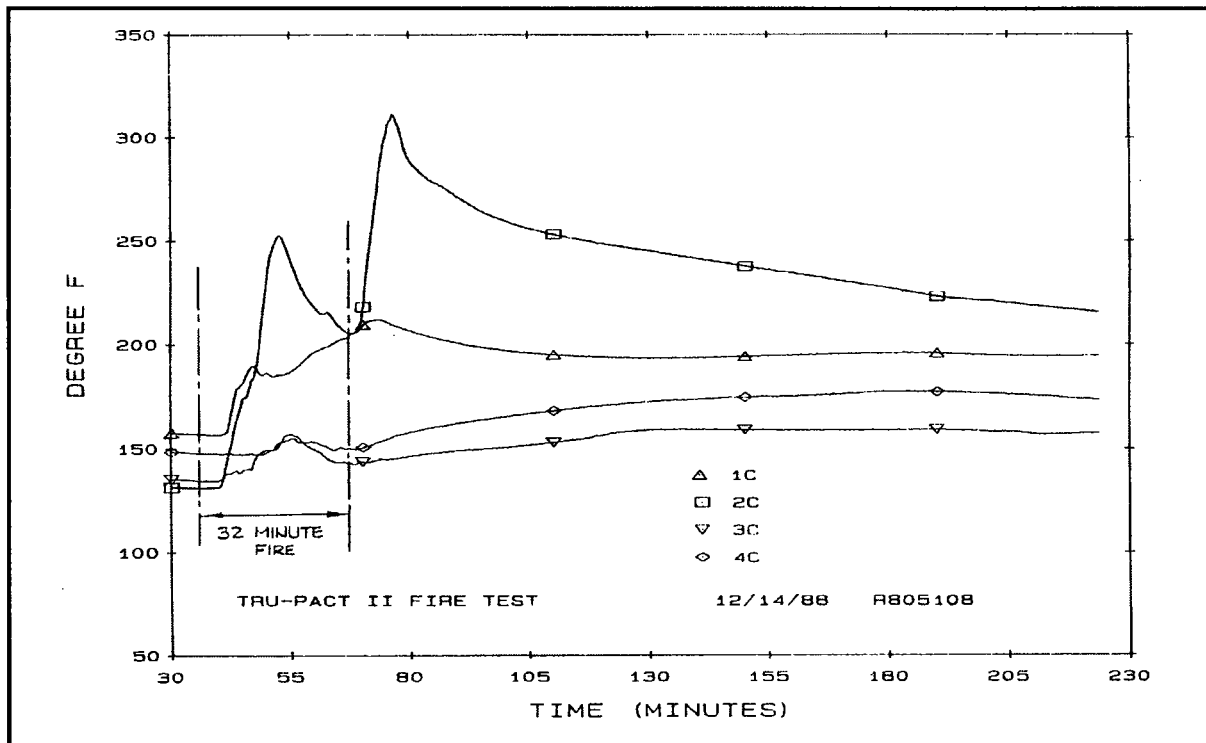


Figure 2.10.3-15 – CTU-1 OCV Thermocouple Data (TH-1D, TH-2D, TH-3D, TH-4D)

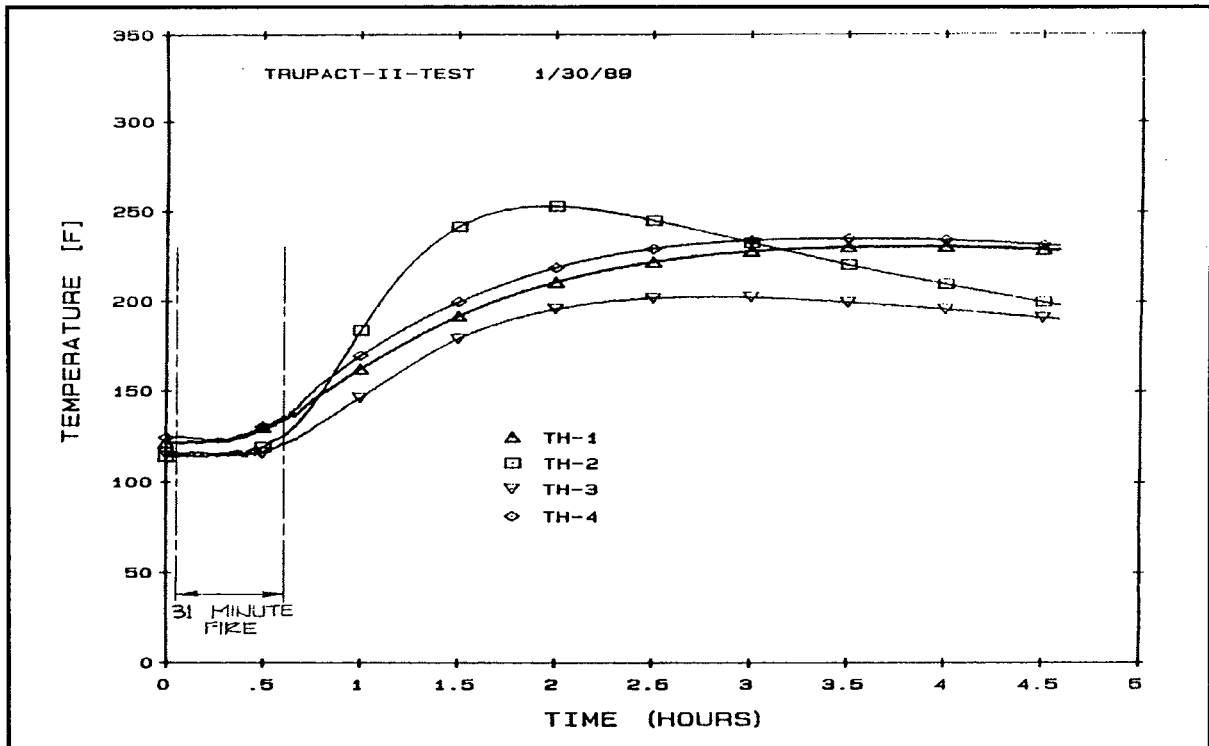


Figure 2.10.3-16 – CTU-2 OCV Thermocouple Data (TH-1, TH-2, TH-3, TH-4)

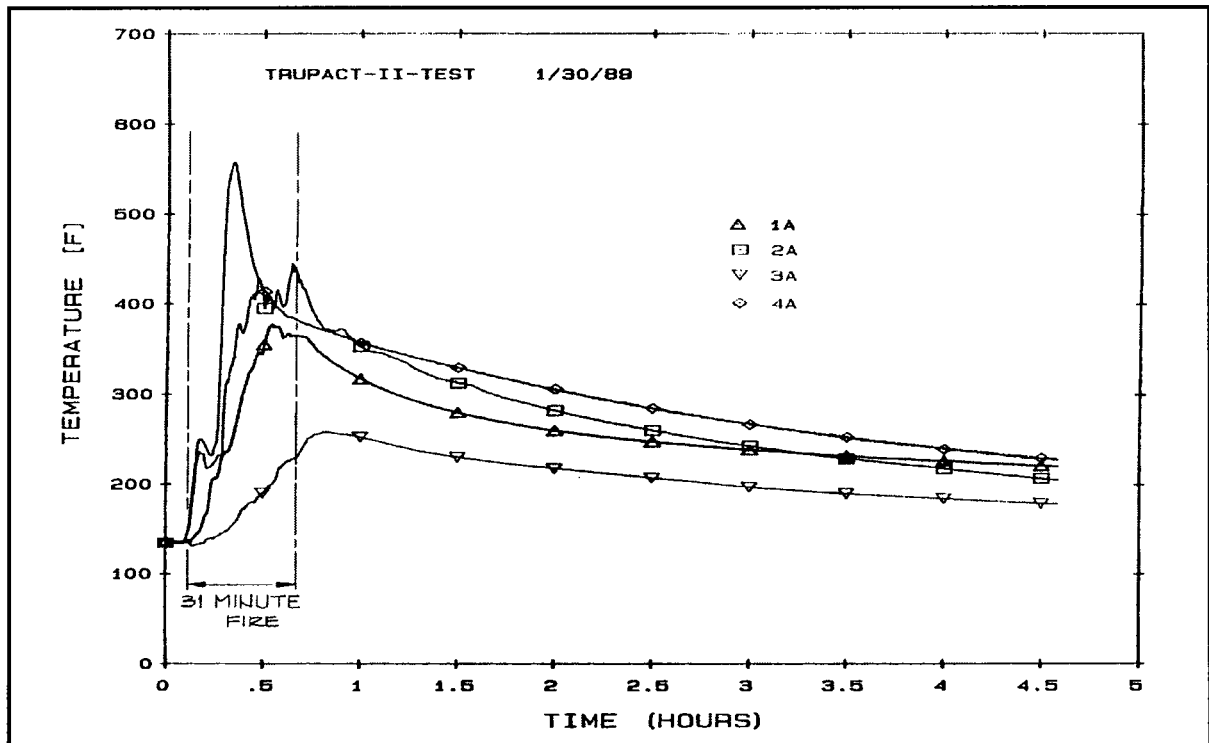


Figure 2.10.3-17 – CTU-2 OCV Thermocouple Data (TH-1A, TH-2A, TH-3A, TH-4A)

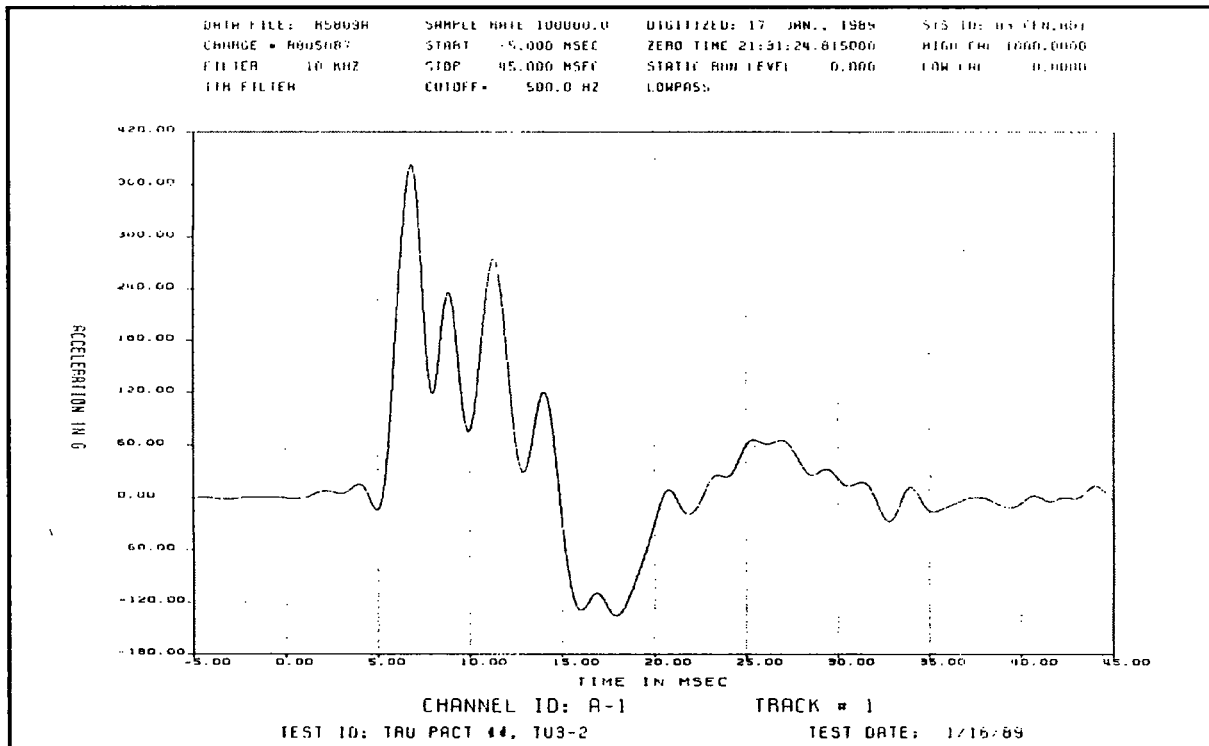


Figure 2.10.3-18 – CTU-2 Free Drop Test No. 2 Accelerometer Data (Gage 1)

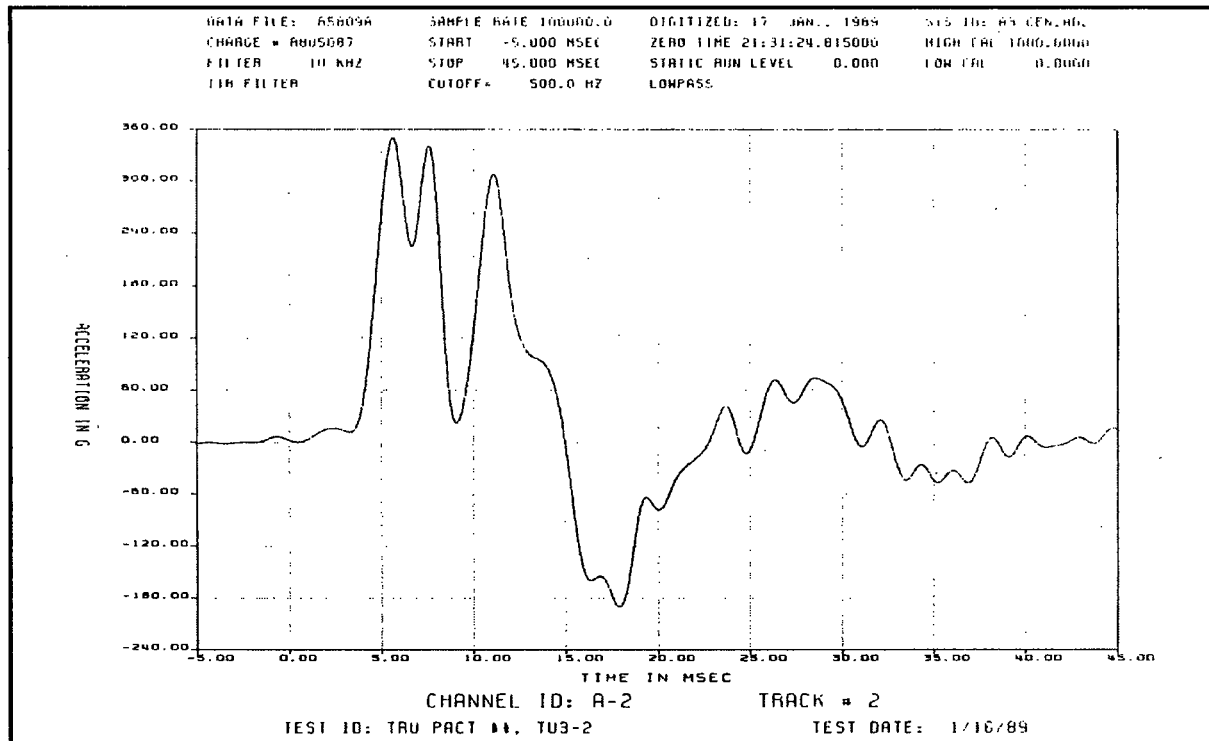


Figure 2.10.3-19 – CTU-2 Free Drop Test No. 2 Accelerometer Data (Gage 2)

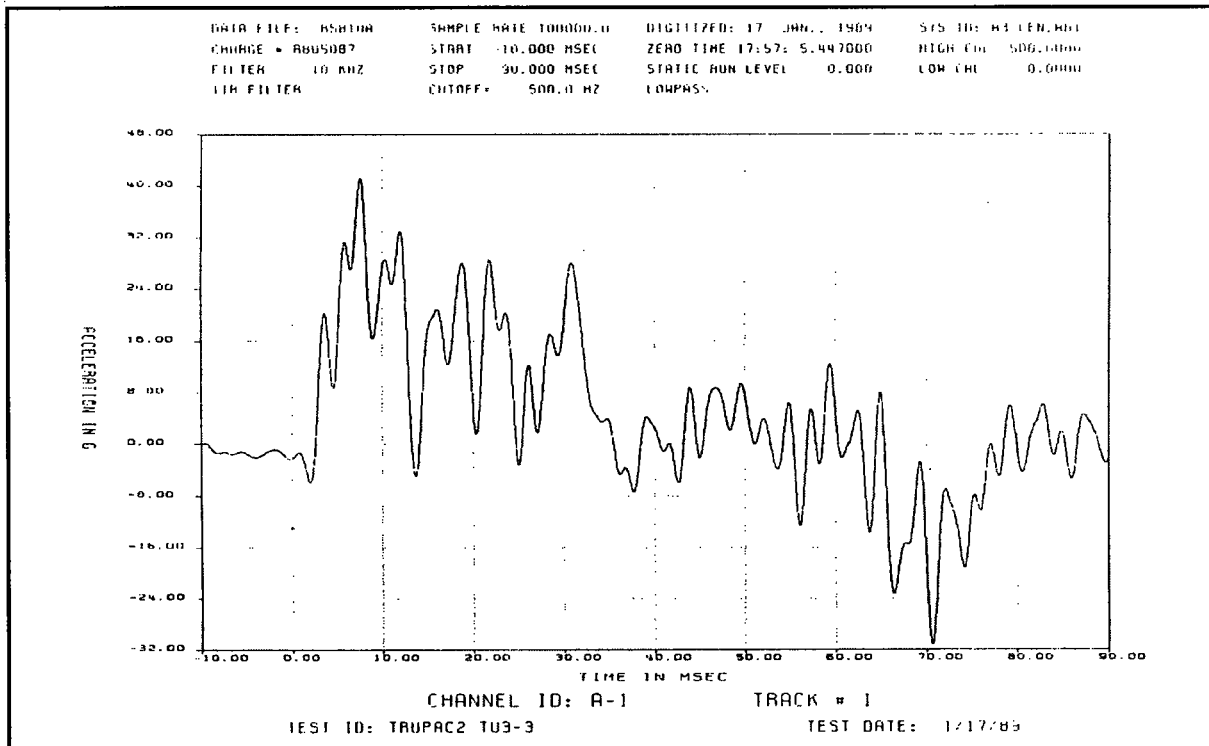


Figure 2.10.3-20 – CTU-2 Free Drop Test No. 3 Accelerometer Data (Gage 1)

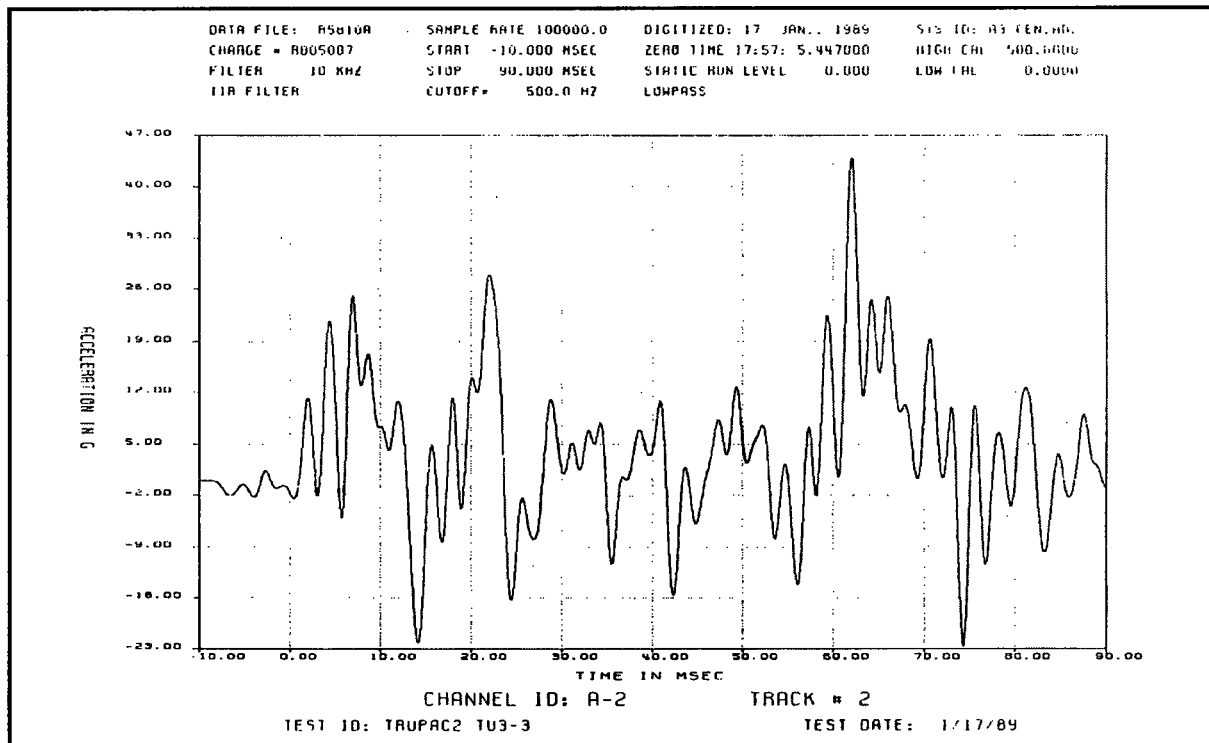


Figure 2.10.3-21 – CTU-2 Free Drop Test No. 3 Accelerometer Data (Gage 2)

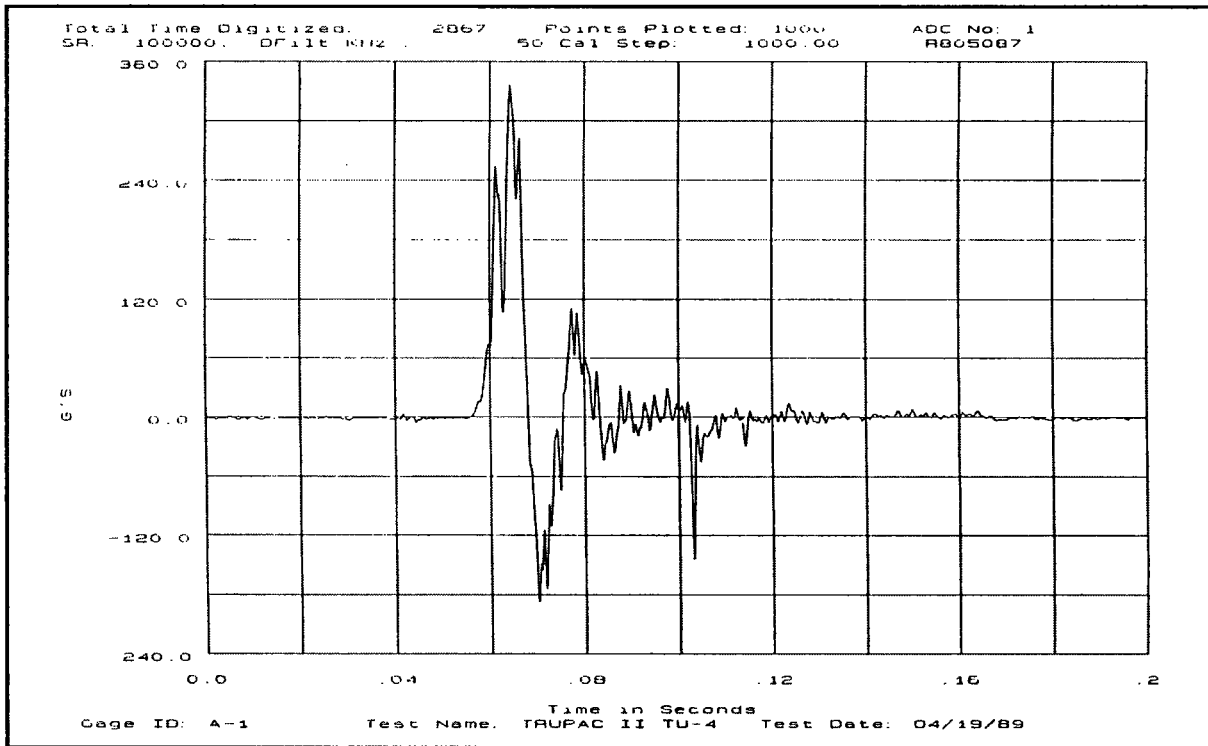


Figure 2.10.3-22 – CTU-3 Free Drop Test No. 2 Accelerometer Data (Gage 1)

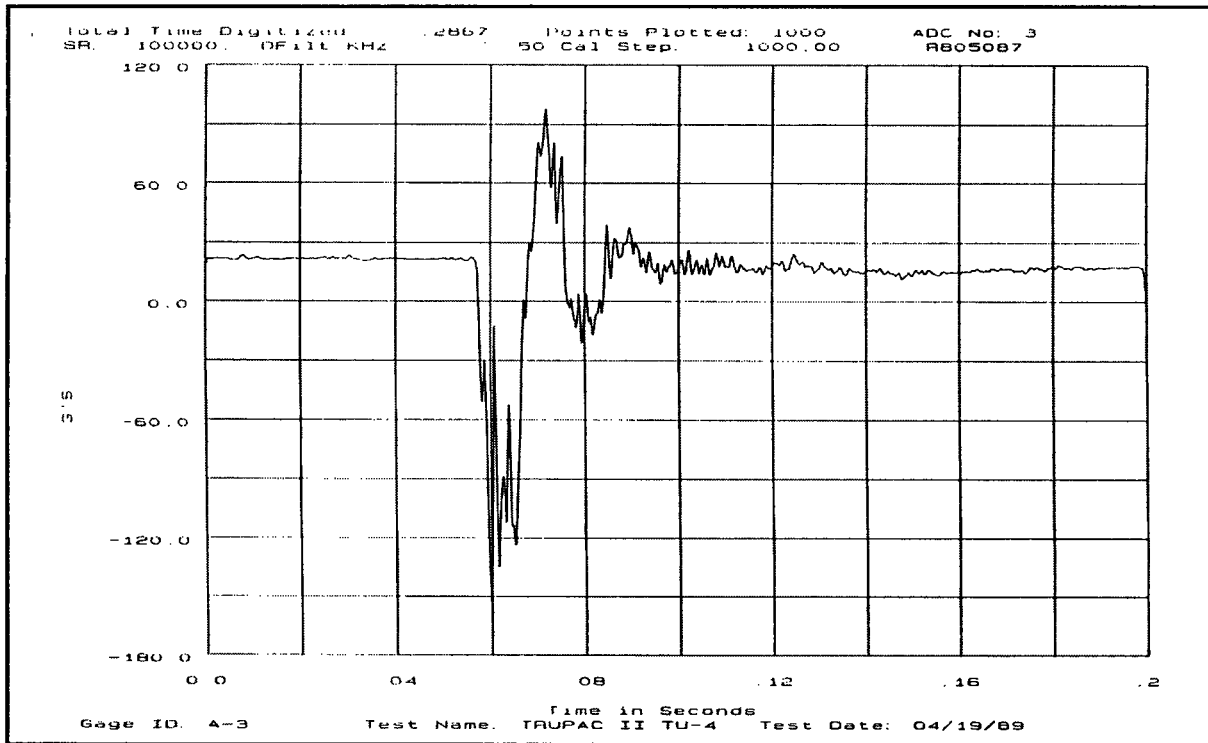


Figure 2.10.3-23 – CTU-3 Free Drop Test No. 2 Accelerometer Data (Gage 2)

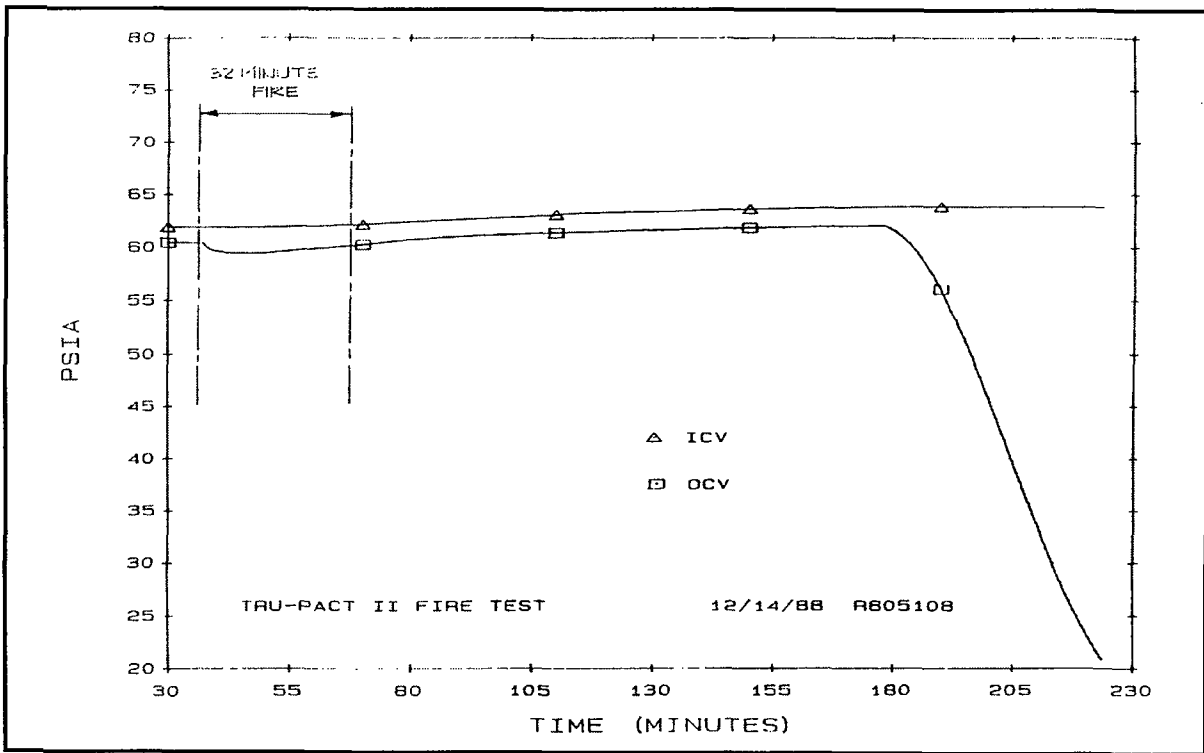


Figure 2.10.3-24 – CTU-1 Pressure Transducer Data During Fire Test No. 10

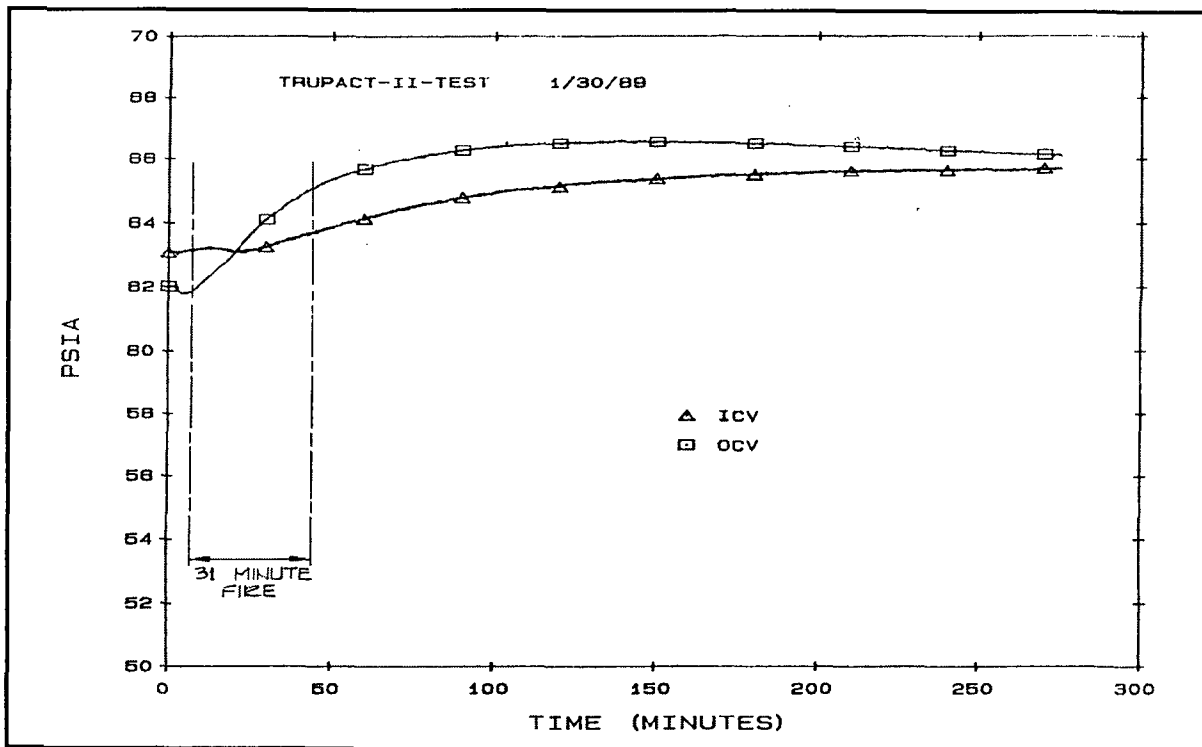
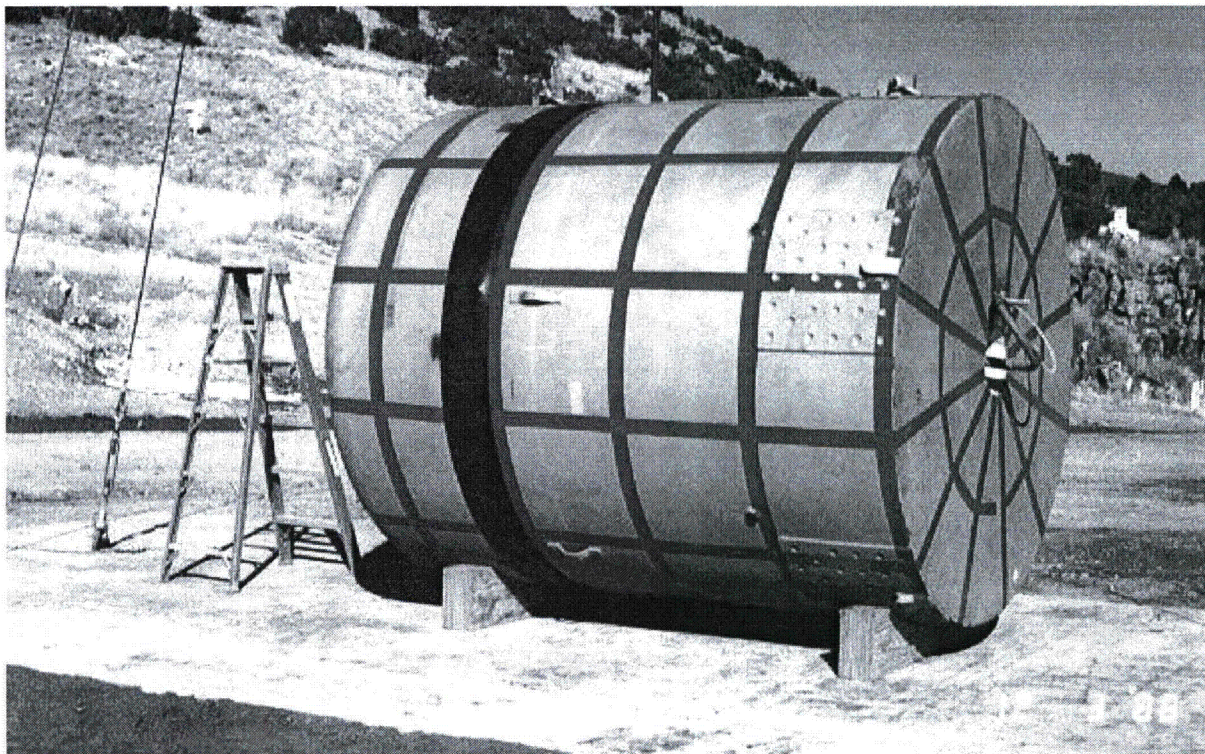
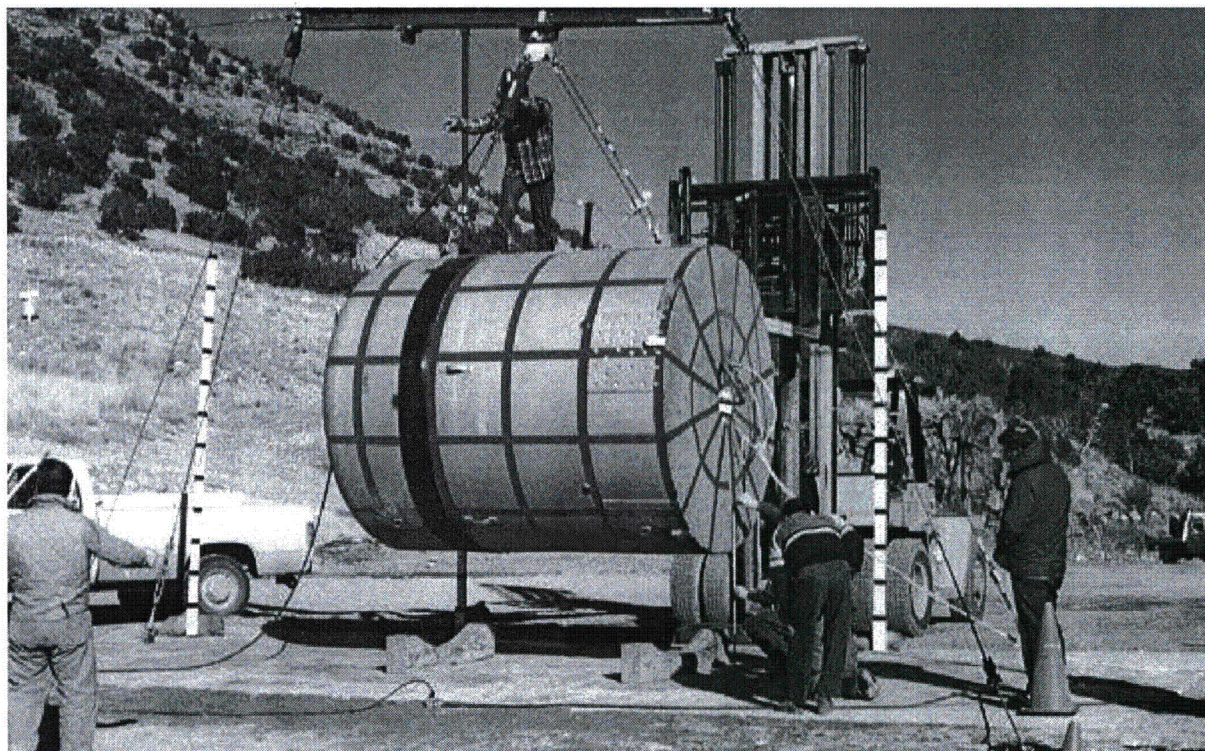


Figure 2.10.3-25 – CTU-2 Pressure Transducer Data During Fire Test No. 9



**Figure 2.10.3-26 – CTU-1 Free Drop No. 1; Initial Preparation for Testing**



**Figure 2.10.3-27 – CTU-1 Free Drop No. 1; Pre-Drop Positioning**

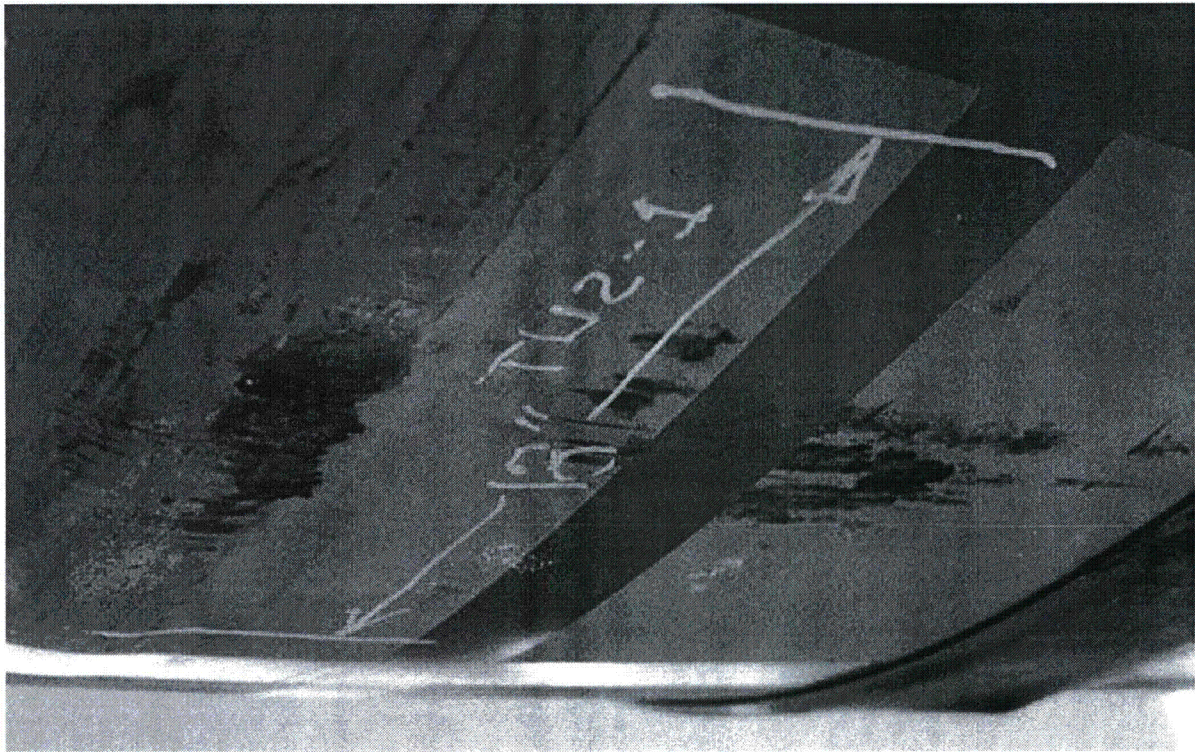


**Figure 2.10.3-28** – CTU-1 Free Drop No. 1; Post-Drop Damage at Top (Lid)

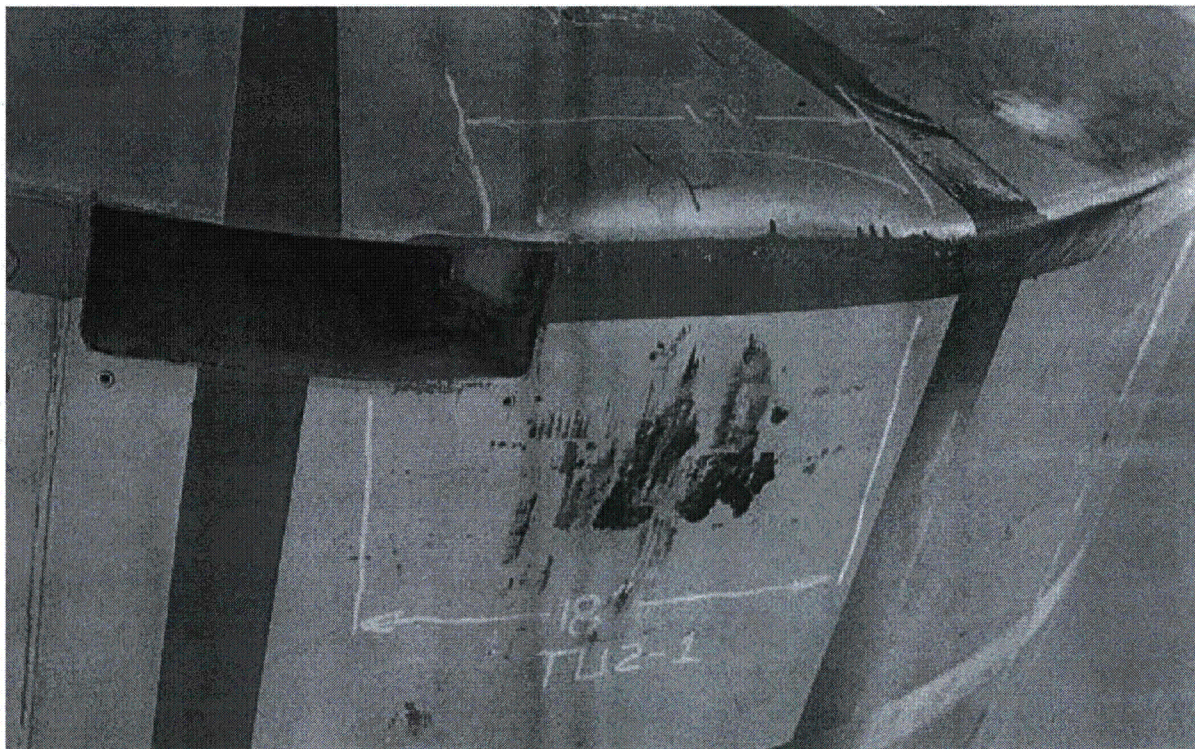


**Figure 2.10.3-29** – CTU-1 Free Drop No. 1; Post-Drop Damage at Bottom (Body)

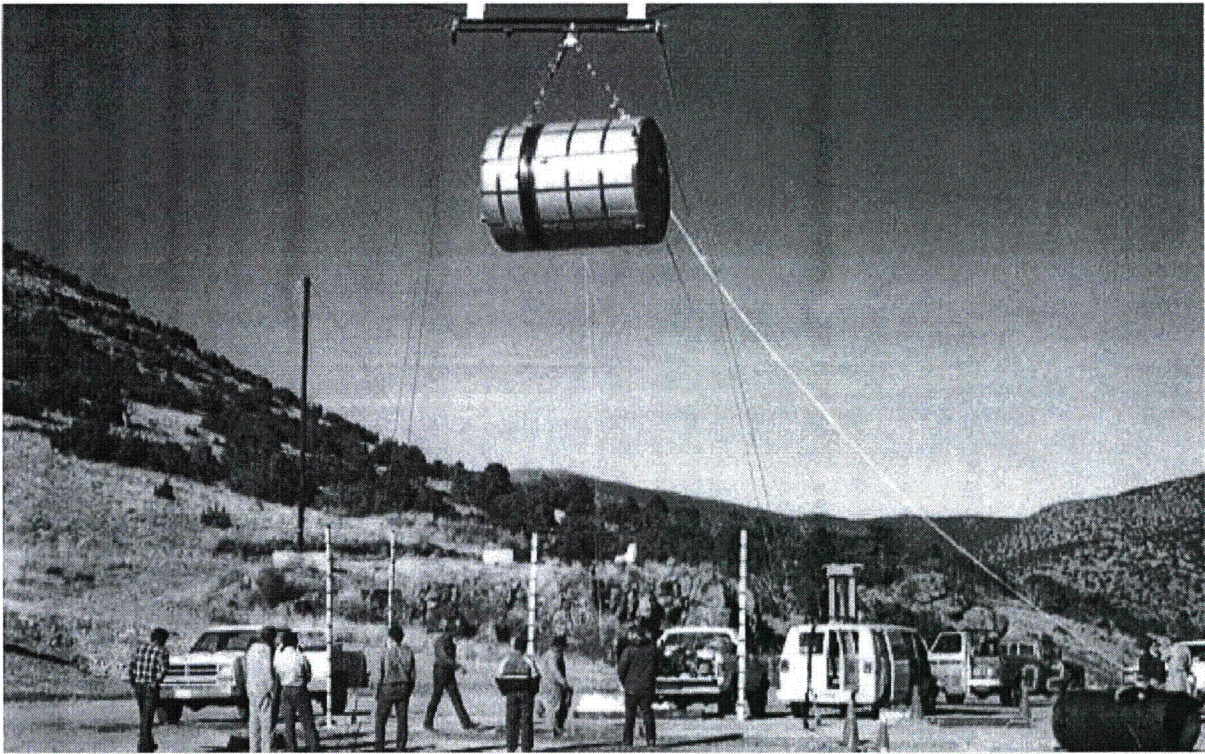


**Figure 2.10.3-30 – CTU-1 Free Drop No. 2; Pre-Drop Positioning**



**Figure 2.10.3-31 – CTU-1 Free Drop No. 2; Post-Drop Damage**



**Figure 2.10.3-32** – CTU-1 Free Drop No. 3; Pre-Drop Positioning

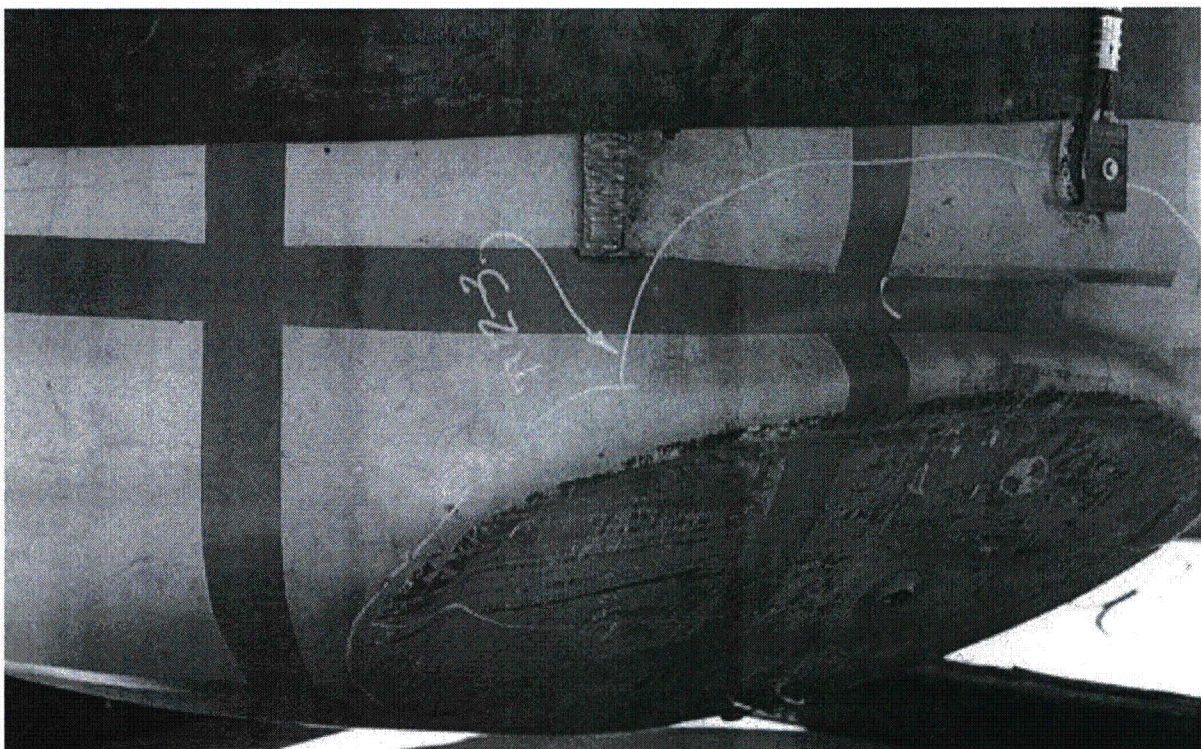


**Figure 2.10.3-33** – CTU-1 Free Drop No. 3; Post-Drop Damage

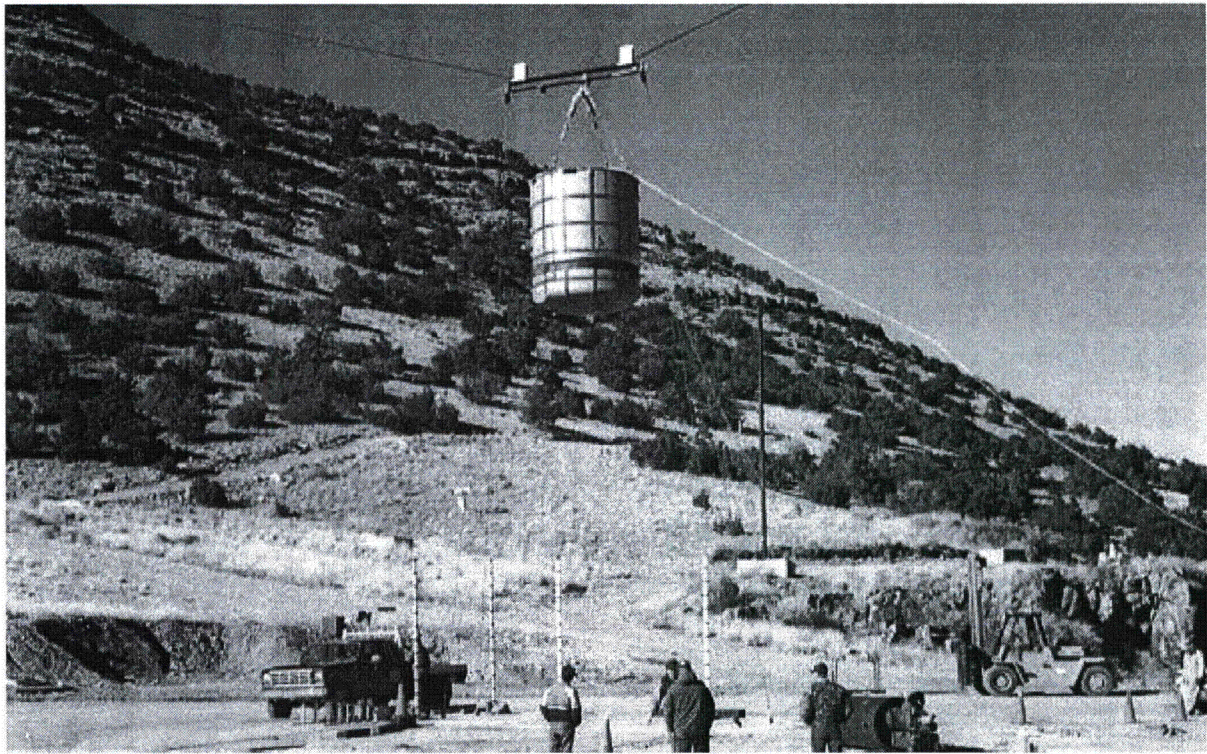


**Figure 2.10.3-34 – CTU-1 Free Drop No. 4; Pre-Drop Positioning**

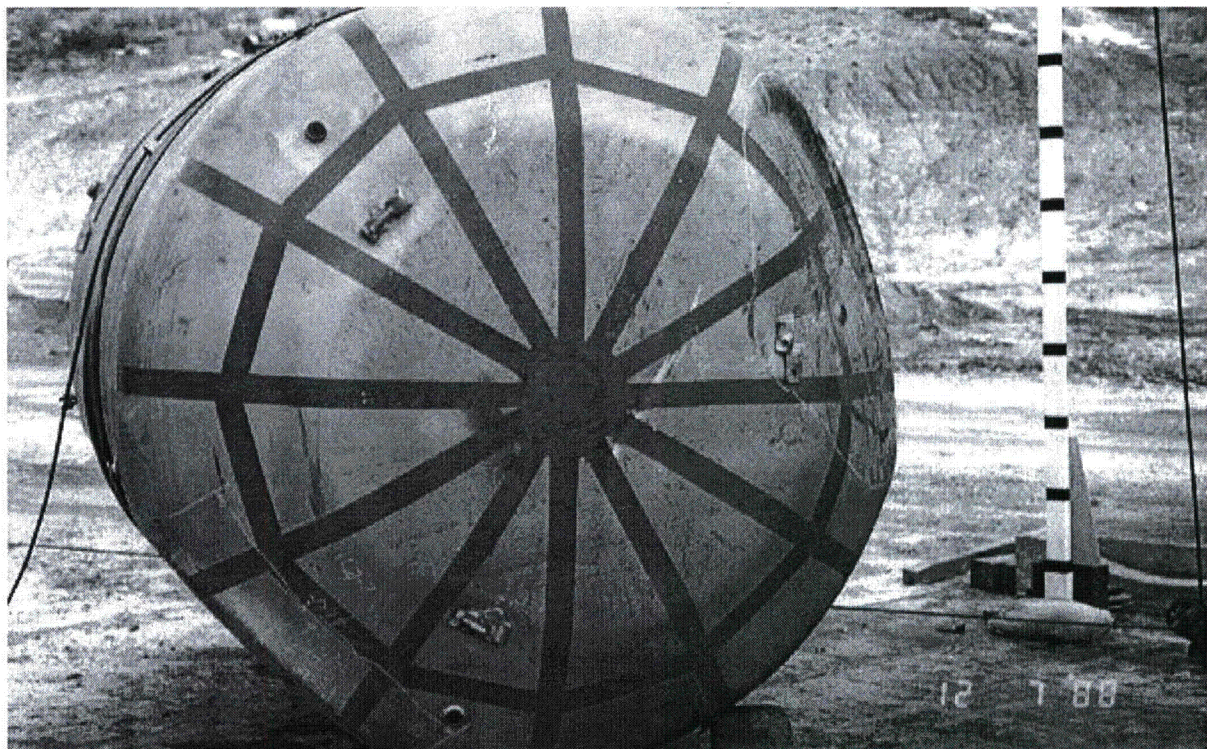


**Figure 2.10.3-35 – CTU-1 Free Drop No. 4; Post-Drop Damage**

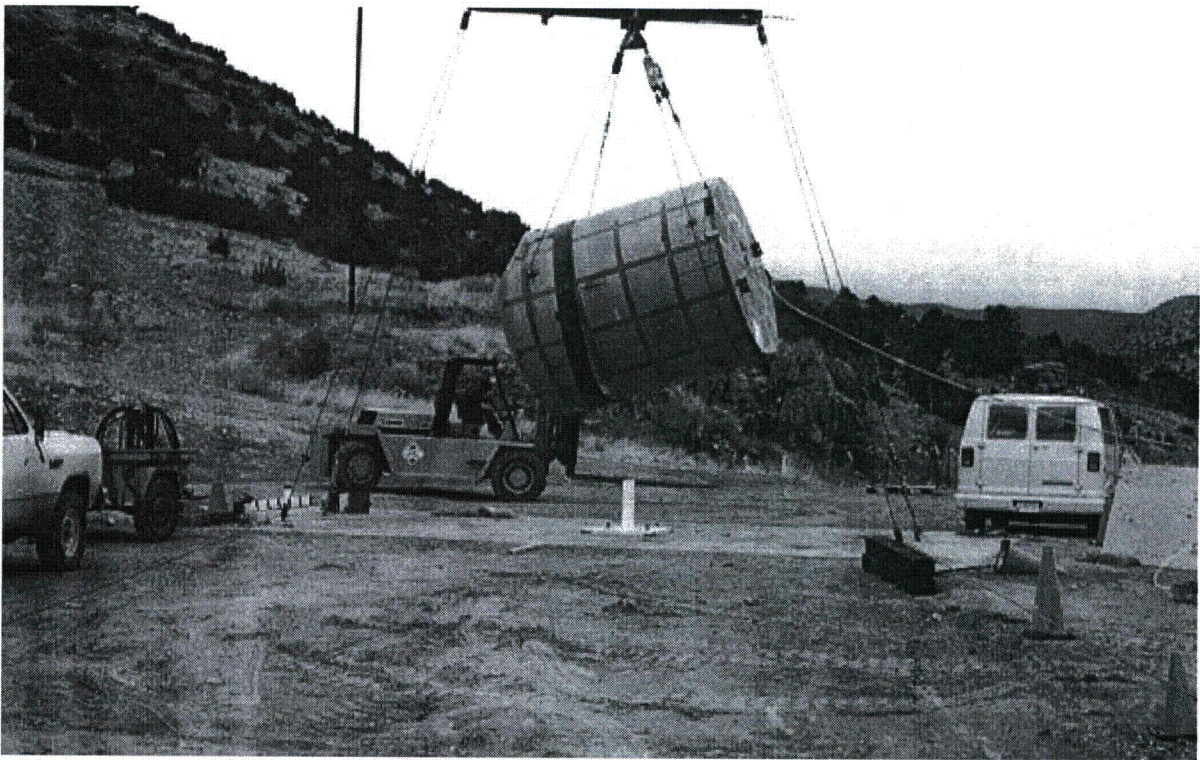


Figure 2.10.3-36 – CTU-1 Puncture Drop No. 5; Pre-Drop Positioning

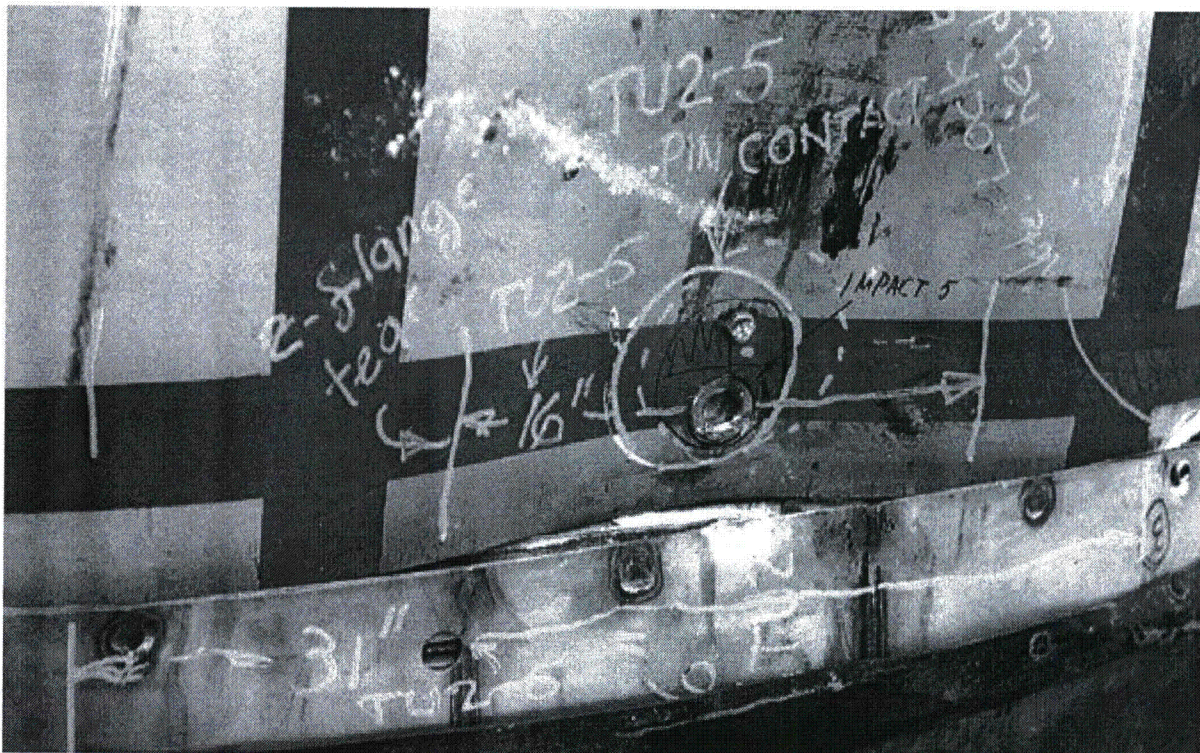


Figure 2.10.3-37 – CTU-1 Puncture Drop No. 5; Post-Drop Damage

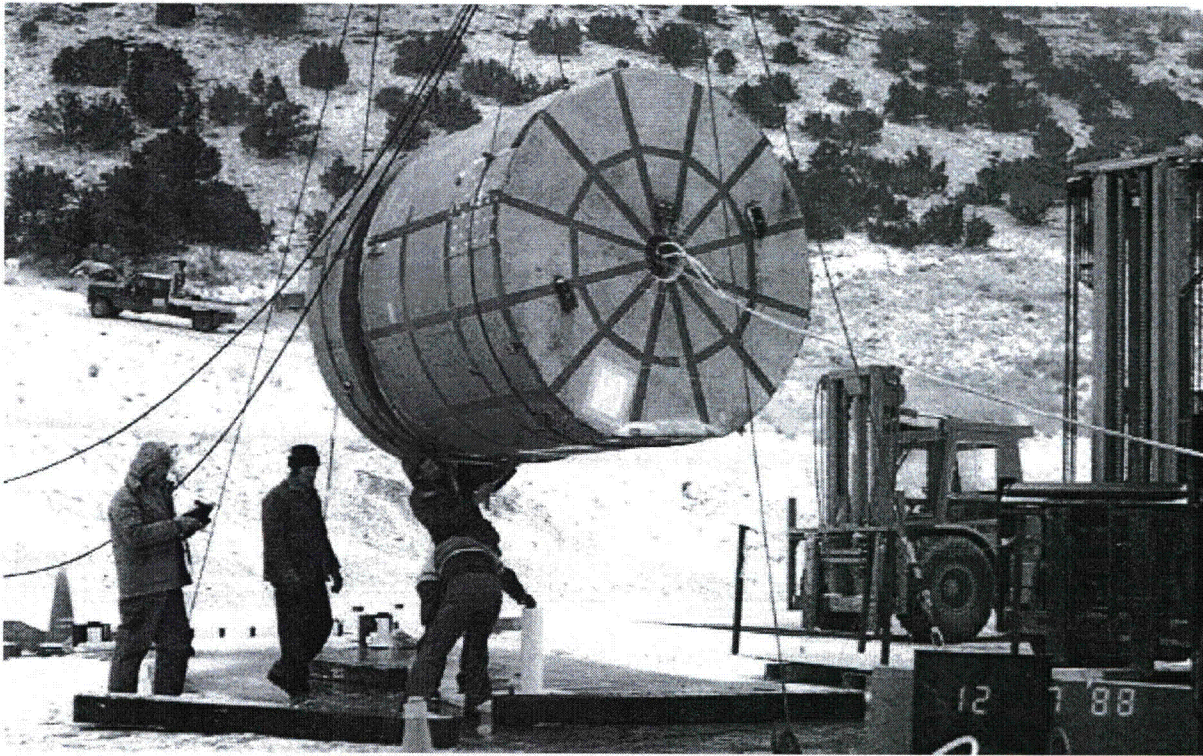


Figure 2.10.3-38 – CTU-1 Puncture Drop No. 6; Pre-Drop Positioning

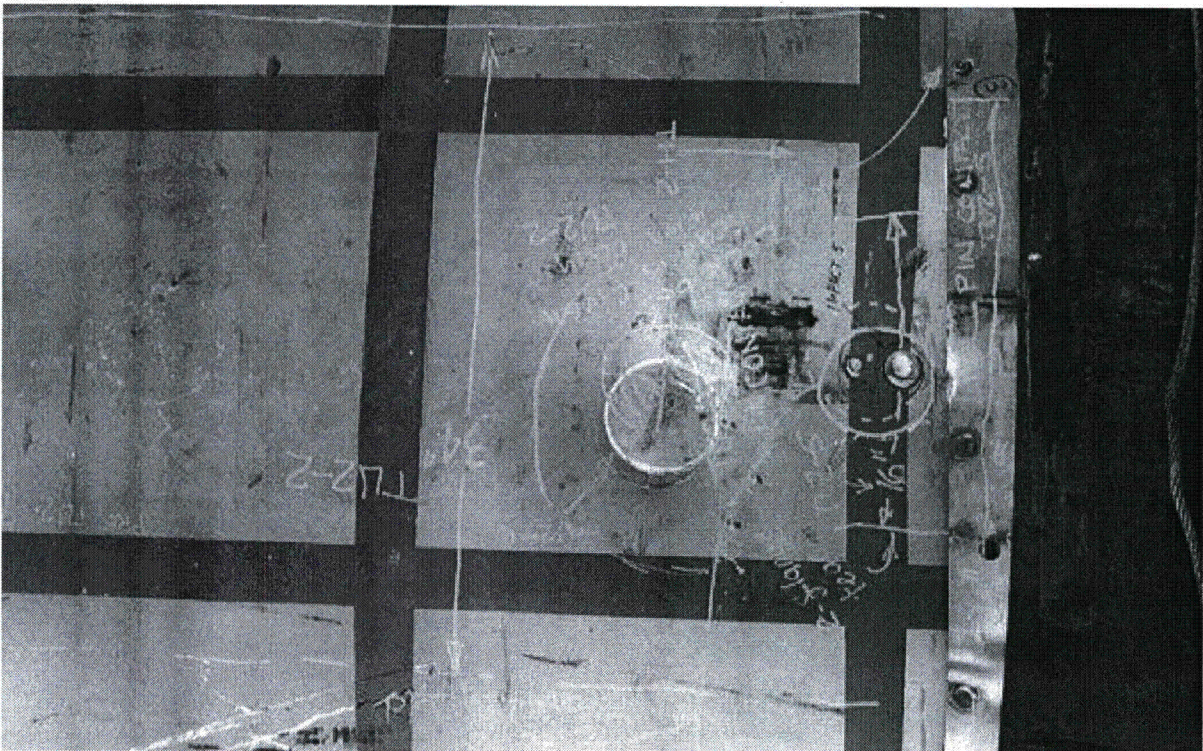
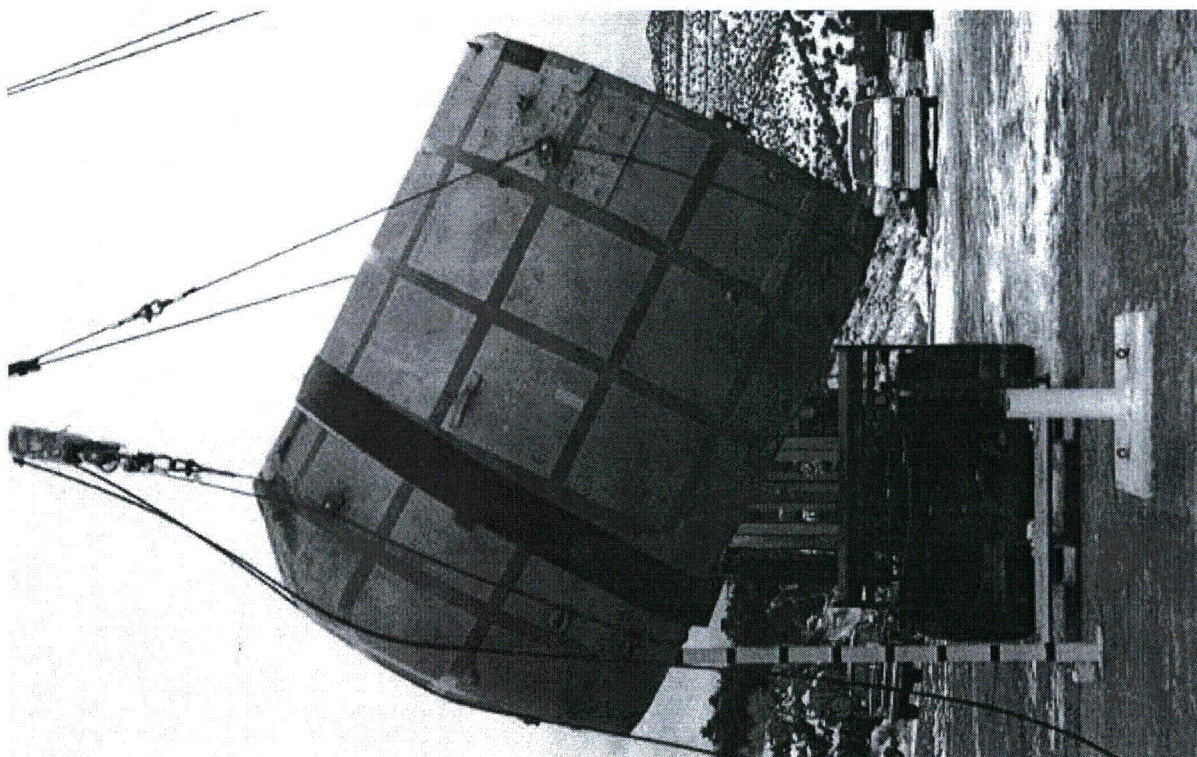
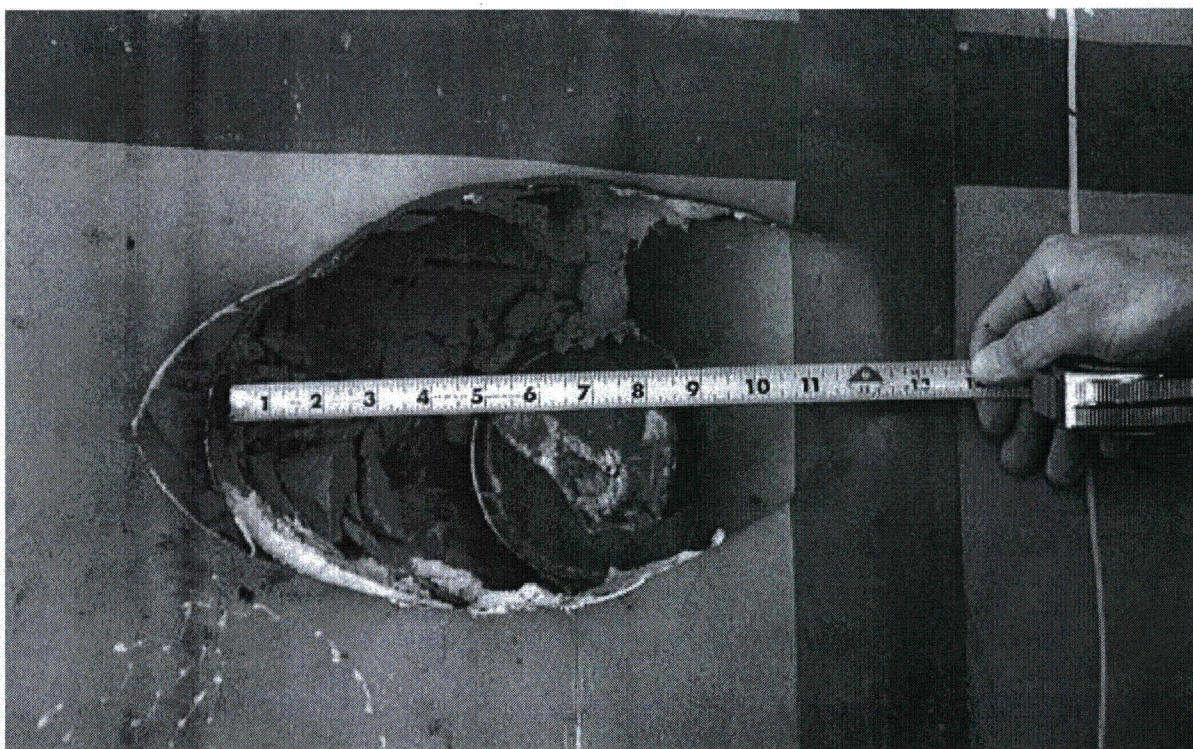


Figure 2.10.3-39 – CTU-1 Puncture Drop No. 6; Post-Drop Damage



**Figure 2.10.3-40** – CTU-1 Puncture Drop No. 7; Pre-Drop Positioning



**Figure 2.10.3-41** – CTU-1 Puncture Drop No. 7; Post-Drop Damage

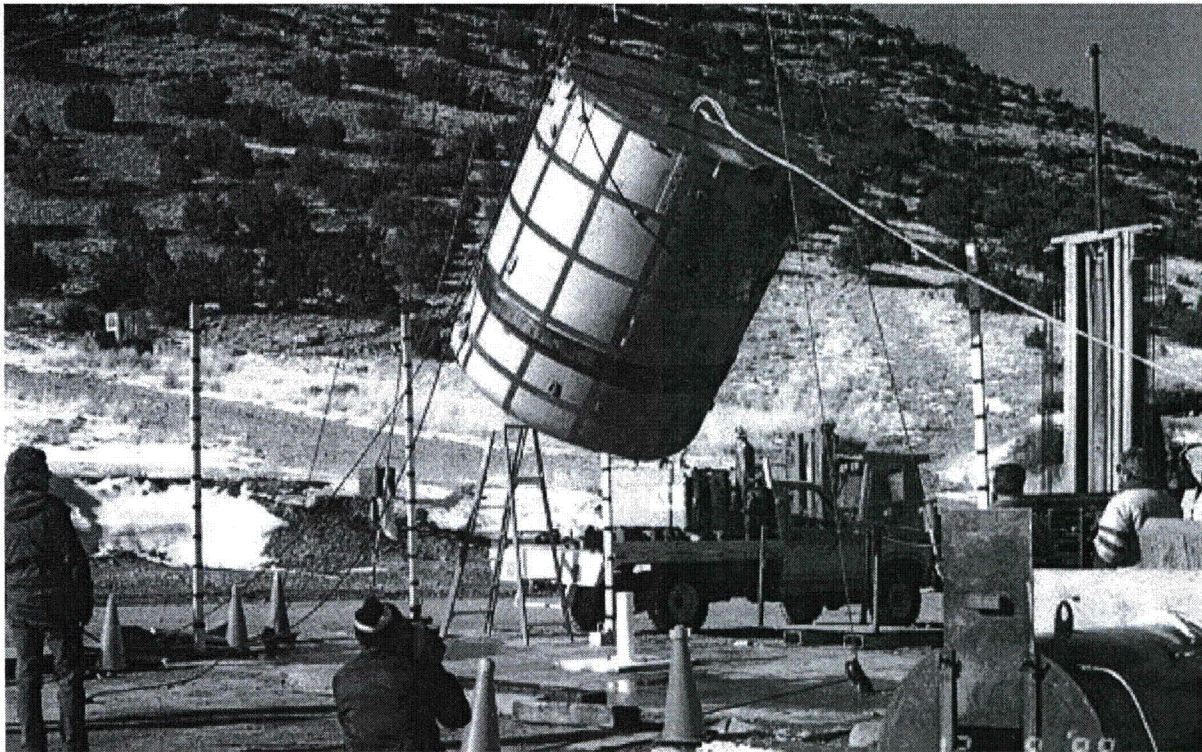


**Figure 2.10.3-42** – CTU-1 Puncture Drop No. 8; Pre-Drop Positioning

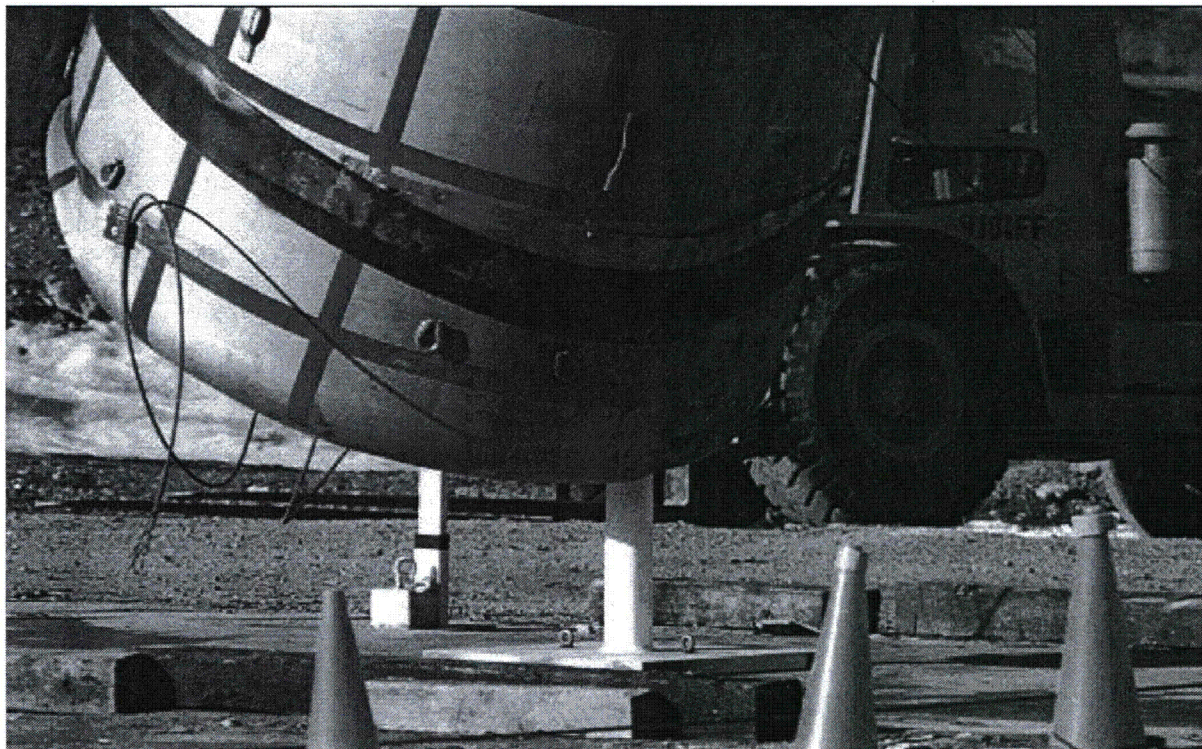


**Figure 2.10.3-43** – CTU-1 Puncture Drop No. 8; Moment of Impact

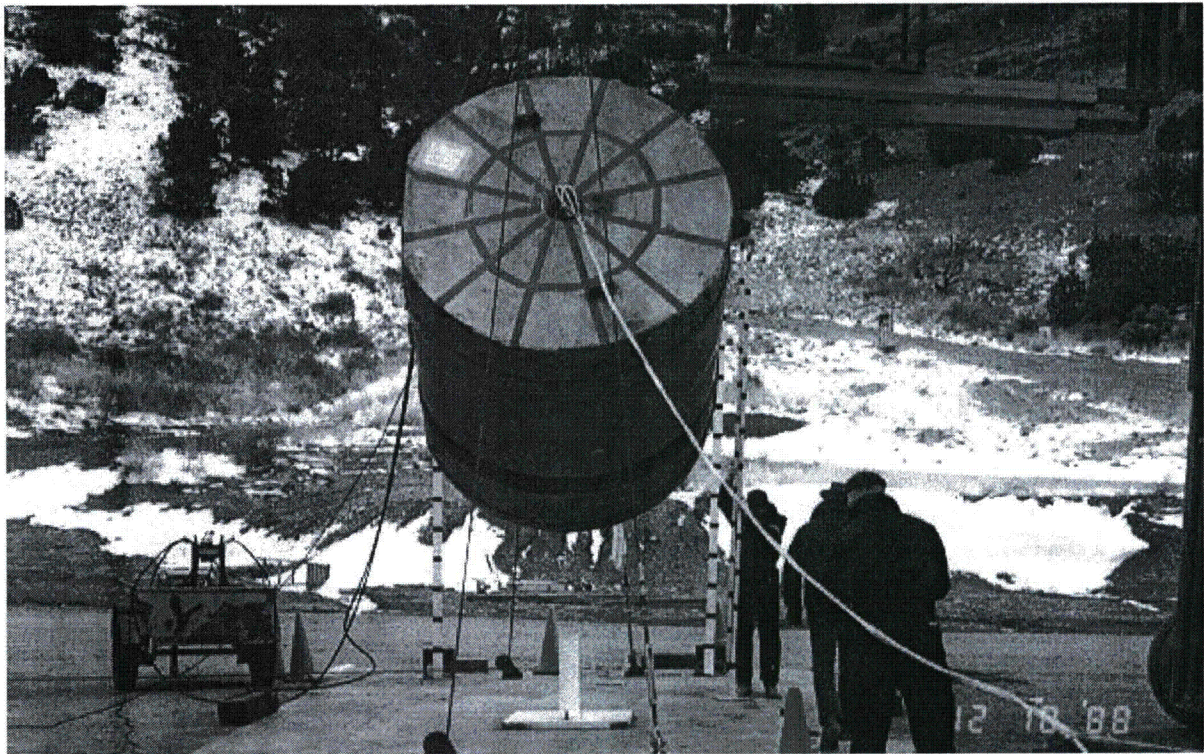


**Figure 2.10.3-44** – CTU-1 Puncture Drop No. 9; Pre-Drop Positioning

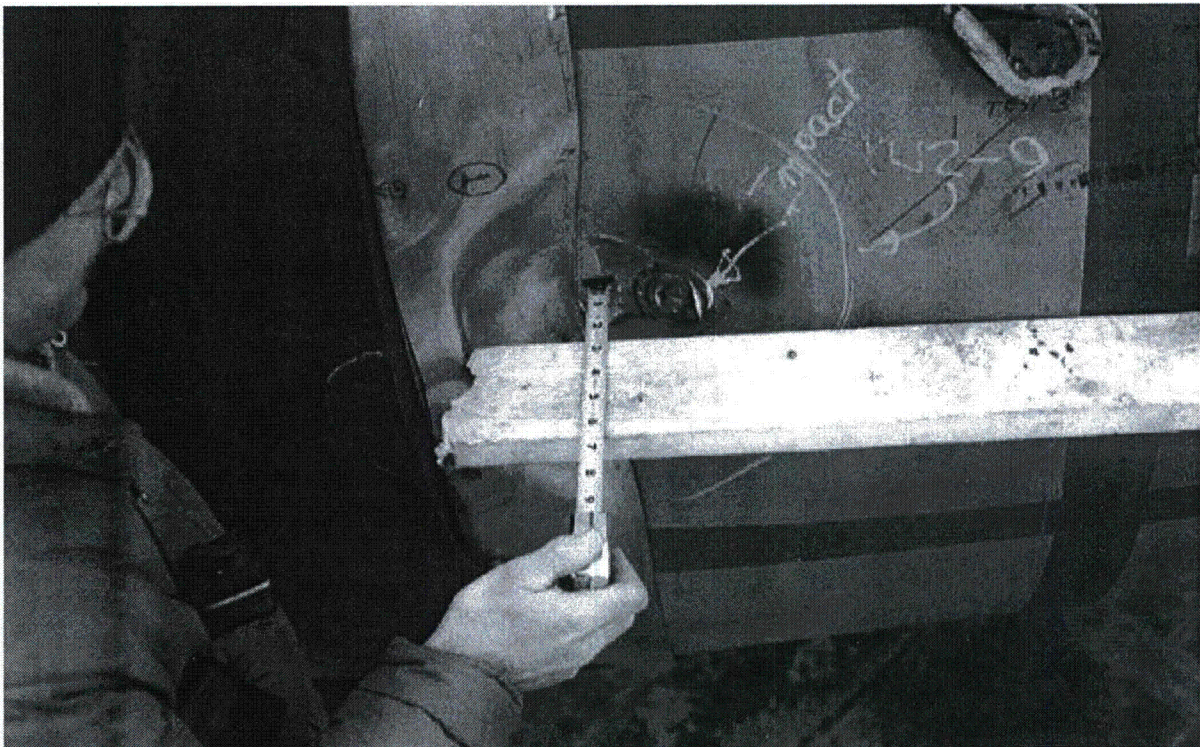


**Figure 2.10.3-45** – CTU-1 Puncture Drop No. 9; Post-Drop Damage

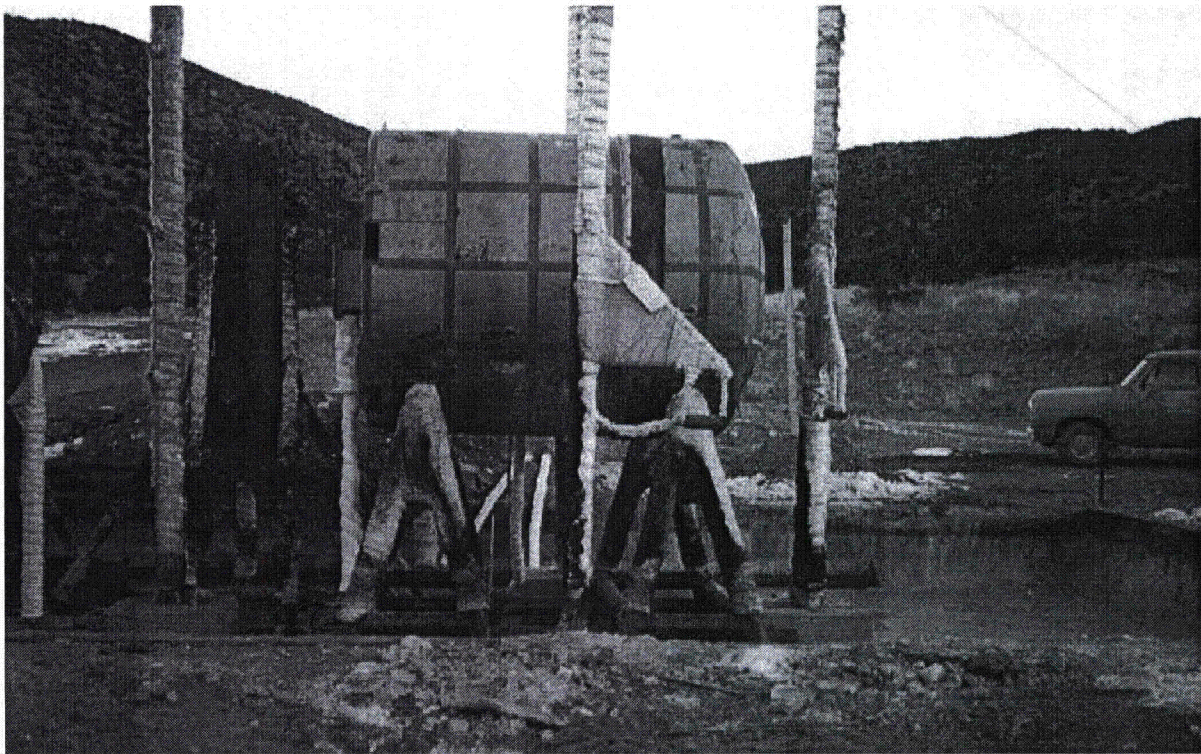


**Figure 2.10.3-46** – CTU-1 Fire No. 10; Pre-Fire Positioning, Side View

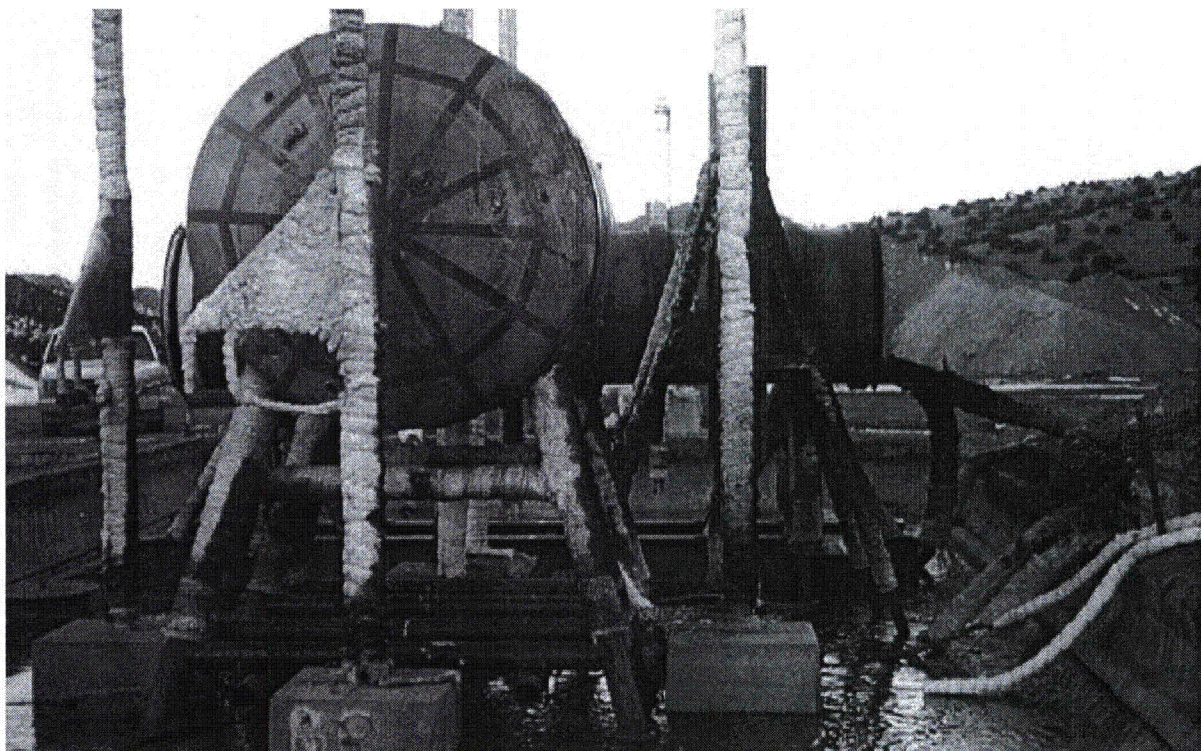


**Figure 2.10.3-47** – CTU-1 Fire No. 10; Pre- Fire Positioning, Top End View



**Figure 2.10.3-48 – CTU-1 Fire No. 10; Fully Engulfing Fire**

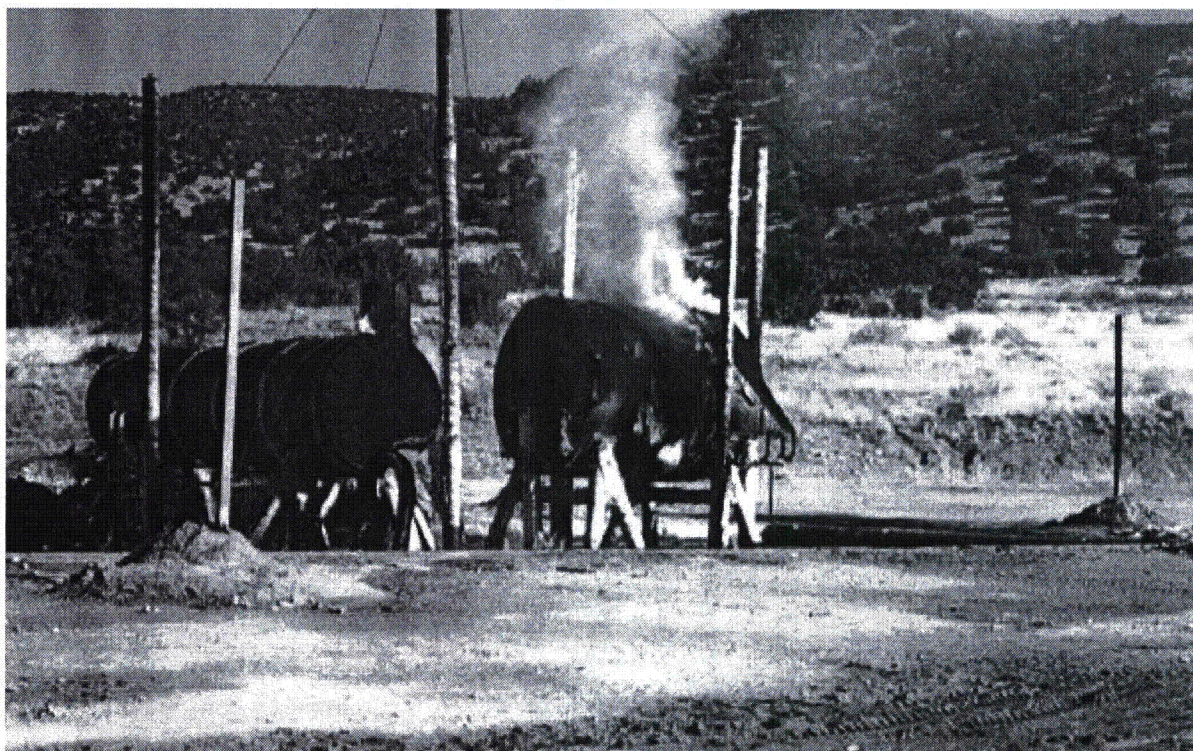


**Figure 2.10.3-49 – CTU-1 Fire No. 10; Post-Fire Cool-Down**

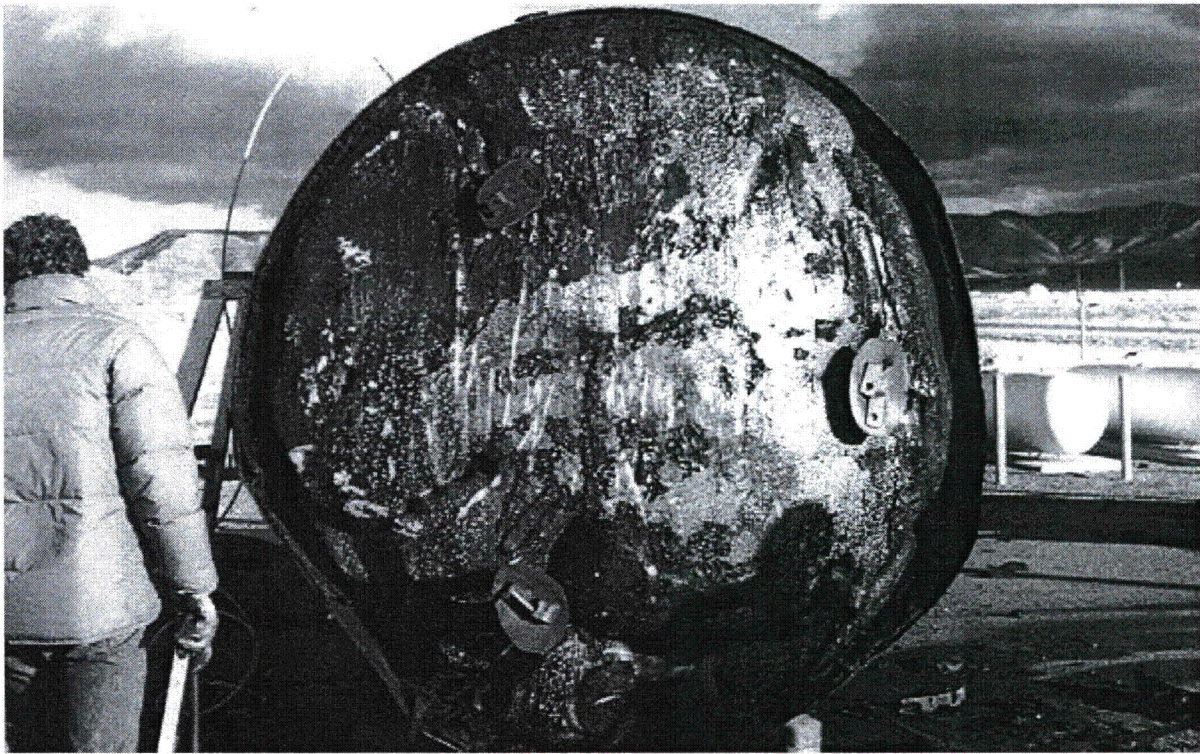


**Figure 2.10.3-50** – CTU-1 Disassembly; OCA Lid Unburned Foam

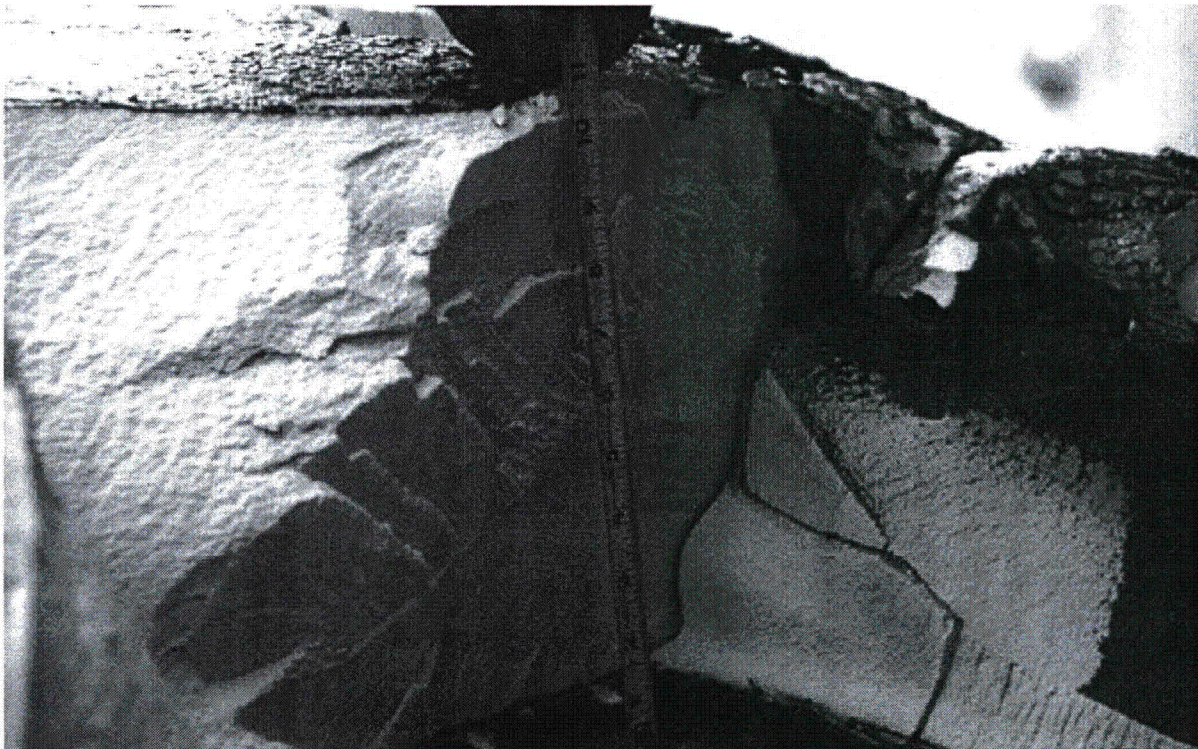


**Figure 2.10.3-51** – CTU-1 Disassembly; OCA Lid Unburned Foam Thickness



**Figure 2.10.3-52** – CTU-1 Disassembly; Payload Drum Removal



**Figure 2.10.3-53** – CTU-1 Disassembly; Loose Debris on Pallet in ICV Body

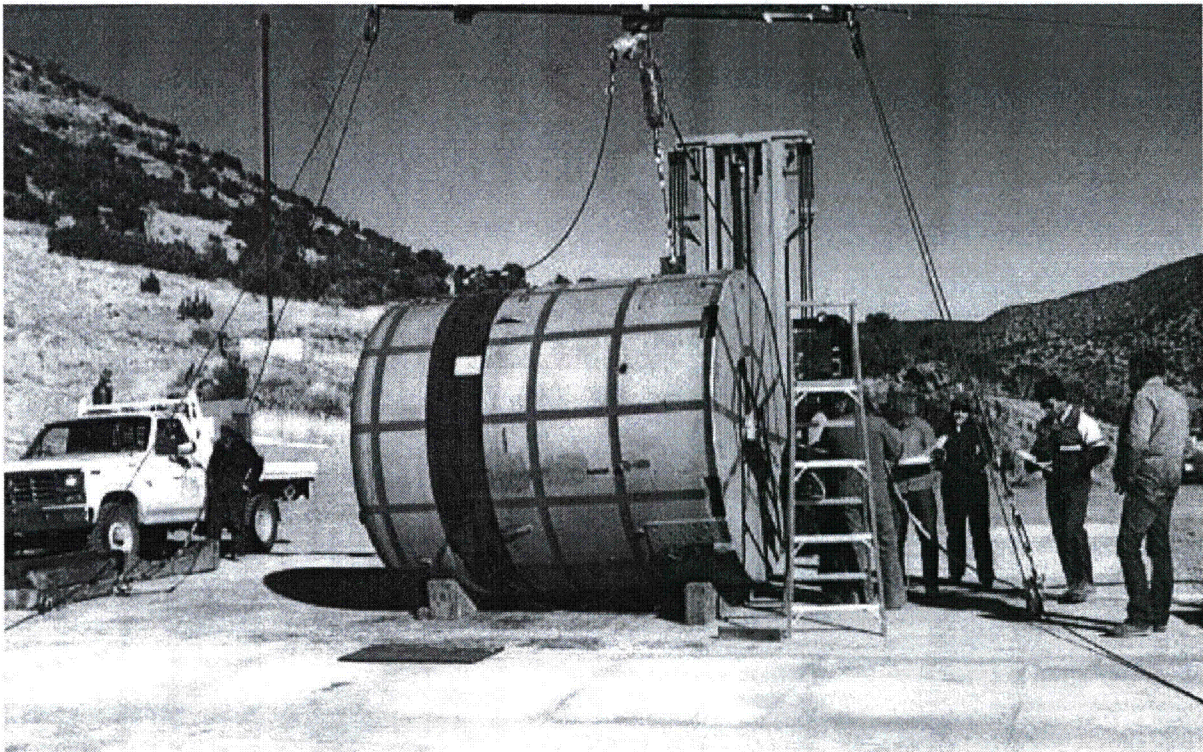


**Figure 2.10.3-54** – CTU-2 Free Drop No. 1; Initial Preparation for Testing

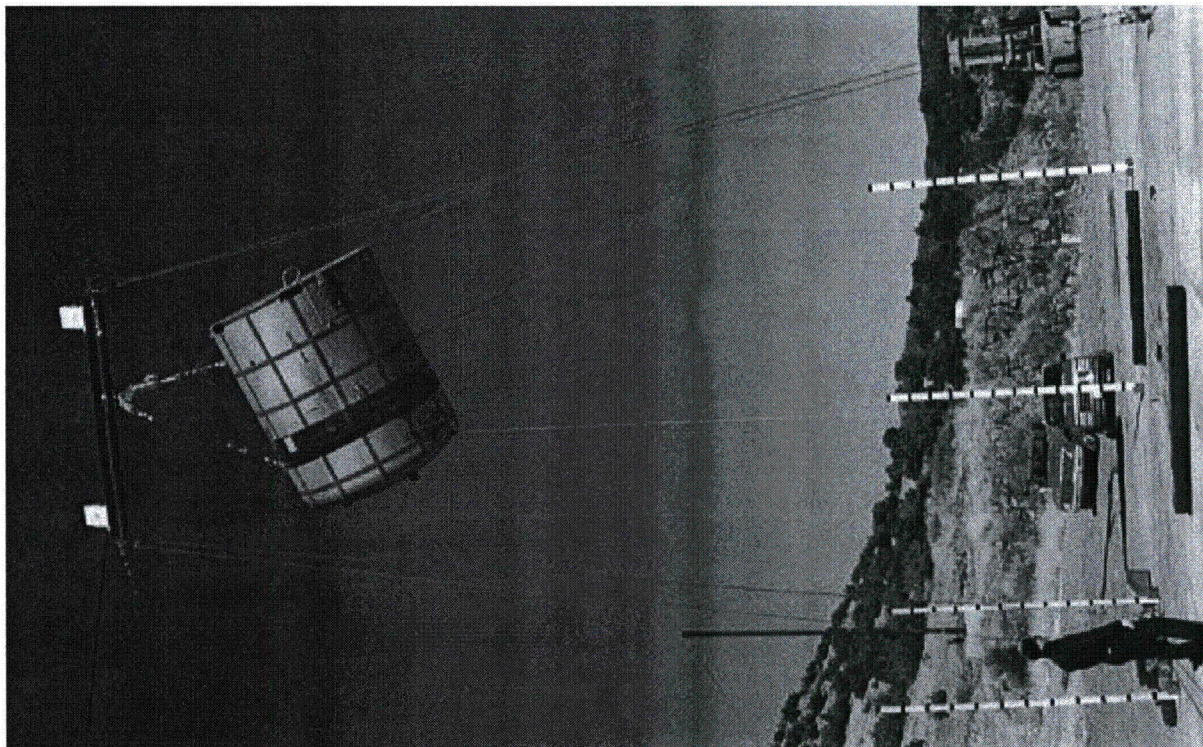


**Figure 2.10.3-55** – CTU-2 Free Drop No. 1; Pre-Drop Positioning

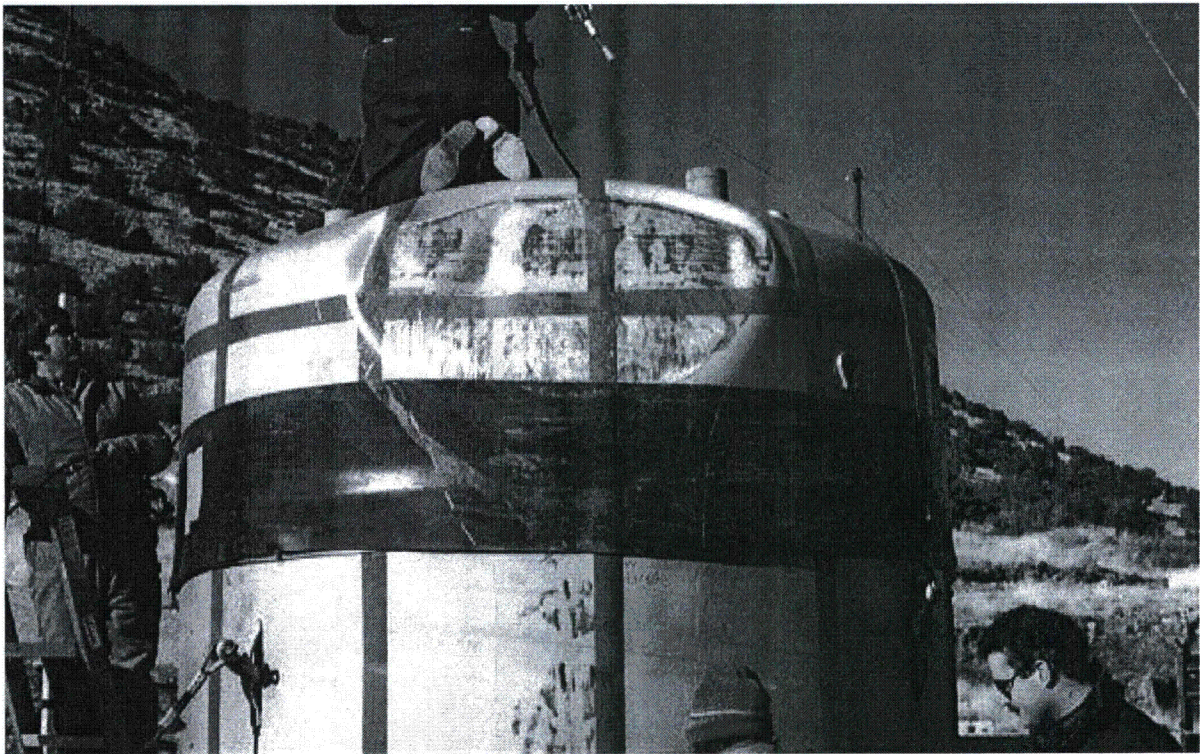


**Figure 2.10.3-56** – CTU-2 Free Drop No. 1; Post-Drop Damage

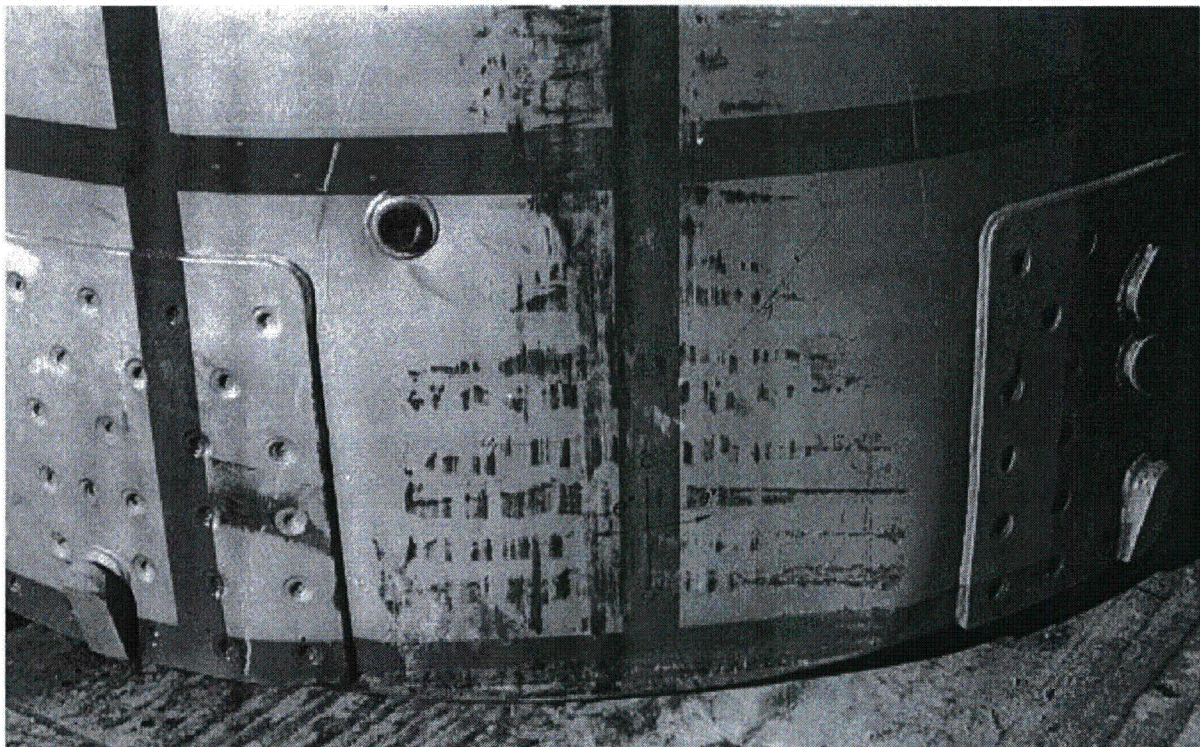


**Figure 2.10.3-57** – CTU-2 Free Drop No. 1; Post-Drop Damage

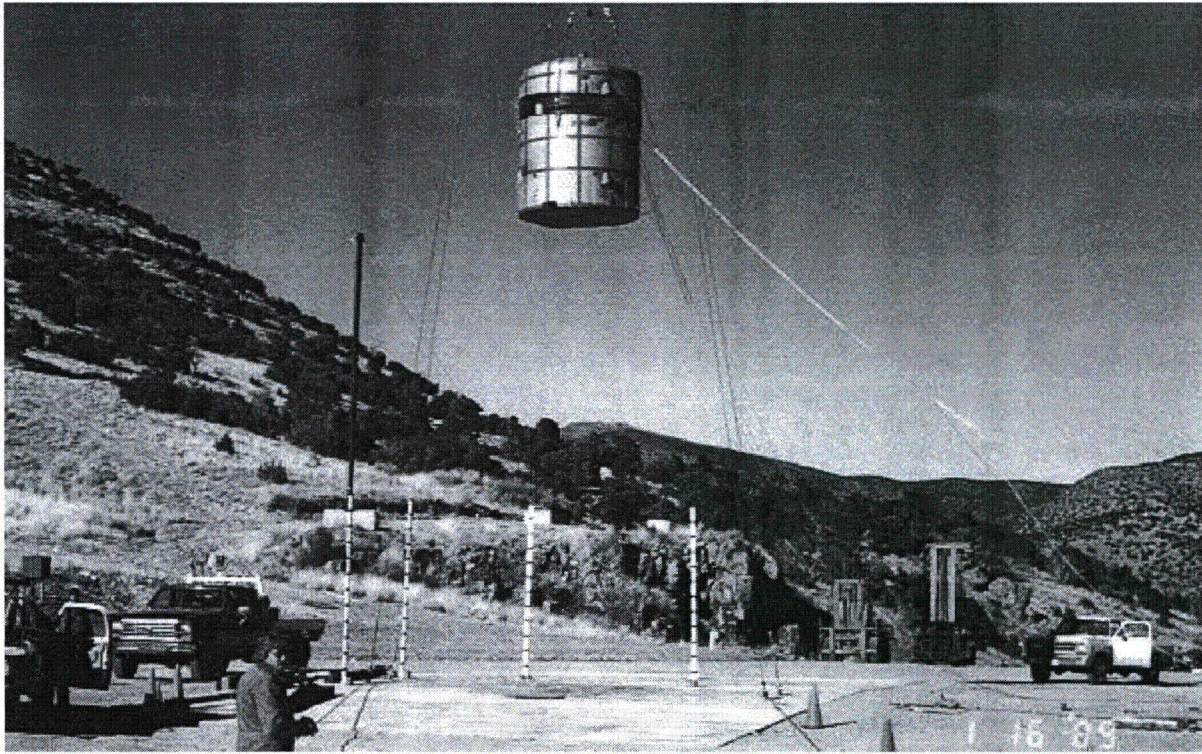


**Figure 2.10.3-58 – CTU-2 Free Drop No. 2; Pre-Drop Positioning**

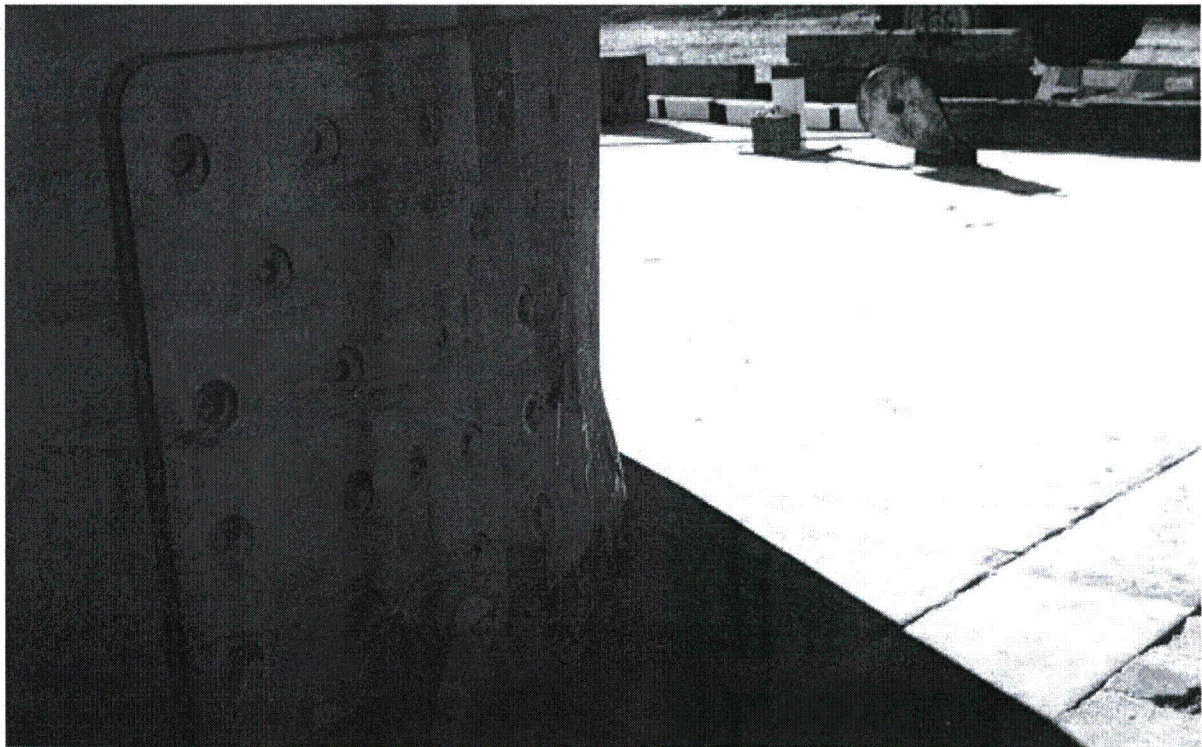


**Figure 2.10.3-59 – CTU-2 Free Drop No. 2; Post-Drop Damage**

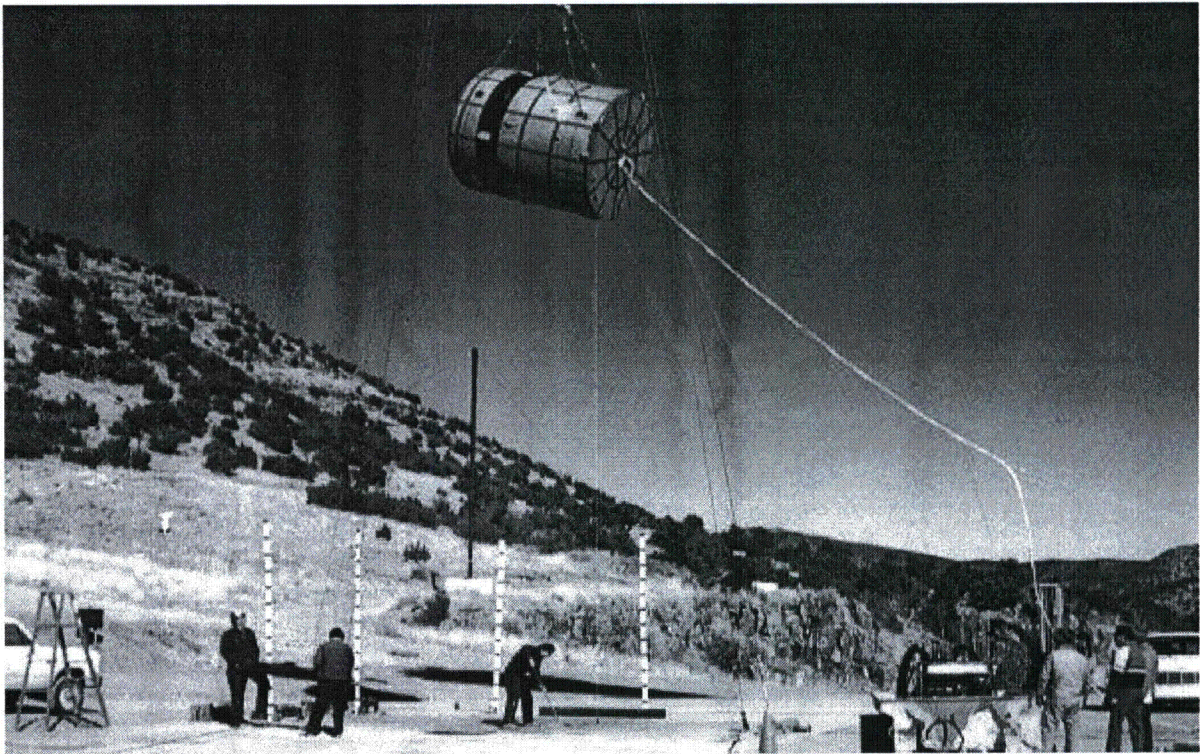


**Figure 2.10.3-60** – CTU-2 Free Drop No. 3; Pre-Drop Positioning

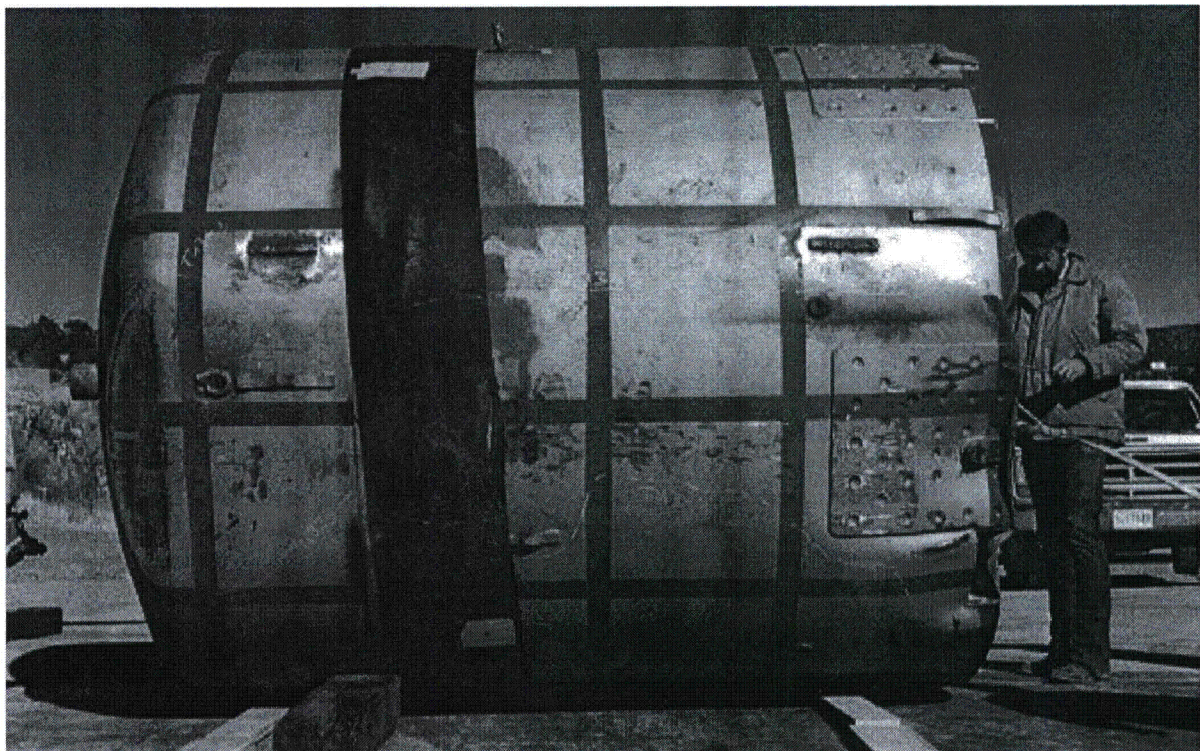


**Figure 2.10.3-61** – CTU-2 Free Drop No. 3; Post-Drop Damage